

NGR- 38-003.036

Orbital Electron Capture by the Nucleus*

W. Bambynek

Bureau Central de Mesures Nucléaires, EURATOM, B-2440 Geel, Belgium

H. Behrens

Zentralstelle für Atomkernenergie-Dokumentation, Kernforschungszentrum

Karlsruhe, 7514 Eggenstein-Leopoldshafen 2,

Germany

M. H. Chen and B. Crasemann

Department of Physics, University of Oregon, Eugene, Oregon 97403,

U. S. A.

M. L. Fitzpatrick and K. W. D. Ledingham

Department of Natural Philosophy, University of Glasgow,

Kelvin Laboratory, N. E. L., East Kilbride,

Lanarkshire, Scotland

H. Genz and M. Mutterer

Institut für Kernphysik, Technische Hochschule Darmstadt,

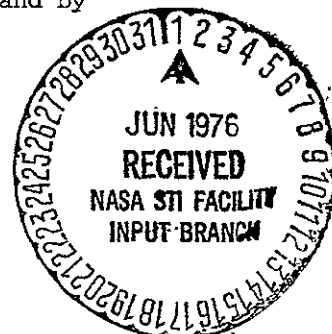
61 Darmstadt, Germany

R. L. Intemann

Department of Physics, Temple University

Philadelphia, Pennsylvania 19122, U.S.A.

*This work was supported in part by Verbundforschung at Ruhr-Universität Bochum, Germany, by the U. S. Army Research Office, and by the National Aeronautics and Space Administration.



N76-23973

Unclass
28097

63/73

(NASA-CR-147953) ORBITAL ELECTRON CAPTURE
BY THE NUCLEUS (Oregon Univ.) 545 P HC
\$13.00 CSCI 20H

The theory of nuclear electron capture is reviewed in the light of current understanding of weak interactions. Experimental methods and results regarding capture probabilities, capture ratios, and EC/β^+ ratios are summarized. Radiative electron capture is discussed, including both theory and experiment. Atomic wave-function overlap and electron exchange effects are covered, as are atomic transitions that accompany nuclear electron capture. Tables are provided to assist the reader in determining quantities of interest for specific cases.

CONTENTS

1.	Introduction.	7
1.1	History.	7
1.2	Energetics	8
1.3	Atomic Effects	10
1.4	Radiative Electron Capture	11
1.5	Significance.	12
1.6	Scope of Review.	12
2.	Electron-Capture Theory	14
2.1	The β -Decay and Electron-Capture Hamiltonian and Transition Rates	14
2.2	Electron-Capture Transition Rates.	30
2.2.1	General Relations for the Transition Probabilities	30
2.2.2	Bound-State Electron Radial Wave Functions.	33
2.2.3	Nuclear Form Factors and Nuclear Matrix Elements.	44
2.2.4	Explicit Expressions for the Quantities $M_K(k_X, k_V)$ and $m_K(k_X, k_V)$	66
2.3	Formulae for Allowed and Forbidden Transitions.	69
2.3.1	Allowed Transitions	69
2.3.2	First-Forbidden Non-Unique Transitions.	70
2.3.3	First-Forbidden Unique Transitions.	71
2.3.4	(L-1)-Forbidden Unique Transitions.	72
2.3.5	Some General Remarks on Higher-Forbidden Non-Unique Transitions.	73

2.4	Electron-Capture to Positron-Decay Ratios:	74
2.4.1	General Expressions	74
2.4.2	Allowed Transitions	77
2.4.3	Non-Unique Forbidden Transitions.	81
2.4.4	Unique Forbidden Transitions.	81
2.5	Atomic Matrix Elements: Exchange and Overlap Corrections:	83
2.5.1	Introduction.	83
2.5.2	Effect of Atomic Overlap and Exchange on Total Capture Rates	84
2.5.3	Overlap and Exchange Corrections on Capture Ratios:	86
2.5.4	Evaluation of Atomic Matrix Elements.	93
2.5.5	Comparison Among Theoretical Exchange Corrections to Capture Ratios	95
2.5.6	Correlation Effects in Electron-Capture Ratios	96
2.5.7	Conclusion:	96
3	Experimental Methods and Results:	98
3.1	Determination of Capture Ratios:	101
3.1.1	Spectrometry with Internal Gas Sources.	102
3.1.2	Spectrometry with Internal Solid Sources.	109
3.1.3	Spectrometry of K and L x Rays with External Sources	112
3.2	Determination of the Relative K-Capture Probability P_K	115
3.2.1	Measurement of K x Rays or Auger Electrons and γ Rays or Conversion Electrons:	115
3.2.2	Coincidence Measurements:	119

3.3	Experimental Capture Probabilities P_K , P_L , and P_M ; Comparison with Theory	127
3.3.1	Experimental Results.	127
3.3.2	Theoretical Predictions	129
3.3.3	Comparison of Experimental and Theoretical Electron-Capture Ratios	131
3.3.4	Conclusions and Recommendations	135
3.4	Determination of K/β^+ and EC/β^+ Ratios	136
3.4.1	Measurements of K/β^+ Ratios with Internal Sources	137
3.4.2	Measurements of K/β^+ Ratios with External Sources	140
3.4.3	Measurements of EC/β^+ Ratios.	144
3.5	Experimental Results and Comparison with Theory for K/β^+ and EC/β^+ Ratios.	150
3.5.1	Results	150
3.5.2	Theoretical Predictions	151
3.5.3	Comparison of Experiment and Theory	153
3.5.4	Conclusions and Recommendations	155
4.	Radiative Electron Capture.	157
4.1	Theory	157
4.1.1	Matrix Elements and Transition Rates.	159
4.1.2	IB Spectra from Allowed Transitions	164
4.1.3	IB Correlation Effects in Allowed Transitions	190
4.1.4	IB Spectra and Correlation Effects in Forbidden Transitions	201
4.2	Experiments.	209
4.2.1	Experiments on Total IB Spectra	212
4.2.2	Experiments on Partial IB Spectra	220

4.2.3	Analysis of IB Pulse-Height Spectra	225
4.2.4	Determination of Electron-Capture Transition Energies from Measured IB Spectra	229
4.2.5	Experimental Results and Comparison with Theory: Allowed and First-Forbidden Nonunique Transitions	234
4.2.6	Experimental Results and Comparison with Theory: IB Spectra from Higher-Forbidden Decays	240
4.2.7	Experiments on IB Correlation Effects	242
4.2.8	Concluding Remarks.	246
5.	Atomic Transitions Accompanying Nuclear Electron Capture. . .	248
5.1	Introduction	248
5.2	Internal Ionization: Nonrelativistic Theory	249
5.3	Relativistic Calculations of Electron Ejection	257
5.4	Electron Ejection from Higher Shells	261
5.5	Measurements of Internal Ionization.	265
5.6	Correlation of x Rays and γ Rays Following Electron Capture.	268
Appendix.	270
A2.1	Expressions for $M_K(k_x, k_\nu)$ and $m_K(k_x, k_\nu)$	270
A2.2	Expansion Coefficients $I(k, m, n, \rho; r)$ up to Order $m=3$. . .	274
Footnotes	276
References.	284
Tables.	341
Figure Captions	465

1. INTRODUCTION

1.1 History

In β decay, a nucleus can capture an electron (or a positron) instead of emitting one. This possibility, inherent in the Fermi (1934) theory of β emission, was first suggested by Yukawa and Sakata (1935, 1936, 1937). The density of atomic bound electrons at the nucleus makes orbital electron capture significant, particularly for s electrons in heavy atoms. Detection of the emitted neutrino is a major experimental undertaking that has not yet met with success (Davis, *et al.*, 1968; see also *Physics Today* 25, August 1972, p. 17; Bahcall, 1972). Even the nuclear recoil from neutrino emission is very difficult to detect (Crane, 1948), unless extraordinary ingenuity is brought to bear (Goldhaber *et al.*, 1958). X rays and Auger electrons emitted in the deexcitation of the ionized daughter provide more readily detectable, albeit indirect, signals of the capture process.

Alvarez (1937) first gained experimental evidence for the existence of nuclear electron capture by detecting Ti K x rays emitted in the decay of ^{48}V . A Geiger counter was employed; positrons were bent away by a magnetic field, and the x-ray energy was established approximately from an Al absorption curve. Gamma-ray internal conversion could not be excluded as a possible origin of the Ti K x rays. A completely conclusive demonstration was brought about the following year, when Alvarez (1938a, b) used differential absorption to identify

Zn K x rays from the decay of ^{67}Ga . Related cloud-chamber experiments were performed by Oldenburg (1938) and by Williams and Pickup (1938), after an unsuccessful attempt by Jacobsen (1937). The capture of L electrons was first observed by Kirkwood *et al.* (1948) and Pontecorvo *et al.* (1949), who mixed radioactive ^{37}Ar with the gas in a proportional counter and found a peak due to Cl L x rays in the spectrum. Dougan (1961) first measured M-electron capture in ^{71}Ge .

Following the work of Fermi (1934) and Yukawa and Sakata (1935, 1936, 1937), the theory of allowed electron capture was developed by Bethe and Bacher (1936) and Møller (1937a, b). Generalizations including forbidden transitions were carried out by Marshak (1942), Bouchez *et al.* (1950; Bouchez, 1952), Brysk and Rose (1958), Hubbard (1965), Robinson (1965), Zweifel (1954, 1957, 1959), Konopinski (1966), and Behrens and Jänecke (1969), among others. The subject has been reviewed by Robinson and Fink (1955, 1960), Bouchez (1963a, 1968a), and Depommier (1960), and Berényi [^] Introductions to the theory are contained in the books by Schopper (1966) and Wu and Moszkowski (1966).

1.2. Energetics

We denote by $W_0 + 1$ the energy (mass) difference between parent and daughter neutral atoms:

$$W_0 = \Delta W_{\text{nucl}} - \Delta |\Sigma E_x|, \quad (1-1)$$

in units such that $\hbar = m_e = c = 1$. Here, ΔW_{nucl} is the energy difference between the parent nucleus (A,Z) and the daughter nucleus (A,Z-1).

The quantity $\Delta |\Sigma E_x|$ is the total change in electron binding energy

between parent and daughter atoms, which arises because all electron energy levels move up in the potential well as the nuclear charge decreases by one unit (the electron cloud "expands"). The binding-energy change $\Delta|\Sigma E_x|$ is not negligible; it amounts to ~ 20 keV for $Z=85$, for example.

Let E_x' be the binding energy of the captured electron in the daughter atom. We neglect the energy of atomic recoil from neutrino emission; its largest value, in ${}^7\text{Be}$ decay, is only 57 eV. Because of imperfect atomic wave-function overlap, the daughter atom's electronic excitation energy will exceed $|E_x'|$ by an amount that we denote by E_R . The average of this rearrangement energy E_R , taken over many atoms, is small (of the order of a few eV), but in those individual transitions in which substantial shakeup or shakeoff (internal ionization) occurs, E_R can be quite significant (Sec. 5). The neutrino energy is

$$q = W_0 + 1 - |E_x'| - E_R \quad (1-2)$$

or

$$q = \Delta W_{\text{nucl}} - \Delta|\Sigma E_x| + 1 - |E_x'| - E_R. \quad (1-3)$$

The atomic excitation energy $|E_x'| + E_R$ is released after the capture event in a cascade of Auger and radiative transitions, except for energy carried into the continuum in shakeoff. The energy threshold for electron capture from orbital x is

$$\Delta W_{\text{nucl}} \geq -1 + \Delta|\Sigma E_x| + |E_x'| + E_R. \quad (1-4)$$

Positron emission is energetically possible, and competes with

orbital electron capture (Secs. 3.4, 3.5) if $W_0 \geq 1$, or

$$\frac{\Delta W_{\text{nucl}}}{\Delta} \geq 1 + \Delta \left| \sum E_x \right| + E_R. \quad (1-5)$$

1.3. Atomic Effects

Nuclear electron capture by its very nature stands at the interface between nuclear and atomic physics. Only in the crudest of approximations can the atomic electron cloud be treated as merely the donor of the electron that is captured. Nevertheless, the importance of treating β decay in general, and electron capture in particular, as transformations of the whole atom was not quantitatively taken into account until Benoist-Gueutal (1950, 1953a, b) wrote her thesis. The idea of including atomic variables in the description of initial and final states was pursued by Odier and Daudel (1956) and formulated elegantly by Bahcall (1962a, 1963a, b).

The fact that the entire atom is transformed in electron-capture decay is reflected in the energetics (Sec. 1.2) and in the effect of imperfect atomic wave-function overlap on the transition rate (Sec. 2.5). Furthermore, atomic transitions such as shakeup and shakeoff (internal ionization) can take place as an integral part of the radioactive decay (Sec. 5), quite distinct from the Auger and x-ray cascade through which the daughter atom is subsequently deexcited. Atomic effects in nuclear decay have recently been reviewed by Emery (1972), Crasemann (1973), Freedman (1974), and Walen and Briançon (1975).

1.4. Radiative Electron Capture

The existence of a low-intensity continuous photon spectrum accompanying β^\pm decay was first observed by Aston (1927) and Bramson (1930). The basic theory of radiative β decay was developed independently by Knipp and Uhlenbeck (1936), who were seeking an explanation for the observed photon continuum, and by Bloch (1936), who was unaware of the experimental work and was motivated by purely theoretical considerations based on Fermi's theory of β decay and Dirac's theory of the positron. Møller (1937a, b) and Morrison and Schiff (1940) pointed out that internal bremsstrahlung (IB) should be emitted in the course of nuclear electron capture as well as in β decay, and independently worked out the theory. Møller (1937a, b) in particular, was interested in differentiating between the Fermi and Konopinski-Uhlenbeck couplings. Internal bremsstrahlung from electron capture was first detected by Bradt *et al.* (1946). A number of reports followed, describing the observation of IB at high energies; all of these data were consistent with the Morrison-Schiff theory. A study of the ^{55}Fe IB spectrum by Madansky and Rasetti (1954), however, showed an unexpected steep rise of the IB intensity at low photon energies. These data were only explained after Glauber and Martin (1956; Martin and Glauber, 1958) developed an elaborate and much more accurate theory of IB in electron capture, in which Coulomb and screening effects are taken into account and capture from L and M shells is included. Although originally restricted to allowed transitions, this theory was later generalized to electron-capture transitions

of arbitrary degree of forbiddenness by Zon and Rapoport (1968; Zon, 1971).

1.5. Significance

Research on electron-capture probabilities and ratios is being pursued as a facet of basic science and because of the importance of applications. Electron capture plays a part in the decay schemes of some 500 radionuclides, 460 of which are commercially available. Nuclear decay by electron capture is not only relevant to nuclear science but also to geochemistry, cosmology and astrophysics (Trimble and Reines, 1973), nuclear medicine (Dillman, 1968, 1970), and technology. The measurement of K/β^+ ratios is one of the more sensitive ^{an} ways of determining an upper limit on the Fierz interference term (Schopper, 1968). Ratios of allowed electron capture from various shells are independent of nuclear factors and reflect purely atomic properties; these ratios are sensitive to bound-electron wave functions at the nuclear surface and to electron exchange and imperfect atomic wave-function overlap (Bahcall, 1962a, 1963a, b).

1.6. Scope of Review

In Sec. 2 of this article, we discuss the theory of allowed and forbidden nuclear electron capture. Formulae and tables are provided that enable the reader to calculate transition rates and ratios of interest. Special attention is paid, in Sec. 2.5, to electron-exchange and atomic wave-function overlap effects on the transition probability. Experimental methods for the measurement of electron-

capture probabilities and ratios and of EC/β^+ ratios are described and compared in Sec. 3. Published data are listed, critically evaluated, and compared with theory. In Sec. 4, the theory of radiative electron capture and experimental work on internal bremsstrahlung are thoroughly reviewed and tables for the calculation of IB spectra are provided. Section 5 is devoted to a discussion of atomic transitions that accompany nuclear electron capture.

We have made an effort at completeness in covering the subject. Some information has been included that is now of merely historical interest, but we have attempted to be adequately critical in the final evaluation and comparison of results. Meson capture, though interesting and closely related to our subject, has not been included.

We hope that this article may prove useful for both theoretical and experimental researchers in need of a complete survey of what is known about nuclear electron capture, and that it will be of help to nuclear physicists and chemists and to workers in radionuclide metrology, nuclear medicine, and in related areas.

2. ELECTRON-CAPTURE THEORY

2.1. The β Decay and Electron-Capture Hamiltonian and Transition Rates

It is usually assumed that all the weak interaction processes can be described by a universal fundamental Hamiltonian density (current-current interaction) (Marshak et al., 1969; Schopper, 1966; Blin-Stoyle, 1973). A general discussion of such phenomenological interaction currents in nuclear systems is given by Lock et al. (1974). For the special case of nuclear β decay, this Hamiltonian density has the form¹

$$H_{\beta}(x) = -G_{\beta} 2^{-1/2} [J_{\mu}(x)L_{\mu}^{+}(x) + \text{h.c.}] \quad (2-1)$$

where J_{μ} and L_{μ} denote the hadron and the lepton current, respectively. The β -decay coupling constant G_{β} is related to the universal weak coupling constant G by

$$G_{\beta} = G \cos\theta, \quad (2-2)$$

where θ is the Cabbibo angle.

Although Eq. (2-1) well describes such processes as β and μ decay, it represents an incomplete theory because it is not renormalizable. Thus, higher-order corrections cannot be calculated. In the last few years, however, renormalizable models (first proposed by Weinberg¹⁹⁶⁷ and Salam, 1968) have been developed.

These models are based on gauge theories unifying the weak and electromagnetic interactions (Abers and Lee, 1973; Lee, 1973; Bernstein, 1974; Weinberg, 1974; Beg and Sirlin, 1974). These gauge theories imply that the weak interaction operates through a neutral current in addition to the previously known charged current. Phenomena induced by neutral currents occur mostly in high-energy physics, but they can be found in atomic physics as well (Bouchiat and Bouchiat, 1974). Nevertheless, for the purposes of the present paper, the Hamiltonian of Eq. (2-1) is sufficient and we shall deal only with this form of the weak-interaction theory.

In nuclear β decay, we must consider the three processes

$$(Z,A) \rightarrow (Z+1,A) + e^- + \bar{\nu}_e \quad (\beta^- \text{ decay})$$

$$(Z,A) \rightarrow (Z-1,A) + e^+ + \nu_e \quad (\beta^+ \text{ decay})$$

$$(Z,A) + e^- \rightarrow (Z-1,A) + \nu_e \quad (\text{electron capture}).$$

Here, (Z,A) signifies an atomic nucleus of mass number A and atomic number Z , e^- denotes an electron and e^+ , a positron, ν_e is the neutrino, and $\bar{\nu}_e$, the antineutrino.

In order to discuss the general features of these weak-interaction processes and their interrelations, we first consider the decay of a single neutron or proton, assuming that the individual nucleons in the nucleus are independent of one another and behave like free particles.

In the case of nuclear β decay, we need only the electron part of the lepton current, which can be expressed as

$$L_\mu(x) = i\bar{\psi}_{\nu_e}(x)\gamma_\mu(1+\gamma_5)\psi_e(x), \quad (2-3)$$

where ψ_{ν_e} and ψ_e are the field operators² and γ_λ the Dirac matrices.³

The nucleons, unlike the leptons, interact strongly as well. This leads to complications, and consequently it is not possible to express the hadron current so simply in terms of field operators (Marshak et al., 1969; Blin-Stoyle, 1973). If, however, we approximately treat the nucleons as point particles, neglecting the influence of the strong interaction, then the hadron current is

$$J_{\mu}(x) = i\bar{\psi}_p \gamma_{\mu} (1 + \lambda \gamma_5) \psi_n, \quad (2-4)$$

where $\lambda = -C_A/C_V = 1.251 \pm 0.009$ (Kropf and Paul, 1974). The Hamiltonian density then has the form

$$H_{\beta}(x) = G_{\beta} 2^{-1/2} \{ \bar{\psi}_p(x) \gamma_{\mu} (1 + \lambda \gamma_5) \psi_n(x) \bar{\psi}_e(x) \gamma_{\mu} (1 + \gamma_5) \psi_{\nu_e}(x) + \text{h.c.} \} \quad (2-5)$$

The corresponding transition matrix elements for the three basic processes in nuclear β decay are

$$n \rightarrow p + e^{-} + \bar{\nu}_e \quad M_{\beta^{-}} = \langle p e^{-} \bar{\nu}_e | \int H_{\beta}(x) d^4x | n \rangle \quad (2-6a)$$

$$p \rightarrow n + e^{+} + \nu_e \quad M_{\beta^{+}} = \langle n e^{+} \nu_e | \int H_{\beta}(x) d^4x | p \rangle \quad (2-6b)$$

$$p + e^{-} \rightarrow n + \nu_e \quad M_{\text{EC}} = \langle n \nu_e | \int H_{\beta}(x) d^4x | p e^{-} \rangle \quad (2-6c)$$

With $H_{\beta}(x)$ according to Eq. (2-5), the transition matrix elements become

$$M_{\beta^{-}} = G_{\beta} 2^{-1/2} (2\pi)^4 \delta(q_p + q_{e^{-}} - q_{\bar{\nu}_e} - q_n) [\bar{u}_p \gamma_{\mu} (1 + \lambda \gamma_5) u_n] [\bar{u}_e \gamma_{\mu} (1 + \gamma_5) v_{\nu}], \quad (2-7a)$$

$$M_{\beta^+} = G_{\beta} 2^{-1/2} (2\pi)^4 \delta(q_n - q_{e^+} + q_{\nu_e} - q_p) [\bar{u}_n \gamma_{\mu} (1 + \lambda \gamma_5) u_p] [\bar{u}_{\nu_e} \gamma_{\mu} (1 + \gamma_5) v_e] \quad (2-7b)$$

$$M_{EC} = G_{\beta} 2^{-1/2} (2\pi)^4 \delta(q_n + q_{\nu_e} - q_p - q_e) [\bar{u}_n \gamma_{\mu} (1 + \lambda \gamma_5) u_p] [\bar{u}_{\nu_e} \gamma_{\mu} (1 + \gamma_5) u_e]. \quad (2-7c)$$

The q 's are the four-momenta of the particles indicated by the subscripts, and $\delta(q)$ is the Dirac delta function.

Equations (2-7) have been derived for the decay of a single, point-like nucleon. To consider the decay of a nucleon in a complex nucleus, we transform the wave function used in Eqs. (2-7) from momentum space to configuration space. For this purpose, the 3-dimensional momentum-dependent part of the delta function is replaced by

$$\delta(\vec{p}) = (2\pi)^{-3} \int e^{-i\vec{p} \cdot \vec{r}} d^3r \quad (2-8)$$

(Blin-Stoyle, 1973). We introduce the plane-wave solutions of the Dirac equation for the particles,

$$\phi_a(\vec{p}_a, \vec{r}) = u_a e^{i\vec{p}_a \cdot \vec{r}}, \quad (2-9a)$$

and for the antiparticles,

$$\phi_b(-\vec{p}_b, \vec{r}) = C \phi_a(\vec{p}_a, \vec{r}) = -\gamma_2 \phi_a^*(\vec{p}_a, \vec{r}) = v_b e^{-i\vec{p}_b \cdot \vec{r}}. \quad (2-9b)$$

Here, a and b denote particles and antiparticles, respectively, and C is the charge conjugation operator. We find

$$M_{\beta^-} = G_{\beta} 2^{-1/2} 2\pi \delta(E_p + E_{e^-} + E_{\nu_e} - E_n) \int \bar{\phi}_p(\vec{p}_p, \vec{r}) \gamma_{\mu} (1 + \lambda \gamma_5) \\ \times \phi_n(\vec{p}_n, \vec{r}) \bar{\phi}_{e^-}(\vec{p}_e, \vec{r}) \gamma_{\mu} (1 + \gamma_5) \phi_{\nu_e}(-\vec{p}_{\nu_e}, \vec{r}); \quad (2-10a)$$

$$\begin{aligned}
M_{\beta+} = & G_{\beta} z^{-1/2} 2\pi \delta(E_n + E_{e^+} + E_{\nu_e} - E_p) \int \bar{\phi}_n(\vec{p}_n, \vec{r}) \gamma_{\mu} (1 + \lambda \gamma_5) \\
& \times \phi_p(\vec{p}_p, \vec{r}) \bar{\phi}_{\nu_e}(\vec{p}_{\nu_e}, \vec{r}) \gamma_{\mu} (1 + \gamma_5) \phi_{e^+}(-\vec{p}_{e^+}, \vec{r}) d^3r; \quad (2-10b)
\end{aligned}$$

$$\begin{aligned}
M_{EC} = & G_{\beta} z^{-1/2} 2\pi \delta(E_n + E_{\nu_e} - E_p - E_{e^-}) \int \bar{\phi}_n(\vec{p}_n, \vec{r}) \gamma_{\mu} (1 + \lambda \gamma_5) \\
& \times \phi_p(\vec{p}_p, \vec{r}) \bar{\phi}_{\nu_e}(\vec{p}_{\nu_e}, \vec{r}) \gamma_{\mu} (1 + \gamma_5) \phi_{e^-}(\vec{p}_{e^-}, \vec{r}) d^3r. \quad (2-10c)
\end{aligned}$$

Inside the nucleus, we replace the nucleon plane waves by bound spinor wave functions, and represent electrons or positrons by wave functions which are solutions of the Dirac equation for an extended charged nucleus surrounded by atomic electrons.⁴ Furthermore, it is convenient to split off the delta function and the factor 2π by writing $M_{\beta} = 2\pi \delta(E_i - E_f) \langle f | H_{\beta} | i \rangle$.

The hadron parts of Eqs. (2-10a-c) can now be expanded into multipoles (Schopper, 1966; Konopinski, 1966; Bouchez and Depommier, 1960; Weidenmüller, 1961):

$$\left[\bar{\phi}_f \gamma_{\mu} (1 + \lambda \gamma_5) \phi_i \right] \gamma_4 \gamma_{\mu} = \sum_{KLSM} (-1)^{K+M} a_{KLS}^M(\vec{r}) T_{KLS}^{-M}(\hat{r}). \quad (2-11)$$

Here, i and f denote initial and final states, and

$$T_{LLO} = i Y_L^M \quad (2-12a)$$

and

$$T_{KL1} = (-1)^{L-K+1} i Y_{KL}^M \cdot \vec{\alpha} \quad (2-12b)$$

are the multipole operators.⁵

The expansion coefficients $a_{KLS}^M(r)$ can be derived from the relation

$$a_{KLS}^M(r) = \int \phi_f^+(1+\lambda\gamma_5) T_{KLS}^M \phi_i d\Omega_{\text{nucl}} \quad (2-13)$$

Inserting Eqs. (2-11) and (2-13) in Eqs. (2-10a-c), we find for the matrix elements

$$\begin{aligned} \langle f | H_{\beta^-} | i \rangle &= G_{\beta} 2^{-1/2} \sum_{KLSM} (-1)^{K+M} \left[\int \phi_p^+(1+\lambda\gamma_5) T_{KLS}^M \phi_n d\Omega_{\text{nucl}} \right] \\ &\times \left[\int \phi_{e^-}^+(Z)(1+\gamma_5) T_{KLS}^{-M} \phi_{\nu_e}^-(\vec{q}) d\Omega_{\text{lept}} \right] r^2 dr; \end{aligned} \quad (2-14a)$$

$$\begin{aligned} \langle f | H_{\beta^+} | i \rangle &= G_{\beta} 2^{-1/2} \sum_{KLSM} (-1)^{K+M} \left[\int \phi_n^+(1+\lambda\gamma_5) T_{KLS}^M \phi_p d\Omega_{\text{nucl}} \right] \\ &\times \left[\int \phi_{\nu_e}^+(\vec{q})(1+\gamma_5) T_{KLS}^{-M} \phi_{e^+}(-Z) d\Omega_{\text{lept}} \right] r^2 dr; \end{aligned} \quad (2-14b)$$

$$\begin{aligned} \langle f | H_{EC} | i \rangle &= G_{\beta} 2^{-1/2} \sum_{KLSM} (-1)^{K+M} \left[\int \phi_n^+(1+\lambda\gamma_5) T_{KLS}^M \phi_p d\Omega_{\text{nucl}} \right] \\ &\times \left[\int \phi_{\nu_e}^+(\vec{q})(1+\gamma_5) T_{KLS}^{-M} \phi_{e^-}(Z) d\Omega_{\text{lept}} \right] r^2 dr. \end{aligned} \quad (2-14c)$$

Here, \vec{q} denotes the momentum for neutrino or antineutrino, and $\phi_{e^{\pm}}(\mp Z)$ is the electron or positron wave function in the Coulomb field of a nucleus of atomic number Z .

We expand the electron (positron) and neutrino (antineutrino) continuum wave functions in partial spherical waves ϕ_{κ}^{μ} (Konopinski, 1966; Schülke, 1964; Weidenmüller, 1961):

$$\phi_{e^-}(Z) = \sum_{\kappa_e \mu_e} a_{\kappa_e \mu_e} \phi_{\kappa_e}^{\mu_e}(Z), \quad (2-15a)$$

$$\phi_{\nu_e}(q) = \sum_{\kappa_{\nu_e}^{\mu_{\nu_e}}} b_{\kappa_{\nu_e}^{\mu_{\nu_e}}} \phi_{\kappa_{\nu_e}^{\mu_{\nu_e}}}^{\mu_{\nu_e}}(q), \quad (2-15b)$$

$$\phi_{e^+}(-Z) = -\gamma_2 \phi_{e^-}^*(Z) = \sum_{\kappa_e^{\mu_e}} (-1)^{j(\kappa_e) + \mu_e} a_{\kappa_e^{\mu_e}}^* \phi_{\kappa_e^{\mu_e}}^{-\mu_e}(-Z), \quad (2-15c)$$

$$\phi_{\bar{\nu}_e}(-q) = -\gamma_2 \phi_{\nu_e}^*(q) = \sum_{\kappa_{\nu_e}^{\mu_{\nu_e}}} (-1)^{j(\kappa_{\nu_e}) + \mu_{\nu_e}} b_{\kappa_{\nu_e}^{\mu_{\nu_e}}}^* \phi_{\kappa_{\nu_e}^{\mu_{\nu_e}}}^{-\mu_{\nu_e}}(-q). \quad (2-15d)$$

The spherical waves ϕ_{κ}^{μ} here have the form

$$\phi_{\kappa}^{\mu}(Z) = \begin{pmatrix} (\text{sign } \kappa) f_{\kappa}(Z, r) \chi_{-\kappa}^{\mu} \\ g_{\kappa}(Z, r) \chi_{\kappa}^{\mu} \end{pmatrix}, \quad (2-16)$$

where we have

$$\chi_{\kappa}^{\mu} = i^{\ell} \sum_m C(\ell \frac{1}{2} j; \mu - m m) Y_{\ell}^{\mu - m} \chi^m, \quad (2-17)$$

the χ^m ($m = \pm \frac{1}{2}$) are two-component Pauli spinors, the $C(\ell \frac{1}{2} j; \mu - m m)$ are Clebsch-Gordan coefficients, and the Y_{ℓ}^{μ} are spherical harmonics. The index κ is

$$\kappa = \begin{cases} \ell, & j = \ell - \frac{1}{2} \\ -(\ell + 1), & j = \ell + \frac{1}{2} \end{cases}, \quad (2-18)$$

and $g_{\kappa}(Z, r)$ and $f_{\kappa}(Z, r)$ are the large and small radial wave functions, respectively.

The antiparticle (positron) wave function is (Rose, 1961)

$$\bar{\phi}_{\kappa}^{\mu}(-Z) = \begin{pmatrix} g_{\kappa}(-Z, r) \chi_{\kappa}^{-\mu} \\ (-\text{sign } \kappa) f_{\kappa}(-Z, r) \chi_{-\kappa}^{-\mu} \end{pmatrix}. \quad (2-19)$$

The neutrino radial wave functions can be written explicitly:

$$\phi_{\kappa}^{\mu}(q) = \begin{bmatrix} j_{\bar{\ell}}(qr) \chi_{-\kappa}^{\mu} \\ j_{\ell}(qr) \chi_{\kappa}^{\mu} \end{bmatrix} \quad (2-20)$$

where $\ell - \bar{\ell} = \text{sign } \kappa$, and $j_{\ell}(qr)$ is the spherical Bessel function.

For the antineutrino we have

$$\bar{\phi}_{\kappa}^{\mu}(-q) = \begin{bmatrix} j_{\ell}(qr) \chi_{\kappa}^{-\mu} \\ -j_{\bar{\ell}}(qr) \chi_{-\kappa}^{-\mu} \end{bmatrix}. \quad (2-21)$$

The expansion coefficients $a_{\kappa\mu}$ and $b_{\kappa\mu}$ in Eqs. (2-15) are determined by the condition that the continuum wave functions $\phi_{e^{-}}(Z)$ and $\phi_{\nu_e}(q)$ become asymptotically equal to a plane wave plus incoming (or outgoing) spherical waves (Schülke, 1964; Weidenmüller, 1961):

$$\begin{aligned} a_{\kappa_e \mu_e}(\vec{p}, s_e) &= 4\pi p^{-1} C(\ell) \frac{1}{e^2} j_{\ell}(\mu_e^{-s_e} s_e) \\ &\quad \times Y_{\ell}^{*\mu_e -s_e}(\hat{p}) e^{-i[\Delta_{\kappa_e} + (\pi/2)(\ell_e + 1)]} \end{aligned} \quad (2-22)$$

$$b_{\kappa_{\nu} \mu_{\nu}}(\vec{q}, s_{\nu}) = 4\pi C(\ell) \frac{1}{\nu^2} j_{\ell}(\mu_{\nu}^{-s_{\nu}} s_{\nu}) Y_{\ell}^{*\mu_{\nu} -s_{\nu}}(\hat{q}) \quad (2-23)$$

Here, Δ_{κ} is the Coulomb phase (Böhning, 1965, 1967).

It is useful, furthermore, to introduce reduced hadron and lepton matrix elements by applying the Wigner-Eckart theorem.

From Eqs. (2-14a-c) and (2-15a-c) we find

$$\begin{aligned}
\langle f | H_{\beta-} | i \rangle &= G_{\beta} 2^{-1/2} \sum_{KLSM} \sum_{\kappa_e^{\mu_e}} (-1)^{J_f - M_f + j_e - \mu_e} \\
&\quad \kappa_v^{\mu_v} \\
&\quad \times (-1)^{K+M+j_v+\mu_v} \begin{Bmatrix} J_f & K & J_i \\ -M_f & M & M_i \end{Bmatrix} \begin{Bmatrix} j_e & K & j_v \\ -\mu_e & -M & -\mu_v \end{Bmatrix} \\
&\quad \times a_{\kappa_e^{\mu_e}}^* b_{\kappa_v^{\mu_v}}^* \langle \phi_p \| (1+\lambda\gamma_5)^T_{KLS} \| \phi_n \rangle \\
&\quad \times \langle \phi_{\kappa_e}(Z) \| (1+\gamma_5)^T_{KLS} \| \phi_{\kappa_v}(-q) \rangle r^2 dr; \tag{2-24a}
\end{aligned}$$

$$\begin{aligned}
\langle f | H_{\beta+} | i \rangle &= G_{\beta} 2^{-1/2} \sum_{KLSM} \sum_{\kappa_e^{\mu_e}} (-1)^{J_f - M_f + j_v - \mu_v} \\
&\quad \kappa_v^{\mu_v} \\
&\quad \times (-1)^{K+M+j_e+\mu_e} \begin{Bmatrix} J_f & K & J_i \\ -M_f & M & M_i \end{Bmatrix} \begin{Bmatrix} j_v & K & j_e \\ -\mu_v & -M & -\mu_e \end{Bmatrix} \\
&\quad \times a_{\kappa_e^{\mu_e}}^* b_{\kappa_v^{\mu_v}}^* \langle \phi_n \| (1+\lambda\gamma_5)^T_{KLS} \| \phi_p \rangle \\
&\quad \times \langle \phi_{\kappa_v}(q) \| (1+\gamma_5)^T_{KLS} \| \phi_{\kappa_e}(-Z) \rangle r^2 dr; \tag{2-24b}
\end{aligned}$$

$$\begin{aligned}
\langle f | H_{EC} | i \rangle &= G_{\beta} 2^{-1/2} \sum_{KLSM} \sum_{\kappa_v^{\mu_v}} (-1)^{J_f - M_f + j_v - \mu_v} \\
&\quad \times (-1)^{K+M} \begin{Bmatrix} J_f & K & J_i \\ -M_f & M & M_i \end{Bmatrix} \begin{Bmatrix} j_v & K & j_x \\ -\mu_v & -M & \mu_x \end{Bmatrix} b_{\kappa_v^{\mu_v}}^* \\
&\quad \times \langle \phi_n \| (1+\lambda\gamma_5)^T_{KLS} \| \phi_p \rangle \\
&\quad \times \langle \phi_{\kappa_v}(q) \| (1+\gamma_5)^T_{KLS} \| \phi_{\kappa_x}(Z) \rangle r^2 dr. \tag{2-24c}
\end{aligned}$$

Here, x ($=K, L_1, L_2, L_3, M_1, \dots$) denotes the different shells and subshells of the atomic cloud from which the electron can be captured. The states of the initial neutron or proton are specified by $|J_i M_i\rangle$, and those of the final nucleon, by $|J_f M_f\rangle$.

The similarity of Eqs. (2-24a), (2-24b), and (2-24c) suggests that we need to derive the final formulae of the observables for only one type of decay (β^- , β^+ , or EC) and can hence obtain results for the other decay modes. For this purpose, we transform Eqs. (2-24b,c) into a form that is similar to that of Eq. (2-24a), by interchanging initial and final states in the reduced lepton matrix elements. Taking into account the relation (Weidenmüller, 1961)

$$\langle f || (1+\gamma_5)^T_{KLS} || i \rangle^* = (-1)^{K-s+j_i-j_f} \langle i || (1+\gamma_5)^T_{KLS} || f \rangle \quad (2-25)$$

and the fact that here the reduced matrix elements are defined as real quantities, we obtain

$$\begin{aligned} \langle f | H_{\beta^+} | i \rangle &= G_{\beta^+} 2^{-1/2} \sum_{KLSM} \sum_{\kappa_e \mu_e} (-1)^{J_f - M_f + j_e - \mu_e} \\ &\quad \kappa_v \mu_v \\ &\times (-1)^{K-s+M+j_v+\mu_v+1} \begin{bmatrix} J_f & K & J_i \\ -M_f & M & M_i \end{bmatrix} \begin{bmatrix} j_e & K & j_v \\ -\mu_e & -M & -\mu_v \end{bmatrix} \\ &\times a_{\kappa_e \mu_e}^* b_{\kappa_v \mu_v}^* \langle \phi_n || (1+\lambda\gamma_5)^T_{KLS} || \phi_p \rangle \\ &\times \langle \phi_{\kappa_e}(-Z) || (1+\gamma_5)^T_{KLS} || \phi_{\kappa_v}(q) \rangle r^2 dr; \end{aligned} \quad (2-26a)$$

$$\begin{aligned}
\langle f | H_{EC} | i \rangle &= G_{\beta} 2^{-1/2} \sum_{KLSM} \sum_{\kappa \mu} (-1)^{J_f - M_f + j_x - \mu_x} \\
&\times (-1)^{K - s + M + j_v + \mu_v + 1} \begin{bmatrix} J_f & K & J_i \\ -M_f & M & M_i \end{bmatrix} \begin{bmatrix} j_x & K & j_v \\ \mu_x & -M & -\mu_v \end{bmatrix} \\
&\times b_{\kappa \nu \mu \nu}^* (-1)^{j_x + \mu_x} \int \langle \phi_n || (1 + \lambda \gamma_5)^T_{KLS} || \phi_p \rangle \\
&\times \langle \phi_{\kappa_x}(Z) || (1 + \gamma_5)^T_{KLS} || \phi_{\kappa_v}(q) \rangle r^2 dr. \tag{2-26b}
\end{aligned}$$

The transition probability per unit time can now be found from standard quantum-mechanical formulae. By applying first-order time-dependent perturbation theory (the "Golden Rule"), the decay constant λ and the half life t are given by

$$\begin{aligned}
\lambda_{\beta^{\pm}} &= (\ln 2)(t_{\beta^{\pm}})^{-1} = 2\pi(2J_i + 1)^{-1} \sum_{M_i, M_f} \sum_{s_e, s_v} \\
&\times \iiint |\langle f | H_{\beta^{\pm}} | i \rangle|^2 p^2 q^2 dp d\Omega_e d\Omega_v (2\pi)^{-6} \tag{2-27}
\end{aligned}$$

for β^{\pm} -decay, and by

$$\begin{aligned}
\lambda_x &= (\ln 2)(t_x)^{-1} = 2\pi(2J_i + 1)^{-1} \sum_{M_i, M_f} \sum_{\mu_x, s_v} \\
&\times \int |\langle f | H_{EC} | i \rangle|^2 q_x^2 d\Omega_v (2\pi)^{-3} \tag{2-28}
\end{aligned}$$

for electron capture from the atomic x-shell. By inserting the matrix element given by Eq. (2-24a) in Eq. (2-27) and making use of the orthogonality relations for Clebsch-Gordan coefficients and $3j$ -symbols, we find

$$\lambda_{\beta^-} = G_{\beta}^2 (2\pi)^{-3} (2J_i + 1)^{-1} \frac{1}{2} \sum_K \sum_{\kappa_e \kappa_\nu} \left\{ \sum_{L_S} (2K+1)^{-1/2} (4\pi)^{1/2} \right. \\ \times \langle \phi_p || (1 + \lambda \gamma_5)^T_{KLS} || \phi_n \rangle \\ \left. \times (4\pi)^{1/2} \langle \phi_{\kappa_e}(Z) || (1 + \gamma_5)^T_{KLS} || \phi_{\kappa_\nu}(-q) \rangle r^2 dr \right\}^2 q^2 dp. \quad (2-29)$$

Similarly, by combining Eqs. (2-26a) and (2-27), we have

$$\lambda_{\beta^+} = G_{\beta}^2 (2\pi)^{-3} (2J_i + 1)^{-1} \frac{1}{2} \sum_K \sum_{\kappa_e \kappa_\nu} \left\{ \sum_{L_S} (-1)^S (2K+1)^{-1/2} (4\pi)^{1/2} \right. \\ \times \langle \phi_n || (1 + \lambda \gamma_5)^T_{KLS} || \phi_p \rangle \\ \left. \times (4\pi)^{1/2} \langle \phi_{\kappa_e}(-Z) || (1 + \gamma_5)^T_{KLS} || \phi_{\kappa_\nu}(q) \rangle r^2 dr \right\}^2 q^2 dp. \quad (2-30)$$

The electron-capture decay constant is found by inserting Eq. (2-26b) in Eq. (2-28):

$$\lambda_x = G_{\beta}^2 (2\pi)^{-3} (2J_i + 1)^{-1} (1/2) \sum_K \sum_{\kappa_\nu} \left\{ \sum_{L_S} (-1)^S (2K+1)^{-1/2} \right. \\ \times (4\pi)^{1/2} \langle \phi_n || (1 + \lambda \gamma_5)^T_{KLS} || \phi_p \rangle \\ \left. \times (4\pi)^{1/2} \langle \phi_{\kappa_x}(Z) || (1 + \gamma_5)^T_{KLS} || \phi_{\kappa_\nu}(q) \rangle r^2 dr \right\}^2 q_x^2. \quad (2-31)$$

The neutrino momentum q_x is given by

$$q_x = W_0 + W_x^i, \quad (2-32)$$

where W_0 is the total transition energy between initial and final states (the difference between the atomic masses, minus $m_0 c^2$, see Sec 1.2), and W_x^i denotes the energy of the bound electron (in the daughter atom). This is $W_x^i = -|E_x^i|$, where E_x^i is the binding energy of the electron. Because the electron and neutrino wave functions

are well-known [Eqs. (2-16)-(2-21)], we can evaluate the reduced lepton matrix elements explicitly (Schülke, 1964; Weidenmüller, 1961). For the three kinds of reduced lepton matrix elements appearing in Eqs. (2-29), (2-30), and (2-31), we have

$$\begin{aligned}
 (4\pi)^{1/2} \langle \phi_{\kappa_e}(-Z) | | (1+\gamma_5) T_{KLS} | | \phi_{\kappa_\nu}(q) \rangle &= g_{\kappa_e}(Z) \left[j_{\ell_\nu} G_{KLS}(\kappa_e, \kappa_\nu) \right. \\
 &+ j_{\ell_\nu} G_{KLS}(\kappa_e, -\kappa_\nu) \left. \right] + (\text{sign } \kappa_e) f_{\kappa_e}(Z) \left[j_{\ell_\nu} G_{KLS}(-\kappa_e, \kappa_\nu) \right. \\
 &\left. + j_{\ell_\nu} G_{KLS}(-\kappa_e, -\kappa_\nu) \right] \quad (2-33)
 \end{aligned}$$

for the electron-neutrino matrix element,

$$\begin{aligned}
 (4\pi)^{1/2} \langle \phi_{\kappa_e}(Z) | | (1+\gamma_5) T_{KLS} | | \phi_{\kappa_\nu}(-q) \rangle &= g_{\kappa_e}(Z) \left[j_{\ell_\nu} G_{KLS}(\kappa_e, \kappa_\nu) - j_{\ell_\nu} G_{KLS}(\kappa_e, -\kappa_\nu) \right] \\
 + (\text{sign } \kappa_e) f_{\kappa_e}(Z) \left[j_{\ell_\nu} G_{KLS}(-\kappa_e, \kappa_\nu) - j_{\ell_\nu} G_{KLS}(-\kappa_e, -\kappa_\nu) \right] \quad (2-34)
 \end{aligned}$$

for the electron-antineutrino matrix element, and

$$\begin{aligned}
 (4\pi)^{1/2} \langle \phi_{\kappa_e}(-Z) | | (1+\gamma_5) T_{KLS} | | \phi_{\kappa_\nu}(q) \rangle &= g_{\kappa_e}(-Z) \left[j_{\ell_\nu} G_{KLS}(\kappa_e, \kappa_\nu) + j_{\ell_\nu} G_{KLS}(\kappa_e, -\kappa_\nu) \right] \\
 + (\text{sign } \kappa_e) f_{\kappa_e}(-Z) \left[j_{\ell_\nu} G_{KLS}(-\kappa_e, \kappa_\nu) + j_{\ell_\nu} G_{KLS}(-\kappa_e, -\kappa_\nu) \right] \quad (2-35)
 \end{aligned}$$

for the positron-neutrino matrix element. The quantity $G_{KLS}(n_1, n_2)$, introduced by Weidenmüller (1961), represents the spin-angular part of these reduced lepton matrix elements:

$$\begin{aligned}
G_{KLS}(n_f, n_i) &= \left\{ (2s+1)(2K+1)[2\ell_f(n_f)+1][2\ell(n_i)+1](2j_f+1)(2j_i+1) \right\}^{1/2} \\
&\quad \times i^{\ell(n_i)+\ell(n_f)+L} (-1)^{j_i-j_f} \\
&\quad \times C\left(\ell(n_f) \ell(n_i) L; 00\right) \left\{ \begin{matrix} K & s & L \\ j_f & \frac{1}{2} & \ell(n_f) \\ j_i & \frac{1}{2} & \ell(n_i) \end{matrix} \right\}. \quad (2-36)
\end{aligned}$$

Here, we have $\ell(n)=n$ if $n>0$ and $\ell(n)=|n|-1$ if $n<0$, where n stands for $+\kappa$ and $-\kappa$; C is a Clebsch-Gordan coefficient, and the braces denote a Wigner $9j$ -symbol.

We now consider the relation between β^- and β^+ decay. It is easily shown that the following relations hold:

$$\begin{aligned}
&(-1)^{1-s}(4\pi)^{1/2} \langle \phi_{\kappa_e}(Z) \| (1-\gamma_5)^T_{KLS} \| \phi_{\kappa_v}(-q) \rangle \\
&= g_{\kappa_e}(Z) \left[j_{\ell_v} G_{KLS}(\kappa_e, \kappa_v) + j_{\ell_v}^- G_{KLS}(\kappa_e, -\kappa_v) \right] \\
&(\text{sign } \kappa_e)^{f_{\kappa_e}}(Z) \left[j_{\ell_v} G_{KLS}(-\kappa_e, \kappa_v) + j_{\ell_v}^- G_{KLS}(-\kappa_e, -\kappa_v) \right]. \quad (2-37)
\end{aligned}$$

Thus, we see from Eq. (2-35) that the product of the two reduced matrix elements in Eq. (2-30) can be replaced as follows:

$$\begin{aligned}
&\langle \| (1+\lambda\gamma_5)^T_{KLS} \| \rangle \langle \| (1-\gamma_5)^T_{KLS} \| \rangle \\
&= \langle \| T_{KLS} \| \rangle \langle \| (1-\gamma_5)^T_{KLS} \| \rangle - \langle \| \lambda\gamma_5^T_{KLS} \| \rangle \langle \| \gamma_5(1-\gamma_5)^T_{KLS} \| \rangle. \quad (2-38)
\end{aligned}$$

Consequently, we can derive the formulae for β^+ decay from those for β^- decay by making the following substitutions:

$$\begin{array}{ccc}
 \beta^- \text{ decay} & & \beta^+ \text{ decay} \\
 \lambda & \rightarrow & -\lambda \\
 Z & \rightarrow & -Z \\
 G & \rightarrow & -G
 \end{array} \tag{2-39}$$

Here, G represents the terms which are due to parity non-conservation (e.g., electron polarization or β - γ circular polarization correlation). The relation between β^+ decay and electron capture is established by the substitutions [cf. Eqs. (2-30), (2-31), (2-33), (2-35)]

$$\begin{array}{ccc}
 \beta^+ \text{ decay} & & \text{électron capture} \\
 f_{\kappa_e}(-Z) & \rightarrow & -f_{\kappa_e}(Z) \\
 g_{\kappa_e}(-Z) & \rightarrow & g_{\kappa_e}(Z)
 \end{array} \tag{2-40}$$

where $g_{\kappa_e}(Z)$ and $f_{\kappa_e}(Z)$ are the large and small components of the bound-state electron radial wave functions, respectively. Alternatively, we can start from β^- decay [cf. Eqs. (2-29) and (2-34) vs. Eqs. (2-31) and (2-33)]:

$$\begin{array}{ccc}
 \beta^- \text{ decay} & \rightarrow & \text{électron capture} \\
 j_{l_v}(qr) & \rightarrow & j_{l_v}(qr) \\
 j_{l_v}^-(qr) & \rightarrow & -j_{l_v}^-(qr)
 \end{array}$$

$$\langle f || (1+\lambda\gamma_5)^T_{KLs} || i \rangle + (-1)^S \langle f || (1+\lambda\gamma_5)^T_{KLs} || i \rangle \tag{2-41a}$$

$$\begin{array}{ccc}
 \text{continuum-electron} & & \text{bound-electron} \\
 \text{wave function} & \rightarrow & \text{wave function}
 \end{array}$$

For the decay probabilities as given in Eqs. (2-29) and (2-31), this prescription can be replaced by one mentioned by Behrens and Jänecke (1969):

$$\begin{array}{ll}
 \beta^- \text{ decay} & \rightarrow \text{electron capture} \\
 q & \rightarrow -q
 \end{array}$$

$$\langle f || (1 + \lambda \gamma_5)^T_{KLs} || i \rangle \rightarrow (-1)^{K-s} \langle f || (1 + \lambda \gamma_5)^T_{KLs} || i \rangle. \quad (2-41b)$$

In this description of the electron-capture and β -decay processes, three important points have not been considered:

1. The hadron current in the form of Eq. (2-4) is an approximation which is only valid for bare nucleons. The exact form of this current is discussed under the heading Induced Interactions in Sec. 2.2.3.

2. The Hamiltonian and transition matrix elements used here refer to a single-particle process. The description must be generalized for the case of many nucleons in the initial and final states. This point is discussed in Sec. 2.2.3.

3. A complete description of the initial and final states must include the electrons of the atomic cloud. Since the nuclear charge and the number of electrons are different in the initial and final states, the atomic-electron wave functions of these two states are not orthogonal, and the overlap between them is not perfect. This leads to some modifications of the transition rate (exchange and overlap corrections) and to higher-

order processes (e.g., autoionization). These points are discussed in Secs. 2.5 and 5.

2.2. Electron-Capture Transition Rates

2.2.1. General Relations for the Transition Probabilities

In discussing transition matrix elements and transition rates for the three weak nuclear decay modes, we have pointed out how these decay types are related. From here on, we consider electron capture only. We simplify Eq. (2-31), discuss the electron and neutrino radial wave functions in the lepton part, and generalize the hadron part through methods of elementary-particle physics.

We first note that Eq. (2-33) is invariant under the substitution $k_\nu \rightarrow -k_\nu$ and set $k_\nu = |k_\nu|$. We also introduce the abbreviation (Bühring, 1963a, 1963b; Behrens and Bühring, 1971)

$$\beta_x \left[M_K(k_x, k_\nu) + (\kappa_x / k_x) m_K(k_x, k_\nu) \right] = \sum_{1s} (4\pi)^{1/2} [(2J_i + 1)(2K + 1)]^{-1/2} (-1)^S$$

$$\times \int \langle \phi_n \| (1 + \gamma_5) T_{KLS} \| \phi_p \rangle \left\{ g_{\kappa_x}(Z) \left[j_{\ell_\nu} G_{KLS}(k_x, k_\nu) \right. \right.$$

$$\left. \left. + j_{\ell_x} G_{KLS}(k_x, -k_\nu) \right] + (\text{sign } \kappa_x) f_{\kappa_x}(Z) \right.$$

$$\left. \times \left[j_{\ell_\nu} G_{KLS}(-k_x, k_\nu) + j_{\ell_x} G_{KLS}(-k_x, -k_\nu) \right] \right\} r^2 dr, \quad (2-42)$$

where $k_x = |\kappa_x|$, and β_x is the Coulomb amplitude (Behrens and Jänecke, 1969) of the bound-state electron radial wave function

(ERWF), discussed in Sec. 2.2.2. For $\kappa_x = -1$ we have $\beta_x = g_{-1}(0)$ equal to the value of the wave function $g_{-1}(r)$ at $r=0$.

For the total capture probability from all atomic shells we then have

$$\lambda_c = (\ln 2)(t_c)^{-1} = G_\beta^2 (2\pi)^3 \sum_x n_x C_x f_x \quad (2-43)$$

(Behrens and Jänecke, 1969; Bouchez and Depommier, 1960; Brysk and Rose, 1958). The sum in Eq. (2-43) extends over all atomic subshells from which an electron can be captured. For closed shells, n_x equals 1. For partially filled shells, n_x is equal to the relative occupation number of electrons in the shell. The quantity C_x corresponds to the shape factor of β decay. Taking into account only the lowest-order terms in the summation over κ and k_v , C_x has the form

$$\begin{aligned} C_x = & \left[M_L(k_x, k_v^{(1)}) + (\kappa_x/k_x) m_L(k_x, k_v^{(1)}) \right]^2 \\ & + \left[M_L(k_x, k_v^{(2)}) + (\kappa_x/k_x) m_L(k_x, k_v^{(2)}) \right]^2 \\ & + \left[M_{L+1}(k_x, k_v^{(2)}) + (\kappa_x/k_x) m_{L+1}(k_x, k_v^{(2)}) \right]^2 \\ & + \delta_{\Delta J, 0} \left[M_0(1, 1) + (\kappa_x/k_x) m_0(1, 1) \right]^2. \end{aligned} \quad (2-44)$$

The classification of allowed and forbidden electron-capture transitions is similar to that in β decay (Schopper, 1966; Konopinski, 1966; Behrens and Jänecke, 1969):

$\Delta J=0,1$	$\pi_i \pi_f = +1$	allowed
$\Delta J=0,1$	$\pi_i \pi_f = -1$	first non-unique forbidden
$\Delta J=n>1$	$\pi_i \pi_f = (-1)^n$	n^{th} non-unique forbidden
$\Delta J=n>1$	$\pi_i \pi_f = (-1)^{n-1}$	$(n-1)^{\text{th}}$ unique forbidden

(2-45)

Here, (J_i, π_i) and (J_f, π_f) denote spins and parities of the initial and final nuclear states, and we have $\Delta J = |J_i - J_f|$. Hence, we can write in Eq. (2-44)

$$\begin{aligned}
 L &= \Delta J & \text{for } \Delta J > 0 \\
 L &= 1 & \text{for } \Delta J = 0 \\
 k_y^{(1)} &= L - k_x + 1 \\
 k_y^{(2)} &= L - k_x + 2.
 \end{aligned}
 \tag{2-46}$$

The quantities κ_x and k_x are related by Eq. (2-18) to the total angular momentum j_x and the orbital angular momentum l_x of the bound electron. Similarly, κ_y and k_y determine j_y and l_y of the continuum wave function of the emitted neutrino.

The values of κ_x for bound electrons are as follows:

K	(1s)	$\kappa_x = -1$		M ₁	(3s)	$\kappa_x = -1$
L ₁	(2s)	$\kappa_x = -1$		M ₂	(3p _{1/2})	$\kappa_x = +1$
L ₂	(2p _{1/2})	$\kappa_x = +1$		M ₃	(3p _{3/2})	$\kappa_x = -2$
L ₃	(2p _{3/2})	$\kappa_x = -2$		M ₄	(3d _{3/2})	$\kappa_x = +2$
				M ₅	(3d _{5/2})	$\kappa_x = -3$

(2-47)

ORIGINAL PAGE IS
OF POOR QUALITY

The function f_x in Eq. (2-43), which corresponds to the integrated Fermi function of β decay, has the form

$$f_x = (\pi/2) q_x^2 \beta_x^2 B_x. \quad (2-48)$$

The factor B_x takes account of the effects of electron exchange and overlap; it is discussed in Sec. 2.5.

2.2.2. Bound-State Electron Radial Wave Functions

The electron radial wave functions $f_k(r)$ and $g_k(r)$ are a solution of the Dirac radial differential equation or of the equivalent integral equation (Rose, 1961; Behrens and Bühring, 1971). It is convenient to consider instead the functions $H_k(r)$, $h_k(r)$, $D_k(r)$, and $d_k(r)$ introduced by Bühring (1963a):

$$f_{k_x}(r) = \beta_x (p_x r)^{k_x-1} [(2k_x-1)!!]^{-1} [H_{k_x}(r) + h_{k_x}(r)] \quad (2-49a)$$

$$g_{k_x}(r) = \beta_x (p_x r)^{k_x-1} [(2k_x-1)!!]^{-1} (r/R) [D_{k_x}(r) + d_{k_x}(r)] \quad (2-49b)$$

$$f_{-k_x}(r) = -\beta_x (p_x r)^{k_x-1} [(2k_x-1)!!]^{-1} \left(\frac{r}{R}\right) [D_{k_x}(r) - d_{k_x}(r)] \quad (2-49c)$$

$$g_{-k_x}(r) = \beta_x (p_x r)^{k_x-1} [(2k_x-1)!!]^{-1} [H_{k_x}(r) - h_{k_x}(r)] \quad (2-49d)$$

Here, R is the nuclear radius, or equivalent radius of a uniformly charged nucleus.

The first of two aspects of the electron radial wave functions that require more detailed consideration is the behavior

of these functions inside the nucleus: the dependence of the electron and neutrino radial wave functions on the distance r from the center of the nucleus must be subsumed into the nuclear matrix elements [cf. Eq. (2-42)]. The r -dependence of the electron radial wave functions inside the nucleus depends essentially on the form of the nuclear charge distribution.

Secondly, the Coulomb amplitudes β_x must be considered; they can only be calculated numerically by solving the Dirac equation for an extended nucleus and for a self-consistent atomic potential. The value of β_x is essentially determined by the shape of the charge distribution of the surrounding atomic electrons.

In many of the earlier papers on β decay and electron capture, the expansion of the functions $H_k(r)$, $D_k(r)$, $h_k(r)$, and $d_k(r)$ in powers of r is carried out (Behrens and Bühring, 1970):

$$H_k(r) = \sum_{n=0}^{\infty} H_n(k)(r/R)^n; \quad (2-50)$$

the different powers of r are then incorporated into the definition of the nuclear matrix elements (Behrens and Jänecke, 1969; Bühring, 1963a,b). The nuclear charge distribution has been approximated throughout by a uniformly charged sphere of radius R , equal to the nuclear radius. Because this charge distribution is discontinuous at R , the power-series expansion of the electron radial wave functions is only valid inside the nucleus. Usable β -decay and electron-capture formulae have been derived by truncating this series and extrapolating the resulting polynomials

outside the nuclear radius (Behrens and Jänecke, 1969; Bühring, 1963a). However, this approach is unsatisfactory: contrary to general belief, a significant contribution (or even the main contribution) to the nuclear matrix elements originates from the region $r > R$, particularly if the initial and final nucleons are in different shells (Behrens and Bühring, 1971; de Raedt, 1968).

It might be expected that this difficulty could be avoided by using a more realistic, smooth nuclear charge distribution, such as a modified Gaussian or a Fermi distribution. However, for such distributions the β -decay and electron-capture formulae do not converge at all (Behrens and Bühring, 1970, 1971), because the nuclear matrix elements are introduced by integrating a power series term by term, a dubious procedure if the upper limit of the integral is infinity. Only if the potential $V(r)$ vanishes identically, as for the neutrino, is this procedure justified. Thus, the neutrino radial wave functions (spherical Bessel functions) can be expanded in powers of r . The electron radial wave functions, on the other hand, can be expanded in powers of the mass and energy parameters of the electron and the nuclear charge. The coefficients in this expansion still are functions of r and depend on the shape of the charge distribution. We find (Behrens and Bühring, 1971)

$$H_{k_x}(r) = \sum_{\mu=0}^{\infty} \sum_{\nu=0}^{\mu} \sum_{\rho=0}^{2\nu} \frac{(2k_x-1)!!}{(2\mu)!!(2\mu+2k_x-1)!!} (-1)^{\nu} \begin{pmatrix} \mu \\ \nu \end{pmatrix} \begin{pmatrix} 2\nu \\ \rho \end{pmatrix} \left(\frac{r}{R}\right)^{2\mu} \\ \times I(k_x, 2\mu, 2\nu, \rho; r) (m_e R)^{2\mu-2\nu} (W_x R)^{2\nu-\rho} (\alpha Z)^{\rho}, \quad (2-51a)$$

$$h_{k_x}(r) = \sum_{\mu=1}^{\infty} \sum_{\nu=1}^{\mu} \sum_{\rho=1}^{2\nu-1} \frac{(2k_x-1)!!}{(2\mu)!!(2\mu+2k_x-1)!!} (-1)^{\nu} \binom{\mu}{\nu} \binom{2\nu-1}{\rho} \left(\frac{r}{R}\right)^{2\mu} \\ \times I(k_x, 2\mu, 2\nu-1, \rho; r) (m_e R)^{2\mu-2\nu+1} (WR)^{2\nu-1-\rho} (\alpha Z)^{\rho} \quad (2-51b)$$

$$D_{k_x}(r) = \sum_{\mu=0}^{\infty} \sum_{\nu=0}^{\mu} \sum_{\rho=0}^{2\nu+1} \frac{(2k_x-1)!!}{(2\mu)!!(2\mu+2k_x+1)!!} (-1)^{\nu} \binom{\mu}{\nu} \binom{2\nu+1}{\rho} \left(\frac{r}{R}\right)^{2\mu} \\ \times I(k_x, 2\mu+1, 2\nu+1, \rho; r) (m_e R)^{2\mu-2\nu} (WR)^{2\nu+1-\rho} (\alpha Z)^{\rho}, \quad (2-51c)$$

$$d_{k_x}(r) = \sum_{\mu=0}^{\infty} \sum_{\nu=0}^{\mu} \sum_{\rho=0}^{2\nu} \frac{(2k_x-1)!!}{(2\mu)!!(2\mu+2k_x+1)!!} (-1)^{\nu} \binom{\mu}{\nu} \binom{2\nu}{\rho} \left(\frac{r}{R}\right)^{2\mu} \\ \times I(k_x, 2\mu+1, 2\nu, \rho; r) (m_e R)^{2\mu+1-2\nu} (WR)^{2\nu-\rho} (\alpha Z)^{\rho}. \quad (2-51d)$$

The symbol m_e has been retained in these equations, even though we use natural units $\hbar=c=m_e=1$, because m_e will be used as an expansion parameter. The expansion coefficients $I(k_x, m, n, \rho; r)$ depend on the form of the nuclear charge distribution and on the parameters k_x , m , n , and ρ . The order m is the sum of the exponents of $(m_e R)$, (WR) , and αZ ; the number n is the sum of the exponents of (WR) and (αZ) . The functions I with $\rho=0$ are trivial:

$$I(k_x, m, n, 0; r) \equiv 1. \quad (2-52)$$

The functions I with $\rho>0$, up to order $m=3$, are listed in Appendix A2.2 (Behrens and Bühring, 1971). For $\alpha Z=0$, Eqs. (2-51) reduce to the usual expansion in powers of r (Bühring, 1963a).

Up to and including terms of order $\mu=0$, the functions

$$H_{k_x}(r), h_{k_x}(r), D_{k_x}(r), \text{ and } d_{k_x}(r) \text{ are}$$

$$H_{k_x}(r) = 1 + \dots \quad (2-53a)$$

$$h_{k_x}(r) = 0 + \dots \quad (2-53b)$$

$$D_{k_x}(r) = \frac{W R}{2k_x + 1} + \frac{\alpha Z}{2k_x + 1} I(k_x, 1, 1, 1; r) + \dots \quad (2-53c)$$

$$d_{k_x}(r) = \frac{m R}{2k_x + 1} + \dots \quad (2-53d)$$

As usual, α is the fine-structure constant, and Z is the atomic number of the parent nucleus.

The important function $I(k_x, 1, 1, 1; r)$, which gives the large Coulomb terms in non-unique forbidden transitions, takes the following forms for the three most widely used charge distributions (Behrens and Böhning, 1970, 1971):

(i) For a uniform charge distribution

$$\rho(r) = \begin{cases} -3\alpha Z/R, & 0 \leq r \leq R \\ 0, & R < r \leq \infty \end{cases} \quad (2-54)$$

we have (Behrens and Böhning, 1971)

$$I(k_x, 1, 1, 1; r) = \begin{cases} \frac{3}{2} - \frac{2k_x + 1}{2(2k_x + 3)} \left(\frac{r}{R}\right)^2, & 0 \leq r \leq R \\ \frac{2k_x + 1}{2k_x} \frac{R}{r} - \frac{3}{2k_x(2k_x + 3)} \left(\frac{R}{r}\right)^{2k_x + 1}, & R \leq r. \end{cases} \quad (2-55)$$

(ii) In a shell-model or modified Gaussian distribution

(Behrens and Böhning, 1970)

$$\rho(r) = N \left\{ 1 + A \left(\frac{r}{a}\right)^2 \right\} e^{-\left(\frac{r}{a}\right)^2}, \quad (2-56a)$$

where

$$N = - \frac{8\alpha Z}{(2+3A)a^3\sqrt{\pi}}, \quad (2-56b)$$

the equivalent uniform radius R is related to the parameters a and A as

$$R = a[5(2+5A)/2(2+3A)]^{1/2}; \quad (2-57)$$

for this distribution, we have

$$I(k_x, 1, 1, 1; r) = \frac{2k_x + 1}{2k_x} \frac{R}{r} \left\{ \operatorname{erf}(y) - \left(1 + \frac{2k_x A}{2+3A}\right) \frac{(2k_x - 1)!!}{2^{k_x} y^{2k_x}} \right. \\ \left. \times \left[\operatorname{erf}(y) - \frac{2}{\sqrt{\pi}} e^{-y^2} \sum_{m=0}^{k_x-1} \frac{2^m y^{2m+1}}{(2m+1)!!} \right] \right\}, \quad (2-58)$$

where $\operatorname{erf}(y)$ is the error function,

$$\operatorname{erf}(y) = 2\pi^{-1/2} \int_0^y e^{-t^2} dt, \quad y = \beta \frac{r}{R}$$

and

$$\beta = [5(2+5A)/2(2+3A)]^{1/2}.$$

(iii) For a Fermi distribution (Behrens and Bühring, 1970)

$$\rho(r) = -3\alpha Z c^{-3} N [1 + e^{(r-c)/b}]^{-1}, \quad (2-59)$$

with

$$N = [1 + \pi^2 (b/c)^2 - 6w_3(b, c; 0)]^{-1},$$

the equivalent uniform radius R is

$$R = c \left[\frac{3c^5 + 10\pi^2 c^3 b^2 + 7\pi^4 c b^4 - 360b^5 w_5(b, c; 0)}{3c^5 + 3\pi^2 c^3 b^2 - 18c^2 b^3 w_3(b, c; 0)} \right]^{1/2} \quad (2-60)$$

The function $I(k_x, 1, 1, 1; r)$ takes the form

$$\begin{aligned}
 I(k_x, 1, 1, 1; r) = & \frac{3}{2} \frac{R}{c} N \left\{ 1 + \frac{1}{3} \pi^2 \left(\frac{b}{c}\right)^2 - \frac{1}{3} \frac{2k_x + 1}{2k_x + 3} \left(\frac{r}{c}\right)^2 \right. \\
 & - 2(2k_x + 1) \frac{c}{r} \left[w_3(b, c; r) - \frac{1}{k_x} w_3(b, c; 0) \right] \\
 & + 2(2k_x + 1)(2k_x + 2) \left(\frac{c}{r}\right)^2 \sum_{m=0}^{2k_x - 1} (-1)^m \\
 & \left. \times \frac{(2k_x - 1)!}{(2k_x - 1 - m)!} \left(\frac{c}{r}\right)^m w_{4+m}(b, c; r) \right\}, \quad (2-61)
 \end{aligned}$$

where the functions w_n are defined as

$$\begin{aligned}
 w_n(b, c; r) &= \begin{cases} \left(\frac{b}{c}\right)^n \sum_{m=1}^{\infty} (-1)^{m-n} \left(e^{\frac{r-c}{b}}\right)^m, & r \leq c \\ \left(\frac{b}{c}\right)^n \sum_{m=0}^{\lfloor \frac{1}{2}n \rfloor} a_m^{(n)} \left(\frac{r-c}{b}\right)^{n-2m} + (-1)^{n-1} \sum_{m=1}^{\infty} (-1)^{m-n} \left(e^{-\frac{r-c}{b}}\right)^m, & r \geq c \end{cases} \\
 & \quad (2-62)
 \end{aligned}$$

(Schucan, 1965). Here, $a_m^{(n)}$ stands for

$$a_m^{(n)} = (-1)^m \frac{(2^{2m} - 2)}{(2m)!(n-2m)!} B_{2m},$$

where the B_{2m} are Bernoulli numbers:

$$B_0 = 1, B_2 = \frac{1}{6}, B_4 = -\frac{1}{30}, B_6 = \frac{1}{42}, \dots$$

At $r=c$, w_n is given by

$$w_n(b, c; c) = \left(\frac{b}{c}\right)^n \sum_{m=1}^{\infty} (-1)^{m-n} = \left(\frac{b}{c}\right)^n (2^{1-n} - 1) \zeta(n), \quad (2-63)$$

where $\zeta(n)$ is the Riemann zeta function.

The functions $I(k_x, 1, 1, 1)$ [Eqs (2-55), (2-58), and (2-61)] have been derived neglecting the small influence of the atomic electron cloud on the r -dependence of the electron radial wave functions inside the nucleus. These functions are illustrated in Fig. 2-1.

We consider next the Coulomb amplitudes β_x of the bound atomic electrons. These quantities can be calculated by integrating the Dirac equation in the potential of the nuclear and atomic charge distributions.⁶ The value of β_x is essentially determined by the potential outside the nucleus, i.e., by the electronic screening of the nuclear electrostatic field. The finite nuclear size and the shape of the nuclear charge distribution have less influence on β_x . The potential produced by the nuclear charge and the atomic electron cloud can be derived approximately from statistical models (Gombas, 1956, 1967), by solving the Thomas-Fermi or the Thomas-Fermi-Dirac equations. A more exact form of the potential can be derived through self-consistent Hartree-Fock methods (Hartree, 1957; Slater, 1960; Mayers, 1972; Burke and Grant, 1967; Grant, 1970; Lindgren and Rosen, 1974).

Both methods of finding the extranuclear potential can only be carried out numerically and have been pursued by many investigators. The Thomas-Fermi and Thomas-Fermi-Dirac equations have been solved for potentials and eigenvalues, for example, by Gombas (1956), Thomas (1954), Latter (1955), Shalitin (1965, 1967), and Yonei (1966, 1967). The self-consistent field methods offer the best possibility for obtaining good atomic electron wave

**ORIGINAL PAGE IS
OF POOR QUALITY**

functions, but require extensive numerical calculations (Hartree, 1957; Slater, 1960; Mayers, 1972; Burke and Grant, 1967; Grant, Lindgren and Rosén, 1974). In a simplification first introduced by Slater (1960, Vol. 2), the exact exchange potential is approximated by the exchange potential of an electron gas with local electron density $\rho(r)$, i.e.,

$$V_{\text{ex}}(r) = \frac{3}{2} \alpha \frac{3\rho(r)}{\pi}^{1/3} \quad (2-64)$$

This Slater exchange potential tends to zero as the radius becomes large, while the exact potential tends to α/r . To correct this discrepancy, Latter (1955) has suggested replacing the Slater term in the region of large radius by α/r . Statistical exchange potentials have been discussed extensively by Gombas (1967).

Herman and Skillman (1963) have tabulated nonrelativistic Hartree-Fock-Slater potentials and wave functions for elements with $Z=2$ to 103, including the Latter tail correction. Extensive nonrelativistic calculations with the exact Hartree-Fock form of the exchange potential have been performed by Froese-Fischer (1972b) and Mann (1967, 1968). Approximate analytic nonrelativistic Hartree-Fock wave functions have been derived by Watson and Freeman (1961a,b), Malli (1966), and Roetti and Clementi (1974).

Because relativistic effects in atomic structure are remarkably important, even for light elements, a number of relativistic self-consistent-field calculations (mostly Hartree-Fock-Slater) have been carried out (Liberian et al., 1965;

Nestor et al., 1966; Tucker et al., 1969). Most comprehensive is the work of Lu et al. (1971), who have published tables of energies and of expectation values of r , r^{-1} , r^{-3} , r^2 , and r^4 for each orbital, of the total energy, and of the potential function. They have included the effect of finite nuclear size, using a Fermi charge distribution.

The possibility of making better approximations than Slater's Kohn and Sham (1965), for the exchange potential has been discussed by Rosén and Lindgren (1968), and Lindgren and Schwarz (1971).

The most sophisticated method of calculating atomic wave functions involves the use of relativistic Hartree-Fock codes; here the exchange term is included without approximation (see e.g. Mann and Waber, 1973; Desclaux, 1973).

Unfortunately, in most published atomic-structure calculations no explicit values are given for the Coulomb amplitudes or electron wave functions at the nuclear radius. For applications to electron capture, special calculations have therefore been carried out; these are listed in Table 2.1. For comparison among the various calculations, the most important electron radial wave-function ratios are listed in Tables 2.2-2.8. For s electrons, the nonrelativistic ratios for a point nucleus are included in the comparison. For $p_{1/2}$ electrons, on the other hand, it is meaningless to compare nonrelativistic wave functions in the field of a point nucleus (proportional to ar at small r) with relativistic electron wave functions in the field of a finite nucleus [proportional to $b(1+cr^2+\dots)$]. We also do not compare

absolute values of electron wave functions, nor do we list other ratios than those contained in Tables 2.2-2.8, because the magnitudes of the nuclear radius R chosen by different authors are not the same, and moreover, some authors report $g_{\kappa}(R)$ and $f_{\kappa}(R)$, while others instead report the amplitudes β_x .

We can draw the following conclusions from Tables 2.2-2.8:

(1) For the s-electron ratios (Tables 2.2-2.5), there is excellent agreement between the nonrelativistic Hartree-Fock calculations of Froese-Fischer (1972b) and Winter (1968) and the relativistic Hartree-Fock calculations of Mann and Waber (1973). An exception is the $g_{O_1}^2/g_{N_1}^2$ ratio. However, here relativistic effects might play some role because of the high atomic numbers ($Z \geq 70$).

(2) Relativistic effects become notable in $g_{L_1}^2/g_K^2$ for $Z > 15$, in $g_{M_1}^2/g_{L_1}^2$ for $Z > 30$, and in $g_{N_1}^2/g_{M_1}^2$ and $g_{O_1}^2/g_{N_1}^2$ for $Z > 60$. For $g_{L_1}^2/g_K^2$, relativistic and nonrelativistic ratios differ by ~50% for very heavy nuclei. For all other ratios, relativistic effects are small (<2% for the $g_{M_1}^2/g_{L_1}^2$ and $g_{N_1}^2/g_{M_1}^2$, <8% for the $g_{O_1}^2/g_{N_1}^2$).

(3) The electron radial wave-function ratios from Hartree-Fock calculations lie systematically below those from Hartree-Fock-Slater and Thomas-Fermi-Dirac calculations, especially for low atomic numbers.

(4) For the K, L, and M ratios, the Hartree-Fock-Slater calculations agree with the Thomas-Fermi-Dirac calculations to within 2.5% for $Z > 40$.

(5) The $g_{L_{\pm}}^2/g_K^2$ ratios of Brysk and Rose (1958) deviate systematically from all other calculations in the range $20 < Z < 80$ (Table 2.2). Therefore, these values should be discarded.

Of the various methods discussed above, the self-consistent relativistic Dirac-Hartree-Fock calculations of atomic structure are based on the soundest theoretical grounds (Mayers, 1972; Burke and Grant, 1967). It might consequently be expected that the wave functions of Mann and Waber (1973) would be most accurate, and should preferably be used for analyzing electron-capture experiments.⁷ Table 2.9 contains a compilation of electron radial wave-function amplitudes according to Mann and Waber (1973). For practical reason, we have listed the products $\beta_{x^k} p_x^{k-1}$ instead of the amplitudes β_x . It is always this product which appears in the formulae for the decay constant [Eq. (2-49)].

Because the electron-capture rate is essentially proportional to the electron density at the nucleus, different chemical environments or other macroscopic perturbations (pressure, temperature, etc.) can affect the decay constant. Such effects are most noticeable in capture from outer electron shells (Emery, 1972; Crasemann, 1973).

2.2.3. Nuclear Form Factors and Nuclear Matrix Elements

Form factors and form factor coefficients. The electron-capture transition matrix elements [Eq. (2-4)] were formulated in Sec. 2.1 under the assumption that the vector and axial vector interactions govern the process. However, the hadron part of this

ORIGINAL PAGE IS
OF POOR QUALITY

transition matrix element is only an approximation. In the most general case, we must make the substitution

$$\langle i \bar{u}_n \gamma_\mu (1 + \lambda \gamma_5) u_p \rangle \rightarrow \langle f | V_\mu - A_\mu | i \rangle \quad (2-65)$$

in Eq. (2-7c), where f and i represent the final and initial nuclear states, respectively. The vector and axial vector hadron weak current are denoted by V_μ and A_μ . According to Stech and Schülke (1964) and Schülke (1964), we decompose this V-A nuclear current into form factors depending on the square of the momentum transfer (Armstrong and Kim, 1972; Bottino and Holstein, 1974). Giochetti, 1973; Donnelly and Walecka, 1972, 1973; \wedge We use a covariant decomposition, which is strictly valid in the Breit system. A transformation in the frame in which the initial nucleus is at rest is easily performed because the decay energies are low compared with the nuclear rest masses. The correction due to this transformation is of the order $|\vec{k}|/M$, where \vec{k} is the momentum of the nucleus and M is its mass. In this approximation, the hadron matrix element depends only on the momentum transfer $\vec{q} = \vec{k}_f - \vec{k}_i$. It can be expanded as

$$\begin{aligned} \langle f | V_\mu - A_\mu | i \rangle \gamma_4 \gamma_\mu &= \sum_{KLSM} (-1)^{J_f - M_f + M} (-1)^L (4\pi)^{1/2} \\ &\times (2J_i + 1)^{1/2} \begin{bmatrix} J_f & K & J_i \\ -M_f & M & M_i \end{bmatrix} T_{KLS}^{-M}(\hat{q}) \frac{(qR)^L}{(2L+1)!!} F_{KLS}(q^2). \end{aligned} \quad (2-66)$$

Here, T_{KLS} is the irreducible tensor defined by Eqs. (2-12);

J_i , J_f and M_i , M_f denote the spins and magnetic quantum numbers

of the initial and final nuclear states, respectively, and R is the nuclear radius.

This treatment of the nuclear current, similar to methods used in elementary-particle physics, has the advantage of being completely independent of any assumption about the detailed form of the β -decay operators. All information about the nuclear current and all effects due to the strong interaction (induced terms, exchange currents, relativistic nucleon motion inside the nucleus, etc.) are contained in the form factors $F_{KLS}(q^2)$; they determine the outcome of β -decay and electron capture experiments and are the only quantities, as far as nuclear structure is concerned, that can be extracted from experimental data.

We neglect, for the moment, the initial electromagnetic interaction between electron and nucleus, i.e. the fact that there is a bound electron in the initial state. Then the form factors $F_{KLS}(q^2)$ can be expanded in powers of q^2 in analogy with the expansion of spherical Bessel functions (Stech and Schülke, 1964)]:

$$F_{KLS}(q^2) = F_{KLS}^0 - \frac{(qR)^2}{2(2L+3)} F_{KLS}^1 + \dots \quad (2-67)$$

The form-factor coefficients are then

$$F_{KLS}^N = \frac{(-1)^N (2N+2L+1)!! (2N)!!}{R^{2N} (2L+1)!! N!} \left(\frac{d}{dq^2} \right)^N F_{KLS}(q^2) \Big|_{q^2=0} \quad (2-68)$$

These form-factor coefficients contain all the information about the initial and final nuclear states and the $V-A$ operator. Since q equals W_0 if the initial nucleus is at rest, we have $qR < 0.1$,

whence the form factors are slowly varying functions of q^2 . Therefore, only the first one or two terms will be significant.

In reality, however, we must take into account the fact that there is a bound-state electron wave function in the initial state. Hence, the momentum transfer \vec{q}_N to the nucleus is $\vec{q}_N = \vec{p}_e - \vec{q}_x$ if the center of mass of the initial nucleus and electron is at rest. The Fourier transform⁸ of the lepton part of Eq. (2-10c) is

$$L(\vec{q}_N) = \int e^{-i\vec{q}_N \cdot \vec{r}} \bar{u}_\nu \gamma_\mu (1 + \gamma_5) \phi_{e^-}(r) d^3r \quad (2-69)$$

or

$$L(\vec{q}_N) = \bar{u}_\nu \gamma_\mu (1 + \gamma_5) \phi_{e^-}(\vec{q}_N + \vec{q}_x) \quad (2-70)$$

(Schopper, 1966; Stech and Schülke, 1964). Hence, Eq. (2-7c) becomes

$$M_{EC} \approx \int \langle f | V_\mu - A_\mu | i' \rangle \bar{u}_\nu \gamma_\mu (1 + \gamma_5) \phi_{e^-}(\vec{q}_N + \vec{q}_x) d\vec{q}_N^i \quad (2-71)$$

The hadron matrix element corresponds to a transition from the initial state i' to the final state f , whereas the Fourier transform $\phi_{e^-}(\vec{q}_N + \vec{q}_x)$ induces an electromagnetic transition from i to i' . The integral over \vec{q}_N^i corresponds to an integration over all momenta of the intermediate initial states, because we have $\vec{q}_N^i = -\vec{k}_1^i - \vec{q}_x$. The Coulomb interaction in the initial state therefore entails that terms of the form

$$\int_0^\infty I(q_N^i) F_{KLS}(q_N^i{}^2) q_N^i{}^2 dq_N^i \quad (2-72)$$

appear in electron-capture formulae (Schülke, 1964), where $I(q_N^i)$ has four different possible forms [Eq. (2-42)]:

$$I(q_N^i) = \frac{(q_N^i R)^L}{(2L+1)!!} \begin{cases} \int g_K(r) j_L(q_X r) j_L(q_N^i r) r^2 dr \\ \int g_K(r) j_L^-(q_X r) j_L(q_N^i r) r^2 dr \\ \int f_K(r) j_L(q_X r) j_L(q_N^i r) r^2 dr \\ \int f_K(r) j_L^-(q_X r) j_L(q_N^i r) r^2 dr. \end{cases} \quad (2-73)$$

By expanding the spherical Bessel functions in powers of r and the electron radial wave functions $g_K(r)$ and $f_K(r)$ as discussed in Sec. 2.2.2. [Eqs. (2-49) and (2-51)], we obtain new form-factor coefficients (Behrens and Bühring, 1971)

$$F_{KLS}^N(k, m, n, \rho) = \int_0^\infty J(q) F_{KLS}(q^2) q^2 dq, \quad (2-74)$$

where

$$J(q) = \frac{2}{\pi} \frac{(qR)^L}{(2L+1)!!} \int_0^\infty \left(\frac{r}{R}\right)^{L+2N} I(k, m, n, \rho; r) j_L(qr) r^2 dr. \quad (2-75)$$

Terms in which these new form factors occur always contain powers of αZ . Terms that are independent of αZ contain the simpler form-factor coefficients F_{KLS}^N [Eqs. (2-67) and (2-68)].

Relation between form-factor coefficients and nuclear matrix elements. The form factors or form-factor coefficients can only be expressed in terms of nuclear matrix elements, in general, if some approximations are made. First, it is assumed that the

nucleons inside the nucleus interact with leptons in the same way as free nucleons do (impulse-approximation treatment). Meson exchange (Blin-Stoyle, 1973; Lock et al., 1974) and other many-body effects are hence neglected.

The β -decay Hamiltonian must be used with various many-body nuclear wave functions that can only be calculated in the framework of specific nuclear models. Thus, the uncertainties of nuclear-structure theory are carried over into the nuclear matrix elements or form-factor coefficients.

Finally, the axial-vector constant λ for nucleons embedded in a complex nucleus is renormalized in a different way from that for free nucleons, because the mesonic currents behave differently for free and bound nucleons, and new mesonic currents appear that are absent for free nucleons. Thus, λ is in principle not a constant over the whole range of nuclei. For light nuclei, a deviation of λ from the free-nucleon value by $\sim 7\%$ has been found (Wilkinson, 1973a, 1973b, 1974a; Szybisz, 1975; Ericson et al., 1973; Ohta and Wakamatsu, 1974).

Under these assumptions, we develop the relation between form-factor coefficients and nuclear matrix elements for a pure V-A nucleon current of the form given in Eq. (2-4). Induced terms will be discussed later. We have (Stech and Schülke, 1964; Behrens and Bühring, 1971)⁹

$$\begin{aligned} V_{F_{KLS}}^N(k_x, m, n, \rho) &= (-1)^{K-L} V_{TKLS}^N(k_x, m, n, \rho) \\ A_{F_{KLS}}^N(k_x, m, n, \rho) &= (-1)^{K-L} \lambda A_{TKLS}^N(k_x, m, n, \rho), \end{aligned} \quad (2-76)$$

where the nuclear matrix elements are denoted by $V_{KLS}^N(k_x, m, n, \rho)$ and $A_{KLS}^N(k_x, m, n, \rho)$. The meaning of the indices has been explained in connection with the form-factor coefficients.

The nuclear matrix elements are [Eq. (2-42)]

$$\begin{aligned}
 & (-1)^{J_f - M_f} \begin{bmatrix} J_f & K & J_i \\ -M_f & M & M_i \end{bmatrix} \left\{ V_{KLS}^N(k_x, m, n, \rho) + \lambda A_{KLS}^N(k_x, m, n, \rho) \right\} \\
 & = [4\pi / (2J_i + 1)]^{1/2} \iint \dots \int \psi_f^+(1, 2, \dots, A; J_f M_f \pi_f) \\
 & \times \sum_{j=1}^A \left\{ \left(\frac{r}{R} \right)^{L+2N} I(k_x, m, n, \rho; r) (1 + \lambda \gamma_5) T_{KLS}^M t^+ \right\}_j \\
 & \times \psi_i(1, 2, \dots, A; J_i M_i \pi_i) d\tau_1 d\tau_2 \dots d\tau_A. \quad (2-77)
 \end{aligned}$$

Here, ψ_f and ψ_i are the nuclear many-particle wave functions of the final and initial state, respectively, which depend on all the coordinates of the A nucleons. The sum over j runs over the A nucleons, and all the operators are single-particle operators operating on the j^{th} nucleon only. The t^+ is the isospin operator changing a proton into a neutron. The term with 1 gives the V matrix element while the term with $\lambda \gamma_5$ leads to the A matrix element. The multipole operators T_{KLS}^M have been defined in Eqs. (2-45).

The nuclear matrix elements of Eq. (2-77) must be calculated on the basis of appropriate nuclear models. This is a complicated problem which requires special considerations for each particular β transition. One-body operators O_K^M must be used in Eq. (2-77), which can be expanded (Bohr and Mottelson, 1969) as

$$0 = \sum_{\alpha, \beta} \langle \alpha | 0 | \beta \rangle a_{\beta} c_{\alpha}^{\dagger}, \quad (2-78)$$

where a_{β} is the annihilation operator for a proton in the single-particle state β and c_{α}^{\dagger} is the creation operator for a neutron in the single-particle state α . Here, α and β represent a complete set of single-particle quantum numbers. We can, therefore, write

$$i_{\text{KLS}}^N(k_x, m, n, \rho) = \sum_{\alpha, \beta} (-1)^{j_{\alpha} + j_{\beta} - K} (2K+1)^{-1/2} \langle \alpha || i_{\text{O}_K}^M || \beta \rangle C_{\alpha\beta}, \quad (2-79)$$

with $i=V;A$ and

$$\begin{aligned} V_{\text{O}_K}^M &= \left(\frac{r}{R}\right)^{L+2N} I(k_x, m, n, \rho; r) T_{\text{KLS}}, \\ A_{\text{O}_K}^M &= \left(\frac{r}{R}\right)^{L+2N} I(k_x, m, n, \rho; r) \gamma_{\text{KLS}}^T. \end{aligned} \quad (2-80)$$

The expansion coefficients $C_{\alpha\beta}$ are

$$C_{\alpha\beta} = \langle \psi_f^J | [\bar{a}_{\beta} c_{\alpha}^{\dagger}]_M^K [\psi_i^J]^J | \psi_f^J \rangle, \quad (2-81)$$

where

$$\bar{a}_{jm} = (-1)^{j+m} a_{j-m}.$$

It follows that, however complicated the nuclear states may be, the exact nuclear matrix elements between many-body states can be expanded in a linear combination of single-particle matrix elements (Donnelly and Walecka, 1972, 1973). For example, methods of calculating the coefficients $C_{\alpha\beta}$ in the framework of the shell model are discussed by de Shalit and Talmi (1963). Formulae for nuclear matrix elements within the isospin formalism are also given by de Shalit and Talmi (1963).

Once the set of numerical coefficients $G_{\alpha\beta}$ has been determined, the nuclear matrix elements can be computed if we are able to deduce reliable values for the single-particle matrix elements. In Eqs. (2-84), we therefore list the single-particle expressions for all the nuclear matrix elements in terms of radial-integral and angular-momentum quantum numbers (Brysk, 1952; Talmi, 1953; Rose and Osborn, 1954; Berthier and Lipnik, 1966; Lipnik and Sunier, 1966; Delabaye and Lipnik, 1966; Strubbe and Callebaut, 1970). The compact form of Eqs. (2-84) is that given by Behrens and Bühring (1971). The orbits of the nucleons are assumed to have definite angular momentum, as in the jj -coupling shell model. In the same notation as used for the electron wave functions [Eqs. (2-16) and (2-17)], the nuclear wave functions can be written

$$\phi_{\kappa}^{\mu}(r) = \begin{cases} (\text{sign } \kappa) f_{\kappa}(r) \chi_{-\kappa}^{\mu} \\ g_{\kappa}(r) \chi_{\kappa}^{\mu} \end{cases} \quad (2-82)$$

The orbit of a nucleon is identified by the number κ , defined as for leptons:

$$|\kappa| = j + (1/2); \begin{cases} \kappa > 0 \text{ if } \ell = j + (1/2) \\ \kappa < 0 \text{ if } \ell = j - (1/2) \end{cases} \quad (2-83)$$

The large component of the nuclear radial wave functions is denoted by g_{κ} and the small component, by f_{κ} . The single-particle values of the nuclear matrix elements then are

$$\begin{aligned}
V_{KKO}^N(k_x, m, n, \rho) &= \sqrt{2}(2J_i+1)^{-1/2} \{ G_{KKO}(\kappa_f, \kappa_i) \\
&\times \int_0^\infty g_f(r, \kappa_f) \left(\frac{r}{R}\right)^{K+2N} I(k_x, m, n, \rho; r) g_i(r, \kappa_i) r^2 dr \\
&\quad + \text{sign}(\kappa_f) \text{sign}(\kappa_i) G_{KKO}(-\kappa_f, -\kappa_i) \\
&\times \int_0^\infty f_f(r, \kappa_f) \left(\frac{r}{R}\right)^{K+2N} I(k_x, m, n, \rho; r) f_i(r, \kappa_i) r^2 dr \}, \quad (2-84a)
\end{aligned}$$

$$\begin{aligned}
A_{KLL}^N(k_x, m, n, \rho) &= \sqrt{2}(2J_i+1)^{-1/2} \{ G_{KLL}(\kappa_f, \kappa_i) \\
&\times \int_0^\infty g_f(r, \kappa_f) \left(\frac{r}{R}\right)^{L+2N} I(k_x, m, n, \rho; r) g_i(r, \kappa_i) r^2 dr \\
&\quad + \text{sign}(\kappa_f) \text{sign}(\kappa_i) G_{KLL}(-\kappa_f, -\kappa_i) \\
&\times \int_0^\infty f_f(r, \kappa_f) \left(\frac{r}{R}\right)^{L+2N} I(k_x, m, n, \rho; r) f_i(r, \kappa_i) r^2 dr \}, \quad (2-84b)
\end{aligned}$$

$$\begin{aligned}
A_{KKO}^N(k_x, m, n, \rho) &= \sqrt{2}(2J_i+1)^{-1/2} \{ \text{sign}(\kappa_i) G_{KKO}(\kappa_f, -\kappa_i) \\
&\times \int_0^\infty g_f(r, \kappa_f) \left(\frac{r}{R}\right)^{K+2N} I(k_x, m, n, \rho; r) f_i(r, \kappa_i) r^2 dr \\
&\quad + \text{sign}(\kappa_f) G_{KKO}(-\kappa_f, \kappa_i) \\
&\times \int_0^\infty f_f(r, \kappa_f) \left(\frac{r}{R}\right)^{K+2N} I(k_x, m, n, \rho; r) g_i(r, \kappa_i) r^2 dr \}, \quad (2-84c)
\end{aligned}$$

$$\begin{aligned}
V_{KL1}^N(k_x, m, n, \rho) = & \sqrt{2(2J_i+1)}^{-1/2} \left\{ \text{sign}(\kappa_i) G_{KL1}(\kappa_f, -\kappa_i) \right. \\
& \times \int_0^\infty g_f(r, \kappa_f) \left(\frac{r}{R}\right)^{L+2N} I(k_x, m, n, \rho; r) f_i(r, \kappa_i) r^2 dr \\
& + \text{sign}(\kappa_f) G_{KL1}(-\kappa_f, \kappa_i) \\
& \left. \times \int_0^\infty f_f(r, \kappa_f) \left(\frac{r}{R}\right)^{L+2N} I(k_x, m, n, \rho; r) g_i(r, \kappa_i) r^2 dr \right\}. \quad (2-84d)
\end{aligned}$$

The indices i and f refer to the initial and final states of the nucleon undergoing decay. The radial quantum numbers of the orbits are not explicitly indicated. The quantity $G_{KLS}(n_f, n_i)$ is defined through Eq. (2-36).

If relativistic nuclear wave functions are used (Miller and Krutov et al., 1974; Green, 1972; Miller, 1972; Krutov and Savashkin, 1973), the nuclear radial wave functions must be normalized to satisfy the condition

$$\int_0^\infty g^2(r, \kappa) r^2 dr + \int_0^\infty f^2(r, \kappa) r^2 dr = 1. \quad (2-85)$$

In most cases, relativistic nuclear wave functions are not known, whence actual calculations must be performed in the context of nonrelativistic nuclear models. It is then necessary to find the small components $f(r, \kappa)$ of the nuclear radial wave functions.¹⁰ It is possible to express $f(r, \kappa)$ in terms of $g(r, \kappa)$ by using the Dirac equation in the nonrelativistic limit, if the spin angular and the radial parts of the wave functions are considered separately (Behrens and Bthring, 1971). In the nonrelativistic limit one then finds

$$f(r, \kappa) = \frac{1}{2M} \left[\frac{d}{dr} + \frac{\kappa+1}{r} \right] g(r, \kappa), \quad (2-86)$$

where M is the nucleon mass, and $g(r, \kappa)$ is the solution of the single-particle Schrödinger equation. In this case, the radial wave functions $g(r, \kappa)$ must be normalized according to

$$\int_0^{\infty} g^2(r, \kappa) r^2 dr = 1. \quad (2-87)$$

The matrix elements of Eqs. (2-84a) and (2-84b) are usually called nonrelativistic because their radial parts depend only on the radial functions $g(r, \kappa)$. The terms containing both $f_f(r, \kappa_f)$ and $f_i(r, \kappa_i)$ constitute small relativistic corrections that can usually be omitted. On the other hand, the matrix elements of Eqs. (2-84c) and (2-84d), which contain $f(r, \kappa)$, are called relativistic matrix elements.

The radial momentum operator p_r is

$$\bar{p}_r = \frac{1}{i} \left(\frac{d}{dr} + \frac{1}{r} \right); \quad (2-88)$$

hence we have

$$f(r, \kappa) = \frac{1}{2M} \left(i p_r + \frac{\kappa}{r} \right) g(r, \kappa). \quad (2-89)$$

For a bound nucleon state in a spherical potential, on the other hand, the relation

$$+\frac{1}{2M} \left(p_r^2 + \frac{\kappa(\kappa+1)}{r^2} \right) g(r, \kappa) = E_{\text{kin}} g(r, \kappa) \quad (2-90)$$

holds, where E_{kin} is the kinetic energy of the nucleon. The ratio of relativistic to nonrelativistic single-particle matrix elements

can, therefore, be estimated as

$$M_R/M_{NR} \approx (E_{kin}/2M)^{1/2} \approx 0.1. \quad (2-91)$$

It has been shown that some approximations must be made in going from relativistic nuclear wave functions to the nonrelativistic limit. Some of the relativistic form-factor coefficients, however, can be related to nonrelativistic coefficients on the basis of CVC theory (Stech and Schülke, 1964; Fujita, 1962; Eich-Schopper, 1966; ler, 1963; Damgaard and Winther, 1965; Blin-Stoyle and Nair, 1966; Blin-Stoyle, 1973). The most important such relations are (Behrens and Bühring, 1971)

$$\begin{aligned} -V_{O11}^{V,N-1}(k_x, m, n, \rho) &= (W_0 + 2.5) \left\{ \int_0^R \left(\frac{x}{R}\right)^{2N-1} I(k_x, m, n, \rho; x) dx T_{000}^V \right\} \\ &- \frac{\alpha Z}{R} \left\{ \int_0^R \left(\frac{x}{R}\right)^{2N-1} I(k_x, m, n, \rho; x) dx U(r)^T_{000} J_0^V \right\} \end{aligned} \quad (2-92)$$

and

$$\begin{aligned} &-(2K+1+2N)[K/(2K+1)]^{1/2} V_{KK-11}^{V,N} - 2N[(K+1)/(2K+1)]^{1/2} V_{KK+11}^{V,N-1} \\ &= (W_0 + 2.5) R V_{KKO}^{V,N} - \alpha Z \left[\int_0^R \left(\frac{r}{R}\right)^{K+2N} U(r)^T_{KKO} J_0^V \right]. \end{aligned} \quad (2-93)$$

Additional relations are given by Behrens and Bühring (1971).

Because the old Cartesian notation for nuclear matrix elements is used in many papers, the connection between form-factor coefficients and nuclear matrix elements is listed in Cartesian notation in Table 2.10.

Induced interactions. As indicated in Sec. 2.1, the hadron current is influenced by the presence of the strong interactions. It can be shown (Delorme and Rho, 1971), that hence the simple nuclear current of Eq. (2-4) must be replaced by the most general current

$$J_{\mu} = i\bar{\psi}_n(p') \sum_{\substack{i=V,S,M, \\ A,P,T}} \left[G_i O_{\mu}^i + F_i (i\vec{\gamma} \vec{p}' + M) O_{\mu}^i + G_i O_{\mu}^i (i\vec{\gamma} \vec{p} + M) + H_i (i\vec{\gamma} \vec{p}' + M) O_{\mu}^i (i\vec{\gamma} \vec{p} + M) \right] \psi_p(p), \quad (2-94)$$

where we have

$$O_{\mu}^V = \gamma_{\mu}, O_{\mu}^S = iq_{\mu}, O_{\mu}^M = \sigma_{\mu\lambda} q_{\lambda}, O_{\mu}^A = \gamma_{\mu} \gamma_5, O_{\mu}^P = iq_{\mu} \gamma_5$$

and

$$O_{\mu}^T = \sigma_{\mu\lambda} q_{\lambda} \gamma_5.$$

Because the binding energy B of the nucleons inside the nucleus is always small compared with their mass M , the off-mass-shell effects are expected to be negligible (of order B/M). In the standard impulse-approximation treatment, the nucleons are therefore taken on their mass shell, i.e., $(i\vec{\gamma} \vec{p} + M)u(p) = 0$ is assumed. Then the terms associated with the coupling constants F_i , G_i , and H_i vanish. On replacing q_{μ} by the corresponding differential operator (Behrens and Bühring, 1971; 1974) we obtain

$$J_{\mu} = i\bar{\psi}_p \left[\gamma_{\mu} + if_M \sigma_{\mu\nu} \left(\frac{\partial}{\partial x_{\nu}} + ieA_{\nu} \right) + f_S \left(\frac{\partial}{\partial x_{\mu}} + ieA_{\mu} \right) + \lambda \gamma_{\mu} \gamma_5 + if_T \sigma_{\mu\nu} \gamma_5 \left(\frac{\partial}{\partial x_{\nu}} + ieA_{\nu} \right) + f_P \gamma_5 \left(\frac{\partial}{\partial x_{\mu}} + ieA_{\mu} \right) \right] \psi_N \quad (2-95)$$

for the case of β^- decay. In β^+ decay and electron capture, the Hermitian conjugate current is

$$\begin{aligned}
 J_{\mu}^{+} = i\bar{\psi}_n \left[\gamma_{\mu} + i f_M \sigma_{\mu\nu} \left(\frac{\partial}{\partial x_{\nu}} - ieA_{\nu} \right) - f_S \left(\frac{\partial}{\partial x_{\mu}} - ieA_{\mu} \right) + \lambda \gamma_{\mu} \gamma_5 \right. \\
 \left. - i f_T \sigma_{\mu\nu} \gamma_5 \left(\frac{\partial}{\partial x_{\nu}} - ieA_{\nu} \right) + f_P \gamma_5 \left(\frac{\partial}{\partial x_{\mu}} - ieA_{\mu} \right) \right] \psi_p. \quad (2-96)
 \end{aligned}$$

By comparing Eqs. (2-95) and (2-96), the formal substitutions can be determined that must be made for the induced coupling constants in going from β^- to β^+ decay, from β^+ decay to electron capture, or from β^- decay to electron capture (Behrens and Bühring, 1974).

Between β^- and β^+ decay, the following correspondences hold [in addition to those indicated in Eq. (2-39)]:

β^- decay	→	β^+ decay	
f_M	→	f_M	
f_S	→	$-f_S$	
f_T/λ	→	$-f_T/\lambda$	(2-97)
f_P/λ	→	f_P/λ	
$-ieA_{\mu}$	→	$-ieA_{\mu}$	

For β^+ decay and electron capture, the hadron current (and therefore also the hadron part of the transition matrix element) has the same form. Thus, beyond the substitutions indicated in Eq. (2-40), it is only necessary to replace W_0 by $W_0 + W_x$ to go from β^+ decay to electron capture.

Starting from β^- decay, on the other hand, the following substitutions apply [in addition to those indicated in Eqs. (2-41) and (2-42)]:

β^- decay	\rightarrow	electron capture	
f_M	\rightarrow	f_M	
f_S	\rightarrow	$-f_S$	
f_T/λ	\rightarrow	$-f_T/\lambda$	(2-98)
f_P/λ	\rightarrow	f_P/λ	
ieA_μ	\rightarrow	$-ieA_\mu$	

The quantities f_M , f_S , f_T and f_P are the coupling constants for the weak magnetic, induced scalar, induced tensor, and induced pseudoscalar interactions, respectively (Marshak et al., 1969; Schopper, 1966; Blin-Stoyle, 1973; Blin-Stoyle and Nair, 1966; Kim, 1974).

The conserved-vector-current theory predicts the values (Blin-Stoyle and Nair, 1966)

$$\begin{aligned} f_M &= (\mu_p - \mu_n)/2M \approx 0.0010, \\ f_S &= 0 \end{aligned} \tag{2-99}$$

for f_M and f_S ; here, μ_p and μ_n are the anomalous magnetic moments of the proton and neutron, and M is the nucleon mass.

The quantity $A_\mu = (A, i\phi)$ in Eq. (2-98) is the potential of the external electromagnetic field, which in this case is the static electric field of the nuclear charge, for which we have $A=0$,

$-e\phi = V(r) = \frac{\alpha Z}{R} U(r)$. The terms containing A_μ must be included to assure gauge invariance of the Hamiltonian.

By applying the Dirac equation, the operator $\frac{\partial}{\partial x_4}$ in Eq. (2-96) can be replaced by the transition energy $W'_0 = W_0 + W_x$.

Like the simple current of Eq. (2-4), the general current given by Eq. (2-96) consists of two parts, one of which Lorentz-transforms like a four-vector, the other like an axial vector. We make use of this property. In the nuclear matrix elements without induced interactions [Eq. (2-77)], the spherical tensor operators T_{KLS} and $\gamma_5 T_{KLS}$ occur:

$$\begin{aligned} 1 \cdot T_{LLO}^M &= 1 \cdot i \cdot Y_L^{LM} \\ \lambda \gamma_5 \cdot T_{LLO}^M &= \lambda \gamma_5 \cdot i \cdot Y_L^{LM} \\ 1 \cdot T_{KL1}^M &= \vec{\alpha} \cdot (-1)^{L-K+1} i \cdot Y_{KL}^{LM} \\ \lambda \gamma_5 \cdot T_{KL1}^M &= \lambda \vec{\sigma} \cdot (-1)^{L-K+1} i \cdot Y_{KL}^{LM} \end{aligned} \quad (2-100)$$

The nuclear operators 1 , $\lambda \gamma_5$, $\vec{\alpha}$ and $\lambda \vec{\sigma}$ behave under rotation like scalars, pseudoscalars, vectors, and axial vectors, respectively. Introduction of the general current of Eq. (2-96) makes it necessary to replace these operators by more complicated operators which have the same transformation properties (Behrens and Bühring, 1971):

$$\begin{aligned}
1 \rightarrow j_0^V &= 1 - if_M \beta \alpha \cdot \nabla + f_S \beta \left[W'_0 - \frac{\alpha Z}{R} U(r) \right], \\
\lambda \gamma_5 \rightarrow j_0^A &= \lambda \gamma_5 + if_T \beta \sigma \cdot \nabla - f_P \beta \gamma_5 \left[W'_0 - \frac{\alpha Z}{R} U(r) \right], \\
\vec{\alpha} \rightarrow -\vec{j}^V &= \vec{\alpha} + f_M \beta [\vec{\sigma} \times \vec{\nabla}] + f_M \beta \vec{\alpha} \left[W'_0 - \frac{\alpha Z}{R} U(r) \right] - if_S \beta \vec{\nabla}, \\
\lambda \vec{\sigma} \rightarrow -\vec{j}^A &= \lambda \vec{\sigma} - f_T \beta [\vec{\alpha} \times \vec{\nabla}] - f_T \beta \vec{\sigma} \left[W'_0 - \frac{\alpha Z}{R} U(r) \right] + if_P \beta \gamma_5 \vec{\nabla}. \quad (2-101)
\end{aligned}$$

These substitutions, in Eq. (2-76) via Eq. (2-77), lead to the form-factor coefficients that correspond to the general nuclear current. The expressions for the observables in terms of form-factor coefficients remain unchanged (Sec. 2.2.3; Stech and Schülke, 1964; Böhning and Schülke, 1965). Only the definition of the form-factor coefficients in terms of nuclear matrix elements and coupling constants is changed.

The form-factor coefficients in terms of nuclear matrix elements appropriate for electron capture are as follows:

$$\begin{aligned}
V_{F_{KKO}}^N(k, m, n, \rho) &= V_{M_{KKO}}^N(k, m, n, \rho) \\
&+ f_M R^{-1} \left\{ [K/(2K+1)]^{1/2} \left(\int (r/R)^{K+2N-1} [(2K+1+2N)I(r) + rI'(r)] \beta T_{KK-11}^{\beta T} \right) \right. \\
&+ \left. [(K+1)/(2K+1)]^{1/2} \left(\int (r/R)^{K+2N-1} [2NI(r) + rI'(r)] \beta T_{KK+11}^{\beta T} \right) \right\} \\
&+ f_S R^{-1} \left(\int (r/R)^{K+2N} I(r) [W'_0 R - \alpha Z U(r)] \beta T_{KKO}^{\beta T} \right), \quad (2-102a)
\end{aligned}$$

$$\begin{aligned}
A_{F_{KKO}}^N(k, m, n, \rho) &= \lambda A_{M_{KKO}}^N(k, m, n, \rho) \\
&- f_T R^{-1} \left\{ [K/(2K+1)]^{1/2} \left(\int (r/R)^{K+2N-1} [(2K+1+2N)I(r) + rI'(r)] \beta \gamma_5^T T_{KK-11}^{\beta T} \right) \right. \\
&+ \left. [(K+1)/(2K+1)]^{1/2} \left(\int (r/R)^{K+2N-1} [2NI(r) + rI'(r)] \beta \gamma_5^T T_{KK+11}^{\beta T} \right) \right\} \\
&- f_P R^{-1} \left(\int (r/R)^{K+2N} I(r) [W'_0 R - \alpha Z U(r)] \beta \gamma_5^T T_{KKO}^{\beta T} \right), \quad (2-102b)
\end{aligned}$$

$$\begin{aligned}
& V_{KKL}^N(k, m, n, \rho) = V_{KKL}^N(k, m, n, \rho) \\
& f_M R^{-1} \left\{ \left[\frac{(K+1)}{(2K+1)} \right]^{1/2} \left(\int (r/R)^{K+2N-1} [(2K+1+2N)I(r) + rI'(r)] \beta \gamma_5^T{}_{KK-11} \right) \right. \\
& \left. \left[\frac{K}{(2K+1)} \right]^{1/2} \left(\int (r/R)^{K+2N-1} [2NI(r) + rI'(r)] \beta \gamma_5^T{}_{KK+11} \right) \right. \\
& \left. + \left(\int (r/R)^{K+2N} I(r) [W'_R - \alpha ZU(r)] \beta \gamma_5^T{}_{KKL} \right) \right\}, \quad (2-102c)
\end{aligned}$$

$$\begin{aligned}
& A_{KKL}^N(k, m, n, \rho) = \lambda A_{KKL}^N(k, m, n, \rho) \\
& - f_T R^{-1} \left\{ \left[\frac{(K+1)}{(2K+1)} \right]^{1/2} \left(\int (r/R)^{K+2N-1} [(2K+1+2N)I(r) + rI'(r)] \beta \gamma_5^T{}_{KK-11} \right) \right. \\
& \left. - \left[\frac{K}{(2K+1)} \right]^{1/2} \left(\int (r/R)^{K+2N-1} [2NI(r) + rI'(r)] \beta \gamma_5^T{}_{KK+11} \right) \right. \\
& \left. + \left(\int (r/R)^{K+2N} I(r) [W'_R - \alpha ZU(r)] \beta \gamma_5^T{}_{KKL} \right) \right\}, \quad (2-102d)
\end{aligned}$$

$$\begin{aligned}
& - V_{KK-11}^N(k, m, n, \rho) = V_{KK-11}^N(k, m, n, \rho) \\
& + f_M R^{-1} \left\{ - \left[\frac{(K+1)}{(2K+1)} \right]^{1/2} \left(\int (r/R)^{K+2N-2} [2NI(r) + rI'(r)] \beta \gamma_5^T{}_{KKL} \right) \right. \\
& \left. + \left(\int (r/R)^{K+2N-1} I(r) [W'_R - \alpha ZU(r)] \beta \gamma_5^T{}_{KK-11} \right) \right\} \\
& - f_S R^{-1} \left[\frac{K}{(2K+1)} \right]^{1/2} \left(\int (r/R)^{K+2N-2} [2NI(r) + rI'(r)] \beta \gamma_5^T{}_{KKO} \right), \quad (2-102e)
\end{aligned}$$

$$\begin{aligned}
& - A_{KK-11}^N(k, m, n, \rho) = \lambda A_{KK-11}^N(k, m, n, \rho) \\
& - f_T R^{-1} \left\{ - \left[\frac{(K+1)}{(2K+1)} \right]^{1/2} \left(\int (r/R)^{K+2N-2} [2NI(r) + rI'(r)] \beta \gamma_5^T{}_{KKL} \right) \right. \\
& \left. + \left(\int (r/R)^{K+2N-1} I(r) [W'_R - \alpha ZU(r)] \beta \gamma_5^T{}_{KK-11} \right) \right\} \\
& + f_P R^{-1} \left[\frac{K}{(2K+1)} \right]^{1/2} \left(\int (r/R)^{K+2N-2} [2NI(r) + rI'(r)] \beta \gamma_5^T{}_{KKO} \right) \quad (2-102f)
\end{aligned}$$

$$\begin{aligned}
& -V_{F_{KK+11}}^N(k, m, n, \rho) = V_{M_{KK+11}}^N(k, m, n, \rho) \\
& + f_{M^R}^{-1} \left\{ [K/(2K+1)]^{1/2} \left(\int (r/R)^{K+2N} [(2K+3+2N)I(r) + rI'(r)] \beta \gamma_5^T{}_{KK1} \right) \right. \\
& \quad \left. + \left(\int (r/R)^{K+1+2N} I(r) [W'_0 R - \alpha Z U(r)] \beta^T{}_{KK+11} \right) \right\} \\
& - f_{S^R}^{-1} [(K+1)/(2K+1)]^{1/2} \left(\int (r/R)^{K+2N} [(2K+3+2N)I(r) + rI'(r)] \beta^T{}_{KK0} \right),
\end{aligned} \tag{2-102g}$$

$$\begin{aligned}
& -V_{F_{KK+11}}^A(k, m, n, \rho) = \lambda^A V_{M_{KK+11}}^A(k, m, n, \rho) \\
& - f_{T^R}^{-1} \left\{ [K/(2K+1)]^{1/2} \left(\int (r/R)^{K+2N} [(2K+3+2N)I(r) + rI'(r)] \beta^T{}_{KK1} \right) \right. \\
& \quad \left. + \left(\int (r/R)^{K+1+2N} I(r) [W'_0 R - \alpha Z U(r)] \beta \gamma_5^T{}_{KK+11} \right) \right\} \\
& + f_{P^R}^{-1} [(K+1)/(2K+1)]^{1/2} \left(\int (r/R)^{K+2N} [(2K+3+2N)I(r) + rI'(r)] \beta \gamma_5^T{}_{KK0} \right).
\end{aligned}$$

For brevity, we have written $I(r)$ instead of $I(k_x, m, n, \rho; r)$; we have $I'(r) \equiv dI/dr$. (2-102h)

In addition to the single-particle matrix elements of Eqs. (2-84), the following are required:

$$\begin{aligned}
& \left(\int (r/R)^{K+2N} \phi(r) \beta^T{}_{KK0} \right) = [2/(2J_i+1)]^{1/2} \left\{ -G_{KK0}(\kappa_f, \kappa_i) \right. \\
& \quad \times \int_0^\infty g_f(r, \kappa_f) (r/R)^{K+2N} \phi(r) g_i(r, \kappa_i) r^2 dr \\
& \quad \left. + \text{sign}(\kappa_f) \text{sign}(\kappa_i) G_{KK0}(-\kappa_f, -\kappa_i) \right. \\
& \quad \left. \times \int_0^\infty f_f(r, \kappa_f) (r/R)^{K+2N} \phi(r) f_i(r, \kappa_i) r^2 dr \right\},
\end{aligned} \tag{2-103a}$$

$$\begin{aligned}
\left(\int (r/R)^{L+2N} \phi(r) \beta \gamma_5^T \text{KLL} \right) &= [2/(2J_i+1)]^{1/2} \left\{ -G_{\text{KLL}}(\kappa_f, \kappa_i) \right. \\
&\times \int_0^\infty g_f(r, \kappa_f) (r/R)^{L+2N} \phi(r) g_i(r, \kappa_i) r^2 dr \\
&+ \text{sign}(\kappa_f) \text{sign}(\kappa_i) G_{\text{KLL}}(-\kappa_f, -\kappa_i) \\
&\left. \times \int_0^\infty f_f(r, \kappa_f) (r/R)^{L+2N} \phi(r) f_i(r, \kappa_i) r^2 dr \right\}, \quad (2-103b)
\end{aligned}$$

$$\begin{aligned}
\left(\int (r/R)^{K+2N} \phi(r) \beta \gamma_5^T \text{KKO} \right) &= [2/(2J_i+1)]^{1/2} \left\{ -\text{sign}(\kappa_i) G_{\text{KKO}}(\kappa_f, -\kappa_i) \right. \\
&\times \int_0^\infty g_f(r, \kappa_f) (r/R)^{K+2N} \phi(r) f_i(r, \kappa_i) r^2 dr + \text{sign}(\kappa_f) G_{\text{KKO}}(-\kappa_f, \kappa_i) \\
&\left. \times \int_0^\infty f_f(r, \kappa_f) (r/R)^{K+2N} \phi(r) g_i(r, \kappa_i) r^2 dr \right\}, \quad (2-103c)
\end{aligned}$$

$$\begin{aligned}
\left(\int (r/R)^{L+2N} \phi(r) \beta \text{T}_{\text{KLL}} \right) &= [2/(2J_i+1)]^{1/2} \left\{ -\text{sign}(\kappa_i) G_{\text{KLL}}(\kappa_f, -\kappa_i) \right. \\
&\times \int_0^\infty g_f(r, \kappa_f) (r/R)^{L+2N} \phi(r) f_i(r, \kappa_i) r^2 dr + \text{sign}(\kappa_f) G_{\text{KLL}}(-\kappa_f, \kappa_i) \\
&\left. \times \int_0^\infty f_f(r, \kappa_f) (r/R)^{L+2N} \phi(r) g_i(r, \kappa_i) r^2 dr \right\}. \quad (2-103d)
\end{aligned}$$

Here, $\phi(r)$ stands for $I(k_x, m, n, \rho; r)$ or $rI'(k_x, m, n, \rho; r)$ or a linear combination of these integrals. The question whether a finite coupling constant f_T exists for the induced tensor interaction has aroused great interest of late. Second-class currents (Weinberg, 1958) manifest themselves in principle only through the

coupling constants f_S and f_T , and f_S vanishes in accord with the conserved vector current theory. Hence, the determination of f_T is connected with the very question of the existence of second-class currents in β decay and electron capture.¹¹ Although this problem has been discussed extensively in the literature (Wilkinson, 1970a, 1971, 1972a, 1971/72, 1974b; Alburger and Wilkinson, 1970; Kim, 1971; Holstein and Treiman, 1971; Vatai, 1971, 1972b; Wilkinson and Alburger, 1971; Blomquist, 1971; Wolfenstein and Henley, 1971; Lipkin, 1970, 1971; Kim and Fulton, 1971; Blin-Stoyle et al., 1971; Laverne and Dang, 1971; Alburger, 1972; Tribble and Garvey, 1974; Towner, 1973; Greenland, 1975) an unambiguous answer concerning the existence of second-class currents has not yet been obtained. An excellent review of this matter has been written by Wilkinson (1971/72).

In view of the uncertainty about second-class currents, Kubodera et al. (1973) have recently pointed out that one cannot neglect the nucleon binding effects, i.e., off-mass-shell phenomena and exchange currents. Thus, at least as far as the axial-vector part is concerned, one should start with the most general current [Eq. (2-94)]. But then the large number of coupling constants complicates the problem to such an extent that it can be dealt with only under some simplifying assumptions, i.e., minimal coupling. Furthermore, special models for the meson exchange current must be used. Following this line of attack, Kubodera et al. (1973) were able to calculate explicitly off-mass-shell and meson-exchange effects for some special cases, and to demonstrate their importance (Eman et al., 1973).

2.2.4. Explicit Expression for the Quantities $M_K(k_x, k_\nu)$ and

$$\underline{m_K(k_x, k_\nu)}$$

By expanding electron and neutrino radial wave functions as outlined in Sec. 2.2.2 and introducing the form-factor coefficients defined in Sec. 2.2.3, we can derive from Eq. (2-42) explicit expansions of the quantities $M_K(k_x, k_\nu)$ and $m_K(k_x, k_\nu)$. If we take into account only dominant terms (of lowest order in the expansion of electron and neutrino radial wave functions), we arrive at the following simple forms for $M_K(k_x, k_\nu)$ and $m_K(k_x, k_\nu)$ (Behrens and Jänecke, 1969; Behrens and Bühring, 1971):

For allowed transitions,

$$\begin{aligned} M_0(1,1) &= V_{F00}^0, \\ M_1(1,1) &= -A_{F10}^0; \end{aligned} \quad (2-104)$$

for first-forbidden transitions,

$$\begin{aligned} M_0(1,1) &= A_{F00}^0 + (1/3)\alpha Z A_{F011}^0(1,1,1,1) - (1/3)W_{0R} A_{F011}^0, \\ m_0(1,1) &= (1/3)R A_{F011}^0, \\ M_1(1,1) &= -V_{F10}^0 + (1/3)\alpha Z (1/3)^{1/2} V_{F110}^0(1,1,1,1) \\ &\quad - (1/3)W_{0R} (1/3)^{1/2} V_{F110}^0 - (1/3)\alpha Z (2/3)^{1/2} \\ &\quad \times A_{F111}^0(1,1,1,1) - (1/3)(W_x + q_x)R (2/3)^{1/2} A_{F111}^0, \\ m_1(1,1) &= (1/3)R \left[(1/3)^{1/2} V_{F110}^0 - (2/3)^{1/2} A_{F111}^0 \right], \end{aligned}$$

$$\begin{aligned}
M_1(1,2) &= -(1/3)q_{xR} \left[(2/3)^{1/2} V_{F_{110}}^0 - (1/3)^{1/2} A_{F_{111}}^0 \right], \\
M_1(2,1) &= -(1/3)p_{xR} \left[(2/3)^{1/2} V_{F_{110}}^0 + (1/3)^{1/2} A_{F_{111}}^0 \right], \\
M_2(1,2) &= -(1/3)q_{xR} A_{F_{211}}^0, \\
M_2(2,1) &= -(1/3)p_{xR} A_{F_{211}}^0. \tag{2-105}
\end{aligned}$$

For higher forbidden transitions, we have

$$\begin{aligned}
M_L(k_x, k_v^{(1)}) &= K_L(p_{xR})^{k_x-1} (q_{xR})^{k_v^{(1)}-1} \left\{ -[(2L+1)/L]^{1/2} V_{F_{LL-11}}^0 \right. \\
&+ (2k_x+1)^{-1/2} \alpha_Z V_{F_{LLO}}^0(k_x, 1, 1, 1) + [(2k_x+1)^{-1} (2k_v^{(1)}+1)^{-1} q_{xR}] \\
&\times V_{F_{LLO}}^0 - (2k_x+1)^{-1} \alpha_Z [(L+1)/L]^{1/2} A_{F_{LL1}}^0(k_x, 1, 1, 1) \\
&\left. - [(2k_x+1)^{-1} w_{xR} + (2k_v^{(1)}+1)^{-1} q_{xR}] [(L+1)/L]^{1/2} A_{F_{LL1}}^0 \right\}, \tag{2-106a}
\end{aligned}$$

$$\begin{aligned}
m_L(k_x, k_v^{(1)}) &= K_L(p_{xR})^{k_x-1} (q_{xR})^{k_v^{(1)}-1} (2k_x+1)^{-1} R \\
&\times \left\{ V_{F_{LLO}}^0 - [(L+1)/L]^{1/2} A_{F_{LL1}}^0 \right\}, \tag{2-106b}
\end{aligned}$$

$$\begin{aligned}
M_L(k_x, k_v^{(2)}) &= -\tilde{K}_L(p_{xR})^{k_x-1} (q_{xR})^{k_v^{(2)}-1} (L+1)^{1/2} [(2k_x-1)(2k_v^{(2)}-1)]^{-1/2} \\
&\times \left\{ V_{F_{LLO}}^0 + (k_x - k_v^{(2)})(L+1)^{-1} [(L+1)/L]^{1/2} A_{F_{LL1}}^0 \right\}, \tag{2-106c}
\end{aligned}$$

$$M_{L+1}(k_x, k_v^{(2)}) = -\tilde{K}_L(p_{xR})^{k_x-1} (q_{xR})^{k_v^{(2)}-1} A_{F_{(L+1)L1}}^0. \tag{2-106d}$$

Here we have introduced the abbreviations

$$K_L = (1/2)^{1/2} [(2L)!! / (2L+1)!!]^{1/2} [(2k_x - 1)!(2k_v^{(1)} - 1)!]^{-1/2}; \quad (2-107a)$$

$$\tilde{K}_L = [(2L)!! / (2L+1)!!]^{1/2} [(2k_x - 1)!(2k_v^{(2)} - 1)!]^{-1/2}. \quad (2-107b)$$

The two quantities K_L and \tilde{K}_L are related by

$$\tilde{K}_{L-1} = [(2L+1)/L]^{1/2} K_L. \quad (2-108)$$

The energy of the bound electron in the parent atom is defined as $W_x = 1 - |E_x|$, where E_x is the binding energy in the parent atom.

The electron momentum p_x is given by

$$p_x = (1 - W_x^2)^{1/2}. \quad (2-109)$$

The form-factor coefficients are $V_{F_{KLs}}^N$, $A_{F_{KLs}}^N$, $V_{F_{KLs}}^N(k_x, m, n, \rho)$ and $A_{F_{KLs}}^N(k_x, m, n, \rho)$; they are related to the nuclear matrix elements as indicated previously. The symbols V and A refer to vector and axial vector; K specifies the rank, L the multipolarity, and s the spin of the spherical tensor operators that are involved. The radial dependence of this operator is r^{L+2N} or $r^{L+2N} I(k_x, m, n, \rho; r)$.

These form-factor coefficients occur in accordance with the expansion of the electron radial wave functions discussed in Sec. 2.2.2.

In Eqs. (2-47) through (2-49) we have only presented the dominant terms of the multipole expansion and the expansion of the electron radial wave functions for linear combinations of form-factor coefficients. Complete expressions are listed in Appendix A2.1 (Behrens and Bühring, 1971). Unless there are strong cancellations between different terms connected with the form-factor coefficients, the higher-order terms can be neglected.

2-3. Formulae for Allowed and Forbidden
Transitions

2.3.1. Allowed Transitions

In allowed transitions, electrons can only be captured from orbits with $\kappa_x = \pm 1$, i.e., from the K, L_1 , L_2 , M_1 , M_2, \dots shells [cf. Eqs. (2-44)-(2-47)]. This result is based on the approximate neglect of contributions from higher-order (so-called second-forbidden) terms (see Appendix A2.2). Capture from orbits with $\kappa = \pm 2$, for example, would be governed by matrix-element combinations $M_1(2,1)$, $M_2(2,1)$, etc., which are smaller than $M_0(1,1)$ and $M_1(1,1)$ by at least a factor $p_x R \approx 0.02$. Consequently, we have

$$C_x(\kappa = \pm 2) \leq 4 \times 10^{-4} C_x(\kappa = \pm 1)$$

[Eq. (2-44)], and capture from orbits with $\kappa = \pm 2$ can be expected to be difficult to observe. However, capture from such states in principle offers a possibility of determining the higher-forbidden contributions separately from the leading terms.

For the quantity C_x we find

$$C_x = (V_{F000}^0)^2 + (A_{F101}^0)^2 \quad (2-110)$$

[Eqs. (2-44) and (2-104)]. Inserting this result in Eq. (2-43) leads to

$$\lambda_c = (g^2/4\pi^2) \left\{ (V_{F000}^0)^2 + (A_{F101}^0)^2 \right\} \left[n_K q_K^2 \beta_K^2 B_K^2 + n_{L_1} q_{L_1}^2 \beta_{L_1}^2 B_{L_1}^2 + n_{L_2} q_{L_2}^2 \beta_{L_2}^2 B_{L_2}^2 + \dots \right] \quad (2-111)$$

for the decay constant. Hence it is easy to derive the ratios of the capture probabilities from different subshells. The L_1/K ratio, for example, is

$$\lambda_{L_1}/\lambda_K = (n_{L_1} q_{L_1}^2 \beta_{L_1}^2 B_{L_1}) / (n_K q_K^2 \beta_K^2 B_K). \quad (2-112)$$

2.3.2. First-Forbidden Non-Unique Transitions

Considering, as before, only the dominant terms in non-unique, first-forbidden transitions, we find that electrons with the quantum numbers $\kappa_x = \pm 1, \pm 2$ are captured. For K, $L_1, L_2, M_1, M_2, \dots$ capture, we have

$$C_x = [M_0(1,1) \mp m_0(1,1)]^2 + [M_1(1,1) \mp m_1(1,1)]^2 + M_1^2(1,2) + M_2^2(1,2) \quad (2-113)$$

[Eqs. (2-44)-(2-46)]. The upper sign holds for K, L_1, M_1, \dots capture and the lower, for L_2, M_2, \dots capture. The quantities $M_L(\kappa_x, \kappa_v)$ in Eq. (2-113) are defined through Eqs. (2-105). If there is no cancellation between the different terms in Eqs. (2-105), we can simplify Eq. (2-113). Because we have $w_x = 1 - |E_K|$, with $|E_K| \leq 0.2$ and $R = 0.0031A^{1/3} < 0.02$, we can usually neglect terms multiplied by R and w_R . Then we find (Vatai, 1973)

$$\begin{aligned} C_x = & \left[A_{F00}^0 + (1/3)\alpha Z A_{F011}^0(1,1,1,1) - (1/3)w_{0R} A_{F011}^0 \right]^2 \\ & + \left[V_{F101}^0 - (\alpha Z/3)(1/\sqrt{3}) \left\{ V_{F110}^0(1,1,1,1) - \sqrt{2} A_{F111}^0(1,1,1,1) \right\} \right. \\ & \quad \left. + (w_{0R}/3)(1/\sqrt{3}) \left\{ V_{F110}^0 + \sqrt{2} A_{F111}^0 \right\} \right]^2 \\ & + (w_{0R})^2/9 \left[(2/3)^{1/2} V_{F110}^0 - (1/\sqrt{3}) A_{F111}^0 \right]^2 + \left[A_{F211}^0 \right]^2. \end{aligned} \quad (2-114)$$

This result shows that, even in the case of first-forbidden non-unique transitions, the quantity C_x to a very good approximation does not depend on the particular subshell from which the electron is captured. As for allowed electron capture, the ratios of the capture probabilities from different subshells are therefore independent of the form-factor coefficients. Thus, these ratios have the same form as given in Eq. (2-81).

In many cases, especially for the heavier nuclei, we have $\alpha Z \gg W_0 R$. Then Eq. (2-114) can be simplified further:

$$C_x = \left[A_{F000}^0 + (1/3)\alpha Z A_{F011}^0(1,1,1,1) \right]^2 + \left[V_{F101}^0 - (\alpha Z/3)(1/\sqrt{3}) \left\{ V_{F110}^0(1,1,1,1) - \sqrt{2} A_{F111}^0(1,1,1,1) \right\} \right]^2. \quad (2-115)$$

For capture from $\kappa = \pm 2$ (L_3, M_3, M_4, \dots) states, we have

$$C_x = \{M_1(2,1)\}^2 + \{M_2(2,1)\}^2, \quad (2-116)$$

or explicitly [cf. Eqs. (2-105)],

$$C_x = [(p_x R)^2/9] \left[\left\{ (2/3)^{1/2} V_{F110}^0 + (1/\sqrt{3}) A_{F111}^0 \right\}^2 + \left\{ A_{F211}^0 \right\}^2 \right]. \quad (2-117)$$

Comparison of Eq. (2-117) with Eq. (2-114) suggests that $\kappa = \pm 2$ capture is negligibly small as against capture from $\kappa = \pm 1$ orbits.

2.3.3. First-Forbidden Unique Transitions

Considering dominant terms in Eqs. (2-105) for unique first-forbidden transitions, we find that subshells with $\kappa = \pm 1, \pm 2$ can contribute (Behrens and Jänecke, 1969). For capture from $\kappa_x = \pm 1$ ($K, L_1, L_2, M_1, M_2, \dots$) states, we have

$$C_x = \left(A_{F211}^0 \right)^2 (R^2/9) q_x^2, \quad (2-118)$$

and for capture from $\kappa_x = \pm 2$ (L_3, M_3, M_4, \dots) orbits, we find

$$C_x = \left(A_{F211}^0 \right)^2 (R^2/9) p_x^2. \quad (2-119)$$

It follows from Eqs. (2-43) and (2-118) that the L_1/K capture ratio is

$$\lambda_{L_1}/\lambda_K = (n_{L_1}^4 q_{L_1}^2 \beta_{L_1}^2 B_{L_1}) / (n_K^4 q_K^2 \beta_K^2 B_K). \quad (2-120)$$

Expressions for the L_2/K , M_1/K , L_2/L_1 , and M_1/L_1 capture ratios are entirely analogous. For the L_3/L_1 ratio, on the other hand, we have

$$\lambda_{L_3}/\lambda_{L_1} = (n_{L_3}^2 p_{L_3}^2 q_{L_3}^2 \beta_{L_3}^2 B_{L_3}) / (n_{L_1}^4 q_{L_1}^2 \beta_{L_1}^2 B_{L_1}). \quad (2-121)$$

Other $k_x = 2$ to $k_x = 1$ capture ratios are analogous to Eq. (2-121).

2.3.4. (L-1)-Forbidden Unique Transitions

Taking only dominant terms in Eq. (2-106d) into account, we have for $L \geq k_x$

$$C_x = \frac{(2L-2)!!}{(2L-1)!!} \left(A_{F_{LL-11}}^0 \right)^2 R^{2(L-1)} \frac{p_x^{2(k_x-1)} q_x^{2(L-k_x)}}{(2k_x-1)! \{2(L-k_x)+1\}!}. \quad (2-123)$$

For $K, L_1, L_2, M_1, M_2, \dots$ capture, for example, we obtain

$$C_x = \left(A_{F_{LL-11}}^0 \right)^2 \{ (2L-1)!! \}^{-2} (q_x R)^{2(L-1)}. \quad (2-124)$$

2.3.5. Some General Remarks on Higher-Forbidden

Non-Unique Transitions

Special formulae for the higher-forbidden non-unique capture rates can easily be derived from Eqs. (2-106) in analogy with the first-forbidden non-unique transition rate [Eqs. (2-113) to (2-115)]. The following general statements can be made regarding such higher-forbidden capture transitions:

(i) As for $\Delta J=1$ first-forbidden non-unique transitions, these capture rates depend only on six different form-factor coefficients, viz., $V_{LL-1}^{(0)}$, $V_{LLO}^{(0)}$, $V_{LLO}^{(0)}(k_x, 1, 1, 1)$, $A_{LL1}^{(0)}$, $A_{LL1}^{(0)}(k_x, 1, 1, 1)$, $A_{L+1,L,1}^{(0)}$. Expressions for these rates are therefore no more complicated than those for first-forbidden transitions.

(ii) If we neglect terms multiplied by R and $W_x R$, as in Eq. (2-114), the capture ratios from shells with the same k_x value do not depend on the nuclear form-factor coefficients. Form-factor coefficients can therefore be determined by investigating capture ratios only if ratios of capture from states with different k_x are measured (e.g. L_2/K , M_2/K) (Vatai, 1973).

(iii) Non-unique L^{th} -forbidden capture rates are always proportional to a factor

$$\{(2L+1)!!\}^{-4} (q_x R)^{2L} (p_x/q_x)^{2k_x}$$

[Eqs. (2-106)]. Consequently, such capture probabilities decrease very rapidly with increasing degree of forbiddenness.

2.4. Electron-Capture to Positron-Decay Ratios

2.4.1. General Expressions

For allowed as well as forbidden transitions, the following general result for EC/ β^+ ratios holds [Eqs. (2-2), (2-7), (2-10)]:

$$\lambda_{EC}/\lambda_{\beta^+} = \left(\sum_x n_x C_x f_x \right) / \left(f_{\beta^+} \overline{C(W)} \right). \quad (2-125)$$

Here, f_{β^+} is the integrated Fermi function (Behrens and Jänecke, 1969):

$$f_{\beta^+} = \int_0^{p_0} p^2 (W_0 - W)^2 F(Z', W) dp, \quad (2-126)$$

where p is the positron momentum (in units of m_0c), the maximum momentum is $p_0 = (W_0^2 - 1)^{1/2}$, W is the positron energy (in units of m_0c^2), Z' is the atomic number of the daughter nucleus, $F(Z, W)$ is the Fermi function, and $\overline{C(W)}$ is the spectrum shape factor, averaged over the β^+ spectrum. The form of the shape factor for different types of β^+ decay has been discussed, for example, by Schopper (1966), Behrens and Jänecke (1969), and Behrens and Bühring (1971).

To calculate the integrated Fermi function f we need the continuum-electron radial wave functions $g_{-1}(r)$ and $f_{+1}(r)$. Conventionally, these functions (and hence the Fermi function) are evaluated at the nuclear radius ($r=R$). However, recent discussions indicate that a less ambiguous result is achieved if the Fermi function is evaluated at the center of the nucleus ($r=0$) (Schopper, 1966; Behrens and Bühring, 1968, 1972; Blin-Stoyle, 1969). This

latter definition of the Fermi function is appropriate for the electron-capture formalism in the present paper (Sec. 2.2.2). A number of detailed calculations and tabulations of the Fermi function $F(Z,W)$ and of the integrated Fermi function $f(Z,W_0)$ exist. However, in many instances finite nuclear size and screening by orbital electrons has not been taken fully into account. The Fermi function for a point nucleus without screening is listed in the National Bureau of Standards tables (1952) and in a paper by Rose and Perry (1953). Dzhelepov and Zyryanova (1956) have calculated the Fermi function and the integrated Fermi function (at $r=R$) by adding corrections for screening and finite size to the functions for a point nucleus. Several authors (Matese and Johnson, 1966; Durand, 1964; Brown, 1964), however, have noted that the screening corrections of Reitz (1950) used by Dzhelepov and Zyryanova are incorrect for higher electron momenta.

Fermi functions evaluated numerically (at $r=R$) from an exact solution of the Dirac equation for a nucleus with finite size, but without screening, have been tabulated by Bhalla and Rose (1960, 1961, 1962, 1964). It was later shown, however, that these tables are not entirely correct for positrons of higher momenta (Bühring, 1967; Huffacker and Laird, 1967; Behrens and Asai and Ogata, 1974). Bühring, 1968; Blin-Stoyle, 1973, p. 38; [^] For a few elements, Bühring (1965) has carried out an exact numerical integration of the Dirac equation, taking into consideration finite nuclear

size and screening. By employing a method similar to that of Böhring, extensive tables of the Fermi function (at $r=0$) and graphs of the integrated Fermi function have been published by Behrens and Jänecke (1969); this calculation takes exact account of both finite nuclear size and electron screening. Numerical integration of the Dirac equation, including finite size and screening, has also been carried out by Suslov (1966, 1967, 1968a). Theoretical K/β^+ ratios have also been listed by Suslov (1970 b). The extensive tabulations of the Fermi function (at $r=R$) and of the integrated Fermi function by Dzhelepov, Zyryanova, and Suslov (1972) are based on these calculations. Suslov, however, included in the electrostatic potential caused by the atomic electrons a Slater exchange term.¹² While the exchange term is applicable to the bound orbital electrons, it is not appropriate for the continuum states; this is self-evident for positrons and has also been shown for emitted β^- particles (Matese and Johnson, 1966; Behrens and Jänecke, 1969, p. 25). It may be for this reason that Suslov's calculations do not agree at low β^+ energies with his Thomas-Fermi-Dirac calculations and with results of other authors (Behrens and Jänecke, 1969; Bhalla and Rose, 1960, 1961, 1962, 1964).

An extensive tabulation of $\log f$ (at $r=R$) and of capture-to-positron ratios, with an accuracy of two to three digits, has been compiled by Gove and Martin (1971). These values were obtained

ORIGINAL PAGE IS
OF POOR QUALITY

by correcting point-nucleus continuum radial wave functions for finite nuclear size and screening.

In all calculations discussed so far, the finite size of the nucleus was represented by the simplest model, *viz.*, a uniformly charged sphere of radius R , equal to the nuclear radius. A more realistic charge distribution has been employed by Behrens and Bühring (1970), who have shown that the influence of the shape of the charge distribution on the Fermi function can be neglected in most cases (see also Asai and Ogata, 1974). An analytical parametrization of the Fermi function and of the integrated Fermi function (for a point-like nucleus), of the screening corrections, the finite nuclear-size effects, and of the dependence of allowed β decay on the nuclear radius has been derived by Wilkinson (1970b, 1970c, 1970d; 1970e, 1972b, 1973c; Wilkinson and Macefield, 1974).

2.4.2. Allowed Transitions

For allowed transitions, for which we have $C(W) = C_x = (F_{000}^0)^2 + (F_{101}^0)^2$, the EC/ β^+ ratio has a very simple form:

$$\lambda_K / \lambda_{\beta^+} = f_K / f_{\beta^+} \quad (2-127)$$

This ratio consequently does not depend on the form-factor coefficients, just like the capture ratios. However, for the EC/ β^+ ratio there are two effects that can lead to small deviations from the result predicted by Eq. (2-127):

(i) If higher-order terms (Appendix A2.1) contribute significantly, the differences between C_x and $C(W)$ must be taken

into account [Sec. 2.1; Eq. (2-40)]. For allowed transitions, the correction factor of Eq. (2-127) can be given explicitly. Neglecting terms in $F_{121}^{(N)}(1, m, n, \rho)$ and form-factor coefficients of rank two, we find (Appendix A2.1; Behrens and Bühring, 1971)¹³

$$\lambda_K/\lambda_{\beta^+} = (f_K/f_{\beta^+}) [1 + (A_1 + y^2 A_2)/(1 + y^2)], \quad (2-128)$$

where

$$\begin{aligned} A_1 = & (2/3)^{3/2} \{2(W_K + \bar{W}) - [1 + (\bar{\mu}_1 \gamma_1)/\bar{W}]\} R(V_{F_{111}}^{(0)}/A_{F_{101}}^{(0)}) \\ & + 2(3)^{-3/2} [1 + (\bar{\mu}_1 \gamma_1)/\bar{W}] R(A_{F_{110}}^{(0)}/A_{F_{101}}^{(0)}) - (2/3)(W_K + \bar{W}) R\alpha Z \\ & \times [(1/9)(A_{F_{101}}^{(1)}(1, 1, 1, 1)/A_{F_{101}}^{(0)}) + (A_{F_{101}}^{(1)}(1, 2, 2, 1)/A_{F_{101}}^{(0)})] \\ & - (1/27)W_0 R^2 [20(W_K + \bar{W}) - 2[1 + (2\bar{\mu}_1 \gamma_1)/\bar{W}]] (A_{F_{101}}^{(1)}/A_{F_{101}}^{(0)}), \end{aligned} \quad (2-129)$$

$$\begin{aligned} A_2 = & -(2/3) [1 + (\bar{\mu}_1 \gamma_1)/\bar{W}] R(V_{F_{011}}^{(0)}/V_{F_{000}}^{(0)}) - (2/3)(W_K + \bar{W}) R\alpha Z \\ & \times [(V_{F_{000}}^{(1)}(1, 2, 2, 1)/V_{F_{000}}^{(0)}) - (V_{F_{000}}^{(1)}(1, 1, 1, 1)/3V_{F_{000}}^{(0)})] \\ & + (2/9)W_0 R^2 \{2(W_K + \bar{W}) - [1 + (\bar{\mu}_1 \gamma_1)/\bar{W}]\} (V_{F_{000}}^{(1)}/V_{F_{000}}^{(0)}), \end{aligned} \quad (2-130)$$

and $y = V_{F_{000}}^{(0)}/A_{F_{101}}^{(0)}$. Here, the energy \bar{W} and the Coulomb function $\bar{\mu}_1$ are averaged over the β^+ spectrum (Behrens and Jänecke, 1969); γ_1 stands for $[1 - (\alpha Z)^2]^{1/2}$.

Equations (2-128) to (2-130) also apply to other allowed EC/ β^+ ratios (L_1/β^+ , L_2/β^+ , M_1/β^+ , ...). In most mixed allowed transitions, the form-factor coefficient $V_{F_{000}}^{(0)}$ is isospin-forbidden,

and hence very small. Thus, we generally have $y \ll 1$ (Blin-Stoyle, 1973; Bertsch and Mekjian, 1972). Hence A_1 is the important correction term. The form-factor coefficient ratio $V_{F_{111}}^{(0)}/A_{F_{101}}^{(0)}$, relativistic over nonrelativistic, depends sensitively on the nuclear structure and is difficult to calculate. This ratio is of the order ~ 0.1 . The ratios $A_{F_{101}}^{(1)}(1,1,1,1)/A_{F_{101}}^{(0)}$, $A_{F_{101}}^{(1)}(1,2,2,1)/A_{F_{101}}^{(0)}$, and $A_{F_{101}}^{(1)}$ can however be estimated more easily. They generally lie in the range 0.5-2.0. Taking into account only the latter form-factor coefficient ratios leads to the estimate $A_1 \approx -0.03$ for $Z=80$.

(ii) A second cause for deviations of the EC/β^+ ratio from the prediction of Eq. (2-127) lies in electromagnetic radiative corrections to the electron-capture and β^+ decay rates, for example for the emission of internal bremsstrahlung. Radiative corrections for allowed β transitions, especially for the superallowed $0^+ \rightarrow 0^+$ transitions, have been discussed extensively (Marshak et al., 1969; Sirlin, 1967; Källen, 1967; Dicus and Norton, 1970; Beg et al., 1972; Jaus and Rasche, 1970; Jaus, 1972; Sirlin, 1974; Roos, 1974; Suzuki and Yokoo, 1975)

For allowed β transitions, the effect of radiative corrections can be described, first, by a renormalization of the vector and axial-vector coupling constants,

$$C_V \rightarrow C_V \left(1 + \frac{\alpha G}{4\pi}\right), \quad (2-131)$$

$$C_A \rightarrow C_A \left(1 + \frac{\alpha D}{4\pi}\right), \quad (2-132)$$

(Blin-Stoyle, 1973), and second, by a known modification of the β spectrum. This second point affects the integrated Fermi function:

$$f_{\beta^+} \rightarrow f_{\beta^+} \{1 + \delta_R(W, Z)\}. \quad (2-133)$$

In Eqs. (2-131) and (2-132), C and D are the so-called model-dependent radiative corrections; they depend on details of the weak and strong interaction theories (Sirlin, 1967; Källen, 1967;

Dicus and Norton, 1970; Beg et al., 1972; Sirlin, 1974; Roos, 1974; Wilkinson, 1975). These model-dependent radiative corrections cannot as yet be calculated without ambiguity, but they cancel in EC/ β^+ ratios. The model-independent radiative correction factor $[1 + \delta_R(W, Z)]$ is well-known to order α (Sirlin, 1967; Källen, 1967; Dicus and Norton, 1970). This correction factor can be found, for example, in the work of Wilkinson and Macefield (1970), where semianalytical formulae and nomograms are given. The terms of order $Z\alpha^2$ and $Z^2\alpha^3$ have also been calculated (Jaus and Räsche, 1970; Jaus, 1972). For electron capture this model-independent part of the radiative correction differs, however, from that discussed for β^+ decay. Unfortunately, no explicit calculation has been carried out as yet.

Some contrary statements notwithstanding (Vatai, 1971, 1972b; Eman et al., 1973), Behrens and Bühring (1974) have pointed out that the existence of second-class currents, i.e., of a finite value of f_T , does not significantly affect EC/ β^+ ratios. This fact follows in principle from the equality¹⁴

of the hadron parts, or of the form-factor coefficients, for electron capture and β^+ decay (Sec. 2.2.3).

2.4.3. Non-Unique Forbidden Transitions

The EC/β^+ ratios for non-unique forbidden transitions are proportional to an additional factor $C_x/\sqrt{C(W)}$. The quantity C_x is given by Eqs. (2-44), (2-105), and (2-106). The corresponding formulae for the shape factor $C(W)$ can, for example, be found in the papers by Behrens and Jänecke (1969) and in Behrens and Bühring (1971). These formulae show that the EC/β^+ ratios for non-unique forbidden transitions generally depend on the relative values of the nuclear form-factor coefficients, i.e., on the details of the nuclear structure.

There is one exception from this rule, however, in the case of non-unique first-forbidden transitions. When the ξ -approximation [Eq. (2-115)] is applicable, the EC/β^+ ratios from $k_x=1$ states are independent of the nuclear matrix elements, and have the same values as for allowed transitions. The applicability of the ξ -approximation can be tested experimentally by investigating the shape factor of the β^+ spectrum.

2.4.4. Unique Forbidden Transitions

For the $(L-1)^{st}$ unique forbidden transitions, explicit expressions for the ratios $C_x/\sqrt{C(W)}$ can be given. The formulae for C_x can be taken from Eq. (2-123), and for $C(W)$, for example, from the work of Behrens and Jänecke (1969). We find

$$\begin{aligned}
C_x/\overline{C(W)} &= \left\{ (2k_x - 1)! [2(L - k_x) + 1]! \right\}^{-1} \left[p_x^{2(k_x - 1)} q_x^{2(L - k_x)} \right] \\
&\times \left\{ \sum_{n=1}^L \overline{\left[\lambda_n p^{2(n-1)} q^{2(L-n)} \right]} \left[(2n-1)! [2(L-n) + 1]! \right]^{-1} \right\}^{-1}. \quad (2-134)
\end{aligned}$$

Here, λ_n is a special Coulomb function defined, for example, by Behrens and Jänecke (1969). As before, barred symbols denote quantities averaged over the β^+ spectrum.

For $K, L_1, L_2, M_1, M_2, \dots$ capture, Eq. (2-134) takes the simpler form

$$\begin{aligned}
C_x/\overline{C(W)} &= [(2L-1)!]^{-1} q_x^{2(L-1)} \\
&\times \left\{ \sum_{n=1}^L \overline{\left[\lambda_n p^{2(n-1)} q^{2(L-n)} \right]} \left[(2n-1)! [2(L-n) + 1]! \right]^{-1} \right\}^{-1}. \quad (2-135)
\end{aligned}$$

2.5. Atomic Matrix Elements: Exchange and Overlap Corrections

2.5.1. Introduction

According to the usual theory of allowed orbital electron capture (Sec. 2.3), the probability that a K electron is captured by the nucleus is

$$\lambda_K \propto G^2 q^2 \xi |\psi_K(0)|^2, \quad (2-136)$$

where G is the β -decay coupling constant, q is the energy of the neutrino that is emitted, ξ is the appropriate combination of nuclear matrix elements, and $|\psi_K(0)|^2$ is the square of the parent atom's 1s electron wave function at the nucleus. In Eq. (2-136), no atomic matrix elements are included.

Benoist-Gueutal (1950, 1953b) first suggested that atomic electrons must be included in a complete description of the nuclear electron-capture process. She estimated the effect of imperfect atomic overlap on the total electron capture rate of ${}^7\text{Be}$ by calculating the electron-capture probability for various final atomic states. Due to the lack of accurately known wave functions for excited Li atoms, Benoist-Gueutal only concluded that the decrease in the total decay rate was less than 30%. Odier and Daudel (1956) made a quantitative calculation of the ${}^{37}\text{Ar}$ L-to-K capture ratio, using wave functions for the entire atom. Odier and Daudel's prediction of 0.10 for the ${}^{37}\text{Ar}$ L-to-K capture ratio has subsequently been verified by experiment.

The discrepancy between the traditional theory of electron capture (Brysk and Rose, 1958) and experiments on L-to-K electron-capture ratios indicated that a critical examination of the theory was needed. Bahcall

(1962a, 1963a,b, 1965a) made a comprehensive study of the role of atomic electrons in the nuclear electron-capture process, emphasizing the importance of the indistinguishability of electrons and of the change in nuclear charge by one unit from initial to final atomic states, aspects which were neglected in the usual theory. In Bahcall's work, ground-state wave functions were used for the initial and final atoms. The importance of the presence of an inner-shell hole in the daughter atom was pointed out by Vatai (1968 b).

In this section, we consider the effect of atomic overlap and exchange corrections on the total electron-capture rate and on various subshell capture ratios. We also discuss the calculation of atomic matrix elements. This subject has recently been reviewed by Genz (1973 a) and Vatai (1973 c). The calculations of electron density at the nuclear surface are discussed in Sec. 2.2.

2.5.2. Effect of Atomic Overlap and Exchange on Total Capture Rates

Bahcall (1963a,b) used second quantization to formulate the nuclear electron-capture process. For allowed transitions, the probability per unit time that a nucleus will capture any of its atomic electrons and leave the daughter atom in the final state $|A'\rangle$ is

$$\lambda(A') = G^2 \xi (2\pi)^{-1} q^2(A') M^\dagger(A') (1 + \gamma_5) M(A'), \quad (2-137)$$

where

$$M(A') \equiv \langle A' | \phi_e(0) | G \rangle \quad (2-138)$$

and

$$q(A') = W_0 + 1 + [E(G) - E(A') - 1]. \quad (2-139)$$

Here, W_0 is the difference between initial and final nuclear masses; $E(G)$ and $E(A')$ are the total energies of the initial and final atomic electrons, including their rest masses.

If one uses a single-particle representation of $|G\rangle$, the total electron-capture rate can be written

$$\lambda \cong \lambda^0 \left[1 + \frac{\lambda'}{\lambda^0} + \frac{\Delta\lambda}{\lambda^0} \right], \quad (2-140)$$

where

$$\lambda^0 \equiv G^2 \xi (2\pi)^{-1} \sum_b q^2(b') |\phi_b(0)|^2 \quad (2-141)$$

is the usual total electron capture rate. We have

$$\begin{aligned} \lambda' &\equiv G^2 \xi \pi^{-1} q(ls') \sum_b |\phi_b(0)|^2 [-\epsilon(ls') + \epsilon(b')] \\ &+ \sum_{A'} \Delta q(A') \langle G | a_b^\dagger | A' \rangle \langle A' | a_b | G \rangle, \end{aligned} \quad (2-142)$$

and

$$\begin{aligned} \Delta\lambda &= q(ls') G^2 \xi \pi^{-1} \sum_{b_1, b_2, A'} \phi_{b_1}^\dagger(0) \phi_{b_2}(0) \Delta q(A') \\ &\times \langle G | a_{b_1}^\dagger | A' \rangle \langle A' | a_{b_2} | G \rangle, \end{aligned} \quad (2-143)$$

and

$$q(ls') \equiv W_0 + E(G) - E(G') - \epsilon(ls'), \quad (2-144)$$

and

$$\Delta q(A') = E(G') - E(A') + \epsilon(ls'), \quad (2-145)$$

where $\epsilon(ls')$ is the K binding energy in the final atom.

The second and third terms in Eq. (2-140) are the contributions due to imperfect atomic overlap and exchange capture, respectively. By applying closure to sum the electron-capture probability over all possible final atomic states, Bahcall found

$$\frac{\lambda'}{\lambda^0} \approx \frac{1}{q(ls')} \frac{\partial^2 E(G)}{\partial Z^2} \quad (2-146)$$

and

$$\frac{\Delta\lambda}{\lambda} \approx \frac{4}{q(ls')} \frac{R_{2s}(0)}{R_{1s}(0)} \left[\left(\frac{1}{r} \right)_{2s,1s} + \sum_{b'} \langle b' 2s | \frac{1}{r_{12}} | b' 1s \rangle \right]. \quad (2-147)$$

The contributions of overlap and exchange are of the opposite sign. They partially cancel each other in the total capture rate. The net effect on the total capture probability does not exceed a few percent if $q(ls')$ is greater than, or of the order of, 50 keV.

2.5.3. Overlap and Exchange Corrections on Capture Ratios

The electron-capture rate, including the atomic matrix element in the theory, can be written

$$\lambda_i = \lambda_i^0 B_i, \quad i = K, L, M, N, \dots, \quad (2-148)$$

where λ_i is the transition rate from the usual theory and B_i is the exchange-correction factor introduced by Bahcall to take account of the exchange and overlap contribution.

For allowed transitions, the L/K capture ratio can then be written

$$\frac{\lambda_L}{\lambda_K} = \left(\frac{\lambda_{L1}^0}{\lambda_K^0} \right) \frac{B_{L1}}{B_K} \left[1 + \left(\frac{\lambda_{L2}^0}{\lambda_{L1}^0} \right) \frac{B_{L2}}{B_{L1}} \right]. \quad (2-149)$$

For unique forbidden transitions, the L/K ratio becomes

$$\frac{\lambda_L}{\lambda_K} = \left(\frac{\lambda_{L1}^0}{\lambda_K^0} \right)_{\Delta J} \frac{B_{L1}}{B_K} \left[1 + \left(\frac{\lambda_{L2}^0}{\lambda_{L1}^0} \right) \frac{B_{L2}}{B_{L1}} + \frac{3(\Delta J-1)(2\Delta J-1)}{(g_{L1} R_0)^2} \frac{g_{L3}^2}{g_{L1}^2} \frac{B_{L3}}{B_{L1}} \right], \quad (2-150)$$

where

$$\left(\frac{\lambda_i}{\lambda_j}\right)^0 = \frac{g_i^2 q_i^2}{g_j^2 q_j^2} \quad (2-151)$$

$$\left(\frac{\lambda_{L_1}}{\lambda_K}\right)_{\Delta J}^0 = \frac{g_{L_1}^2}{g_K^2} \left(\frac{q_{L_1}^2}{q_K^2}\right)^{\Delta J} \quad (2-152)$$

The q 's are neutrino energies and the g 's, charge densities at the nuclear surface.

In Eqs. (2-149) and (2-150), the difference in binding energy among the L subshells has been neglected.

A similar expression applies for M/L capture ratios:

$$\frac{\lambda_M}{\lambda_L} = \left(\frac{\lambda_{M_1}}{\lambda_{L_1}}\right)^0 \frac{B_{M_1}}{B_{L_1}} \left[1 + \left(\frac{\lambda_{M_2}}{\lambda_{M_1}}\right)^0 \frac{B_{M_2}}{B_{M_1}} - \left(\frac{\lambda_{L_2}}{\lambda_{L_1}}\right)^0 \frac{B_{L_2}}{B_{L_1}} \right] \quad (2-153)$$

Most theoretical and experimental work has been done on K, L and M capture for allowed transitions. Little research has been performed on N capture. We proceed to review various theoretical calculations dealing with the overlap and exchange corrections.

Bahcall's approach. In order to overcome the difficulty of calculating and summing an infinite number of separate contributions from the final atomic states, Bahcall (1962a, 1963a, b, 1965a) used the following approximations: (1) The innermost electrons are almost inert. (2) The outer-electron states (outside the 3s shell) form a practically complete set. (3) The energy available for a given nuclear transition is nearly independent of the particular states occupied by the outer electrons in the final atom.

Bahcall separated the atomic state vectors into two independent parts,

$$|\text{atomic}\rangle = |\text{inner}\rangle \times |\text{outer}\rangle. \quad (2-154)$$

He then invoked closure to perform the sum over the infinite number of final atomic states, obtaining

$$\lambda_i = \lambda_i^0 B_i, \quad (2-155)$$

where λ_i^0 is the usual electron-capture rate, and we have

$$B_i = \left| \frac{f_i}{\psi_i(0)} \right|^2. \quad (2-156)$$

The capture amplitudes are

$$\begin{aligned} f(3s') &= \langle 1s' | 1s \rangle \langle 2s' | 2s \rangle \psi_{3s}(0) - \langle 1s' | 3s \rangle \langle 2s' | 2s \rangle \psi_{1s}(0) \\ &\quad - \langle 2s' | 3s \rangle \langle 1s' | 1s \rangle \psi_{2s}(0); \end{aligned} \quad (2-157)$$

$$\begin{aligned} f(2s') &= \langle 1s' | 1s \rangle \langle 3s' | 3s \rangle \psi_{2s}(0) - \langle 1s' | 2s \rangle \langle 3s' | 3s \rangle \psi_{1s}(0) \\ &\quad - \langle 3s' | 2s \rangle \langle 1s' | 1s \rangle \psi_{3s}(0); \end{aligned} \quad (2-158)$$

$$\begin{aligned} f(1s') &= \langle 2s' | 2s \rangle \langle 3s' | 3s \rangle \psi_{1s}(0) - \langle 2s' | 1s \rangle \langle 3s' | 3s \rangle \psi_{2s}(0) \\ &\quad - \langle 3s' | 1s \rangle \langle 2s' | 2s \rangle \psi_{3s}(0). \end{aligned} \quad (2-159)$$

The primed orbitals pertain to the daughter atom.

The L_1 -to-K and M_1 -to- L_1 capture ratios can be written

$$\frac{\lambda_{L_1}}{\lambda_K} = \left(\frac{\lambda_{L_1}}{\lambda_K} \right)^0 \frac{B_{L_1}}{B_K} = \left(\frac{\lambda_{L_1}}{\lambda_K} \right)^0 \times^{L_1/K} \quad (2-160)$$

and

$$\frac{\lambda_{M_1}}{\lambda_{L_1}} = \left(\frac{\lambda_{M_1}}{\lambda_{L_1}} \right)^0 \frac{B_{M_1}}{B_{L_1}} = \left(\frac{\lambda_{M_1}}{\lambda_{L_1}} \right)^0 \times^{M_1/L_1}, \quad (2-161)$$

where the exchange correction factors are

$$X_{L_1/K} = \frac{B_{L_1}}{B_K} = \left| \frac{f(2s')\psi_{1s}(0)}{f(1s')\psi_{2s}(0)} \right|^2 \quad (2-162)$$

$$X_{M_1/L_1} = \frac{B_{M_1}}{B_{L_1}} = \left| \frac{f(3s')\psi_{2s}(0)}{f(2s')\psi_{3s}(0)} \right|^2 \quad (2-163)$$

To compare these calculated capture ratios with measurements, correction must be made for capture from $p_{1/2}$ states.

To calculate the atomic matrix elements $\langle ns' | ns \rangle$, Bahcall used nonrelativistic Hartree-Fock ground-state wave functions for parent and daughter atoms. (Watson, 1960; Watson and Freeman, 1961b).

The following comments can be made on Bahcall's theory:

(1) The assumption that the neutrino energy is independent of final states of the atom, and the use of the closure approximation without correction for occupied states, tend to lead toward underestimation of the overlap correction.

(2) The overlap correction is small for K and L_1 capture, but is much larger for M_1 capture. Therefore, Bahcall's approach will overestimate the M_1 -to- L_1 capture ratio correction factor X_{M_1/L_1} .

(3) Multiple exchange processes and the exchange between inner and outer electrons are neglected.

(4) The effect of the inner-shell vacancy in the daughter atom is neglected.

1973b)

Vatai's ansatz. Vatai (1968b, 1970a) calculated the capture transition to the most prominent state $|A\rangle$ of the final atom. In state $|A\rangle$,

except for the captured electron, all the other electrons retain their quantum numbers. Vatai obtained the exchange and overlap correction coefficients as

$$B_i = \left| \frac{f_i}{\psi_i(0)} \right|^2 \quad (2-164)$$

and

$$\begin{aligned} f_K &= \psi_{1s}(0) \langle 2s' | 2s \rangle \langle 2p' | 2p \rangle \langle 3s' | 3s \rangle \dots \\ &\quad - \psi_{2s}(0) \langle 2s' | 1s \rangle \langle 2p' | 2p \rangle \langle 3s' | 3s \rangle \dots \\ &\quad - \psi_{3s}(0) \langle 3s' | 1s \rangle \langle 2s' | 2s \rangle \langle 2p' | 2p \rangle \dots \end{aligned} \quad (2-165)$$

Similar expressions for f_L and f_M are obtained by exchange of 1s with 2s and 1s with 3s, respectively, in the f_K expression. If overlap corrections for p and d electrons are neglected, one obtains the same f_i expressions as those of Bahcall [Eqs. (2-157) to (2-159)].

In Vatai's calculation, the effect of the inner hole in the daughter atom on the exchange integral is estimated by perturbation theory.

Vatai used the analytic Hartree-Fock wave functions of Watson and Freeman (1961b) for the initial state and as unperturbed wave functions for the final-state calculation. He estimated the overlap correction for the inner p and d electrons including the multiplicity by calculating the overlap integral with the wave functions of Watson and Freeman for both parent and daughter atoms. The overlap integrals of outer electrons are set equal to 1 in Vatai's calculation.

With regard to Vatai's approach, we note the following points:

(1) Some contributions due to processes involving shakeup or shakeoff are neglected.

(2) The use of perturbation theory to calculate the exchange integrals introduces a discrepancy of 10-40% in the value of these integrals compared with Froese's HF calculations (Faessler et al., 1970).

(3) The overlap corrections are only rough estimates.

(4) Vatai, like Bahcall, neglects multiple exchange processes.

Faessler's calculation. Faessler et al. (1970) recalculated the Bahcall exchange corrections, taking into account the inner-shell vacancy that after electron capture exists in the daughter atom. Faessler et al. used the Herman-Skillman (1963) Hartree-Fock-Slater and Froese-Fischer (1965, 1969) Hartree-Fock programs to calculate hole-state wave functions and exchange and overlap integrals. Although some of the exchange integrals calculated with the two programs differ by as much as 50%, the exchange correction factors agree to within 3%. This indicates that the exchange correction, being a ratio, is insensitive to the model wave functions, due to cancellation of errors. Faessler et al. concluded that the influence of rearrangement effects on the L/K and M/L capture ratios is far too small to account for the discrepancy between theory and experiment, although it does affect the theoretical capture ratios in the right direction.

Relativistic calculations. Suslov (1970a) followed Bahcall's approach and used relativistic Hartree-Fock-Slater wave functions to

calculate the exchange and overlap corrections for $14 \leq Z \leq 98$. The wave functions were obtained by numerical integration of Dirac's equation, using a nonrelativistic potential (Herman and Skillman, 1963) for $14 \leq Z \leq 73$, and an analogous relativistic potential (Lieberman *et al.*, 1965) for $Z \geq 74$. Finite nuclear size was included through the uniformly-charged-sphere model. For $15 \leq Z \leq 37$, the new relativistic values of B_K , B_{L_1} , B_{M_1} , $X^{L/K}$, and X^{M/L_1} are quite close to Bahcall's (1963a, b) results; the differences do not exceed 5%. For $Z \geq 38$, the exchange correction decreases as Z increases, and for large Z it is nearly constant. The relativistic exchange-corrected capture ratios do not narrow the gap between theory and experiment.

Martin and Blichert-Toft (1970) performed another relativistic calculation of electron-capture ratios for $6 \leq Z \leq 98$ using the same approach as Vatai's. The required wave functions and electron radial densities were calculated with a relativistic Hartree-Slater program with finite nuclear size. The K and L_1 electron radial density at the nuclear surface, calculated by Martin and Blichert-Toft (1970), agrees with other calculations (Zyryanova and Suslov, 1968; Behrens and Jänecke, 1969; Winter, 1968; Suslov, 1970a) within 1%, and the exchange-overlap factors agree very well with the present results based on Vatai's approach.

2.5.4. Evaluation of Atomic Matrix Elements.

Atomic matrix elements $\langle ms' | ns \rangle$ are not only required for the calculation of exchange and overlap corrections, but also for determining autoionization rates in β -decay and electron-capture transitions, and for shake-up calculations (Sec. 5). The degree of orthogonality of the wave functions is the important point in the evaluation of the overlap integrals $\langle ms' | ns \rangle$. Overlap integrals that involve ground-state wave functions from parent to daughter atoms are not very sensitive to the choice of the atomic potential, because the inner shells are closed shells. Overlap integrals calculated with the analytic Hartree-Fock wave functions of Watson and Freeman, with Herman-Skillman Hartree-Fock-Slater wave functions, or with Froese-Fischer Hartree-Fock wave functions, all agree to better than 5% (Faessler *et al.*, 1970). However, for calculations of inner-shell vacancy states (e.g., 1s and 2s hole states), the atomic model is important, as the hole-state wave functions are sensitive to the potential. In the Herman-and-Skillman (1963) code, single electronic configurations having open shells are treated on the same basis as configurations having only closed shells. Consequently, the wave function of an electron in an open shell is not necessarily orthogonal to a single-electron wave function that describes an electron of the same symmetry species and in the same configuration, but from a closed shell. For example, the 1s electron wave function for an atom

with a K vacancy may not be orthogonal to the 2s wave function of the atom, if it has a full L_1 subshell. The overlap integrals between open-shell and closed-shell single-electron wave functions, involving the ground state of the parent atom and a deep hole state of the daughter, can therefore contain a sizable error if it is computed with Herman-Skillman wave functions (Faessler *et al.*, 1970).

In Froese-Fischer's (1965, 1969) and Bagus' (1964, 1965) approaches, the orthogonality between self-consistent field orbital wave functions with the same symmetry is taken into account by introducing off-diagonal Lagrangian multipliers into the Hartree-Fock equations. For closed shells, a unitary transformation can be found between the occupied orbitals, such that the Lagrangian multipliers are in diagonal form. The additional requirement that the off-diagonal Lagrangian multipliers be zero serves as a unique definition of the self-consistent field orbitals. For open-shell systems, it is not possible to reduce the Lagrangian multipliers that couple open and closed shells of the same symmetry to zero (Roothaan, 1960; Roothaan and Bagus, 1963).

The Ne-like and Ar-like ns hole states have been calculated by Bagus (1964, 1965). The off-diagonal Lagrangian multipliers between open and closed shells $\theta_{ns,ms}$, are large for 1s hole states and become smaller for 3s hole states. The effect of including the off-diagonal Lagrangian multipliers for Ar-like ions is that the 1s orbitals of the 1s-hole states have a node; an extended tail appears in the 1s wave functions (Bagus, 1964). For large r, $P_{1s}(r)$ becomes

$$P_{1s}(r) \approx -\frac{\theta_{2s,1s}}{\epsilon_{1s}} P_{2s}(r) - \frac{\theta_{3s,1s}}{\epsilon_{1s}} P_{3s}(r). \quad (2-166)$$

The features introduced by the off-diagonal Lagrangian multipliers in the Froese-Fischer Hartree-Fock hole-state wave functions explain the differences between overlap integrals obtained by using Herman-Skillman and Froese-Fischer wave functions in the work of Faessler et al. (1970).

To resolve the discrepancy between the overlap matrix elements $\langle n'l|nl \rangle$ of Faessler et al. and of Vatai, we have recalculated these matrix elements for Ar K-, L-, and M-capture with Bagus' accurate analytic Hartree-Fock Ar ground-state and Cl⁻ ns hole-state wave functions (Bagus, 1964). Our results from Bagus' wave functions agree with the overlap matrix elements calculated by Faessler et al. (1970) with the Hartree-Fock program of Froese-Fischer to better than 1%.

2.5.5. Comparison Among Theoretical Exchange Corrections to Capture Ratios

In Sec. 2.5.4, we have described evidence that the Hartree-Fock program of Froese-Fischer is best suited for the evaluation of the exchange and overlap integrals. We have therefore recalculated the exchange correction factors using the Froese-Fischer program (Froese-Fischer, 1972a) and have included the effect of the ns hole present in the daughter atom. Two sets of values were computed, one based on Bahcall's approach, the other following Vatai's ansatz that includes the overlap correction for both inner and outer electrons (Table 2.11). The results computed by various workers according to Bahcall's approach (Faessler et al., 1970; Suslov, 1970a; Bahcall, 1963a,b, 1965a, and our (Table 2.12). present calculations) agree very well (within 5%) \wedge The results of

Martin and Blichert-Toft (1970) coincide with our present calculations based on Vatai's approach. In Figs. 2-2 and 2-3, the exchange correction factors $X_{L_1/K}^{L_1/K}$ and $X_{L_1/L_1}^{M_1/L_1}$ are shown, as recalculated by us with the Froese-Fischer (1972a) code. For comparison, the results from the two relativistic calculations (Suslov, 1970a; Martin and Blichert-Toft, 1970) are also included. In general, the results from Vatai's approach are smaller than those following Bahcall's theory.

2.5.6. Correlation Effects in Electron-Capture Ratios

All theoretical work reviewed in Sec. 2.5.3 contains the independent-particle approximation. Effects due to electron correlations are neglected.

Goverse and Blok (1974c) have observed that the experimental L/K capture ratios seem to oscillate about the theoretical curve, and suggested that correlation effects between the orbital electrons might cause this discrepancy. This assertion remains to be proven.

2.5.7. Conclusion

The exchange and overlap correction factors are not very sensitive to the choice of the atomic potential, due to compensation between the electron density at the nucleus and the atomic matrix element $\langle ns | ms' \rangle$. The importance of including an appropriate inner-shell hole in the daughter atom after electron capture, stressed by Vatai (1968b, 1970a), is not borne out by the work of Faessler *et al.* (1970) nor by our present calculations, if Bahcall's approach is followed. On the other hand, the presence of the inner hole has a significant effect on these correction factors if they are calculated with Vatai's formulae.

The effect of exchange on electron-capture ratios has been treated in a similar way in the two existing theories, those of Bahcall (1963a,b, 1965a) and Vatai (1970), while the overlap corrections are treated differently. Because the overlap corrections are important for low-Z elements, the difference in exchange and overlap correction factors between Bahcall's and Vatai's approaches shows up clearly in light atoms.

Our recalculated correction factors permit a direct comparison of results based on Bahcall's and Vatai's approaches. Vatai's formulation causes an underestimation of L/K capture ratios at low-Z, but leads to M/L capture ratios in fair agreement with experiment. On the other hand, Bahcall's approach yields better agreement to L/K ratios with experiment, but overestimates the M/L capture ratios.

To solve this problem, a new calculation is needed in which overlap corrections are treated more carefully. Electron correlation must be included, at least by means of configuration interactions. More accurate experimental capture ratios in the low-Z region are needed to provide a better test of theory.

3. EXPERIMENTAL METHODS AND RESULTS

The experimental determination of nuclear electron-capture ratios from various atomic shells and of K-capture to positron-emission (K/β^+) ratios has been the subject of considerable effort because of the importance of these quantities in various contexts. Aspects of orbital electron capture have been reviewed by Robinson and Fink (1955, 1960), Bouchez and Depommier (1960, 1965), Depommier (1968), Fink (1965; 1966, 1968; 1969), Berényi (1963a, 1965a, 1968a), Genz (1971b, 1973a), and Fitzpatrick (1973). In recent years, several new measurements of L/K, M/L and K/β^+ ratios have been performed and much effort has been devoted to reducing experimental uncertainties, so that comparisons can be made with different theoretical calculations of atomic wave functions and of electron exchange and imperfect atomic wave-function overlap effects.

In this section we classify the methods employed to determine capture ratios and compare their potential reliability. From the vast body of experimental data reported in the literature, we select a limited list of capture and K/β^+ ratios that can be considered highly reliable and use these values for comparison with theory.

Relative transition probabilities are commonly used in experimental work; these are related as follows to the transition probabilities per unit time as defined in Eqs. (2-27), (2-28) and (2-43):

$$P_{EC} = \frac{\lambda_c}{\lambda_{tot}}, \quad P_{\beta^+} = \frac{\lambda_{\beta^+}}{\lambda_{tot}}, \quad P_{\beta^-} = \frac{\lambda_{\beta^-}}{\lambda_{tot}}, \quad (3-1)$$

where

$$P_{EC} + P_{\beta^+} + P_{\beta^-} = 1, \quad (3-2)$$

and

$$P_K = \frac{\lambda_K}{\lambda_C}, \quad P_L = \frac{\lambda_L}{\lambda_C}, \quad P_M = \frac{\lambda_M}{\lambda_C}, \quad \dots \quad (3-3)$$

where

$$P_K + P_L + P_M + \dots = 1. \quad (3-4)$$

Corresponding relations hold for capture from subshells.

The probability of orbital electron capture from the K shell or from any of the L or M subshells depends upon the nature and energy of the transition. The capture process cannot be detected directly because of the extremely low interaction probability of the emitted neutrino. The capture rate can therefore only be determined from the intensity of subsequently emitted radiation, such as x rays or Auger electrons given off during reorganization of the electronic cloud after capture and γ rays or conversion electrons from the daughter nucleus. In principle, the recoil of the final nucleus can also be measured, but the recoil kinetic energy is always very small. The largest recoil (57 eV) occurs in the transition ${}^7\text{Be} \rightarrow {}^7\text{Li}$.

Methods for measuring capture probabilities vary according to the decay scheme of the radionuclide, the energy and relative intensity of the emitted radiation, available detectors, and requirements for necessary corrections. The methods can be classified according to the information they provide.

One group of methods yields ratios of capture probabilities from

different shells,

$$\frac{P_L}{P_K} = \frac{\lambda_L}{\lambda_K}, \quad \frac{P_M}{P_L} = \frac{\lambda_M}{\lambda_L} \quad (3-5)$$

From these ratios, a consistent set of capture probabilities can be deduced with the aid of Eq. (3-4):

$$P_K = \left\{ 1 + \frac{P_L}{P_K} \left[1 + \frac{P_M}{P_L} \left(1 + \frac{P_N}{P_M} \right) \right] \right\}^{-1},$$

$$P_L = P_K \left(\frac{P_L}{P_K} \right), \quad (3-6)$$

$$P_M = P_L \left(\frac{P_M}{P_L} \right).$$

Equations (3-6) can also be used with reliable theoretical capture ratios.

Some methods pertain to situations in which the L and M x-ray or Auger-electron peaks cannot be resolved. Such methods lead to the determination of a capture ratio $P_{LM...}/P_K$, from which the relative K-capture probability can be obtained directly:

$$\frac{P_{LM...}}{P_K} = \frac{1}{P_K} - 1. \quad (3-7)$$

In several other methods, $P_K \omega_K$ is determined, where ω_K is the K-shell fluorescence yield. With the appropriate value for ω_K (Bambynek *et al.*, 1972), the relative K-capture probability can be calculated.

If the transition energy exceeds twice the electron rest energy ($2mc^2$), then positron emission is possible as an alternative nuclear

decay process. In such cases, it is of interest to measure ratios of K-capture to positron-emission probability or of the total electron-capture to positron-emission rate,

$$\frac{P_K}{P_{\beta^+}} = \frac{\lambda_K}{\lambda_{\beta^+}}, \quad \frac{P_{EC}}{P_{\beta^+}} = \frac{\lambda_c}{\lambda_{\beta^+}}. \quad (3-8)$$

Table 3.1 contains a compilation of methods reported in the literature; these are discussed in Secs. 3.1, 3.2, and 3.4. The usual corrections for background, dead time, detector efficiency, etc., are taken for granted.

3.1. Determination of Capture Ratios

Capture ratios have been determined both with external and internal sources. In general, it is difficult to measure capture ratios with external sources, because large corrections are required for source self-absorption, air scattering, window absorption, and fluorescence yields. During the last few years, capture ratios have therefore more frequently been measured by internal-source techniques in which these difficulties are avoided, provided the radioactive atoms can be dispersed throughout the sensitive volume of the counter. Internal-source methods fall into two major classes: at low atomic numbers, gaseous compounds are mixed with the counting gas of a proportional counter, while at high Z crystal scintillators are preferred that have the radioactive atoms built into the lattice, thus minimizing distortions due to escape of x rays from the sensitive counter volume.

1.1. Spectrometry with Internal Gas Sources

A radioactive gas or the vapor of a radioactive metal-organic compound is added to the counting gas of a proportional counter. The prompt cascade of x rays and Auger electrons, which follows the capture event, is integrated by the detector to produce a single K peak at the K-electron binding energy of the daughter atom. Similarly, L, M, ... peaks are produced by events from higher shells. It is usually assumed that all L and M x rays and Auger electrons are completely absorbed inside the counter. However, as Vatai (1968d, 1970b) has pointed out, the escape of L x rays is not always negligible a priori, and becomes especially important if the L x-ray energy lies just below the K-shell binding energy of the counter gas. The L peak contains a contribution from K-capture events which arises from K x rays that escape from the sensitive volume of the counter.

Typical K, L, and M peaks from an internal ^{71}Ge source are shown in Fig. 3-1. From the measured intensities I_K , I_L , I_M of these peaks, the ratio of capture probabilities can be deduced:

$$\frac{P_L}{P_K} = \frac{I_L}{I_K} [1 - \omega_K (k_{\alpha} P_{K\alpha} + k_{\beta} P_{K\beta})] - \omega_K k_{\alpha} P_{K\alpha} \quad (3-9)$$

$$\frac{P_M}{P_L} = \frac{I_M}{I_L} \left[1 + \frac{P_K}{P_L} \omega_K P_{K\alpha} k_{\alpha} \right] - \frac{P_K}{P_L} \omega_K P_{K\beta} k_{\beta} - P_{K\alpha} \omega_L \left[1 + \frac{P_K}{P_L} \omega_K P_{K\alpha} k_{\alpha} \right] \quad (3-10)$$

Here, ω_K and ω_L are the K- and L-shell fluorescence yields of the daughter atom; and k_α , k_β , and l_α the fractions of $K\alpha$, $K\beta'$, and $L\alpha$ x rays in the K and L series. The K and L x-ray escape probabilities from the detector sensitive volume are denoted by $P_{K\alpha}$, $P_{K\beta}$ and $P_{L\alpha}$.

There are two limiting cases. The first of these is Method 1 of Table 3.1, in which escape of x rays from the counter volume is avoided. Then Eqs. (3-9) and (3-10) have the simple form

$$\frac{P_L}{P_K} = \frac{I_L}{I_K}; \quad \frac{P_M}{P_L} = \frac{I_M}{I_L}. \quad (3-11)$$

Absence of x-ray escape can be realized approximately when the counter is operated at high pressure. Gas fillings of argon-propane and argon-methane mixtures at up to 22 atm have been used. Since the development of the wall-less multiwire proportional counter (Drever *et al.*, 1957a, 1957b), this type of detector has been employed successfully by various groups. The principal advantage of such a multiwire counter is that escape can be made very small. A central counter is surrounded by a ring of additional counters (Fig. 3-2). An inner circle of wires serves as the cathode for the central counter. Alternate wires in an outer circle serve as anodes and cathodes of a set of ring counters. The sensitive volume of the detector is then separated into two parts. The main central counter and the ring counters are operated in anticoincidence.

A block diagram of electronics for the operation of a multiwire proportional counter is shown in Fig. 3-3. Negative high voltage is often applied to the outer case of the counter and to the field tubes.

This approach is superior to grounding the cathode and using positive high voltage on the center wire, with a large potential difference across the coupling capacitor between center wire and the first preamplifier stage, leading to problems of leakage and spurious discharge.

For the determination of L/K ratios at $Z < 20$ and M/L ratios at $Z < 40$ it is necessary to detect Auger electrons and soft x rays below 500 eV, down to a few eV. Most recent advances in low-energy proportional-counter technique are related to the electronic system (Dougan et al., 1962a; Renier et al., 1968; Genz et al., 1971a). Proportional-counter spectrometry of radiation below ~ 500 eV is affected by certain problems that are less important or negligible at higher energies: (1) After-pulses from primary ionizing events can occur (Dougan et al., 1962a; Renier et al., 1968; Genz et al., 1971a; Campion, 1968, 1973); (2) degradation tails from peaks of higher energy can appear (Renier et al., 1968; Genz et al., 1971a; Heuer, 1966; Vaninbroukx and Spornol, 1965; Spornol, 1967); (3) small pulses can be mutually induced between ring and center counters in multiwire detectors (Genz et al., 1971a; Drever et al., 1957); (4) the anticoincidence gate may cause front- and back-edge clipping of large pulses, producing smaller pulses (Dougan et al., 1962a; Renier et al., 1968; Genz et al., 1971a); (5) large deadtime may arise when radiation of higher energy is present in high intensity (Dougan et al., 1962a; Renier et al., 1968; Genz et al., 1971a). The electronic system shown in Fig. 3-3 is designed to overcome these problems, except for long deadtime and degradation tails.

The shape of the spectrum produced by events between a few and 500 eV

depends on the initial number of ion pairs. The energy required to produce an ion pair in an argon-propane mixture is ~ 27 eV. Peaks produced by several ion pairs can be satisfactorily fitted with a Poisson distribution (Campbell and Ledingham, 1966), while the spectrum due to single-electron events cannot be represented accurately by an exponential or quasi-exponential function, as it varies with gas multiplication (Gold and Bennet, 1966; Genz, 1968, 1973b).

Corrections for several effects must be applied. (1) Escape probabilities $P_{K\alpha}$ and $P_{K\beta}$ of $K\alpha$ and $K\beta$ x rays from the sensitive volume of the counter must be accounted for. These escape probabilities can be separated into the additive probabilities P_1 , that a K x ray escapes from the central counter through the ends, P_2 , that a K x ray escapes from the central counter and hits a cathode wire, and P_3 , that an x ray escapes from the central counter and passes through a ring counter without being detected. All these corrections can be kept below 1%. A careful study of the escape probability in multiwire counters has been made by Vatai (1970b). (2) An important correction must be made for degraded L and K events in the energy region below the peaks. The total contribution from such events can be determined by extrapolation parallel to the energy axis to low energy, as has been demonstrated down to 80 eV (Genz *et al.*, 1971a). The degradation correction can amount to several percent but has not been taken into account in many investigations. This leads to appreciable differences in results (Heuer, 1966; Totzek and Hoffmann, 1967; Genz *et al.*, 1971a; Pengra *et al.*, 1972). (3) Condensation of radioactive metal-organic

vapor on the counter wall can lead to an increase in background. (4)
 Values of the fluorescence yield ω_K and of the $K\alpha/K\beta'$ x-ray intensity ratios can usually be taken from literature. The largest source of error in this method arises from the uncertainty in the I_L/I_K or I_M/I_L intensity ratio. In the determination of M/L capture ratios, errors in P_L/P_K largely cancel [see Eq. (3-10)]. Uncertainties in k_α and k_β have been greatly reduced since the new calculations of Scofield (1974) became available, which agree very well with experiment (Scofield, 1975).

If transitions take place to several levels in the daughter nucleus, then only mean capture ratios are measured. Several of the most reliable mean ratios have been measured by internal gas-source spectrometry. In the use of nuclides that decay by electron capture to a level that is deexcited by a γ transition, coincidences can be measured between K and L events detected in a multiwire counter and γ rays detected with NaI(Tl) scintillators surrounding the proportional counter. The capture ratio for transitions to the excited state can be deduced from the measured intensities $I_{L-\gamma}$ and $I_{K-\gamma}$ of L and K events gated by the γ rays. Equation (3-9) applies, with I_L and I_K replaced by $I_{L-\gamma}$ and $I_{K-\gamma}$. An analogous procedure can be employed in M/L-ratio measurements. In addition to the corrections already mentioned, accidental and sum coincidences must be taken into account.

In the second limiting case of internal gas spectrometry (Method 2 of Table 3.1), all K x rays are allowed to escape from the sensitive volume of the counter. Then we have $P_{K\alpha}=1$ and $P_{K\beta}=1$, Eq. (3-9) yields

$$\frac{P_L}{P_K} = \frac{I_L}{I_K} (1 - \omega_K) - \omega_K k_\alpha, \quad (3-12)$$

and Eq. (3-10) becomes

$$\frac{P_M}{P_L} = \frac{I_M}{I_L} \left[1 + \frac{P_K}{P_L} \omega_K k_\alpha \right] - \frac{P_K}{P_L} \omega_K k_\beta \quad (3-13)$$

Here, L x-ray escape is considered negligible. Experimentally, total K x-ray escape has been approximated with single-wire proportional counters filled with a low-Z gas at low pressure (Pontecorvo et al., 1949; Langevin, 1954^b, 1955, 1956; Langevin and Radvanyi, 1954^a, 1955; Radvanyi, 1955a; Scobie, 1957^a; Kiser and Johnston, 1959). Corrections are needed to account for (1) non-escape of K x rays, (2) escape of L x rays, (3) wall and end effects, (4) the fluorescence yield ω_K , and (5) the fraction k_α of $K\alpha$ x rays in the total x-ray group. Additional uncertainties may arise from separation of the K and L peaks and from their degradation tails.

With single-wire proportional counters containing a gaseous radioactive source mixed with the counter gas, reliable measurements are no longer limited to events with energies above ~ 200 eV. Recent advances in single-wire proportional-counter techniques (No. 3 in Table 3.1) have extended the sensitivity of precision measurements to make possible the detection of single- and few-electron events down to essentially zero energy, even in the presence of intense more energetic radiation (Fink, 1968; Genz, 1968, 1973a). These improvements were attained with more sophisticated low-noise electronics and through an understanding of the degradation spectrum (Genz et al., 1971a) and of after-pulses (Genz et al., 1968). Single- and few-electron peaks have been resolved on the basis of their spectral shape (Renier et al., 1968) or by fitting

a Poisson distribution (Genz et al., 1971a, 1972; Pengra et al., 1972). The techniques of single-electron spectrometry have been applied by Renier et al. (1968) in a precision measurement of the M/L capture ratio of ^{37}Ar . In this case, the peak due to capture of L-shell electrons has a mean energy of 280 eV, and the M spectrum is a single-electron peak because the energy released in a capture event (~ 5 eV) is lower than that required to produce an ion pair (~ 26.5 eV in argon-propane). The spectrum due to single electrons was determined experimentally by introducing ultraviolet photons into the counter to produce photoelectrons of only a few eV. This experimentally determined single-electron spectrum was fitted in the M region (Fig. 3-4) of the composite M and L spectrum (Fig. 3-5) and extrapolated to zero energy. The small afterpulses which may follow a primary event in the counter gas were kept from entering the analyzer by introducing an electronic paralysis time of up to 3.8 ms following each primary pulse. A block diagram of the electronic circuit is shown in Fig. 3-6.

The principal errors in this method arise from fitting the single-electron spectrum to the M-peak shape and from establishing the zero-energy calibration of the analyzer. The spectrum must be corrected for background and degradation tails. The ratio P_M/P_L is a very sensitive function of k_α , but it is rather insensitive to ω_K [Eq. (3-13)].

Internal gas spectrometry for the precision determination of electron-capture ratios is limited to sources with atomic numbers below ~ 50 , because with heavier atoms too many x rays escape from the sensitive counter volume, even at high counting-gas pressures. Although

this escape probability can be calculated in principle, the accuracy of the measurements is severely affected.

In earlier days, some L/K capture ratios were determined by measuring trajectories produced in a cloud chamber by K and L events from a radioactive gas (Radvanyi, 1952a, 1955a). This approach is included in Table 3.1 for historical reasons as Method 4.

3.1.2. Spectrometry with Internal Solid Sources

The internal gas spectrometry technique fails at high Z because too many K x rays escape. To circumvent the problem, the proportional counter can be replaced by scintillation crystals if the radioactive atoms can be built into the crystal lattice (der Mateosian; 1953). From the measured intensities of K, L, and M events the capture ratios can then be deduced. The advantage of the method (No. 5 in Table 3.1) is that self-absorption of the emitted radiation can be neglected. It is required, however, that the scintillation behavior not be disturbed by addition of the source material. Clustering must be avoided.

The source crystal can be placed directly on the photocathode of the multiplier tube. Groups at Heidelberg have used NaI(Tl) and CsI(Na) crystals doped with appropriate isotopes for the determination of electron-capture ratios by the internal-source technique. Leutz *et al.* (1966) grew NaI(Tl) crystals containing ^{202}Tl and ^{204}Tl as a constituent of the crystal lattice, and Schulz (1967a) doped the scintillator with ^{83}Rb and ^{185}Os . Furthermore, ^{131}Cs has been built into the lattice of CsI(Na) scintillation crystals. To use doped crystals for spectrometry it is necessary that the radioactive nuclei

be uniformly distributed in the scintillator. To avoid absorption effects caused by possible surface concentration and precipitation of activity at grain boundaries, Ravn and Bøgeholt (1971) used $\text{Cs}_2 \text{Pt}(\text{CN})_4 \cdot \text{H}_2\text{O}$ doped with ^{193}Pt for the determination of the M/L capture ratio in the decay of ^{193}Pt . This scintillator material has several advantages. Platinum being one of the main constituents of the crystal, ^{193}Pt is for chemical reasons ensured a completely uniform distribution. The crystal exhibits light yields and relaxation times comparable to those of $\text{NaI}(\text{Tl})$.

Two principal sources of error must be overcome in this method. The radioactive source must form a true solution; if the radioactivity lodges non-uniformly at dislocations or grain boundaries, absorption effects occur. Schulz (1967b) has investigated the problem and has developed a chemical and a physical criterion to decide which radioactive isotopes form true mixed crystals with $\text{NaI}(\text{Tl})$. She finds that Rb, Cs, Ba, Os, Tl, and Pb do form such mixed crystals, whereas P, Ca, Mn, Zn, As, Y, Sn, Ce, and Bi do not. Joshi *et al.* (1963) have studied the effects of non-uniformity of mixing and the phenomena of over-activation and poisoning. The second main source of error arises from K x-ray escape from regions near the surface, which results in the recording of K-capture events as L- or M-capture events.

To correct for x-ray escape, basically two methods have been used. A well-type $\text{NaI}(\text{Tl})$ hollow crystal can be employed to surround the $\text{NaI}(\text{Tl})$ crystal that contains the internal radioactive source (Fig. 3-7). Escaping K x rays from electron capture and iodine K x rays

associated with the detection process are absorbed in the outer crystal and are recorded as simultaneous events, so that no x-ray escape corrections are required. The method has been used by Joshi and Lewis (1960), Joshi (1961), Smith and Lewis (1966), Goedbloed (1970a), and by Goedbloed et al. (1968, 1970b) who have discussed it in detail.

An alternative approach to correct for x-ray escape involves measurement of the ratios of the areas A, B, and C of the K, L, and M peaks for several source crystals of different sizes (Figs. 3-8 and 3-9). Leutz et al. (1966) have shown that correction for escape can be most accurately performed by plotting the ratios $A/(A+B)$ and C/B against the surface-to-volume ratio of the doped crystal and extrapolating linearly to a surface-to-volume ratio of zero. Thus, values of $P_K/(P_K+P_L)$ and P_M/P_L are found that correspond to a measurement with an infinitely large crystal.

Corrections must be applied for (1) sum effects, (2) self-absorption, if clustering occurs, (3) possible influence of internal conversion or β^- background (as in the case of ^{204}Tl). K x-ray escape is accounted for if one of the above-described techniques is used. The method of internal solid source spectrometry can be made very accurate.

A reduction in the noise level was attained by Rayn and Bøgeholt (1971) by means of a coincidence system in which two low-noise photomultiplier tubes were coupled to a ^{193}Pt -doped crystal. Crystal and photomultiplier assembly were cooled to -35°C to reduce dark current (Fig. 3-10).

In the case of nuclides that undergo electron capture to an excited state, internal solid-source spectrometry with coincident γ rays is possible. The intensities of L and K events are measured in the source crystal in coincidence with ensuing γ rays (Fig. 3-11). Accidental coincidences must be taken into account. In favorable cases this method can be made quite accurate.

3.1.3. Spectrometry of K and L x Rays with External Sources

This method (No. 6 in Table 3.1) is based on the determination of the intensities I_{LX} of L x rays and I_{KX} of K x rays from singles spectra as measured with proportional counters or NaI(Tl) detectors. The sources, placed outside the sensitive volume of the detector, are usually prepared by drop deposition, but metal grains (Johns et al., 1957), sources prepared by painting (Fujiwara et al., 1964), and vacuum-evaporated sources (Venugopala Rao and Crasemann, 1965) have been used. The L/K ratio is deduced from the relation

$$\frac{P_L}{P_K} = \frac{I_{LX} \omega_K}{I_{KX} \omega_{LL}} - \frac{\omega_{LK}}{\omega_{LL}} n_{KL}, \quad (3-14)$$

where ω_K is the K-shell fluorescence yield, ω_{LL} is the partial L-shell fluorescence yield following L capture, ω_{LK} is the partial L fluorescence yield following $K\alpha$ x-ray emission, and n_{KL} is the number of L-shell vacancies produced on the average when a K-shell vacancy is filled.

Corrections must be made to account for (1) self-absorption, (2) absorption between source and detector, (3) solid angle, if different

detectors are used for the measurement of L and K x rays, (4) efficiency of the detectors, (5) interfering effects due to γ rays and internal-conversion electrons. There is some uncertainty in n_{KL} and in the fluorescence yields ω_K , ω_{LK} , and ω_{LL} , which can usually be found in the literature (Bambynek et al., 1972). An additional uncertainty can arise from degraded L x rays at the low-energy side of the L peak.

Capture ratios can be determined by this method in the case of nuclides that decay from ground state to ground state or to an excited metastable state. For nuclei that decay by a prominent transition, among others, to the ground state of the daughter, mean L/K ratios can be obtained. Though often used, the method is not very accurate, because P_L/P_K is a small difference between two large quantities, and the partial L-shell fluorescence yields greatly affects the result.

Venugopala Rao and Crasemann (1965), and Venugopala Rao et al. (1966a) have measured the L and K x-ray intensities relative to the K x-ray intensity of a ^{109}Cd reference source and thus deduced P_L/P_K of ^{181}W and ^{204}Tl . Kramer et al. (1956) have determined P_L/P_K of ^{202}Tl by comparing the intensity ratio I_{LX}/I_{KX} with that of a ^{203}Hg reference source. In addition to the need for corrections indicated earlier, the quantities n_{KL} , ω_{LL} , ω_{LK} and the internal conversion coefficients α_L and α_K of the reference source must be known. With an appropriately chosen reference nuclide these corrections can partly cancel.

For nuclides decaying to an excited state that is followed by γ -ray emission, coincidences can be determined between K x rays and γ rays and between L x rays and γ rays. From the measured coincidence

counting rates $I_{KX-\gamma}$ and $I_{LX-\gamma}$ and from the singles rate I_γ , the L/K-capture ratio can be found:

$$\frac{P_L}{P_K} = \left(\frac{I_{LX-\gamma}/I_\gamma}{I_{KX-\gamma}/I_\gamma} \right) \frac{\omega_K}{\omega_{LL}} - n_{KL} \left(\frac{\omega_{KL}}{\omega_{LL}} \right). \quad (3-15)$$

The L x rays have usually been measured with proportional counters, and the K x rays and γ rays, with NaI(Tl) detectors. This method is an extension of that based on Eq. (3-14). It requires the same principal corrections and suffers from the same uncertainties; accidental and sum coincidences must also be taken into account.

A special technique was employed by McCann and Smith (1968) in their work on ^{133}Ba . These authors used a NaI(Tl) detector to measure the L and K x-ray spectra gated by the sum coincidence peak of the 356-keV and 81-keV γ rays, which were absorbed in another NaI(Tl) detector.

Measurement of (L-event)-(K-x-ray) Coincidences. This method (No. 7 in Table 3.1) has been employed by Christmas (1964) to determine the L/K-capture ratio of ^{204}Tl . Coincidences between L x rays and K x rays were measured by means of two NaI(Tl) detectors, and P_L/P_K was deduced. In a similar approach, Konstantinov and Perepelkin (1961) used a 4π proportional counter filled with a Xe-CH₄ mixture. Coincidences between L events (L x rays and L Auger electrons) in the top part and K x rays in the bottom part of the counter were detected. A sufficiently thick backing material permitted only K x rays to penetrate to the bottom counter.

The method requires corrections for (1) self-absorption of L x rays

and Auger electrons, (2) absorption of K x rays in the backing foil, (3) escape of K x rays from the detectors, (4) detector efficiencies, including solid angle, (5) accidental and sum coincidences, and (6) influence of possible γ rays. Values of n_{KI} and K-shell and L-shell^s fluorescence yields can usually be found in the literature (Bambynek et al., 1972); they contribute to the overall uncertainty. The method yields mean P_L/P_K values if the nuclide decays by more than one electron-capture branch.

3.2. Determination of the Relative

K-Capture Probability P_K

In addition to the determination of capture ratios, there are various other methods from which the relative capture probability P_K can be deduced. Some of these constitute a direct measurement of P_K . In various others the product $P_K \omega_K$ is determined. All measurements described in this section employ external sources, placed outside the sensitive volume of the detector.

3.2.1. Measurement of K x Rays or Auger Electrons and

γ Rays or Conversion Electrons

Spectrometry of K x rays and γ rays. The principle of this method (No. 8 in Table 3.1) is to measure the intensities I_{KX} of the emitted K x rays and I_γ of the γ rays and hence to deduce the K-capture probability:

$$I_{KX}/I_\gamma = \alpha_K \omega_K [1 + P_K (1 + \alpha)/\alpha_K]. \quad (3-16)$$

Here, ω_K is the K-shell fluorescence yield, while α_K and α are the K-shell and total conversion coefficients. Sources have been prepared by simple drop deposition. Proportional counters as well as NaI(Tl) and Ge(Li) detectors have been used.

Principal corrections are required for (1) self-absorption of the K x rays, (2) absorption between source and sensitive volume of the detectors, (3) efficiencies of the detectors for K x rays and γ rays, and (4) solid angles. Values for the fluorescence yield ω_K and the conversion coefficients are required. If internal conversion can be neglected, Eq. (3-16) becomes simply $I_{KX}/I_\gamma = P_K \omega_K$.

Bayer *et al.* (1972) used this method to measure the K x-ray intensities in the $^{140}\text{Nd} \rightarrow ^{140}\text{Pr} \rightarrow ^{140}\text{Ce}$ decay chain and to deduce P_K of ^{140}Nd . Wapstra *et al.* (1954, 1957) and Friedlander and Orr (1951b) employed two nuclides that decay to the same excited level in the daughter nucleus, one by electron capture and the other by β^- emission. The intensity ratio of the K x rays and γ rays from the two nuclides was determined and hence the K-capture probability:

$$\left(\frac{I_{KX}}{I_\gamma}\right)_{EC} \left(\frac{I_{KX}}{I_\gamma}\right)_{\beta}^{-1} = 1 + P_K (1 + \alpha) / \alpha_K \quad (3-17)$$

Corrections are required mainly for (1) sum effects, and (2) contributions of radiation from higher levels. K-shell and total conversion coefficients are usually taken from the literature.

Spectrometry of K x rays or Auger electrons and K conversion electrons. The principle of this method (No. 9) is to measure the intensity I_{KX} of K x rays and I_{eK} of K conversion electrons (Avignon

et al., 1955). The K-capture probability is found from the equation

$$I_{KX}/I_{eK} = \omega_K [1 + P_K(1 + \alpha)/\alpha_K]. \quad (3-18)$$

Moussa and Juillard (1956) have measured the intensities I_{KA} of K Auger electrons and I_{eK} of K conversion electrons and used a relation similar to Eq. (3-18) with I_{KX} and ω_K replaced by I_{KA} and $(1 - \omega_K)$, respectively. Magnetic β^- spectrometers were used to detect the electrons and a NaI(Tl) scintillation counter for the x rays.

Corrections must be made for (1) self-absorption of the K x rays or Auger electrons, (2) absorption between source and detector; (3) efficiencies of the detectors including solid angles; and (4) radiation from higher levels, if present. Fluorescence yields and internal conversion coefficients are usually taken from the literature.

Determination of K x-ray emission rate and disintegration rate.

This method (No. 10) requires determination of the K x-ray emission rate I_{KX} , preferably with a large proportional counter filled to a sufficient pressure to absorb all K x rays. In addition, the disintegration rate I_0 must be determined, preferably by means of a coincidence technique as used in absolute standardization of radioactive sources. The value $P_K \omega_K$ is found from the relationship

$$P_K \omega_K = I_{KX}/I_0, \quad (3-19)$$

where ω_K is the K-shell fluorescence yield.

The method is described in detail by Taylor and Merritt (1965). To check the K x-ray emission rate, a second fairly independent approach

can be used (Bambynek, 1967a) utilizing a medium-solid-angle arrangement with a proportional counter or a thin NaI(Tl) crystal as detector (Bambynek et al., 1966; Bambynek, 1967b). The detection system for determining the disintegration rate has been described by Campion (1959). It consists of a 4π flow-type pillbox proportional counter placed between two NaI(Tl) detectors. A calibrated γ spectrometer (Vaninbroukx and Grosse, 1966) ^{also} has been used to determine the disintegration rate.

Radioactive sources have been prepared for experiments of this type by drop deposition, electrodeposition, and evaporation in vacuum. Sources have been mounted on thin metallized plastic foils for the determination of the disintegration rates, then they were sandwiched between absorber foils to stop all Auger electrons, so that K x-ray emission rates could be measured in a high-pressure proportional counter.

The principal corrections that must be applied in the K x-ray measurements are for (1) self-absorption, (2) foil absorption, (3) x-ray counter efficiency (normally near unity), and (4) the effect of γ rays and β^+ particles, if present. The corrections in the determination of the disintegration rate by the coincidence method are small and well-understood, and involve only parameters that can be determined experimentally as an integral part of the measurement. The fluorescence yield ω_K is usually taken from the literature (Bambynek et al., 1972).

This method has been applied in laboratories specializing in the standardization of radionuclides, and has yielded several of the most reliable $P_K \omega_K$ values.

3.2.2. Coincidence Measurements

With nuclides that decay by electron capture to an excited level in the daughter nucleus, coincidences can be measured between x rays or Auger electrons (from the capture process) and γ rays or conversion electrons (from the deexcitation of the daughter state). Such measurements can serve to determine capture probabilities or their ratios.

Measurement of K x-ray and γ -ray coincidences. In this method (No. 11), coincidences are measured between K x rays in one detector and γ rays in another detector. One finds

$$P_K \omega_K = I_{KX-\gamma} / I_\gamma \quad (3-20)$$

where $I_{KX-\gamma}$ is the (K x-ray)-(γ -ray) coincidence counting rate, I_γ is the singles γ rate, and ω_K is the K-shell fluorescence yield of the daughter atom. Sources for such experiments have mostly been prepared by drop evaporation; however, plated (Grotheer et al., 1969), electroplated (Thomas et al., 1963), gaseous external sources (Bresesti et al., 1964; Winter et al., 1965b) and metal powders (Perrin, 1960; Millar et al., 1959) have also been used.

Different combinations of detectors have been employed; in most cases proportional counters served for the K x rays and NaI(Tl) detectors for the γ rays or for both radiations. Solid state detectors have also been used recently: NaI(Tl)-Ge(Li) (Raeside et al., 1969; Myslek et al., 1971); Ge(Li)-Ge(Li) (Schmidt-Ott and Fink, 1972), and Si(Li)-Ge(Li) (Genz et al., 1973c).

Corrections must be applied principally for the following effects:

(1) self-absorption and absorption of K x-rays between source and sensitive volume of the detector, (2) efficiency of the K x-ray detector, including solid angle, (3) detection of γ rays or conversion electrons in the x-ray detector, (4) contributions from positrons, if present, and (5) sum and accidental coincidences. Values of the fluorescence yield ω_K can usually be taken from the literature. In order to avoid uncertainties due to the insufficiently known fluorescence yields, De Wit and Wapstra (1965) in their measurements on ^{195}Au and ^{197}Hg compared the intensity ratios $I_{\text{KX-}\gamma}/I_\gamma$ with that of a ^{202}Hg reference source. With an appropriately chosen reference nuclide, the fluorescence yields practically cancel. On the other hand, knowledge of P_K of the reference nuclide is required.

With nuclides decaying to an excited level that is followed by a γ - γ cascade to the ground state, triple coincidences have been measured. The K-capture probability can then be found from the relation

$$P_K \omega_K = \frac{I_{\text{KX-}\gamma_1-\gamma_2}}{I_{\gamma_1-\gamma_2}}, \quad (3-21)$$

where $I_{\text{KX-}\gamma_1-\gamma_2}$ is the rate of the (K x-ray)-(γ_1)-(γ_2) triple coincidences, and $I_{\gamma_1-\gamma_2}$ is the (γ_1)-(γ_2) coincidence rate. In addition to the corrections mentioned previously, directional correlations must be taken into account.

The coincidence method permits determination of the K-capture probability for transitions to an excited level in the daughter nucleus. By appropriate choice of γ -ray window settings one can select a particular electron-capture transition among several in the same decay.

This technique (No. 12) has been employed to determine the ratio of K-capture probabilities to different levels (denoted here by 1 and 2):

$$\frac{P_{K1}}{P_{K2}} = \left(\frac{I_{KX-\gamma 1}}{I_{\gamma 1}} \right) / \left(\frac{I_{KX-\gamma 2}}{I_{\gamma 2}} \right). \quad (3-22)$$

The result does not depend upon the fluorescence yield and the efficiency of the K x-ray detector. In most cases, NaI(Tl) detectors have been used for the K x rays and γ rays (Lewin et al., 1965), but NaI(Tl)-Ge(Li) (Schmidt-Ott et al., 1968; Schmidt-Ott, 1970; Cook and Johns, 1969; Lourens et al., 1970) and Si(Li)-Ge(Li) combinations (Lourens, et al., 1970) have also been employed. The method has been used mostly to determine the energies of electron capture transitions.

Measurement of (K x-ray and Auger-electron)-(γ -ray) coincidences.

If coincidences between K x rays or Auger electrons and γ rays are measured (Method 13), the K-capture probability P_K can be directly deduced:

$$P_K = \frac{I_{K-\gamma}}{I_{\gamma}}. \quad (3-23)$$

Very thin (e.g., vacuum-evaporated) sources of large area are required to keep self-absorption down. Kramer et al. (1962a) employed this method with a double proportional counter operated at sufficiently high pressure to detect all K x rays and Auger electrons. The source was placed so as to attain a $\sim 4\pi$ solid angle. Gamma rays were detected with a NaI(Tl) scintillation counter. Vatai and Hohmuth (1968) employed a 4π CsI(Tl) detector system to register K events and a CsI(Tl) detector for the γ rays.

ORIGINAL PAGE IS
OF POOR QUALITY

Corrections are required for (1) self-absorption of K x rays and Auger electrons, (2) absorption of x rays and electrons in the backing foil of the source, (3) incomplete realization of the 4π solid angle, (4) accidental coincidences, (5) detection of γ rays in the K-event detector, and (6) influence of positrons, if present.

Measurement of (K x-ray)-(γ -ray) sum coincidences. In this method (No. 14), which was first used by Gupta and Iha (1956), the pulse-height spectrum of K x rays and γ rays is measured in one single detector. The spectrum (Fig. 3-12) contains a K x-ray peak, a γ -ray peak, and a sum peak arising from (K x-ray)-(γ -ray) coincidences in the detector. From the measured areas A_γ and A_{XY} of these peaks, the capture probability can be deduced:

$$P_{K^0 K} = \frac{I_{KX-\gamma}}{I_\gamma} = \frac{A_{XY}}{A_\gamma + A_{XY}} \quad (3-24)$$

In most cases, a NaI(Tl) detector has been employed for measurements of this type. Das Mahapatra and Mukherjee (1974) used a Ge(Li) detector, and Campbell and McNelles (1972) employed a sandwich detector consisting of two CsI(Tl) crystals with the source in between.

Corrections must be made for (1) self-absorption and absorption of K x rays between source and sensitive volume of the detector, (2) efficiency of the K x-ray counter, including solid angle, (3) accidental coincidences, and (4) separation of overlapping parts of the γ -ray and sum peaks.

Gupta (1958) has used this method with triple sum coincidences. He observed the pulse-height spectrum in a single NaI(Tl) detector and

**ORIGINAL PAGE IS
OF POOR QUALITY**

determined the areas A_{X12} and A_{12} of $Kx-\gamma_1-\gamma_2$ and $\gamma_1-\gamma_2$ sum coincidence peaks. The K-capture probability is

$$P_{K^0} = \frac{I_{KX+\gamma_1+\gamma_2}}{I_{\gamma_1+\gamma_2}} = \frac{A_{X12}}{A_{12}+A_{X12}} \quad (3-25)$$

Instead of employing a single detector, it is possible to measure coincidences between K x rays in one NaI(Tl) detector and sum coincidences of γ_1 and γ_2 in a second NaI(Tl) detector. The K x rays are then gated by the $\gamma_1+\gamma_2$ sum coincidences. The ratio of the corresponding intensities is equal to P_{K^0} . In a few cases, in which K capture is forbidden due to energetics, the L-capture fraction can be measured directly (Wapstra et al., 1962; de Beer et al., 1964; Pengra, 1976).

Measurement of (K x-ray)-(γ-ray) and (K x-ray)-(K x-ray) or (K x-ray)-(K conversion electron) coincidences. This method (No. 15)

can be applied to nuclides that decay to an excited level in the daughter nucleus that is deexcited by a converted γ transition. The approach was developed by Pruett and Wilkinson (1954); it is based on measuring coincidences between K x rays from the electron-capture process and γ rays from the daughter nucleus, and additionally, coincidences between K x rays from the electron capture process and K x rays from internal conversion. The K-capture probability can be deduced from the relation

$$2(I_{KX-\gamma}/I_{\gamma})/(I_{KX-KX}/I_{KX}) = 1+P_K(1+\alpha)/\alpha_K \quad (3-26)$$

where $I_{KX-\gamma}$ and I_{KX-KX} are the coincidence counting rates, and I_{γ} and I_{KX} the corresponding singles rates. Drop-deposited sources and NaI(Tl) detectors were used in these experiments. Results are independent of the fluorescence yields, but the K-shell and total con-

coincidences must be applied.

Hansen (1975) has determined P_K of ^{139}Ce by measuring coincidences between K x rays and γ rays and K x rays and K conversion electrons. The photons were measured by Si(Li) and NaI(Tl) detectors, and the electrons, by means of a magnetic β spectrometer. P_K can be deduced from the relation

$$\frac{1+P_K}{P_K} = \left(\frac{I_{\text{KX-eK}}}{I_{\text{eK}}} \right) / \left(\frac{I_{\text{KX-}\gamma}}{I_{\gamma}} \right). \quad (3-27)$$

In addition to the usual corrections, sum and accidental coincidences must be considered. Fluorescence yield and conversion coefficients need not be known. The method is only applicable to nuclides with a simple decay scheme lacking a γ cascade in the daughter.

Measurements of coincidences between K x rays or Auger electrons and conversion electrons. Coincidence measurements of this type (Method 16) for the determination of P_K were first made by Brosi *et al.* (1959), who observed the K x-ray spectrum gated by K- and L-conversion electrons (Fig. 3-13) and determined coincidence and singles intensities. The K-capture probability can be deduced from the relation

$$\frac{1+P_K}{P_K} = \left(\frac{I_{\text{KX-eK}}}{I_{\text{eK}}} \right) / \left(\frac{I_{\text{KX-eL}}}{I_{\text{eL}}} \right), \quad (3-28)$$

where $I_{\text{KX-eK}}$ and $I_{\text{KX-eL}}$ are the (K x-ray)-(K-conversion electron) and (K x-ray)-(L-conversion electron) intensities, respectively, and I_{eK} and I_{eL} are the corresponding singles rates. The K x rays have been measured with NaI(Tl) detectors, and the conversion electrons, with magnetic β spectrometers. Knowledge of the K-shell fluorescence yield

and the x-ray and electron detector efficiencies is not required. Corrections must be made to account for (1) accidental coincidences, (2) sum effects due to K x rays from electron capture and internal conversion, (3) possible effects of other converted γ transitions in cascade, and (4) possible effects of electron capture to higher levels.

Instead of utilizing coincidences between x rays and conversion electrons, it is possible to determine P_K from coincidences between K Auger electrons and K or L conversion electrons. From the measured intensities, P_K is found:

$$\frac{1+P_K}{P_K} = \left(\frac{I_{KA-eK}}{I_{eK}} \right) / \left(\frac{I_{KA-eL}}{I_{eL}} \right). \quad (3-29)$$

Here, I_{KA-eK} and I_{KA-eL} are the coincidence rates between K Auger electrons and K and L conversion electrons, respectively. This method (No. 17) has been used by Marelius et al. (1967), who employed two magnetic spectrometers. The necessary corrections are essentially the same as those in Method 16.

A slight variation of this approach has been used by Sparrman et al. (1966), who measured the K Auger-electron spectrum in coincidence with K and L conversion electrons by means of two long-lens spectrometers. The value for P_K was found from

$$\frac{1+P_K}{P_K} = \left(\frac{I_{KA-eK}}{I_{KA-eL}} \right) \frac{\alpha_L}{\alpha_K}. \quad (3-30)$$

The K and L conversion coefficients must be known. In addition to the corrections mentioned above, efficiencies for detecting K and L conversion electrons and the absorption of these electrons between source

and detector must be taken into account.

Pich et al. (1971) measured the K x-ray spectrum in a Ge(Li) detector gated by K conversion electrons which were detected in a proportional counter. By this method (No. 18), they determined P_K from the ratio of the (K x-ray)-(K-conversion electron) coincidence rate I_{KX-eK} and the K conversion-electron singles intensity I_{eK} :

$$(1+P_K)\omega_K = I_{KX-eK}/I_{eK}. \quad (3-31)$$

Corrections are needed for (1) accidental and sum coincidences, (2) self-absorption and absorption of K x rays between source and detector, and (3) efficiency of the K x-ray detector.

With nuclides decaying to a metastable level of the daughter, Durosini-Etti et al. (1966) have measured K x rays by means of a NaI(Tl) detector in coincidence with K conversion electrons detected with a surface barrier detector. The K-capture probability was deduced from the equation

$$P_K = \frac{I_{KX} I_{eK}}{I_{\gamma} I_{KX-eK}} \frac{1}{1+\alpha} - \frac{\alpha_K}{1+\alpha}. \quad (3-32)$$

Here, I_{KX} , I_{eK} , and I_{γ} are the measured intensities of K x rays, K conversion electrons, and γ rays, respectively; I_{KX-eK} is the (K x-ray)-(K-conversion electron) coincidence rate, α_K is the K conversion coefficient, and α , the total conversion coefficient. These conversion coefficients must be known. Corrections are needed for (1) X and γ detector efficiencies, including solid angle; (2) absorption between source and detectors, and (3) overlap of spectrum peaks.

Measurement of triple coincidences between K x rays, γ rays, and internal-conversion electrons. This method (No. 19) was used by Thun et al. (1966), who determined the triple coincidence rate $I_{KX-\gamma-eL}$ measuring K x rays with a NaI(Tl) crystal, γ rays with a Ge(Li) detector, and L conversion electrons with a magnetic spectrometer; the coincidence rate $I_{\gamma-eL}$ between γ rays and L conversion electrons was simultaneously determined. Then we have

$$P_{K^0 K} = \frac{I_{KX-\gamma-eL}}{I_{\gamma-eL}} \quad (3-33)$$

A different approach was taken by Törnkvist and Ström (1968) in their measurements on ^{133}Ba decay. These workers determined P_K directly from triple coincidences between K x rays, γ rays, and K or L conversion electrons detected with a lens spectrometer. The K-capture probability was deduced from

$$\frac{1+P_K}{P_K} = \left(\frac{I_{KX-\gamma-eK}}{I_{\gamma-eK}} \right) / \left(\frac{I_{KX-\gamma-eL}}{I_{\gamma-eL}} \right) \quad (3-34)$$

Sources were prepared by evaporation in vacuum. Corrections must account for (1) accidental and sum coincidences, (2) directional correlations (which can be minimized by proper choice of the angle between detectors), and (3) escape of iodine K x rays from the NaI(Tl) detector.

3.3. Experimental Capture Probabilities P_K , P_L , and P_M ;

Comparison with Theory

3.3.1. Experimental Results

All experimentally determined, published values of P_L/P_K , P_M/P_L , P_{LM}/P_K , $P_{K^0 K}$, and P_K are listed in Table 3.2. In the many cases in

which authors quote P_K while they actually have measured $P_K \omega_K$, we list the latter product, recalculated from the authors' P_K and ω_K . In some cases, authors do not specify the value of ω_K which they used; these are indicated by "+." Some entries in Table 3.2 have been revised from the original publication. For example, the $P_{LM..}/P_K$ ratio for ^{109}Cd (Moler and Fink, 1965) was revised by the authors, who communicated this to Durosini-Etti (1966). Vatai (1968b, 1970b) has noted that the ^{109}Cd P_M/P_L value of Moler and Fink (1965) was not corrected for escape of Ag L x rays. Applying a corresponding correction and making use of newly reported values for k_α and k_β , (Salem et al., 1974) and ω_K (Bambynek et al., 1972) and a theoretical P_L/P_K ratio yields $P_M/P_L = 0.205 \pm 0.020$. Similar corrections have been made to the ^{113}Sn P_M/P_L ratio of Manduchi et al. (1964b).

From among the entries in Table 3.2, we have selected those results that can with certainty be judged as reliable, because they were derived from measurements with pure, carefully prepared sources, all necessary corrections being determined and clearly described. (The importance of pure sources has been emphasized, for example, by Raman et al. (1973), who suggest that discrepancies in measured P_L/P_K ratios of ^{113}Sn may be due to variable amounts of ^{250}d ^{119}Sn present in the ^{115}d ^{113}Sn .) We have omitted results published without indication of error limits, or with errors in excess of 15%. The information provided in most publications is unfortunately less than complete. It is therefore probable that we have omitted some "good" results from the list of selected values. The selected P_L/P_K measurements are

listed in Table 3.3, the P_M/P_L ratios in Table 3.4, and selected values of $P_{LM..}/P_K$, $P_{K\omega_K}$, and P_K in Table 3.5. The K-shell fluorescence yields used to deduce the capture ratios P_K in Table 3.5 were calculated from the equation

$$\left(\frac{\omega_K}{1-\omega_K}\right)^{1/4} = A+BZ+CZ^3. \quad (3-35)$$

The constants A, B, C were determined by fitting this expression to the selected "most reliable" experimental fluorescence yields listed by Bambynek et al. (1972), with exception of those deduced from $P_{K\omega_K}$ measurements. The fluorescence yields calculated in this manner are practically the same as those recommended by Bambynek et al. (1972); slight changes in the last digit are within the stated error limits.

We use the transition energies Q_{EC} evaluated by Wapstra and Gove (1971), except in cases where these were deduced from measurements of electron capture ratios. In those cases, we have used Q_{EC} determined from measurements of internal-bremsstrahlung spectra or (p,n) reaction thresholds. For a few transitions, no independent Q_{EC} energies were available; these are indicated by an asterisk in Tables 3.3 and 3.5.

3.3.2. Theoretical Predictions

The last three columns of Tables 3.3 and 3.5 contain theoretical L/K and M/L ratios. These were calculated (see Sec. 2) from the relations

$$\frac{P_L/P_K}{(q_{L_1}/q_K)^2} = \left(\frac{g_{L_1}}{g_K}\right)^2 \left[1 + \left(\frac{f_{L_2}}{g_{L_1}}\right)^2 \right] X^{L/K} \quad (3-36)$$

and

$$\frac{P_M/P_L}{(q_{M_1}/q_{L_1})^2} = \left(\frac{g_{M_1}}{g_{L_1}}\right)^2 \left[\frac{1+(f_{M_2}/g_{M_1})^2}{1+(f_{L_2}/g_{L_1})^2} \right] X^{M/L} \quad (3-37)$$

for allowed transitions; and

$$\frac{P_L/P_K}{(q_{L_1}/q_K)^4} = \left(\frac{g_{L_1}}{g_K}\right)^2 \left[1 + \left(\frac{f_{L_2}}{g_{L_1}}\right)^2 + \left(\frac{P_{L_3} g_{L_3}}{q_{L_3} g_{L_1}}\right)^2 \right] X^{L/K} \quad (3-38)$$

for unique first-forbidden transitions. The electron radial wavefunction amplitudes g_K , g_{L_1} , f_{L_2} , g_{M_1} , f_{M_2} , as well as $P_{L_3} g_{L_3}$ were taken from the relativistic Hartree-Fock calculations of Mann and Waber (1973) as listed in Table 2.9. The exchange and overlap correction factors $X^{L_1/K} = B_{L_1}/B_K$ and $X^{M_1/L_1} = B_{M_1}/B_{L_1}$ were recalculated in the present work according to the ansatz of Bahcall (1963a,c, 1965a) and that of Vatai (1968b, 1970a) as described in Sec. 2.5. For $Z > 32$, the correction factors of Suslov (1970) are used in continuation of the Bahcall factors, and those of Martin and Blichert-Toft (1970) in extension of the recalculated Vatai factors. Assumptions and approximations underlying the calculation of these correction factors are discussed in Sec. 2.5. Equations (3-36)-(3-38) contain the simplifications

$$(q_{L_2}/q_{L_1})^2 = (q_{L_3}/q_{L_1})^2 = (q_{M_2}/q_{M_1})^2 = 1 \quad (3-39)$$

and

$$X^{L_2/L_1} = X^{L_3/L_1} = X^{M_2/M_1} = 1. \quad (3-40)$$

These approximations affect the capture ratios by less than 0.04% for $Z=20$ and less than 0.3% for $Z=75$.

The theoretical K-capture probabilities P_K listed in the last column of Table 3.5 were calculated from theoretical capture ratios P_L/P_K , P_M/P_L , P_N/P_M for $Z > 37$ and also P_O/P_N for $Z > 67$, according to Eq. (3-6). Exchange and overlap corrections $X^{L/K}$ and $X^{M/L}$ were applied as discussed above, using our recalculated factors for $Z \leq 32$ and those of Suslov or Martin and Blichert-Toft for heavier atoms. For the outer shells no exchange correction was made, none being available.

The theoretical capture ratios and probabilities listed in Tables 3.3-3.5 for first-forbidden non-unique transitions are calculated for allowed transitions. This approximation is justified because for such transitions the ratios of capture probabilities from the $ns_{1/2}$ and $np_{1/2}$ subshells are independent of the form-factor coefficients (Sec. 2.3.2).

3.3.3. Comparison of Experimental and Theoretical Electron Capture Ratios

For comparison with theory, the selected experimental L/K and M/L ratios for allowed and non-unique first-forbidden transitions (Tables 3.3 and 3.4) were divided by the energy-dependent factors

$$\left(\frac{q_{L_1}}{q_K}\right)^2 = \left(\frac{E_{EC} - E_{L_1}}{E_{EC} - E_K}\right)^2 \quad (3-41)$$

and

$$\left(\frac{q_{M_1}}{q_{L_1}}\right)^2 = \left(\frac{E_{EC} - E_{M_1}}{E_{EC} - E_{L_1}}\right)^2 \quad (3-42)$$

respectively, where the capture transition energy is

$$E_{EC} = Q_{EC} - E_\gamma \quad (3-43)$$

and E_K , E_{L_1} and E_{M_1} are electron binding energies taken from Bearden and Burr (1967). In the case of measurements pertaining to transitions to several levels, we divided the measured mean L/K capture ratios by the factor

$$\overline{\left(\frac{q_{L_1}}{q_K}\right)^2} = \sum_v a_v \left(\frac{q_{L_1}}{q_K}\right)_v^2. \quad (3-44)$$

The index v labels the final-state levels; the a_v are branching ratios subject to $\sum a_v = 1$. A corresponding procedure was used for mean M/L ratios. The branching ratios were taken from the Nuclear Data Sheets edited by the Nuclear Data Group, Oak Ridge National Laboratory.

The reduced experimental capture ratios $(P_L/P_K)/(q_{L_1}/q_K)^2$ and $(P_M/P_L)/(q_{M_1}/q_{L_1})^2$ are compared with theoretical ratios (Tables 3.3 and 3.4) in Figs. 3-12 and 3-13. For clarity, we have combined results for each atomic number and plotted weighted mean values and their uncertainties.

P_L/P_K capture ratios. Figure 3-12 shows that agreement between experimentally determined L/K capture ratios and exchange-corrected theoretical predictions is fairly good for all atomic numbers, both for allowed and for non-unique first-forbidden transitions. The difference between theoretical ratios, due to different exchange and overlap corrections, is largest for light atoms (Sec. 2.5).

In cases in which the electron-capture transition energy is not much larger than the K-shell binding energy, the $(q_{L_1}/q_K)^2$ ratio is very sensitive to Q_{EC} . Errors in Q_{EC} can then lead to erroneous conclusions in the comparison with theory. Such is the case for ^{206}Bi , and probably also for ^{109}Cd , ^{133}Ba , ^{159}Dy , ^{195}Au , and ^{202}Tl . More accurate

measurements on ^{79}Kr and ^{159}Dy should be performed. For ^{126}I a mean L/K ratio has been measured, due to 60% non-unique and 40% unique first-forbidden transitions. The experimental result agrees well with predictions for either type of transition. The few available measurements pertaining to pure unique first-forbidden transition also agree well with theory. Table 3.3 includes the 4 measured L/K ratios for non-unique second-forbidden transitions, but these are not compared with theoretical ratios.

Vatai (1973a, 1974) has suggested that the ratio of non-relativistic to relativistic nuclear matrix elements could be estimated from L_3/K ratios, and attempted to do this by evaluating the L_3/K fraction of the measured L/K ratios of ^{93}Mo (Hohmuth *et al.*, 1964) and ^{97}Tc (Katcoff, 1958), and the LM.../K ratio of ^{138}La (Turchinets and Pringle, 1956). The fact that the $(L_1+L_2)/K$ ratio is independent of nuclear matrix elements made the separation possible. The experimental ratios unfortunately are not very accurate; improved measurements on these cases and on additional second and higher forbidden non-unique transitions would be useful. Vatai (1973a, 1974) has further pointed out that in the presence of K capture determinations of M/K ratios would be more useful than of M/L ratios, because the former are more sensitive to nuclear matrix elements. Chew *et al.* (1974a) have followed Vatai's suggestion and calculated the ratio of nuclear matrix elements

$$R = \left(\frac{V_{F220}^0}{V_{F221}^0} - \sqrt{3/2} \cdot \frac{A_{F221}^0}{V_{F221}^0} \right) / \frac{V_{F221}^0}{V_{F221}^0}$$

in the decay of ^{59}Ni from L_3/K deduced from the total measured L/K ratio. Daniel (1969) has noticed that for allowed transitions the reduced capture ratios $(P_L/P_K)/(q_L/q_K)^2$ are in surprisingly good agreement with the ratios of the M1 internal conversion coefficients α_L/α_K .

P_M/P_L capture ratios. From Fig. 3-13 it is seen that experimental

ORIGINAL PAGE IS
OF POOR QUALITY

calculations for all Z. Precision measurements of additional M/L ratios of light atoms would be most useful to test exchange and overlap corrections.

A new more precise measurement on ^{65}Zn is needed. Further experimental evidence is also required in the medium-Z region; the M/L capture ratios in the decay of ^{81}Kr , ^{109}Cd and ^{127}Xe should be determined.

P_N/P_X capture ratios. The only measurement of an N/M capture ratio performed to date is that of Fengra (1976) on ^{205}Pb . With a gaseous source of ^{205}Pb tetramethyl, Fengra determined $P_M/P_L = 0.524 \pm 0.010$ and $P_N/P_M = 0.286 \pm 0.020$. Comparison with theory is impeded by lack of reliable information on the transition energy. An indirect determination of the (N+...)/M ratio of ^{202}Tl has been made from measurements of (K+N+...)/L and M/L ratios (Leutz *et al.*, 1966), but the accuracy of this result is insufficient for meaningful comparison with theory.

Capture probability P_K . Selected K-capture probabilities for allowed and first-forbidden transitions are compared in Table 3.5 with theoretical predictions for allowed transitions. Two selected measurements on ^{40}K are compared with theoretical capture probabilities for unique first-forbidden transitions. The K-capture probability, unless the reduced capture ratio, depends on the transition energy as well as on the atomic number. In Fig. 3-14 we have plotted the ratio of experimental to theoretical P_K vs. Z. The recalculated exchange and overlap corrections according to Bahcall (1963a,c, 1965a) (Sec. 2.5) were used in the theoretical calculations. For several nuclides (e.g. ^{133}Ba , ^{145}Pn , ^{151}Gd , ^{195}Au), the energy Q_{EC} is not known with sufficient accuracy.

New, more accurate measurements for P_K are desirable for some nuclides, e.g. for ^{73}As , ^{75}Se , ^{83}Rb , ^{84}Rb , ^{166}Yb , and ^{195}Au . The spin of the 307-keV level of ^{151}Eu is not exactly known, it is quoted as $(3/2)^+$ or $(7/2)^+$. The transition from the $(7/2)^-$ ^{151}Gd ground state to this level can therefore be non-unique or unique first-forbidden. Comparison of the measured $P_K = 0.811 \pm 0.021$ with the theoretical $P_K = 0.740$ for a non-unique and $P_K = 0.428$ for a unique transition supports the $(7/2)^+$ assignment.

Experimental and theoretical K-capture ratios are seen from Fig. 3-14 to agree within $\sim 5\%$; there is no systematic difference between allowed and first-forbidden non-unique transitions.

3.3.4. Conclusions and Recommendations

From Tables 3.3-3.5 and from Figs. 3-12, 3-13, and 3-14 we find that experimental and theoretical electron-capture data agree rather well, viz., on the average to $\sim 3\%$ in the case of L/K ratios, $\sim 9\%$ for M/L ratios, and 5% for P_K values. The experimental accuracy is insufficient to distinguish between the theoretical correction factors for exchange and overlap effects. These effects are expected to be largest in the decay of ^7Be (Odier and Daudel, 1956; Bahcall, 1963). Experiments to measure the P_L/P_K ratio of ^7Be have been unsuccessful due to experimental limitations (Renier et al., 1968).

New, more accurate measurements of capture ratios and P_K should be performed. More accurate results for second- and higher-order forbidden transitions would be useful to deduce nuclear matrix elements. Furthermore, more accurate Q_{EC} energies are very much needed.

3.4 Determination of K/β^+ and \bar{EC}/β^+ Ratios

In Secs. 3.4 and 3.5 we list all available experimental K/β^+ and \bar{EC}/β^+ ratios and describe the experimental techniques involved in these measurements. We compare experimental ratios for allowed, unique first-forbidden and non-unique first-forbidden transitions with the appropriate theoretical values.

Source preparation is an important aspect of these measurements. Allowed β^+ emitters are generally short-lived, many of them having half-lives of the order of seconds, minutes or hours (Fig. 3-15). In order to study β^+ emitters with comparative ease a continuous supply of the source is therefore often necessary. Positron emitting nuclei are normally deficient in neutrons, hence one cannot prepare them by slow-neutron bombardment of stable isotopes in reactors. Instead, the stable isotopes are usually converted to radioactive isotopes by such reactions as (γ, n) , using machines like synchrotrons or electron linear accelerators, or by $(n, 2n)$ reactions with fast neutrons from such devices as Cockroft-Walton generators or high-current electrostatic accelerators. Cyclotron irradiation with protons, deuterons or alpha particles to produce proton-rich (neutron-deficient) nuclei is another useful method of preparing positron emitters.

The radioactive source must be transported to the detector in a time that is short compared with the half-life. This problem has been solved, for example, by fast pneumatic transfer systems in which solid sources can be conveyed from the irradiation site to the detector in a fraction of a second. Continuous gas flow systems (Fig. 3-16) have also been

used extensively (Ledingham et al., 1965); if narrow-bore tubing is used in conjunction with a gas pressure of several atmospheres, the radioactive source (in gaseous form) can be conveyed to the detector in a very short time. Where the sources cannot be obtained in suitable solid or gaseous forms, the problem can often be solved by using liquids under pressure with the radioactive source dissolved in the medium or in suspension.

The main types of measurement used to determine K/β^+ and EC/β^+ ratios are summarized in Table 3.1. These various techniques and the sources of error involved in them are described in Secs. 3.4.1-3.

3.4.1. Measurements of K/β^+ Ratios with Internal Sources

Internal-source proportional counter. In this method (No. 20), the radioactive source in gaseous form is mixed with the normal proportional-counter gas. If the half-life of the source is sufficiently long, the gases may be static, but for short-lived nuclei continuous production of the source and gas flow through the counter is employed. The electron-capture events are detected as discrete peaks superimposed on the positron continuum. A major part of the error in these measurements comes from the procedure adopted in separating the K-capture peak from the continuum.

Measurements of K/β^+ ratios by this technique have generally been made under conditions where K x-ray escape from the counter is very small. For high-Z nuclei, the proportional counter must therefore be operated at high pressure. For low Z nuclei, counters can be operated at normal pressure, but for such nuclei the K/β^+ ratio is usually

extremely small, whence it is often difficult to resolve the K peak from the positron spectrum.

We assume that the radioactive source can be produced with negligible competing activities, a situation which is usually attainable in practice. The positrons and K-capture events are detected with practically 100% efficiency. Then we have

$$\frac{P_K}{P_{\beta^+}} = \frac{I_K}{I_{\beta^+}}, \quad (3-45)$$

where I_K and I_{β^+} are the measured intensities of the K peak and the β^+ spectrum, respectively. Corrections have to be applied to I_{β^+} to account for the number of positrons which, unlike the K x rays and Auger electrons, may enter the sensitive volume from the ends of the proportional counter. This correction was calculated to be 4.6% in the case of ^{18}F (Drever et al., 1956).

Solid internal sources may also be employed (e.g. Avignon, 1956) but corrections for the absorption of the x rays, Auger electrons and positrons in the source itself must then be taken into account.

In cases where the decay leads to an excited state of the daughter nucleus it is sometimes possible to measure coincidences between the spectrum in the proportional counter and the de-excitation γ ray, thus reducing the background. This technique was applied by Kramer et al. (1962b) to the decay of ^{58}Co .

Internal-source proportional counter with anticoincidence. This technique (No. 21) is similar to Method 20 and is particularly suitable

generally very much less intense than the positrons. In order to resolve weak K-capture peaks from the positron continuum, an anti-coincidence counter is employed. One such counter with a plastic scintillator as anticoincidence detector is shown in Fig. 3-17. Both the positron and electron-capture events are detected in the central proportional counter; only the positrons can reach the surrounding counter. Thus, if signals from the central counter are taken in anti-coincidence with those from the surrounding plastic scintillator, a well-resolved K peak is obtained. Figure 3-18 shows a typical K peak from ^{30}P , measured with the counter shown in Fig. 3-17.

From the total spectrum in the central counter and the K peak in the anticoincidence spectrum, I_K and I_{β^+} are obtained and Eq. (3-45) applies as in Method 20.

Unless high-pressure counters are employed, this method becomes complicated for nuclei with $Z \geq 18$ because corrections for x-ray escape must be made. The method then becomes intrinsically less accurate, and hence, has so far been employed only in the low-Z region.

Internal-source scintillation counter. In this technique (Method 22), the radioactive source is distributed in a scintillating crystal (usually NaI) by introducing it into the melt from which the crystal is grown. The capture and positron events are detected in the scintillator, with the K x rays and K Auger electrons producing a well-defined peak so that the K/β^+ ratio can be determined. The interpolation of the continuum under the peak is a major source of error. Examples of this technique are the measurements of the K/β^+ ratios for ^{22}Na with an error

of 9% (McCann and Smith, 1969) and for ^{60}Co with an error of 2% (Joshi and Lewis, 1961). In both of these isotopes the decay leads to an excited state of the daughter nucleus which then de-excites by γ -ray emission. To reduce background, the positron and electron-capture events were measured in coincidence with the de-excitation gamma rays, detected in a second scintillation counter.

Corrections must be applied for the escape of positrons from the source crystal before they have deposited sufficient energy to be detected. If coincidences are taken with a de-excitation gamma ray, allowance should furthermore be made for the loss of positron counts due to the summing of the gamma ray with a 511-keV positron-annihilation photon. A K peak from ^{22}Na (McCann and Smith, 1969) is shown in Fig. 3-19. The difficulty of obtaining peaks at these very low energies with a scintillation counter is considerable. Specially selected low-noise photomultiplier tubes must be used in conjunction with an electronic system that is capable of eliminating afterpulses from long-lived phosphorescence associated with large energy deposition by positrons in the radioactive scintillator.

Because the positrons and the K-capture events are detected with approximately 100% efficiency, Eq. (3-45) again applies, allowing for the corrections described above.

3.4.2. Measurements of K/β^+ Ratios with External Sources

Spectroscopy of positrons and K Auger electrons. In this type of measurement (No. 23), the areas under the Auger lines and the positron spectrum are measured. Since the Auger electrons and the positrons are

oppositely charged, a magnetic spectrometer with a Geiger, proportional, or scintillation counter is often used to analyze the radiations. The difficulty of subtracting a β^+ spectrum from a K peak is thus avoided.

In order to determine a K/β^+ ratio from such measurements, the value of the K-shell fluorescence yield ω_K must be known. There were often fairly large errors in the values of ω_K employed in the early experiments. However, Bambynek et al. (1972) have selected reliable measurements of ω_K and carried out a semi-empirical fit to these values. Thus, for many cases, uncertainty in ω_K need no longer seriously limit the accuracy of this method.

The relation

$$\frac{P_K}{P_{\beta^+}} = \frac{I_{KA}}{(1-\omega_K)I_{\beta^+}}, \quad (3-46)$$

applies, where I_{KA} is the total intensity of the K Auger lines. Corrections for absorption of low-energy Auger electrons and β^+ in the source are very important and contribute significantly to the errors involved in this technique.

Spectroscopy of K x rays and positrons. In this method (No. 24), a solid source is placed outside of semiconductor or scintillation counters. The K x rays and positron continuum are detected either in the same or separate counters, the Auger electrons generally being absorbed before reaching the detectors. A major uncertainty again arises from the subtracting of the β^+ spectrum from the K x-ray peak. As with Method 23, this technique requires knowledge of the fluorescence yield. Assuming that there are no competing activities, and correcting for

absorption, the equation applicable to this method is

$$\frac{P_{\text{K}}}{P_{\beta^+}} = \frac{I_{\text{KX}}}{I_{\beta^+\omega\text{K}}} \quad (3-47)$$

Account must be taken of any differences in solid angle for the detection of K x rays and positrons. Self-absorption of x rays in the source is an important factor in this technique and makes the use of thin sources desirable.

Figure 3-20 shows how clearly the K x rays may be separated from the continuum in the decay of ^{91}Mo (Fitzpatrick et al., 1975). This spectrum was obtained from a 5-mg/cm² thick, activated molybdenum foil placed 2 cm from a Si(Li) detector (area 30 mm², thickness 5 mm). The K α and K β x rays of Nb are well resolved and the fluorescent K x rays of Mo caused by positron excitation of the foil can also be seen. Although the intensity of the K-capture branch in the decay of ^{91}Mo is small (~5%), the error in estimating the areas of the K x-ray peaks can easily be kept as low as 1%. There is, however, a difficulty in ensuring that the solid angles for the x rays and the positrons are the same, even when a single detector is employed. This difficulty can be reduced by using a detector with a large surface area. The K x-ray spectrum of ^{91}Mo measured with a 5.1-cm \times 0.63-cm NaI(Tl) detector is shown in Fig. 3-21. The fine structure in the spectrum of Fig. 3-20 is unfortunately lost due to the intrinsically inferior resolution of NaI(Tl). Corrections are required for absorption of the K x rays and positrons and for the scattering of positrons out of the detector before they have deposited sufficient energy to be detected.

An interesting development of this technique is shown in Fig. 3-22 (Campbell *et al.*, 1975). Here, the radioactive sample is placed between two $\text{CaF}_2(\text{Eu})$ scintillators in a 4π arrangement. This arrangement overcomes the problem caused by positrons being scattered out of the detector before depositing sufficient energy to be detected, or being scattered into the detector from surrounding material.

Many of the early K/β^+ measurements in this category (Method 24) employed absorption techniques, typically with a Geiger counter and different absorbers to determine the relative intensities of the K x rays and the positrons. The accuracy of these measurements is very poor.

Spectroscopy of K x rays and β^+ annihilation photons. This technique (No. 25) is similar to the previous method, but instead of detecting the β^+ continuum, the positrons are stopped in an absorber and the 511-keV annihilation photons are detected. The source must be surrounded by sufficient material to ensure that all positrons are stopped at a well-defined position, as close to the source as possible. The K x rays and the annihilation photons may be counted simultaneously, with corrections applied to both intensities to allow for the presence of the β^+ absorber. Alternatively, when the half-life of the source is sufficiently long, spectra taken with and without the absorber may be used to determine I_{511} and I_{KX} respectively.

The K/β^+ ratio is deduced from the relation

$$\frac{P_K}{P_{\beta^+}} = \frac{2I_{KX}}{\omega_K I_{511}} \quad (3-48)$$

A correction must be applied to I_{511} for the loss of 511-keV γ -rays due to the summing of two such γ rays; the size of this correction depends on details of geometry and the type of detector. The effect on I_{511} of β^+ annihilation in flight (e.g. Kantele and Valkonen, 1973) must also be considered, although in many cases this has been assumed to be negligibly small.

3.4.3. Measurements of EC/ β^+ Ratios

EC/ β^+ ratios are determined by measuring the number of positrons emitted by the parent leading to an excited state of the daughter nucleus, and the number of γ rays or conversion electrons from that level in a given time interval. Since the total number of γ rays plus conversion electrons is equal to the total number of positrons and electron capture events--corrected with reference to the decay scheme where necessary--the ratio EC/ β^+ of total electron capture to β^+ emission can be determined. Errors in these measurements can be kept very small, especially if the decay scheme is well-known. For example, the EC/ β^+ ratios for ^{22}Na and ^{58}Co have been determined to $\sim 0.3\%$ and $\sim 0.7\%$, respectively. Errors in the decay scheme can, however, be large, and have led to large systematic errors in many of these measurements.

Spectroscopy of γ rays or conversion electrons and β^+ annihilation photons. One of the simplest forms of EC/ β^+ measurements consists of a comparison of the relative photopeak intensities of the de-excitation γ rays and the β^+ annihilation photons in, for example, a scintillation or semiconductor detector (Method 26). As for Method 25, the source

must be surrounded by sufficient material to annihilate the positrons near the source to ensure that the solid angle is the same for both the nuclear and the annihilation photons. Corrections are required for absorption in the source and detector window, for decays to other levels in the daughter nucleus, for summing, and for annihilation of positrons in flight. In cases where the energy of the de-excitation γ rays is high it may be necessary to correct for a contribution to the annihilation photons due to internal and external pair production (e.g., Rupnik, 1972).

The total capture to β^+ emission ratio is given by

$$\frac{P_{EC}}{P_{\beta^+}} = \frac{2I_{\gamma}(1+\alpha)}{I_{511}} - 1, \quad (3-49)$$

where I_{γ} and I_{511} are the photopeak areas of the de-excitation γ ray and β^+ annihilation photons, respectively, and α is the internal conversion coefficient.

A variation of this technique which has often been employed, particularly in the early measurements, is the comparison of the photopeak areas of the 511-keV and de-excitation γ rays for the source being investigated with similar areas for a source with a known EC/β^+ ratio. Thus, if the subscripts a and b refer to the source with known and unknown EC/β^+ ratio, respectively, we have

$$\left(\frac{P_{EC}}{P_{\beta^+}}\right)_b = \left(\frac{I_{\gamma}}{I_{511}}\right)_b \left(\frac{I_{511}}{I_{\gamma}}\right)_a \frac{\epsilon_{\gamma a}}{\epsilon_{\gamma b}} \left[\left(\frac{P_{EC}}{P_{\beta^+}}\right)_a + 1 \right] \left(\frac{1+\alpha_b}{1+\alpha_a}\right) - 1. \quad (3-50)$$

This method is suitable when the de-excitation γ rays for the two sources are of similar energy, since the ratio of efficiencies $\epsilon_{\gamma a}/\epsilon_{\gamma b}$

is then approximately unity. Hence the EC/β^+ ratio is then independent of detector efficiency. The accuracy of this method is obviously limited by the error in the EC/β^+ ratio of the standard source. Often ^{22}Na was used for this comparison but the range of reported EC/β^+ values for this isotope is large (Table 3.6). Some authors did not even state which comparison value they employed.

A less common variation of this technique consists of measuring the intensities of the β^+ annihilation photons and the conversion electrons, rather than the de-excitation γ rays. This method is only feasible in special cases where the internal conversion coefficient is high.

Several measurements have been carried out employing a similar technique in which the positron activity was determined from the area under the β^+ spectrum rather than from the intensity of the annihilation photons. As above, comparison with an isotope with a well-known EC/β^+ ratio was often employed. The results reported from this technique, however, have very large errors (>20%).

Measurement of β^+ - γ -ray coincidences. The principle of this method (No. 27) is to determine the number of γ rays, I_γ , and of positron- γ -ray coincidences, $I_{\beta^+-\gamma}$. Various combinations of detectors may be employed. Typically, scintillation or semiconductor detectors have been used for the γ rays while the positrons were detected in proportional or scintillation counters. A 4π proportional counter or an internal-source scintillation counter (Leutz and Wenninger, 1967) have also been employed to detect the positrons.

The EC/β^+ ratio is given by

$$\frac{P_{EC}}{P_{\beta^+}} = \frac{I_{\gamma}}{I_{\beta^+-\gamma}} - 1. \quad (3-51)$$

Comparison of I_{γ} and $I_{\beta^+-\gamma}$ with measurements for a source of known EC/ β^+ ratio has often been employed.

Sum-coincidence technique. In this more sophisticated coincidence technique (No. 28), the quantities measured are the positron intensity I_{β^+} , the γ -ray intensities I_{γ_N} and I_{γ_S} , and the positron- γ -ray coincidence intensities $I_{\beta^+-\gamma_N}$ and $I_{\beta^+-\gamma_S}$, where γ_N refers to the normal de-excitation γ ray and γ_S is the sum of a β^+ annihilation photon and γ_N . It can be shown (Williams, 1964) that the relation

$$\frac{I_{\beta^+} + I_{\gamma_N}}{I_{\beta^+-\gamma_N}} = I_0 \quad (3-52)$$

holds, where I_0 represents the total number of disintegrations.

Furthermore, we have

$$\frac{I_{\beta^+} + I_{\gamma_S}}{I_{\beta^+-\gamma_S}} = I_0 P_{\beta^+}, \quad (3-53)$$

whence

$$\frac{P_{EC}}{P_{\beta^+}} = \frac{I_{\beta^+-\gamma_S} + I_{\gamma_N}}{I_{\beta^+-\gamma_N} + I_{\gamma_S}} - 1. \quad (3-54)$$

In a measurement of the EC/ β^+ ratio for ^{22}Na (Williams, 1964), the β^+ activity was determined with a 4π proportional counter. For the detection of γ_S , two large NaI(Tl) crystals were used to obtain a high efficiency for the summation events. For γ_N , one smaller NaI(Tl) crystal was used to minimize the efficiency to summation events. The simplifying assumptions involved in Eq. (3-54) and the corrections which must be applied are discussed in detail by Williams (1964).

Measurement of triple coincidences. The EC/β^+ ratio can be obtained by taking the γ -ray spectrum in triple coincidence with two β^+ annihilation photons (Method No. 29). The two counters for annihilation photons are placed opposite each other with analyzer channels set to record the 511-keV photopeaks only. Due to the nature of the annihilation process, the efficiency for the detection of coincidences of two 511-keV γ rays at 180° is sufficiently increased over other coincidences that even very weak positron emission can be detected. A typical electronic arrangement for this type of measurement is shown in Fig. 3-23. The γ -ray singles intensity I_γ and of the triple coincidence intensity I_C are measured. If similar measurements are made for a source a whose EC/β^+ ratio is known, then the unknown EC/β^+ ratio source b is

$$\left(\frac{P_{EC}}{P_{\beta^+}}\right)_b = \left(\frac{I_\gamma}{I_C}\right)_b \left(\frac{I_C}{I_\gamma}\right)_a \left[\left(\frac{P_{EC}}{P_{\beta^+}}\right)_a + 1 \right] \left(\frac{1+\alpha_b}{1+\alpha_a}\right) - 1. \quad (3-55)$$

Corrections are required for such effects as summing, β^+ annihilation in flight, differences in the detection of annihilation radiation for the two sources due to possible differences in solid angle and in summing of the γ rays and the annihilation radiation, and the possibility of coincidences due to Compton events from high-energy γ rays being registered in the analyzer window of the annihilation detectors.

Measurement of (γ -ray)-(β^+ -annihilation-photon) coincidences. The various coincidence techniques are very similar in principle and this method (No. 30) is essentially a variation of Method 27. The quantities measured are the number of nuclear γ rays I_γ and the number of coincidences of nuclear and β^+ annihilation photons $I_{511-\gamma}$. The usual corrections

for absorption, summing, and β^+ annihilation in flight are required.

The EC/ β^+ ratio is given by

$$\frac{P_{EC}}{P_{\beta^+}} = \frac{2I_{\gamma}}{I_{511-\gamma}} - 1. \quad (3-56)$$

Miscellaneous. The experiments in this group (No. 31) do not fall readily into any of the other categories. Many of the experiments were carried out by employing various combinations of methods 20-30. No loss of accuracy need be implied. This category also includes methods which have been employed in only very few, exceptional cases and because of their limited application do not warrant description as a separate technique. Also included in the miscellaneous category are a few experimental results whose methods are in doubt due to incomplete details provided in the published papers.

One different approach to EC/ β^+ measurements is the technique employed by Allen et al. (1955) for the determination of the EC/ β^+ ratio for ^{22}Na . This involves a comparison of the number of positrons emitted from the source with the number of daughter atoms produced (Alvarez, 1937). The positron activity was determined using a 4π Geiger counter and the rate of evolution of the daughter (Ne) was determined by gas analysis.

Another interesting technique has been applied by Gleason (1959) to ^{65}Zn which decays by electron capture and β^+ emission to the ground state and by electron capture to the first excited state of ^{65}Cu . Using a measured value for the efficiency of detection of the de-excitation γ ray, the total electron capture decay rate and the electron capture

branching ratio were determined from measurements of the K x-ray counting rate, the γ -ray singles rate and (K-x-ray)-(γ -ray) coincidence counting rate. The assumption was made that the ratio of K-electron capture to total electron capture was the same for both branches. The β^+ emission rate was determined by counting coincidences of annihilation photons in two detectors at 180° and thus the EC/β^+ ratio for the ground state transition was found. The important feature of this technique is that although K x rays were used to indicate the occurrence of electron capture, the deduced value of the EC/β^+ ratio is independent of the fluorescence yield.

3.5. Experimental Results and Comparison with Theory for K/β^+ and EC/β^+ Ratios

3.5.1. Results

All published experimental K/β^+ and EC/β^+ ratios are listed in Table 3.6. Table 3.7 contains selected experimental K/β^+ and EC/β^+ ratios for allowed transitions. Only ratios for transitions to a single final state in the daughter nucleus are included. Unfortunately, information provided on some measurements was not complete and these results had to be rejected. Where the ω_K values were stated, results were recalculated using the latest reliable fluorescence yields, derived with the aid of Eq. (3-35).

The remaining K/β^+ and EC/β^+ ratios were found to lie in two distinct groups, one with errors ranging up to 12.5% and the other, consisting mainly of the earlier measurements, with considerably larger errors. Since the two groups are well separated only the results from the former are considered further.

Tables 3.8 and 3.9 contain selected results for first-forbidden unique and first-forbidden non-unique transitions. Results with errors greater than 25% or without quoted errors were excluded.

3.5.2. Theoretical Predictions

Allowed transitions. The theoretical K/β^+ ratios for allowed transitions in Table 3.7 have been calculated according to the relation

$$\frac{P_K}{P_{\beta^+}} = \frac{\pi \beta_K^2 (W_0 + W_K)^2 B_K}{2 \int_0^{p_0} p^2 (W_0 - W)^2 F(Z', W) dp} \quad (3-57)$$

[See Eqs. (2-111), (2-125), and (2-126)]. Small corrections [Eq. (2-128)] were neglected. The values of β_K were taken from Mann and Waber (1973) (Sec. 2.2.2) and the intensity of the β^+ spectrum was computed with the tables of Fermi functions of Behrens and Jänecke (1969). The energies W_0 were taken from the atomic mass tables of Wapstra and Gove (1971). Errors in the theoretical K/β^+ ratios in Table 3.7 reflect only the uncertainty in W_0 obtained from Wapstra and Gove. The value of B_K used in these calculations is discussed in Sec. 3.5.3.

The theoretical EC/β^+ ratio for allowed transitions is

$$\frac{P_{EC}}{P_{\beta^+}} = \frac{P_K}{P_{\beta^+}} \frac{P_{EC}}{P_K} = \frac{P_K}{P_{\beta^+}} \frac{\Sigma q_x^2 \beta_x^2 B_x}{q_K^2 \beta_K^2 B_K}, \quad (3-58)$$

where x stands for $K, L_1, L_2, M_1,$ or M_2 , and P_K/P_{β^+} is the theoretical K/β^+ ratio for an allowed transition [Eq. (3-58)].

Unique forbidden transitions. In general, the K/β^+ ratio for forbidden transitions is

$$\frac{P_K}{P_{\beta^+}} = \frac{\pi \beta_K^2 (W_0 + W_K)^2 C_{KBK}}{2 \int_0^{P_0} p^2 (W_0 - W)^2 \overline{F(Z', W) C(W)} dp}, \quad (3-59)$$

where C_K and $C(W)$ are shape factors and the bar represents averaging over the β^+ spectrum [Eq. (2-134)]. The shape factors contain matrix elements and are functions of W and W_0 . For unique forbidden transitions it is possible to separate the matrix-element and the energy dependence of C_K and $C(W)$ to give explicit expressions for the ratio $C_K/\overline{C(W)}$ (Sec. 2.4.4).

The first-forbidden unique transitions Eq. (2-135) is simplified to

$$\frac{C_K}{\overline{C(W)}} = \frac{(W_0 + W_K)^2}{q^2 + \lambda_2 p^2}, \quad (3-60)$$

where q is the neutrino momentum, p is the positron momentum, and the bar represents averaging over the β^+ spectrum. The theoretical first-forbidden unique K/β^+ ratios shown in Table 3.8 have been calculated using these expressions, with values of λ_2 from the tables of Behrens and Jänecke (1969). For comparison of theory and experiments, one can

use the approximations $W_K \approx 1$ and $q^2 + \lambda_2 p^2 \approx 2(W_0^2 - 1)$, whence

$$\frac{C_K}{C(W)} \approx \frac{2(W_0 + 1)}{W_0 - 1} \quad (3-61)$$

Equation (3-61) has an accuracy of a few percent.

Non-unique forbidden transitions. For non-unique forbidden transitions, K/β^+ ratios cannot, in general, be calculated explicitly (Sec. 2.4.3). For the special case of non-unique first forbidden transitions, however, which exhibit a β^+ spectrum with an allowed shape, the K/β^+ ratio is expected to be the same as for allowed transitions. Information about the shapes of some β spectra is given by Paul (1966) and Daniel (1968). For many of the non-unique first-forbidden decays listed in Table 3.9, however, details of the spectrum shape are not available. Nevertheless, to provide a general comparison, allowed theoretical K/β^+ and EC/β^+ ratios are indicated for all cases.

3.5.3. Comparison of Experiment and Theory

Allowed transitions. Theoretical and selected experimental values for K/β^+ and EC/β^+ ratios are listed in Table 3.7. Exchange and overlap corrections have been neglected in the theoretical ratios; they affect the total capture probability and β^+ emission rate only slightly (Bahcall, 1963a). The EC probability for ${}^7\text{Be}$, e.g., is affected by $<0.1\%$, and that of ${}^{37}\text{Ar}$, by $<0.1\%$ through exchange and overlap; the ${}^{65}\text{Zn}$ β^+ decay rate is affected by $\sim 0.1\%$, and that of ${}^{14}\text{O}$, by $<0.1\%$. The theoretical K/β^+ ratios in Table 3.7 include a correction factor according to Bahcall (Table 2.11); from $Z > 32$, the factors of

Suslov (1970) were used. At present, EC/β^+ -ratio measurements (Table 3.7) are not nearly accurate enough to help decide between the two sets of exchange and overlap correction factors listed in Table 2.11.

Figure 3-24 shows the ratio of experimental to theoretical values for all the results in Table 3.7. The interesting and very accurate point for ^{22}Na is plotted in the inset. For most of the decays, the experiment/theory ratio is less than unity; exceptions are ^{11}C , ^{15}O , ^{19}Ne , ^{89}Zr , $^{89\text{m}}\text{Zr}$, and ^{111}Sn . The disagreement between experiment and theory apparently increases with Z .

In the theory of allowed transitions, only s-wave leptons are considered and the EC/β^+ and K/β^+ ratios are independent of nuclear matrix elements. In the general case, leptons do not leave the nucleus only radially, and small contributions from p and d waves must be considered. This gives rise to higher-order matrix elements that do not cancel in the ratios (Sec. 2.4.2). A correction factor has been determined [Eq. (2-128)] that slightly reduces the theoretical ratios, by as much as 3% at $Z=80$.

The possible existence of second-class currents does not significantly affect electron-capture to positron-emission ratios (Behrens and Bühring, 1974).

First-forbidden unique transitions. For these transitions the experimental K/β^+ ratios are compared in Table 3.8 with first-forbidden unique theoretical ratios. There is agreement within the errors between experiment and theory, but the experimental accuracy is fairly poor.

First-forbidden non-unique transitions. The experimental K/β^+ and EC/β^+ ratios for these transitions are compared in Table 3.9 with the corresponding theoretical ratios for allowed transitions. The comparison is made for interest only; a complete theoretical treatment requires knowledge of the nuclear matrix elements which for these transitions do not cancel.

3.5.4. Conclusions and Recommendations

It can be seen from Fig. 3-24 that theoretical allowed K/β^+ and EC/β^+ ratios are systematically larger than experimental ratios; the discrepancy apparently increases with Z . Higher-order effects, such as second-class currents, corrections of the type described by Eq. (2-128), and radiative corrections are insufficient to resolve the difficulty. The question of radiative corrections is still unsettled; it has been shown (Sec. 2.4.2) that these corrections partially cancel out. There remains a model-independent part of the radiative corrections, however, which differs in the case of electron capture from that in positron emission. This model-independent correction includes the well-known emission of real photons (internal bremsstrahlung). Calculations for β^+ emission have been carried out to order α , e.g. by Wilkinson and Macefield (1970); an increase in the probability of β^+ emission is found which thus reduces the theoretical capture-to-positron ratios. The correction factor increases as W_0 decreases and as Z increases and amounts to 1.5% for ^{58}Co (Williams, 1970) if it is assumed that the correction is multiplicative and not additive. Radiative corrections for electron capture

have not yet been calculated.

It would be of interest to establish with greater accuracy the Z dependence of the trend shown in Fig. 3-24, if indeed such a simple functional dependence on Z exists. Remeasurements, preferably using different techniques, for any of the decays in Table 3.7 would be useful. The decays of ^{65}Zn , ^{111}Sn and any high-Z isotope are possibly the most interesting for study. The question of whether there is real agreement between theory and experiment in the case of first-forbidden unique transitions is still open; measurements on ^{84}Rb , ^{122}Sb and ^{126}I should be repeated with greater accuracy.

The theory of atomic exchange and imperfect wave-function overlap effects needs to be refined and calculations must be extended to low Z. Critical experiments on capture/ β^+ ratios which would differentiate between theoretical approaches have yet to be carried out. The problem of establishing the overlap and exchange correction for the K shell cannot be resolved by measuring K/β^+ ratios alone. The most sensitive isotope for study is ^7Be which decays solely by electron capture; a measurement of P_K for this isotope is very desirable (Sec. 3.3.4).

Some new and interesting EC/β^+ ratios have recently been reported by Firestone *et al.* (1974, 1975a). Anomalously high ratios are found for hindered allowed transitions in ^{145}Gd and ^{143}Sm ; these are attributed to the interference of higher-order nuclear matrix elements. It would be of great value to verify this experimental finding.

Theoretically K/β^+ ratios for allowed transitions are plotted in Figs. 3-25 and 3-26 as functions of Z and of the β^+ end-point kinetic energy. These ratios were calculated according to Eq. (3-58) with $B_K = 1$; the graphs may be used where an accuracy of $\sim 10\%$ is sufficient.

4. RADIATIVE ELECTRON CAPTURE

4.1. Theory

Radiative electron capture consists of processes which lead to the production of a continuous spectrum of electromagnetic radiation during electron capture (EC) decays. Such processes involve the emission of one or more photons during a single EC event. The energy released in the decay is shared statistically among these photons and the neutrino, thus accounting for the continuous nature of the resulting spectra. The most probable radiative electron capture events are those in which a single photon accompanies the neutrino. The radiation emitted even in this mode is quite weak, the total probability for the emission of a single photon being of the order of 10^{-4} per EC event. Radiative electron capture processes in which more than one photon is emitted occur with far smaller probabilities.¹⁵ Their contributions to the radiation spectra are completely insignificant and will not be considered further.

From the point of view of perturbation theory, radiative electron capture is a second-order process involving both beta and electromagnetic radiative transitions. The two transitions connect the initial and final states of the system through a set of virtual intermediate states. In general, there are two fundamentally different types of intermediate states through which the process can proceed. They are represented pictorially by the

Feynman diagrams shown in Fig. 4-1. The first type [Fig. 4-1(a)] involves only excited electronic states, and the radiation is produced by the sudden acceleration of charge and magnetic moment associated with the orbital electron's capture. This radiation is commonly referred to as internal bremsstrahlung (IB). The second type [Figs. 4-1(b) and (c)] involves excited nuclear states and the radiation arises from a nuclear transition which may either precede or follow the virtual EC decay. These two decay modes are variously denoted as electronic beta-gamma and nuclear beta-gamma transitions or, more simply, direct and detour transitions. In allowed decays, detour transitions are expected to occur at a $\sim 10^6$ times smaller rate than direct transitions. In forbidden decays, this difference can be less pronounced (Longmire, 1949; Horowitz, 1952).

Extensive calculations on detour transitions were carried out by Rose et al. (1962) and Lassiila (1963) for the especially interesting situation in which the initial and intermediate nuclear states, connected by a virtual EC transition, are almost degenerate. It was shown that the spectrum of the radiation arising from detour transitions is sharply peaked near the end point under these circumstances, in contrast to the usual IB spectrum. It was hoped that this deviation of the photon spectrum from its IB form might be observable, revealing the presence of detour transitions, even though their contribution was still expected to be quite small. An experiment designed to test these ideas was reported shortly thereafter by Schmorak (1963), who

studied ^{59}Ni , a nucleus possessing a decay scheme with the required characteristics, and found that the observed spectrum did indeed show a very small distortion from the predicted IB form near the end point. Attributing this distortion to the presence of detour transitions, Schmorak (1963) concluded that such transitions account for no more than $\sim 0.6\%$ of the total radiative K-capture transition rate.

While the contribution of detour transitions is of great interest for the study of nuclear structure, such transitions usually do not significantly affect the shape or intensity of radiative electron-capture spectra.¹⁶ For this reason, and because available theoretical results on detour transitions are very limited, such transitions will be disregarded here and all calculations will be confined to the determination of the direct-transition amplitude shown diagrammatically in Fig. 4-1(a). Clearly, a highly accurate theory of the direct-transition process will be necessary to permit the identification of any detour-transition contributions in observed spectra.

4.1.1. Matrix Elements and Transition Rates

Radiative electron capture is expected to occur with significant probability only for the innermost electrons of the atom. Since the available energy is usually greater than the K-shell binding energy, the K electrons, which spend the most time in the neighborhood of the nucleus, are expected to provide the dominant contribution to the IB spectra (except at very low photon

energies where 2p-state capture provides the dominant contribution). In all but the very lightest atoms, the potential in which the innermost electrons move is primarily the Coulomb potential of the nucleus. For this reason, all electron-electron interactions and the screening and correlation effects for which they are responsible are neglected in current theories, and it is assumed that each orbital electron is initially moving under the influence of only the nuclear Coulomb field.

Accordingly, the unperturbed electron-field operator $\Psi_e(x)$ is chosen to satisfy a Dirac equation containing the nuclear Coulomb field,

$$(\gamma_\mu \partial_\mu + 1 + \gamma_4 Z\alpha/r)\Psi_e(x) = 0. \quad (4-1)$$

In this representation, the interaction Hamiltonian density is

$$H_I(x) = H_Y(x) + H_{EC}(x), \quad (4-2)$$

where H_Y represents the interaction of the electron field with the Maxwell field and H_{EC} represents the EC interaction, assumed to be of the standard $V-\lambda A$ form. The matrix element associated with diagram (a) of Fig. 4-1 is derivable by standard quantum-field theoretic methods. As Glauber and Martin (1956) have shown, it can be written

$$M_\alpha = ieC_V(2\pi/k)^{1/2} \int d\underline{r}_N j_\mu^N(\underline{r}_N) \overline{\Psi}^V(\underline{r}_N) \Gamma_\mu \int d\underline{r} G_E(\underline{r}_N, \underline{r}) \times \underline{\gamma} \cdot \underline{e}^* e^{-ik \cdot \underline{r}} \underline{\Phi}_\alpha(\underline{r}), \quad (4-3)$$

with the matrix element of the nuclear EC current density defined by

$$j_{\mu}^N(\underline{r}_N) = \langle N_f | \bar{\psi}_N(\underline{r}_N, 0) \Lambda_{\mu} \psi_p(\underline{r}_N, 0) | N_i \rangle. \quad (4-4)$$

In these equations, C_V is the weak-interaction vector coupling constant, and we have $\lambda = |C_A/C_V|$, $\Lambda_{\mu} = \gamma_{\mu}(1 + \lambda \gamma_5)$, and $\Gamma_{\mu} = \gamma_{\mu}(1 + \gamma_5)$. The ψ_n and ψ_p are the nucleon field operators, and ϕ^{ν} and ϕ_{α} are the Dirac spinor wave functions for a neutrino of momentum \underline{P}_{ν} and an initial electron in state α , respectively. The one-photon state, characterized by momentum \underline{k} and polarization \underline{e} , has been normalized to a unit volume. The intermediate-state sum which appears in Eq. (4-3) has been identified as the eigenfunction expansion for the Dirac-Coulomb Green's function,

$$G_E(\underline{r}_N, \underline{r}) = \sum_{\beta} \frac{\phi_{\beta}(\underline{r}_N) \bar{\phi}_{\beta}(\underline{r})}{(E_{\beta} - E)}, \quad (4-5)$$

with $E = E_{\alpha} - k$, where E_{α} is the relativistic energy of the orbital electron undergoing capture.

Two comments on the structure of the matrix element are in order. First, it should be noted that the role played by positrons in the radiative capture process is included implicitly in the structure of M_{α} . One type of path through which the radiative capture process can proceed is the emission of a virtual positron by the nucleus followed by its single-quantum annihilation with an orbital electron. Such paths are accounted for by the presence of the various negative-energy eigenstates in the expansion of the Green's function. Thus, the structure of the

Green's function is such that complete account is taken of the role of positrons in the radiative capture process.

Since the theory developed so far assumes the presence of any number of orbital electrons moving independently in the Coulomb field of the nucleus, the Pauli exclusion principle forbids virtual radiative transitions to intermediate states which are already occupied. Presumably such occupied intermediate states should then be excluded from the eigenfunction expansion. However, as was first pointed out quite generally by Feynman (1949) and emphasized by Glauber and Martin (1956) in reference to radiative electron capture, the presence of an obstructing electron makes another path possible for the radiative capture process, which is not otherwise available. This path consists of virtual EC of the obstructing electron followed by a radiative transition. Feynman has shown that, for a noninteracting system, the total amplitude for such a new path exactly compensates for that of the forbidden intermediate states; thus one may perform the calculation as if all the other states were unoccupied.

Feynman's result is easily generalized to include the presence of a static external field, such as the field of the nucleus, and consequently it has been assumed valid in all theoretical studies on radiative electron capture. However, as pointed out by Persson and Koonin (1972), radiation before capture takes place in the Coulomb field of element Z , while radiation following capture takes place in the field of element $Z-1$. Consequently, those terms in the eigenfunction expansion for the Green's function which

correspond to occupied atomic states should really be represented by Coulomb eigenfunctions for element $Z-1$ rather than element Z . Undoubtedly, for $Z \gg 1$ the corrections resulting from such a modification of the eigenfunction expansion are entirely negligible. However, for very low- Z elements, especially at the lower photon energies ($k \lesssim Z\alpha$) where the poles corresponding to the bound states contribute strongly to the transition amplitude, such a modification of the Green's function may prove to be of importance.

The Green's function introduced in Eq. (4-3) and defined by the eigenfunction expansion [Eq. (4-5)] is seen to satisfy the inhomogeneous differential equation

$$G_E(\underline{r}_N, \underline{r}) \gamma_4 [H_c(\underline{r}) - E] = \delta(\underline{r}_N - \underline{r}), \quad (4-6)$$

where H_c is the Dirac-Coulomb Hamiltonian. As Glauber and Martin (1956) have shown, the evaluation of M_α is facilitated by the introduction of the second-order Dirac-Coulomb Green's function $g_E(\underline{r}_N, \underline{r})$, defined by

$$G_E(\underline{r}_N, \underline{r}) = g_E(\underline{r}_N, \underline{r}) [\gamma_4 \nabla + \gamma_4 (E + Z\alpha/r) + 1] \quad (4-7)$$

and satisfying the inhomogeneous second-order equation

$$g_E(\underline{r}_N, \underline{r}) [\nabla^2 + (E + Z\alpha/r)^2 - 1 - iZ\alpha \frac{\alpha \cdot (\nabla 1/r)}{r}] = -\delta(\underline{r}_N - \underline{r}). \quad (4-8)$$

With the introduction of Eq. (4-7), the matrix element of Eq. (4-3) lends itself to considerable simplification and can be written

$$M_\alpha = ieC_V (2\pi/k)^{1/2} \int d\underline{r}_N j_\mu^N(\underline{r}_N) \bar{\psi}^N(\underline{r}_N) \Gamma_\mu \int d\underline{r} g_E(\underline{r}_N, \underline{r}) e^{-i\mathbf{k} \cdot \underline{r}} \times [-2e^* \frac{\nabla + e^*}{\lambda} \Sigma_{\lambda\delta} k_\delta] \psi_\alpha(\underline{r}). \quad (4-9)$$

In the Secs. 4.1.2-4.1.4, the evaluation of M_{α}^{ν} and related quantities is described and final results are presented for allowed and first-forbidden transitions. We note that the differential transition rate is determined by the usual formula of time-dependent perturbation theory (Fermi's "Golden Rule No. 2") and is given by

$$dw_{\alpha}^{\nu} = (2\pi)^{-5} |M_{\alpha}^{\nu}|^2 \delta(E_{\nu} + k - q_{\alpha}) dP_{\nu}^{\nu} dk, \quad (4-10)$$

where $q_{\alpha} = Q_{EC} - B_{\alpha}$ has been introduced to represent the total available energy, shared between the photon and the neutrino.

4.1.2. IB Spectra from Allowed Transitions

For allowed transitions, the lepton functions of r_N are usually replaced by their values at $r_N = 0$. However, one must exercise some caution in doing this since the Coulomb Green's function $g_E(r_N, r)$ is known to be weakly singular at $r_N = 0$. To get around this difficulty it is necessary to take account of the fact that the EC interaction actually takes place over a finite nuclear volume, by averaging the Green's function over this volume.¹⁷ This averaged Green's function will be denoted by $\langle g_E(r_N, r) \rangle_{\Omega}$. Thus, for allowed transitions the matrix element of Eq. (4-9) is simplified to

$$M_{\alpha}^{\nu} = ieC_{\nu}^{\nu} (2\pi/k)^{1/2} \int_{\mu}^{\nu} \Phi_{\mu}^{\nu}(0) \Gamma_{\mu}^{\nu} \int_{\Omega} dr \langle g_E(r_N, r) \rangle_{\Omega} e^{-ik \cdot r} \times [-2e_{\nu}^* \cdot \nabla + e_{\nu}^* \cdot \Sigma_{\lambda} \lambda \delta_{\lambda} k] \Phi_{\alpha}(r), \quad (4-11)$$

where the nuclear EC transition current has been introduced,

ORIGINAL PAGE IS
OF POOR QUALITY

defined by $J_{\mu}^N = \int d\mathbf{r}_N j_{\mu}^N(\mathbf{r}_N)$. A nonrelativistic approximation for the nuclear motion leads to $J_{\mu}^N = (i\lambda \langle \sigma \rangle, \langle l \rangle)$, where $\langle l \rangle$ and $\langle \sigma \rangle$ are the familiar matrix elements associated with Fermi and Gamow-Teller transitions.

Coulomb-Free Theory

The earliest theory of IB spectra in allowed transitions was developed independently by Møller (1937a) and by Morrison and Schiff (1940).¹⁸ This theory is presently of interest because of its simplicity and because it yields IB spectra that are accurate at high photon energies. The more sophisticated theory developed later by Glauber and Martin (1956) may be viewed as providing correction factors for the basic results.

Morrison and Schiff (1940) simplified the problem by neglecting the momentum (and binding energy) of the initial electron and by neglecting the influence of the Coulomb field on the intermediate electron states. The first of these assumptions is only valid when the recoil momentum of the electron after photon emission greatly exceeds its initial momentum (of average value $Z\alpha$). The second approximation consists of assuming a Born-approximation treatment of the intermediate states. For its validity, this approximation requires that $Z\alpha/v \ll 1$, where v is the velocity of the electron after photon emission. It is evident that both approximations restrict the results to photons in the high-energy region where k is much larger than $Z\alpha$.

Ignoring the Coulomb field in the intermediate states amounts to using the free-particle relativistic Green's function found by

solving Eq. (4-8) with $Z=0$. The initial momentum of the electron is neglected by approximating its wave function by a constant, equal to the value of the wave function at the origin. Under these approximations, the calculation of the matrix element of Eq. (4-11) is greatly simplified and leads to the result

$$M_{ns} = ieC_v (\pi/2k)^{1/2} J_{\mu}^{N\nu} \phi_{ns}(0) \sum_{\lambda} e_{\lambda}^* k_{\lambda} \phi_{ns}(0). \quad (4-12)$$

It is important to note that as a consequence of neglecting the momentum of the initial electron, radiative electron capture from an initial electron state of nonvanishing angular momentum is forbidden. Both the electric and magnetic contributions to the IB radiation vanish under these circumstances; this is immediately evident from the structure of the matrix element of Eq. (4-12).

When Eq. (4-12) is substituted into Eq. (4-10) and the appropriate momentum and spin summations are completed, the IB spectra associated with ns-state capture are found to be

$$dw_{ns} = \frac{2\alpha}{\pi} C_v^2 J^N \cdot J^{N*} |\phi_{ns}(0)|^2 k(q_{ns} - k)^2 dk. \quad (4-13)$$

The ratio of the radiative capture rate to that for ordinary K capture is

$$\frac{dw_{ns}}{w_K} = \frac{\alpha}{\pi} \frac{|\phi_{ns}(0)|^2}{|\phi_{1s}(0)|^2} \frac{k(q_{ns} - k)^2}{q_{1s}^2} dk. \quad (4-14)$$

Hence the total radiative capture rate per K-capture event is

$$\frac{w_{ns}}{w_K} = \frac{1}{w_K} \int_0^{q_{ns}} \frac{dw_{ns}}{dk} dk = \frac{\alpha}{\pi} \frac{q_{ns}^2}{12} \frac{|\phi_{ns}(0)|^2}{|\phi_{1s}(0)|^2} \left(\frac{q_{ns}}{q_{1s}}\right)^2. \quad (4-15)$$

More generally, if only photons with $k \geq k_0$ are detected, the integrated radiative capture rate per K-capture event is given by

$$\frac{w_{ns}(k_0)}{w_K} = \frac{1}{w_K} \int_{k_0}^{q_{ns}} \frac{dw_{ns}}{dk} dk = \frac{w_{ns}}{w_K} [4(1-k_0/q_{ns})^3 - 3(1-k_0/q_{ns})^4]. \quad (4-16)$$

For radiative K capture in particular, these formulas are simplified. The $\beta\beta$ spectrum then is

$$\frac{dw_{1s}}{w_K} = \frac{\alpha}{\pi} q_{1s}^2 \epsilon(1-\epsilon)^2 d\epsilon, \quad (4-17)$$

where we have $\epsilon = k/q_{1s}$. The total radiative K-capture rate is

$$\frac{w_{1s}}{w_K} = \frac{\alpha}{\pi} \frac{q_{1s}^2}{12}. \quad (4-18)$$

Equations (4-17) and (4-18) were first derived by Møller (1937a) and by Morrison and Schiff (1940).¹⁹ The more general results for arbitrary s-state capture [Eqs. (4-14) and (4-15)] were first reported by Glauber and Martin (1956).

Theory of Glauber and Martin

The results of the Coulomb-free theory of Møller (1937a) and Morrison and Schiff (1940) are expected to hold only for large k and small Z ; otherwise it is essential to include Coulomb effects in the evaluation of the matrix element M_{α} . Such calculations, in

which account is taken of both relativistic and Coulomb effects, have been reported by Glauber and Martin in two well-known papers.

In their first paper on the subject, Glauber and Martin (1956) developed the general formalism for allowed transitions (Sec. 4.1.1.) and evaluated M_c to a relative accuracy of order $Z\alpha$ for both s- and p-state capture. Certain relativistic corrections that are important for s-state capture at low energies were also calculated. In their second paper, Martin and Glauber (1958) developed more elaborate methods which make detailed calculations possible in which relativistic and Coulomb effects are included to all orders in $Z\alpha$. These results lead to certain integrals which cannot be evaluated exactly in closed form or tabulated easily. To obtain numerical results, Martin and Glauber developed $Z\alpha$ expansions for these integrals and carried out their evaluation to a relative accuracy of order $(Z\alpha)^2$. This limitation on their otherwise exact results for radiative K capture has been removed recently however, by Intemann (1971), who has shown how to evaluate the integrals exactly using partly numerical methods. We briefly outline this theory and summarize its final results.

Nonrelativistic calculations. For moderately light nuclei it is expected that the initial electronic states can be described adequately by nonrelativistic Coulomb wave functions, especially for capture from the higher shells. In view of the greater complexity attendant to the use of Dirac-Coulomb wave functions, it is natural that nonrelativistic calculations be considered first. In general, these are expected to yield results with a relative

accuracy of order $Z\alpha$. In order to preserve this level of accuracy at all photon energies, however, it is necessary to employ somewhat more accurate wave functions, in order to correct for certain relativistic effects which have a pronounced influence on the low-energy portions of the s-state spectra (Glauber and Martin, 1956).

A particular advantage of introducing the second-order Green's function is that, consistent with the use of nonrelativistic wave functions, an approximate Green's function $g_E^I(\underline{r}, \underline{r})$ can be employed,²⁰ which has a particularly simple structure. This Green's function, obtained by neglecting the $(Z\alpha/r)^2$ and $Z\alpha \underline{\alpha} \cdot (\underline{v}/r)$ terms in Eq. (4-8) and solving the resulting equation, has been studied in considerable detail by Glauber and Martin (1956). In particular, $g_E^I(0, r)$ has been shown to possess the integral representation²¹

$$g_E^I(0, r) = (\mu/2\pi) e^{-\mu r} \int_0^\infty ds s^{-\eta} (1+s)^{\eta} e^{-2\mu r s}, \quad (4-19)$$

where $\mu = (1-E^2)^{1/2}$ and $\eta = Z\alpha E/\mu$.

(i) s-state radiative capture. For radiative capture from an s state, the contribution to M_α from the $e^{*} \underline{\alpha} \cdot \underline{V}$ term vanishes from symmetry considerations; when terms of order $Z\alpha$ are neglected, the remaining contribution can be evaluated using only very general properties of the Green's function.²² Final results for the transition rates are identical with those of the Coulomb-free theory [Eq. (4-14) et seq.]. The calculations of Glauber and Martin (1956) reveal, however, that the range of validity of the Coulomb-

free theory is much greater than could have been anticipated on the basis of the calculations of Møller (1937a) or Morrison and Schiff (1940). Indeed, it was established by Glauber and Martin (1956) that the Coulomb-free theory yields results for the IB spectra associated with s-state capture which are formally correct to order $Z\alpha$ for all photon energies. It is also true however, that for the low-energy portion of s-state spectra, the factor of $Z\alpha$ is partially compensated by an increased probability of radiation. Consequently, in order to obtain results for which the actual error is not greater than order $Z\alpha$, it is necessary to carry the calculations to the next order in $Z\alpha$ and omit only those terms which are actually of order $Z\alpha$ or less. Glauber and Martin (1956) accomplished this by means of a Foldy-Wouthysen transformation applied to the Dirac-Coulomb wave functions and Green's function. The result, valid for $\eta < 2$ and $k \lesssim \alpha$, is

$$M_{ns} = ieC_V (\pi/2k^3)^{1/2} \int_{\mu}^{\infty} \phi_{ns}^{(0)}(0) \Gamma_{\mu} [\Sigma \cdot \underline{e} \times \underline{k} + ik \cdot \underline{e} B_{ns}^*] \phi_{ns}^{(0)}(0). \quad (4-20)$$

The function $B_{ns}(k)$ is defined by

$$B_{ns}(k) = 1 + \frac{2}{3\phi_{ns}^{(0)}(0)} \int dr g_E^{(1)}(0,r) r \frac{d}{dr} \phi_{ns}(r), \quad (4-21)$$

where $g_E^{(1)}(0,r)$ is the p-wave contribution to the partial-wave expansion of the approximate Green's function $g_E^i(\underline{r}_N, \underline{r})$, $g_E^i(\underline{r}_N, \underline{r}) = g_E^i(0,r) + g_E^{(1)}(0,r) \underline{r}_N \cdot \underline{r} + \dots$. The transition rate is calculated as before, with the result

$$\frac{dw_{ns}}{w_K} = \left(\frac{dw_{ns}}{w_K} \right)_{CF} R_{ns} = \frac{\alpha}{\pi} \frac{|\phi_{ns}^{(0)}|^2}{|\phi_{1s}^{(0)}|^2} \frac{k(q_{ns} - k)^2}{q_{1s}^2} R_{ns} dk. \quad (4-22)$$

The correction factor $R_{ns}(k)$, which describes the modification of the Coulomb-free result brought about by inclusion of the most important relativistic and Coulomb effects, is defined by

$$R_{ns}(k) = (1/2)(1+B_{ns}^2). \quad (4-23)$$

The evaluation of the functions $B_{ns}(k)$ has been described in great detail by Glauber and Martin (1956). Here we quote only the final results,

$$B_{1s}(k) = 1 - \frac{4}{3} \frac{\eta_1}{(1+\eta_1)} \left\{ 1 + \frac{\eta_1}{(1-\eta_1)} [2K(\lambda_1) - 1] \right\}, \quad (4-24)$$

with $\lambda_1 = (1-\eta_1)/(1+\eta_1)$, and

$$B_{2s}(k) = 1 - \frac{\eta_2}{(1-\eta_2^2/4)} \left(\frac{4}{3} + \frac{5}{6} \eta_2^2 \right) - \frac{\eta_2^2}{(1-\eta_2^2/4)^2} \times \left[\frac{8}{3} (1-\eta_2^2) K(\lambda_2) - 3 - \eta_2 + \frac{5}{4} \eta_2^2 \right], \quad (4-25)$$

with $\lambda_2 = (2-\eta_2)/(2+\eta_2)$. The function $K(\lambda)$ is

$$K(\lambda) = \lambda \int_0^1 \frac{dX X^{-\eta}}{(1+\lambda X)}. \quad (4-26)$$

For the purpose of evaluation, $K(\lambda)$ can be represented conveniently by the rapidly converging series expansion

$$K(\lambda) = \ln(1+\lambda) - \eta \sum_{j=1}^{\infty} \frac{(-\lambda)^j}{j(j-\eta)}. \quad (4-27)$$

In arriving at these final results, advantage has been taken of the fact that E may be set equal to one in the correction term,

so that $\eta = Z\alpha/\mu$. Consequently, the two parameters Z and k , upon which the functions B_{ns} depend, enter only in the single combination η which, in the present approximation, is given by $\eta_{1s} = (1+k/B_{1s})^{-1/2}$ for 1s-state capture and by $\eta_{2s} = (1/4+k/B_{1s})^{-1/2}$ for 2s-state capture. Here, B_{1s} is the 1s-state binding energy. This simplification greatly facilitates tabulation of final results.

With the aid of Eq. (4-27), we have evaluated Eq. (4-24) and Eq. (4-25) numerically (Tables 4.1 and 4.2). Although for energies not greatly exceeding the binding energy, $B_{1s}(k)$ increases quite rapidly from its value of zero at $k=0$, the function approaches its asymptotic value of unity quite slowly. The correction factor $R_{1s}(k)$ therefore remains substantially less than unity, even at energies very much larger than the binding energy. Like $R_{1s}(k)$, $R_{2s}(k)$ also slowly approaches unity for large k . Unlike $B_{1s}(k)$, however, $B_{2s}(k)$ does not go to zero as k approaches zero; rather, as may be shown analytically, $B_{2s}(0) = 3/2$.

The functions $B_{ns}(k)$ for $n \geq 3$ can be evaluated similarly. However, the contributions to radiative electron capture from ns states with $n \geq 3$ can usually be neglected entirely, compared with contributions from 1s and 2s states. For example, according to the above results the 3s-state intensity is only ~4% of the 1s-state intensity; when screening effects are taken into account, its contribution is reduced even more.

(ii) p-state radiative capture. From the calculations of Morrison and Schiff (1940) it can be concluded that the p-state

capture contribution to the IB spectrum is negligibly small for $k \gg Z\alpha$. As the calculations of Glauber and Martin (1956) bear out, however, the p-state intensity becomes quite appreciable for $k \lesssim Z\alpha$ and indeed exceeds the s-state spectrum over a large part of this range. Discussion of p-state radiative capture can therefore be restricted to photon energies $k \lesssim Z\alpha$. In this energy region, the transition matrix element can be reduced to

$$M_{np} = -2ieC_v (2\pi/k)^{1/2} J_{\mu}^{N\Phi} v(0) \Gamma_{\mu} \int d\underline{r} g_E^I(0, \underline{r}) \underline{e} \cdot \underline{\nabla} \phi_{np}(\underline{r}) \quad (4-28)$$

when terms of order $Z\alpha$ are neglected. It is clear that the IB radiation associated with p-state capture is distributed isotropically.

Since the three np-state wave functions transform like the components of a vector under rotations, one of them can conveniently be chosen to be the component in the direction of \underline{e} . The remaining two component states then do not contribute to the matrix element, and a single calculation takes into account the contributions from all three magnetic substates. On this basis, the matrix element can be written

$$M_{np} = -2ieC_v (Z\alpha/k)^{1/2} J_{\mu}^{N\Phi} v(0) \Gamma_{\mu} X_{np} Q_{np}, \quad (4-29)$$

where X_{np} is the spin part of the np-state wave function, and the integral $Q_{np}(k)$ is

$$Q_{np}(k) = (2\pi/Z\alpha)^{1/2} \int d\underline{r} g_E^I(0, \underline{r}) \underline{e} \cdot \underline{\nabla} \phi_{np}(\underline{r}). \quad (4-30)$$

The transition rate is calculated as before, with the result

$$\frac{dw_{np}}{w_K} = \frac{4}{\pi Z^2 \alpha} [\mathcal{Q}_{np}(k)]^2 \frac{k(q_{np}-k)^2}{q_{1s}^2} dk. \quad (4-31)$$

Evaluation of the integrals $\mathcal{Q}_{np}(k)$ is similar to that of $B_{ns}(k)$ and has also been described in detail by Glauber and Martin (1956). The final results are

$$\mathcal{Q}_{2p}(k) = \frac{\eta_2^2}{4(1-\eta_2^2/4)^2} [1 + (2/3)\eta_2 - (7/12)\eta_2^2 + (4/3)\eta_2^2 E(\eta_2)] \quad (4-32)$$

and

$$\mathcal{Q}_{3p}(k) = \frac{4}{27} \frac{\eta_3^2}{(1-\eta_3^2/9)^3} \left\{ (1-\eta_3/3) [1-\eta_3 - 2(\eta_3/3)^2 - 2(\eta_3/3)^3] + (4/3)\eta_3^2 (1-\eta_3^2/3) E(\lambda_3) \right\}, \quad (4-33)$$

where $\eta_3 = (1/9 + k/B_{1s})^{-1/2}$, all other quantities having been defined previously. Evaluation of Eqs. (4-32) and (4-33) yields the results shown in Table 4.3.

(iii) Results. To illustrate the results of the theory of Glauber and Martin (1956), the predicted spectra associated with 1s-, 2s-, 2p-, and 3p-state radiative capture in ^{55}Fe have been plotted in Fig. 4-2. As stated, terms of order $Z\alpha$ were neglected, introducing an error of ~20% for ^{55}Fe . It is evident from Fig. 4-2 that the s-state spectra do not differ greatly in form from the simple $k(q_{ns}-k)^2$ shape predicted by the Coulomb-free theory. Figure 4-2 also shows the existence of very intense p-state spectra at low photon energies. Indeed, p-state contributions to

the IB spectrum become more dominant with increasing charge and decreasing available energy.

For states of still higher orbital angular momentum, the radiative capture probability is expected to be much smaller than for capture from s or p states, because the probability of finding the electron in the neighborhood of the nucleus is smaller and the radiation emitted is of a higher multipole order than the predominantly M1 and E1 radiation associated with s- and p-state radiative capture, respectively. Indeed, within the framework defined by the approximations used in treating p-state capture, the transition amplitude for radiative capture from a state of orbital angular momentum >1 vanishes.

Relativistic calculations. The preceding calculations were intended to provide results with a relative accuracy of order $Z\alpha$. To achieve even this level of accuracy requires that some consideration be given to relativistic effects when treating radiative capture from s states. The importance of relativistic effects in s-state capture, even for moderately light nuclei, is primarily due to the fact that such transitions involve a spin flip, a process which results in large photon energies, and hence, in a relativistic recoil by the electron. Furthermore, a nonrelativistic calculation does not take account of paths that involve virtual positron emission and neglects electron capture through intermediate p states, a path made possible by spin-orbit coupling.

The results described above are usually adequate to determine the IB spectra of moderately light nuclei for photon energies that

are small compared with the electron rest energy. For heavy nuclei or large photon energies, these results are wholly inadequate. Martin and Glauber (1958) therefore developed a more general theory, taking full account of relativistic and Coulomb effects. The nonrelativistic results indicate that relativistic and Coulomb effects to all orders in $Z\alpha$ are most important in radiative capture from $1s$ states, hence Martin and Glauber (1958) applied their full theory to this specific calculation.

It should be noted that Yukawa (1956) has also attempted a fully relativistic calculation of the K-capture IB spectrum. Yukawa found it necessary, however, to introduce an approximation in constructing a usable form for the relativistic Coulomb Green's function; it is not entirely clear how reliable this approximation is. The results of Yukawa (1956) are at least as complicated as those of Martin and Glauber (1958) and have the serious drawback of being inapplicable to heavy nuclei. For these reasons, we do not discuss Yukawa's calculations further.

(i) $1s$ -state radiative capture. The starting point for the fully relativistic calculations of Martin and Glauber (1958) is the general expression (4-11) for the allowed-transition matrix element. To evaluate this matrix element exactly within the one-electron Coulomb approximation, appropriate forms for ϕ_{1s} and $G_E(\underline{r}_N, \underline{r})$ must first be introduced. For ϕ_{1s} , the usual ground-state solution of the Dirac equation for an electron moving in the Coulomb field of a nuclear charge Ze is chosen. For the exact second-order Green's function $G_E(\underline{r}_N, \underline{r})$, Martin and Glauber (1958)

ORIGINAL PAGE IS
OF POOR QUALITY

constructed an eigenfunction expansion from the solutions of Eq. (4-8). The smallness of the nuclear radius ($2\mu r_N \leq 10^{-3}$) allows some simplification. The region occupied by the nucleus may be safely neglected in integrating over r , and those functions in the Green's-function expansion which depend on r_N can be replaced by the first term in their power-series expansion. The errors associated with the use of this simplified form of the exact Green's function are expected to be no greater than $\sim 10^{-3}$.

Using the above representations, Martin and Glauber (1958) calculated the transition matrix element for allowed radiative K capture without further approximations,

$$M_{1s} = \frac{ieC}{k} (\pi/k)^{1/2} \sum_{\lambda} \langle \phi_{1s} \rangle_{\Omega} \bar{\psi}^{\nu}(0) \Gamma_{\lambda} [A_{1s} \Sigma \cdot e^{-ik} + ik B_{1s} \alpha \cdot e^{-ik}] \chi_{+}^{\mu}. \quad (4-34)$$

The particular angular-momentum substate of the initial K electron is represented through the spin function $\chi_{+}^{\mu} = \begin{pmatrix} \chi^{\mu} \\ 0 \end{pmatrix}$, where χ^{μ} are the usual two-component Pauli spinors, and the integrals $A_{1s}(k)$ and $B_{1s}(k)$ are defined by

$$A_{1s}(k) = \frac{(\lambda_1+1)k}{\Gamma(2\lambda_1+1)\mu} \int_0^{\infty} dr \int_0^{\infty} ds$$

$$\left\{ j_0(kr) \left[1 + \frac{a^2}{3(\lambda_1+1)^2} \right] - \frac{j_1(kr)2a^2}{kr(\lambda_1+1)^2} - \frac{j_2(kr)2a^2}{3(\lambda_1+1)^2} \right\}$$

$$\times s^{-\eta+\lambda_1-1} (1+s)^{\eta+\lambda_1-1} (2\mu r)^{2\lambda_1} e^{-(2s+1)\mu r} e^{-ar}, \quad (4-35a)$$

$$\begin{aligned}
B_{1s}(k) &= \frac{(\lambda_1+1)k}{\Gamma(2\lambda_1+1)\mu} \int_0^{\infty} dr \int_0^{\infty} ds \\
&\left\{ j_0(kr) \left[1 - \frac{4a}{3(\lambda_1+1)} \left(\frac{\lambda_1}{kr} - \frac{a}{k} \right) + \frac{a^2}{3(\lambda_1+1)^2} \right] + j_2(kr) \left[\frac{4a}{3(\lambda_1+1)} \right. \right. \\
&\quad \left. \left. \times \left(\frac{a}{k} + \frac{(3-2\lambda_1)}{2kr} \right) - \frac{2a^2}{3(\lambda_1+1)^2} \right] \right\} \\
&\times s^{-\eta+\lambda_1-1} (1+s)^{\eta+\lambda_1-1} (2\mu r)^{2\lambda_1} e^{-(2s+1)\mu r} e^{-ar}. \quad (4-35b)
\end{aligned}$$

In Eqs. (4-35), the previous definitions of μ and η have been retained, and we have $a=Z\alpha$ and $\lambda_1=(1-a^2)^{1/2}=\epsilon_{1s}$.

The energy spectrum of the IB, calculated as before, is

$$\frac{dw_{1s}}{w_K} = \frac{\alpha}{\pi} \frac{k(q_{1s}-k)^2}{q_{1s}^2} R_{1s} dk. \quad (4-36)$$

This expression is the same as Eq. (4-22) for 1s capture, except that $R_{1s}(k)$ is defined by

$$R_{1s}(k) = \frac{1}{2} (A_{1s}^2 + B_{1s}^2), \quad (4-37)$$

with $A_{1s}(k)$ and $B_{1s}(k)$ given by Eqs. (4-35). Unfortunately, the integrals appearing in Eqs. (4-35) cannot be evaluated exactly analytically in closed form and depend separately on Z and k , rather than on the single combined parameter $k/(Z\alpha)^2$ as do the integrals B_{ns} and Q_{np} discussed earlier.

A number of limited and, in most cases, approximate analytic results for A_{1s} and B_{1s} are reported by Martin and Glauber (1958).

For example, Eqs. (4-35) can be simplified, transformed, and expanded if one neglects terms of order $(Z\alpha)^2$ or smaller and the remaining contribution to $B_{1S}(k)$ from the $j_2(kr)$ term. The results are

$$A_{1S}(k) = \text{Im} \left[2/(\mu+a-ik) + (\eta\mu/k)(\lambda_1+ia)\zeta \right], \quad (4-38a)$$

$$B_{1S}(k) = A_{1S}(k) \left(1 + \frac{2}{3} a^2/k - \frac{2}{3} (a/k)^2 \frac{\eta}{\mu} \zeta \right), \quad (4-38b)$$

where

$$\zeta = 2 \left[\ln \left(\frac{\mu+a+ik}{2\mu} \right) + \eta \sum_{n=1}^{\infty} \frac{1}{n(n-\eta)} \left(\frac{a+ik-\mu}{a+ik+\mu} \right)^n \right] \quad (4-39)$$

Because of the underlying approximations, these expressions are expected to hold well only at low photon energies and for elements which are not too heavy.

For $k \gg 1$, it is feasible to expand the Green's function and the initial-state wave function in powers of $Z\alpha$. Carried to first order in $Z\alpha$, such expansions yield

$$A_{1S}(k) = 1 - Z\alpha \left\{ (\mu/k) + 2 \left(1 - \frac{1}{k} \right) \tan^{-1}(k/\mu) \right\}, \quad (4-40a)$$

$$B_{1S}(k) = 1 - Z\alpha \left\{ (\mu/k) \left(1 + \frac{1}{k} \right) + 2 \left(1 - \frac{1}{k^2} \right) \tan^{-1}(k/\mu) \right\}. \quad (4-40b)$$

For three particular photon energies, more accurate results can easily be obtained because of special circumstances which simplify the calculation in each case. In the neighborhood of $k=0$, A_{1S} and B_{1S} are given, exact to all orders in $Z\alpha$, by

$$A_{1s}(k) = \frac{(2\lambda_1+1)}{3} (1-k), \quad (4-41a)$$

$$B_{1s}(k) = O(k/Z\alpha). \quad (4-41b)$$

The integrals can be evaluated conveniently to second order in $Z\alpha$ for $k=\lambda_1$ ($\eta=0$),

$$A_{1s}(k) = 1-Z\alpha+\pi(Z\alpha)^2/4, \quad (4-42a)$$

$$B_{1s}(k) = 1-2Z\alpha+(4-\pi/2)(Z\alpha)^2, \quad (4-42b)$$

and for $k=1+\lambda_1$ ($\mu=0$),

$$A_{1s}(k) = 1-\pi Z\alpha/2+2(Z\alpha)^2, \quad (4-43a)$$

$$B_{1s}(k) = 1-3\pi Z\alpha/4+9(Z\alpha)^2/2. \quad (4-43b)$$

These approximate results are expected to be fairly reliable for the lighter elements. In general, however, it is necessary to resort to numerical procedures. The above results are still of interest, though, since they provide a valuable check on the accuracy of numerical computations.

A relatively simple procedure for obtaining exact numerical results for A_{1s} and B_{1s} for arbitrary k and Z has been reported by Intemann (1971). The integration over r in Eqs. (4-35) is performed first, then the change of variable $x=s/(1+s)$ is made in the remaining integrals. After algebraic reduction, one finds

$$A_{1s}(k) = C \int_0^1 dx x^{-\eta+\lambda_1-1} f_A(x), \quad (4-44a)$$

$$B_{1s}(k) = \frac{C}{2k(1-\lambda_1)} \int_0^1 dx x^{-\eta+\lambda_1-1} f_B(x), \quad (4-44b)$$

where $C = -(2\mu)^{2\lambda_1-1} / [\lambda_1(2\lambda_1-1)k^2]$. To define f_A and f_B , it is convenient to introduce the definitions

$$\begin{aligned} \Sigma &= k^2 + (\mu+a)^2, & s &= \Sigma + \epsilon x + \delta x^2, \\ \epsilon &= 2(\mu^2 - a^2 - k^2), & \sigma &= a + \mu(1+x)/(1-x), \\ \delta &= k^2 + (\mu-a)^2, & \theta &= \tan^{-1}(k/\sigma). \end{aligned}$$

whence f_A and f_B can be written

$$f_A(x) = [2k\lambda_1\sigma \cos(2\lambda_1\theta) - \sigma^2 \sin(2\lambda_1\theta)] / s^{\lambda_1}, \quad (4-45a)$$

$$\begin{aligned} f_B(x) &= (2k\lambda_1\sigma [\sigma - 2a^2 + (1-\lambda_1)k] \cos(2\lambda_1\theta) \\ &+ \{k^2(2\lambda_1-1)[k(\lambda_1-1) - 2a^2 + \sigma] + \sigma^2[2a^2 - k(1-\lambda_1) - \sigma]\} \sin(2\lambda_1\theta) / s^{\lambda_1}. \end{aligned} \quad (4-45b)$$

Now f_A and f_B are very slowly varying functions of x over the entire range of integration, for all physical values of k and Z of interest. After an integration by parts to remove the weak singularity in each of the integrands at $x=0$, the remaining integrals which appear in A_{1s} and B_{1s} thus can easily be evaluated

in this manner for several nuclides of interest, are displayed in Fig. 4-3:

It is considerably easier to evaluate A_{1s} and B_{1s} by means of the low- k approximation [Eqs. (4-38) and (4-39)] or the high- k approximation [Eqs. (4-40)], rather than by employing the exact results [Eqs. (4-44)]. Therefore it is of interest to compare the functions $R_{1s}(k)$ obtained in these three ways, in order to assess the circumstances under which either of the approximate results can be employed without significant error. We have evaluated $R_{1s}(k)$ exactly and in the high- and low- k approximations for three very different values of Z . The results, shown in Fig. 4-4, are indistinguishable for very small Z over almost the entire energy range. For intermediate Z , the low- k approximation fits the exact curve quite well, even in the high-energy region where it does better than the high- k approximation. For large Z , neither approximation fits the exact result very well, and both approximations are totally wrong in their description of the low-energy behavior of $R_{1s}(k)$.

To compare the various calculations and indicate the importance of relativistic and Coulomb effects, we have plotted in Fig. 4-5 the $1s$ -state radiative capture spectra predicted for the moderately light nucleus ^{55}Fe . It is evident from Fig. 4-5 that the shape of the $1s$ spectrum is not substantially altered by the inclusion of relativistic and Coulomb effects, but that the overall intensity experiences a very significant reduction. As is to

exact calculation (MG) and that in which terms of order $Z\alpha$ are neglected (GM) agree fairly well. There will be no such agreement for heavy nuclei or for photon energies $k \gg 1$.

(ii) L- and M-shell radiative capture. Although Martin and Glauber (1958) limited their fully relativistic calculations to 1s-state capture, their relativistic theory provides an equally valid basis for describing radiative capture from an arbitrary atomic shell. The general results of such a calculation are given by Zon (1971). The complexity of the expressions has precluded the derivation of analytical results; not even approximate results have been derived in which only terms through first order in $Z\alpha$ are retained. Zon (1971) does however report the construction of a computer program which permits numerical evaluation of the amplitude for radiative capture from the L and M shells, although few details are given and the only spectra reported in Zon's paper are those for ^{165}Er (Fig. 4-6).

Two general features of the ^{165}Er spectra are worth noting since they undoubtedly will be exhibited by the radiative capture spectra of other nuclei as well. A resonance in the 2s-state capture spectrum appears which is associated with a forbidden 2s-1s atomic transition. This resonance is quite sharp and therefore modifies the result of Glauber and Martin (1956) only in the binding-energy region. Elsewhere, the results of Zon (1971) and of Glauber and Martin (1956) are indistinguishable. Also to be noted are the modifications of the p-state spectra brought about by the inclusion of all relativistic and Coulomb effects. While

these modifications appear to be only slight for capture from 3p states, they are quite important for the 2p-state spectrum (at least for heavy nuclei). In the case of ^{165}Er , they cause a reduction by a factor of ~ 2 in the overall intensity of the 2p-state spectrum. There is, however, no appreciable change in the form of the p-state capture energy distributions.

Some years ago it was suggested by Koh et al. (1962), and again by Koh (1965), that the IB spectrum possesses a cusp-shaped irregularity in the neighborhood of the positron threshold. To confirm this idea, Zon and Rapoport (1968) carried out extensive calculations. Their results, accurate to order $(Z\alpha)^2$, show however that the form factor for radiative K capture varies continuously in this region, and thus, there is no such anomaly in the predicted spectrum at this level of accuracy.

Influence of Uncaptured Atomic Electrons

In all of the foregoing calculations, only the electron which undergoes radiative capture is considered, and the presence of all other atomic electrons has been ignored. We now consider how, and to what extent, the one-electron results are modified when the presence of the remaining atomic electrons is taken into account.

Screening corrections. Screening by the remaining electrons affects the amplitude for radiative capture both by altering the initial configuration of the electron to be captured and by altering the probability amplitude for an electron to reach the nucleus

after the virtual emission of a photon. To analyze these effects most simply, Martin and Glauber (1958) employed an independent-particle model in which the stationary states of the individual electrons are determined as the self-consistent-field solutions for the full many-body atomic Hamiltonian. In this approximation, no further account of the remaining electrons needs to be taken when the radiative transition probability for a single electron is calculated.

By far the more important effect of screening is the modification of the wave function that describes the initial electronic state. This modification is quite similar to that which occurs in ordinary electron capture, except that the effective size of the region from which capture can occur is somewhat larger. In ordinary electron capture, this region is determined by the nuclear radius, while in radiative electron capture it is determined by the range of the Green's function. For photon energies of greatest practical interest, above the binding energy of the initial electron and below the threshold for positron production, the range of the Green's function is of the order of the electron's Compton wavelength. While it is much larger than the nuclear radius, this range is still very small on an atomic scale. Thus, it is argued by Martin and Glauber (1958) that a simple and seemingly reasonable procedure for taking into account screening effects on the initial state of an electron undergoing radiative capture is to multiply the unscreened results for the radiative capture probability amplitude by the ratio of the screened to

unscreened initial-state wave functions, evaluated in the neighborhood of the origin.

The second effect of screening, the alteration in the structure of the Green's function, is expected to be quite small; this can be understood qualitatively from the following considerations (Martin and Glauber, 1958). Over the relatively small region defined by the range of the Green's function, the electron field is well approximated by the nuclear Coulomb field. Indeed, if the electronic charge cloud associated with the remaining atomic electrons did not penetrate this region at all, its external presence would simply result in a shift in the zero of energy and thus produce no physical effects. For all but the lowest-energy photons, the range of the Green's function is so small that penetration of the electronic charge cloud into the region defined by this range is not expected to be appreciable, and therefore no significant modification in the Green's function is expected. It should be emphasized, however, that this reasoning is not valid for photon energies near the binding energy, where the range of the Green's function becomes quite large and a more elaborate treatment of screening is required.

To establish in quantitative terms the accuracy of the simple approximation scheme of Martin and Glauber (1958), these authors carried out more extensive calculations in which the screened Coulomb potential was approximated by a Hulthen potential. The results of these calculations indicate that the above conclusions are quite well-founded. In particular, Martin and Glauber (1958)

calculated the screening corrections for the 2p state of Fe to lowest order in the Hulthen parameter. The results were compared with unscreened results multiplied by the ratio of the screened to unscreened probability densities at the origin. At a photon energy equal to the K-shell binding energy in Fe, the difference between these two results was found to be ~20% (i.e., of order $Z\alpha$), while at a photon energy three times as large the difference is only ~2%. Thus it appears that, except at very low photon energies (in the immediate neighborhood of the K-shell binding energy), screening effects can be taken into account satisfactorily by simply multiplying the unscreened rate for radiative capture from the state α by the screening factor

$$S_{\alpha} = \left| \frac{\psi_{\alpha}^{sc}(R_N)}{\psi_{\alpha}(R_N)} \right|^2, \quad (4-46)$$

where R_N is the nuclear radius.

From results of Brysk and Rose (1958) and available Hartree calculations, Martin and Glauber (1958) have constructed a graph of S_{α} vs. Z for initial states of interest (see Fig. 4-7). It appears that the intensities of the IB spectra for radiative capture from the L shell are considerably reduced by screening effects and those for radiative capture from higher shells become insignificant.

If the intensities of the various IB spectra are normalized to a single K-capture event, or to a single EC event, then only the ratios S_{α}/S_{1s} appear in the final formulas. To evaluate these ratios for the most important case, the L shell, results of

Sec. 2.2.2 can be used when a high degree of accuracy is desired.²³ The ratios are

$$\frac{S_{2s}}{S_{1s}} = \left| \frac{G_K}{G_{L_1}} \frac{g_{L_1}}{g_K} \right|^2 \quad (4-47a)$$

and

$$\frac{S_{2p}}{S_{1s}} = \left| \frac{G_K}{F_{L_2}} \frac{f_{L_2}}{g_K} \right|^2 \quad (4-47b)$$

Here, G_K , G_{L_1} , and F_{L_2} are the large components of the unscreened Dirac wave function for the 1s, 2s, and 2p states, respectively, evaluated at the nuclear radius of a hydrogenic atom. The large components are denoted by g_K , g_{L_1} , and f_{L_2} , respectively, when the effects of screening are included.

Plots of G_K , G_{L_1} , and F_{L_2} for a point nucleus and corrections for finite nuclear size are given by Brysk and Rose (1958) (finite-nuclear-size corrections to the L-shell screening ratios are always <1%).²⁴ As discussed in Sec. 2.2.2, the ratios $(g_{L_1}/g_K)^2$ and $(f_{L_2}/g_{L_1})^2$ have been calculated by several authors; the most reliable results being those displayed in Table 2.9. These ratios were computed with a relativistic Hartree-Fock self-consistent potential with allowance for finite nuclear size.

The procedure described above is but one possible way in which screening effects can be treated. Alternatively, Zon (1971) has included screening effects by employing relativistic initial-state Coulomb wave functions with effective charges. These effective charges, as suggested by work on internal conversion, were taken to be $Z_{\text{eff}} = Z - \sigma$, with $\sigma_K = 0.3$, $\sigma_L = 3.5$, and $\sigma_M = 5$. Zon (197

has carried out several numerical calculations but does not compare his results with those obtained by the simpler procedure of Martin and Glauber (1958).

Exchange and overlap corrections. All results described so far, including screening corrections, are based on independent-particle approximations and take no account of exchange and overlap effects which result from the many-particle nature of the atom (see also Sec. 2.5). Corrections for such effects have been applied to the Martin-Glauber theory by Persson and Koonin (1972), using a procedure analogous to that applied by Bahcall (1962) to L/K electron-capture ratios. The calculations of Persson and Koonin (1972) deal specifically with the electron-capturing nucleus ${}^7\text{Be}$, but are easily generalized.

It is found that, for EC decays of ${}^7\text{Be}$ to the 477-keV state of ${}^7\text{Li}$, the predominant effect of exchange and overlap corrections is to increase the ratio of 2s-state radiative capture to 1s-state radiative capture w_{2s}/w_{1s} by a factor of 2.9. The ratio of the 1s-state radiative capture rate to the total (K+L) nonradiative capture rate $w_{1s}/(w_K+w_L)$ is decreased by 7%. However, the net effect on the ratio $(w_{1s}+w_{2s})/(w_K+w_L)$ is found to be negligibly small (<1%). Changes in the shape of the IB spectrum at energies above 50 keV are found to be negligible.

Calculations of overlap and exchange effects in radiative EC of ${}^{51}\text{Cr}$ and ${}^{54}\text{Mn}$ are reported by Koonin and Persson (1972), who find that w_{2s}/w_{1s} is increased by 15% over the Martin-Glauber predictions. This increase is cancelled, however, by a similar

increase in the corresponding ratio for nonradiative capture, so that the correction to the ratio $(w_{1s} + w_{2s}) / (w_K + w_L)$ is again found to be insignificant ($< 0.5\%$).

4.1.3. IB Correlation Effects in Allowed Transitions

With the discovery of parity nonconservation in weak interactions, interest in radiative electron capture shifted to studies of those correlation effects whose existence requires a parity-violating interaction. Calculations on such phenomena were reported by Cutkosky (1957), Koh et al. (1957, 1962), Berestetskii (1958), Martin and Glauber (1958), Gandel'man (1959), Bloom and Uretsky (1960), and Timashev and Kaminskii (1960).

Cutkosky (1957) first showed that a two-component neutrino theory predicts that IB radiation will be circularly polarized. Terms of order $Z\alpha$ were neglected in Cutkosky's calculations, but a determination of the polarization of the IB associated with K capture, valid to all orders in $Z\alpha$, was reported shortly thereafter by Martin and Glauber (1958). Only the polarization of the $1s$ -state contribution to the IB spectrum is considered in these papers, yet it is evident from the results of Sec. 4.1.2. that at low photon energies the contributions from L- and M-shell radiative capture must also be taken into account. For allowed transitions, this is easily accomplished using the theory of Glauber and Martin (1958). More elaborate calculations, based on a generalization of the Martin-Glauber theory, are reported by Zon (1971), who lists numerical results for ^{37}Ar .

The parity-nonconserving character of the weak interaction is also responsible for the existence of an anisotropy in the angular distribution of the IB radiation emitted from oriented nuclei, as may be inferred from the work of Cutkosky (1957). This makes IB angular-distribution studies of interest as a potential source of information on nuclear spin changes and the relative magnitudes of the EC nuclear matrix elements. The angular distribution of the IB emitted from oriented nuclei during K capture was first calculated by Timashev and Kaminskii (1960) and by Koh et al. (1962), assuming a nonrelativistic description of the electronic motion and neglecting all Coulomb effects on the intermediate states of the electron. The results of these calculations are quite simple, but they have proved inadequate to explain the experimental data at low photon energies, where both intermediate-state Coulomb effects and the contributions from L- and M-shell radiative capture become important. More exact and extensive calculations, based on the work of Glauber and Martin, have been reported by Intemann (1971) and by Zon (1971).

While the existence of the IB correlation effects described above depends on the parity-nonconserving property of the weak interaction, a variety of other correlation phenomena exist which could arise even if parity were conserved. (From the point of view of testing weak-interaction theory, these phenomena are of little interest, but they can provide information on nuclear structure.) In particular, Koh et al. (1957, 1962) have studied

the correlations between the direction of nuclear spin, the momentum of the IB photon, and the momentum of a subsequent nuclear γ ray, and have reported detailed results on the correlation between the directions of the IB photon and the nuclear γ ray. These calculations were, however, carried out for allowed and first-forbidden transitions and neglect Coulomb effects on the intermediate electron states; thus they are limited to high photon energies. More extensive calculations of this correlation function, based on a generalization of the work of Martin and Glauber (1958), have been reported by Zon (1971). This latter work includes a determination of the correlation between the directions of the IB photon and a subsequently emitted atomic x ray.

IB Circular Polarization

The polarization $P_\alpha(k)$ of the IB accompanying electron capture from the state α is defined as the difference in the intensities of the right- and left-circularly polarized radiation, divided by their sum:

$$P_\alpha(k) = \frac{d\omega_\alpha^{+1} - d\omega_\alpha^{-1}}{d\omega_\alpha^{+1} + d\omega_\alpha^{-1}} . \quad (4-48)$$

For 1s-state radiative capture, the required expressions for the intensity of the polarized radiation are obtained from Eq. (4-34) by squaring and summing over all final states of the unobserved neutrino and over the spin states of the initial electron. The

result for randomly oriented nuclei is

$$dw_{1s}^s(k) \propto [A_{1s}(k) + sB_{1s}(k)]^2, \quad (s = \pm 1).$$

The polarization of the IB accompanying 1s-state capture is found to be

$$P_{1s}(k) = \frac{(A_{1s} + B_{1s})^2 - (A_{1s} - B_{1s})^2}{(A_{1s} + B_{1s})^2 + (A_{1s} - B_{1s})^2} = A_{1s}B_{1s}/R_{1s}. \quad (4-49)$$

At low photon energies, the 1s-state radiation is almost completely unpolarized since $B_{1s}(k) \rightarrow 0$ as $k \rightarrow 0$. At high energies, we have $A_{1s} = B_{1s} = 1$, neglecting terms of order $Z\alpha$, and due to cancellation, $P_{1s}(k) = +1$ neglecting terms of order $(Z\alpha)^2$. More precisely, the high-energy form of $P_{1s}(k)$ is

$$P_{1s}(k) = 1 - (Z\alpha)^2 \left\{ (\mu/k) + 2\left(1 - \frac{1}{k}\right) \tan^{-1}(k/\mu) \right\}^2 / 2k^2, \quad (4-50)$$

which follows from Eq. (4-40).

The polarization of the 2s-state radiation can be analyzed similarly, starting with Eq. (4-20). The final result has the same structure as Eq. (4-49) except that, in the approximation which underlies Eq. (4-20), $A_{2s}(k) = 1$. Thus, we have

$$P_{2s}(k) = B_{2s}/R_{2s}. \quad (4-51)$$

While it is expected in the high-energy limit that $P_{2s}(k) = 1 - O(Z\alpha)^2$, the results which follow from Eq. (4-20) are not sufficiently accurate to allow the determination of the coefficient of the $(Z\alpha)^2$ term. The low-energy limit of $P_{2s}(k)$ is easily obtained, however,

by using the fact that $B_{2s}(0) = -3/2$. From this result it follows that $P_{2s}(0) = -12/13$.

To illustrate the above results, the functions A_{1s} , B_{1s} , B_{2s} and the resulting polarization functions have been evaluated for two nuclei of interest, *viz.* ^{37}Ar and ^{119}Sb (Figs. 4-8 and 4-9).

It is evident from Eqs. (4-29) and (4-30) that, when terms of order $Z\alpha$ are neglected, p-state radiation should be completely unpolarized. At low photon energies, where the p-state spectra dominate, one therefore expects an even greater reduction of the IB polarization than predicted by the function $P_{1s}(k)$. The overall polarization of the total IB radiation accompanying electron capture is

$$P(k) = \frac{\sum_{n=1}^2 s_{ns} P_{ns}(k) dw_{ns}}{\sum_{\alpha} s_{\alpha} dw_{\alpha}}, \quad (4-52)$$

where the sum on α extends over 1s, 2s, 2p, and 3p states.

Angular Distribution of IB from Oriented Nuclei

When the initial nuclei are aligned, it is convenient to represent each by its polarization vector $P_M = \langle J_i M | J_i | J_i M \rangle / J_i$, where J is the angular-momentum operator and J_i, M are the angular-momentum eigenvalues which label the initial nuclear state. In this case, squaring Eq. (4-34) and summing over all final states of the neutrino, the spin states of the initial electron, and the final magnetic substates of the nucleus leads to the following result for 1s-state radiative capture:

$$dw_{1s}^s(k) \propto (A_{1s} + sB_{1s})^2 [1 + sa_k P_M \cos \theta]. \quad (4-53)$$

Here, θ is the angle between the vectors P_M and k . The factor a_k vanishes for a pure Fermi transition, while for a pure Gamow-Teller transition we have

$$a_k = \begin{cases} -J_i/(J_i+1) & \text{if } J_f = J_i+1 \\ 1/(J_i+1) & \text{if } J_f = J_i \\ 1 & \text{if } J_f = J_i-1, \end{cases} \quad (4-54)$$

where J_f is the angular-momentum quantum number of the final nuclear state. For transitions in which both allowed EC matrix elements are operative, a_k is given by

$$a_k = \left[\frac{\lambda^2 |R|^2}{(J_i+1)} + \frac{\lambda J_i (R+R^*)}{[J_i(J_i+1)]^{1/2}} \right] (1 + \lambda^2 |R|^2)^{-1} \quad (4-55)$$

with

$$R = \langle f || \sigma || i \rangle / \langle f || 1 || i \rangle.$$

If the circular polarization s of the IB is measured, then the angular-distribution function has the simple form

$$w_{1s}(\theta, s) = 1 + sa_k P_M \cos \theta, \quad (4-56)$$

whence the shape of the angular distribution is seen to be independent of the energy of the IB photon.

If the photon polarization is not measured, Eq. (4-53) must be summed over $s = \pm 1$. This leads to an angular-distribution function of the form

$$w_{1s}(\theta) = 1 + \alpha_{1s}(k) a_k P_M \cos \theta. \quad (4-57)$$

The function $\alpha_{1s}(k)$ is defined by

$$\alpha_{1s}(k) = A_{1s} B_{1s} / R_{1s} \quad (4-58)$$

and is seen to be identical with the polarization function $P_{1s}(k)$ discussed earlier. Indeed, this one function is sufficient to account for the IB energy dependence of all 1s-state capture correlations considered here.

The angular distribution of the IB radiation accompanying 2s-state capture can be determined in a similar manner, starting with Eq. (4-20). It is found that the distribution function $W_{2s}(\theta, s)$ is identical with $W_{1s}(\theta, s)$. The function $W_{2s}(\theta)$ has the same general form as that for 1s-state capture, viz.,

$$W_{2s}(\theta) = 1 + \alpha_{2s}(k) a_{k^2} P_2 \cos^2 \theta, \quad (4-59)$$

but $\alpha_{2s}(k)$ is defined as

$$\alpha_{2s}(k) = B_{2s} / R_{2s}, \quad (4-60)$$

describing the dependence of the angular-distribution function on the energy of the IB photon. Again we have $\alpha_{2s}(k) = P_{2s}(k)$.

With regard to p-state radiation, it has already been noted that the structure of Eq. (4-29) implies an isotropic distribution, i.e., $\alpha_{np}(k) = 0$. This result is expected to be valid only to a relative accuracy of order $Z\alpha$. Indeed, Zon (1971) reports that exact computer calculations for α_{np} show α_{2p} and α_{3p} to be small negative quantities.

The overall angular-distribution function is given by

$$W(\theta) = \frac{\sum_{\alpha} s_{\alpha} \, d\omega_{\alpha} W_{\alpha}(\theta)}{\sum_{\alpha} s_{\alpha} \, d\omega_{\alpha}} = 1 + A(k) a_k P_M \cos \theta, \quad (4-61)$$

with the overall asymmetry function $A(k)$ defined by

$$A(k) = \frac{\sum_{\beta} s_{\beta} \, d\omega_{\beta} \alpha_{\beta}}{\sum_{\beta} s_{\beta} \, d\omega_{\beta}}. \quad (4-62)$$

In view of the equality of the asymmetry function and the polarization function for both s and p states, it follows that the overall asymmetry function $A(k)$ is identical with the overall polarization function $P(k)$ [Eq. (4-52)].

Correlation of IB and Subsequent Nuclear γ Rays

The simplest type of decay scheme for which the directional correlation between an IB photon and a subsequent nuclear γ ray can be studied is one in which the radiative capture transition leads to an excited nuclear state $|N_f^*\rangle$ from which there is a single γ -ray mode for deexcitation, leading to the final nuclear state $|N_f\rangle$. To determine the correlation between the directions of emission of the IB and γ -ray photons, a knowledge of the radiative capture matrix element must be combined with results from the theory of nuclear angular correlations (Frauenfelder and Steffen, 1966). The required calculation is straightforward but employs much mathematical machinery from the theory of angular momentum (Edmonds, 1960) and will not be described here. Such calculations were first reported by Gandel'man (1959) for allowed transitions, and by Koh *et al.* (1962) for allowed and

first-forbidden transitions. Although Coulomb effects on the intermediate electron states are neglected in these calculations, Zon (1971) has reported results of much more extensive calculations based on a generalization of the Martin-Glauber theory to radiative capture from arbitrary shells and for any order of forbiddenness of the EC transition. Only for the case of allowed radiative K capture, however, has Zon's theory been worked out in complete detail, and we shall restrict our discussion to this particular case.

For allowed K-capture transitions, the radiative capture matrix element of Zon (1971) reduces to that of Martin and Glauber (1958). For this particular case, Zon's final results can be summarized as follows. For an IB quantum of circular polarization s and a nuclear γ quantum of circular polarization t , the directional correlation function is of the form

$$W_{\gamma}(\theta, s, t) \propto (A_{1s} + sB_{1s})^2 + \frac{t}{\sqrt{2}} A_1 (LL' J_{ff} J_f) b_k S (A_{1s} + sB_{1s})^2 \cos \theta, \quad (4-63)$$

where the quantum numbers J_f and J_{ff} refer to the angular momentum of the nuclear states $|N_f^*\rangle$ and $|N_f\rangle$ respectively, and θ is the angle between the directions of the two photons. The factor b_k vanishes for a pure Fermi transition, while for a pure Gamow-Teller transition it is

$$b_k = \begin{cases} [(J_f+1)/J_f]^{1/2} & \text{if } J_f = J_i+1 \\ 1/[J_f(J_f+1)]^{1/2} & \text{if } J_f = J_i \\ -[J_f/(J_f+1)]^{1/2} & \text{if } J_f = J_i-1. \end{cases} \quad (4-64)$$

For transitions in which both EC matrix elements are operative, we have

$$b_k = \left[\frac{\lambda^2 |R|^2}{[J_f(J_f+1)]^{1/2}} + \lambda(R+R^*) \right] (1+\lambda^2 |R|^2)^{-1}. \quad (4-55)$$

The coefficient A_1 , familiar from the theory of angular correlations, is defined by

$$A_1(LL'J_{ff}J_f) = [F_1(LLJ_{ff}J_f) + 2\delta F_1(LL'J_{ff}J_f) + \delta^2 F_1(L'L'J_{ff}J_f)] \times (1+\delta^2)^{-1}, \quad (4-66)$$

where the angular-momentum and parity quantum numbers $L\pi$ and $L'\pi'$ characterize the multipolarities of the γ transition, and the ratio of the corresponding reduced matrix elements is $\delta = \langle J_{ff} || L'\pi' || J_f \rangle \langle J_{ff} || L\pi || J_f \rangle^{-1}$. For pure multipole radiation, we have $L'=L$ and $\pi'=\pi$. The F coefficients are defined by

$$F_1(LL'J_{ff}J_f) = (-1)^{J_{ff}+J_f-1} [(2L+1)(2L'+1)(2J_f+1)3]^{1/2} \times \begin{pmatrix} L & L' & 1 \\ 1 & -1 & 0 \end{pmatrix} \left\{ \begin{matrix} L & L' & 1 \\ J_f & J_f & J_{ff} \end{matrix} \right\}, \quad (4-67)$$

where the standard designations $\begin{pmatrix} & & \\ & & \end{pmatrix}$ and $\left\{ \begin{matrix} & & \\ & & \phantom{J_{ff}} \end{matrix} \right\}$ indicate Wigner 3j and 6j symbols.

It is immediately apparent from the form of Eq. (4-63) that the circular polarization of the γ -ray photon must be measured if one is to observe any correlation between the directions of the two photons. If the circular polarization of the IB photon is also measured, then the directional correlation function is

$$W_{\gamma}(\theta, s, t) = 1 + \frac{ts}{\sqrt{3}} A_1(LL'J_{ff}J_f) b_k \cos \theta, \quad (4-68)$$

independent of the IB-photon energy. If the polarization of the IB photon is not measured, Eq. (4-63) must be summed over $s=\pm 1$. In this case, the directional correlation function is given by

$$W_{\gamma}(\theta, t) = 1 + \frac{t}{\sqrt{3}} A_1(LL'J_{ff}J_f) b_k a_{1s}(k) \cos \theta, \quad (4-69)$$

and shows a dependence on the energy of the IB photon characterized by the asymmetry function $a_{1s}(k)$ previously discussed.

The above results are exact, but in the derivation of the IB- γ directional-correlation functions it is assumed that no forces act on the nucleus while it is in the intermediate state $|N_f^*\rangle$. Generally, this assumption is not well satisfied, because the hole in the atomic shell produces strong magnetic and inhomogeneous electric fields at the nucleus, leading to a perturbation of the directional correlations.

Correlations of IB and Succeeding Atomic X Rays

The determination of the directional correlation function for an IB photon and a succeeding x-ray quantum requires a calculation which is essentially analogous to that of IB-photon- γ -ray directional correlations. Zon (1971) has carried out such a calculation and reported final formulas for the case of radiative X capture. For allowed transitions, these results can be summarized as follows.

For an IB quantum of circular polarization s , and an atomic x-ray quantum of circular polarization t , the directional-

correlation function is of the form

$$w_x(\theta, s, t) \propto (2J+1)(A_{1s} + sB_{1s})^2 + (-1)^{J+\frac{1}{2}} \frac{ts}{3} (A_{1s} + sB_{1s})^2 \cos \theta, \quad (4-70)$$

where θ is the angle between the directions of the two photons and $J=1/2, 3/2$ is the angular momentum of the atomic electron which fills the hole in the K shell.

Further results are parallel to those for the nuclear γ -ray case. For example, it is evident from Eq. (4-70) that, in order to observe a directional correlation between the two photons, the circular polarization of the x-ray photon must be measured. If the circular polarization of the IB photon is also measured, we have

$$w_x(\theta, s, t) = 1 + \frac{(-1)^{J+1/2}}{(2J+1)} \frac{ts}{3} \cos \theta, \quad (4-71)$$

and the directional correlation shows no dependence on the energy of the IB photon. If the polarization of the IB photon is not measured, we have

$$w_x(\theta, t) = 1 + \frac{(-1)^{J+1/2}}{(2J+1)} \frac{t}{3} a_{1s}(k) \cos \theta, \quad (4-72)$$

and the correlation function again displays a dependence on the energy of the IB photon characterized by the asymmetry function $a_{1s}(k)$.

4.1.4. IB Spectra and Correlation Effects in Forbidden Transitions

Early attempts to formulate a theory of IB for forbidden transitions were made by Cutkosky (1954), Turovtsev and Shapiro (1954),

Yukawa (1956), and Koh *et al.* (1957, 1962). Turovtsev and Shapiro calculated the radiative K-capture spectrum for first-forbidden transitions, assuming vector and tensor couplings, while Cutkosky derived the matrix element for radiative K capture for arbitrary coupling, neglecting terms strictly of order $Z\alpha$ or smaller and terms contributing only to third- or higher-order transitions. Cutkosky's principal result was a theorem, often referred to as the "Cutkosky rule," which relates the spectra and angular correlations of the K-capture IB to the spectra and angular correlations of positrons. Basically, these calculations are extensions of the work of Morrison and Schiff (1940) to forbidden transitions. Yukawa (1956) made an attempt to include relativistic and Coulomb effects in the calculation of allowed and first-forbidden K-capture IB spectra. The formulas he obtained proved to be so complicated that this work has never led to useful results. Koh *et al.* (1957, 1962) first reported correlation studies for first-forbidden transitions; Coulomb effects were neglected in these calculations.

The modern theory of radiative electron capture in forbidden transitions is due to Zon and Rapoport (1968), who developed a generalization of the theory of Martin and Glauber (1958) to transitions of arbitrary order of forbiddenness. They also derived general formulas for the IB energy spectra. For K capture, detailed results were obtained. Zon (1971) developed this theory further for radiative capture from an arbitrary atomic shell, derived general formulas for various correlation and polarization

effects, and obtained detailed results for the case of K capture.

The theory of Zon and Rapoport (1968) starts from Eqs. (4-9) and (4-10) for the radiative capture matrix element and transition rate. In order to evaluate the matrix element (4-9) exactly, including relativistic and Coulomb effects to all orders in $Z\alpha$, Zon and Rapoport first decompose and simplify it by introducing the irreducible tensor operators and the second-order Dirac-Coulomb Green's function of Martin and Glauber. This decomposition makes the angular-momentum dependence of the transition amplitude explicit. Integration over the angular coordinates is then completed through extensive use of the methods of the theory of angular momentum.

In evaluating the transition amplitude, Zon and Rapoport introduce the Konopinski-Uhlenbeck approximation,

$$\int_0^{R_N} dr r^{\lambda_L} \dots \approx R_N^{\lambda_L - L} \int_0^{R_N} dr r^L,$$

where $\lambda_L = (L^2 - a^2)^{1/2}$, and the ξ approximation which is based on the assumption $(Q_{EC} - 1)R_N \ll Z\alpha$, a condition that is always well-satisfied when competing positron emission is not energetically possible. Under only these approximations, Zon and Rapoport obtain a general expression for the transition rate for radiative electron capture from an arbitrary shell. The form of the result reveals that for radiative electron capture in the ξ approximation, just as in β decay, nonunique forbidden spectra have

the same shape as the unique spectra of the next-lower order of forbiddenness.

Only for K capture do Zon and Rapoport carry their calculations to completion. For capture from higher shells, the theory is developed further by Zon (1971), but the resulting expressions prove to be too complicated to permit exact analytic evaluation or even the development of expressions that are correct to first order in $Z\alpha$. Indeed, the only detailed results which have so far been reported are those contained in the table of Zon (1973) for the L - and M -shell IB spectra associated with the first-forbidden unique transition in ^{41}Ca ; these results were derived through completely numerical procedures.

Zon and Rapoport's transition rate for radiative K capture can be summarized as follows. Assuming the polarization of the IB radiation is not observed, the transition rate can be written

$$dw_{1s} = \frac{8\alpha}{\pi} \left| \langle \phi_{1s} \rangle_Q \right|^2 k (q_{1s} - k)^2 F_{1s}(k) dk. \quad (4-73)$$

The form factor $F_{1s}(k)$ is defined in terms of two correction factors, $R_{1s}^{(1)}(k)$ and $R_{1s}^{(2)}(k)$, and the appropriate combination of nuclear matrix elements $R_{Nj_v}^A$:

$$F_{1s}(k) = \sum_{ANj_v} (2\mu R_N)^{2(\lambda_N - \lambda_1) - 2(N-1)} \left[\frac{2^{N-1}(N-1)!}{(2j_v)!!(2N-1)!} \right]^2 \left| R_{Nj_v}^A \right|^2 \\ \times R_{1s}^{(N)}(q_{1s} - k)^{2j_v - 1} k^{2N-2}, \quad (4-74)$$

Here, R_N is the nuclear radius, and λ_N equals $(N^2 - a^2)^{1/2}$. The quantities $F_{\nu j \nu}^A$, for all contributing values of A , N , and j_ν , have been tabulated by Zon and Rapoport for up to third-forbidden transitions (Table 4.4.). The correction factors $R_{1s}^{(H)}$ are defined in terms of the more fundamental quantities $A_{1s}^{N, \dots}$ and $B_{1s}^{N, M}$, which are generalizations of the functions A_{1s} and B_{1s} of Martin and Glauber (1958):

$$R_{1s}^{(H)} = \frac{1}{4N} \left[(N-1) \left(\left| A_{1s}^{N, N-1} \right|^2 + \left| B_{1s}^{N, N-1} \right|^2 \right) + (N+1) \left(\left| A_{1s}^{N, N} \right|^2 + \left| B_{1s}^{N, N} \right|^2 \right) \right]. \quad (4-75)$$

To specify the transition rate, formulas for A and B are required. Zon and Rapoport (1968) have developed exact general expressions for these functions, but these formulae contain a large number of integrals involving Whittaker functions, none of which can be evaluated exactly analytically.

For moderately light nuclei, it may be sufficient to expand the above-mentioned integrals in powers of $Z\alpha$ and thereby evaluate A and B to first order in $Z\alpha$. Such calculations are reported by Zon and Rapoport (1968) with the result

$$A_{1s}^{N, M} (B_{1s}^{N, M}) = 1 - Z\alpha \sum_{n=0}^{\infty} [a_n (\mu/k) + b_n \tan^{-1}(k/\mu)] (1/k)^n. \quad (4-76)$$

The coefficients a_n and b_n are listed in Table 4.5. At the present time, Eq. (4-76) is the only formula available for the determination of A and B . Unfortunately, even for light elements these formulas are not valid for low k . The nature of the expansion underlying Eq. (4-76) is such that these results are expected to break down for $k \lesssim Z\alpha$. For the special case $k \rightarrow 0$, however, A and B

can be evaluated exactly to all order in $Z\alpha$. The $k \rightarrow 0$ results, listed in the last column of Table 4.5, are valuable for estimating the low-energy behavior of A and B and to test numerical procedures for the exact evaluation of A and B for arbitrary k .

In examining the predicted IB spectra for K capture in further detail, we restrict our discussion to first-forbidden transitions.

Nonunique First-Forbidden Transitions

In the ξ approximation, the K-capture IB spectrum of a nonunique first-forbidden transition is predicted to have the allowed shape. Indeed, when the above results are evaluated for this case and normalized by the corresponding nonradiative K-capture rate, exactly the same result is obtained as for the allowed case,

$$\frac{dw_{1s}}{w_K} = \frac{\alpha}{\pi} \frac{k(q_{1s} - k)^2}{q_{1s}^2} R_{1s}^{(1)} dk, \quad (4-77)$$

where $R_{1s}^{(1)}$ is easily identified as the function R_{1s} of Martin and Glauber (1958), defined by Eq. (4-37) and displayed in Fig. 4-3.

Unique First-Forbidden Transitions

In unique forbidden transitions, only one nuclear matrix element contributes and the ξ approximation becomes irrelevant. For unique first-forbidden electron capture, the radiative transition rate normalized by the corresponding nonradiative K-capture rate is

$$\frac{dw_{1s}}{w_K} = \frac{\alpha}{\pi} \frac{k(q_{1s}-k)^2}{q_{1s}^2} \times [R_{1s}^{(1)}(1-k/q_{1s})^2 + (2\mu R_N)^{2(\lambda-\lambda_N)-2} R_{1s}^{(2)}(k/q_{1s})^2] dk. \quad (4-78)$$

The factor in the brackets replaces the function $R_{1s}^{(1)}$ which appears in the allowed result.

While the factor $R_{1s}^{(1)}$ has been evaluated exactly numerically and in several analytic approximations, this has not been done for $R_{1s}^{(2)}$. The only available basis for the evaluation of $R_{1s}^{(2)}$ is Eq. (4-76), from which $R_{1s}^{(2)}$ can be calculated to first order in $Z\alpha$, with results only valid for $k \geq Z\alpha$. For $k \rightarrow 0$, it follows from Table 4.5 that $R_{1s}^{(2)} \propto 1/k^2$. Thus, it may be expected that $R_{1s}^{(2)}$ will contribute substantially to the determination of the IB spectrum at all photon energies. Little is therefore gained by evaluating $R_{1s}^{(1)}$ to any greater accuracy than $R_{1s}^{(2)}$. To illustrate the behavior of the correction factors, we have evaluated the functions $R_{1s}^{(1)}$ and $R_{1s}^{(2)}$ to first order in $Z\alpha$, using Eqs. (4-75) and (4-76), for two atomic numbers (Fig. 4-10).

It is of interest to consider the limit $Z \rightarrow 0$, corresponding to the neglect of Coulomb effects on the intermediate electron states and the momentum of the initial electron. In this limit, $\lambda_N = N$, $R_{1s}^{(1)} = R_{1s}^{(2)} = 1$, and Eq. (4-78) is simplified to

$$\left(\frac{dw_{1s}}{w_K} \right)_{CF} = \frac{\alpha}{\pi} \frac{k(q_{1s}-k)^2}{q_{1s}^2} [(1-k/q_{1s})^2 + (k/q_{1s})^2] dk. \quad (4-79)$$

This result can also be obtained by extending the calculations of Morrison and Schiff (1940) to unique first-forbidden transitions. Equation (4-79) is interesting because of its simplicity but is not expected to be very accurate, although it does describe the general shape of the IB spectrum. The expression is useful for estimating the integrated intensity over any given portion of the spectrum, providing an upper bound.

In order to assess the importance of Coulomb effects in unique first-forbidden transitions and to illustrate the difference between allowed and forbidden shapes, we have plotted several different predictions for the K-capture IB spectrum of ^{41}Ca in Fig. 4-11.

The two Morrison-and-Schiff curves, labeled MS-A and MS-F, illustrate the basic differences in spectral shape between allowed and first-forbidden unique transitions. The behavior of the Zon-Rapoport (ZR) result at $k > Z\alpha$ suggests that, for unique first-forbidden transitions, the main effect resulting from the inclusion of Coulomb effects is an overall reduction in the intensity of the IB spectrum, similar to that found in the allowed case.

ORIGINAL PAGE IS
OF POOR QUALITY

4.2. Radiative Electron Capture--Experiments

Experimental studies of the radiative capture process are valuable for providing information on electron-capture decay, analogous to the information on β decay derived from the study of β spectra. The energy spectrum and the intensity of internal-bremsstrahlung (IB) photons provide a measure of the total energy release and the change of spin and parity in the decay. Experiments on the circular polarization and on various angular correlations provide basic information on weak interaction and nuclear structure. Furthermore, bremsstrahlung experiments may yield supplementary data for the characterization of nuclear decay schemes and for the determination of capture ratios from various subshells.

Precise experimental investigations of radiative electron capture do, however, require rather complicated techniques for experiment and analysis, due to the very low intensity ($\sim 10^{-4}$ photons per capture event) and the continuous nature of the IB spectra. The interpretation of experimental results is made difficult by the fact that electrons captured from different atomic subshells contribute to the emitted radiation.

Much effort has been devoted to IB experiments during the last thirty years. Critical reviews were compiled by Zylicz (1968) and Kádár (1972), and to a lesser extent by Bouchez and Depommier (1965), Petterson (1965), Schopper (1966), and Berényi (1968). Considerable progress has been achieved since, especially in the development of experimental techniques.

The low probability of radiative capture makes its observation sensitive to interference from other electromagnetic radiation. Especially nuclear γ rays, annihilation radiation and x rays emitted in the course of radioactive decay can considerably limit the energy range of an IB measurement and distort the measured IB pulse-height spectrum through pileup and summing effects. The measurement of coincidences between such primary radiation and the rare IB photons requires sophisticated techniques. In decays with competing β^+ or β^- branches or with highly converted γ transitions, corrections may be required for other types of electromagnetic radiation, comparable in intensity with IB: (i) internal bremsstrahlung accompanying β^+ or β^- decays, (ii) external bremsstrahlung emitted during absorption of β particles or conversion electrons in the source or surrounding materials, and (iii) continuously distributed annihilation radiation for positron annihilation in flight. In view of the large number of possible interfering effects, it is not surprising that IB measurements performed up to now have been restricted to electron-capture transitions in simple decay schemes. In most of the many nuclei decaying by electron capture, radiative capture has not yet been investigated.

It is also evident that IB experiments are very sensitive to small amounts of γ -ray emitting impurities in the sources. Experimental results therefore are only reliable if the source material is carefully checked and purified if necessary to remove spurious contaminants. Impurity checks of the required sensitivity were hardly possible before the advent of high-resolution Ge(Li) spectrometers,

whence older experimental results must be regarded with reservations.

On reviewing the experimental literature, it appears that most measurements of IB spectra have been performed only to derive electron-capture transition energies from the IB end-point energies. This procedure was initiated by the early theory of Morrison and Schiff (1940) and Jauch's proposition to linearize IB spectra in a way that resembles the construction of Kurie plots for β spectra (Jauch, 1951; Bell *et al.*, 1952). For this purpose, most IB spectra were measured without normalization to the electron-capture rate. These shape measurements qualitatively confirmed the spectral shapes predicted by theory for s- and p-type radiation; in the case of forbidden decays, they yielded an estimate of the relative abundance of detour transitions. Measurements of spectral shapes alone, however, are not adequate for a detailed test of modern IB theory (Martin and Glauber, 1958; Intemann, 1971): as shown in Sec. 4.1, relativistic and Coulomb effects, screening, exchange and overlap influence the absolute IB yield, while affecting spectral shapes only slightly. Absolute IB measurements are, however, scarce. Some early results exist, of poor accuracy, pertaining to ground-state transitions; a few results on decays that include γ transitions were obtained recently.

In Secs. 4.2.1-4.2.2, we have compiled the available experimental material and classified the techniques employed in the measurement of normalized IB spectra associated with different decay schemes. We do, however, frequently refer to incomplete studies and list all experiments known to us, to provide a guide for accurate future investigations.

4.2.1. Experiments on Total IB Spectra

An IB spectrum that is not measured in coincidence with x rays or Auger electrons constitutes the total spectrum dw_{IB} , which is a superposition of partial spectra dw_{nl} due to electron capture from different atomic states nl . This spectrum is mainly determined by s radiation for energies above $\nu Z\alpha$ (in units of mc^2) and by p radiation at lower energies; contributions from the innermost 1s and 2p shells dominate.

Experimental techniques applicable to the determination of total spectra can be divided broadly into two categories: single-spectrum methods and coincidence methods. In single-spectrum methods, IB spectra are measured relative to other emitted radiation that can be normalized to the ordinary capture rate. Measurements in coincidence with γ rays or conversion electrons permit separation of the IB spectra associated with individual electron-capture branches in a given decay.

In Table 4.6, we list published experiments on total IB spectra and indicate what methods and spectrometers were used and what quantities were deduced. A somewhat more detailed description of experimental methods follows.

Spectrometry of IB and of x rays and Auger electrons. Total IB spectra can most advantageously be observed in pure ground-state transitions and in decays that feed only low-energy transitions. Table 4.6 shows that numerous total IB measurements have been performed on such simple decays, viz., on $^{37}_{Ar}$, $^{41}_{Ca}$, $^{49}_{V}$, $^{55}_{Fe}$, $^{71}_{Ge}$, $^{119}_{Sb}$, $^{125}_{I}$, $^{131}_{Cs}$,

^{145}Sm , ^{159}Dy , ^{165}Er , ^{181}W and ^{193}Pt . NaI(Tl) and Ge(Li) spectrometers have been used. In cases in which the electron-capture transition energy is high compared with the K x-ray or γ -ray energy, a large fraction of the IB spectrum can be measured. Counting problems produced by the much higher x-ray or γ -ray rates can be avoided by placing suitable absorbers between source and spectrometer. For example, Fig. 4-12 shows IB pulse-height spectra of ^{131}Cs recorded with a NaI(Tl) spectrometer, a variety of Cu absorbers having been interposed (Saraf, 1954a). The procedure fails for transition energies not far above the K x-ray energy; in such cases, pileup from the K x-ray pulses strongly affects the IB spectrum. Methods for pileup reduction and correction are described below.

In most cases listed in Table 4.6, only IB spectral shapes were measured, and the accuracy is generally poor. Precise shape determinations with different types of NaI(Tl) spectrometers have been performed on ^{55}Fe (Berényi *et al.*, 1965b), and on the forbidden spectra from ^{36}Cl (Berényi *et al.*, 1965a, b; Smirnov and Batkin, 1973) and ^{59}Ni (Schmorak, 1963). Only recently were Ge(Li) spectrometers used, resulting in accurate shape measurements on ^{41}Ca (MysZek *et al.*, 1973) and ^{59}Ni (Berényi *et al.*, 1976) and on the IB spectrum from higher shells only in ^{193}Pt (Hopke and Naumann, 1969).

To obtain normalized IB spectra, the ordinary K-capture rate w_K must be determined from separate measurements of the K x-ray or K Auger-electron emission rates. Normalized IB spectra have been determined in only a few cases: for ^{37}Ar (Saraf, 1956), ^{55}Fe (Michalowicz, 1953; Saraf, 1956), ^{71}Ge (Bisi *et al.*, 1955a), ^{119}Sb

(Olsen et al., 1957), ^{131}Cs (Michalowicz, 1956), ^{145}Sm (Sujkowski et al., 1968), ^{159}Dy (Sujkowski et al., 1965) and ^{165}Er (Zylicz et al., 1963; Sujkowski et al., 1965). All these workers used NaI(Tl) crystals to detect the K x rays, with the exception of Saraf (1956), who applied a low-geometry proportional counter for the K x rays in ^{55}Fe and used internal gas counting to determine the K Auger-electron rate from ^{37}Ar . In the cases of ^{145}Sm and ^{159}Dy , the K x rays could not be resolved from low-energy γ rays, and decay-scheme corrections were applied. The accuracy of these early normalized IB spectra is generally poor (rarely better than 50%); considerable improvements would be possible today (see Sec. 3). New measurements of total IB spectra would be of great value, especially for pure ground-state transitions which are listed in Table 4.7.

IB and γ -ray spectrometry. For decays that involve emission of energetic γ rays, the measurement of total IB spectra is much more complicated. On the other hand, the γ rays make it possible to normalize the IB spectra, independently of fluorescence yields. If no IB- γ coincidences are measured, the available energy range is generally limited to energies above the highest γ energy. These measurements depend strongly on the details of the decay scheme, such as γ and electron-capture energies and branching ratios, and internal-conversion coefficients.

To date, IB and γ spectroscopy has only been applied to relatively simple decays, such as that of ^7Be (Mutterer, 1973b), ^{51}Cr (Bisi et al., 1955b; Cohen and Ofer, 1955; Van der Kooi and Van der Bold, 1956;

Ofer and Wiener, 1957; Murty and Jnanananda, 1967; Ribordy and Huber, 1970; and Mutterer, 1973a) and ^{113}Sn (Phillips and Hopkins, 1960). The isotopes ^7Be and ^{51}Cr have favorable decay schemes for this type of measurement. Both nuclides decay by two electron-capture branches, $\sim 90\%$ to the ground state and $\sim 10\%$ to an excited state with an energy of $Q_{\text{EC}}/2$. Thus, a large fraction of the IB spectrum associated with the ground-state branch can be measured without interference from the second electron-capture branch. A single γ spectrometer can be used to determine dw_{IB} relative to the γ emission rate. In order to normalize dw_{IB} to the ground-state electron-capture rate, the γ branching ratio $P_{\gamma} = N_{\gamma}/N_0$ is found precisely from measurements of the disintegration rate N_0 through 4π (x-ray, Auger)- γ coincidence counting, and of the γ rate N_{γ} by integral γ counting (Mutterer, 1971; De Roost and Lagoutine, 1973).

Above the γ -ray energy, the IB spectrum must be corrected for γ -ray pileup. In early measurements on ^{51}Cr and ^{113}Sn , NaI(Tl) spectrometers were used. With these, poor resolution and long pulse rise times cause the pileup spectra to be smeared out (Waibel, 1969, 1970) and it is not clear whether the measured IB spectra are free of pileup distortions. These measurements were considerably refined by Ribordy and Huber (1970) and Mutterer (1973a, b) who used Ge(Li) spectrometers with electronic pileup-rejection systems. Such systems prevent pileup of pulses spaced by ≥ 100 ns and can reduce total pileup by an order of magnitude. Furthermore, the residual pileup spectra show sharp sum peaks that can be distinguished from the smooth IB spectra (Fig. 4-13). A complete separation of the IB spectrum from

the residual pileup spectrum cannot, however, be achieved in a single measurement, even with a weak ^{51}Cr source (Ribordy and Huber, 1970); an extrapolation from measurements with sources of different strengths is required. The extrapolation procedure used by Mutterer (1973a) is illustrated in Fig. 4-14. This technique has yielded normalized IB spectra of ^7Be and ^{51}Cr (Fig. 4-15) of good accuracy.

The spectrometry of IB in the presence of γ rays could be further improved by using large Ge(Li) detectors and suitable absorbers, in order to optimize the ratio of IB to γ -ray counting rates, and by using low-background arrangements. The reduction of background, either by applying optimal shielding or by using anticoincidence devices (Persson and Koonin, 1972), allows the use of weak sources and reduces the pileup correction accordingly. It would also be interesting to apply Ge(Li) anti-Compton spectrometers operated with pileup rejectors, because here pileup is confined to the region of the coincidence sum peaks. It can be expected that with improved techniques the accuracy with which total IB spectra of ^{51}Cr and ^7Be are now measured can also be attained in cases of decay schemes with higher P_γ , larger ratios of γ -ray energy to Q_{EC} , or with several γ branches. Spectrometry of the ground-state bremsstrahlung offers the possibility of determining ground-state branching ratios that in complex decays can otherwise only be obtained (often with very poor accuracy) from total γ and x-ray intensities.

IB spectrometry in coincidence with γ rays. Spectrometry of internal bremsstrahlung in coincidence with γ rays or conversion

electrons permit one to separate the IB spectra accompanying decay to different excited states. Spectra can be measured over their entire energy range, above the K x-ray region, for EC transitions that feed states which decay by prompt γ -ray emission to the ground state or to a lower-lying metastable state of the daughter nucleus. Normalization is easily accomplished by dividing a coincidence IB spectrum by the singles γ counting rate.

IB- γ coincidence experiments have been performed on EC transitions to excited states in the decays of ^7Be (Lancman and Lebowitz, 1971a; Persson and Koonin, 1972), ^{51}Cr (Koonin and Persson, 1972); ^{54}Mn (Lancman and Lebowitz, 1969; Kádár *et al.*, 1970; Koonin and Persson, 1972), ^{57}Co (Lancman and Lebowitz, 1971b), and ^{113}Sn (Bosch *et al.*, 1967). The main difficulty in IB- γ coincidence spectrometry arises from the large difference in intensity ($\sim 10^{-4}$) between IB and γ radiation, because the γ -ray spectra usually cover the same energy range as the weak IB spectra. Very short coincidence resolving times and high-efficiency detectors are therefore necessary to attain good true-to-chance coincidence ratios within reasonable counting times. Furthermore, scattering between the IB and γ detectors must be avoided to prevent false prompt coincidences and counting losses produced by sum effects in both channels. To meet these conditions, NaI(Tl) scintillators have been used as IB and γ detectors, arranged in close face-to-face geometry. Scattering has been reduced with suitable absorbers (Lancman and Lebowitz, 1969, 1971a, b), sometimes combined with lead collimators (Persson and Koonin, 1972; Koonin and Persson, 1972) (Fig. 4-16). Kádár *et al.* (1970) employed a 90° crystal

arrangement of lower geometry with lead collimators. Timing was accomplished by Bosch et al. (1967), Lancman and Lebowitz (1969, 1971a, b), and Kádár et al. (1970) with conventional fast-slow coincidence circuits of 20-35 nsec resolving time. Even so, random coincidences between γ events in both detectors made the main contribution to the measured coincidence spectra. Bremsstrahlung spectra were found by subtracting singles γ spectra, recorded with the IB detector, from the measured coincidence spectra; both sets of spectra had been normalized to equal photopeak areas (Fig. 4-17).

A considerable improvement in technique was achieved by Persson and Koonin (1972) by using a fast time-to-pulse-height converter and applying two-parameter analysis: the IB pulse-height spectrum and the energy-dependent delay between IB and γ pulses were recorded simultaneously. A block diagram of the electronic circuit is shown in Fig. 4-18. This technique has led to effective coincidence resolving times of ~ 4 nsec over the entire IB-spectrum range. Persson and Koonin (1972) have furthermore reduced the background rate by surrounding both crystals with a plastic-scintillator anticoincidence shield, allowing the use of weak sources. With this technique, random coincidences could be reduced to a much lower level, and accurate IB spectra could be measured for ^7Be , ^{51}Cr , and ^{54}Mn . The result for ^7Be is shown in Fig. 4-19.

It would undoubtedly be of interest to apply this IB- γ coincidence technique to additional cases. Large Ge(Li) detectors or plastic scintillators might be used. In cases that involve low-energy γ transitions, measurements might be performed in coincidence with conversion electrons; this has been done only with ^{145}Sm (Sujkowski et al., 1965).

Spectrometry of IB and of positrons or annihilation radiation.

For high-energy transitions in which electron capture competes with positron emission, total IB spectra can be measured relative to the β^+ decay rate or to the annihilation radiation (γ_A) produced by the positrons in suitable source encapsulations. Methods for measuring EC/ β^+ ratios, with which the IB spectra can be normalized, are discussed in Sec. 3.4. Interference of annihilation radiation with the IB spectrum can be reduced by measuring γ_A - γ_A anticoincidences with a detector placed opposite the IB detector. Alternatively, very thin sources and backings can be used and the β^+ particles can be magnetically bent away from the IB detector. This technique has been applied by Berényi and Varga (1969) to measure internal bremsstrahlung from β^- emission with minimal contribution from external bremsstrahlung. In isotopes that decay by electron capture and β^+ emission, the positrons give rise to such other continuously distributed radiation as internal and external bremsstrahlung and photons from positron annihilation in flight (Kantele and Valkonen, 1973). The EC bremsstrahlung spectra will be affected by these effects at energies below the β^+ end point and in the neighborhood of 511 keV.

The only reported IB measurements on a nuclide decaying by EC and β^+ emission are on ^{36}Cl , which has a very weak (0.001%) β^+ branch and decays 98.1% of the time by β^- emission. The bremsstrahlung accompanying the 1.9% EC branch has been studied by Dougan et al. (1962), Berényi (1962, 1963b, 1965a), Lipnik et al. (1964), Berényi et al. (1965b), and Smirnov and Batkin (1973) with various types of NaI(Tl) spectrometers. The latter two experiments yielded very

accurate results on the IB spectrum shape at energies above the β^- end point at 712 keV. No attempt was made, however, to normalize the spectra to the electron-capture rate.

Bremsstrahlung studies on isotopes that decay by electron capture and β^+ emission do not contribute decay-scheme information that could not be derived more readily from β^+ spectrometry. Measurements of normalized IB spectra at high energies would, however, be extremely useful to check the treatment of relativistic and Coulomb effects in the theory, which predicts that these effects reduce the IB yield with increasing energy (Fig. 4-3).

4.2.2. Experiments on Partial IB Spectra

Supplementary to the experiments described in Sec. 4.2.1, considerable effort has been expended to measure partial IB spectra associated with electron capture from specific shells, mainly the 1s IB spectrum associated with K capture. Such spectra can be observed by IB spectrometry in coincidence with x rays or Auger electrons. Higher-shell spectra can be determined by subtracting accurately measured 1s IB spectra from total IB spectra.

The 1s IB spectrum. Spectrometry of internal bremsstrahlung in coincidence with K x rays or K Auger electrons singles out the 1s IB spectrum $d\omega_{1s}$. The spectrum can be normalized to the corresponding K-capture rate by dividing the coincidence IB spectrum by the singles K x-ray (K Auger-electron) counting rate.

Only IB-K-x-ray coincidence experiments have been reported

(Table 4.8). Most of these experiments have yielded only spectral shapes. Normalized spectra have been determined only for some simple decays, viz., for ^{55}Fe (Biavati et al., 1962), ^{131}Cs (Michalowicz, 1956; Biavati et al., 1962) (Fig. 4-20), ^{145}Sm (Sujkowski et al., 1968), and ^{165}Er (Zylicz et al., 1963; Sujkowski et al., 1965). NaI(Tl) detectors were used in these experiments for both the IB and K x-ray photons; interference of K x-rays in the IB spectrometer was avoided with absorbers. For all isotopes but ^{145}Sm and ^{165}Er , only poor accuracy was achieved in these early experiments.

Measurements of bremsstrahlung in coincidence with K x rays can also be performed in the presence of higher-energy γ rays, with the restriction that prompt γ rays limit the observable ls radiation to energies above the γ energy. Spectra accompanying EC decays that feed a state deexcited by prompt γ rays of energies in excess of the EC transition energy cannot be obtained by IB-K-x-ray coincidences with any degree of accuracy. One IB result on such a cascade in ^{54}Mn , reported by Jung and Pool (1956), should be disregarded. Delayed γ rays, such as arise if electron capture feeds isomeric states, have no direct influence but may contribute considerably to the random-coincidence rate below the γ energy. This was the case in the older coincidence experiments on ^{85}Sr by McDonnell and Ramaswamy (1969), ^{109}Cd by Gopinathan and Rubinson (1968), and ^{113}Sn by Jung and Pool (1956). Modern coincidence techniques, as used by Persson and Koonin (1972) in IB- γ spectrometry, would permit measurements of entire ls IB spectra. Some results on ls spectra have been reported for EC transitions to isomeric states with mean lives of the order of the

coincidence resolving time, viz., on ^{125}I (Gopinathan and Rubinson, 1968), ^{145}Sm (Sujkowski et al., 1968), and ^{197}Hg (Jasinski et al., 1965). In such cases, only the spectrum above the γ -ray energy is usually observable, and normalization is complicated.

In all measurements of coincidences between bremsstrahlung and K x rays on radioisotopes that emit prompt or delayed γ rays, a correction must be applied for the γ contribution in the K x-ray channel. This correction is determined through a second measurement with a discriminator window setting above the K x-ray line. Corrections for K x rays from internal conversion must also be considered.

Bremsstrahlung from ls capture can be measured in coincidence with K x rays even in cases where β^+ or β^- decay competes with electron capture because the only K vacancies created in β decay are the few produced by K-shell internal ionization or shakeup (Sec. 5). Thallium-204 has often been investigated; this isotope decays by 97.9% β^- emission and 2.1% electron capture. Lancmann and Bond (1973) have pointed out that double internal bremsstrahlung associated with the β^- branch may have to be considered.

Most measurements of ls IB spectra could be considerably improved today. Careful new measurements on pure ground-state decays and EC decays to isomeric states would be especially useful.

Higher-shell IB spectra. The possibilities for measuring the bremsstrahlung that accompanies electron capture from higher shells are more limited. Radiation from ns capture, $n>1$, has very similar shape to ls radiation and constitutes only $\sim 10\%$ of the total

bremsstrahlung in the energy range above $\sim Z\alpha$. The radiation accompanying capture of p electrons dominates only at low energies, $k < Z\alpha$; for low Z, this is difficult to separate from the characteristic x-ray lines.

The IB spectra associated with capture from higher shells are quite easily observed in the few low-energy transitions in which K capture is energetically forbidden, e.g., ^{193}Pt and ^{163}Ho . An accurate IB shape measurement on ^{193}Pt was performed by Hopke and Naumann (1969) with a Ge(Li) spectrometer (Fig. 4-21). In more energetic transitions, however, such spectra are very difficult to measure with good accuracy.

The 2s IB spectrum, associated with radiative capture of L_1 electrons, can only be singled out in coincidence with L x rays if it is possible to gate on the $L\beta_3$ and $L\beta_4$ lines. Other L x rays can also arise from $L_{2,3}$ capture or follow $K\alpha$ x-ray emission after K capture. The method is thus restricted to high-Z atoms for which the L x-ray components can be resolved and the K fluorescence yield is large. For other nuclides, the 2s spectrum (including s spectra from higher shells) can only be obtained indirectly by comparing accurately measured 1s and total IB spectra. No experimental results on separated 2s IB spectra have been reported.

The 2p IB spectrum associated with radiative capture of electrons from the L_2 subshell (plus the small amount captured from the L_3 subshell) can be singled out by coincidence IB spectrometry in cases in which K capture is forbidden, such as ^{193}Pt . Here, an IB measurement in coincidence with those L x rays that fill L_2 and L_3 vacancies (all

but $L\beta_3$ and $L\beta_4$) can be performed. The total p radiation, however, that differs strongly in spectral shape from s radiation, can be determined by subtracting from the total IB spectrum measured at energies below $Z\alpha$ the s IB spectrum that is measured at higher energies and extrapolated to the p IB region. Alternatively, one can subtract the $1s$ IB spectrum measured by IB-K-x-ray coincidences and corrected for the $\sim 10\%$ contribution from higher s states (Biavati et al., 1962).

Measurements of total IB spectra at low energies where p IB dominates, have been performed on several nuclides, viz., on ^{55}Fe by Biavati et al. (1962), ^{131}Cs by Michalowicz (1956), Hoppes and Haywards (1966), and Biavati et al. (1962) (Fig. 4-20), ^{145}Sm by Sujkowski et al. (1968), and ^{159}Dy and ^{165}Er by Sujkowski et al. (1965). Relative intensities of p radiation and s radiation were determined for ^{145}Sm , ^{159}Dy and ^{165}Er . In all these experiments, NaI(Tl) detectors were used. With scintillation detectors, however, distortions of the IB spectrum due to pileup contributions from K x rays and K-L x-ray sum effects are difficult to control in the vicinity of the K x-ray energy. For the measurement of p radiation, Ge(Li) spectrometers should be used, preferably with pileup rejectors, and corrections for residual pileup should be considered. Platinum-193 would be a good case for study.

of

The measurement of the relative intensity I_{IB} from s and p capture represents an independent method to determine the capture ratios; this may supplement corresponding x-ray and Auger-electron experiments.

4.2.3. Analysis of IB Pulse-Height Spectra

In this Section, we consider methods for deriving IB energy spectra $dw_{IB}(k)$ or $dw_{nl}(k)$ from measured pulse-height distributions. For continuous spectra, spectrometer calibration is more complicated and analysis more laborious than for line spectra. The calibration procedure must include determination of total detector response over the entire range of energy k and pulse height E that is covered by the continuous spectrum. The pulse-height spectrum $dn(E)$ and the corresponding photon energy spectrum $dw(k)$ are, in general, related as follows:

$$dn(E) = \int_0^k \max R(E,k) dw(k). \quad (4-80)$$

The response function $R(E,k)dE$ defines the probability that a photon emitted with energy k produces a pulse of height between E and $E+dE$ when detected. The accuracy to which a measured spectrum $dn(E)$ can be compared with a predicted IB spectrum $dw_{IB}(k)$ depends both on the accuracy of R and the method used to solve Eq. (4-80).

In analogy to extensive work on β spectra, various methods for making response corrections on continuous γ spectra have been worked out that are applicable to measurements with NaI(Tl) and Ge(Li) spectrometers. In the present paper, we can only make a few remarks on essential features. Electron-capture bremsstrahlung spectra have been subjected successively to procedures designed to correct for resolution, Compton distribution, total efficiency, iodine K x-ray escape, etc. (Lidén and Starfelt, 1954; Lindqvist and Wu, 1955; Persson and Koonin, 1972). As an example, Fig. 4-22 shows the various

corrections applied by Lindqvist and Wu (1955) to the IB spectrum of ^{37}Ar . These procedures depend very much on the peculiarities of the detector arrangement and can differ considerably in accuracy. We discuss, instead, more generally applicable methods based on the application of complete response functions.

Determination of response functions for NaI(Tl) and Ge(Li) spectrometers. The response function R [Eq. (4-80)], which varies strongly with the type of spectrometer and the measured energy range (see e.g. Heath, 1963), can in principle be calculated in terms of the different fundamental absorption processes in the detector. Monte-Carlo calculations have been performed, e.g., by Beattie and Byrne (1972) for scintillators and by Meixner (1974) for Ge(Li) spectrometers. These calculations have reached a high level of accuracy; their application, however, is limited by the fact that the true dimensions of the detector's sensitive volume and the thickness of dead zones and encapsulations are often not accurately known. In fact, calculations deviate from measured response functions, especially at low energies.

All pertinent effects are correctly taken into account if the response function is determined empirically by interpolation, starting from pulse-height spectra produced by monoenergetic γ rays of known energies and intensities.

For NaI(Tl) spectrometers, numerous peak-fitting procedures have been developed (e.g., Prescott, 1963); these allow one to derive the energy dependence of the fitting parameters. For the interpolation

of Compton distributions, Chester et al. (1963) have fitted parametrized analytical curves to measured spectra and determined the sets of parameters as functions of the energy k . Wapstra and Oberski (1963) and others have interpolated between calibration spectra that were transformed so as to bring all Compton edges to a common value of the transformed pulse height. Under special conditions, e.g. with large crystals in close geometry yielding a small Compton-to-peak ratio, it may suffice to approximate the Compton distributions by simple rectangular or trapezoidal shapes. The possibility of such simplification has been demonstrated by Persson and Koonin (1972) for IB spectra measured with a 3×3-in. NaI(Tl) crystal (Fig. 4-16).

With Ge(Li) spectrometers, the correct determination of peak areas is important, whereas the peak shapes can be approximated because the continuous spectra vary little over an energy interval corresponding to a peak width. On the other hand, correct fitting of the Compton distribution is of the utmost importance, especially for small detectors, because the Compton-to-peak ratio is large. Methods for interpolating Compton distributions by fitting parametrized curves (Ribordy and Huber, 1970) and by interpolating transformed calibration spectra (Mutterer, 1973a, c) were reported. Both procedures have yielded accurate Ge(Li)-response functions (Fig. 4-23).

Correction methods. With a known response function, a measured IB pulse-height spectrum dn_{IB} can be compared in either of two ways with a theoretical spectrum dw_{IB} : (i) the theoretical spectrum can be converted according to Eq. (4-80) into a "predicted" pulse-height

spectrum that is compared with the measured spectrum (folding method), or the measured pulse-height spectrum can be converted into an experimental energy spectrum by solving Eq. (4-80) (unfolding method).

The folding method has been applied most often in the evaluation of IB results; e.g. for ^7Be by Lancman and Lebowitz (1971b), and Mutterer (1973b, c), ^{37}Ar by Anderson and Wheeler (1953), Lindqvist and Wu (1955), and Saraf (1956), ^{49}V by Hayward and Hoppes (1956), ^{51}Cr by Mutterer (1973a, c), ^{54}Mn by Lancman and Lebowitz (1969), ^{55}Fe by Maeder and Preiswerk (1951), Michalowicz (1953), and Biavati, *et al.* (1962), ^{57}Co by Lancman and Lebowitz (1971a), ^{113}Sn by Phillips and Hopkins (1962), ^{165}Er by Ryde *et al.* (1963a), and ^{204}Tl by Lancman and Bond (1973). The folding method is simplest but has the great disadvantage that no direct experimental energy spectrum dw_{IB} is obtained. It is thus less valuable for a detailed comparison of IB experiments with theory. Furthermore, the important method for determining the transition energy E_{EC} by constructing a Jauch plot of dw_{IB} (Sec. 4.2.4) cannot be applied. Instead, a variational procedure has often been used to determine E_{EC} : dn_{IB} is calculated from IB theory and the known detector response as a function of the end-point energy q , and q is varied to give the best fit to the measured spectrum (Fig. 4-24). To obtain experimental results for the IB yield as well as E_{EC} , both a constant factor and q have often been varied in fitting calculated to experimental IB pulse-height spectra (e.g., Lancman and Lebowitz, 1969, 1971a, b). Experimental results on the IB yield obtained by this method evidently imply theoretical assumptions on the spectral shape.

The unfolding method is consequently to be preferred. Various procedures have been reported in ^{the} literature. The solution of Eq. (4-80) by matrix inversion usually has to be limited to small matrices. This difficulty can be overcome by iterative methods, such as the correction-factor method of Scofield (1963) and the Gauss-Seidel method (e.g., Zurmühl, 1965). Both of these methods, which also have often been used for unfolding measured β spectra, normally lead to quite rapid convergence if the diagonal elements ($E=k$) in the response function dominate. Ribordy and Huber (1970) have compared different iterative methods for unfolding the IB spectrum of ^{51}Cr and find comparable results. The Gauss-Seidel method was applied to the ^{51}Cr IB spectra by Mutterer (1973a, ^{b,} c), who found rapid convergence of the iteration, provided that the response function was renormalized to unit peak areas. These unfolding techniques performed with the aid of modern computers have yielded accurate response corrections for bremsstrahlung spectra: It should be noted, however, that some problems remain concerning the propagation of statistical experimental errors (Weise, 1968).

4.2.4. Determination of Electron-Capture Transition

Energies from Measured IB Spectra

The determination of IB endpoint energies is of particular interest because it provides a direct method for measuring EC transition energies E_{EC} and the corresponding isobaric atomic mass differences Q_{EC} . The endpoint of an IB spectrum is equal to the energy q of the neutrino emitted during ordinary (nonradiative) electron

capture and, consequently, the transition energy is obtained by adding to the endpoint energy the atomic binding energy (in the daughter atom) of the shell from which capture has occurred (Rubinson, 1971).

Transition energies have been determined in most IB experiments. In Tables 4.6 and 4.8, E_{EC} results are listed which were obtained from measurements of total and ls IB spectra. Tables 4.6 and 4.8 also contain E_{EC} values deduced from the atomic-mass compilation of Wapstra and Gove (1971). With few exceptions (^{113}Sn , ^{125}I , ^{197}Hg and ^{204}Tl), the IB data are in fair agreement with the atomic-mass differences. It should, however, be noted that the two sets of data are not independent. Wapstra and Gove (1971) have considered part of the listed IB data in assigning the isobaric mass differences, supplementing data from nuclear reaction thresholds and electron-capture ratios. Especially in the medium and high-Z region (e.g., ^{103}Pd , ^{109}Cd , ^{119}Sb , ^{131}Cs , ^{145}Sm and ^{181}W), the listed E_{EC} values from IB experiments appear, with slight changes, also in the atomic mass tables.

Because of the great importance of accurate mass differences, some comments on the determination of IB endpoint energies are in order. Many electron-capture transition energies listed in Tables 4.6 and 4.8 originate from early experiments and are of low accuracy. These measurements could be much improved with modern techniques. The overall accuracy of E_{EC} , however, depends also upon the theoretical model which is used to extract the IB endpoint energy q from a measured IB spectrum. This dependence on theory is most obvious in E_{EC} determinations based on the fitting of calculated spectra to measured

ones, with q_{1s} as the fitting parameter (Sec. 4.2.3). That different theoretical assumptions in this procedure can yield quite different values of q_{1s} was demonstrated by Lancman and Bond (1973) in the case of the first forbidden unique EC decay of ^{204}Tl : fitting procedures with different allowed IB shapes yielded E_{EC} values that differ by 25 keV. Shape functions from theories for forbidden transitions were, however, not considered. Berényi *et al.* (1976) studied the variation of E_{EC} of ^{59}Ni , obtained from an accurately measured ^{59}Ni IB spectrum, by fitting spectra calculated from different theoretical approaches to forbidden radiative capture; they found differences of a few keV.

Most experimental transition-energy determinations from (unfolded) IB spectra dw_{IB} (or dw_{1s}) have been made by linearizing the spectra in a way that resembles the construction of Kurie plots for β spectra. The procedure for constructing such a Jauch plot (Jauch, 1951; Bell *et al.*, 1952) is based on the elementary shape of the 1s IB spectrum (Eq. 4-17) as predicted by the early Coulomb-free theory of Morrison and Schiff (1940). A linear plot is obtained by converting a measured spectrum dw_{1s} into Jauch coordinates by plotting $(dw_{1s}/k)^{1/2}$ vs. k . Because of the predicted proportionality

$$(dw_{1s}/k)^{1/2} \propto k - q_{1s}, \quad (4-81)$$

the intercept with the k -axis occurs at q_{1s} . The accuracy of this procedure evidently depends on how closely the investigated spectrum is approximated by the Morrison-Schiff theory. For a strictly correct linearization, various corrections to the spectrum must be considered which appear in the modern theory for allowed decays (Sec. 4.1.2) and for forbidden decays (Sec. 4.1.4).

The 1s IB spectrum from allowed and first-forbidden nonunique decays can be linearized more strictly on the basis of the relation

$$\left[\frac{dw_{1s}}{kR_{1s}(k)} \right]^{1/2} \propto k - q_{1s}. \quad (4-82)$$

The 1s IB shape function $R_{1s}(k)$ corrects for relativistic and Coulomb effects; it can be calculated exactly from Eq. (4-44). This shape function is displayed in Fig. 4-3 for various atomic numbers. The influence of R_{1s} on the determination of q_{1s} has been studied by Zylicz *et al.* (1963) in the case of the ^{165}Er IB spectrum (Fig. 4-5). It was found that a Jauch plot according to the relation (4-82) yields an endpoint energy that differs by 3 keV from that obtained with a simple plot based on the proportionality (4-81). In this analysis, however, an approximate result for the relativistic shape factor R_{1s} was used, as derived by Martin and Glauber (1958). For ^{165}Er ($Z=68$) and in the measured energy range, $150 \text{ keV} \leq k \leq 300 \text{ keV}$, the approximate function deviates considerably from the exact function R_{1s} (Fig. 4-4), so that a greater effect of R_{1s} on q_{1s} is expected. Larger differences are also expected in the case of IB spectra that cover wider energy intervals and are not measured as close to the endpoint.

In order to determine 1s IB endpoint energies from measured total IB spectra dw_{IB} , a correction must be applied for the higher-shell components which have endpoints q_{nl} larger than q_{1s} . In the energy range $k < q_{1s}$, this correction can be written

$$dw_{\text{IB}} = dw_{1s} \left[1 + \left(\sum_{nl} \frac{dw_{nl}}{dw_{1s}} \right) \right]; \quad (4-83)$$

this leads to an additional energy-dependent correction $f(k)$ in the Jauch coordinate:

$$[\text{dw}_{\text{IB}}/kR_{1s}(k)f(k)]^{1/2} \propto k - q_{1s}. \quad (4-84)$$

The k -dependence of $f(k)$ is complicated because it generally contains the higher-shell shape functions R_{ns} and Q_{np}^2 (Tables 4.2 and 4.3) as well as corrections for the different endpoint energies q_{nl} . In most practical cases, however, only higher-shell s radiation is important at higher energies. The correction for the dominant $2s$ radiation is adequately taken into account by

$$f(k) = 1 + \frac{P_L R_{2s}(k)}{P_K R_{1s}(k)} \left(1 + \frac{k_{Kx}}{q_{1s} - k} \right)^2. \quad (4-85)$$

Here, P_L/P_K is the L/K electron-capture ratio, and the K x-ray energy k_{Kx} has been written for the difference $q_{2s} - q_{1s}$. The term containing k_{Kx} constitutes an important correction for experimental data that are close to q_{1s} , within a few times k_{Kx} . Because this term implicitly also contains q_{1s} , the correction (4-85) can only be calculated iteratively.

Equation (4-84) has been used by Mutterer (1973a, b) in determining the IB endpoint energies of ^7Be and ^{51}Cr , with R_{ns} functions calculated from Martin and Glauber's theory, setting $R_{1s} = R_{2s} = 1$.

In total IB spectra that accompany low-energy transitions between high- Z nuclei, p radiation dominates; a correction function $f(k)$ can be calculated from theory, using shape functions Q_{np}^2 and the corresponding subshell capture ratios. Because p -type spectra deviate considerably from the Morrison-Schiff spectrum, it is expected

that a simple Jauch plot according to Eq. (4-81) may yield quite incorrect results. Consequently, the result for E_{EC} of ^{193}Pt derived by Hopke and Naumann (1969) from both the L- and M-capture bremsstrahlung (Fig. 4-21) by using Eq. (4-81) should be regarded with reservations.

It is clear that reliable theoretical calculations are necessary for obtaining accurate E_{EC} values from measured IB spectra. A strong argument for the performance of accurate new IB experiments is implied. Measurements on those decays for which accurate E_{EC} values are available from independent experiments are most valuable for testing IB theories.

4.2.5. Experimental Results and Comparison with Theory:

Allowed and First-Forbidden Nonunique Transitions

Most experiments described so far deal with allowed EC decays. They are to be compared with the theory of Martin and Glauber (1958) which, in the ξ approximation, is expected to apply also for first-forbidden nonunique decays.

In most experiments, only spectral shapes have been determined. The results, of varying accuracy, generally agree with theory. This agreement is found both for total IB spectra (experiments listed in Table 4.6) with dominating s- and p-type radiation and for 1s IB spectra singled out by IB-K-x-ray coincidences (Table 4.8). The situation is illustrated in Figs. 4-15, 4-26, and 4-27 for the s IB spectra of ^{51}Cr , ^{49}V , and ^{55}Fe , which cover different energy ranges. Figure 4-20 contains a comparison with theory of the 1s IB spectrum of ^{131}Cs and of the total IB spectrum which in this case covers an

energy range below αZ , so that p radiation dominates. Measured s IB spectra (including 1s IB spectra) however, are generally not sufficiently accurate to reveal the weak energy dependence of the predicted IB shape factors (mainly R_{1s}). The measured IB shapes can therefore not be used to distinguish between the theory of Martin and Glauber and the pioneering work of Møller (1937a) and Morrison and Schiff (1940). It is seen from Fig. 4-3 that R_{1s} depends on the energy k quite differently for different atomic numbers and in different energy regions. The most precise measurement of an allowed IB shape was performed by Berényi et al. (1965b) on ^{55}Fe . In Fig. 4-27, their result is displayed in terms of the effective shape factor R_{eff} , defined by

$$R_{\text{eff}}(k) \propto dw_{\text{IB}}(k)/[k(q_{1s} - k)^2]. \quad (4-86)$$

The function R_{eff} is equal to R_{1s} , multiplied by the correction function $f(k)$ for higher-shell contributions [Eq. (4-85)]. The accuracy of the experiment of Berényi et al. (1965b) is comparable with the accuracy attainable in determinations of β shape factors. The constancy of R_{eff} within 1%, found in this measurement, can also be compared in this special case with the Martin-Glauber theory. It is seen from Fig. 4-3 that, for $Z=26$, the theoretical 1s shape factor has a flat maximum between 100 and 218 keV, ^{the} range covered by the ^{55}Fe experiment. To reveal the dependence of R_{1s} on k , accurate shape measurements below ~ 100 keV and on transitions of high energy (e.g. ^{37}Ar and ^{49}V) should be performed.

Only in a few experiments has the IB intensity been measured in

addition to the shape. Some of the data on normalized IB spectra have been compiled and compared with theory by Bouchez and Depommier (1965), Kádár et al. (1970), Lancman and Lebowitz (1971a), Vanderleeden et al. (1971), Kádár (1971), Koonin and Perssón (1972), and Mutterer (1973c). Conclusions from these summaries were partly inconsistent, depending on whether or not theoretical values were recalculated and which values for the transition energies E_{EC} were inserted. Here we therefore compare experimental results with consistently calculated theoretical values.

The selected experimental data on normalized IB spectra from allowed and first forbidden nonunique decays are compiled in Table 4.9. These data represent integral values $I_{IB}(k_1, k_2)$ of normalized spectra dw_{IB} , measured between energy limits k_1 and k_2 . The upper limits k_2 are always equal to or slightly below the endpoint energies q . We did not consider data for which k_1 and k_2 were not specified, as in measurements on ^{51}Cr by Cohen and Ofer (1955), Ofer and Wiener (1957), Murty and Jnanananda (1957), and Ribordy and Huber (1970). In these experiments, the γ branching ratio in ^{51}Cr was determined by comparing IB and γ intensities. We also have omitted results on ^{51}Cr reported by Vanderleeden et al. (1971) and Kuphal et al. (1973), which were deduced from measurements of circularly polarized bremsstrahlung, because the measured energy range could not be inferred clearly. It is to be noted that experimental I_{IB} values obtained from measured IB pulse-height spectra through the folding method (Sec. 4.2.3) also do not exactly represent the IB intensity within stated limits, but

rather constitute ratios of counting rates between corresponding limits E_1 and E_2 . These values are included in the comparison, but are specially identified in Table 4.9. In this Table, we distinguish between values for 1s IB intensities I_{1s} and intensities of total IB spectra, measured relative to the ordinary K or total EC rates.

The experimental values listed in Table 4.9 are compared with predictions according to different approaches to the theory of allowed radiative capture. Predictions for 1s IB intensities (which dominate as well in most of the listed total spectra) have been calculated from the Coulomb-free theory of Morrison and Schiff (MS) (1940) and from the theory of Martin and Glauber (MG) (1958). Results are listed from both the (analytical) low-energy approximation of Eq. (4-38) (MG) and the (numerically calculated) exact solution [Eq. (4-44)] as derived by Intemann (Int) (1971). The higher-shell contributions were consistently calculated from the approximate relativistic Martin-Glauber theory (Glauber and Martin, 1956) with screening corrections of Fig. 4-7. We consistently used transition energies E_{EC} derived from the atomic mass compilation of Wapstra and Gove (1971) and, for EC decays to excited states, from γ energies as evaluated by Meixner. Energies $q_{n\ell}$ were calculated from atomic binding energies (Bearden and (1971) \wedge). The only exception is ^{197}Hg , where the E_{EC} value of 338 ± 20 Burr, 1967) keV derived from the mass table (which originates from a $P_{K\omega_K}$ measurement by DeWit and Wapstra, 1965) falls completely outside of the range of the measured IB spectrum. Uncertainties in the calculated intensities which are due to the stated errors in the energy E_{EC} were estimated from the Coulomb-free theory by differentiating Eq. (4-16) with respect to q_{1s} . These uncertainties were found to be generally

below 1%, except for ^{71}Ge , ^{131}Cs , ^{145}Sm and ^{165}Er , where they lie between 2% and 7%, and for ^{197}Hg , where it is 40%.

In Figs. 4-28 to 4-30, ratios $\rho_{E,T}$ of experimental and theoretical bremsstrahlung intensities are plotted as a function of atomic number. We have included only data which pertain predominantly to s radiation. The indicated error bars correspond to the sum of experimental and theoretical errors.

In Table 4.10, unweighted average values $\langle \rho_{E,T} \rangle$ of independent measurements are listed.

The summary of experimental and theoretical IB intensities proves the advantage of the theory of Martin and Glauber over the Coulomb-free approach. The measured data, although widely scattered, clearly reveal the predicted reduction of the IB intensity, increasing with Z , that is caused by relativistic and Coulomb effects. While this lowering of the intensity is most obvious in the heavier nuclides with $51 \leq Z \leq 80$, it can also be noted, on the average, in the data on lighter nuclides with $18 \leq Z \leq 32$.

The ratios $\rho_{E,T}$ between measured data and theoretical intensity according to either MG or Int deviate from unity by up to 50%; the deviations in most cases are larger than the error bars. The available data do not allow one to distinguish between the approximate solution of MG and the exact solution of Int. The average values $\langle \rho_{E,T} \rangle$ in Table 4.10 provide no evidence that experiments deviate systematically from the Martin-Glauber theory, either at low Z or in general, contrary to indications in previous surveys by Lancman and Lebowitz (1971a) and Vanderleeden *et al.* (1971). On the other hand, the

inconsistency between experimental results makes it difficult to assign a limit within which the present theory correctly seems to describe the intensity of bremsstrahlung.

Inspection of the experimental data shows that there is a special discrepancy between some of the most recent results obtained by different groups of authors, with quoted probable errors of 6% to 20%. The IB- γ coincidence experiments of Lancman and Lebowitz (1969, 1971a, b) on ^7Be , ^{54}Mn , and ^{57}Co yielded intensities that fall 20% to 50% below theoretical predictions, whereas similar experiments, performed with improved techniques by Persson and Koonin (1972) and Koonin and Persson (1972) on ^7Be , ^{51}Cr , and ^{54}Mn led to results that exceed theoretical intensities by up to 30%. The spectrometry of IB and γ rays in ^7Be and ^{51}Cr by Mutterer (1973a, b) yielded IB intensities which are in agreement with theory to within $\leq 8\%$. This inconsistency suggests that unknown sources of systematic errors of $\leq 10\%$ remain in the experimental techniques and in the procedures applied for the response correction.

Double IB. Experimental evidence for the simultaneous emission of two IB photons during electron capture, or double internal bremsstrahlung, has been reported by Ljubičić *et al.* (1974). Coincidences between two IB photons from ^{37}Ar were measured at an angle of 90° to each other. In the energy range from 210 to 810 keV, the ratio of double IB to single IB was found to be $(4.8 \pm 0.4) \times 10^{-5}$, which is comparable to the IB/EC rate, as might be expected. The only presently available theoretical results on double IB are those of

Menhardt (1957), which unfortunately are not applicable to the experimental situation realized by Ljubičić et al. (1974).

4.2.6. Experimental Results and Comparison with Theory:

IB Spectra from Higher-Forbidden Decays

Experimental information on IB spectra that accompany higher-forbidden transitions is limited to a few cases of ground-state transitions by EC alone (^{41}Ca and ^{59}Ni) or with competing β^- branches (^{36}Cl and ^{204}Tl). Some of these decays have been measured extensively (Tables 4.6 and 4.8).

Bremsstrahlung from first-forbidden unique transitions has been studied with ^{41}Ca and ^{204}Tl . The total IB spectrum from ^{41}Ca was measured with a Ge(Li) spectrometer by Myslek et al. (1973). The observed shape (Fig. 4-31) is not in accord with the theory of Zon and Rapoport (1968) and Zon (1971). The shape agrees with theory only at low energies, $k < 250$ keV; at higher energies the spectrum has nearly allowed shape. Myslek et al. have also derived a crude value for the IB intensity by estimating the K capture rate from the weight of the source. A value of 3.9×10^{-4} IB photons between 90 and 421.5 keV per EC event was found, much in excess of theoretical predictions. For forbidden transitions, theory in the Coulomb-free approach of Eq. (4-79) leads to an upper limit of 5.7×10^{-5} IB photons per decay. The low- Z expansion of Zon and Rapoport (1968) results in a value of 3.3×10^{-5} photons and more detailed calculations of Zon (1973) have yielded 4.9×10^{-5} photons per EC transition.

On ^{204}Tl , several IB-K-x-ray coincidence experiments have been

performed to measure the 1s IB spectrum that accompanies the 2.1% EC branch to the ground state of ^{204}Hg . Severe doubts exist regarding the reliability of early experiments by Der Mateosian and Smith (1952), Jung and Pool (1956), and Biavati *et al.* (1962), because no corrections for the bremsstrahlung from the 97.9% β^- branch to ^{204}Pb were applied. It was first pointed out by Goudsmit *et al.* (1966) and established by a recent experiment of Lancman and Bond (1973) that scattering effects due to the β^- bremsstrahlung and double-IB emission can cause a continuous spectrum that closely resembles the IB spectrum expected from the weak EC branch. The shape of the IB spectrum measured by Lancman and Bond, taking account of corrections for these effects, agrees well with the theory for allowed transitions. Such agreement is expected because only a small energy range is involved. The intensity per K capture was found to be 2.8×10^{-6} IB photons above 103 keV. This result is to be compared with an upper limit of 1.08×10^{-5} , from Eq. (4-79). More accurate theoretical results are not available. Zon (1973) has reported only values for the shape factors, and the $Z\alpha$ expansion of Zon and Rapoport (1968) is not applicable for ^{204}Tl , because the entire IB spectrum lies in the region of the K binding energy.

Bremsstrahlung spectra from second-forbidden nonunique transitions were studied with ^{36}Cl and ^{59}Ni by several groups. It has been well established that the total IB spectrum of ^{36}Cl closely follows an allowed shape at energies above 600 keV. This observation agrees with the calculation of Zon (1971), which predicts a noticeable deviation from allowed shape only at lower energies. The result of the

most recent IB measurement on ^{36}Cl by Smirnov and Batkin (1973) is shown in Fig. 4-32. An attempt was made to look for possible contributions from detour transitions; a clear indication could, however, not be established.

In the case of ^{59}Ni , a distinct deviation of the IB spectrum from allowed shape was observed already in an early measurements by Saraf (1956); the IB intensity above 100 keV was reported to be 1.4 ± 0.4 times the theoretical value calculated from the early theory of Cutkowsky (1954). The shape of the ^{59}Ni IB spectrum was very carefully measured by Schmorak (1963), who used 3×3-in. and 5×5-in. NaI(Tl) detectors. An apparent deviation from the calculated shape, observed near the endpoint, was attributed to destructive interference with detour transitions, as predicted by Rose *et al.* (1962). Schmorak (1963) estimated the amount of detour transitions as between 6×10^{-3} and 5×10^{-4} of the total IB intensity. A careful Ge(Li) measurement of the ^{59}Ni IB spectrum was recently performed by Berényi *et al.* (1976), who report that the measured shape agrees well with calculations of Zon (1971) and shows no evidence for detour transitions.

In most experiments performed hitherto, only spectral shapes have been determined albeit often with high precision. Without question, accurate measurements of normalized spectra would be of great value to improve our present knowledge of radiative capture in forbidden EC transitions. Pertinent EC nuclides are listed in Table 4.7.

4.2.7. Experiments on IB Correlation Effects

Experiments on the various IB correlation effects that are

-4.1.4 to allowed decays and discussed in Secs. 4.1.3 are scarce. They are confined to measurements of circular polarization and to some work on the angular distribution of IB photons emitted from oriented nuclei.

Circular polarization of internal bremsstrahlung. Experiments on the circular polarization of the IB accompanying electron capture are listed in Table 4.11. Polarimeters employed in these measurements are based on the effect of spin-dependent Compton scattering from electrons in magnetized iron. Usually, forward-scattering magnets have been used, but in the most recent experiment by Kuphal *et al.* (1974), a specially designed radial-transmission magnet was employed.

The polarization P , defined by Eq. (4-48), is proportional to the relative change $\Delta N/N$ of the measured intensity when the magnetic field in the scattering magnet is reversed:

$$P \propto \Delta N/N = 2(N_+ - N_-) / (N_+ + N_- - 2N_0). \quad (4-87)$$

Here, N_+ (N_-) is the counting rate with the electron spins in iron parallel (antiparallel) to the incident-photon momentum. The counting rate N_0 is due to background, including γ impurities in the source. If nuclides are measured which emit also nuclear γ rays, the denominator in Eq. (4-87) is represented by the counting rate of the unpolarized γ rays. The measured effect is then extremely low.

The polarization of IB in pure ground-state transitions was studied in early measurements on ^{37}Ar by Hartwig and Schopper (1958) and Mann *et al.* (1959), ^{55}Fe by Paf'anova (1960), and ^{71}Ge by Bernardini *et al.* (1958). Only recently, IB polarization has also been measured in the presence of a background of much more intense

γ rays. In such experiments on ^{51}Cr , Vanderleeden et al. (1971) used a Ge(Li) detector, whereas Kuphal et al. (1974) used a ring of 8 NaI(Tl) scintillators. In both experiments, very strong ^{51}Cr sources of up to 500 Ci were employed, and current integration was applied instead of counting techniques. The statistical errors could be kept below 10^{-6} . Clearly, the polarimeter efficiency must be accurately known to derive the absolute polarization from the measured rate $\Delta N/N$. This efficiency has generally been calculated from basic assumptions. Kuphal et al. (1974) have tested their calculation by measuring polarized (internal and external) bremsstrahlung from several β^- -decaying nuclides.

Measurements summarized in Table 4.11 confirm within errors that s-type bremsstrahlung is nearly 100% right-circularly polarized, due to the parity-nonconserving character of the weak interaction. The measured polarization of IB from ^{37}Ar (Hartwig and Schopper, 1958) is displayed in Fig. 4-33. Figure 4-34 shows $\Delta N/N$ values measured for ^{51}Cr , compared with calculations from theory. The incomplete polarization observed in ^{37}Ar at low energies and the low result for ^{71}Ge found by Germanoli et al. (1958) can qualitatively be explained by Coulomb effects and the influence of unpolarized p-type bremsstrahlung. Both effects, which enter in the overall polarization function $P(k)$ according to Eq. (4-52), reduce the polarization at low energies. A noticeable reduction of P is not expected, however, in the high-energy bremsstrahlung from ^{51}Cr ; the low value of 0.67 ± 0.07 found by Vanderleeden et al. (1971) can probably be attributed to an erroneous calculation of the polarimeter efficiency, in view of the work of Kuphal et al. (1974).

Angular distribution of IB emitted from oriented nuclei. Anisotropy of IB emitted from oriented nuclei has been observed only once. Brewer and Shirley (1968) studied the forward-backward asymmetry of IB from oriented ^{119}Sb . Carrier-free ^{119}Sb had been implanted in an iron lattice, cooled to $\sim 0.02^\circ\text{K}$, and magnetized in a field of 2.3 kOe. The IB radiation was measured with two 3x3-in. NaI(Tl) detectors placed at 0° and 180° relative to the direction of the magnetic field. Figure 4-35 shows the measured asymmetry $W(\pi)/W(0)$ as a function of the sample temperature T that defines the degree of source polarization. The measurement of this ratio for different energy intervals has revealed an unexpected energy dependence of the asymmetry.

The experimental results of Brewer and Shirley have been compared with theory by Intemann (1971) in terms of the overall asymmetry function $A(k)$ of Eq. (4-62). It was found that the measured decrease of $A(k)$ at low energies can be well explained (Fig. 4-36). This decrease is consistent with the observed decrease of the overall polarization, described above. Other nuclei that might be suitable for measuring IB angular correlations have been listed by Koh et al. (1962).

A preliminary measurement of the angular correlation between bremsstrahlung and nuclear γ rays in the decay of ^{84}Rb has been performed by Chasan and Chandra (1967). The result was reported to be in approximate agreement with calculations of Koh et al. (1962). The experimental error, however, is $\sim 50\%$ and details of the measurement have not been fully reported, so that a detailed comparison with theory is not feasible.

4.2.8. Concluding Remarks

The study of second-order effects, such as internal bremsstrahlung, is of particular interest in electron-capture decay because experimental information on the primary process is very limited because of the extremely low interaction probability of the emitted neutrino. The main features of the low-intensity radiative-capture process are generally understood today. There is still a great need, however, for experimental work to test the details of the theory. Open questions remain concerning the influence of screening and exchange and overlap effects (Persson and Koonin, 1972) on the shape and intensity of IB spectra. Experimental information is still very scarce on forbidden decays, where nuclear matrix elements play an important role.

Precise measurements of normalized IB spectra are very much needed. The same holds for measurements of partial spectra that accompany the capture of electrons from specific atomic subshells. Experimental techniques have been developed to high accuracy in recent years. This applies especially to the determination of electron-capture rates, to coincidence experiments with bremsstrahlung, and to calibration procedures for γ spectrometers which yield complete response functions. It can be expected that it will be possible to measure normalized IB spectra in the near future with an overall accuracy of a few percent, at least in some favorable decays such as pure ground-state transitions. As pointed out before, precise experiments are also very valuable for providing accurate isobaric atomic-mass differences, supplementary data on subshell capture ratios, and spectroscopic information on branching ratios. In this context, refined computa-

tions of higher-shell IB spectra, based on the present theory, would be of interest.

The variety of IB correlation effects, discussed in Secs. 4.1.3 - 4.1.4 opens another wide field for future experimental work, from which valuable information on the weak interaction and nuclear structure can be expected. Bremsstrahlung measurements may also help to solve some specific problems of radionuclide metrology (Spernol *et al.*, 1973; Mutterer, 1973c), such as the (relative and absolute) determination of disintegration rates of pure EC nuclides.

5. ATOMIC TRANSITIONS ACCOMPANYING NUCLEAR

ELECTRON CAPTURE

5.1. Introduction

In first approximation, the probability of allowed capture of a K electron by the nucleus is

$$\lambda_K \propto G^2 q^2 \xi |\psi^{(K,Z)}(0)|^2, \quad (5-1)$$

where G is the β -decay coupling constant, q is the energy of the emitted neutrino, ξ the appropriate combination of nuclear matrix elements, and $\psi^{(K,Z)}(0)$ is the 1s-electron wave function, evaluated at the origin (Sec. 2). The only electron wave function contained in this formulation is that of the electron which is destroyed. Two significant aspects of the problem are neglected in Eq. (5-1): (1) the indistinguishability of electrons, and (2) the nuclear charge change by one unit, which entails that parent and daughter atomic wave functions are eigenfunctions of different Hamiltonians.

The importance of treating β decay and nuclear electron capture as transformations of the whole atom, and hence, of including atomic variables in the description of initial and final states, was first emphasized by Benoist-Gueutal (1950, 1953a, b), pursued by Odier and Daudel (1956), and comprehensively formulated by Bahcall (1962a, 1963a, b). In fact, an infinite number of final atomic states, including continuum states, contribute to any given electron-capture probability. The effect on transition rates is discussed in Sec. 2. In the present section, we consider observable atomic effects that result during

nuclear decay by electron capture. Atomic rearrangements that take place after the decay process are not included in this discussion, even though x rays emitted in the course of such rearrangements have led to the discovery of the process (Alvarez, 1937, 1938a, b) and constitute the most readily detectable signals indicating that capture has taken place. Details of the rearrangement process have been surveyed by Rao et al. (1972) and Bambynek et al. (1972). Here, we consider atomic transitions that take place in the course of the electron-capture decay process, due to imperfect overlap between parent and daughter atomic wave functions. This effect is variously denoted as electron shakeup and shakeoff, autoionization, or internal ionization.

5.2. Internal Ionization: Nonrelativistic Theory

Nuclear electron capture is accompanied by the emission of low-intensity, continuous photon and electron spectra. The internal-bremsstrahlung photon spectrum emitted during radiative electron capture was first calculated by Møller (1937a) and by Morrison and Schiff (1940); this subject is discussed in Sec. 4. The process of internal ionization was first treated by Primakoff and Porter (1953), who calculated the probability of K-electron ejection during K capture and derived an expression for the ejected-electron spectrum, in analogy with work by Migdal (1941) and Feinberg (1941) on orbital-electron ejection accompanying β -particle emission.

The weak interaction which is responsible for nuclear electron capture is of very short range. On the atomic time scale, the

transformation of the parent nucleus with Z protons into the daughter nucleus with atomic number Z' can be assumed to be instantaneous. One can gain an intuitive feeling for the mechanism that causes internal ionization by considering the nucleus plus the orbital vacancy created by the capture simply as the source of a suddenly changing Coulomb potential. A $1s$ electron, for example, with the wave function $\psi^{(K,Z)}$ in the parent atom does not have time to adjust its wave function adiabatically to the change in potential; the sudden approximation of time-dependent perturbation theory applies. The amplitude of the probability that the electron retains its original quantum numbers is then proportional to the overlap of its original wave function with the $1s$ wave function in the daughter ion with one inner vacancy:²⁵

$$P_{\text{remain}} \propto \left| \int \psi^{(K,Z')}^*(\vec{r}) \psi^{(K,Z)}(\vec{r}) d\vec{r} \right|^2. \quad (5-2)$$

Similarly, the overlap of $\psi^{(K,Z)}$ with excited- and continuum-state wave functions in the potential of the daughter ion provides an indication of the probability amplitudes of excitation or ejection of the K electron. The Pauli principle excludes excitation into occupied orbitals, and conservation of angular momentum allows only $\ell=0$ final states for s -electron shakeup or shakeoff.

It is a gross oversimplification, however, to consider the nucleus-plus-vacancy as a mere source of an abruptly changing electrostatic potential, and the internal excitation and ionization probabilities as determined by wave-function overlap alone. In particular, energy conservation and the demands of quantum

statistics are not included unless the process is treated as a transformation of the whole atom, and nuclear and lepton variables (including those characterizing the pertinent atomic electrons) are incorporated in the description of the initial and final states of the system. Especially, the available energy is shared statistically between ejected electron and neutrino, and the transition probability is weighted by the density of available final states. The energy-conserving delta function must be included in the expression for the transition probability.

Quantitatively, the transition probability can be expressed in the sudden perturbation approximation through "Fermi's Golden Rule No. 2." The general applicability of this approach to the present problem has been examined by Bahcall (1963a). The transition rate for K-electron ejection during K capture is —

$$dw = 2\pi \int (1/2) \sum |M|^2 \delta(W_0 + 1 - |E'_K| - W - q) d\vec{q} d\vec{p}, \quad (5-3)$$

where \vec{p} and W are the momentum and total relativistic energy of the ejected electron, \vec{q} is the neutrino momentum and q its energy, $1 - |E'_K|$ is the total energy of a K electron in the daughter atom (with binding energy E'_K), and $W_0 + 1$ is the energy difference between the parent atom and the neutral daughter atom (Sec. 1.2). The matrix element M is discussed below. The units used throughout this discussion are such that $\hbar = m = c = 1$, and hence, $e^2 = \alpha \approx 1/137$. The summation sign in Eq. (5-3) indicates summing over spin states of ejected electron and neutrino, and over spin states of the two initial K electrons. One must also sum over final nuclear spin states and

average over initial nuclear spin states. Because $\Sigma |M|^2$ is independent of \vec{q} , the integration over all possible neutrino momenta can be carried out at this stage.²⁶ The result, after performing the spin summations, is

$$dw = 16\pi^3 (W_0 + 1 - |E'_K| - W)^2 P^2 dp \Sigma |M|^2 \quad (5-4)$$

(Intemann, 1972).

In a representation in which the interaction Hamiltonian consists of the β interaction H_β alone, the matrix element for K-electron ejection during K capture can be written

$$M = (1 - P_{12}) \int \psi^{(\infty, Z')}^*(\vec{r}) \psi_\nu^*(0) \psi_N^* |H_\beta| \psi_N \psi_{1,2}^{(K, Z)}(0, \vec{r}) d\vec{r}. \quad (5-5)$$

Here, ψ_N , and ψ_N are the final and initial nuclear wave functions, respectively, and ψ_ν is the neutrino wave function. The wave functions of the leptons that participate in the β interaction have been replaced by their values at the origin. It is assumed that all but the two K electrons retain their original quantum numbers, and that their initial and final wave functions overlap perfectly. The exchange operator P_{12} exchanges the two K electrons.

The main difficulty in explicitly writing out the matrix element (5-5) resides in expressing the initial-state two-electron wave function $\psi_{1,2}^{(K, Z)}$, including correlation effects between the two electrons. Primakoff and Porter (1953), in their classic calculation, used an approximate wave function of the form

$$\psi_{1,2}^{(K, Z)}(r_1, r_2) = N \psi_1^{(K, Z)}(r_1) \psi_2^{(K, Z)}(r_2) e^{\alpha \gamma_1 r_{12}} e^{\alpha \gamma_2 (r_1 + r_2)}, \quad (5-6)$$

where ψ_1 and ψ_2 are hydrogenic 1s wave functions, and N is chosen to assure normalization. The factor $e^{\alpha\gamma_1 r_{12}}$ takes account of the effect of the electron-electron Coulomb interaction on their spatial correlation, and the factor $e^{\alpha\gamma_2 (r_1+r_2)}$ accounts for screening of the nucleus, effectively replacing Z by $Z-\gamma_2$ in ψ_1 and ψ_2 . The parameters γ_1 and γ_2 were chosen so that ψ_{12} is a good approximation to the Hylleraas variational wave function for a two-electron atom. With a Coulomb wave function $\psi^{(\infty, Z')}$ to describe the ejected electron and a plane wave to describe the neutrino, the matrix element (5-5), and hence, the transition rate (5-3) were computed. Dividing by the transition rate w_K for ordinary allowed K capture, Primakoff and Porter derived an expression for the probability, per K-capture event, for ejection of the other K electron with a momentum in the range dp . This result can be written

$$dw_{\text{ejec}} = \frac{dw}{w_K} = \frac{16\alpha^2 \zeta^4 p^4 e^{-(4\zeta/p) \tan^{-1}(p/\zeta)}}{(\zeta^2 + p^2)^4 (1 - e^{-2\pi\zeta/p})} \left[1 - \frac{p^{2/2 + |E'_K|}}{W_0 + 1} \right]^2 dp. \quad (5-7)$$

Again, W_0 and the K-electron binding energy E'_K are in units of mc^2 , the ejected-electron momentum p is in multiples of mc , and ζ stands for αZ . We have neglected $\gamma_1 + \gamma_2 \approx 0.5$ and unity compared with Z in the final result, and have set $\beta = p$, i.e., $W \approx 1$ for the ejected electrons, whose kinetic energy is generally very much smaller than mc^2 . As before, $W_0 + 1 = \Delta W_{\text{nucl}} - \Delta(\Sigma E_x) + 1$ is the mass difference between parent and daughter neutral atoms: ΔW_{nucl} is the nuclear energy release, and $\Delta(\Sigma E_x)$ is the change in the total electronic binding energy between parent and daughter atoms--a positive quantity in electron capture (Sec. 1.2).

A very different method for constructing the initial two-electron wave function was devised by Intemann and Pollock (1967), who calculated it from perturbation theory. They treated the electron-electron interaction as a perturbation on the nuclear Coulomb interaction, including it in the perturbed part of the Hamiltonian, rather than in the unperturbed part as Primakoff and Porter had done. In essence, they performed a perturbation expansion on the exact two-electron wave function, with the perturbation taken to be the electron-electron interaction. With this approach, the problem of K-shell internal ionization during K capture is one in third-order perturbation theory, involving a sum over intermediate electron states. Intemann and Pollock found it possible to represent this sum in closed form by drawing upon the analogy between internal ionization and internal-bremsstrahlung emission. In fact, the electron-ejection process can be looked upon as a radiative capture process in which the emitted photon is virtual, and is absorbed by the electron that is ejected. Exploiting this aspect of the problem, Intemann and Pollock were able to take advantage of a crucial observation made by Glauber and Martin (1956; Martin and Glauber, 1958) in their development of the theory of radiative capture, *viz.*, that the sum over intermediate electron states which appears in the calculation is the Green's function for the Dirac equation with a nuclear Coulomb potential and can be represented in closed form. This approach made a more exact analysis of the internal-ionization process possible. The result for the differential transition rate per K-capture event is

$$d_{w_{eject}} = \frac{64\alpha^2 \zeta^4 p e^{-(4\zeta/p) \tan^{-1}[p/(2\zeta+\mu)]}}{(\mu+\zeta)^4 [(2\zeta+\mu)^2 + p^2]^2 (1-e^{-2\pi\zeta/p})} \times [(1-p^2)/2(W_0+1)]^2 I^2 dp. \quad (5-8)$$

Here, we have $\mu = [2(1-\epsilon)]^{1/2}$, where ϵ is the intermediate-state energy (in units of mc^2) of the electron undergoing capture: $\epsilon = \epsilon_1 + \epsilon_2 - W$, where ϵ_1 and ϵ_2 are the energies of the initial K electrons, and W is the energy of the ejected electron. In the Intemann-Pollock treatment, the relation $\epsilon = 1 - \zeta^2 - p^2/2$ holds, because $\epsilon_1 = \epsilon_2 = 1 - \zeta^2/2$ and $W = 1 + p^2/2$.

The integral I is

$$I = 1 + \eta \int_0^1 x^{-\eta-1} [1 - (1-x)^4 f(x)] dx, \quad (5-9)$$

where

$$f(x) = \frac{e^{-(2\zeta/p) \tan^{-1}[(2\zeta+\mu)/p]} e^{(2\zeta/p) \tan^{-1}[(2\zeta/p) + \mu(1+x)/p(1-x)]}}{(1+\lambda x)^2 (1+\sigma x) (1+\sigma^* x)} \quad (5-10)$$

and the remaining symbols are defined as $\eta = \zeta/\mu$,

$\sigma = (\mu - 2\zeta - ip)/(\mu + 2\zeta + ip)$, $\lambda = (\mu - \zeta)/(\mu + \zeta)$. Fortunately, a rapidly converging Maclaurin series exists for I :

$$I = \eta \sum_{n=0}^{\infty} \frac{f^{(n)}(0)}{n!} \left[-\frac{1}{(n-\eta)} + \frac{4}{(n+1-\eta)} - \frac{6}{(n+2-\eta)} + \frac{4}{(n+3-\eta)} - \frac{1}{(n+4-\eta)} \right]. \quad (5-11)$$

Intemann and Pollock find that, for $Z=26$, an error only of order ζ^2 results from breaking the series off after the first three terms.

The energy spectrum of electrons ejected from ^{55}Fe , predicted by this more exact theoretical approach, does not appear to differ materially from that of Eq. (5-7) when placed on a semi-logarithmic plot (Intemann and Pollock, 1967). Some writers have consequently assumed that the results of the two theories are truly identical. This is not the case. In fact, the momentum spectra from the two approaches differ appreciably on a linear plot; they have approximately the same shape, but the Intemann-Pollock spectrum has somewhat lower intensity. Hence it yields significantly smaller values for the total ejection rate than the Primakoff-Porter theory (Intemann, private communication). That the difference is not greater appears to indicate that Primakoff and Porter's variational wave function takes unexpectedly accurate account of screening and correlations in the initial two-electron state. Improving the accuracy of the continuum wave function to take screening in the final state into consideration is only expected to affect the results of Eqs. (5-7) and (5-8) by $\lesssim 5\%$ for $Z=26$.

The neglect of relativistic effects inherently limits the accuracy of the results to a relative error of order αZ , even at the lowest ejection energies. The nonrelativistic calculations were pushed to this limit in a refinement, due to Intemann (1972), of the Intemann-Pollock approach, which involves the use of a more elaborate Coulomb Green function. This modification has the effect of considerably reducing the calculated K ejection probabilities w_{ejec} , particularly at high Z , as compared with the Intemann-Pollock results

(Intemann, 1974). The reduction in the predicted intensity of the ejected-electron spectrum can be understood in the following terms (Intemann, 1975). In all calculations based on the Intemann-Pollock approach (including the one discussed in Sec. 5.3), retardation effects are neglected and the interaction between the two electrons is taken to be an instantaneous Coulomb interaction, so that the exchange of only longitudinal and scalar virtual photons can be considered. In the approximation used by Intemann and Pollock (1967), only s-wave intermediate states make a contribution to the transition amplitude, and thus, only scalar photon exchange is taken into account. In his later paper, Intemann (1972) employed the more accurate Green's function used by Glauber and Martin (1956). In this more refined calculation, p-wave intermediate states also contribute to the amplitude, and thus, longitudinal photon exchange is also being taken into account. The relative importance of longitudinal photon exchange is indicated by the extent to which the intensity of the electron spectrum is reduced (Fig. 5-1).

5.3. Relativistic Calculations of Electron Ejection

Both of the basic approaches described in Sec. 5.2 have been extended to include relativistic effects. Intemann (1969) modified the work of Intemann and Pollock (1967), using the solutions of the symmetric Hamiltonian of Biedenharn and Swamy (1964). This is a relativistic Hamiltonian with symmetry so that the radial parts of the spinor components of its solutions are formally nonrelativistic. The solutions form a complete canonical basis, and their close

correspondence to the nonrelativistic problem leads to substantial computational simplifications. The Biedenharn Hamiltonian differs from the exact Dirac-Coulomb Hamiltonian by a precisely known fine-structure term; the eigenfunctions differ from the exact Dirac-Coulomb eigenfunctions by terms of order $(\alpha Z)^2$.

Except for the use of semi-relativistic Coulomb eigenfunctions in the overlap integral and an appropriately modified expression for the density of final states available to the ejected electron, the calculation of Intemann (1969) follows the lines of his earlier work, i.e., the interaction between the two K electrons is treated as a perturbation along with the weak interaction, leading to an exact calculation of the electron ejection probability without the need of introducing adjustable parameters such as screening constants or effective nuclear charges. Even though relativistic effects partly cancel the reduction in w_{eje} that arises when longitudinal photon exchange is included, the ejected-electron spectrum calculated semirelativistically by Intemann (1969) is considerably less intense than that derived from the Primakoff-Porter (1953) approach (Fig. 5-2).

An independent relativistic calculation of auto-ionization in electron-capture decay was performed by Law and Campbell (1973b), in terms of second-quantization formalism and in analogy with extensive work by the same authors on internal ionization accompanying β decay (Campbell et al., 1971; Campbell and Law, 1972; Law and Campbell, 1972a, 1972b, 1973a). It was, however, shown by Intemann (1974) that the model of Law and Campbell (1973b) is actually identical with that of Intemann and Pollock (1967) and Intemann

(1969), and that the large difference in the results can be traced to the fact that Law and Campbell cut off the eigenfunction expansion for the Coulomb Green function too soon. Law and Campbell approximated the infinite series by a few terms because it appeared to converge rapidly; Intemann (1974), drawing upon an analogous calculation by Paquette (1962), pointed out that the sum over discrete eigenstates in the Green function expansion does indeed converge rapidly, but that continuum states make a large contribution that cannot be neglected.

The (historically older) alternative to the Intemann approach for the calculation of internal ionization is the "overlap" ansatz, used in the pioneering work of Primakoff and Porter (1953). As indicated in Sec. 5.2, in this method one attempts to take account of all screening and correlation effects in the initial two-electron wave function by an adjustable parameter, viz.; the effective nuclear charge. The calculations are simplified considerably, but it is difficult to make a choice of the key parameter, and some arbitrariness is bound to remain. Moreover, the near-orthogonality of the wave functions makes the overlap integral very sensitive to the exact form of the wave functions and to the values chosen for the effective charges. Thus, the accuracy of the results cannot be established a priori, as in the Intemann approach; on the other hand, the overlap method does not rely on the condition $Z \gg 1$, and hence, may be superior for very light elements.

The most recent and complete calculation based on the "overlap"

method is due to Mukoyama et al. (1973). In their formulation, Mukoyama et al. draw upon the work of Stephas (1969), who had employed an atomic matrix element calculated from analytic hydrogenic relativistic wave functions for the purpose of studying internal ionization accompanying β decay (Stephas and Crasemann, 1967, 1971; Crasemann and Stephas, 1969). However, in their evaluation of the wave-function overlap integral, Stephas and Crasemann (1967) made an approximation that causes their expression to diverge at low electron momenta, where most electrons are ejected; thus, the result cannot meaningfully be integrated to compute total electron-ejection probabilities (Isozumi and Shimizu, 1971; Kitahara et al., 1972; Nagy et al., 1972). Mord (1972, 1973) and, independently, Mukoyama et al. (1973) have calculated the atomic matrix element by alternative techniques and derived a result that is exact, within the limitations stated above; it agrees in the non-relativistic limit with the formulae of Primakoff and Porter (1953) and Stephas and Crasemann (1971).

The screening constants σ that determine the effective nuclear charge $Z_{\text{eff}} = Z - \sigma$, to take account of electron-electron interaction, are determined by Mukoyama et al. (1973) in the following manner.

In the parent atom, they take

$$\sigma = Z(1 - \bar{r}_Z / \bar{r}_{\text{SCF}}), \quad (5-12)$$

where \bar{r}_Z is the mean value of r determined from the relativistic hydrogenic wave functions, and \bar{r}_{SCF} is \bar{r} from relativistic self-consistent field wave functions, as computed by Carlson et al. (1970).

For the continuum electron, Mukoyama et al. use the same screening constant as for the bound electron to be ejected. They take account of the fact that a vacancy resulting from electron capture is present in the daughter atom by reducing σ from Eq. (5-12) by the ratio of the appropriate Slater screening constant for an atom that is ionized in an inner shell to that for a neutral atom (Slater, 1930).

The total K-electron ejection probabilities per K capture, calculated by Mukoyama et al. (1973), agree with those of Intemann (1969, 1974) as well as could be expected, given the uncertainties in the choice of screening parameters (Table 5.1).

Excitation to a bound state ("shakeup") of the second K electron, while the first one is captured, has also been computed by Mukoyama et al. (1973). Such calculations are important for comparison with experiments, in which double K x-ray emission is measured. The main difficulty here is to make adequate provision for omitting occupied final states to which shakeup is forbidden by the Pauli principle. Mukoyama et al. (1973) find that the probability for double K-vacancy production (including excitation), just as the K electron-ejection probability, is reduced when relativistic effects are included, compared with the nonrelativistic results of Primakoff and Porter (1953) (Table 5.2).

5.4. Electron Ejection from Higher Shells

It was first emphasized by Wolfsberg (1954) that a spectrum of electrons ejected during nuclear electron capture, measured in coincidence with a single K x ray, contains contributions from L

electrons shaken off during K capture and from K electrons ejected during L capture. Wolfsberg evaluated these effects in terms of the Primakoff-Porter formalism. Internal ionization of this type, resulting in K and L_1 vacancies, has also been discussed by Law and Campbell (1973a, b). The energy distribution of K electrons ejected during nuclear electron capture from higher shells was considered by Ryde et al. (1963).

The subject has been extensively treated in terms of the wavefunction overlap approach by Mukoyama and Shimizu (1974). Starting with the formalism of Stephas (1969), but using the relativistic hydrogenic atomic matrix element of Mukoyama et al. (1973), these workers have computed the probability per K capture for L_1 -shell electron ejection with total energy W:

$$P_{Ki}(W) dW = \frac{n_i}{2\pi^2} |M_{Ki}|^2 \frac{S(W_K - W)}{S(W_0)} \frac{(W_K - W)^2}{W_0^2} pWdW. \quad (5-13)$$

Here, W_0 is the transition energy for K capture, W_K is the maximum total energy of the ejected electron, and n_i is the number of electrons in the L_i shell. S is the shape factor, and the wavefunction overlap integral is

$$M_{Ki} = \langle \psi(Z-1, W) | \cdot \psi(Z, L_i) \rangle. \quad (5-14)$$

Similarly, Mukoyama and Shimizu have computed the K-shell internal ionization probability per L_1 capture, expressed as a ratio to the K-capture probability:

$$P_{iK}(W) dW = \frac{n_i}{2\pi^2} \frac{\epsilon_i}{\epsilon_K} |M_{iK}|^2 \frac{S(W_K - W)}{S(W'_0)} \frac{(W_K - W)^2}{W'_0{}^2} pWdW, \quad (5-15)$$

where ϵ_i/ϵ_K is the L_i -to-K capture ratio, and W'_0 is the mass difference between initial and final nuclei, minus the L_i binding energy, plus one (in units of mc^2). The atomic matrix element is

$$M_{iK} = \langle \psi(Z-1, W) | \psi(Z, K) \rangle. \quad (5-16)$$

The authors construct a properly antisymmetrized expression for the total probability for the direct and exchange processes (5-13) and (5-15) and evaluate the result for cases of practical interest (Table 5.1). It is predicted that the L-shell internal-ionization probability accompanying K capture is of almost the same order of magnitude as the K ejection probability during L capture. The probability that the atom undergoing electron capture and internal ionization is left with holes in the K and L shells increases with Z, relative to the double K-hole production probability. The L-shell ionization probability decreases more slowly with Z than the K-electron ejection probability, per K capture.

Calculated spectra of electrons ejected during K and L capture of ^{55}Fe are shown in Fig. 5-2. It is predicted that electrons ejected from the L_1 shell contribute substantially over the entire spectrum.

Comparable calculations of L-shell internal ionization accompanying L capture have been carried out by Mukoyama

et al. (1974).

In this context, it should be noted that only allowed transitions have so far been treated by the Intemann-Pollock approach. By contrast, because of its simplicity, the overlap-integral approach has led to results for arbitrary beta transitions. The simplifying feature of this approach is the assumption that the initial state of the two electrons involved in the process is describable in terms of an independent-particle model, i.e., the two-electron wave function can be written as an uncorrelated product of one-electron wave functions. It is this assumption which permits the factorization of the matrix element. For forbidden transitions, however, with the entrance of higher beta moments, it is to be expected that the amplitude for internal ionization will be more sensitive to the details of the structure of the initial electronic configuration, and therefore the overlap-integral approach will be less reliable. On the other hand, relativistic effects, which are of particular importance for forbidden transitions, are much more easily included in this approach than in the Intemann-Pollock approach.

Furthermore, in connection with all wave-function overlap calculations, on which the most extensive predictions of internal-ionization probabilities are based, it must be kept in mind that near-orthogonality makes the atomic matrix element exceedingly sensitive to the accuracy of the wave functions. This point is discussed in detail in Sec. 2.5. It is likely that quantitative results derived from hydrogenic wave functions may lack in accuracy, particularly in the case of outer shells.

5.5. Measurements of Internal Ionization

Excellent critical reviews of experimental work on internal ionization and excitation accompanying electron capture have been compiled by Law and Campbell (1973), Mukoyama *et al.* (1973), Freedman (1974), and Walen and Briançon (1975); somewhat earlier results have been discussed by Stephas (1969).

Experiments on shakeup and shakeoff during electron capture are made difficult *a priori* by the fact that the probability of these processes is much lower, perhaps by an order of magnitude, than in β decay: the effect of the sudden increase in nuclear charge upon the Coulomb field seen by the atomic electrons is, to a considerable extent, compensated by the reduction in screening that ensues when one K electron is captured. Consequently, the experimental information on the subject is quite limited; it is confined to the five isotopes with simple ground-state-to-ground-state decays listed in Tables 5.1 and 5.2, and to some recent work on ^7Be (Mutterer, 1970).

Relatively least difficult are measurements of the probability of double K-vacancy production through the detection of coincidences between two K x rays (or K Auger electrons, or both). Two decades ago, Charpak (1953) used two 2π proportional counters for such measurements on ^{55}Fe . Langevin (1957, 1958) measured the K Auger-electron sum peak in a single proportional counter with a gaseous internal ^{71}Ge source. Miskel and Perlman (1954) and Kiser and Johnston (1959) measured K Auger electrons and K shakeoff electrons from ^{37}Ar in a proportional counter.

Upon the advent of NaI(Tl) scintillation detectors, these were employed in several measurements (Daniel et al., 1960; Lark and Perlman, 1960; Ryde et al., 1963; Smith, 1964). A further advance in the technique was made possible when solid state detectors were developed with which K x rays from elements with adjoining atomic numbers can be resolved, so that one can discriminate sensitively against impurities. Nagy et al.

(1972) used a Si(Li) semiconductor detector in coincidence with a scintillation counter in double K-vacancy production measurements on ^{131}Cs and ^{165}Er .

The creation of double K holes can also be determined by detecting radiative transitions to the empty K shell. Such transitions produce $K\alpha$ x-ray "hypersatellites" that are shifted up in energy with respect to the diagram line. A hypersatellite measurement was first used by Oertzen (1964), who employed a bent-crystal diffraction spectrometer to determine the double K-vacancy production rate in ^{71}Ge ; the result agrees extremely well with that of Langevin (1957, 1958). Briand et al. (1971) measured the $K\alpha$ hypersatellite from ^{71}Ge decay in coincidence with the ensuing $K\alpha_{3,4}$ satellite.

Results of all these measurements of double K-vacancy production probability during nuclear K capture are included in Table 5.2.

Total electron ejection probabilities are much more difficult to determine. Spectrum measurements necessarily have a low-energy threshold, determined by detector noise, electron scattering, and window transmission problems. Because most electrons are ejected with very low energies (Fig. 5-3), total ejection probabilities can only

be inferred from measured spectra, that extend over a limited range, by fitting the data to some theoretical spectral shape. The admixture of L electrons ejected during K capture, and of K electrons ejected during L capture, introduces additional uncertainties that are difficult to account for, unless the electron counts are gated by double K x-ray events. The results depend so heavily on the theoretical model in terms of which the data are interpreted and often contain such large probable errors that they have not been included in Table 5.1. Pertinent information can be found in the original literature and in the papers by Stephas (1969), Mukoyama *et al.* (1973), Freedman (1974), and Walen and Briançon (1975).

While ejected-electron spectrum measurements have not, in the past, led to unequivocal and precise determinations of the total electron ejection probability, they are nevertheless of value for testing theoretically predicted spectrum shapes. The ^7Be electron spectrum has been measured by Mutterer (1970), and that of ^{37}Ar , by Miskel and Perlman (1954), with proportional counters. Pengra and Crasemann (1963) gated on Mn K x rays, detected with a scintillation counter, to measure the ^{55}Fe electron spectrum with a proportional counter, at low energies, and with an early solid state detector, at higher energies. Modern measurements of the ^{55}Fe electron spectrum have been performed by Nagy (1971) with two plastic scintillators in coincidence, and by Kitahara and Shimizu (1975), who performed a triple-coincidence (x-x-p) experiment with proportional counters. The ^{71}Ge spectrum was determined by Langevin (1958) with a proportional counter. Daniel *et al.* (1960) used a

magnetic spectrometer to study the spectrum from ^{131}Cs ; this spectrum was measured more recently by Sujkowski *et al.* (1973) with a Si(Li) detector placed at the focus of a zero-dispersion homogeneous magnetic-field spectrometer. A magnetic β -ray spectrometer was used by Ryde *et al.* (1963) on ^{165}Er .

The measured spectra appear to agree, within errors, with the general shape that all theories predict; this shape is largely determined by the statistical factor. Without question, precise absolute measurements of ejected-electron spectra, preferably in coincidence with two K x rays, would be of great value as a guide for more refined computations of the atomic matrix element.

5.6. Correlation of x Rays and γ Rays Following Electron Capture

If aligned nuclei undergo electron capture, the atomic inner-shell vacancies created thereby can be polarized, and subsequently emitted x rays can be circularly polarized (for an illustrative example, see Emery, 1975). Dolginov (1956-1957, 1958a, b) has described these circular polarization effects and pointed out that even in the decay of unaligned atoms a correlation can exist between the circular polarization of x rays and of γ rays emitted following the nuclear decay.

An unisotropic directional correlation of the type

$$W(\theta) = 1 + A_2 P_2(\cos\theta) \quad (5-17)$$

can exist between x rays and γ rays emitted after nuclear electron

capture if the intermediate atomic state is characterized by a vacancy with $j > 1/2$. The theory has been developed by Dolginov (An early discussion of the problem is given by Tolhoek *et al.*, (1958b). Somewhat simplified expressions based on Dolginov's theory (1955)). are given by Rupnik and Crasemann (1972), who also worked out the directional-correlation function for x rays emitted in transitions to the L_3 level and γ rays, following second-forbidden nonunique electron capture transitions.²⁷

The experimental detection of anisotropic x- γ correlations is hampered by the condition that the intermediate atomic vacancy must have $j > 1/2$, whence only L_3 capture is of interest.²⁸ The L_3/L_1 capture ratio in allowed transitions is always small ($< 10^{-7}$); one must choose a radioisotope that decays through a second or higher forbidden electron-capture transition to a short-lived excited state of the daughter. The only readily available isotope that fulfills these requirements is ^{207}Bi , but its decay scheme is cluttered with other transitions. Efforts to detect anisotropy in the x- γ directional correlation from ^{207}Bi decay have been unsuccessful (Rupnik and Crasemann, 1972; Cambiaggio *et al.*, 1975), although the results are not inconsistent with theoretical predictions.

ACKNOWLEDGMENTS

We are indebted to many colleagues for helpful discussions and for making their results available to us in advance of publication. In particular, we wish to thank H. Appel of the Universität and Kernforschungszentrum Karlsruhe, W. Bühring of the Universität Heidelberg, M. S. Freedman of the Argonne National Laboratory, and B. E. Persson of the Technische Hochschule Darmstadt for reading and criticizing parts of early drafts of this paper. J. B. Mann of the Los Alamos Scientific Laboratory, University of California, kindly supplied us with unpublished wave functions, and B. Fricke of the Gesamthochschule Kassel generously made his Hartree-Fock-Slater computer codes available. One of us (M. L. F.) is indebted to the University of Glasgow for a research fellowship.

Appendix

A2.1. Expressions for $M_K(k_x, k_y)$ and $m_K(k_x, k_y)$

Only the dominant terms of the quantities $M_K(k_x, k_y)$ and $m_K(k_x, k_y)$ are given in Eqs. (2-106). The complete formulae for $k_v^{(1)}$ and $k_v^{(2)}$ follow (Behrens and Böhning, 1971, modified for electron capture).

$$1. \quad k_v = k_v^{(1)} = K - k_x + 1$$

$$\begin{aligned}
 M_x(k_x, k_y) = & \sqrt{\frac{K!}{(2K+1)!! (2k_x-1)!! (2k_y-1)!! (k_x-1)! (k_y-1)!}} (qR)^{k_x-1} (qR)^{k_y-1} \\
 & \times \sum_{\lambda=0}^{\infty} \sum_{\mu=0}^{\infty} \frac{(2k_x-1)!!}{(2\mu)!! (2\mu+2k_x-1)!!} \frac{(2k_y-1)!!}{(2\lambda)!! (2\lambda+2k_y-1)!!} (qR)^{2\lambda} \sum_{\sigma=0}^{\mu} (-1)^{\lambda+\sigma} \binom{\mu}{\sigma} \\
 & \times \sum_{\rho=0}^{2\sigma+1} (m_e R)^{2\mu-2\sigma} (W_x R)^{2\sigma-\rho} (\alpha Z)^{\rho} \left\{ -\sqrt{\frac{2K+1}{K}} \left[\binom{2\sigma}{\rho} F_{KK-11}^{\mu+\lambda}(k_x, 2\mu, 2\sigma, \rho) \right. \right. \\
 & \left. \left. - \frac{1}{2K+1} \frac{1}{2\lambda+2k_y+1} \frac{1}{2\mu+2k_x+1} qR W_x R \binom{2\sigma+1}{\rho} F_{KK-11}^{\mu+\lambda+1}(k_x, 2\mu+1, 2\sigma+1, \rho) \right] \right. \\
 & \left. + \left[\frac{1}{2\mu+2k_x+1} W_x R \binom{2\sigma+1}{\rho} F_{KK0}^{\mu+\lambda}(k_x, 2\mu+1, 2\sigma+1, \rho) \right. \right. \\
 & \left. \left. - \frac{1}{2\lambda+2k_y+1} qR \binom{2\sigma}{\rho} F_{KK0}^{\mu+\lambda}(k_x, 2\mu, 2\sigma, \rho) \right] - \sqrt{\frac{K+1}{K}} \right. \\
 & \left. \times \left[\frac{1}{2\mu+2k_x+1} W_x R \binom{2\sigma+1}{\rho} F_{KK1}^{\mu+\lambda}(k_x, 2\mu+1, 2\sigma+1, \rho) \right. \right. \\
 & \left. \left. + \frac{1}{2\lambda+2k_y+1} qR \binom{2\sigma}{\rho} F_{KK1}^{\mu+\lambda}(k_x, 2\mu, 2\sigma, \rho) \right] - \sqrt{\frac{K+1}{2K+1}} \right. \\
 & \left. \times \frac{2}{2\lambda+2k_y+1} \frac{1}{2\mu+2k_x+1} qR W_x R \binom{2\sigma+1}{\rho} F_{KK+11}^{\mu+\lambda}(k_x, 2\mu+1, 2\sigma+1, \rho) \right\},
 \end{aligned} \tag{2-A1}$$

$$\begin{aligned}
m_K(k_x, k_v) &= \sqrt{\frac{K!}{(2K+1)!!} \frac{1}{(2k_x-1)!!(2k_v-1)!!(k_x-1)!(k_v-1)!}} (pR)^{k_x-1} (qR)^{k_v-1} \\
&\times \sum_{\lambda=0}^{\infty} \sum_{\mu=0}^{\infty} \frac{(2k_x-1)!!}{(2\mu)!!(2\mu+2k_x-1)!!} \frac{(2k_v-1)!!}{(2\lambda)!!(2\lambda+2k_v-1)!!} (qR)^{2\lambda} \sum_{\sigma=0}^{\mu} (-1)^{\lambda+\sigma} \binom{\mu}{\sigma} \\
&\times \sum_{\rho=0}^{2\sigma} (m_o R)^{2\mu-2\sigma} (W_x R)^{2\sigma-\rho} (\alpha Z)^{\rho} \left\{ -\sqrt{\frac{2K+1}{K}} \left[m_o R (W_x R)^{-1} \Delta \binom{2\sigma-1}{\rho} \right. \right. \\
&\times F_{KK-11}^{\mu+\lambda}(k_x, 2\mu, 2\sigma-1, \rho) - \frac{1}{2K+1} \frac{1}{2\lambda+2k_v+1} \frac{1}{2\mu+2k_x+1} qR m_o R \binom{2\sigma}{\rho} \\
&\times F_{KK-11}^{\mu+\lambda+1}(k_x, 2\mu+1, 2\sigma, \rho) \left. \right] + \left[\frac{1}{2\mu+2k_x+1} m_o R \binom{2\sigma}{\rho} F_{KK0}^{\mu+\lambda}(k_x, 2\mu+1, 2\sigma, \rho) \right. \\
&- \frac{1}{2\lambda+2k_v+1} qR m_o R (W_x R)^{-1} \Delta \binom{2\sigma-1}{\rho} F_{KK0}^{\mu+\lambda}(k_x, 2\mu, 2\sigma-1, \rho) \left. \right] - \sqrt{\frac{K+1}{K}} \\
&\times \left[\frac{1}{2\mu+2k_x+1} m_o R \binom{2\sigma}{\rho} F_{KK1}^{\mu+\lambda}(k_x, 2\mu+1, 2\sigma, \rho) + \frac{1}{2\lambda+2k_v+1} qR m_o R (W_x R)^{-1} \Delta \right. \\
&\times \binom{2\sigma-1}{\rho} F_{KK1}^{\mu+\lambda}(k_x, 2\mu, 2\sigma-1, \rho) \left. \right] - \sqrt{\frac{K+1}{2K+1}} \frac{2}{2\lambda+2k_v+1} \frac{1}{2\mu+2k_x+1} qR m_o R \\
&\times \binom{2\sigma}{\rho} F_{KK+11}^{\mu+\lambda}(k_x, 2\mu+1, 2\sigma, \rho) \left. \right\}, \quad (2-A2)
\end{aligned}$$

$$2. \quad k_v = k_v^{(2)} = K - k_x + 2$$

$$\begin{aligned}
M_K(k_x, k_v) &= \sqrt{\frac{K!}{(2K+1)!!} \frac{1}{(2k_x-1)!!(2k_v-1)!!(k_x-1)!(k_v-1)!}} (pR)^{k_x-1} (qR)^{k_v-1} \\
&\times \sqrt{\frac{K+1}{(2k_x-1)(2k_v-1)}} \sum_{\lambda=0}^{\infty} \sum_{\mu=0}^{\infty} \frac{(2k_x-1)!!}{(2\mu)!!(2\mu+2k_x-1)!!} \frac{(2k_v-1)!!}{(2\lambda)!!(2\lambda+2k_v-1)!!} \\
&\times (qR)^{2\lambda} \sum_{\sigma=0}^{\mu} (-1)^{\lambda+\sigma} \binom{\mu}{\sigma} \sum_{\rho=0}^{2\sigma+1} (m_o R)^{2\mu-2\sigma} (W_x R)^{2\sigma-\rho} (\alpha Z)^{\rho} \\
&\times \left\{ \left[\binom{2\sigma}{\rho} F_{KK0}^{\mu+\lambda}(k_x, 2\mu, 2\sigma, \rho) + \frac{1}{2\lambda+2k_v+1} \frac{1}{2\mu+2k_x+1} qR W_x R \right. \right. \\
&\times \binom{2\sigma+1}{\rho} F_{KK0}^{\mu+\lambda+1}(k_x, 2\mu+1, 2\sigma+1, \rho) \left. \right] + \frac{k_x - k_v}{K+1} \sqrt{\frac{K+1}{K}} \\
&\times \left[\binom{2\sigma}{\rho} F_{KK1}^{\mu+\lambda}(k_x, 2\mu, 2\sigma, \rho) - \frac{1}{2\lambda+2k_v+1} \frac{1}{2\mu+2k_x+1} qR W_x R \right. \\
&\times \binom{2\sigma+1}{\rho} F_{KK1}^{\mu+\lambda+1}(k_x, 2\mu+1, 2\sigma+1, \rho) \left. \right] + \sqrt{\frac{1}{K(2K+1)}} \\
&\times \left[2(k_v-1) \frac{1}{2\mu+2k_x+1} W R \binom{2\sigma+1}{\rho} F_{KK-11}^{\mu+\lambda+1}(k_x, 2\mu+1, 2\sigma+1, \rho) \right. \\
&- \frac{2(k_x-1)}{2\lambda+2k_v+1} qR \binom{2\sigma}{\rho} F_{KK-11}^{\mu+\lambda+1}(k_x, 2\mu, 2\sigma, \rho) \left. \right] + \sqrt{\frac{1}{(K+1)(2K+1)}} \\
&\times \left[(2k_x-1) \frac{1}{2\mu+2k_x+1} W_x R \binom{2\sigma+1}{\rho} F_{KK+11}^{\mu+\lambda}(k_x, 2\mu+1, 2\sigma+1, \rho) \right. \\
&- \left. \left. \frac{2k_v-1}{2\lambda+2k_v+1} qR \binom{2\sigma}{\rho} F_{KK+11}^{\mu+\lambda}(k_x, 2\mu, 2\sigma, \rho) \right] \right\}, \quad (2-A3)
\end{aligned}$$

$$\begin{aligned}
m_K(k_x, k_v) = & \sqrt{\frac{K!}{(2K+1)!!}} \frac{1}{(2k_x-1)!!(2k_v-1)!!(k_x-1)!(k_v-1)!} (p_x R)^{k_x-1} (q_x R)^{k_v-1} \\
& \times \sqrt{\frac{K+1}{(2k_x-1)(2k_v-1)}} \sum_{\lambda=0}^{\infty} \sum_{\mu=0}^{\infty} \frac{(2k_x-1)!!}{(2\mu)!!(2\mu+2k_x-1)!!} \frac{(2k_v-1)!!}{(2\lambda)!!(2\lambda+2k_v-1)!!} \\
& \times (q_x R)^{2\lambda} \sum_{\sigma=0}^{\mu} (-1)^{\lambda+\sigma} \binom{\mu}{\sigma} \sum_{\rho=0}^{2\sigma} (m_e R)^{2\mu-2\sigma} (W_x R)^{2\sigma-\rho} (\alpha Z)^{\rho} \\
& \times \left\{ \left[m_e R (W_x R)^{-1} \Delta \binom{2\sigma-1}{-\rho} F_{KK0}^{\mu+\lambda}(k_x, 2\mu, 2\sigma-1, \rho) \right. \right. \\
& + \frac{1}{2\lambda+2k_v+1} \frac{1}{2\mu+2k_x+1} q_x R m_e R \binom{2\sigma}{\rho} F_{KK0}^{\mu+\lambda+1}(k_x, 2\mu+1, 2\sigma, \rho) \left. \right] \\
& + \frac{k_x-k_v}{K+1} \sqrt{\frac{K+1}{K}} \left[m_e R (W_x R)^{-1} \Delta \binom{2\sigma-1}{\rho} F_{KK1}^{\mu+\lambda}(k_x, 2\mu, 2\sigma-1, \rho) \right. \\
& - \frac{1}{2\lambda+2k_v+1} \frac{1}{2\mu+2k_x+1} q_x R m_e R \binom{2\sigma}{\rho} F_{KK1}^{\mu+\lambda+1}(k_x, 2\mu+1, 2\sigma, \rho) \left. \right] \\
& + \sqrt{\frac{1}{K(2K+1)}} \left[2(k_v-1) \frac{1}{2\mu+2k_x+1} m_e R \binom{2\sigma}{\rho} F_{KK-11}^{\mu+\lambda+1}(k_x, 2\mu+1, 2\sigma, \rho) \right. \\
& - \frac{2(k_x-1)}{2\lambda+2k_v+1} q_x R m_e R (W_x R)^{-1} \Delta \binom{2\sigma-1}{\rho} F_{KK-11}^{\mu+\lambda+1}(k_x, 2\mu, 2\sigma-1, \rho) \left. \right] \\
& + \sqrt{\frac{1}{(K+1)(2K+1)}} \left[(2k_x-1) \frac{1}{2\mu+2k_x+1} m_e R \binom{2\sigma}{\rho} F_{KK+11}^{\mu+\lambda}(k_x, 2\mu+1, 2\sigma, \rho) \right. \\
& \left. \left. - \frac{2k_v-1}{2\lambda+2k_v+1} q_x R m_e R (W_x R)^{-1} \Delta \binom{2\sigma-1}{\rho} F_{KK+11}^{\mu+\lambda}(k_x, 2\mu, 2\sigma-1, \rho) \right] \right\}. \tag{2-A4}
\end{aligned}$$

In these expressions, we have

$$\Delta = \begin{cases} 0 & \text{if } \mu=0 \\ 0 & \text{if } \sigma=0 \\ 0 & \text{if } \rho=0 \\ 1 & \text{otherwise.} \end{cases}$$

For n^{th} -forbidden unique transitions, Eqs. (2-A1) through (2-A4) apply, with $K=n+1$, $A_{F(n+1)n1}$, $A_{F(n+1)(n+1)0}$, $V_{F(n+1)(n+1)1}$,

$A_{F(n+1)(n+2)1}$. For n^{th} forbidden non-unique transitions, Eqs. (2-A1)-(2-A4) apply with $K=n$, $V_{F_{n(n-1)1}}$, $V_{F_{nn0}}$, $A_{F_{nn1}}$, $V_{F_{n(n+1)1}}$. If $n=1$, there is a further contribution from Eqs. (2-A3)-(2-A4) with $K=0$, $A_{F_{000}}$, $A_{F_{011}}$. Allowed transitions involve Eqs. (2-A3) and (2-A4) with $K=0$, $V_{F_{000}}$, $V_{F_{011}}$ and Eqs. (2-A1) and (2-A2) with $K=1$, $A_{F_{101}}$, $A_{F_{110}}$, $V_{F_{111}}$, $A_{F_{121}}$. The magnitude of the various terms in Eqs. (2-A1) through (2-A4) is determined, first, by powers of the factors $(p_x R)$, $(q_x R)$, $(w_x R)$, $(m_e R)$, and (αZ) ; and second, by the difference of one order of magnitude between the relativistic and nonrelativistic form-factor coefficients. Thus, the dominant terms of Eqs. (2-A1)-(2-A4) are a subset of the terms with $\lambda=0$, $\mu=0$ [Eqs. (2-104)-(2-106)]. The correction terms of the next order are

(i) terms with $\mu=0$, $\lambda=0$ which were not included in Eqs. (2-104)-(2-106);

(ii) terms with $\mu=0$, $\lambda=1$ and $\mu=1$, $\lambda=0$ corresponding to the terms with $\mu=0$, $\lambda=0$ of Eqs. (2-104)-(2-106).

All terms, however, with powers of $m_e R$ and $w_x R$ can usually be omitted since $m_e R$ and $w_x R$ are generally much smaller than αZ . It should be noted that for electron capture the correction terms are important only in cases where cancellations occur among the dominant terms.

A2.2. Expansion Coefficients $I(k, m, n, \rho; r)$ up to Order $m=3$

The expansion coefficients $I(k, m, n, \rho; r)$ of the electron radial wave functions; up to order $m=3$, are as follows (Behrens and Böhning, 1971):

$$I(k, 1, 1, 1; r) = (2k+1)r^{-2k-1} \int_0^r x^{2k} U(x) dx,$$

$$I(k, 2, 2, 2; r) = 2(2k+1)r^{-2} \int_0^r U(y)y^{-2k} \int_0^y x^{2k} U(x) dx dy,$$

$$I(k, 2, 2, 1; r) = -\frac{2k+1}{2k-1} r^{-2k-1} \int_0^r x^{2k} U(x) dx + \frac{4k}{2k-1} r^{-2} \int_0^r x U(x) dx,$$

$$I(k, 2, 1, 1; r) = +\frac{2(2k+1)}{2k-1} r^{-2k-1} \int_0^r x^{2k} U(x) dx - \frac{4}{2k-1} r^{-2} \int_0^r x U(x) dx,$$

$$I(k, 3, 3, 3; r) = 2(2k+1)(2k+3)r^{-2k-3} \int_0^r z^{2k} U(z) \int_0^z U(y)y^{-2k} \int_0^y x^{2k} U(x) dx dy dz,$$

$$I(k, 3, 3, 2; r) = \frac{2}{3}(2k+3)r^{-2} \int_0^r U(y)y^{-2k} \int_0^y x^{2k} U(x) dx dy + \frac{8k(2k+3)}{3(2k-1)} r^{-2k-3} \\ \times \int_0^r y^{2k} U(y) \int_0^y x U(x) dx dy - \frac{8k(2k+3)}{3(2k-1)} r^{-2k-3} \int_0^r y U(y) \int_0^y x^{2k} U(x) dx dy,$$

$$I(k, 3, 2, 2; r) = 2(2k+3)r^{-2} \int_0^r U(y)y^{-2k} \int_0^y x^{2k} U(x) dx dy - \frac{4(2k+3)}{2k-1} r^{-2k-3} \\ \times \int_0^r y^{2k} U(y) \int_0^y x U(x) dx dy + \frac{4(2k+3)}{2k-1} r^{-2k-3} \int_0^r y U(y) \int_0^y x^{2k} U(x) dx dy,$$

$$I(k, 3, 3, 1; r) = \frac{4k(2k+3)}{3(2k+1)} r^{-2k-3} \int_0^r x^{2k+2} U(x) dx - \frac{(2k+1)(2k+3)}{3(2k-1)} r^{-2k-1} \\ \times \int_0^r x^{2k} U(x) dx + \frac{8k(2k+3)}{3(2k+1)(2k-1)} r^{-2} \int_0^r x U(x) dx,$$

$$I(k, 3, 2, 1; r) = \frac{2(2k+3)}{2k+1} r^{-2} \int_0^r x U(x) dx - \frac{2(2k+3)}{2k+1} r^{-2k-3} \int_0^r x^{2k+2} U(x) dx,$$

$$I(k, 3, 1, 1; r) = \frac{4(k+1)(2k+3)}{2k+1} r^{-2k-3} \int_0^r x^{2k+2} U(x) dx - \frac{(2k+1)(2k+3)}{2k-1} r^{-2k-1} \\ \times \int_0^r x^{2k} U(x) dx + \frac{4(2k+3)}{(2k+1)(2k-1)} r^{-2} \int_0^r x U(x) dx.$$

The function $U(x)$ in these expressions is defined by

$$V(x) = -(\alpha Z/R)U(x), \quad (2-A6)$$

where $V(x)$ is the potential of the nuclear and atomic charge distributions.

Footnotes

¹We have $A^+ = \{A_1^+, A_2^+, A_3^+, -A_4^+\}$.

²The field operators are given by

$$\psi(x) = V^{-1/2} \sum_q \sum_r \{e^{iqx} a_r(q) u_r(q) + b_r^+(q) v_r(q) e^{-iqx}\},$$

$$\bar{\psi}(x) = V^{-1/2} \sum_q \sum_r \{e^{-iqx} a_r^+(q) \bar{u}_r(q) + b_r(q) \bar{v}_r(q) e^{iqx}\};$$

$$r = 1, 2.$$

The $a_r(q)$ and $a_r^+(q)$ are the annihilation and creation operators for a fermion of momentum q and spin r , respectively, $b_r(q)$ and $b_r^+(q)$ are the corresponding operators for the anti-particles. The $u_r(q)$ and $v_r(q)$ are both the free-particle Dirac spinors. We have $\bar{u}_r(q) = u_r^+(q) \gamma_4$ and $\bar{v}_r(q) = v_r^+(q) \gamma_4$.

³We use the Dirac equation $(-\vec{\alpha} \cdot \vec{p} - \beta m - W) \psi = 0$ and the notation

$$\gamma_\mu = -i\beta \alpha_\mu, \gamma_4 = -\beta, \gamma_5 = \gamma_1 \gamma_2 \gamma_3 \gamma_4, \vec{\sigma} = \vec{\alpha} \gamma_5, \vec{\alpha} = \vec{\sigma} \gamma_5 \text{ and } \sigma_{\mu\nu} = \frac{1}{2} i (\gamma_\mu \gamma_\nu - \gamma_\nu \gamma_\mu).$$

⁴In the following, we use natural units $\hbar = m_e = c = 1$.

⁵We have $\hat{r} = \vec{r}/r$, and $d\Omega$ is the solid angle.

⁶The electron radial wave functions can also be calculated approximately as hydrogenic wave functions for a point nucleus of charge reduced by the appropriate Slater screening constants (Slater, 1930).

⁷However, for the inner shells and for medium and high atomic numbers, there is only a negligible difference between the wave functions of Mann and Waber (1973) and those from Hartree-

Fock-Slater calculations (Suslov, 1969 and 1970b; Dzhelepov et al., 1972; Martin and Blichert-Toft, 1970) or Thomas-Fermi-Dirac calculations (Behrens and Jänecke, 1969; Band et al., 1956, 1958).

⁸The Fourier transform of the electron wave function $\phi_{e^-}(\mathbf{r})$ is

$$\phi_{e^-}(\vec{p}_e) = \int e^{-i\vec{p}_e \cdot \vec{r}} \phi_{e^-}(\vec{r}) d\mathbf{r}^3.$$

⁹In the formulae for β^- and β^+ decay, the axial-vector coupling constant λ has the opposite sign [Sec. 2.1, Eq. (2-39)]. For electron capture, there are hence two ways of defining the axial-vector form-factor coefficients in terms of matrix elements and coupling constants, i.e., by using the same sign definition for λ as in the β^- -decay formulae or the same as in the β^+ -decay formulae. In the present work, the definition of the form-factor coefficients corresponds, as in Behrens and Jänecke (1969), to those in β^- decay. Consequently, in addition to the substitution indicated in Eq. (2-40), we must replace $A_{F_{KLs}}^A$ by $-A_{F_{KLs}}^A$ when going from β^+ decay to electron capture.

¹⁰There is another possibility of going to the nonrelativistic limit. By applying the Foldy-Wouthuysen transformation on the total (nuclear plus β -decay) Hamiltonian, one can construct an effective V-A transition operator that can be used with nonrelativistic single-particle wave functions (Rose and Osborn, 1954; Blin-Stoyle, 1973; Konopinski, 1966).

The operators $\vec{\alpha}$ and γ_5 which appear in the relativistic matrix elements are replaced in the nuclear space by

$$\alpha \rightarrow -\frac{\vec{p}}{M}; \quad \gamma_5 \rightarrow \frac{\vec{\sigma} \cdot \vec{p}}{M}.$$

This treatment of the relativistic nuclear single-particle matrix elements is fully equivalent to that described in the text.

11. First- and second-class currents are defined on the basis of their behavior under a G operation. If we split the hadron current into first- and second-class terms (Weinberg, 1958; Kim and Primakoff, 1969),

$$J_\mu = J_\mu^I + J_\mu^{II},$$

we have

$$2J_\mu^I = J_\mu + GJ_\mu G^{-1}$$

$$2J_\mu^{II} = J_\mu - GJ_\mu G^{-1},$$

and hence,

$$GJ_\mu^I G^{-1} = +J_\mu^I$$

$$GJ_\mu^{II} G^{-1} = -J_\mu^{II}.$$

Here, J_μ^I is a first-class element of the hadron current, and J_μ^{II} is a second-class element. The G operator is defined as

$$G = Ce^{\frac{i\pi T_2}{2}},$$

where C is the charge-conjugation operator, and T_2 is the second isospin component.

¹² Goslov used the nonrelativistic self-consistent Hartree-Fock-Glater potential of Herman and Skillman (1963).

¹³₁. Note that $1_{\bar{x}} = W_x + \bar{W}$. A correction formula given by Firestone et al. (1975b) might contain an error of sign and therefore should not be used.

b. Form-factor coefficients not included in Table 2.10 are related as follows to the nuclear matrix elements (without induced terms):

$$V_{F100}(1) = \int \left(\frac{r}{R}\right)^2 ;$$

$$V_{F101}(0) = \int \frac{\vec{r}}{R} ;$$

$$V_{F100}(K) (k, m, n, g) = \int \left(\frac{r}{R}\right)^{2N} J(k, m, n, g; r) ;$$

$$V_{F111}(0) = -\sqrt{\frac{3}{2}} \int \frac{\vec{r} \times \vec{r}}{R} ;$$

$$A_{F110}(0) = \lambda \sqrt{3} \int \sqrt{5} \frac{\vec{r}}{R} ;$$

$$A_{F101}(1) = -\lambda \int \vec{\sigma} \left(\frac{r}{R}\right)^2 ;$$

$$A_{F101}(K) (k, m, n, g) = -\lambda \int \vec{\sigma} \left(\frac{r}{R}\right)^{2N} J(k, m, n, g; r) .$$

ORIGINAL PAGE IS
OF POOR QUALITY

¹⁴ There is only a small difference between the form-factor coefficients for electron capture and β^+ decay, because of the different decay energies. In the former case, the decay energy is $W_0^+ = W_0 + W_x$, while in the latter case it is W_0 . This energy difference leads to the

following correction factor (Behrens and Böhning, 1974) :

$$\frac{\lambda_K}{\lambda_{\beta^+}} = \frac{f_K}{f_{\beta^+}} \left\{ 1 + 2 \frac{f_T}{\lambda} \left[W_K - \frac{1}{3} \left(1 + \frac{\bar{\mu}_1 \gamma_1}{W} \right) \right] \right\}.$$

Because we can assume $|f_T/\lambda| < 3 \times 10^{-3}$ (Blin-Stoyle, 1973; Wilkinson, 1970a; Alburger and Wilkinson, 1970; Wilkinson and Alburger, 1971; Eman et al., 1973), we obtain a correction

$$\left| \frac{f_T}{\lambda} \right| \left\{ W_K - \frac{1}{3} \left(1 + \frac{\bar{\mu}_1 \gamma_1}{W} \right) \right\} \leq 2 \times 10^{-3}.$$

This value is smaller than the contributions from higher-order terms [Eqs. (2-128)-(2-131)] and from the radiative corrections.

- 15 The total integrated intensity of a two-photon spectrum, for example, is expected to be no greater than νI_0^{-4} times that of the corresponding one-photon spectrum. Two-photon IB and the directional correlation between the photons have been studied by Menhardt (1957).
- 16 The adequacy of this procedure has been questioned by Koonin and Persson (1972), but it underlies all theoretical work reported so far.
- 17 For a possible exception to this statement, see Smirnov and Batkin (1974).
- 18 Unfortunately, Möller's work is much less well-known than that of Morrison and Schiff. Thus, the theory has come to be known by the names of the latter authors. Yet, it was Möller who first envisaged IB as arising from the emission of a virtual positron, followed by its single-quantum annihilation with one of the K electrons.
- 19 Winter (1957) has shown how to construct a simple classical model for radiative K capture which correctly predicts the low-energy portion of the IB spectrum [Eq. (4-17)] and, to within a factor of $\ln 2$, the total radiative capture rate [Eq. (4-18)]. Neither the high-energy portion of the IB spectrum, however, nor the IB angular distribution are correctly given by the model.

- ²⁰ Because $g_E^i(r_N, r)$ is well behaved as $r_N \rightarrow 0$, it is unnecessary to average it over the nuclear volume.
- ²¹ Of greatest interest are those EC transitions for which competing positron emission is energetically impossible. Then we have $k \leq 2 - B_\alpha$ and $|E| < 1$. In this case, the Green's function cannot represent a freely propagating wave. Rather, it decreases rapidly with distance from the nucleus and has a range which depends on k .
- ²² In this approximation, Glauber and Martin neglect the retardation factor $e^{ik \cdot r}$ for photon energies $k \leq Z\alpha$. This approximation is discussed further and a calculation of the 1s-state capture spectrum of ^{37}Ar in which this approximation is not made is given by Paquette (1962).
- ²³ As pointed out in Sec. 2.2.2, the $(g_{L1}/g_K)^2$ -ratios given in Brysk and Rose (1958) deviate systematically from all other reported calculations on screened electron wave functions. However, these deviations, and the resulting uncertainties in Fig. 4-7, appear to be never greater than about 5-6%. The errors, of order $Z\alpha$, associated with the results of Glauber and Martin (1956) for the 2s, 2p, 3p -spectra are always much larger (except for the special case of ^4Be). Thus the results displayed in Fig. 4-7 are more than adequate for present purposes and, as a convenience, will be used to determine all screening corrections in Sec. 4.2 unless otherwise noted.
- ²⁴ An excellent summary of these results is given by Schopper (1966).

- ²⁵The vacancy created by nuclear electron capture tends to counteract the effect of the decrease in nuclear charge from Ze to $(Z-1)e$. For this reason, the overlap integral of Eq. (5-2) is smaller than its analogs in β^\pm decay.
- ²⁶The upper limit of the neutrino energy is only approximately $W_0 + 1 - |E'_K| - W$ as implied by the energy-conserving delta function in Eq. (5-3). The neutrino energy is reduced by the binding energy of the second K electron in the daughter atom that already contains one K hole, and increased by the additional relaxation energy of the electron cloud.
- ²⁷The directional correlation function for x rays from L_3 -shell internal conversion of an M4 γ transition and a cascade γ ray in ^{207}Bi , given by Rupnik and Crasemann (1972) [their Eqs. (36) and (37)] is in error: contrary to these authors' assumption, the radial integrals cannot be factored out of the correlation expression (J. S. Geiger, private communication, 1974). New calculations are being carried out by Geiger and Ferguson (1974) and Carvalho *et al.* (1975).
- ²⁸While nuclear electron capture as a rule occurs predominantly from s states, it is interesting to note that $\sim 97\%$ of the primary vacancies produced in the decay of ^{202}Pb and ^{205}Pb are in the L_3 shell (Emery, 1975; Bambynek *et al.*, 1974).

REFERENCES

- Abdurazakov, A.A., G. Beyer, K.Ya. Gromov, E. Herrmann,
T.A. Islamov, M. Jachim, F. Molnar, G. Musiol,
H.-U. Siebert, H. Strusny, H. Tyrroff, and S.A. Usmanova,
1974, Joint Institute for Nuclear Research, Dubna Report
JINR, E6-8008 (unpublished).
- Abers, E.S., and B.W. Lee, 1973, *Physics Reports* 9C, 1.
- Adam, I., K.S. Toth, and R.A. Meyer, 1967a, *Phys. Rev.* 159, 985.
- Adam, N., K. Wilsky, Zh. Zhelev, M. Jorgensen, M. Krivopostov,
V. Kuznetsov, O.B. Nielsen, and M. Finger, 1967b, *Izv.*
Akad. Nauk. SSSR, Ser. Fiz. 31, 122 [*Bull. Acad. Sci.*
USSR, Phys. Ser. 31, 114].
- Adamovicz, B., Z. Moroz, Z. Preibisz, and A. Zglinski, 1968,
Acta Phys. Polonia 34, 529.
- Albrecht, G., and J.W. Hammer, 1975, *Z. Phys.* A273, 405.
- Alburger, D.E., 1972, *Phys. Rev.* C6, 1167.
- Alburger, D.E., and D.H. Wilkinson, 1970, *Phys. Letters* 32B, 190.
- Aleksandrov, V.S., V.S. Buttsev, T. Vylov, K.Y. Gromov, and
V.G. Kalinnikov, 1972, Joint Institute for Nuclear Research,
Dubna, Report JINR-P6-6794, (unpublished).
- Allen, R.A., W.E. Burcham, K.F. Chackett, G.L. Munday,
and P. Reasbeck, 1955, *Proc. Phys. Soc. (London)* 68A 681.
- Alvarez, L.W., 1937, *Phys. Rev.* 52, 134.
- Alvarez, L.W., 1938a, *Phys. Rev.* 53, 606.
- Alvarez, L.W., 1938b, *Phys. Rev.* 54, 486.

- Anderson, C.E., G.W. Wheeler, and W.W. Watson, 1952,
Phys. Rev. 87, 668.
- Anderson, C.E., G.W. Wheeler, and W.W. Watson, 1953,
Phys. Rev. 90, 606.
- Andersson, G., G. Rudstam, and G. Sörensen, 1965, Ark. Fys.
28, 37.
- Arbman, E., and N. Svartholm, 1955, Ark. Fys. 10, 1.
- Armstrong, L., and C.W. Kim, 1972, Phys. Rev. C6, 1924.
- Asai, J., and H. Ogata, 1974, Nucl. Phys. A233, 55.
- Aston, G.H., 1927, Proc. Cambr. Phil. Soc. 22, 935.
- Auble, R.L., 1971a, Nucl. Data Sheets B5, 568.
- Auble, R.L., 1971b, Nucl. Data Sheets B5, 588.
- Avignon, P., 1953, J. Phys. Radium 14, 637.
- Avignon, P., 1956, Ann. Phys. (Paris) 1, 10.
- Avignon, P., A. Michałowicz, and R. Bouchez, 1955, J. Phys.
Radium 14, 404.
- Avotina, M.P., E.P. Grigor'ev, Zh.T. Zhelev, A.V. Zolotavin,
and V.O. Sergeev, 1965a, Dubna Report 2272, (unpublished)
quoted by Berényi, 1967.
- Avotina, M.P., E.P. Grigor'ev, A.V. Zolotavin, N.A. Lebedev,
and V.O. Sergeev, 1965b, Dubna Report 2271, (unpublished)
quoted by Berényi, 1967.

- Avotina, M.P., E.P. Grigor'ev, A.V. Zolotavin, V.O. Sergeev,
V.E. Ter-Nersesyants, J. Vrzal, N.A. Lebedev, J. Liptak,
and Ya. Urbanets, 1966, Izv. Akad. Nauk. SSSR, Ser. Fiz.
30, 1292 [Bull. Acad. Sci. USSR, Phys. Ser. 30, 1350].
- Azman, A., A. Moljk, and J. Pahor, 1968, Z. Phys. 208, 234.
- Bagus, P.S., 1964, Argonne National Laboratory Report No. ANL-
6959 (unpublished).
- Bagus, P.S., 1965, Phys. Rev. 139, A619.
- Bahcall, J.N., 1962a, Phys. Rev. Letters 9, 500.
- Bahcall, J.N., 1962b, Phys. Rev. 128, 1297.
- Bahcall, J.N., 1963a, Phys. Rev. 129, 2683.
- Bahcall, J.N., 1963b, Phys. Rev. 131, 1756.
- Bahcall, J.N., 1963c, Phys. Rev. 132, 362.
- Bahcall, J.N., 1965a, Nucl. Phys. 71, 267.
- Bahcall, J.N., 1965b, in Proceedings of the International Conference
on the Role of Atomic Electrons in Nuclear Transformations
(Nuclear Energy Information Center, Warsaw), p. 336.
- Bahcall, J.N., 1972, Comments Nuclear Particle Phys. 5, 59.
- Bakhru, H., and I.L. Preiss, 1967, Phys. Rev. 154, 1091.
- Bambynek, W., 1967a, Z. Phys. 206, 66.
- Bambynek, W., 1967b, Standardization of Radionuclides (International
Atomic Energy Agency, Vienna), p. 373.

- Bambynek, W., B. Crasemann, R.W. Fink, H.-U. Freund,
Hans Mark, C.D. Swift, R.E. Price, and P. Venugopala Rao,
1972, *Rev. Mod. Phys.* 44, 716, and 1974, 46, 853.
- Bambynek, W., E. De Roost, and E. Funck, 1968, in Berényi,
(1968b) p. 253.
- Bambynek, W., O. Lerch, and A. Spornol, 1966, *Nucl. Inst.*
Methods 39, 104.
- Bambynek, W., and D. Reher, 1968a, *Z. Phys.* 214, 374.
- Bambynek, W., and D. Reher, 1970, *Z. Phys.* 238, 49.
- Bambynek, W., and D. Reher, 1973, *Z. Phys.* 264, 253.
- Band, I.M., L.N. Zyryanova, and Tsin Chen-Zhui, 1956, *Izv.*
Akad. Nauk. SSSR, Ser. Fiz. 20, 1387 [*Bull. Acad. Sci.*
USSR, Phys. Ser. 20, 1269].
- Band, I.M., L.M. Zyryanova, and Yu.P. Suslov, 1958, *Izv. Akad.*
Nauk. SSSR, Ser. Fiz. 22, 952 [*Bull. Acad. Sci. USSR,*
Phys. Ser. 22, 943].
- Baskova, K.A., S.S. Vasil'ev, No Seng Ch'ang, and L.Ya. Shavtvalov,
1961, *Zhur. Eksp. Teor. Fiz.* 41, 1484 [1962, *Sov. Phys.*
JETP 14, 1060].
- Baskova, K.A., S.S. Vasil'ev, M.A. Khamo-Leila, and
L.Ya. Shavtvalov, 1964, *Zhur. Eksp. Teor. Fiz.* 47, 1162.
[1965, *Sov. Phys. JETP* 20, 781].
- Bayer, G., V.S. Butsev, K.Ya. Gromov, V.G. Kalinnikov,
K.O. Mortensen, G.L. Nilssen, and N.A. Tikhonov, 1972,
Izv. Akad. Nauk. SSSR, Ser. Fiz. 36, 782 [*Bull. Acad. Sci.*
USSR, Phys. Ser. 36, 705].

- Bayer, G., V.S. Butsev, Ts. Vylov, V.G. Kalinnikov, and I. Penev, 1974, *Programma i tezisy dokladov* 24. Soveshchaniya po yadernoj spektroskopii i strukture atomnogo yadra. Khar'kov, 29 yanvarga-1 fevraiya, p. 91. [Program and abstracts of 24. conference on nuclear spectroscopy and nuclear structure, Kharkov, 29 January-1 February, p. 91, INIS-mf-1850].
- Bearden, J.A., and A.F. Burr, 1967, *Rev. Mod. Phys.* 39, 125.
- Beattie, R.J.D., and J. Byrne, 1971, *Nucl. Phys.* A161, 650.
- Beattie, R.J.D., and J. Byrne, 1972, *Nucl. Inst. Methods* 104, 163.
- Beery, D.B., W.H. Kelly, and W.C. McHarris, 1968, *Phys. Rev.* 171, 1283.
- Beg, M.A., B.J. Bernstein, and A. Sirlin, 1972, *Phys. Rev.* D6, 2597.
- Beg, M.A., and A. Sirlin, 1974, *Ann. Rev. Nucl. Science* 24, 379.
- Behrens, H., and W. Bühring, 1968, *Nucl. Phys.* A106, 433.
- Behrens, H., and W. Bühring, *Nucl. Phys.* A150, 481.
- Behrens, H., and W. Bühring, 1971, *Nucl. Phys.* A162, 111.
- Behrens, H., and W. Bühring, 1972, *Nucl. Phys.* A179, 297.
- Behrens, H., and W. Bühring, 1974, *Nucl. Phys.* A232, 230.
- Behrens, H., and J. Jänecke, 1969, *Landolt-Börnstein, Numerical Data and Functional Relationships in Science and Technology, New Series, Group I, Vol. 4: Numerical Tables for β -Decay and Electron Capture (Springer-Verlag, Berlin).*

- Bell, P.R., J.M. Jauch, and J.M. Cassidy, 1952, *Science* 15, 12.
- Belyanin, Yu.I., E.I. Biryukov, and N.S. Shimanskaya, 1966,
 Izv. Akad. Nauk. SSSR, Ser. Fiz. 30, 1130 [Bull. Acad.
 Sci. USSR, Phys. Ser. 30, 1182].
- Benoist-Gueutal, P., 1950, C.R. Acad. Sci. 230, 624.
- Benoist-Gueutal, P., 1953a, Thèses (Masson, Paris, unpublished).
- Benoist-Gueutal, P., 1953b, Ann. Phys. (Paris) 8, 593.
- Berényi, D., 1962, Phys. Letters 2, 332.
- Berényi, D., 1963a, Nucl. Phys. 48, 121.
- Berényi, D., 1963b, Acta Phys. Hung. 16, 101.
- Berényi, D., 1965a, in Role of Atomic Electrons in Nuclear Transformations (Nuclear Energy Information Center, Warsaw, Poland), p. 609.
- Berényi, D., 1967, Acta Phys. Hung. 22, 25.
- Berényi, D., 1968a, Rev. Mod. Phys. 40, 390.
- Berényi, D., ed. 1968b, Proceedings of the Conference on the Electron Capture and Higher Order Processes in Nuclear Decays (Eötvös Lőránd Physical Society, Budapest).
- Berényi, D., 1970, Magyar Fiz. Folyóirat 18, 23.
- Berényi, D., Gs. Újhelyi and J. Fehér, 1965b, Phys. Letters 18, 293.
- Berényi, D., and L. Kazai, 1965c, Nucl. Phys. 61, 657.
- Berényi, D., and D. Varga 1969, Nucl. Phys. A138, 685.
- Berényi, D., A. Szalay, D. Varga, F. Molénar, and J. Uchrin,
 1970, Acta Phys. Hung. 28, 431.

- Berényi, D., G. Hock, A. Ménes, G. Szekely, Cs. Ujhelyi,
and B.A. Zon, 1976, Nucl. Phys. A256, 205.
- Berestetskii, V.B., 1958, Nuovo Cimento 10, 385.
- Bergström, I., 1951, Phys. Rev. 82, 112.
- Bergström, I., 1952, Ark. Phys. 5, 191.
- Bernardini, M., P. Broveto, S. Debenedetti, and S. Ferroni,
1958, Nuovo Cimento 7, 419.
- Bernstein, J., 1974, Rev. Mod. Phys. 46, 7.
- Berthier, J., and P. Lipnik, 1966, Nucl. Phys. 78, 448.
- Bertmann, U., F. Krahn, and E. Huster, 1972, Z. Phys. 251, 382.
- Bertolini, G., A. Bisi, E. Lazzarini, and L. Zappa, 1954,
Nuovo Cimento 11, 539.
- Bertrand, F.E., 1974, Nucl. Data Sheets 11, 473.
- Bertsch, G.F., and A. Mekjian, 1972, Ann. Rev. Nucl. Science 22, 25.
- Bethe, H.A., and R.F. Bacher, 1936, Rev. Mod. Phys. 8, 82.
- Bhalla, C.P., 1964, National Bureau of Standards Monograph NBS-81.
- Bhalla, C.P., and M.E. Rose, 1960, Oak Ridge National Laboratory
Report ORNL-2954.
- Bhalla, C.P., and M.E. Rose, 1961, Oak Ridge National Laboratory
Report ORNL-3207.
- Bhalla, C.P., and M.E. Rose, 1962, Phys. Rev. 128, 774.
- Bhat, M.R., and M.L. Pool, 1962, Phys. Rev. 127, 1704.
- Bhatki, K.S., R.K. Gupta, S. Jha, and B.K. Madan, 1957,
Nuovo Cimento 6, 1461.

- Bhattacharjee, S.K., and S. Raman, 1956, Nucl. Phys. 1, 486.
- Biavati, M.H., 1959, Thesis, Columbia University N.Y., U.S.
Atomic Energy Commission Rep. CU-190 (unpublished).
- Biavati, M.H., S.J. Nassiff, and C.S. Wu, 1962, Phys. Rev. 125,
1364.
- Biedenharn, L.C., and N.V.V.J. Swamy, 1964, Phys. Rev. 133, B1353
- Biryukov, E.I., and N.S. Shimanskaya, 1962, Izv. Akad. Nauk.
SSSR, Ser. Fiz. 26, 215 [Bull. Acad. Sci. USSR, Phys. Ser.
26, 215].
- Biryukov, E.I., and N.S. Shimanskaya, 1963a, Izv. Akad. Nauk.
SSSR, Ser. Fiz. 27, 1402 [Bull. Acad. Sci. USSR, Phys. Ser.
27, 1377].
- Biryukov, E.I., and N.S. Shimanskaya, 1970, Yadern. Fiz. 11, 246
(Sov. J. Nucl. Phys. 11, 138).
- Biryukov, E.I., O.I. Grigor'ev, B.S. Kuznetsov, and N.S. Shimanskaya,
1960, Izv. Akad. Nauk. SSSR, Ser. Fiz. 24, 1135 [Bull. Acad.
Sci. USSR, Phys. Ser. 24, 1138].
- Biryukov, E.I., V.T. Novikov, and N.S. Shimanskaya, 1963b, Izv.
Akad. Nauk. SSSR, Ser. Fiz. 27, 1406 [Bull. Acad. Sci. USSR,
Phys. Ser. 27, 1383].
- Biryukov, E.I., V.T. Novikov, and N.S. Shimanskaya, 1965, Izv.
Akad. Nauk. SSSR, Ser. Fiz. 29, 151 [Bull. Acad. Sci. USSR,
Phys. Ser. 29, 148].

- Biryukov, E.I., E.G. Zaletskii, and N.S. Shimanskaya, 1966,
Izv. Akad. Nauk. SSSR, Ser. Fiz. 30, 504 [Bull. Acad.
Sci. USSR, Phys. Ser. 30, 514].
- Bisi, A., E. Germagnoli, L. Zappa, and E. Zimmer, 1955a,
Nuovo Cimento 2, 290.
- Bisi, A., E. Germagnoli, and L. Zappa, 1955b, Nuovo Cimento 2, 1052.
- Bisi, A., E. Germagnoli, and L. Zappa, 1956b, Nucl. Phys. 1, 593.
- Bisi, A., E. Germagnoli, and L. Zappa, 1957, Nuovo Cimento 6, 299.
- Bisi, A., E. Germagnoli, and L. Zappa, 1959, Nuovo Cimento 11, 843.
- Bisi, A., S. Terrani, and L. Zappa, 1955c, Nuovo Cimento 1, 651.
- Bisi, A., and L. Zappa, 1954, Nuovo Cimento 12, 539.
- Bisi, A., L. Zappa, and E. Germagnoli, 1956a, Nuovo Cimento 4, 764.
- Bisi, A., L. Zappa, and E. Zimmer, 1956c, Nuovo Cimento 4, 307.
- Bjorken, J.D., and S.D. Drell, 1965, Relativistic Quantum Fields
(McGraw-Hill, New York).
- Blin-Stoyle, R.J., 1969, Phys. Letters 29B, 12.
- Blin-Stoyle, R.J., 1973, Fundamental Interactions and the Nucleus
(North Holland Publ. Co., Amsterdam).
- Blin-Stoyle, R.J., J.A. Evans, and A.M. Knau, 1971, Phys. Letters
36B, 202.
- Blin-Stoyle, R.J., and S.C.K. Nair, 1966, Adv. in Physics 15, 493.
- Bloch, F., 1936, Phys. Rev. 50, 272.
- Blok, L., T.J. de Boer, and J. Blok, 1959, Physica 25, 333.
- Blok, L., W. Goedbloed, E. Mastenbroek, and J. Blok, 1962,
Physica 28, 993.

- Blomquist, J., 1971, Phys. Letters 35B, 375.
- Bloom, S.D., and J.L. Uretsky, 1960, Nuovo Cimento 17, 304.
- Blue, J.W., and E. Bleuler, 1955, Phys. Rev. 100, 1324.
- Bock, R., 1955, private communication to K. Way, R.W. King,
C.L. McGinnis, and R. van Lieshout, 1955, Nuclear Level
Schemes, United States Atomic Energy Commission Report
TID-5300 (unpublished).
- Bohr, A., and B.R. Mottelson, 1969, Nuclear Structure
(W.A. Benjamin, Inc., New York, Amsterdam).
- Bolotin, H.H., 1964, Phys. Rev. 136B, 1566.
- Bolotin, H.H., A.C. Li, and A. Schwarzschild, 1961, Phys. Rev.
124, 213.
- Bonacalza, E.C.O., P. Thieberger, and I. Bergström, 1962,
Ark. Fys. 22, 111.
- Bosch, H.E., M.A. Fariolli, N. Martin, and M.C. Simon, 1969,
Nucl. Inst. Methods 73, 323.
- Bosch, H.E., M.C. Simon, E. Szichman, L. Gatto, and S.M. Abecasis,
1967, Phys. Rev. 159, 1029.
- Bottino, A., and G. Ciocchetti, 1973, Phys. Letters 43B, 170.
- Bouchez, R., 1952, Physica 18, 1171.
- Bouchez, R., S.R. de Groot, R. Nataf, and H.A. Tolhoek, 1950,
J. Phys. Radium 11, 105.
- Bouchez, R., and P. Depommier, 1960, Rept. Prog. Phys. 23, 395.

- Bouchez, R., and P. Depommier, 1965, in Role of Atomic Electrons in Nuclear Transformations (Nuclear Energy Information Center, Warsaw, Poland), p. 30.
- Bouchez, R., and G. Kayas, 1949, J. Phys. Radium 10, 110.
- Bouchiat, M.A., and C. Bouchiat, 1974, J. Phys. (Paris) 35, 899.
- Bouchiat, M.A., and C. Bouchiat, 1975, J. Phys. (Paris) 36, 493.
- Brabec, V., B. Kracík, and M. Vobecký, 1960, Czech. J. Phys. 10, 855.
- Bradt, H., P.C. Gugelot, O. Huber, H. Medicus, P. Preiswerk, and P. Scherrer, 1945, Helv. Phys. Acta 18, 351.
- Bradt, H., P.C. Gugelot, O. Huber, H. Medicus, P. Preiswerk, P. Scherrer, and R. Steffen, 1946, Helv. Phys. Acta 19, 222.
- Bramson, S., 1930, Z. Phys. 66, 721.
- Breستي, M., F. Cappellani, and A.M. Del Turco, 1964, Nucl. Phys. 58, 491.
- Brewer, H.R., D.S. Harmer, and D.H. Hay, 1961, Phys. Rev. Letters 7, 319, Georgia Institute of Technology Report GIT-ES-B 151-1 (unpublished).
- Brewer, W.D., and D.A. Shirley, 1968, Phys. Rev. Letters 20, 885.
- Briand, J.P., P. Chevallier, M. Tavernier, and J.P. Rozet, 1971, Phys. Rev. Letters 27, 777.
- Brosi, A.R., B.H. Ketelle, H.C. Thomas, and R.J. Kerr, 1959, Phys. Rev. 113, 239.
- Brown, L.S., 1964, Phys. Rev. B135, 314.

- Browne, C.I., J.O. Rasmussen, J.P. Surls, and D.F. Martin,
1952, Phys. Rev. 85, 146.
- Brysk, H., 1952, Phys. Rev. 86, 996.
- Brysk, H., and M.E. Rose, 1955, Oak Ridge National Laboratory Report
ORNL-1830, (unpublished).
- Brysk, H., and M.E. Rose, 1958, Rev. Mod. Phys. 30, 1169.
- Bühring, W., 1963a, Nucl. Phys. 40, 472.
- Bühring, W., 1963b, Nucl. Phys. 49, 190.
- Bühring, W., 1965, Nucl. Phys. 61, 110.
- Bühring, W., 1967, Kernforschungszentrum Karlsruhe Report KFK 559.
- Bühring, W., and L. Schülke, 1965, Nucl. Phys. 65, 369.
- Burke, V.M., and I.P. Grant, 1967, Proc. Phys. Soc. (London)
90, 297.
- Cambiaggio, M.C., J. Davidson, V. Silbergleit, and M. Behar,
1975, Phys. Rev. C12, 699.
- Campbell, J.L., and K.W.D. Ledingham, 1966, Brit. J. Appl.
Phys. 17, 786.
- Campbell, J.L., W. Leiper, K.W.D. Ledingham, and R.W.P. Drever,
1967, Nucl. Phys. A96, 279.
- Campbell, J.L., L.A. McNelles, and J. Law, 1971, Can. J. Phys.
49, 3142.
- Campbell, J.L., and J. Law, 1972, Can. J. Phys. 50, 2451.
- Campbell, J.L., and L.A. McNelles, 1972, Nucl. Inst. Methods 98, 433.
- Campbell, M., K.W.D. Ledingham, A.D. Baillie, M.L. Fitzpatrick,
J.Y. Gourlay, and J.G. Lynch, 1975, Nucl. Phys. A249, 349.

- Campion, P.J., 1959, Int. J. Appl. Rad. Isotopes 4, 232.
- Campion, P.J., 1968, Int. J. Appl. Rad. Isotopes 19, 219.
- Campion, P.J., 1973, Nucl. Inst. Methods 112, 75.
- Carey, W.E., R.P. Sullivan, M.R. Bhat, and M.L. Pool, 1958,
Bull. Am. Phys. Soc., Sec. II, 3, 63.
- Carlson, T.A., C.C. Lu, T.C. Tucker, C.W. Nestor, and
F.B. Malik, 1970, Oak Ridge National Laboratory Report
ORNL-4614 (unpublished).
- Carvalho, M.J., A. Barroso, and F.B. Gil, 1975, private communi-
cation
- Casson, H., L.S. Goodman, and V.E. Krohn, 1953, Phys. Rev. 92, 1517.
- Charpak, G., 1953, C.R. Acad. Sci. B237, 243.
- Charpak, G., 1955, J. Phys. Radium 16, 62.
- Chasan, B., and R. Chandra, 1967, Bull. Am. Phys. Soc. 12, 74.
- Chen, M.H., B. Crasemann, P. Venugopala Rao, J.M. Palms, and
R.E. Wood, 1971, Phys. Rev. A4, 846.
- Chester, R.O., R.W. Peelle, and F.C. Maienschein, 1963, in
O'Kelley (1963), p. 201.
- Chew, W.M., J.C. McGeorge, and R.W. Fink, 1973, in Proceedings
of the International Conference on Inner Shell Ionization Phenomena
and Future Applications, edited by R.W. Fink, S.T. Manson,
J.M. Palms, P. Venugopala Rao, U.S. Atomic Energy Commission
Report No. CONF-720404 (unpublished), p. 197.

- Chew, W.M., A.C. Xenoulis, R.W. Fink, and J.J. Pinajian,
1974a, Nucl. Phys. A218, 372.
- Chew, W.M., A.C. Xenoulis, R.W. Fink, F.J. Schima, and
W.B. Mann, 1974b, Nucl. Phys. A229, 79.
- Chilosi, G., S. Monaro, and R.A. Ricci, 1962, Nuovo Cimento 26, 440.
- Christmas, P., 1964, Nucl. Phys. 55, 577; 1965, 61, 352.
- Chu, Y.Y., 1971, Phys. Rev. C4, 642.
- Cohen, S.G., and S. Ofer, 1955, Phys. Rev. 100, 856.
- Cook, C.S., and L.M. Langer, 1948, Phys. Rev. 74, 1241.
- Cook, C.S., and F.M. Tomnovec, 1956, Phys. Rev. 104, 1407.
- Cook, W.B., and M.W. Johns, 1969, Can. J. Phys. 47, 1899.
- Cooper, J.A., J.M. Hollander, M.I. Kalkstein, and J.O. Rasmussen,
1965, Nucl. Phys. 72, 113.
- Crane, H.R., 1948, Rev. Mod. Phys. 20, 278.
- Crasemann, B., 1973, Nucl. Inst. Methods 112, 33.
- Crasemann, B., and P. Stephas, 1969, Nucl. Phys. A134, 641.
- Creager, C.B., C.W. Kocher, and A.C.G. Mitchell, 1959/60,
Nucl. Phys. 14, 578.
- Cretzu, T., K. Hohmuth, and J. Schintmeister, 1965, Nucl. Phys.
70, 129.
- Cretzu, T., K. Hohmuth, and G. Winter, 1964, Nucl. Phys. 56, 415.
- Cutkosky, R.E., 1954, Phys. Rev. 95, 1222.
- Cutkosky, R.E., 1957, Phys. Rev. 107, 330.
- Damgaard, J., and A. Winther, 1965, Phys. Letters 23, 345.

- Danby, G. T., J.S. Foster, and A.L. Thomson, 1958, *Can. J. Phys.* 36, 1487.
- Daniel, H., 1968, *Rev. Mod. Phys.* 40, 659.
- Daniel, H., 1969, *Z. Phys.* 223, 150.
- Daniel, H., G. Schupp, and E.N. Jensen, 1960, *Phys. Rev.* 117, 823.
- Dasmahapatra, B., 1972, *Radiochem. Radioanal. Letters* 12, 185.
- Dasmahapatra, B., 1975a, *Phys. Rev. C* 12, 702.
- Dasmahapatra, B., 1975b, *Pramana.* 4, 218.
- Das Mahapatra, B.K., and P. Mukherjee, 1974, *J. Phys. A* 7, 388.
- Davis, R., D.S. Harmer, and K.C. Hoffman, 1968, *Phys. Rev. Letters* 20, 1205.
- de Beer, A., H.P. Blok, and J. Blok, 1964, *Physica* 30, 1938.
- Delabaye, M., and P. Lipnik, 1966, *Nucl. Phys.* 86, 668.
- Delorme, J., and M. Rho, 1971, *Nucl. Phys.* B34, 317.
- Depommier, P., 1968 in Berényi (1968b), p. 202.
- Der Mateosian, E., 1953, *Phys. Rev.* 92, 938.
- Der Mateosian, E., and A. Smith, 1952, *Phys. Rev.* 88, 1186.
- de Raedt, J., 1968, in *Proceedings Beta Spectroscopy and Nuclear Structure* (Natuurkundig Laboratorium, Rijksuniversiteit, Groningen) p. 78.
- De Roost, E., and F. Lagoutine, 1973, in Grinberg *et al.* (1973), *Atomic Energy Review* 11, 515.
- Desclaux, J.P., 1973, *Atomic and Nuclear Data* 12, 311.
- de Shalit, A., and I. Talmi, 1963, *Nuclear Shell Theory* (Academic Press, New York and London)..

- de Wit, S.A., and A.H. Wapstra, 1965, Nucl. Phys. 73, 49.
- Dicus, D.A., and R.E. Norton, 1970, Phys. Rev. D1, 1360.
- Dillman, L.T., 1968, J. Nucl. Medicine 10, Suppl. 2.
- Dillman, L.T., 1970, J. Nucl. Medicine 11, Suppl. 4.
- Dillman, L.T., J.J. Kraushaar, and J.D. McCullen, 1963,
Nucl. Phys. 42, 383.
- Dobrilović, L., V. Voljin, D. Bek-Uzarov, K. Buraei, and
A. Milojević, 1972, V Kongres na matematikarite, fizikarite
i astronomite na Jugoslavia (Zbornik na trudorite, Tom. II,
Fizika, Skopje), p. 151.
- Dolginov, A.Z., 1956/1957, Nucl. Phys. 2, 723.
- Dolginov, A.Z., 1958a, Nucl. Phys. 6, 460.
- Dolginov, A.Z., 1958b, Zh. Eksp. Teor. Fiz. 34, 931 [Soviet Phys.
JETP 34, 644].
- Donnelly, T.W., and J.D. Walecka, 1972, Phys. Letters 41B, 275.
- Donnelly, T.W., and J.D. Walecka, 1973, Phys. Letters 44B, 330.
- Dougan, P.W., 1961, Ph. D. Thesis, University of Glasgow,
(unpublished).
- Dougan, P.W., K.W.D. Ledingham, and R.W.P. Drever, 1962a,
Phil. Mag. 7, 475.
- Dougan, P.W., K.W.D. Ledingham, and R.W.P. Drever, 1962b,
Phil. Mag. 7, 1223.
- Drever, R.W.P., 1959, private communication to R.W. Fink,
quoted in Robinson and Fink, 1960.
- Drever, R.W.P., and A. Moljk, 1957a, Phil. Mag. 2, 427.

- Drever, R.W.P., A. Moljk, and S.C. Curran, 1957b, Nucl. Inst. Methods 1, 41.
- Drever, R.W.P., A. Moljk, and J. Scobie, 1956, Phil. Mag. 1, 942.
- Durand, III, L., 1964, Phys. Rev. B135, 310.
- Durosinmi-Etti, I.O., D.R. Brundrit, and S.K. Sen, 1966, in International Conversion Processes, edited by J.H. Hamilton (Academic Press, New York), p. 201.
- Dzhelepov, B.S., and L.N. Zyryanova, 1956, Influence of Atomic Electric Fields on Beta Decay (Akad. Nauka, Moscow).
- Dzhelepov, B.S., L.N. Zyryanova, and Yu.P. Suslov, 1972, Beta Processes, Functions for the Analysis of Beta-Spectra and Electron Capture (Nauka, Leningrad).
- Edmonds, A.R., 1960, Angular Momentum in Quantum Mechanics (Princeton Univ. Press, Princeton).
- Eichler, J., 1963, Z. Phys. 171, 463.
- Ellis, Y.A., 1973, Nucl. Data Sheets 9, 353.
- Eman, B., B. Gubertina, and D. Tadić, 1973, Phys. Rev. C8, 1301.
- Emery, G.T., 1972, Ann. Rev. Nucl. Science 22, 165.
- Emery, G.T., 1975, in Atomic Inner Shell Processes, edited by B. Crasemann (Academic Press, New York), Vol. 1, p. 201.
- Emery, G.T., W.R. Kane, M. McKeown, M.L. Perlman, and G. Scharff-Goldhaber, 1963, Phys. Rev. 129, 2597.
- Emmerich, W.S., S.E. Singer, and J.D. Kurbatov, 1954, Phys. Rev. 94, 113
- Ericson, M., A. Figureau, and C. Thévenet, 1973, Phys. Letters 45B, 19.

- Evans, J.L., J.R. Cooper, D.M. Moore, and W.L. Alford,
1972, Phys. Rev. C6, 1372.
- Faessler, A., E. Huster, O. Krafft, and F. Krahn, 1970,
Z. Phys. 238, 352.
- Fasoli, U., C. Manduchi, and G. Zannoni, 1962 Nuvo Cimento.
23, 1126.
- Fermi, E., 1934, Z. Phys. 88, 161, translated in The Development
of Weak Interaction Theory, edited by P.K. Kabir (Gordon
and Breach, New York, 1963).
- Feinberg, E.L., 1941, J. Phys. USSR 4, 423.
- Feynman, R.P., 1949, Phys. Rev. 76, 749.
- Fink, R.W., 1965, in Role of Atomic Electrons in Nuclear Trans-
formations (Nuclear Energy Information Center, Warsaw,
Poland), p. 365.
- Fink, R.W., 1968a, in Berényi, (1968b) p. 23.
- Fink, R.W., 1968b, Nucl. Phys. A110, 379.
- Fink, R.W., 1969, Phys. Rev.; 180, 1220.
- Fink, R.W., G. Andersson, and J. Kantele, 1961, Ark. Fys. 19, 323.
- Fink, R.W., and K.W.D. Ledingham, 1966, Bull. Am. Phys. Soc.
11, 352.
- Firestone, R.B., R.A. Warner, W.C. McHarris, and W.H. Kelly,
1974, Phys. Rev. Letters 33, 30.
- Firestone, R.B., R.A. Warner, W.C. McHarris, and W.H. Kelly,
1975a, Phys. Rev. Letters 35, 401.

- Firestone, R.B., R.A. Warner, W.C. McHarris, and W.H. Kelly,
1975b, Phys. Rev. Letters 35, 713.
- Fitzpatrick, M.L., 1973, Ph.D. Thesis, University of Glasgow
(unpublished).
- Fitzpatrick, M.L., K.W.D. Ledingham, M. Campbell, A.D. Baillie,
J.Y. Gourlay, and J.G. Lynch, 1976, to be published.
- Ford, G.W., and C.F. Martin, 1969, Nucl. Phys. A134, 457.
- Ford, J.W., A.V. Ramaya, and J.J. Pinajian, 1970, Nucl. Phys.
A146, 397.
- Frauenfelder, G., and R.M. Steffen, 1966, in Alpha-, Beta-, and
Gamma-Ray Spectroscopy, edited by K. Siegbahn (North-Holland
Publ. Co., Amsterdam).
- Freedman, M.S., 1974, Ann. Rev. Nucl. Science 24, 209.
- Freedman, M.S., F. Wagner, Jr., F.T. Porter, and H.H. Bolotin,
1966, Phys. Rev. 146, 791.
- Frevert, L.; R. Schöneberg, and A. Flammersfeld, 1965, Z. Phys.
182, 439.
- Fricke, B., W. Greiner, and J.T. Waber, 1971, Theoret. Chim.
Acta 21, 235.
- Friedlander, G., and J.M. Miller, 1951a, Phys. Rev. 84, 588.
- Friedlander, G., and W.C. Orr, 1951b, Phys. Rev. 84, 484.
- Friedlander, G., M.L. Perlman, D. Alburger, and A.W. Sunyar,
1950, Phys. Rev. 80, 30.

- Friedlander, G., and L. Yaffe, 1962, *Can. J. Phys.* 40, 1249.
- Froese-Fischer, C., 1965, *Phys. Rev.* 137, A1644.
- Froese-Fischer, C., 1969, *Comp. Phys. Com.* 1, 151.
- Froese-Fischer, C., 1972a, *Comp. Phys. Com.* 4, 107.
- Froese-Fischer, C., 1972b, *Atomic Data* 4, 301.
- Fujita, J.I., 1962, *Phys. Rev.* 126, 202.
- Fujioka, M., K. Hisatake, and K. Takahashi, 1964, *Nucl. Phys.* 60, 294.
- Fujiwara, I., S. Iwata, T. Nishi, S. Goda, M. Tabushi, and T. Shigematsu, 1964, *Nucl. Phys.* 50, 346.
- Funk Jr., E.G., J.W. Mihelich, and C.F. Schwerdtfeger, 1962, *Nucl. Phys.* 39, 147.
- Funke, L., H. Graber, K.H. Kaun, H. Sodan, and L. Werner, 1965, *Nucl. Phys.* 70, 347.
- Gallagher, C.J., H.L. Nielsen, and O.B. Nielsen, 1961, *Phys. Rev.* 122, 1590.
- Gandel'man, G.M., 1959, *J. Exptl. Theoret. Phys. (USSR)* 36, 585 [*Soviet Physics JETP* 36, 406 (1959)].
- Geiger, J.S., and A.J. Ferguson, 1974 (private communication).
- Genz, H., 1968, in Berényi (1968b), p. 81.
- Genz, H., 1971b, Ph.D. Thesis, Emory University, Atlanta, (unpublished).
- Genz, H., 1973a, in Proceedings of the International Conference on Inner-Shell Ionization Phenomena, edited by R.W. Fink, S.T. Manson, J.M. Palms, and P. Venugopala Rao, U.S. Atomic Energy Commission Report No. CONF-720404 (unpublished), p. 1965.

- Genz, H., 1973b, Nucl. Inst. Methods 112, 83.
- Genz, H., D.S. Harmer, and R.W. Fink, 1968, Nucl. Inst. Methods 60, 195.
- Genz, H., J.P. Renier, and R.W. Fink, 1972, in Radioactivity in Nuclear Spectroscopy, edited by J.H. Hamilton and J.C. Manthuruthil (Gordon and Breach, Science Publ., New York) p. 1335.
- Genz, H., J.P. Renier, J.G. Pengra, and R.W. Fink, 1971a, Phys. Rev. C3, 172.
- Genz, H., R.E. Wood, J.M. Palms, and P. Venugopala Rao, 1973c, Z. Phys. 260, 47.
- Gindler, J.E., J.R. Huizenga, and D.W. Engelkemeir, 1958, Phys. Rev. 109, 1263.
- Girgis, R.K., and R. van Lieshout, 1959a, Physica 25, 133.
- Girgis, R.K., R.A. Ricci, R. van Lieshout, and J. Konijn, 1959b, Nucl. Phys. 13, 473.
- Glauber, R.J. and P.C. Martin, 1955a, J. Phys. Radium 16, 573.
- Glauber, R.J., P.C. Martin, T. Lindqvist, and C.S. Wu, 1955b, Phys. Rev. 101, 905.
- Glauber, R.J., and P.C. Martin, 1956, Phys. Rev. 104, 158.
- Glaubman, M.J., 1955, Phys. Rev. 98, 645.
- Gleason, G.I., 1959, Phys. Rev. 113, 287.

- Gnatovich, I., V. Svols'ka, Y. Svols'ki, Y. Rjikovska, M. Fisher, and I. Yursik, 1974, *Programma i tezisy dokladov 24. soveshchaniya po yadernoj spektroskopii i strukture atomnogo yadra*, Khar'kov, 29 yanvarya - 1 fevraiya, p. 136 [Program and abstracts of 24. conference on nuclear spectroscopy and nuclear structure Khar'kov, 29 January - 1 February, p. 136, INIS-mf-1850].
- Goedbloed, W., 1968, in Berényi (1968b), p. 92.
- Goedbloed, W., 1970, Ph. D. Thesis, Vrije Universiteit, Amsterdam (unpublished).
- Goedbloed, W., S.C. Gøverse, A. Brinkman, and J. Blok, 1970c, *Nucl. Phys.* A159, 409.
- Goedbloed, W., S.C. Gøverse, C.P. Gerneř, A. Brinkman, and J. Blok, 1970a, *Nucl. Inst. Methods* 88, 197.
- Goedbloed, W., S.C. Gøverse, C.P. Gerneř, A. Brinkman, and J. Blok, 1970b, *Nucl. Phys.* A159, 417.
- Goedbloed, W., E. Mastenbroek, A. Kemper, and J. Blok, 1964, *Physica* 30, 2041.
- Gold, R., and E.F. Bennett, 1966, *Phys. Rev.* 147, 201.
- Goldhaber, M., E. der Mateosian, G. Scharff-Goldhaber, A.W. Sunyar, M. Deutsch, and N.S. Wall, 1951, *Phys. Rev.* 83, 661L.
- Goldhaber, M., L. Grodzins, and A.W. Sunyar, 1958, *Phys. Rev.* 109, 1015.
- Gombás, P., 1956, in Handbuch der Physik, edited by S. Flügge (Springer-Verlag, Berlin), Vol. 36, p. 109.

- Gombás, P., 1967, Pseudopotentiale (Springer-Verlag, Wien, New York)
- Good, W.M., and W.C. Peacock, 1946, Phys. Rev. 69, 680.
- Good, W.M., D. Peaslee, and M. Deutsch, 1946, Phys. Rev. 69, 313.
- Goodier, I.W., M.J. Woods, and A. Williams, 1971, in Chemical Nuclear Data edited by M.L. Hurrel (The British Nuclear Energy Society, London) p. 175.
- Gopinathan, K.P., and W. Rubinson, 1968, Bull. Am. Phys. Soc. 13, 1452.
- Gopych, P.M., I.I. Gromova, A.F. Novgorodov, Kh.-G. Urtlepp, and A. Yasinski, 1974, Programma i tezisy dokladov 24. soveshchaniya po yadernoj spektroskopii i strukture atomnogo yadra, Khar'kov, 29 yanvarya - 1 fevraiya, p. 85 [Program and abstracts of 24. conference on nuclear spectroscopy and nuclear structure, Kharkov 29 January - 1 February, p. 85, INIS-mf-1850]
- Goudsmit, P.F.A., J.F.W. Jansen, B.J. Mijneer, and A.H. Wapstra, 1966, Physica 32, 2161.
- Gove, N.B., and M.J. Martin, 1971, Nucl. Data A10, 205.
- Goverse, S.C., and J. Blok, 1974c, Phys. Letters 50A, 135.
- Goverse, S.C., J. van Pelt, J. van den Berg, J.C. Klein, and J. Blok, 1973, Nucl. Phys. A201, 326.
- Goverse, S.C., J.C. Klein, J. Kuijper, and J. Blok, 1974a, Nucl. Phys. A227, 506.
- Goverse, S.C., J. Kuijper, and J. Blok, 1974b, Z. Phys. 269, 111.
- Grant, I.P., 1970, Adv. in Physics 19, 747.

- Grator, I., M. le Pape, J. Olkowsky, and G. Ranc, 1959,
Nucl. Phys. 13, 303.
- Greenland, P.T., 1975, J. Phys. G1, 1.
- Greenwood, R.C., and E. Brannen, 1960, Phys. Rev. 120, 1411.
- Greenwood, R.C., and E. Brannen, 1961, Phys. Rev. 122, 1849.
- Grigor'ev, E.P., B.S. Dzheleпов, A.V. Zolotavin, V.Ia. Mishin,
V.P. Prikhodtseva, Iu.V. Khol'nov, and G.E. Shchukin,
1958a Izv. Akad. Nauk. SSSR, Ser. Fiz. 22, 831 [Bull. Acad.
Sci. USSR, Phys. Ser. 22, 825].
- Grigor'ev, O.I., B.S. Kuznetsov, N.S. Shimanskaia, and I.A. Iutlandov,
1958b, Izv. Akad. Nauk, SSSR, Ser. Fiz. 22, 850, [Bull. Acad.
Sci., USSR, Phys. Ser. 22, 845].
- Grinberg, B., J.P. Brethon, F. Lagoutine, Y. Le Gallic, J. Legrand,
A.H. Wapstra, H.M. Weiss, W. Bambynek, E. De Roost,
H.H. Hansen, and A. Spornol, Atomic Energy Review 1973, 11, 516.
- Grissom, J.T., D.R. Koehler, and W.I., Alford, 1966, Phys. Rev.
142, 725.
- Grodzins, L., and H. Motz, 1956, Phys. Rev. 102, 761.
- Gromov, K.Ya., Zh.T. Zhelev, V. Zvol'ska, and V.G. Kalinnikov,
1965, Yadern. Fiz. 2, 783 [Sov. J. Nucl. Phys. 2, 559].
- Grotheer, H.H., J.W. Hammer, and K.-W. Hoffmann, 1969,
Z. Phys. 225, 293.
- Gupta, R.K., 1958a, Proc. Phys. Soc. (London), 71, 330.
- Gupta, R.K., 1960, Ark. Fys. 17, 337.

- Gupta, R.K., and S. Jha, 1956, *Nuovo Cimento* 4, 88.
- Gupta, R.K., and S. Jha, 1957, *Nuovo Cimento* 5, 1524.
- Gupta, R.K., S. Jha, M.C. Joshi, and B.K. Madan, 1958b,
Nuovo Cimento 8, 48.
- Hagedoorn, H.L., 1958, Ph. D. Thesis, Technische Hogeschool,
Delft (unpublished).
- Hagedoorn, H.L., and J. Konijn, 1957, *Physica* 23, 1069.
- Hamers, H.C., A. Marseille, and T.J. de Boer, 1957, *Physica* 23,
1056.
- Hamilton, J.H., K.E.G. Löbner, A.R. Sattler, and R. van Lieshout,
1964, *Physica* 30, 1802.
- Hammer, J.W., 1968, *Z. Phys.* 216, 355.
- Hansen, H.H., and D. Mouchel, 1975, *Z. Phys.* 274, 335.
- Hanson, R.J., P.G. Hansen, H.L. Nielsen, and G. Sørensen,
1968, *Nucl. Phys.* A115, 641.
- Harmer, D.S., and M.L. Perlman, 1959, *Phys. Rev.* 114, 1133.
- Harris, J.R., G.M. Rothberg, and N. Benczer-Koller, 1965, *Phys.*
Rev. 138, B554.
- Hartree, D.R., 1957, *The Calculation of Atomic Structures* (John Wiley
& Sons, Inc., New York).
- Hartwig, G., and H. Schopper, 1958, *Z. Phys.* 152, 314.
- Hayashi, T., and J.R. Comerford, Jr., 1968, U.S. Atomic Energy
Commission Report TID-6080 (unpublished).
- Hayward, R.W., 1950, *Phys. Rev.* 79, 541.

- Hayward, R.W., and D.D. Hoppes, 1956, Phys. Rev. 104, 183.
- Heath, R.L., 1963, in O'Kelley (1963), p. 93.
- Heintze, J., 1954, Z. Naturforschung 9a, 469.
- Henry, E.A., 1974, Nucl. Data Sheets 11, 529.
- Herman, F., and S. Skillman, 1963, Atomic Structure Calculations
(Prentice-Hall Inc. Englewood Cliffs, New Jersey).
- Heuer, W., 1966, Z. Phys. 194, 224.
- Heuer, W., and E. Huster, 1964, Z. Naturforschung 19a, 517.
- Hinrichsen, P.F., 1968, Nucl. Phys. A118, 538.
- Hoff, R.W., 1953, University of California, Radiation Laboratory
Report UCRL-2325 (unpublished).
- Hoff, R.W., J.L. Olsen, and L.G. Mann, 1956, Phys. Rev., 102, 805.
- Hoffman, E.J., and D.G. Sarantites, 1969, Phys. Rev. 177, 1640.
- Hoffmann, D.C., and B.J. Dropesky, 1958, Phys. Rev. 109, 1282.
- Hohmuth, K., G. Müller, and J. Schintlmeister, 1964, Nucl. Phys.
52, 590.
- Holstein, B.R., 1974, Rev. Mod. Phys. 46, 789.
- Holstein, B.R., and S.B. Treiman, 1971, Phys. Rev. C3, 1921.
- Hopke, P.K., and R.A. Naumann, 1969, Phys. Rev. 4, 185.
- Hoppes, D.D., and R.W. Hayward, 1956, Phys. Rev. 104, 368.
- Horen, D.J., W.E. Meyerhof, J.J. Kraushaar, D.O. Wells,
E. Brun, and J.E. Neighbor, 1959, Phys. Rev. 113, 875.
- Horowitz, J., 1952, J. Phys. Radium 13, 429.

- Huber, O. R. Rüetschi, and P. Scherrer, 1949, *Helv. Phys. Acta* 22, 375.
- Huffaker, J.N., and E. Greuling, 1963, *Phys. Rev.* 132, 738.
- Huffaker, J.N., and C.E. Laird, 1967, *Nucl. Phys.* A92, 584.
- Huizenga, J.R., and C.M. Stevens, 1954, *Phys. Rev.* 96, 548.
- Intemann, R.L., and F. Pollock, 1967, *Phys. Rev.* 157, 41.
- Intemann, R.L., 1969, *Phys. Rev.* 178, 1543, corrected in *Phys. Rev.* 188, 1963.
- Intemann, R.L., 1971, *Phys. Rev.* C3, 1.
- Intemann, R.L., 1972, *Phys. Rev.* C6, 211.
- Intemann, R.L., 1974, *Nucl. Phys.* A219, 20.
- Isozumi, Y., and S. Shimizu, 1971, *Phys. Rev.* C4, 522.
- Jacobsen, J.C., 1937, *Nature* 139, 879.
- Jaffe, H., 1954, University of California, Radiation Laboratory Report, UCRL-2537 (unpublished).
- Jasinski, A., and C.J. Herrlander, 1968, *Ark. Fys.* 37, 585.
- Jasinski, A., J. Kownacki, H. Lancman, J. Ludziejewski, S. Chojnacki and I. Yutlandov, 1963, *Nucl. Phys.* 41, 303.
- Jasinski, A., J. Kownacki, H. Lancman, and J. Ludziejewski, 1965, Role of Atomic Electrons in Nuclear Transformations [Nuclear Energy Information Center, Warsaw, Poland] p. 625.

- Jastram, P.S., W.L. Skeel, and M.K. Ramaswamy, 1961, Bull. Am. Phys. Soc. 6, 38.
- Jastrzebski, J., and P. Kilcher, 1961, J. Phys. Radium 22, 525.
- Jauch, J.M., 1951, Oak Ridge National Laboratory Report, ORNL-1102 (unpublished).
- Jaus, W., 1972, Phys. Letters 40, 616.
- Jaus, W., and G. Rasche, 1970, Nucl. Phys. A143, 202.
- Jha, S., and H.G. Devare, 1959, Nuovo Cimento 14, 509.
- Jha, S., R.K. Gupta, H.G. Devare, and G.C. Pramila, 1961, Nuovo Cimento 20, 1067.
- Johansson, S., Y. Cauchois, and K. Siegbahn, 1951, Phys. Rev. 82, 275.
- Johns, M.W., S.V. Nablo, and W.J. King, 1957, Can. J. Phys. 35, 1159.
- Jopson, R.C., Hans Mark, C.D. Swift, and J.H. Zenger, 1961, Phys. Rev. 124, 157.
- Joshi, B.R., 1961, Proc. Phys. Soc. (London) 77, 1205.
- Joshi, B.R., and G.M. Lewis, 1960, Proc. Phys. Soc. (London) 76, 349.
- Joshi, B.R., and G.M. Lewis, 1961, Proc. Phys. Soc. (London) 78, 1056.
- Joshi, B.R., G.M. Lewis, and K.M. Smith, 1963, Nucl. Inst. Methods 24, 77.
- Juliano, J.O., C.W. Kocher, T.D. Nainan, and A.C.G. Mitchell, 1959, Phys. Rev. 113, 602.

- Jung, R.G., and M.L. Pool, 1956, Bull. Am. Phys. Soc. 1, 172.
- Kabasakal, Y., and M.K. Ramaswamy, 1969, Nuovo Cimento 61B, 220.
- Kádár, I., 1971, ATOMKI Közlem. 13, 29, also Fiz. Szemle 1972, 22, 10.
- Kádár, I., D. Berényi, and B. Mysłek, 1970, Nucl. Phys. A153, 383.
- Källen, G., 1967, Nucl. Phys. B1, 225.
- Kalkstein, M.I., 1957, private communication, quoted by Thomas et al. (1957).
- Kantele, J., and M. Valkonen, 1973, Nucl. Inst. Methods 112, 501.
- Karraker, D.G., and D.H. Templeton, 1950, Phys. Rev. 80, 646.
- Karttunen, E., H.-U. Freund, and R.W. Fink, 1969, Nucl. Phys. A131, 343.
- Katcoff, S., 1958, Phys. Rev. 111, 575.
- Katcoff, S., and H. Abrash, 1956, Phys. Rev. 103, 966.
- Ketelle, B.H., A.R. Brosi, and J.R. van Hise, 1971, Phys. Rev. C4, 1431.
- Ketelle, B.H., H. Thomas, and A.R. Brosi, 1956, Phys. Rev. 103, 190.
- Kim, C.W., 1971, Phys. Letters 34B, 383.
- Kim, C.W., 1974, Riv. Nuovo Cimento 4, 189.
- Kim, C.W., and T. Fulton, 1971, Phys. Rev. C4, 390.
- Kim, C.W., and H. Primakoff, 1969, Phys. Rev. 180, 1502.
- Kirkwood, D.H.W., B. Pontecorvo, and G.C. Hanna, 1948, Phys. Rev. 74, 497.

- Kiselev, B.G., and V.R. Burmistrov, 1969, *Yadern. Fiz.* 10, 1105. [*Sov. J. Nucl. Phys.* 10, 629].
- Kiser, R.W., and W.H. Johnston, 1959, *J. Am. Chem. Soc.* 81, 1810.
- Kitahara, T., Y. Isozumi, and S. Shimizu, 1972, *Phys. Rev.* C5, 1810.
- Kitahara, T., and S. Shimizu, 1975, *Phys. Rev.* C11, 920.
- Klein, H., and H. Leutz, 1966, *Nucl. Phys.* 79, 27.
- Knipp, J.K., and G.E. Uhlenbeck, 1936, *Physica* 3, 425.
- Koerts, L., P. Macklin, B. Farrelly, R. van Lieshout, and C.S. Wu, 1955, *Phys. Rev.* 98, 1230.
- Koh, Y., 1965, in Role of Atomic Electrons in Nuclear Transformations, (Nuclear Energy Information Center, Warsaw) p. 637.
- Koh, Y., O. Miyatake, and Y. Watanabe, 1957, *Progr. Theor. Phys.* 18, 663.
- Koh, Y., O. Miyatake, and Y. Watanabe, 1962, *Nucl. Phys.* 32, 246.
- Kohn, W., and L.J. Sham, 1965, *Phys. Rev.* A140, 1133.
- Koićki, S.D., A.M. Mijatović, and J.M. Simić, 1958, *Bull. Inst. Nucl. Sci., Boris Kidrich*, 8, 1.
- Konijn, J., B. van Nooijen, P. Mostert, and P.M. Endt, 1956, *Physica* 22, 887.
- Konijn, J., H.L. Hagedoorn, H. van Krugten, and J. Slobben, 1958a, *Physica* 24, 931.
- Konijn, J., H.L. Hagedoorn, and B. van Nooijen, 1958b, *Physica* 24, 129.
- Konijn, J., B. van Nooijen, and H.L. Hagedoorn, 1958c, *Physica* 24, 377.

- Konijn, J., B. van Nooijen, H.L. Hagedoorn, and A.H. Wapstra, 1958/59, Nucl. Phys. 9, 296.
- Konijn, J., B. van Nooijen, and A.H. Wapstra, 1960, Nucl. Phys. 16, 683.
- Konijn, J., E.W.A. Lingeman, and S.A. de Wit, 1967a, Nucl. Phys. A90, 558.
- Konijn, J., W.H.G. Lewin, B. van Nooijen, H.F. van Beek, S.A. de Wit, and E.W.A. Lingeman, 1967b, Nucl. Phys. A102, 129.
- Konopinski, E.J., 1966, The Theory of Beta Radioactivity (Clarendon Press, Oxford).
- Konstantinov, A.A., and V.V. Perepelkin, 1961, Izv. Akad. Nauk. SSSR, Ser. Fiz. 25, 106 [Bull. Acad. Sci., USSR, Phys. Ser. 25, 103].
- Koonin, S.E., and B.I. Persson, 1972, Phys. Rev. C6, 1713.
- Krafft, O., 1970, Z. Phys. 238, 78.
- Krahn, F., 1972, Z. Phys. 251, 375.
- Kramer, P., E.C. Bos, A. de Beer, and J. Blok, 1962a, Physica 28, 569.
- Kramer, P., A. de Beer, and J. Blok, 1962b, Physica 28, 587.
- Kramer, P., H.C. Hamers, and G. Meijer, 1956, Physica 22, 208.
- Kreger, W.E., 1954, Phys. Rev. 96, 1554.
- Kroger, L.A., and C.W. Reich, 1973, Nucl. Data Sheets 10, 447.
- Kropf, A., and H. Paul, 1974, Z. Phys. 267, 129.
- Krutov, V.A., and L.N. Savashkin, 1973, J. Phys. A6, 93.
- Krutov, V.A., V.N. Fomenko, and L.N. Savashkin, 1974, J. Phys. A7, 37

- Kubodera, K., J. Delorme, and M. Rho, 1973, Nucl. Phys. B66, 253.
- Kuhlmann, E., and K.E.G. Löbner, 1969, Z. Phys. 222, 144.
- Kuphal, E., P. Dewes, and E. Kankeleit, 1974, Nucl. Phys. A234,
308.
- Kyles, J., J.C. McGeorge, F. Shaikh, and J. Byrne, 1970, Nucl. Phys.
A150, 143.
- Lancman, H., and A. Bond, 1973, Phys. Rev. C7, 2600.
- Lancman, H., and J.M. Lebowitz, 1969, Phys. Rev. 188, 1683.
- Lancman, H., and J.M. Lebowitz, 1971a, Phys. Rev. C3, 188.
- Lancman, H., and J.M. Lebowitz, 1971b, Phys. Rev. C3, 465.
- Langer, L.M., and R.D. Moffat, 1950, Phys. Rev. 80, 651.
- Langevin, M., 1954b, C.R. Acad. Sci. 239, 1625.
- Langevin, M., 1954d, C.R. Acad. Sci. 238, 2518.
- Langevin, M., 1955a, J. Phys. Radium, 16, 516.
- Langevin, M., 1955b, C.R. Acad. Sci. 240, 289.
- Langevin, M., 1956, Ann. Phys. (Paris) 1, 57.
- Langevin, M., 1957, C.R. Acad. Sci. 245, 664.
- Langevin, M., 1958, J. Phys. Radium 19, 34.
- Langevin, M., and N. Marty, 1954c, J. Phys. Radium 15, 127.
- Langevin, M., and P. Radvanyi, 1954a, C.R. Acad. Sci. 238, 77.
- Langevin, M., and P. Radvanyi, 1955c, C.R. Acad. Sci. 241, 33.
- Langhoff, H., P. Kilian, and A. Flammersfeld, 1961, Z. Phys. 165, 393.
- Langhoff, H., L. Frevert, W. Schött, and A. Flammersfeld, 1966,
Nucl. Phys. 79, 145.
- Lark, N.L., and M.L. Perlman, 1960, Phys. Rev. 120, 536.

- Lassila, K.E., 1963, Phys. Rev. 131, 807.
- Latter, R., 1955, Phys. Rev. 99, 510.
- Laverne, A., and G.Do. Dang, 1971, Nucl. Phys. A177, 665.
- Law, J., and J.L. Campbell, 1972a, Nucl. Phys. A185, 529.
- Law, J., and J.L. Campbell, 1972b, Nucl. Phys. A187, 525.
- Law, J., and J.L. Campbell, 1973a, in Proceedings of the International Conference on Inner-Shell Ionization Phenomena, edited by R.W. Fink, S.T. Manson, J.M. Palms, and P. Venugopala Rao, U.S. Atomic Energy Commission Report No. CONF-720404 (unpublished) p. 2110.
- Law, J., and J.L. Campbell, 1973b, Nucl. Phys. A199, 481.
- Lederer, C.M., J.M. Hollander, and I. Perlman, 1967, Table of Isotopes, (John Wiley and Sons, Inc., New York).
- Ledingham, K.W.D., J.A. Payne, and R.W.P. Drever, 1965, Role of Atomic Electrons in Nuclear Transformations, (Nuclear Information Centre, Warsaw) p. 359.
- Ledingham, K.W.D., J.Y. Gourlay, J.L. Campbell, M.L. Fitzpatrick, J.G. Lynch, and J. McDonald, 1971, Nucl. Phys. A170, 663.
- Lee, T.D., 1973, Physics Reports 9C, 143.
- Leiper, W., and R.W.P. Drever, 1972, Phys. Rev. C6, 1132.
- Leiper, W., and O.P. Jolly, 1971, Can. J. Phys. 49, 582.
- Leistner, M., and K. Friedrich, 1965, Atomkernenergie 10, 311.
- Leutz, H., 1960, Z. Phys. 159, 462.
- Leutz, H., K. Schneckenberger, and H. Wenninger, 1965, Nucl. Phys. 63, 263.

- Leutz, H., G. Schulz, and H. Wenninger, 1966, Nucl. Phys. 75, 81.
- Leutz, H., and H. Wenninger, 1967, Nucl. Phys. A99, 55.
- Leutz, H., and K. Ziegler, 1962, Z. Phys. 166, 582.
- Leutz, H., and K. Ziegler, 1964, Nucl. Phys. 50, 648.
- Levi, C., and L. Papineau, 1954, C.R. Acad. Sci. 238, 2313.
- Levi, C., and L. Papineau, 1957, C.R. Acad. Sci. 244, 1358.
- Levi, C., L. Papineau, C. Latapie-Redon, and N. Saunier, 1959,
C.R. Acad. Sci. 249, 410.
- Lewin, W.H.G., J. Bezemer, and C.W.E. van Eijk, 1965a,
Nucl. Phys. 62, 337.
- Lewin, W.H.G., J. Lettinga, B. van Nooijen, and A.H. Wapstra,
1965b, Nucl. Phys. 65, 337.
- Liberman, D., J.T. Waber, and Don T. Cromer, 1965, Phys. Rev.
A137, 27.
- Liden, K., and N. Starfelt, 1954, Ark. Fys. 7, 427.
- Lindgren, I., and A. Rosen, 1974, Case Studies in Atomic Physics 4,
93.
- Lindgren, I., and K. Schwarz, 1971, Phys. Rev. A5, 542.
- Lindner, M., and I. Perlman, 1948, Phys. Rev. 73, 1202.
- Lindqvist, T., and C.S. Wu, 1955, Phys. Rev. 100, 145.
- Lipnik, P., G. Pralong, and J.W. Sunier, 1964, Nucl. Phys. 59, 504.
- Lipnik, P., and J.W. Sunier, 1966, Phys. Rev. 145, 746.
- Lipkin, H.J., 1970, Phys. Letters 34B, 202.
- Lipkin, H.J., 1971, Phys. Rev. Letters 27, 432.

- Ljubičić, A., R.T. Jones, and B.A. Logan, 1974, Nucl. Phys. A236, 158.
- Lock, J.A., L.L. Foldy, and F.R. Buskirk, 1974, Nucl. Phys. A220, 103.
- Longmire, C.L., 1949, Phys. Rev. 75, 15.
- Lourens, W., B.O. ten Brink, and A.H. Wapstra, 1970, Nucl. Phys. A152, 463.
- Lu, C.C., T.A. Carlson, F.B. Malik, T.C. Tucker, and C.W. Nestor, Jr., 1971, Atomic Data 3, 1.
- Lu, D.C., and G. Schlupp, 1962, Bull. Am. Phys. Soc. 7, 353.
- MacMahon, T.D., and A.P. Baerg, 1970, Bull. Am. Phys. Soc., Ser. II, 15, 755; 1970, Physics in Canada, 26, no. 4.
- Madansky, L., and R. Rasetti, 1954, Phys. Rev. 94, 407.
- Maeder, D., and P. Preiswerk, 1951, Phys. Rev. 84, 595.
- Magnusson, L.B., A.M. Friedman, D. Engelkemeir, P.R. Fields, and F. Wagner, Jr., 1956, Phys. Rev. 102, 1097.
- Major, J.K., 1952, Phys. Rev. 86, 631.
- Malli, G., 1966, Can. J. Phys. 44, 3121 and 3131.
- Manduchi, C., G. Nardelli, M.T. Russo-Manduchi, and G. Zannoni, 1964a, Nuovo Cimento 31, 1380.
- Manduchi, C., G.C. Nardelli, M.T. Russo-Manduchi, and G. Zannoni, 1964b, Nuovo Cimento 33, 49.
- Manduchi, C., and G. Zannoni, 1961, Nuovo Cimento 22, 462.
- Manduchi, C., and G. Zannoni, 1962a, Nucl. Phys. 36, 497.
- Manduchi, C., and G. Zannoni, 1962b, Nuovo Cimento 24, 181.

- Manduchi, C., and G. Zannoni, 1963, *Nuovo Cimento* 27, 251.
- Mann, J.B., 1967, Atomic Structure Calculations, Los Alamos Scientific Laboratory Report No. LA-3690 (unpublished).
- Mann, J.B., 1968, Atomic Structure Calculations, Los Alamos Scientific Laboratory Report No. LA-3691 (unpublished).
- Mann, J.B., and J.T. Waber, 1973, for $57 \leq Z \leq 70$ Atomic Data 5, 201, for the other Z private communication.
- Mann, L.G., J.A. Miskel, and S.D. Bloom, 1958, *Phys. Rev. Letters* 1, 82.
- Marelius, A., P. Sparrman, and S.-E. Håggglund, 1967, *Nucl. Phys.* A95, 632.
- Marquez, L., and I. Perlman, 1950, *Phys. Rev.* 78, 189.
- Marshak, R.E., 1942, *Phys. Rev.* 61, 431.
- Marshak, R.E., Riazuddin, and C.P. Ryan, 1969, Theory of Weak Interactions in Particle Physics (John Wiley & Sons, Inc., New York).
- Martin, M.J., and P.H. Blichert-Toft, 1970, *Nucl. Data* A8, 1.
- Martin, P.C., and R.J. Glauber, 1958, *Phys. Rev.* 109, 1307.
- Marty, N., H. Langevin, and P. Hubert, 1953, *J. Phys. Radium* 14, 663.
- Matese, J.J., and R. Johnson, 1966, *Phys. Rev.* 150, 846.
- Matuszek Jr., J.M., and T.T. Sugihara, 1963, *Nucl. Phys.* 42, 582.
- Mayers, D.F., 1972, Relativistic Self-Consistent Fields in New Direction in Atomic Physics, Vol. 1, edited by F.U. Condon and O. Sinanoglu (Yale University Press, New Haven and London).

- McCann, M.F., G.M. Lewis, and K.M. Smith, 1967, Nucl. Phys. A98, 577.
- McCann, M.F., and K.M. Smith, 1968, Nucl. Phys. A121, 233.
- McCann, M.F., and K.M. Smith, 1969, J. Phys. A2, 392.
- McCown, D.A., L.L. Woodward, and M.L. Pool, 1948a, Phys. Rev. 74, 1311.
- McCown, D.A., L.L. Woodward, and M.L. Pool, 1948b, Phys. Rev. 74, 1315.
- McDonnell, M., and M.K. Ramaswamy, 1968, Phys. Rev. 168, 1393.
- McDonnell, M., and M.K. Ramaswamy, 1969, Nucl. Phys. A127, 531.
- McGinnis, C.L., 1951, Phys. Rev. 81, 734.
- McGinnis, C.L., 1955, Phys. Rev. 97, 93.
- Medicus, H., P. Preiswerk, and P. Scherrer, 1950, Helv. Phys. Acta 23, 299.
- Menhardt, W., 1957, Acta Phys. Austriaca 11, 101.
- Meixner, C.H., 1971, KfA Jülich Report, JÜL-811-Rx (unpublished).
- Meixner, C.H., 1974, Nucl. Inst. Methods 119, 521.
- Merz, E.R., and A.A. Caretto Jr., 1961, Phys. Rev. 122, 1558.
- Michalowicz, A., 1953, J. Phys. Radium 14, 214.
- Michalowicz, A., 1956, C.R. Acad. Sci. 242, 108.
- Migdal, A., 1941, J. Phys. USSR 4, 449.
- Millar, C.H., T.A. Eastwood, and J.C. Roy, 1959, Can. J. Phys. 37, 1126.
- Miller, L.D., 1972, Phys. Rev. Letters 28, 1281.
- Miller, L.D., and A.E.S. Green, 1972, Phys. Rev. C5, 241.

- Miller, M.M., and R.G. Wilkinson, 1951, Phys. Rev. 83, 1050.
- Miskel, J.A., and M.L. Perlman, 1954, Phys. Rev. 94, 1683.
- Mitchell, A.C.G., J.O. Juliano, C.B. Creager, and C.W. Kocher,
1959, Phys. Rev. 113, 628.
- Møller, C., 1937a, Phys. Z. Sowjet. 11, 9.
- Møller, C., 1937b, Phys. Rev. 51, 84.
- Moler, R.B., and R.W. Fink, 1963, Phys. Rev. 131, 821.
- Moler, R.B., and R.W. Fink, 1965, Phys. Rev. 139, B282.
- Monaro, S., G.B. Vingiani, and R. van Lieshout, 1961, Physica 27, 985.
- Monaro, S., G.B. Vingiani, R.A. Ricci, and R. van Lieshout,
1962, Physica 28, 63.
- Mord, A.J., 1972, Nucl. Phys. A192, 305.
- Mord, A.J., 1973, in Proceedings of the International Conference on
Inner-Shell Ionization Phenomena, edited by R.W. Fink,
S.T. Manson, J.M. Palms, and P. Venugopala Rao,
U.S. Atomic Energy Commission Report No. CONF-720404,
(unpublished) p. 2079.
- Morrison, P., and L.I. Schiff, 1940, Phys. Rev. 58, 24.
- Moussa, A., and A. Juillard, 1956, C.R. Acad. Sci. 243, 1515.
- Muir, Jr., A.H., and F. Boehm, 1961, Phys. Rev. 122, 1564.
- Mukerji, A., T.M. Carlton, and G.D. Cole, 1965, Bull. Am.
Phys. Soc. 10, 93.

- Mukerji, A., and L. Chin, 1973, in Proceedings of the International Conference on Inner Shell Ionization Phenomena and Future Applications, edited by R.W. Fink, S.T. Manson, J.M. Palms, P. Venugopala Rao (U.S. Atomic Energy Commission, Report No. CONF-720404 (unpublished), p. 164.
- Mukerji, A., and J.B. McGouch, Jr., 1967a, Nucl. Phys. A94, 95.
- Mukerji, A., J.B. McGouch, Jr., and G.D. Cole, 1967b, Nucl. Phys. A100, 81.
- Mukoyama, T., Y. Isozumi, T. Kitahara, and S. Shimizu, 1973, Phys. Rev. C8, 1308.
- Mukoyama, T., T. Kitahara, and S. Shimizu, 1974, Phys. Rev. C9, 2307.
- Mukoyama, T., and S. Shimizu, 1974, Phys. Rev. C9, 2300.
- Murty, K.N., and S. Jnanananda, 1967, Ind. J. Pure Appl. Phys. 5, 557.
- Mutterer, M., 1971, in A.B. Smith (ed.) Neutron Standards and Flux Normalization, AEC Symp. Ser. 23, (U.S. Atomic Energy Commission Rep. CONF-701002, (unpublished), p. 452.
- Mutterer, M., 1973a, Phys. Rev. C8, 1370.
- Mutterer, M., 1973b, Phys. Rev. C8, 2089.
- Mutterer, M., 1973c, Ph. D. Thesis, Technische Universität München, Germany (unpublished).
- Muziol', G., 1966, Dubna Report 6-2920 (unpublished), quoted by Berényi, 1968a.
- Mysłek, B., B. Pietrzyk, Z. Sujkowski, and J. Szczepankowski, 1971, Acta Phys. Polonica B2, 441.

- Myszek, B., Z. Sujkowski, and J. Zylicz, 1973, Nucl. Phys. A215, 79.
- Nagy, J., 1971, ATOMKI Közlem. 13, 101.
- Nagy, H.J., G. Schupp, and R.R. Hurst, 1972, Phys. Rev. C6, 607.
- Narang, V., and H. Houtermans, 1968, in Berényi, (1968b), p. 97.
- National Bureau of Standards, 1952, Applied Mathematics Series,
No. 13: Tables for the Analysis of Beta Spectra.
- Naumann, R.A., and P.K. Hopke, 1967, Phys. Rev. 160, 1035.
- Naumann, R.A., F.L. Reynolds, and I. Perlman, 1950, Phys. Rev.
77, 398.
- Nestor, C.W., T.C. Tucker, T.A. Carlson, L.D. Roberts,
F.B. Malik, and C. Froese, 1966, Oak Ridge National Laboratory
Report, ORNL-4027 (unpublished).
- Nielsen, H.L., K. Wilsky, J. Zylicz, and G. Sprensen, 1967, Nucl.
Phys. A93, 385.
- Norris, A.E., G. Friedlander, and E.M. Franz, 1966, Nucl. Phys.
86, 102.
- Odiot, S., and R. Daudel, 1956, J. Phys. Radium 17, 60.
- Ofer, S., and R. Wiener, 1957, Phys. Rev. 107, 1639.
- Ohta, K., and M. Wakamatsu, 1974, Nucl. Phys. A234, 445.
- Oldenburg, O., 1938, Phys. Rev. 53, 35.
- Olsen, J.L., L.G. Mann, and M. Lindner, 1957, Phys. Rev. 106, 985.
- O'Kelley, G.D., (ed.), 1963, Applications of Computers to Nuclear and
Radiochemistry, U.S. Atomic Energy Commission Report,
NAS-NS 3107 (unpublished).
- Orth, D.A., and G.D. O'Kelley, 1951, Phys. Rev. 82, 758.

- Paquette, G., 1962, Can. J. Phys. 40, 1765.
- Parfenova, V.P., 1960, Zh. Eksp. Teor. Fiz. 38, 56, [Sov. Phys. JETP 11, 42].
- Paul, H., 1966, Nucl. Data A2, 281.
- Penev, I., K. Zuber, Ya. Zuber, A. Lyatushinsk, and A. Potemka, 1974, Programma i tezis y dokladov 24. soveshchaniya po yadernoj spektroskopii i strukture atomnogo yadra, Khar'kov, 29 yanvarya - 1 fevraiya, p. 93 [Program and abstracts of 24. conference on nuclear spectroscopy and nuclear structure, Kharkov 29 January - 1 February, p. 93, INIS-mf-1850].
- Pengra, J.G., and B. Crasemann, 1963, Phys. Rev. 131, 2642.
- Pengra, J.G., H. Genz, J.P. Renier, and R.W. Fink, 1972, Phys. Rev. C5, 2007.
- Pengra, J. G., 1976, in Abstracts of Contributed Papers, Second International Conference on Inner Shell Ionization Phenomena, University Freiburg, p. 194.
- Perkins, J.F., and S.K. Haynes, 1953, Phys. Rev. 92, 687.
- Perlman, M.L., and J.P. Welker, 1954, Phys. Rev. 95, 133.
- Perlman, M.L., W. Bernstein, and R.B. Schwartz, 1953, Phys. Rev. 92, 1236.
- Perlman, M.L., J.P. Welker, and M. Wolfsberg, 1958, Phys. Rev. 110, 381.
- Perrin, N.N., 1960, Ann. Phys. (Paris) 5, 71.
- Persson, B.I., and S.E. Koonin, 1972, Phys. Rev. C5, 1443.
- Persson, L., H. Ryde, and K. Oelsner-Ryde, 1963, Nucl. Phys. 44, 653.
- Persson, L., and Z. Sujkowski, 1961, Ark. Fys. 19, 309.

- Petel, M., and H. Houtermans, 1967, in Standardization of Radio-nuclides (International Atomic Energy Agency, Vienna), p. 301 and private communication to W. Bambynek.
- Petterson, B.G., 1965, in K. Siegbahn (1965), p. 1569.
- Phillips, W.E., and J.E. Hopkins, 1960, Phys. Rev. 119, 1315.
- Plassmann, E., and F.R. Scott, 1951, Phys. Rev. 84, 156.
- Plch, J., J. Zderadička, and I. Bučina, 1971, Radioisotopy 12, 131.
- Plch, J., and J. Zderadička, 1974a, Czech. J. Phys. B24, 1311.
- Plch, J., J. Zderadička, and L. Kokta, 1974b, Int. J. Appl. Rad. Isotopes 25, 433.
- Plch, J., J. Zderadička, and O. Dragoun, 1975, Int. J. Appl. Rad. Isotopes, 26, 579.
- Polak, H.L., W. Schoo, B.L. Schram, R.K. Girgis, and R. van Lieshout, 1958, Nucl. Phys. 5, 271.
- Pontecorvo, B., D.H.W. Kirkwood, and G.C. Hanna, 1949, Phys. Rev. 75, 982.
- Prescott, J.R., 1954, Proc. Phys. Soc. (London) A67, 254.
- Prescott, J.R., 1963, Nucl. Inst. Methods 22, 256.
- Primakoff, H., and F.T. Porter, 1953, Phys. Rev. 89, 930.
- Pruet, C.H., and R.G. Wilkinson, 1954, Phys. Rev. 96, 1340.
- Radvanyi, P., 1952b, C.R. Acad. Sci. 235, 289.
- Radvanyi, P., 1952a, C.R. Acad. Sci. 235, 428.
- Radvanyi, P., 1955b, Ann. Phys. (Paris) 10, 584.
- Radvanyi, P., 1955a, J. Phys. Radium 16, 509.

- Raeseide, D.E., M.A. Ludington, J.J. Reidy, and M.L. Wiedenbeck, 1969, Nucl. Phys. A130, 677.
- Raj, K., and M.K. Ramaswamy, 1969, Am. J. Phys. 37, 70.
- Raman, S., H.J. Kim, T.A. Walkiewicz and M.J. Martin, 1973, Phys. Letters 44B, 225.
- Ramaswamy, M.K.; 1959a, Ind. J. Phys. 33, 285.
- Ramaswamy, M.K., 1959b, Nucl. Phys. 10, 205.
- Ramaswamy, M.K., 1961, Ind. J. Phys. 35, 610.
- Ramaswamy, M.K., W.L. Skeel, and P.S. Jastram, 1960, Nucl. Phys. 19, 299.
- Rao, P. Venugopala, and B. Crasemann, 1965, Phys. Rev. 137, B64.
- Rao, P. Venugopala, and B. Crasemann, 1966a, Phys. Rev. 142, 768.
- Rao, P. Venugopala, M.H. Chen, and B. Crasemann, 1972, Phys. Rev. A5, 997.
- Rao, P. Venugopala, D.K. McDaniels, and B. Crasemann, 1966b, Nucl. Phys. 81, 296.
- Rasmussen, J.O., 1957, private communication to D. Strominger, J.M. Hollander, and G.T. Seaborg, 1958, Rev. Mod. Phys. 30, 585.
- Ravn, H.L., and P. Bøgeholt, 1971, Phys. Rev. C4, 601.
- Rehfuss, D.E., and B. Crasemann, 1959, Phys. Rev. 114, 1609.
- Reitz, J.R., 1950, Phys. Rev. 77, 10.
- Renier, J.P., H. Genz, K.W.D. Ledingham, and R.W. Fink, 1968, Phys. Rev. 166, 935.
- Reynolds, J.R., 1950, Phys. Rev. 79, 789.

- Ribordy, C., and O. Huber, 1970, *Helv. Phys. Acta* 43, 345.
- Ricci, R.A., R.K. Girgis, and R. van Lieshout, 1960, *Nucl. Phys.* 21, 177.
- Rietjens, L.H.Th., H.J. Van den Bold, and P.M. Endt, 1954, *Physica* 20, 107.
- Rightmire, R.A., J.R. Simanton, and T.P. Kohman, 1959, *Phys. Rev.* 113, 1069.
- Ristinen, R.A., A.A. Bartlett, and J.J. Kraushaar, 1963, *Nucl. Phys.* 45, 321.
- Rivier, J., and R. Moret, 1971, *C.R. Acad. Sci.* B272, 1022.
- Robinson, B.L., 1963, private communication quoted by Klein and Leutz, 1966.
- Robinson, B.L., and R.W. Fink, 1955, *Rev. Mod. Phys.* 27, 424.
- Robinson, B.L., and R.W. Fink, 1960, *Rev. Mod. Phys.* 32, 117.
- Robinson, B.L., N.R. Johnson, and E. Eichler, 1962, *Phys. Rev.* 128, 252.
- Roetti, C., and E. Clementi, 1974, *J. Chem. Phys.* 60, 3342, and refs. quoted therein.
- Roos, M., 1974, *Nucl. Phys.* B77, 420.
- Roothaan, C.C.J., 1960, *Rev. Mod. Phys.* 32, 179.
- Roothaan, C.C.J., and P.S. Bagus, 1963, Methods in Computational Physics (Academic Press, New York), Vol. 2.

- Rose, M.E., 1961, Relativistic Electron Theory (John Wiley & Sons, New York).
- Rose, M.E., and R.K. Osborn, 1954, Phys. Rev. 93, 1315 and 1326.
- Rose, M.E., R. Perrin, and L.L. Foldy, 1962, Phys. Rev. 128, 1776.
- Rose, M.E., and C.L. Perry, 1953, Phys. Rev. 90, 479.
- Rosén, A., and I. Lindgren, 1968, Phys. Rev. 176, 114.
- Rubinson, W., 1971, Nucl. Phys. A169, 629.
- Rubinson, W., and K.P. Gopinathan, 1968, Phys. Rev. 170, 969.
- Rupnik, T., 1972, Phys. Rev. C6, 1433.
- Rupnik, T., and B. Crasemann, 1972, Phys. Rev. C6, 1780. See erratum in Phys. Rev. C 13, 89C (1976).
- Ryde, H., L. Persson, and K. Oelsner-Ryde, 1962a, Ark. Fys. 23, 17
- Ryde, H., L. Persson, and K. Oelsner-Ryde, 1962b, Ark. Fys. 23, 19
- Ryde, H., L. Persson, and K. Oelsner-Ryde, 1963, Nucl. Phys. 47, 614
- Sakai, M., J.L. Dick, W.S. Anderson, and J.D. Kurbatov, 1954, Phys. Rev. 95, 101.
- Salam, A., 1968, Nobel Symposium, edited by N. Svartholm. (18th Meeting of Nobel Laureates, Lindau, Germany).
- Salem, S.I., S.L. Panossian, and R.A. Krause, 1974, Atomic Data and Nuclear Data Tables 14, 91.
- Santos Ocampo, A.G., 1961, Ph. D. Thesis, Purdue University, TID Report 13490 (unpublished).
- Santos Ocampo, A.G., and D.C. Conway, 1960, Phys. Rev. 120, 2196.
- Santos Ocampo, A.G., and D.C. Conway, 1962, Phys. Rev. 128, 258.
- Saraf, B., 1954a, Phys. Rev. 94, 642.

- Saraf, B., 1954b, Phys. Rev. 95, 97.
- Saraf, B., 1956, Phys. Rev. 102, 466.
- Saraf, B., J. Varma, and C.F. Mandeville, 1953, Phys. Rev. 91, 1216.
- Schima, F., E.G. Funk, Jr., and J.W. Mihelich, 1963, Phys. Rev. 132, 2650.
- Schmidt-Ott, W.-D., 1970a, Z. Phys. 232, 298.
- Schmidt-Ott, W.-D., 1970b, Z. Phys. 236, 445.
- Schmidt-Ott, W.-D., and R.W. Fink, 1972, Z. Phys. 249, 286.
- Schmidt-Ott, W.-D., W. Weirauch, F. Smend, H. Langhoff, and D. Gföller, 1968, Z. Phys. 217, 282.
- Schmorak, M., 1963, Phys. Rev. 129, 1668.
- Schopper, H.F., 1966, Weak Interactions and Nuclear Beta Decay (North-Holland Publ. Co., Amsterdam).
- Schopper, H.F., 1968, in Berényi 1968b, p. 488.
- Schucan, T.H., 1965, Nucl. Phys. 61, 417.
- Schülke, L., 1964, Z. Phys. 179, 331.
- Schulz, G., 1967a, Nucl. Phys. A101, 177.
- Schulz, G., 1967b, Nucl. Inst. Methods 53, 320.
- Schulz, G., 1967c, Z. Phys. 203, 289.
- Schulz, G., and K. Ziegler, 1967d, Nucl. Phys. A104, 692.
- Scobie, J., 1957a, Nucl. Phys. 3, 465.
- Scobie, J., and E. Gabathuler, 1958, Proc. Phys. Soc. (London) 72, 437.

- Scobie, J., and G.M. Lewis, 1957b, *Phil. Mag.* 2, 1089.
- Scobie, J., R.B. Moler, and R.W. Fink, 1959, *Phys. Rev.* 116, 657.
- Scofield, J.E., 1974, *Atomic Data and Nucl. Data Tables* 14, 121.
- Scofield, J.E., 1975, in *Atomic Inner-Shell Processes*, edited by B. Crasemann, (Academic Press, New York, San Francisco, London) Vol. I, p. 265.
- Scofield, N.E., 1963, in O'Kelley (1963), p. 108.
- Scott, F.R., 1951, *Phys. Rev.* 84, 659.
- Sehr, R., 1954, *Z. Phys.* 137, 523.
- Shalitin, D., 1965, *Phys. Rev.* A140, 1857.
- Shalitin, D., 1967, *Phys. Rev.* 155, 20.
- Sherr, R., and R.H. Miller, 1954, *Phys. Rev.* 93, 1076.
- Shore, F.J., W.L. Bendel, H.N. Brown, and R.A. Becker, 1953, *Phys. Rev.* 91, 1203.
- Siegbahn, K., (ed.) 1965, *Alpha-, Beta- and Gamma-Ray Spectroscopy* (North-Holland Publishing Co., Amsterdam).
- Singh, B., and H.W. Taylor, 1970, *Nucl. Phys.* A147, 12.
- Sirlin, A., 1967, *Phys. Rev.* 164, 1767.
- Sirlin, A., 1974, *Nucl. Phys.* B71, 29.
- Slater, J.C., 1930, *Phys. Rev.* 36, 57.
- Slater, J.C., 1960, *Quantum Theory of Atomic Structures* (McGraw Hill Book Company, Inc., New York), Vol. 1 and 2.

- Smirnov, Yu. G., and I.S. Batkin, 1973, *Yad. Fiz.* 18, 239
[*Sov. J. Nucl. Phys.* 18, 122].
- Smith, K.M., 1964, Ph. D. Thesis, University of Glasgow
(unpublished).
- Smith, K.M., and B.R. Joshi, 1963, *Proc. Phys. Soc. (London)*
82, 918.
- Smith, K.M., and G.M. Lewis, 1966, *Nucl. Phys.* 89, 561.
- Snyder, J.W., and M.L. Pool, 1965, *Phys. Rev.* 138B, 770.
- Sparman, P., T. Sundström, and A. Marelus, 1966, *Nucl.*
Phys. 81, 548.
- Spernol, A., 1967, Standardization of Radionuclides (International
Atomic Energy Agency, Vienna), p. 277.
- Spernol, A., E. De Roost, and M. Mutterer, 1973, *Nucl. Inst.*
Methods 112, 169.
- Stanford, Jr., A.L., C.H. Braden, and L.D. Wyly, 1960, *Bull.*
Am. Phys. Soc. 5, 449.
- Stech, B., and L. Schülke, 1964, *Z. Phys.* 179, 314.
- Stephas, P., 1969, *Phys. Rev.* 186, 1013.
- Stephas, P., and B. Crasemann, 1967, *Phys. Rev.* 164, 1509.
- Stephas, P., and B. Crasemann, 1971, *Phys. Rev.* C3, 2495.
- Sterk, M.J., A.H. Wapstra, and R.F.W. Kropveld, 1953, *Physica*
19, 135.
- Steyn, J., and A.S.M. De Jesus, 1966, South African CSIR
Special Report FIS 15 (unpublished).
- Stover, B.J., 1951, *Phys. Rev.* 81, 8.

- Strubbe, H.J., and D.K. Callebaut, 1970, Nucl. Phys. A143, 537.
- Sujkowski, Z., J. Jastrzebski, A. Zgliński, and J. Zylicz, 1965,
in Role of Atomic Electrons in Nuclear Transformations,
(Nuclear Energy Information Center, Warsaw, Poland), p. 614.
- Sujkowski, Z., B. Myszek, J. Lukasiak, and B. Kotlinska-Filipek,
1973, in Proceedings of the International Conference on Inner-
Shell Ionization Phenomena, edited by R.W. Fink, S.T. Manson,
J.M. Palms, and P. Venugopala Rao, U.S. Atomic Energy
Commission Report No. CONF-720404, (unpublished) p. 2005.
- Sujkowski, Z., B. Myszek, A. Zgliński, and B. Adamowicz, 1968,
in Berényi (1968b) p. 163.
- Suslov, Yu. P., 1966, Izv. Akad. Nauk SSSR, Ser. Fiz. 30, 1248.
[Bull. Acad. Sci. USSR, Phys. Ser. 30, 1305].
- Suslov, Yu. P., 1967, Izv. Akad. Nauk SSSR, Ser. Fiz. 31, 688.
[Bull. Acad. Sci. USSR, Phys. Ser. 31, 684].
- Suslov, Yu. P., 1968a, Izv. Akad. Nauk SSSR, Ser. Fiz. 32, 213.
[Bull. Acad. Sci. USSR, Phys. Ser. 32, 192].
- Suslov, Yu. P., 1968b, in Berényi (1968b), p. 51.
- Suslov, Yu. P., 1969, Izv. Akad. Nauk SSSR, Ser. Fiz. 33, 78.
[Bull. Acad. Sci. USSR, Phys. Ser. 33, 74].
- Suslov, Yu. P., 1970a, Izv. Akad. Nauk SSSR, Ser. Fiz. 34, 97
[Bull. Acad. Sci. USSR, Phys. Ser. 34, 91].
- Suslov, Yu. P., 1970b, Izv. Akad. Nauk SSSR, Ser. Fiz. 34, 2223.
[Bull. Acad. Sci. USSR, Phys. Ser. 34, 1983].

- Suzuki, Sh., and Y. Yokoo, 1975, Nucl. Phys. B94, 431.
- Szybisz, L., 1975, Z. Phys. A273, 277.
- Takekoshi, E., Z. Matsumoto, M. Ishi, K. Sugiyama,
S. Hayashibe, H. Sekiguchi, and H. Natsume, 1964,
J. Phys. Soc. Japan 19, 587.
- Talmi, I., 1953, Phys. Rev. 91, 122.
- Taylor, H.W., G.N. Whyte, and R. McPherson, 1963, Nucl. Phys.
41, 221.
- Taylor, J.G.V., and J.S. Merritt, 1965, in Role of Atomic Electrons
in Nuclear Transformations (Nuclear Energy Information Center,
Warsaw, Poland), p. 465.
- Thomas, H.C., C.F. Griffin, W.E. Phillips, and E.C. Davis Jr.,
1963, Nucl. Phys. 44, 268.
- Thomas, L.H., 1954, J. Chem. Phys. 22, 1758.
- Thomas, T.D., R. Vandenbosch, R.A. Glass, and G.T. Seaborg,
1957, Phys. Rev. 106, 1228.
- Thulin, S., 1955, Ark. Fys. 9, 137.
- Thulin, S., J. Moreau, and H. Atterling, 1954a, Ark. Fys. 8, 219.
- Thulin, S., J. Moreau, and H. Atterling, 1954b, Ark. Fys. 8, 229.
- Thun, J.E., S. Törnkvist, K.B. Nielsen, H. Snellman, F. Falk,
and A. Mocoroa, 1966, Nucl. Phys. 88, 289.
- Timashev, S.F., and V.A. Kaminskii, 1960, Zh. Eksp. Teor. Fiz.
38, 284 [Sov. Phys. - JETP 11, 206].

- TSA, Lofsted, G., and S. Alfaro, 1969, Arch. Phys. 39, 261.
- Tobler, J., H.B. Baker, M.E. Chubbuck, and E.W. Fitch,
1977, Z. Phys. 269, 253.
- Tobler, E.L., C.D. Bertozzi, and J.B. de Groot, 1995,
J. Phys. Radium 16, 615.
- Totzek, D., and K.-H. Hoffmann, 1967, Z. Phys. 205, 137.
- Towner, I.S., 1973, Nucl. Phys. A216, 589.
- Tribble, R.E., and G.T. Garvey, 1974, Phys. Rev. Letters 32, 314.
- Trimble, V., and F. Reines, 1973, Rev. Mod. Phys. 45, 1.
- Tucker, T.C., L.D. Roberts, C.W. Nestor, Jr., T.A. Carlson,
and F.B. Malik, 1969, Phys. Rev. 178, 998.
- Turchinets, W., and R.W. Pringle; 1956, Phys. Rev. 103, 1000.
- Turovtsev, V.V., and I.S. Shapiro, 1954, Doklady Akad. Nauk.
SSSR 95, 777.
- Unik, J.P., and J.O. Rasmussen, 1959, Phys. Rev. 115, 1687.
- van der Kooi, J.B., and H.J. van den Bold, 1956, Physica 22, 681.
- Vanderleeden, J.C., F. Boehm, and E.D. Lipson, 1971, Phys. Rev.
C4, 2218.
- Van Hise, J.R., B.H. Ketelle, and A.R. Brosi, 1967, Phys. Rev.
153, 1287.
- Van Nooijen, B., J. Konijn, A. Heyligers, J.F. van der Brugge,
and A.H. Wapstra, 1957; Physica 23, 753.
- van Nooijen, B., H. van Krugten, W.J. Wieseahn, and A.H. Wapstra,
1962, Nucl. Phys. 31, 406.
- Van Patter, D.M., and S.M. Shafroth, 1964, Nucl. Phys. 50, 113.
- Vaninbrouckx, R., and G. Grosse, 1966, Int. J. Appl. Rad.
Isotopes 17, 41.

- Vaninbrouckx, R., and A. Spérnol, 1965, Int. J. Appl. Rad. Isotopes 16, 289.
- Varga, D., 1970, ATOMKI Közlem. 12, 165.
- Vartanov, N.A., 1963, Zh. Eksp. Teor. Fiz. 45, 1875
[1964, Sov. Phys. JETP 18, 1286].
- Vatai, E., 1966, Acta Phys. Hung. 20, 217.
- Vatai, E., 1968b, in Berényi (1968b), p. 71.
- Vatai, E., 1968d, in Berényi (1968b), p. 112.
- Vatai, E., 1970a, Nucl. Phys. A156, 541.
- Vatai, E., 1970b, Acta Phys. Hung. 28, 103.
- Vatai, E., 1971, Phys. Letters B34, 395.
- Vatai, E., 1972b, ATOMKI Közlem. 14, 233.
- Vatai, E., 1973a, Nucl. Phys. A212, 413.
- Vatai, E., 1973b, ATOMKI Közlem. 15, 225.
- Vatai, E., 1973c, in Proceedings of the International Conference on Inner-Shell Ionization Phenomena, edited by R.W. Fink, S.T. Manson, J.M. Palms, and P. Venugopala Rao, U.S. Atomic Energy Commission Report No. CONF-720404 (unpublished), p. 1957.
- Vatai, E., 1974, ATOMKI Közlem. Suppl. 16/2, 91.
- Vatai, E., and K. Hohmuth, 1968a, in Berényi (1968b) p. 88.
- Vatai, E., D. Varga, and J. Uchrin, 1968c, Nucl. Phys. A116, 637.
- Vatai, E., A.C. Xenoulis, K.R. Baker, F. Tolea, and R.W. Fink, 1974, Nucl. Phys. A219, 595.

- Vitnam, V.D., B.S. Dzhelepov, A.A. Pavlov, S.V. Semenov,
and S.A. Shestopalova, 1960, *Izv. Akad. Nauk SSSR*,
Ser. Fiz. 24, 934 [*Bull. Acad. Sci. USSR, Phys. Ser.*
24, 931].
- von Oertzen, W., 1964, *Z. Phys.* 182, 130.
- Wahlgren, M.A., and W.W. Meinke, 1960, *Phys. Rev.* 118, 181.
- Waibel, E., 1969, *Nucl. Inst. Methods* 74, 69.
- Waibel, E., 1970, *Nucl. Inst. Methods* 86, 29.
- Walen, R.J., and C. Briançon, 1975, in Atomic Inner-Shell
Processes, edited by B. Crasemann (Academic Press, New York),
Vol. 1, p. 233.
- Wapstra, A.H., and N.B. Gove, 1971, *Nucl. Data Tables* A9, 267.
- Wapstra, A.H., J.F.W. Jansen, P.F.A. Goudsmit, and J. Oberski,
1962, *Nucl. Phys.* 31, 575.
- Wapstra, A.H., D. Maeder, G.J. Nijgh, and L.T.M. Ornstein,
1954, *Physica* 20, 169.
- Wapstra, A.H., G.J. Nijgh, and R. van Lieshout, 1959, Nuclear
Spectroscopy Tables (North Holland Publ. Co., Amsterdam).
- Wapstra, A.H., and J. Oberski, 1963, in O'Kelley (1963), p. 137.
- Wapstra, A.H., and W. van der Eijk, 1957, *Nucl. Phys.* 4, 325.
- Watase, Y., J. Itoh, and E. Takeda, 1940, *Proc. Phys.-Math. Soc.*
Japan 22, 90.
- Watson, R.E., 1960, *Phys. Rev.* 118, 1036.
- Watson, R.E., and A.J. Freeman, 1961a, *Phys. Rev.* 123, 521.

- Watson, R.E., and A.J. Freeman, 1961b, Phys. Rev. 124, 1117.
- Weidenmüller, H.A., 1961, Rev. Mod. Phys. 33, 574.
- Weinberg, S., 1958, Phys. Rev. 112, 1375.
- Weinberg, S., 1967, Phys. Rev. Letters 19, 1964.
- Weinberg, S., 1974, Rev. Mod. Phys. 46, 255.
- Weise, K., 1968, Nucl. Inst. Methods 65, 189, and private communication.
- Welker, J.P., and M.L. Perlman, 1955, Phys. Rev. 100, 74.
- West, Jr., H.I., L.G. Mann, and R.J. Nagle, 1961, Phys. Rev. 124, 527.
- Wilkinson, D.H., 1970a, Phys. Letters B31, 447.
- Wilkinson, D.H., 1970b, Nucl. Phys. A143, 365.
- Wilkinson, D.H., 1970c, Nucl. Inst. Methods 82, 122.
- Wilkinson, D.H., 1970d, Nucl. Phys. A150, 478.
- Wilkinson, D.H., 1970e, Nucl. Phys. A158, 476.
- Wilkinson, D.H., 1971, Phys. Rev. Letters 27, 1018.
- Wilkinson, D.H., 1971/72, Proc. Roy. Soc. Edinburgh, A70, 307.
- Wilkinson, D.H., 1972a, Nucl. Phys. A179, 289.
- Wilkinson, D.H., 1972b, Nucl. Inst. Methods 105, 505.
- Wilkinson, D.H., 1973a, Phys. Rev. C7, 930.
- Wilkinson, D.H., 1973b, Nucl. Phys. A209, 470.
- Wilkinson, D.H., 1973c, Nucl. Phys. A205, 363.
- Wilkinson, D.H., 1974a, Nucl. Phys. A225, 365.
- Wilkinson, D.H., 1974b, Phys. Letters B48, 169.
- Wilkinson, D.H., 1975, Nature 257, 189.

- Wilkinson, D.H., and D.E. Alburger, 1971, Phys. Rev. Letters 18, 1127.
- Wilkinson, D.H., and B.E.F. Macefield, 1970, Nucl. Phys. A158, 110.
- Wilkinson, D.H., and B.E.F. Macefield, 1974, Nucl. Phys. A232, 58.
- Wilkinson, G., and H.G. Hicks, 1949, Phys. Rev. 75, 1370, 1687.
- Williams, A., 1964, Nucl. Phys. 52, 324.
- Williams, A., 1968, Nucl. Phys. A117, 238.
- Williams, A., 1970, Nucl. Phys. A153, 665.
- Williams, E.J., and E. Pickup, 1938, Nature 141, 199.
- Wilson, R.G., 1969, Phys. Rev. 178, 1949.
- Wilson, R.G., and M.L. Pool, 1960, Phys. Rev. 119, 262.
- Wilson, R.G., A.A. Bartlett, J.J. Kraushaar, J.D. McCullen, and R.A. Ristinen, 1962, Phys. Rev. 125, 1655.
- Winter, G., 1968, Nucl. Phys. A113, 617.
- Winter, G., K. Hohmuth, and J. Schintlmeister, 1964, Exp. Technik Phys. 12, 141.
- Winter, G., K. Hohmuth, R. Ross, H. Kästner, and J. Schintlmeister, 1965a, Ann. Phys. 16, 207.
- Winter, G., K. Hohmuth, R. Ross, H. Kästner, and J. Schintlmeister, 1967, Z. Phys. Chem. 234, 305.
- Winter, G., K. Hohmuth, and J. Schintlmeister, 1965b, Nucl. Phys. 73, 91.

- Winter, R.G., 1957, Am. J. Phys. 25, 79.
- Wolfenstein, L., and E.M. Henley, 1971, Phys. Letters B36, 28.
- Wolfsberg, M., 1954, Phys. Rev. 96, 1712.
- Wolczek, O., Tat-To Nguyen, and I. Yutlandov, 1963, Institute
for Nuclear Research, Warsaw, Report INR-430/1 (unpublished).
- Woodward, L.L., D.A. McCown, and M.L. Pool, 1948a, Phys.
Rev. 74, 761.
- Woodward, L.L., D.A. McCown, and M.L. Pool, 1948b, Phys.
Rev. 74, 870.
- Wu, C.S., and S.A. Moszkowski, 1966, Beta Decay (Wiley,
New York).
- Yonei, K., 1966, J. Phys. Soc. Japan 21, 142.
- Yonei, K., 1967, J. Phys. Soc. Japan 22, 1127.
- Yuasa, T., 1952, Physica 18, 1267.
- Yukawa, J., 1956, Progr. Theor. Phys. 15, 561.
- Yukawa, H., and S. Sakata, 1935, Proc. Phys.-Math. Soc. Japan
17, 467.
- Yukawa, H., and S. Sakata, 1936, Proc. Phys.-Math. Soc. Japan
18, 128.
- Yukawa, H., and S. Sakata, 1937, Phys. Rev. 51, 677.
- Zhelev, Zh., and G. Muziol', 1967, Yadern, Fiz. 4, 1 [Sov. J.
Nucl. Phys. 4, 1].
- Zoller, W.H., W.B. Walters, and C.D. Coryell, 1969, Phys. Rev.
185, 1537.
- Zon, B.A., 1971, Yad. Fiz. 13, 963 [Sov. J. Nucl. Phys. 13, 554].

- Zon, B.A., 1973, *Izv. Akad. Nauk SSSR, Ser. Fiz.* 37, 1978
[*Bull. Acad. Sci. USSR, Phys. Ser.* 37, 153].
- Zon, B.A., and L.P. Rapoport, 1968, *Yad. Fiz.* 7, 528
[*Sov. J. Nucl. Phys.* 7, 330].
- Zurmühl, R., 1965, Praktische Mathematik für Ingenieure und Physiker (Springer Verlag, Berlin, Heidelberg and New York, p. 157.
- Zumwalt, L.R., 1947, Plutonium Project Report, Mon N-432, 54
(unpublished).
- Zweifel, P.F., 1954, *Phys. Rev.* 96, 1572.
- Zweifel, P.F., 1957, *Phys. Rev.* 107, 329.
- Zweifel, P.F., 1958, Proc. Rehovoth Conf. Nucl. Structure edited
by H.L. Lipkin (North-Holland Publ. Co., Amsterdam) p. 300.
- Zylicz, J., 1968, in D. Berényi (1968b) p. 123.
- Zylicz, J., Z. Sujkowski, J. Jastrzebski, and O. Wołczek, 1963,
Nucl. Phys. 42, 330.
- Zyryanova, L.N., and Yu. P. Suslov, 1968, in Berényi (1968b) p. 45.
- Zyryanova, L.N., and Yu. P. Suslov, 1969, *Izv. Akad. Nauk SSSR,*
Ser. Fiz. 33, 1693 [*Bull. Acad. Sci. USSR, Phys. Ser.* 33, 1553].
- Zyryanova, L.N., and Yu. P. Suslov, 1970, *Izv. Akad. Nauk SSSR,*
Ser. Fiz. 34, 101 [*Bull. Akad. Sci. USSR, Phys. Ser.* 34, 95].

TABLE 2.1. List of calculations of electron radial wave functions inside or near the nucleus.

Reference	R/NR ^a	Atomic potential ^b	Nuclear charge distribution	Z	Shells	Remarks
Brysk and Rose (1955)	R	TFD	uniform	10-100	K, L	Results presented graphically
Band <i>et al.</i> (1956, 1958)	R	TFD	uniform	18-98	K, L	
Brewer <i>et al.</i> (1961)	R	TFD	uniform	55-90	M	Every fifth atomic number is listed
Watson and Freeman (1961)	NR	HF	point	3-42	all	Analytical wave functions are used
Herman and Skillman (1963)	NR	HFS	point	2-100	all	
Winter (1968)	NR ^c	HF	point	3-42	K, L	L ₁ /K ratios only
Behrens and Jänecke (1969)	R	HF (Z < 36) TFD (Z > 36)	uniform	1-102	K, L, M	
Suslov (1969, 1970b)	R	NR HFS (Z < 72) R HFS (Z > 72)	uniform	2-98	K, L, M N ₁ , N ₂	
Martin and Blichert-Toft (1970)	R	HFS ^d	Fermi	5-98	K, L	
Froese-Fischer (1972b)	NR	HF	point	2-86	all	
Mann and Waber (1973)	R	HF	Fermi	1-102	all	

^aNR=nonrelativistic; R=relativistic.

^bTFD=Thomas-Fermi-Dirac; HF=Hartree-Fock; HFS=Hartree-Fock-Slater.

^cSupplementary relativistic corrections are applied to results from NR analytic wave functions of Watson and Freeman (1961) and Malli (1966).

^dNestor *et al.* (1966); Tucker *et al.* (1969); Lu *et al.* (1971).

TABLE 2.2. Calculated electron radial wave-function ratios $\epsilon_{L_1}^2 / \epsilon_K^2$.

Z	Nonrelativistic			Relativistic							
	HFS	HF		TFD			HFS		HF		
	Herman and Skillman (1963)	Froese-Fischer (1972 b)	Winter (1968)	Brysk and Rose (1958)	Band <u>et al.</u> (1956, 1958)	Behrens and Jänecke (1969)	Suslov (1969, 1970)	Martin and Blichert-Toft (1970)	Calculated ^a with the codes of Fricke <u>et al.</u> (1971)	Winter (1968), ^b corrected	Mann and Waber (1973)
5	0.049	0.041	0.041				0.049	0.041	0.049	0.041	0.041
10	0.058	0.055	0.055	0.075			0.059	0.058	0.059	0.055	0.055
15	0.075	0.074	0.074	0.079		0.077	0.076	0.076	0.076	0.074	0.074
20	0.085	0.084	0.084	0.083	0.085	0.086	0.086	0.086	0.086	0.086	0.086
30	0.095	0.095	0.095	0.093	0.099	0.100	0.100	0.100	0.100	0.099	0.099
40	0.101	0.101		0.103	0.109	0.109	0.109	0.109	0.109	0.108	0.109
50	0.104	0.105		0.113	0.118	0.118	0.119	0.118	0.118		0.118
60	0.107	0.107		0.125	0.128	0.128	0.128	0.128	0.128		0.127
70	0.109	0.109		0.137	0.139	0.140	0.140	0.139	0.139		0.138
80	0.110	0.111		0.151	0.153	0.154	0.152	0.152	0.152		0.151
90	0.111			0.166	0.169	0.170	0.167	0.167	0.168		0.167
100	0.112			0.184		0.190			0.187		0.186

^aThe parameters in the Slater exchange term [Eq. (6) of Fricke et al. (1971)] are C=1, n=1, and m=1.

^bNonrelativistic results multiplied by a correction factor for relativistic effects.

TABLE 2.3. Calculated electron radial wave-function ratios $g_{M_1}^2/g_{L_1}^2$.

Z	Nonrelativistic			Relativistic				
	HFS	HF		TFD		HFS		HF
	Herman and Skillman (1963)	Watson and Freeman (1961)	Froese-Fischer (1972 b)	Brewer et al. ^a (1961)	Behrens and Jänecke (1969)	Suslov (1969, 1970)	Calculated with the codes of Fricke et al. (1971)	Mann and Waber (1973)
15	0.095	0.075	0.076			0.095	0.095	0.076
20	0.132	0.118	0.119			0.133	0.133	0.119
25	0.144	0.134	0.136			0.145	0.145	0.136
30	0.148	0.144	0.143		0.162	0.150	0.150	0.144
40	0.174		0.172		0.184	0.176	0.176	0.174
50	0.194		0.193		0.201	0.197	0.196	0.195
60	0.208		0.208	0.216	0.214	0.212	0.211	0.210
70	0.218		0.218	0.228	0.224	0.224	0.222	0.222
80	0.225		0.225	0.237	0.233	0.231	0.231	0.230
90	0.231			0.242	0.240	0.237	0.238	0.237
100	0.235				0.245		0.243	0.242

^aHere, $g_{L_1}^2$ has been taken from the tables of Behrens and Jänecke (1969).

TABLE 2.4. Calculated electron radial wave-function ratios $\epsilon_{N_1}^2 / \epsilon_{M_1}^2$.

Z	Nonrelativistic			Relativistic		
	HFS	HF		HFS	HF	
	Herman and Skillman (1963)	Watson and Freeman (1961)	Froese-Fischer (1972b)	Suslov (1969, 1970); Dzhelepov <i>et al.</i> (1972)	Calculated with the codes of Fricke <i>et al.</i> (1971)	Mann and Waber (1973)
35	0.116	0.094	0.094		0.116	0.094
40	0.162		0.143	0.163	0.162	0.143
45	0.184		0.168	0.186	0.185	0.167
50	0.203		0.188	0.206	0.204	0.189
60	0.233		0.224	0.236	0.235	0.225
70	0.237		0.232	0.245	0.243	0.236
80	0.251		0.248	0.257	0.257	0.251
90	0.266			0.271	0.271	0.267
100	0.279				0.283	0.279

TABLE 2.5. Calculated electron radial wave-function ratios g_{01}^2 / g_{N1}^2 .

Z	Nonrelativistic		Relativistic	
	HFS	HF	HFS	HF
	Herman and Skillman (1963)	Froese-Fischer (1972b)	Calculated with the codes of Fricke <i>et al.</i> (1971)	Mann and Waber (1973)
70	0.155	0.135	0.161	0.146
75	0.182	0.163	0.186	0.171
80	0.203	0.183	0.208	0.192
85	0.229	0.211	0.232	0.216
90	0.252		0.252	0.239
95	0.263		0.266	0.254
100	0.272		0.278	0.279

TABLE 2.6. Calculated relativistic electron radial wave-function ratios $f_{L_2}^2 / g_{L_1}^2$.

Z	TFD			HFS			HF
	Brysk and Rose (1955)	Band <i>et al.</i> (1956, 1958)	Behrens and JHnecke (1969)	Suslov (1969, 1970b); Dzhelepov <i>et al.</i> (1972)	Martin and Blichert- Toft (1970)	Calculated with the codes of Fricke <i>et al.</i> (1971)	Mann and Waber (1973)
10	0.001			0.00052	0.00053	0.00052	0.00046
15	0.002		0.00160	0.00155	0.00155	0.00155	0.00143
20	0.003	0.00235	0.00318	0.00308	0.00306	0.00306	0.00290
25	0.005	0.00492	0.00525	0.00515	0.00512	0.00512	0.00489
30	0.007	0.00751	0.00786	0.00778	0.00774	0.00774	0.00746
40	0.013	0.0145	0.0149	0.0148	0.0147	0.0147	0.0143
50	0.022	0.0241	0.0247	0.0246	0.0244	0.0244	0.0238
60	0.034	0.0368	0.0377	0.0376	0.0371	0.0371	0.0364
70	0.052	0.0538	0.0548	0.0546	0.0538	0.0538	0.0527
80	0.077	0.0757	0.0771	0.0755	0.0755	0.0754	0.0741
90	0.111	0.1056	0.1068	0.1043	0.1042	0.1041	0.1023
100	0.154		0.1474			0.1432	0.1407

TABLE 2.7. Calculated relativistic electron radial wave-function ratios $f_{M_2}^2 / g_{M_1}^2$.

Z	TFD		HFS		HF
	Brewer <u>et al.</u> (1961)	Behrens and Jänecke (1969)	Suslov (1969, 1970 b); Dzhelepov <u>et al.</u> (1972)	Calculated with the codes of Fricke <u>et al.</u> (1971)	Mann and Waber (1973)
15			0.00112	0.00111	0.00102
20			0.00282	0.00281	0.00259
25			0.00495	0.00492	0.00470
30		0.0079	0.00766	0.00761	0.00730
40		0.0158	0.0156	0.0155	0.0150
50		0.0268	0.0267	0.0264	0.0258
60	0.0409	0.0416	0.0415	0.0409	0.0400
70	0.0601	0.0610	0.0609	0.0599	0.0588
80	0.0834	0.0865	0.0848	0.0847	0.0831
90	0.1179	0.1201	0.1176	0.1173	0.1153
100		0.1661		0.1616	0.1589

TABLE 2.8. Calculated relativistic electron radial wave-function ratios $f_{N_2}^2 / f_{N_1}^2$.

Z	HFS		HF
	Suslov (1969, 1970b); Dzhelepov <i>et al.</i> (1972)	Calculated with the codes of Fricke <i>et al.</i> (1971)	Mann and Waber (1973)
35		0.0078	0.0076
40	0.0134	0.0133	0.0126
45	0.0185	0.0182	0.0176
50	0.0247	0.0244	0.0237
60	0.0400	0.0394	0.0385
70	0.0594	0.0583	0.0572
80	0.0836	0.0836	0.0821
90	0.117	0.117	0.115
100		0.162	0.160

TABLE 2.9. Amplitudes $\beta_{x^k} p_{x^k}^{-1}$ of the bound electron radial wave functions. (After Mann and Waber, 1973 and private communication.) Columns are headed by atomic numbers Z. (Outermost electrons have been omitted.)

	1	2	3	4	5	6	7	8
K	0.12470E-02	0.29658E-02	0.57843E-02	0.91767E-02	0.13059E-01	0.17346E-01	0.22175E-01	0.27256E-01
LI	0.0	0.0	0.90318E-03	0.15727E-02	0.26379E-02	0.37220E-02	0.49069E-02	0.61904E-02
LII	0.0	0.0	0.0	0.0	0.0	0.0	0.67149E-04	0.10080E-03
	9	10	11	12	13	14	15	16
K	0.37762E-01	0.38634E-01	0.44867E-01	0.51461E-01	0.59405E-01	0.69766E-01	0.73354E-01	0.81364E-01
LI	0.75954E-02	0.90927E-02	0.10394E-01	0.13042E-01	0.15235E-01	0.17560E-01	0.20013E-01	0.22594E-01
LII	0.14302E-03	0.19456E-03	0.27250E-03	0.36644E-03	0.47827E-03	0.60905E-03	0.75949E-03	0.92853E-03
LIII	0.0	0.0	0.53674E-03	0.71972E-03	0.93526E-03	0.11950E-02	0.14771E-02	0.17979E-02
MI	0.0	0.0	0.0	0.0	0.35174E-02	0.45117E-02	0.55193E-02	0.65660E-02
MII	0.0	0.0	0.0	0.0	0.0	0.0	0.17636E-03	0.23345E-03
	17	18	19	20	21	22	23	24
K	0.89721E-01	0.93431E-01	0.10754E 00	0.11702E 00	0.12684E 00	0.13707E 00	0.14770E 00	0.15875E 00
LI	0.25904E-01	0.23140E-01	0.31122E-01	0.34259E-01	0.37522E-01	0.40930E-01	0.44491E-01	0.48189E-01
LII	0.11205E-02	0.13357E-02	0.15773E-02	0.18455E-02	0.21416E-02	0.24673E-02	0.28241E-02	0.32161E-02
LIII	0.21640E-02	0.25728E-02	0.30760E-02	0.35272E-02	0.40780E-02	0.46902E-02	0.53356E-02	0.60669E-02
MI	0.76570E-02	0.87964E-02	0.10259E-01	0.11812E-01	0.13221E-01	0.14649E-01	0.16113E-01	0.17694E-01
MII	0.25983E-03	0.37310E-03	0.48051E-03	0.60071E-03	0.71956E-03	0.84951E-03	0.99208E-03	0.11444E-02
MIII	0.0	0.0	0.0	0.0	0.13690E-02	0.16056E-02	0.19610E-02	0.21192E-02
MIV	0.0	0.0	0.0	0.0	0.0	0.0	0.0	0.24081E-04
	25	26	27	28	29	30	31	32
K	0.17020E 00	0.13710E 00	0.10641E 00	0.20724E 00	0.27043E 00	0.23416E 00	0.24871E 00	0.26401E 00
LI	0.52039E-01	0.56057E-01	0.60226E-01	0.64591E-01	0.69038E-01	0.73778E-01	0.78837E-01	0.84170E-01
LII	0.36406E-02	0.41043E-02	0.46073E-02	0.51525E-02	0.57410E-02	0.63726E-02	0.70509E-02	0.77909E-02
LIII	0.60132E-02	0.74395E-02	0.89769E-02	0.94707E-02	0.10497E-01	0.11584E-01	0.12741E-01	0.13974E-01
MI	0.19173E-01	0.20932E-01	0.22505E-01	0.24260E-01	0.25929E-01	0.27577E-01	0.29094E-01	0.32464E-01
MII	0.11611E-02	0.14794E-02	0.16756E-02	0.18075E-02	0.21231E-02	0.23886E-02	0.26924E-02	0.30065E-02
MIII	0.24395E-02	0.27666E-02	0.31189E-02	0.34989E-02	0.38709E-02	0.43410E-02	0.48945E-02	0.53655E-02
MIV	0.32569E-04	0.40024E-04	0.48020E-04	0.58104E-04	0.66018E-04	0.81368E-04	0.98443E-04	0.11862E-03
MV	0.0	0.0	0.0	0.0	0.0	0.0	0.19943E-03	0.22760E-03
	33	34	35	36	37	38	39	40
K	0.27925E 00	0.27397E 00	0.31735E 00	0.32721E 00	0.34474E 00	0.36289E 00	0.38172E 00	0.40117E 00
LI	0.88070E-01	0.94430E-01	0.10914E 00	0.11221E 00	0.11221E 00	0.11221E 00	0.11221E 00	0.13222E 00
LII	0.75645E-02	0.94029E-02	0.10304E-01	0.11264E-01	0.12204E-01	0.13191E-01	0.14567E-01	0.15915E-01
LIII	0.15294E-01	0.16674E-01	0.18149E-01	0.17709E-01	0.21360E-01	0.23104E-01	0.24947E-01	0.26897E-01
MI	0.34767E-01	0.37281E-01	0.39903E-01	0.42689E-01	0.45570E-01	0.48524E-01	0.51598E-01	0.54799E-01
MII	0.33581E-02	0.37399E-02	0.41571E-02	0.45965E-02	0.50783E-02	0.55957E-02	0.61544E-02	0.67509E-02
MIII	0.55906E-02	0.66320E-02	0.73220E-02	0.80609E-02	0.88473E-02	0.96852E-02	0.10576E-01	0.11570E-01
MIV	0.14102E-03	0.16612E-03	0.19417E-03	0.22532E-03	0.26001E-03	0.29883E-03	0.34100E-03	0.38744E-03
MV	0.26930E-03	0.31692E-03	0.36641E-03	0.42759E-03	0.49216E-03	0.56145E-03	0.64194E-03	0.72763E-03
MVI	0.96508E-02	0.10747E-01	0.12273E-01	0.13630E-01	0.15491E-01	0.17294E-01	0.19022E-01	0.20827E-01
MVII	0.0	0.0	0.0	0.0	0.15185E-02	0.17470E-02	0.20624E-02	0.23381E-02
MVIII	0.0	0.0	0.0	0.0	0.0	0.0	0.35534E-02	0.40141E-02

ORIGINAL PAGE IS
OF POOR QUALITY

	41	42	43	44	45	46	47	48
K	0.42135E 00	0.44216E 00	0.46370E 00	0.48609E 00	0.50929E 00	0.53319E 00	0.55811E 00	0.58364E 00
LI	0.13943E 00	0.14691E 00	0.15469E 00	0.16279E 00	0.17123E 00	0.17984E 00	0.18911E 00	0.19853E 00
LII	0.17154E-01	0.19572E-01	0.20084E-01	0.21697E-01	0.23413E-01	0.25230E-01	0.27170E-01	0.29219E-01
LIII	0.28936E-01	0.31089E-01	0.33351E-01	0.35731E-01	0.38233E-01	0.40853E-01	0.43609E-01	0.46486E-01
MI	0.56504E-01	0.62071E-01	0.65796E-01	0.69664E-01	0.73707E-01	0.77893E-01	0.82290E-01	0.86934E-01
MII	0.73915E-02	0.80738E-02	0.88053E-02	0.95859E-02	0.10420E-01	0.11307E-01	0.12257E-01	0.13265E-01
MIII	0.12520E-01	0.13579E-01	0.14699E-01	0.15880E-01	0.17127E-01	0.18440E-01	0.19825E-01	0.21279E-01
MIV	0.43977E-03	0.49583E-03	0.55730E-03	0.62364E-03	0.69641E-03	0.77478E-03	0.86027E-03	0.95764E-03
MV	0.82127E-03	0.92367E-03	0.10347E-02	0.11560E-02	0.12871E-02	0.14295E-02	0.15827E-02	0.17463E-02
NI	0.22468E-01	0.24297E-01	0.26341E-01	0.28121E-01	0.30132E-01	0.32082E-01	0.34366E-01	0.36788E-01
NII	0.26015E-02	0.29193E-02	0.32805E-02	0.36188E-02	0.40027E-02	0.43908E-02	0.48462E-02	0.53399E-02
NIII	0.44583E-02	0.49474E-02	0.55075E-02	0.60306E-02	0.65751E-02	0.71345E-02	0.78125E-02	0.85417E-02
NIV	0.0	0.12877E-03	0.16111E-03	0.19017E-03	0.20928E-03	0.23174E-03	0.27549E-03	0.32276E-03

	49	50	51	52	53	54	55	56
K	0.61024E 00	0.63774E 00	0.66627E 00	0.69549E 00	0.72657E 00	0.75913E 00	0.79123E 00	0.82511E 00
LI	0.20840E 00	0.21961E 00	0.22927E 00	0.24025E 00	0.25197E 00	0.26393E 00	0.27652E 00	0.28949E 00
LII	0.31404E-01	0.33717E-01	0.36175E-01	0.38766E-01	0.41559E-01	0.44495E-01	0.47611E-01	0.50902E-01
LIII	0.44505E-01	0.52668E-01	0.55979E-01	0.59429E-01	0.63071E-01	0.66951E-01	0.70819E-01	0.74943E-01
MI	0.91596E-01	0.96536E-01	0.10170E 00	0.10703E 00	0.11271E 00	0.11854E 00	0.12468E 00	0.13101E 00
MII	0.14344E-01	0.15491E-01	0.16713E-01	0.18006E-01	0.19401E-01	0.20969E-01	0.22442E-01	0.24102E-01
MIII	0.22812E-01	0.24422E-01	0.26117E-01	0.27892E-01	0.29742E-01	0.31731E-01	0.33795E-01	0.35949E-01
MIV	0.10526E-02	0.11604E-02	0.12747E-02	0.14016E-02	0.15367E-02	0.16812E-02	0.18367E-02	0.20030E-02
MV	0.19231E-02	0.21129E-02	0.23165E-02	0.25345E-02	0.27685E-02	0.30179E-02	0.32847E-02	0.35688E-02
NI	0.39331E-01	0.42001E-01	0.44809E-01	0.47729E-01	0.50843E-01	0.54054E-01	0.57449E-01	0.60973E-01
NII	0.58811E-02	0.64674E-02	0.70932E-02	0.77606E-02	0.84838E-02	0.92499E-02	0.10076E-01	0.10954E-01
NIII	0.92266E-02	0.10163E-01	0.11057E-01	0.12004E-01	0.13017E-01	0.14077E-01	0.15196E-01	0.16372E-01
NIV	0.37449E-03	0.43054E-03	0.49217E-03	0.55884E-03	0.63135E-03	0.70954E-03	0.79451E-03	0.88633E-03
NV	0.68149E-03	0.78300E-03	0.89168E-03	0.10087E-02	0.11352E-02	0.12711E-02	0.14196E-02	0.15773E-02
NVI	0.0	0.0	0.11399E-04	0.12700E-04	0.14044E-04	0.15406E-04	0.17255E-04	0.19179E-04
NVII	0.0	0.0	0.0	0.0	0.0	0.0	0.13933E-06	0.16136E-06

	57	58	59	60	61	62	63	64
K	0.86070E 00	0.89769E 00	0.93616E 00	0.97557E 00	0.10166E 01	0.10590E 01	0.11034E 01	0.11485E 01
LI	0.30317E 00	0.31746E 00	0.33242E 00	0.34771E 00	0.36370E 00	0.38063E 00	0.39823E 00	0.41623E 00
LII	0.54419E-01	0.59159E-01	0.62134E-01	0.66315E-01	0.70755E-01	0.75454E-01	0.80464E-01	0.85706E-01
LIII	0.79271E-01	0.83801E-01	0.88541E-01	0.93459E-01	0.98595E-01	0.10395E 00	0.10954E 00	0.11533E 00
MI	0.13765E 00	0.14468E 00	0.15201E 00	0.15955E 00	0.16745E 00	0.17566E 00	0.18429E 00	0.19314E 00
MII	0.25880E-01	0.27774E-01	0.29793E-01	0.31920E-01	0.34183E-01	0.36581E-01	0.39147E-01	0.41831E-01
MIII	0.38216E-01	0.40601E-01	0.43107E-01	0.45712E-01	0.48439E-01	0.51288E-01	0.54273E-01	0.57366E-01
MIV	0.21417E-02	0.23735E-02	0.25790E-02	0.27975E-02	0.30308E-02	0.32794E-02	0.35462E-02	0.38277E-02
MV	0.38720E-02	0.41975E-02	0.45463E-02	0.49137E-02	0.53040E-02	0.57178E-02	0.61553E-02	0.66161E-02
NI	0.64675E-01	0.68271E-01	0.71798E-01	0.75635E-01	0.79632E-01	0.83777E-01	0.89146E-01	0.92798E-01
NII	0.11898E-01	0.12841E-01	0.13789E-01	0.14841E-01	0.15958E-01	0.17142E-01	0.18409E-01	0.19788E-01
NIII	0.17614E-01	0.18815E-01	0.19984E-01	0.21218E-01	0.22634E-01	0.24043E-01	0.25527E-01	0.27137E-01
NIV	0.58640E-03	0.10839E-02	0.11789E-02	0.12895E-02	0.14077E-02	0.15337E-02	0.16693E-02	0.18212E-02
NV	0.17483E-02	0.19125E-02	0.20714E-02	0.22547E-02	0.24488E-02	0.26542E-02	0.28746E-02	0.31207E-02
NVI	0.20571E-04	0.22909E-04	0.24839E-04	0.28825E-04	0.33151E-04	0.37857E-04	0.43037E-04	0.50527E-04
NVII	0.18147E-06	0.11285E-05	0.11532E-05	0.12115E-05	0.12714E-05	0.13331E-05	0.77773E-04	0.92061E-04

ORIGINAL PAGE IS
 OF POOR QUALITY

	65	66	67	68	69	70	71	72
K	0.11964E 01	0.12459E 01	0.12969E 01	0.13501E 01	0.14058E 01	0.14627E 01	0.15227E 01	0.15944E 01
LI	0.43539E 00	0.45516E 00	0.47592E 00	0.49761E 00	0.52034E 00	0.54776E 00	0.56959E 00	0.59411E 00
LII	0.91339E-01	0.97268E-01	0.10356E 00	0.11028E 00	0.11739E 00	0.12488E 00	0.13297E 00	0.14130E 00
LIII	0.12141E 00	0.12772E 00	0.13431E 00	0.14117E 00	0.14833E 00	0.15574E 00	0.16349E 00	0.17152E 00
MI	0.20756E 00	0.21230E 00	0.22252E 00	0.23320E 00	0.24441E 00	0.25597E 00	0.26917E 00	0.28082E 00
MII	0.44732E-01	0.47789E-01	0.51040E-01	0.54497E-01	0.58179E-01	0.62055E-01	0.66195E-01	0.70564E-01
MIII	0.60628E-01	0.64019E-01	0.67568E-01	0.71275E-01	0.75149E-01	0.79172E-01	0.83395E-01	0.87765E-01
MIV	0.41318E-02	0.44529E-02	0.47950E-02	0.51586E-02	0.55492E-02	0.59540E-02	0.63970E-02	0.68449E-02
MV	0.71069E-02	0.76238E-02	0.81705E-02	0.87478E-02	0.93595E-02	0.99886E-02	0.10675E-01	0.11385E-01
NI	0.97362E-01	0.10226E 00	0.10741E 00	0.11278E 00	0.11841E 00	0.12422E 00	0.13051E 00	0.13709E 00
NII	0.21163E-01	0.22669E-01	0.24272E-01	0.25976E-01	0.27791E-01	0.29702E-01	0.31799E-01	0.34030E-01
NIII	0.28683E-01	0.30366E-01	0.32126E-01	0.33944E-01	0.35897E-01	0.37993E-01	0.40048E-01	0.42271E-01
NIV	0.19633E-02	0.21250E-02	0.22972E-02	0.24804E-02	0.26752E-02	0.28915E-02	0.31120E-02	0.33595E-02
NV	0.37550E-02	0.36166E-02	0.38939E-02	0.41870E-02	0.44972E-02	0.48240E-02	0.51851E-02	0.55703E-02
NVI	0.54763E-04	0.61389E-04	0.68582E-04	0.76377E-04	0.84820E-04	0.93936E-04	0.10466E-03	0.12007E-03
NVII	0.98950E-04	0.11086E-03	0.12376E-03	0.13765E-03	0.15263E-03	0.16886E-03	0.18717E-03	0.21628E-03
OI	0.0	0.0	0.41330E-01	0.43291E-01	0.45323E-01	0.47427E-01	0.50722E-01	0.54179E-01
OII	0.0	0.0	0.0	0.0	0.0	0.0	0.11189E-01	0.12214E-01

	73	74	75	76	77	78	79	80
K	0.16409E 01	0.17159E 01	0.17956E 01	0.18753E 01	0.19330E 01	0.20112E 01	0.20932E 01	0.21775E 01
LI	0.62103E 00	0.64910E 00	0.67893E 00	0.70890E 00	0.74123E 00	0.77477E 00	0.81010E 00	0.84665E 00
LII	0.15029E 00	0.15979E 00	0.16959E 00	0.18054E 00	0.19195E 00	0.20401E 00	0.21697E 00	0.23043E 00
LIII	0.17900E 00	0.19961E 00	0.19769E 00	0.20707E 00	0.21699E 00	0.22708E 00	0.23770E 00	0.24969E 00
MI	0.29412E 00	0.30799E 00	0.32256E 00	0.33764E 00	0.35362E 00	0.37025E 00	0.38779E 00	0.40594E 00
MII	0.75224E-01	0.80168E-01	0.85426E-01	0.90977E-01	0.96925E-01	0.10322E 00	0.10995E 00	0.11704E 00
MIII	0.92343E-01	0.97114E-01	0.10210E 00	0.10727E 00	0.11269E 00	0.11833E 00	0.12422E 00	0.13034E 00
MIV	0.73309E-02	0.78453E-02	0.83900E-02	0.89649E-02	0.95750E-02	0.10219E-01	0.10902E-01	0.11621E-01
MV	0.12134E-01	0.12922E-01	0.13751E-01	0.14621E-01	0.15538E-01	0.16500E-01	0.17512E-01	0.18570E-01
NI	0.14404E 00	0.15134E 00	0.15902E 00	0.16701E 00	0.17559E 00	0.18435E 00	0.19371E 00	0.20345E 00
NII	0.36424E-01	0.39997E-01	0.41705E-01	0.44596E-01	0.47704E-01	0.51004E-01	0.54541E-01	0.58287E-01
NIII	0.46719E-01	0.47234E-01	0.49979E-01	0.52644E-01	0.55556E-01	0.58605E-01	0.61800E-01	0.65127E-01
NIV	0.36254E-02	0.39102E-02	0.42129E-02	0.45344E-02	0.48781E-02	0.52430E-02	0.56320E-02	0.60444E-02
NV	0.55810E-02	0.64171E-02	0.69817E-02	0.73735E-02	0.78956E-02	0.84500E-02	0.90362E-02	0.96501E-02
NVI	0.13489E-03	0.15095E-03	0.16857E-03	0.18762E-03	0.20824E-03	0.23052E-03	0.25454E-03	0.28039E-03
NVII	0.24279E-03	0.27149E-03	0.30205E-03	0.33510E-03	0.37077E-03	0.40900E-03	0.45029E-03	0.49477E-03
OI	0.57835E-01	0.61666E-01	0.65728E-01	0.69952E-01	0.74415E-01	0.79983E-01	0.83625E-01	0.89077E-01
OII	0.13314E-01	0.14488E-01	0.15929E-01	0.17252E-01	0.18782E-01	0.20346E-01	0.22085E-01	0.24004E-01
OIII	0.0	0.0	0.18681E-01	0.20049E-01	0.21489E-01	0.22840E-01	0.24404E-01	0.25192E-01

	91	92	93	94	95	96	97	98
K	0.22651E 01	0.29569E 01	0.24532E 01	0.25542E 01	0.26604E 01	0.27606E 01	0.28746E 01	0.29917E 01
L I	0.98436E 00	0.92911E 00	0.96756E 00	0.10123E 01	0.10599E 01	0.11049E 01	0.11543E 01	0.12094E 01
L II	0.24491E 00	0.26716E 00	0.27654E 00	0.29404E 00	0.31275E 00	0.33146E 00	0.35247E 00	0.37462E 00
L III	0.26011E 00	0.27206E 00	0.28441E 00	0.29734E 00	0.31092E 00	0.32430E 00	0.33890E 00	0.35377E 00
M I	0.42494E 00	0.44497E 00	0.46610E 00	0.48839E 00	0.51193E 00	0.53661E 00	0.56227E 00	0.58943E 00
M II	0.12459E 00	0.13263E 00	0.14124E 00	0.15044E 00	0.16028E 00	0.17015E 00	0.18123E 00	0.19291E 00
M III	0.13671E 00	0.14136E 00	0.15032E 00	0.15759E 00	0.16519E 00	0.17282E 00	0.18104E 00	0.18955E 00
M IV	0.12390E 01	0.13184E 01	0.14035E 01	0.14935E 01	0.15884E 01	0.16885E 01	0.17927E 01	0.19032E 01
M V	0.15680E 01	0.20846E 01	0.22071E 01	0.23456E 01	0.24796E 01	0.26091E 01	0.27567E 01	0.29109E 01
N I	0.21368E 00	0.22446E 00	0.23596E 00	0.24700E 00	0.25766E 00	0.26805E 00	0.27900E 00	0.30142E 00
N II	0.62293E 01	0.66563E 01	0.71146E 01	0.76055E 01	0.81320E 01	0.86627E 01	0.92591E 01	0.98970E 01
N III	0.69607E 01	0.72255E 01	0.76095E 01	0.80101E 01	0.84311E 01	0.88571E 01	0.93153E 01	0.97915E 01
N IV	0.64924E 02	0.67482E 02	0.74438E 02	0.77706E 02	0.81307E 02	0.85307E 02	0.89736E 02	0.10399E 02
N V	0.10799E 01	0.10993E 01	0.11705E 01	0.12467E 01	0.13271E 01	0.14102E 01	0.14991E 01	0.15923E 01
N VI	0.30824E 03	0.33829E 03	0.37064E 03	0.40545E 03	0.44292E 03	0.48262E 03	0.52567E 03	0.57171E 03
N VII	0.54753E 03	0.59393E 03	0.64998E 03	0.70788E 03	0.77100E 03	0.83901E 03	0.91014E 03	0.98702E 03
O I	0.24751E 01	0.10079E 00	0.10719E 00	0.11392E 00	0.12119E 00	0.12930E 00	0.13826E 00	0.14658E 00
O II	0.26097E 01	0.29317E 01	0.30908E 01	0.33426E 01	0.36246E 01	0.39129E 01	0.42152E 01	0.45786E 01
O III	0.28110E 01	0.30145E 01	0.32313E 01	0.34603E 01	0.37022E 01	0.39511E 01	0.42152E 01	0.44909E 01
O IV	0.27149E 02	0.27999E 02	0.26699E 02	0.29593E 02	0.32664E 02	0.35861E 02	0.39317E 02	0.42989E 02
P V	0.0	0.0	0.41515E 02	0.45797E 02	0.50297E 02	0.54962E 02	0.60011E 02	0.65339E 02
Q VI	0.0	0.0	0.0	0.0	0.0	0.0	0.44033E 04	0.48652E 04

	99	90	91	92	93	94	95	96
K	0.31189E 01	0.37429E 01	0.33781E 01	0.35119E 01	0.36613E 01	0.38136E 01	0.39697E 01	0.41326E 01
L I	0.12673E 01	0.13236E 01	0.13859E 01	0.14493E 01	0.15191E 01	0.15907E 01	0.16649E 01	0.17425E 01
L II	0.39992E 00	0.42327E 00	0.45059E 00	0.47846E 00	0.50949E 00	0.54208E 00	0.57644E 00	0.61309E 00
L III	0.36959E 00	0.39547E 00	0.40251E 00	0.41971E 00	0.43899E 00	0.45700E 00	0.47444E 00	0.49672E 00
M I	0.61574E 00	0.64392E 00	0.67551E 00	0.70961E 00	0.74189E 00	0.77777E 00	0.81499E 00	0.85399E 00
M II	0.29569E 00	0.21862E 00	0.23106E 00	0.24782E 00	0.26475E 00	0.28152E 00	0.29974E 00	0.31918E 00
M III	0.19586E 00	0.20764E 00	0.21739E 00	0.22720E 00	0.23785E 00	0.24876E 00	0.26004E 00	0.27178E 00
M IV	0.29217E 01	0.21437E 01	0.22762E 01	0.24110E 01	0.25570E 01	0.27097E 01	0.28699E 01	0.30393E 01
M V	0.30735E 01	0.32407E 01	0.34199E 01	0.36023E 01	0.37999E 01	0.39994E 01	0.42099E 01	0.44297E 01
M VI	0.31715E 00	0.33259E 00	0.34991E 00	0.36692E 00	0.38599E 00	0.40560E 00	0.42599E 00	0.44731E 00
M VII	0.19577E 00	0.11279E 00	0.12998E 00	0.12998E 00	0.12998E 00	0.14699E 00	0.15679E 00	0.16739E 00
M VIII	0.10296E 00	0.10309E 00	0.11356E 00	0.11914E 00	0.12511E 00	0.13129E 00	0.13769E 00	0.14437E 00
M IX	0.11108E 01	0.11347E 01	0.12634E 01	0.13456E 01	0.14342E 01	0.15270E 01	0.16247E 01	0.17279E 01
N V	0.16910E 01	0.17372E 01	0.19019E 01	0.20144E 01	0.21341E 01	0.22599E 01	0.23999E 01	0.25267E 01
N VI	0.62130E 03	0.67374E 03	0.73077E 03	0.79091E 03	0.85573E 03	0.92512E 03	0.99993E 03	0.10759E 04
N VII	0.10694E 02	0.11544E 02	0.12494E 02	0.13477E 02	0.14529E 02	0.15640E 02	0.16823E 02	0.18073E 02
N VIII	0.15355E 00	0.16246E 00	0.17209E 00	0.18169E 00	0.19230E 00	0.20313E 00	0.21457E 00	0.22662E 00
O I	0.49541E 01	0.53937E 01	0.57471E 01	0.61751E 01	0.66487E 01	0.71393E 01	0.76722E 01	0.82471E 01
O II	0.47836E 01	0.50829E 01	0.53907E 01	0.56927E 01	0.60239E 01	0.63560E 01	0.67082E 01	0.70957E 01
O III	0.46960E 02	0.51117E 02	0.54869E 02	0.59091E 02	0.63611E 02	0.68310E 02	0.73136E 02	0.78749E 02
O IV	0.70990E 02	0.76787E 02	0.82391E 02	0.88376E 02	0.94669E 02	0.10094E 03	0.10771E 03	0.11519E 03
O V	0.53293E 04	0.57651E 04	0.62409E 04	0.67624E 04	0.73099E 04	0.78999E 04	0.82597E 04	0.87159E 04
O VI	0.41185E 06	0.47732E 06	0.50266E 06	0.53807E 06	0.57445E 06	0.61281E 06	0.53152E 03	0.61603E 03
Q VII	0.0	0.0	0.06413E 06	0.10439E 06	0.11309E 06	0.12065E 06	0.38582E 05	0.41339E 05
Q VIII	0.0	0.0	0.0	0.0	0.0	0.0	0.44033E 04	0.48652E 04
Q IX	0.0	0.0	0.0	0.0	0.0	0.0	0.0	0.93045E 07

ORIGINAL PAGE IS
 OF POOR QUALITY

	97	99	99	100	101	102
K	0.47053E 01	0.44959E 01	0.46741E 01	0.448776E 01	0.50826E 01	0.53013E 01
L I	0.19256E 01	0.19127E 01	0.20040E 01	0.21031E 01	0.27040E 01	0.23121E 01
L I I	0.65263E 00	0.69489E 00	0.73976E 00	0.78990E 00	0.84026E 00	0.89589E 00
L I I I	0.51790E 00	0.53939E 00	0.56255E 00	0.58667E 00	0.61124E 00	0.63696E 00
M I	0.99567E 00	0.93953E 00	0.98530E 00	0.10351E 01	0.10859E 01	0.11402E 01
M I I	0.34018E 00	0.36262E 00	0.38645E 00	0.41257E 00	0.43986E 00	0.46943E 00
M I I I	0.28410E 00	0.29692E 00	0.31022E 00	0.32429E 00	0.33971E 00	0.35786E 00
M I V	0.32169E -01	0.34049E -01	0.36022E -01	0.38123E -01	0.40310E -01	0.42626E -01
M V	0.46603E -01	0.47010E -01	0.51518E -01	0.54159E -01	0.56891E -01	0.59754E -01
N I	0.47017E 00	0.49421E 00	0.51932E 00	0.54661E 00	0.57449E 00	0.60433E 00
N I I	0.17882E 00	0.19106E 00	0.20408E 00	0.21839E 00	0.23327E 00	0.24745E 00
N I I I	0.15138E 00	0.15970E 00	0.16630E 00	0.17435E 00	0.18263E 00	0.19132E 00
N I V	0.18372E -01	0.19527E -01	0.20742E -01	0.22040E -01	0.23394E -01	0.24831E -01
N V	0.26699E -01	0.29205E -01	0.29778E -01	0.31438E -01	0.33162E -01	0.34972E -01
N V I	0.11584E -02	0.12463E -02	0.13177E -02	0.14395E -02	0.15449E -02	0.16569E -02
N V I I	0.19411E -02	0.20923E -02	0.22715E -02	0.23905E -02	0.25577E -02	0.27357E -02
N I	0.23925E 00	0.24257E 00	0.26671E 00	0.28193E 00	0.29752E 00	0.31420E 00
N I I	0.89601E -01	0.95209E -01	0.10255E 00	0.10997E 00	0.11807E 00	0.12686E 00
N I I I	0.74587E -01	0.79589E -01	0.82745E -01	0.87135E -01	0.91654E -01	0.96401E -01
N I V	0.84260E -02	0.90304E -02	0.96671E -02	0.10346E -01	0.11056E -01	0.11810E -01
N V	0.17221E -01	0.12999E -01	0.13913E -01	0.14671E -01	0.15564E -01	0.16503E -01
N V I	0.40021E -03	0.44077E -03	0.48370E -03	0.52957E -03	0.57811E -03	0.62986E -03
N V I I	0.65359E -03	0.71010E -03	0.79783E -03	0.86069E -03	0.93711E -03	0.10163E -02
N V I I I	0.43218E -05	0.45721E -05	0.48331E -05	0.51159E -05	0.54055E -05	0.57155E -05

TABLE 2.10. Relations between form-factor coefficients and nuclear matrix elements in Cartesian notation. (After Behrens and Jänecke, 1969; Bühring, 1963b; Bühring and Schülke, 1965.)

Type of transition	Form-factor coefficient	Matrix element in Cartesian notation
Allowed	$V_{F000}^{(0)}$	$\int 1.$
	$A_{F101}^{(0)}$	$-\lambda \int \vec{\sigma}$
First forbidden nonunique	$A_{F000}^{(0)}$	$\lambda \int \gamma_5$
	$A_{F011}^{(0)}$	$\lambda \int i \frac{\vec{\sigma} \cdot \vec{r}}{R}$
	$A_{F011}^{(0)}(1,1,1,1)$	$\lambda \int i \frac{\vec{\sigma} \cdot \vec{r}}{R} I(1,1,1,1;r)$
	$V_{F101}^{(0)}$	$\int \vec{\alpha}$
	$V_{F110}^{(0)}$	$\sqrt{3} \int i \frac{\vec{r}}{R}$
	$V_{F110}^{(0)}(1,1,1,1)$	$\sqrt{3} \int i \frac{\vec{r}}{R} I(1,1,1,1;r)$
	$A_{F111}^{(0)}$	$-\lambda(3/2)^{1/2} \int \frac{\vec{\sigma} \cdot \vec{r}}{R}$
	$A_{F111}^{(0)}(1,1,1,1)$	$-\lambda(3/2)^{1/2} \int \frac{\vec{\sigma} \cdot \vec{r}}{R} I(1,1,1,1;r)$
	$A_{F211}^{(0)}$	$-\lambda \sqrt{3/2} \int \frac{iB_{ij}}{R}$

TABLE 2:10. Continued.

Type of transition	Form-factor coefficient	Matrix element in Cartesian notation
L^{th} forbidden nonunique	$V_{F_{LLO}}^{(0)}$	$\left(\frac{(2L+1)!!}{L!}\right)^{\frac{1}{2}} \int \frac{i^{L-1} R_{i_1 \dots i_L}}{R^L}$
	$V_{F_{LLO}}^{(0)}(k, l, l, l)$	$\left(\frac{(2L+1)!!}{L!}\right)^{\frac{1}{2}} \int \frac{i^{L-1} R_{i_1 \dots i_L}}{R^L} I(k, l, l, l; r)$
	$V_{F_{L, L-1, l}}^{(0)}$	$\frac{1}{L!} \left(\frac{(2L-1)!!}{(L-1)!}\right)^{\frac{1}{2}} \int \frac{i^{L-1} A_{i_1 \dots i_L}}{R^{L-1}}$
	$A_{F_{LlL}}^{(0)}$	$\lambda \frac{1}{L!} \left(\frac{(2L+1)!!}{L!} \frac{L}{L+1}\right)^{\frac{1}{2}} \int \frac{i^{L+1} T_{i_1 \dots i_L}}{R^L}$
	$A_{F_{LlL}}^{(0)}(k, l, l, l)$	$\lambda \frac{1}{L!} \left(\frac{(2L+1)!!}{L!} \frac{L}{L+1}\right)^{\frac{1}{2}} \int \frac{i^{L+1} T_{i_1 \dots i_L}}{R^L} I(k, l, l, l; r)$
	$A_{F_{L+1, L, l}}^{(0)}$	$-\lambda \frac{1}{(L+1)!} \left(\frac{(2L+1)!!}{L!}\right)^{\frac{1}{2}} \int \frac{i^{L+1} B_{i_1 \dots i_{L+1}}}{R^L}$
First forbidden unique	$A_{F_{211}}^{(0)}$	$-\lambda \sqrt{3/2} \int \frac{i^2 B_{ij}}{R}$
$(L-1)^{\text{st}}$ forbidden unique	$A_{F_{L, L-1, l}}^{(0)}$	$-\lambda \frac{1}{L!} \left(\frac{(2L-1)!!}{(L-1)!}\right)^{\frac{1}{2}} \int \frac{i^{L-1} B_{i_1 \dots i_L}}{R^{L-1}}$

Table 2.11. Exchange and overlap correction factors E_{ij} for 1- α 100-
 'ron capture and $Z^{1/3}$ for 1/j capture ratios, recalculated with the
 Hartree-Fock code of Froese-Fischer. Columns labeled "W" are calcu-
 lated according to the approach of Vekal; columns labeled "P" are
 calculated with Sobel's formulas. In both approaches, the effect
 of the hole in the daughter atom has been included. Asterisks indicate
 the elements for which the calculations were performed ab initio;
 the remaining factors were determined by a 4-point Lagrangian inter-
 polation procedure. (K. S. Chen, private communication).

Z	B(K)		E(L1)		B(M1)		o(N1)		X(L1/K)		X(M1/L1)		X(N1/M1)		
	V	B	V	B	V	B	V	B	V	B	V	B	V	B	
4*	.816	.900	2.222	3.045						2.723	3.363				
5	.806	.924	1.875	2.432						2.104	2.633				
6	.903	.941	1.636	2.009						1.611	2.134				
7*	.928	.954	1.482	1.738						1.547	1.622				
8	.944	.962	1.391	1.586						1.474	1.642				
9	.953	.967	1.341	1.496						1.408	1.547				
10*	.957	.970	1.309	1.444						1.368	1.494				
11	.979	.971	1.272	1.399						1.327	1.441				
12*	.961	.972	1.209	1.309	1.551	2.134				1.256	1.347	1.366	1.630		
13	.964	.973	1.185	1.272	1.541	1.960				1.230	1.307	1.300	1.541		
14	.966	.974	1.167	1.242	1.463	1.829				1.208	1.275	1.255	1.473		
15*	.968	.975	1.152	1.219	1.411	1.733				1.190	1.250	1.225	1.422		
16	.970	.976	1.140	1.200	1.375	1.661				1.170	1.230	1.206	1.383		
17	.972	.977	1.130	1.181	1.346	1.603				1.163	1.213	1.193	1.353		
18*	.973	.978	1.121	1.171	1.322	1.549				1.152	1.197	1.179	1.323		
19	.974	.979	1.111	1.157	1.288	1.488				1.140	1.162	1.160	1.287		
20*	.975	.980	1.099	1.141	1.239	1.414	1.593	2.130		1.127	1.154	1.127	1.239	1.286	1.506
21	.976	.981	1.090	1.133	1.239	1.390				1.117	1.155	1.133	1.227		
22	.977	.981	1.084	1.125	1.230	1.369				1.109	1.147	1.135	1.217		
23*	.978	.982	1.078	1.119	1.225	1.350	1.334	1.800		1.103	1.140	1.135	1.206	1.093	1.333
24	.979	.983	1.076	1.113	1.220	1.333	1.329	1.746	1.079	1.133	1.134	1.197	1.090	1.312	
25	.979	.983	1.074	1.108	1.214	1.317	1.318	1.700	1.096	1.127	1.131	1.189	1.086	1.291	
26*	.980	.984	1.072	1.103	1.208	1.303	1.308	1.658	1.094	1.121	1.127	1.181	1.083	1.272	
27	.981	.985	1.071	1.098	1.202	1.290	1.297	1.621	1.092	1.116	1.123	1.175	1.079	1.256	
28	.981	.985	1.069	1.094	1.197	1.279	1.287	1.588	1.090	1.110	1.119	1.169	1.076	1.242	
29	.982	.986	1.067	1.090	1.191	1.266	1.276	1.561	1.087	1.105	1.116	1.164	1.071	1.231	
30*	.983	.986	1.064	1.087	1.186	1.258	1.265	1.538	1.082	1.100	1.115	1.159	1.067	1.223	
31	.984	.987	1.063	1.083	1.174	1.243	1.250	1.519	1.080	1.098	1.105	1.147	1.071	1.222	
32*	.985	.987	1.061	1.081	1.164	1.230	1.252	1.499	1.077	1.095	1.097	1.138	1.076	1.219	
33	.986	.987	1.059	1.078	1.155	1.219	1.247	1.479	1.075	1.092	1.091	1.130	1.079	1.213	
34	.986	.988	1.057	1.075	1.147	1.209	1.242	1.459	1.072	1.089	1.085	1.124	1.083	1.207	
35	.986	.988	1.055	1.072	1.140	1.200	1.236	1.439	1.070	1.085	1.081	1.119	1.086	1.199	
36*	.986	.988	1.053	1.069	1.134	1.192	1.234	1.420	1.068	1.082	1.077	1.115	1.088	1.191	
37	.986	.988	1.051	1.066	1.128	1.185	1.230	1.402	1.066	1.079	1.074	1.111	1.090	1.184	
38	.986	.988	1.049	1.064	1.123	1.177	1.226	1.386	1.063	1.070	1.071	1.107	1.092	1.177	
39	.986	.989	1.047	1.061	1.117	1.170	1.221	1.371	1.061	1.074	1.067	1.102	1.093	1.171	
40*	.987	.990	1.045	1.060	1.112	1.162	1.216	1.359	1.059	1.072	1.064	1.096	1.094	1.170	
41	.987	.989	1.043	1.058	1.108	1.157	1.211	1.347	1.057	1.069	1.062	1.093	1.093	1.164	
42	.988	.990	1.042	1.056	1.105	1.152	1.206	1.335	1.055	1.067	1.060	1.091	1.091	1.159	
43	.988	.990	1.041	1.054	1.102	1.147	1.201	1.324	1.054	1.065	1.058	1.088	1.090	1.154	
44*	.988	.990	1.040	1.053	1.099	1.143	1.196	1.314	1.053	1.064	1.057	1.089	1.088	1.150	
45	.988	.990	1.039	1.052	1.097	1.139	1.191	1.304	1.052	1.062	1.055	1.083	1.086	1.145	
46	.988	.991	1.038	1.050	1.094	1.135	1.187	1.295	1.051	1.060	1.054	1.081	1.085	1.141	
47	.989	.991	1.036	1.049	1.092	1.132	1.182	1.287	1.050	1.059	1.052	1.078	1.083	1.137	
48*	.989	.991	1.037	1.046	1.090	1.128	1.178	1.279	1.045	1.058	1.051	1.076	1.081	1.134	
49	.989	.991	1.036	1.047	1.088	1.125	1.174	1.271	1.047	1.056	1.050	1.074	1.079	1.130	
50	.990	.991	1.035	1.045	1.086	1.121	1.169	1.264	1.046	1.055	1.049	1.073	1.077	1.127	
51*	.990	.991	1.034	1.044	1.083	1.118	1.165	1.257	1.044	1.053	1.047	1.071	1.076	1.124	
52	.990	.991	1.033	1.042	1.080	1.115	1.161	1.250	1.043	1.052	1.046	1.069	1.074	1.122	
53	.990	.991	1.031	1.041	1.077	1.111	1.156	1.244	1.042	1.050	1.044	1.067	1.073	1.119	
54*	.990	.991	1.030	1.039	1.074	1.107	1.151	1.237	1.040	1.048	1.043	1.065	1.072	1.117	

FOLOUT FRAME

12a
 TABLE 2.A Comparison of published exchange and overlap corrections (B_K)
 for selected values of Z.

		Exchange and overlap corrections B_K					Recalculated in this work as described in Sec. 2.5 after :	
Z	El.	Bahcall (1963)	Vatai (1970)	Martin and Blichert-Toft (1970)	Suslov (1970)	Bahcall	Vatai	
4	Be					0.900	0.816	
5	B					0.924	0.866	
6	C			0.938		0.941	0.903	
7	N			0.948		0.954	0.928	
8	O			0.958		0.962	0.944	
9	F			0.964		0.967	0.953	
10	Ne			0.969		0.970	0.957	
11	Na			0.973		0.971	0.959	
12	Mg			0.974		0.972	0.961	
13	Al		0.987	0.975		0.973	0.964	
14	Si	0.924	0.988	0.976	0.9231	0.974	0.966	
15	P	0.939	0.988	0.977	0.9391	0.975	0.968	
16	S	0.947	0.988	0.978	0.9479	0.976	0.970	
17	Cl	0.954	0.988	0.979	0.9542	0.977	0.972	
18	Ar	0.959	0.988	0.980	0.9589	0.978	0.973	
19	K	0.963	0.988	0.981	0.9600	0.979	0.974	
20	Ca	0.966	0.989	0.982	0.9650	0.980	0.975	
25	Mn	0.976	0.990	0.985	0.9731	0.983	0.979	
30	Zn	0.981	0.991	0.987	0.9794	0.986	0.983	
35	Br	0.983	0.992	0.989	0.9822	0.988	0.986	
40	Zr			0.990	0.9844	0.989	0.987	
50	Sn			0.991	0.9878	0.991	0.990	
60	Nd			0.992	0.9888			
70	Yb			0.992	0.9896			
80	Hg			0.992	0.9898			
90	Th			0.992	0.9899			

12b
 TABLE 2.A Comparison of published exchange and overlap corrections (B_L)
 for selected values of Z

Z	El	Exchange and overlap corrections				B_{L_1}		B_{L_2}, B_{L_3}
		Bahcall (1963)	Vatai (1970)	Martin and Blichert-Toft (1970)	Suslov (1970)	Recalculated in this work as described in Sec. 2.5 after :		Martin and Blichert-Toft (1970)
						Bahcall	Vatai	
4	Be					3.045	2.222	
5	B					2.432	1.875	
6	C					2.009	1.636	
7	N			1.475		1.738	1.482	
8	O			1.405		1.580	1.391	
9	F			1.360		1.496	1.341	
10	Ne			1.309		1.449	1.309	
11	Na			1.283		1.399	1.272	
12	Mg			1.248		1.309	1.209	
13	Al		1.250	1.212		1.272	1.185	
14	Si	1.199	1.229	1.186	1.205	1.242	1.167	0.921
15	P	1.193	1.211	1.169	1.189	1.219	1.152	0.929
16	S	1.181	1.196	1.154	1.179	1.200	1.140	0.935
17	Cl	1.172	1.183	1.143	1.168	1.185	1.130	0.940
18	Ar	1.162	1.170	1.132	1.159	1.171	1.121	0.944
19	K	1.153	1.158	1.120	1.150	1.157	1.111	0.946
20	Ca	1.145	1.149	1.113	1.140	1.141	1.099	0.948
25	Mn	1.112	1.116	1.085	1.108	1.108	1.074	0.958
30	Zn	1.090	1.095	1.070	1.090	1.085	1.067	0.967
35	Br	1.075	1.077	1.060	1.075	1.072	1.055	0.971
40	Zr			1.050	1.064	1.060	1.045	0.974
50	Sn			1.037	1.050	1.045	1.035	0.978
60	Nd			1.029	1.040			0.980
70	Yb			1.025	1.035			0.981
80	Hg			1.022	1.031			0.982
90	Th			1.021	1.028			0.982

TABLE 2. Comparison of published exchange and overlap corrections
(B_M and B_N) for selected values of Z

		Exchange and overlap corrections B_{M_1}					B_N				
Z	El	Bahcall (1963)	Vatai (1970)	Martin and Bichert-Toft (1970)	Suslov (1970)	Recalculated in this work as described in Sec. 2.5 after		Vatai (1970)	Recalculated in this work as described in Sec.2.5 after		
						Bahcall	Vatai			Bahcall	Vatai
4	Be										
5	B										
6	C										
7	N										
8	O										
9	F										
10	Ne										
11	Na										
12	Mg					2.134	1.651				
13	Al		1.432	1.628		1.960	1.541				
14	Si	1.804	1.408	1.510	1.769	1.829	1.463				
15	P	1.711	1.385	1.434	1.686	1.733	1.411				
16	S	1.639	1.369	1.388	1.621	1.661	1.375				
17	Cl	1.579	1.346	1.358	1.567	1.603	1.348				
18	Ar	1.530	1.327	1.328	1.522	1.549	1.322				
19	K	1.489	1.315	1.285	1.486	1.489	1.288				
20	Ca	1.454	1.299	1.255	1.453	1.414	1.239		2.139	1.593	
25	Mn	1.335	1.241	1.226	1.339	1.317	1.214	1.283	1.700	1.318	
30	Zn	1.266	1.202	1.190	1.273	1.258	1.186	1.236	1.538	1.265	
35	Br	1.222	1.170	1.150		1.200	1.140	1.215	1.459	1.238	
40	Zr			1.121		1.162	1.112		1.359	1.216	
50	Sn			1.093		1.121	1.086		1.264	1.169	
60	Nd			1.070							
70	Yb			1.062							
80	Hg			1.056							
90	Th			1.051							

12d
 TABLE 2. Comparison of exchange and overlap corrections for L/K ratios

		Exchange and overlap corrections $X^{L/K}$						Recalculated in this work as described in Sec. 2.5 after:	
Z	El	Bahcall (1963)	Vatai (1970)	Martin and Blichert-Toft (1970)	Suslov (1970)	Faessler et al. (1970)	Faessler et al. (1970)*	Bahcall	Vatai
4	Be					3.504	2.947	3.383	2.723
5	B							2.633	2.164
6	C							2.134	1.811
7	N			1.556				1.822	1.597
8	O			1.467				1.642	1.474
9	F			1.411				1.547	1.408
10	Ne			1.351				1.494	1.368
11	Na			1.319				1.441	1.327
12	Mg			1.281				1.347	1.258
13	Al		1.266	1.243				1.307	1.230
14	Si	1.298	1.244	1.215	1.293			1.275	1.208
15	P	1.271	1.226	1.197	1.266			1.250	1.190
16	S	1.248	1.210	1.180	1.243			1.230	1.176
17	Cl	1.228	1.197	1.168	1.224			1.213	1.163
18	Ar	1.212	1.184	1.155	1.208	1.207	1.195	1.197	1.152
19	K	1.197	1.171	1.142	1.194			1.182	1.140
20	Ca	1.184	1.162	1.133	1.181			1.164	1.127
25	Mn	1.139	1.127	1.102	1.139	1.135	1.127	1.127	1.096
30	Zn	1.112	1.104	1.084	1.113	1.110	1.103	1.100	1.082
35	Br	1.093	1.085	1.072	1.094			1.085	1.070
40	Zr			1.061	1.081			1.072	1.059
50	Sn			1.046	1.063			1.055	1.046
60	Nd			1.037	1.052				
70	Yb			1.033	1.046				
80	Hg			1.030	1.042				
90	Th			1.029	1.038				

* Takes into account rearrangement in final state

TABLE 2.A Comparison of exchange and overlap corrections for M/L ratios

Z	El	Exchange and overlap corrections $X^{M/L}$					Recalculated in this work as described in Sec. 2.5 after		
		Bahcall	Vatai	Martin and Blichert-Toft	Suslov	Faessler et al.	Faessler et al.	Bahcall	Vatai
		(1963)	(1970)	(1970)	(1970)	(1970)	(1970)*		
10	Ne								
11	Na								
12	Mg							1.630	1.366
13	Al	1.584	1.146	1.343				1.541	1.300
14	Si	1.505	1.146	1.273	1.482			1.473	1.255
15	P	1.433	1.144	1.227	1.419			1.422	1.225
16	S	1.387	1.140	1.203	1.375			1.383	1.206
17	Cl	1.347	1.138	1.188	1.341			1.353	1.193
18	Ar	1.316	1.134	1.173	1.314	1.311	1.289	1.323	1.179
19	K	1.291	1.137	1.147	1.292			1.287	1.160
20	Ca	1.270	1.123	1.128	1.275			1.239	1.127
25	Mn	1.201	1.112	1.130	1.209	1.190	1.178	1.189	1.131
30	Zn	1.161	1.098	1.112	1.168	1.153	1.147	1.159	1.115
35	Br	1.137	1.086	1.085	1.143			1.119	1.081
40	Zr			1.068	1.126			1.094	1.061
50	Sn			1.054	1.101			1.073	1.049
60	Nd			1.040	1.086				
70	Yb			1.036	1.076				
80	Hg			1.033	1.070				
90	Th			1.029	1.066				

* Takes into account rearrangement in final state

12f
 TABLE 2. Comparison of exchange and overlap corrections for N/M ratios

Z	El	Vatai (1970)	Recalculated in this work as described in Sec. 2.5 after :	
			Bahcall	Vatai
18	Ar			
19	K			
20	Ca		1.506	1.286
25	Mn	1.034	1.291	1.086
30	Zn	1.028	1.223	1.067
35	Br	1.038	1.199	1.086
40	Zr		1.170	1.094
50	Sn		1.127	1.077
60	Nd			
70	Yb			
80	Hg			
90	Th			

TABLE 3.1 Methods that have been used for the determination of electron capture probabilities.

No.	Method	Source	Detectors ^a	Measured	Deduced	Estimated accuracy of the method (percent)
1	Spectroscopy of K, L and M events without x-ray escape	internal	mw	$I_L/I_K, I_M/I_L$	P_L/P_K	1
		gaseous	NaI(Tl)	$I_{L-\gamma}/I_{K-\gamma}$	P_M/P_L	
2	Spectroscopy of K and L events with complete K x-ray escape	internal	pc	I_L/I_K	P_L/P_K	5
		gaseous				
3	Spectroscopy of K, L and M events	internal	pc	I_L/I_K	P_L/P_K	1
		gaseous		I_M/I_L	P_M/P_L	
4	Cloud chamber technique	internal	cc	I_L/I_K	P_L/P_K	20
		gaseous				
5	Spectroscopy of K, L and M events	internal	NaI(Tl)	I_L/I_K	P_L/P_K	1
		solid	CsI(Tl)	I_M/I_L	P_M/P_L	
			CsI(Na)			
			$Cs_2Pt(CN)_4 \cdot H_2O$ Ge(Li)	$I_{L-\gamma}/I_{K-\gamma}$		
6	Spectroscopy of K and L x rays	external	pc	I_{LX}/I_{KX}	P_L/P_K	10
		solid	NaI(Tl)	$I_{LX-\gamma}/I_{KX-\gamma}$		

TABLE 3.1 (continued)

No.	Method	Source	Detectors ^a	Measured	Deduced	Estimated accuracy of the method (percent)
7	Measurement of (K x-ray)-(L x-ray) coincidences	external	pc	I_{KX-LX}	P_L/P_K	8
		solid	NaI(Tl)	I_{LX}, I_{KX}		
8	Spectroscopy of K x rays and γ rays	external	pc, NaI(Tl)	I_{KX}/I_γ	P_K	8
		solid	Ge(Li)			
9	Spectroscopy of K x rays or K Auger electrons and K conversion electrons	external	sd	I_{KX}/I_{eK}	P_{K^wK}	15
		solid	NaI(Tl)	I_{KA}/I_{eK}		
10	Determination of K x ray emission rate and disintegration rate	external	pc	I_{KX}, I_o	P_{K^wK}	1
		solid	NaI(Tl)			
11	Measurement of (K x-ray)-(γ -ray) coincidences	external	pc, NaI(Tl)	$I_{KX-\gamma}/I_\gamma$	P_{K^wK}	5
		solid	Ge(Li)			
			Si(Li)	$I_{KX-\gamma_1-\gamma_2}/I_{\gamma_1-\gamma_2}$		
12	Measurement of (K x-ray)-(γ -ray) coincidences at different levels	external	NaI(Tl)	$I_{KX-\gamma_1}/I_{\gamma_1}$	P_{K1}/P_{K2}	5
		solid	Ge(Li)			
			Si(Li)	$I_{KX-\gamma_2}/I_{\gamma_2}$		
13	Measurement of (K-event)-(γ -ray) coincidences	external	pc, NaI(Tl)		P_K	3
		solid	CsI(Tl)	$I_{K-\gamma}/I_\gamma$		

TABLE 3.1 (continued)

No.	Method	Source	Detectors. ^a	Measured	Deduced	Estimated accuracy of the method (percent)
14	Measurement of (K x-ray)-(γ-ray)sum coincidences.	external solid	NaI(Tl) CsI(Tl) Ge(Li)	$I_{KX+\gamma}/I_{\gamma}$ $I_{KX+\gamma 1+\gamma 2}/I_{\gamma 1+\gamma 2}$	$P_{K^w K}$	8.
15	Measurement of (K x-ray)-(γ-ray) and (K x-ray)-(K x-ray) or (K x-ray)-(K conversion electron) coincidences	external solid	NaI(Tl) Si(Li) sd	$I_{KX-\gamma}/I_{\gamma}$ I_{KX-KX}/I_{KX} I_{KX-eK}/I_{eK}	P_K	3
16	Measurement of (K x-ray)-(K conversion electron) and (K x-ray)-(L conversion electron) coincidences	external solid	NaI(Tl) sd	I_{KX-eK}/I_{eK} I_{KX-eL}/I_{eL}	P_K	3
17	Measurement of (K Auger electron)-(K conversion electron) and (K Auger electron)-(L conversion electron) coincidences	external solid	sd, sl	I_{KA-eK}/I_{eK} I_{KA-eL}/I_{eL}	P_K	3
18	Measurement of (K x-ray)-(K conversion electron) coincidences	external solid	pc, sc NaI(Tl) Ge(Li)	I_{KX-eK}/I_{eK} I_{KX-eK}/I_{KX} $I_{eK} I_{KX}$	$P_{K^w K}$ P_K	5 7

TABLE 3.1 (continued)

No.	Method	Source	Detectors ^a	Measured	Deduced	Estimated accuracy of the method (percent)
19	Measurement of (K x-ray)-(γ-ray)- (K or L conversion electron) coincidences	external	NaI(Tl)	$I_{KX-\gamma-e_L} / I_{\gamma-e_L}$	$P_{K^w K}$	5
		solid	Ge(Li) sd	$I_{KX-\gamma-e_K} / I_{\gamma-e_K}$	P_K	
20	Spectroscopy of K events and positrons (no K x ray escape)	internal gaseous	pc	I_K / I_{β^+}	P_K / P_{β^+}	6
21	Spectroscopy of K events and positrons (no K x ray escape)	internal gaseous	apc	I_K / I_{β^+}	P_K / P_{β^+}	3
22	Spectroscopy of K events and positrons	internal solid	NaI(Tl)	I_K / I_{β^+}	P_K / P_{β^+}	2
23	Spectroscopy of K Auger electrons and positrons	external solid	gm, pc	I_{KA} / I_{β^+}	P_K / P_{β^+}	9
24	Spectroscopy of K x rays and positrons	external solid	NaI(Tl), Si(Li), pc	I_{KX} / I_{β^+}	P_K / P_{β^+}	1
25	Spectroscopy of K x rays and β^+ annihilation photons	external solid	NaI(Tl), Si(Li), pc, Ge(Li)	I_{KX} / I_{511}	P_K / P_{β^+}	1.5

ORIGINAL PAGE IS
OF POOR QUALITY

TABLE 3.1 (continued)

No.	Method	Source	Detectors ^a	Measured	Deduced	Estimated accuracy of the method (percent)
26	Spectroscopy of nuclear and β^+ annihilation photons	external solid	NaI(Tl), Ge(Li)	I_{γ} / I_{511}	P_{EC} / P_{β^+}	3
27	Measurement of (positron)-(γ ray) coincidences	external solid	pc, pl NaI(Tl), Ge(Li)	$I_{\gamma} \cdot I_{\beta-\gamma}$	P_{EC} / P_{β^+}	2.5
28	Measurement of (positron)-(γ ray)N and (positron)-(γ ray)S coincidences	external solid	pc, NaI(Tl)	$I_{\beta^+} \cdot I_{\gamma N} \cdot I_{\gamma S}$ $I_{\beta^+ \gamma N} \cdot I_{\beta^+ \gamma S}$	P_{EC} / P_{β^+}	0.3
29	Measurement of (γ ray)-511 keV γ -(511 keV γ) triple coincidences	external solid	NaI(Tl)Ge(Li)	$I_{\gamma} \cdot I_{\text{triple}}$	P_{EC} / P_{β^+}	2
30	Measurement of (γ ray)-511 keV β^+ annihilation, photon coincidences	external solid	NaI(Tl), Ge(Li)	$I_{\gamma} \cdot I_{\gamma-511}$	P_{EC} / P_{β^+}	3
31	Miscellaneous	-	-	-	-	-

^a The following abbreviations are used: apc, anticoincidence proportional counter; cc, cloud chamber; gm, Geiger-Müller counter; pc, proportional counter; pl, plastic scintillator; mw, multi-wire proportional counter; sc, semiconductor; sd, double-focussing spectrometer; se, lens spectrometer.

TABLE 3.2 Experimental electron capture values

Z	Q_{EC} A (keV) ^a	Final state (keV)	$J_i^{\pi_i} \rightarrow J_f^{\pi_f}$	P_L/P_K	P_M/P_L	$P_{LM..}/P_K$	P_{K^wK} ^b	P_K	Me- thod ^c	Reference
17 Cl	36 1144	0	$2^+ - 0^+$	0.112 \pm 0.008					1	Dougan(1962b)
18 Ar	37 814	0	$\frac{3^+}{2} - \frac{3^+}{2}$	0.092 \pm 0.010					2	Langevin(1955c)
				-0.005					2	Kiser(1959)
				0.102 \pm 0.008					1	Santos-Ocampo(1960)
				0.103 \pm 0.003					1	Manduchi(1961)
				0.0971 \pm 0.0005					1	Dougan(1962a)
				0.102 \pm 0.004					1	Winter(1964)
				0.102 \pm 0.003					1	Heuer(1966)
				0.097 \pm 0.003					1	Totzek(1967)
				0.098 \pm 0.003					3	Renier(1968)
				0.104 \pm 0.007						
				-0.003						
				0.098 \pm 0.002					1	Krahn(1972)
19 K	40 1505	1460;0	$4^- - 2^+, 0^+$			1.34 \pm 0.35			8	Heintze(1954)
						0.34 \pm 0.08			5	McCann(1967)
						0.44 \pm 0.09			8	Azman(1968)
23 V	48 4015	several	$4^+ - 4^+$	0.104 \pm 0.004					1	Bertmann(1972)
				0.115 \pm 0.015					1	Bertmann(1972)
23 V	49 601	0.	$\frac{7^-}{2} - \frac{7^-}{2}$	0.106 \pm 0.004			0.2005 \pm 0.0030		11	Albrecht(1975)
									1	Krahn(1972)

TABLE 3.2 (continued)

Z	A	Q_{EC}^a (keV)	Final state (keV)	$J_i^{\pi_i} \rightarrow J_f^{\pi_f}$	P_L/P_K	P_M/P_L	$P_{LM..}/P_K$	$P_{K^w}^b$	P_K	Me- thod	Reference			
24	Cr	51	751	320;0	$\frac{7^-}{2} \rightarrow \frac{5^-}{2}, \frac{7^-}{2}$	0.10 \pm 0.02	0.1026 \pm 0.0004			7	Konstantinov(1961)			
										1	Fasioli(1962)			
										320	$\frac{7^-}{2} \rightarrow \frac{5^-}{2}$	0.227 \pm 0.003	10	Taylor(1963)
										320		0.1044 \pm 0.0021	1	Heuer(1966)
										320;0		0.1033 \pm 0.0031	1	Heuer(1966)
			320			0.196 \pm 0.016	11	Mukerji(1967b)						
25	Mn	54	1374	835.5	$3^+ \rightarrow 2^+$	0.098 \pm 0.006	0.106 \pm 0.003			0.901 \pm 0.006	13	Kramer(1962a)		
											1	Moler(1963)		
											0.257 \pm 0.004	10	Taylor(1963)	
											0.106 \pm 0.003	1	Manduchi(1963)	
											0.243 \pm 0.012	10	Leistner(1965)	
											0.2514 \pm 0.0017	10	Bambynek(1967a)	
											0.250 \pm 0.005	10	Petel(1967)	
											0.2492 \pm 0.0017	11	Hammer(1968)	
											0.900 \pm 0.014	10	Dobrilović(1972)	
											0.247 \pm 0.009	11	Mukerji(1973)	

TABLE 3.2 (continued)

Z	Q_{EC} ^a A (keV)	Final state (keV)	$J_i^{\pi} \rightarrow J_f^{\pi}$	P_L/P_K	P_M/P_L	$P_{LM}./P_K$	$P_{K^w_K}$ ^b	P_K	Me- thod ^c	Reference	
26 Fe	55 232	0	$\frac{3^-}{2} \rightarrow \frac{5^-}{2}$	0.108 \pm 0.006					1	Scobie(1959)	
				0.106 \pm 0.003					1	Manduchi(1962a)	
				0.106 \pm 0.005					1	Moler(1963)	
				0.117 \pm 0.001	0.157 \pm 0.003				1	Pengra(1972)	
27 Co	57 837	136	$\frac{7^-}{2} \rightarrow \frac{5^-}{2}$			0.20 \pm 0.13			9	Moussa (1956)	
							0.254 \pm 0.011		11	Kramer(1962a)	
				136					1	Moler(1963)	
				136;706	$\frac{7^-}{2} \rightarrow \frac{5^-}{2}; \frac{5^-}{2}$	0.099 \pm 0.011					
				136			0.262 \pm 0.008		11	Thomas(1963)	
				136			0.3044 \pm 0.0043		11	Rubinson(1968)	
				136			0.15 \pm 0.02		0.87 \pm 0.02 ⁺	11	Bosch(1969)
27 Co	58 2308	1675;810	$2^+ \rightarrow 2^+; 2^+$	0.107 \pm 0.004					1	Moler(1963)	
							0.3050 \pm 0.0022		10	Bambynek(1968b)	
28 Ni	56 2133	1720	$0^+ \rightarrow 1^+$	0.115 \pm 0.006					1	Winter(1967)	
28 Ni	57 3243	several		0.100 \pm 0.006					1	Winter(1967)	
28 Ni	59 1073	0	$\frac{3^-}{2} \rightarrow \frac{7^-}{2}$	0.121 \pm 0.002					1	Chew(1974a)	

ORIGINAL PAGE IS
OF POOR QUALITY

TABLE 3.2 (continued)

Z	Q_{EC} ^a A (keV)	Final state (keV)	$J_i^\pi \rightarrow J_f^\pi$	P_L/P_K	P_M/P_L	$P_{LM..}/P_K$	P_{K^0K} ^b	P_K	Me- thod ^c	Reference
30 Zn	65 1350	1115	$\frac{5^-}{2} \rightarrow \frac{5^-}{2}$				0.369 \pm 0.023		11	Perrin(1960)
		1115;0	$\frac{5^-}{2} \rightarrow \frac{5^-}{2}, \frac{3^-}{2}$	0.13 \pm 0.002					7	Konstantinov(1961)
		1115;0		0.119 \pm 0.007					1	Santos-Ocampo(1962)
		1115						0.878 \pm 0.006	13	Kramer(1962a)
		1115;0					0.400 \pm 0.006		10	Taylor(1963)
		1115;0		0.111 \pm 0.006					1	Totzek(1967)
		1115		0.117 \pm 0.007					5	McCann(1968)
		1115					0.3927 \pm 0.0026		11	Hammer(1968)
		1115;0					0.3894 \pm 0.0016		10	Bambynek(1968a)
		1115;0		0.118 \pm 0.003					1	Krafft(1970)
		1115		0.120 \pm 0.003	0.153 \pm 0.020				1	Krafft(1970)
		1115					0.386 \pm 0.010		11	Mukerji(1973)
32 Ge	71 235	0	$\frac{1^-}{2} \rightarrow \frac{3^-}{2}$	0.30 \pm 0.02					2	Langevin(1956)
				0.116 \pm 0.005					1	Drever(1959)
				0.13 \pm 0.02					7	Konstantinov(1961)
				0.1187 \pm 0.0008	0.142 \pm 0.010				1	Manduchi(1962)
				0.117 \pm 0.001	0.162 \pm 0.003				1	Genz(1971a)
33 As	73 340	67	$\frac{3^-}{2} \rightarrow \frac{1^-}{2}$					0.85 \pm 0.05	16	Kyles(1970)

TABLE 3.2 (continued)

Z	Q_{EC} A (keV)	^a Final state (keV)	$J_i^\pi \rightarrow J_f^\pi$	P_L/P_K	P_M/P_L	$P_{LM..}/P_K$	$P_{K^wK}^b$	P_K	^c Me- thod	Reference
33 As	74 2564	several		0.085 \pm 0.020					2	Scobie(1957)
34 Se	75 865	401	$\frac{5^+}{2} \rightarrow \frac{5^+}{2}$				0.457 0.460 \pm 0.004 0.462 \pm 0.012 0.516 \pm 0.021		11 11 11 11	Perrin(1960) Rao(1966b) Raeside(1969) Chew(1973)
36 Kr	79 1631	several		0.27 \pm 0.09 0.26 \pm 0.03 0.108 \pm 0.005					4 2 1	Radvanyi(1955a) Langevin(1955a) Drever(1959)
36 Kr	81 290	0	$\frac{7^+}{2} \rightarrow \frac{3^-}{2}$	0.146 \pm 0.005					1	Chew(1974b)
37 Rb	83 1038	571;562	$\frac{5^-}{2} \rightarrow \frac{3^-}{2}; \frac{3^-}{2}$	0.121 \pm 0.002					5	Schulz(1967a)
		571		0.128 \pm 0.002					5	Goedbloed(1970 b)
		562		0.132 \pm 0.002		0.164 \pm 0.002			5	Goedbloed(1970b)
37 Rb	84 2680	880	$2^- \rightarrow 2^+$				0.580 \pm 0.025		11	Welker(1955)
				0.116 \pm 0.002					5	Schulz(1967a)
				0.119 \pm 0.002					5	Goedbloed(1970 b)
38 Sr	85 1064	514	$\frac{9^+}{2} \rightarrow \frac{9^+}{2}$					0.88 \pm 0.04 ⁺	11	Bisi(1956 a)
							0.5959 \pm 0.0035		11	Grootheer(1969)
							0.586 \pm 0.003		10	Bambynek(1970)

 ORIGINAL PAGE IS
 OF POOR QUALITY

TABLE 3.2 (continued)

Z	Q_{EC} ^a A (keV)	Final state (keV)	$J_i^\pi \rightarrow J_f^\pi$	P_L/P_K	P_M/P_L	$P_{LM..}/P_K$	$P_{K^w K}$ ^b	P_K	Me- thod ^c	Reference
39 Y	88 3619	2734	$4^- \rightarrow 3^-$				0.6290 ± 0.0032		11	Grootheer(1969)
		2734;1836	$4^- \rightarrow 3^-, 2^+$				0.613 ± 0.004		10	Bambynek(1973)
42 Mo	93 398	30;0	$\frac{5^+}{2} \rightarrow \frac{1^-}{2}, \frac{9^+}{2}$	0.36 ± 0.04					6	Hohmuth(1964)
43 Tc	97 347	0	$\frac{9^+}{2} \rightarrow \frac{5^+}{2}$	0.21 ± 0.14 -0.10					6	Katcoff(1958)
45 Rh	101 554	325;127	$\frac{1^-}{2} \rightarrow \frac{1^-}{2}, \frac{3^+}{2}$				0.65		11	Perrin (1960)
46 Pd	103 553	several					0.56 ± 7		8	Avignon(1953)
							0.95		9	Avignon(1955)
47 Ag	105 1341	344	$\frac{1^-}{2} \rightarrow \frac{1^+}{2}$	0.128 ± 0.003					5	Schulz(1967d)
		1088	$\frac{1^-}{2} \rightarrow \frac{3^-}{2}$	0.152 ± 0.002					5	Schulz(1967d)
48 Cd	109 182	87.7	$\frac{5^+}{2} \rightarrow \frac{7^+}{2}$			0.28 ± 0.03			5	Der Mateosian(1953)
				0.32 ± 0.04					6	Bertolini(1954)
				0.195 ± 0.005		0.228 ± 0.003		0.805 ± 0.027	8	Wapstra(1957)
			0.237 ± 0.015	0.223 ± 0.020	0.267 ± 0.015			5	Leutz(1965)	
					0.26 ± 0.03			2	Moler(1965)	
		0.193 ± 0.003		0.226 ± 0.003			18	Durosini-Etti(1966)		
								5	Goedbloed(1970a)	

TABLE 3.2 (continued)

Z	^a Q _{EC} A (keV)	Final state (keV)	J _i ^π → J _f ^π	P _L /P _K	P _M /P _L	P _{LM..} /P _K	^b P _K ^ω P _K	P _K	^c Method	Reference
49	In 111 826	419	$\frac{9}{2}^+ \rightarrow \frac{7}{2}^+$					0.867 ± 0.007	17	Sparrman(1966)
49	In 114 ^m 1623	1283	$5^+ \rightarrow 4^-$					0.75	11	Perrin(1960)
50	Sn 113 1025	648	$\frac{1}{2}^+ \rightarrow \frac{3}{2}^-$				0.26 +0.09 -0.07		11	Bhatki(1957)
		648						1.01 ± 0.17 ⁺	11	Greenwood(1961)
		648;393	$\frac{1}{2}^+ \rightarrow \frac{3}{2}^-; \frac{1}{2}^-$	0.44 ± 0.04	0.223 ± 0.020 ^g				1	Manduchi(1964)
		393	$\frac{1}{2}^+ \rightarrow \frac{1}{2}^-$	0.16 ± 0.02					18	Durosini-Etti(1966)
		648	$\frac{1}{2}^+ \rightarrow \frac{3}{2}^-$					0.75 ± 0.10 ⁺	11	Bosch(1967)
53	I 125 177 ^q	35.5	$\frac{5}{2}^+ \rightarrow \frac{3}{2}^+$					0.77 ± 0.08	8	Friedlander(1951b)
						0.23 ± 0.03			5	Der Mateosian(1953)
						0.2543 ± 0.0027			5	Leutz(1964)
						0.253 ± 0.005			5	Smith(1966)
							0.685 ± 0.018		11	Karttunen(1969)
							0.699 ± 0.030		11	Tolea(1974)
							0.685 ± 0.012		11	Plch(1974a)

ORIGINAL PAGE IS
OF POOR QUALITY

TABLE 3.2 (continued)

Z	^a Q _{EC} A (keV)	Final state (keV)	J _i ^π → J _f ^π	P _L /P _K	P _M /P _L	P _{LM} /P _K	^b P _K ^w /P _K	P _K	^c Me- thod	Reference
53 I	126 2151	several		0.142					5	Scobie(1958)
54 Xe	127 664	375	$\frac{1}{2}^+ \rightarrow \frac{1}{2}^+$				0.705 ± 0.004		11	Bresesti(1964)
		203	$\frac{1}{2}^+ \rightarrow \frac{3}{2}^+$				0.750 ± 0.016		11	Bresesti(1964)
		375	$\frac{1}{2}^+ \rightarrow \frac{1}{2}^+$				0.53 ± 0.05		11	Winter(1965b)
		375;203;0	$\frac{1}{2}^+ \rightarrow \frac{1}{2}^+; \frac{3}{2}^+; \frac{5}{2}^+$		0.183	± 0.025			1	Winter(1965b)
55 Cs	131 355	0	$\frac{5}{2}^+ \rightarrow \frac{3}{2}^+$	0.153					5	Joshi(1960)
				0.155					5	Schulz(1967a)
							0.734 ± 0.006		11	Plch(1974b)
55 Cs	132 2099	several		0.136					5	Goverse(1974a)
56 Ba	128 700	273	0 ⁺ → 1 ⁻					0.71 ± 0.05 ⁺	11	Goych(1974)
56 Ba	131 1340	696;620		0.135					5	Smith(1963)
56 Ba	133 516 ^h	137	$\frac{1}{2}^+ \rightarrow \frac{1}{2}^+$		0.202				11	Koishi(1955)
							0.219 ± 0.015	0.46 ± 0.05 ⁺	11	Gupta(1958b)
							0.319 ± 0.013	± 0.04	11	Ramaswamy(1960)
									19	Thun(1966)
				0.371					5	Schulz(1967c)
		384	$\frac{1}{2}^+ \rightarrow \frac{3}{2}^+$	0.221					5	Schulz(1967c)

TABLE 3.2 (continued)

Z	^a Q _{EC} A (keV)	Final state (keV)	J _i ^π →J _f ^π	P _L /P _K	P _M /P _L	P _{LM..} /P _K	^b P _K ^w _K	P _K	^c Me- thod	Reference
56 Ba 133	516 ^h	437		0.67 ±0.15					6	McDonnel(1968)
		437				0.45 ±0.04			19	Törnkvist(1968)
		437					0.576±0.038		14	Narang(1968)
		437						0.47 ±0.02 ⁺	6	Bosch(1969)
		437					0.644±0.034		11	Schmidt-Ott(1972)
		384					0.72 ±0.06		11	Schmidt-Ott(1972)
		437						0.76 ±0.06 ⁺	14	Das Mahapatra(1974)
		384						0.87 ±0.014 ⁺	14	Das Mahapatra(1974)
		437;384						0.79 ±0.07 ⁺	14	Das Mahapatra(1974)
		57 La 138	1794	1426	5 ⁻ -2 ⁺			1.4 ±0.25		
58 Ce 134	500	0	0 ⁺ -1 ⁺					0.72 ±0.08	8	Aleksandrov(1972)
58 Ce 139	275	165	$\frac{3}{2}^+ - \frac{5}{2}^+$			0.21			15	Pruett(1954)
		165				0.37 ±0.02			15	Ketelle(1956)
		165						0.83 ±0.04 ⁺	11	Stanford(1960)
		165						0.68 ±0.02	17	Marelius(1967)
		165						0.750±0.010	16	Adamowicz(1968)
		165						0.69 ±0.02	13	Vatai(1968)
		165						0.707±0.018	11	Schmidt-Ott(1972)
		165						0.649±0.017	14	Campbell(1972)
		165						0.639±0.006	11	Bayer(1974) Plch(1975)
		165							0.726±0.010	15
165						0.66±0.06	0.73±0.07	14	Das Mahapatra (1975b)	

ORIGINAL PAGE IS
OF POOR QUALITY

TABLE 3.2 (continued)

Z	Q_{EC} A (keV)	^a Final state (keV)	$J_i^{\pi_i} \rightarrow J_f^{\pi_f}$	P_L/P_K	P_M/P_L	$P_{LM..}/P_K$	$P_{K^u K}$ ^b	P_K	^c Me- thod	Reference
60 Nd	140 470	0	$0^+ - 1^+$	0.8					6	Vitman(1960)
								0.745 ± 0.048	8	Bayer(1972)
61 Pm	145 170 ^h	several		1.8					6	Carey(1958)
		67	$\frac{5^+}{2} - \frac{3^-}{2}$			0.85 ± 0.03			16	Brosi(1959)
		67	$\frac{7^-}{2} - \frac{5^+}{2}$				0.559 ± 0.022		11	Tolea(1974)
		72	$\frac{5^+}{2} - \frac{5^-}{2}$				0.509 ± 0.022		11	Tolea(1974)
62 Sm	145 647 ⁱ	several		2.0					6	Carey(1958)
		492	$\frac{7^-}{2} - \frac{3^+}{2}$			0.61 ± 0.10			15	Brosi(1959)
		61	$\frac{7^-}{2} - \frac{5^+}{2}$			0.20 ± 0.02			16	Brosi(1959)
		several		0.6					6	Vitman(1960)
		492						0.27 ± 0.03 ⁺	11	Myslek(1971)
63 Eu	152 1886 1529	1529	$3^- - 2^-$					0.78	11	Perrin(1960)
		1529						0.79 ± 0.02		Lu(1962)
		1529				0.71 ± 0.08			14	Dasmahapatra(1975a)
		1234	$3^- - 3^+$			0.82 ± 0.10			14	Dasmahapatra(1975a)
		several				0.55 ± 0.02			8	Dasmahapatra(1972)
63 Eu	152 ^m 1935 950	950	$0^- - 1^-$					0.82	11	Perrin(1960)
64 Gd	151 484 ^r 350	350	$\frac{7^-}{2} - \frac{9^-}{2}$				0.664 ± 0.009		11	Genz(1973c)
		307	$\frac{7^-}{2} - \frac{3^+}{2}$				0.754 ± 0.014		11	Genz(1973c)
64 Gd	153 490 ^j	103	$\frac{3^+}{2} - \frac{3^+}{2}$				0.679 ± 0.020		14	Gupta(1956)
		103				0.42			15	Bhattacharjee(1956)
		103					0.543 ± 0.006		14	Bisi(1956 b)
		97;103	$\frac{3^+}{2} - \frac{5^-}{2} - \frac{3^+}{2}$			0.34 ± 0.02			5	Leutz(1960)
		173	$\frac{3^+}{2} - \frac{5^+}{2}$			0.85 ± 0.30			5	Leutz(1960)

TABLE 3.2 (continued)

Z	A	Q_{EC}^a (keV)	Final state (keV)	$J_i^{\pi} \rightarrow J_f^{\pi}$	P_L/P_K	P_M/P_L	$P_{LM..}/P_K$	$P_{K^wK}^b$	P_K	Method	Reference
64	Gd 153	490 ^j	173					0.375±0.022		11	Blok (1962)
			103					0.66 ±0.07		11	Blok(1962)
			97					0.67 ±0.05		11	Blok(1962)
			173					0.35 ±0.03		11	Cretzu(1964)
65	Tb 157	64 ^{*k}	0	$\frac{3^+}{2} \rightarrow \frac{3^-}{2}$	2.64 2.18 2.65 ±0.20					6	Ehat(1962)
										6	Fujiwara(1964)
										6	Naumann(1967)
66	Dy 159	365	0;58	$\frac{3^-}{2} \rightarrow \frac{3^+}{2}; \frac{5^+}{2}$	1.0 ±0.3					6	Grigorev(1958b)
			0;58		0.3 ±0.7 -0.3					6	Vitman(1960)
			58	$\frac{3^-}{2} \rightarrow \frac{5^+}{2}$					0.85 ±0.11 [†]	11	Greenwood(1960)
			0	$\frac{3^-}{2} \rightarrow \frac{3^+}{2}$	0.198±0.009					5	Leiper(1971)
			58	$\frac{3^-}{2} \rightarrow \frac{5^+}{2}$				0.752±0.024		11	Genz(1973c)
67	Ho 160	2920	several		1.2 ±3.8 -1.1					6	Vitman(1966)
68	Er 160	800	60	$0^+ \rightarrow 2^+$					0.795±0.020	8	Aleksandrov(1972)
69	Er 165	371	0	$\frac{5^-}{2} \rightarrow \frac{7^-}{2}$	1.2 ±0.4					6	Grigorev(1958b)
70	Yb 166	260 [*]	82	$2^+ \rightarrow 2^+$				0.68 ±0.06 -0.02		14	Jasinski(1963a)
72	Hf 175	607 [*]	433	$\frac{5^+}{2} \rightarrow \frac{7^+}{2}$				0.64 ±0.04		11	Funke(1965)
			433						0.712±0.008	16	Jasinski(1968)
			343	$\frac{5^+}{2} \rightarrow \frac{5^+}{2}$					0.767±0.030 -0.016	16	Jasinski(1968)

ORIGINAL PAGE IS
OF POOR QUALITY

TABLE 3.2 (continued)

Z	^a Q _{EC} A (keV)	Final state (keV)	J _i ^π → J _f ^π	P _L /P _K	P _M /P _L	P _{LM..} /P _K	^b P _{K^ωK}	P _K	^c Me- thod	Reference
73 Ta	177 1158	1058	$\frac{7}{2}^+ \rightarrow \frac{7}{2}^-$					0.42 ± 0.07 ⁺	16	West(1961)
73 Ta	179 119*	0	$\frac{7}{2}^+ \rightarrow \frac{9}{2}^+$	1.4 ± 0.4					6	Bisi(1956c)
				0.63 ± 0.06					6	Jopson(1961)
74 W	178 89	0	0 ⁺ → 1 ⁺					0.29 ± 0.02	8	Nielsen(1967)
74 W	181 193 ¹	0;6	$\frac{9}{2}^+ \rightarrow \frac{7}{2}^-; \frac{9}{2}^-$	1.54					6	Bisi(1955c)
				0.23 ± 0.05					6	Jopson(1961)
				0.358 ± 0.070					6	Muir(1961)
				0.27 ± 0.05					6	Kao(1966a)
75 Re	183 558*	453	$\frac{5}{2}^+ \rightarrow \frac{3}{2}^-$				0.38 ± 0.07		11	Kuhlmann(1969)
76 Os	185 1015	several		0.35 ± 0.15					6	Miller(1951)
		several		0.38 ± 0.07					6	Johns(1957)
		875	$\frac{1}{2}^- \rightarrow \frac{3}{2}^+$				0.457 ± 0.008		11	Bisi(1957)
		873;878	$\frac{1}{2}^- \rightarrow \frac{3}{2}^+; \frac{1}{2}^+$	0.600 ± 0.006					5	Schulz(1967a)
		646	$\frac{1}{2}^- \rightarrow \frac{1}{2}^+$	0.228 ± 0.004	0.254 ± 0.005				5	Schulz(1967a)
77 Ir	192 1050	691	4 ⁻ → 3 ⁺				0.67 ± 0.06		14	Dasmahapatra(1975)

TABLE 3.2 (continued)

Z	Q_{EC} ^a A (keV)	Final state (keV)	$J_i^\pi \rightarrow J_f^\pi$	P_L/P_K	P_M/P_L	$P_{LM..}/P_K$	P_{K^wK} ^b	P_K	Me- thod ^c	Reference	
78 Pt 188 540*		195	$0^+ - 1^-$					0.744±0.020	16	Hanson(1968)	
		187	$0^+ - 1^-$					0.766±0.023	16	Hanson(1968)	
78 Pt 193 61		0	$\frac{1}{2}^- - \frac{3}{2}^+$		0.386±0.014				5	Ravn(1971)	
79 Au 195 229*		130	$\frac{3}{2}^+ - \frac{5}{2}^-$				0.143±0.019		11	Bisi(1959, 1954)	
		130					0.146±0.010		11	Goedbloed(1964)	
		130					0.188±0.005		11	De Wit(1965)	
		130					0.123±0.009		11	Harris(1965)	
		99	$\frac{3}{2}^+ - \frac{3}{2}^-$				0.38 ±0.09		11	Harris(1965)	
		99							0.458±0.012	16	Jasinski(1968)
		99			0.873±0.044	0.478±0.020 ^P	1.28 ±0.06		0.438±0.011	5	Goverse(1973)
		130			3.055±0.086	0.697±0.078 ^P	5.25 ±0.66		0.160±0.017	5	Goverse(1973)
79 Au 196 1482		0	$\frac{3}{2}^+ - \frac{1}{2}^-$	0.337±0.007					5	Goverse(1973)	
		689	$2^- - 2^+$		0.31 ±0.05				14	Gupta(1958a)	
80 Hg 197 684 ^m		268	$\frac{1}{2}^- - \frac{3}{2}^+$				0.52 ±0.06		11	De Wit(1965)	
		268;77	$\frac{1}{2}^- - \frac{3}{2}^+; \frac{1}{2}^+$				0.741±0.012		18	Plch(1971)	

TABLE 3.2 (continued)

Z	Q_{EC} A (keV) ^a	Final state (keV)	$J_i^\pi \rightarrow J_f^\pi$	P_L/P_K	P_M/P_L	$P_{LM..}/P_K$	$P_K^{w_K}$ ^b	P_K	Me- thod ^c	Reference
81	Tl 201 484 ⁿ	167	$\frac{1}{2}^+ \rightarrow \frac{1}{2}^+$				0.67 \pm 0.04		11	Gupta(1960)
81	Tl 202 1372 ⁰	several						0.7	6	Huizenga(1954)
		several		0.90 \pm 0.27					6	Kramer(1956)
		440	$2^- \rightarrow 2^+$				0.613 ^{+0.014} -0.013		14	Gupta(1957)
		440		0.638 \pm 0.030			0.523 \pm 0.011		6;11	Hamers(1957)
		440		0.23 \pm 0.05			0.76 \pm 0.05		8;11	Hagedoorn(1958)
		440					0.761 ^{+0.015} -0.008		14	Jha(1959)
		440					0.751 \pm 0.014		14	Blok(1959)
		440					0.75 \pm 0.03		11	Gupta(1960)
		965	$2^- \rightarrow 2^+$				0.50 \pm 0.05		11	Gupta(1960)
		440		0.196 \pm 0.002	0.269 \pm 0.007	0.265 \pm 0.010			5	Leutz(1966)
		440			0.35 \pm 0.04 ^P				5	Leutz(1966)
		965		0.305 \pm 0.020					5	Leutz(1966)
		0	$2^- \rightarrow 0^+$	0.22 \pm 0.02 -0.015					5	Leutz(1966)
81	Tl 204 345	0	$2^- \rightarrow 0^+$	0.33					6	Jaffe(1954)
		0		0.42 \pm 0.05					5	Joshi(1961)
		0		0.41 \pm 0.03					5	Leutz(1962)
		0		0.60 \pm 0.055					7	Christmas(1964)
		0		0.48 \pm 0.04						Robinson(1963)
		0		0.43 \pm 0.16					6	Rao(1965)
		0		0.52 \pm 0.02					5	Klein(1966)

TABLE 3.2 (continued)

Z	A	^a Q _{EC} (keV)	Final state (keV)	J _i ^π → J _f ^π	P _L /P _K	P _M /P _L	P _{LM..} /P _K	^b P _{K^wK}	P _K	^c Method	Reference
82	Pb 203	982	279	$\frac{5^-}{2} \rightarrow \frac{3^+}{2}$				0.82 ± 0.05		11	Prescott(1954)
			680	$\frac{5^-}{2} \rightarrow \frac{5^+}{2}$				0.70 ± 0.05		11	Prescott(1954)
			279						0.74 ± 0.05	8	Wapstra(1954)
			680		0.36 ± 0.07			0.66 ± 0.04		6; 11	Hagedoorn(1958)
82	Pb 205	~43	279		0.208 ± 0.005		0.524 ± 0.010	0.755 ± 0.014		6; 11	Hagedoorn(1958)
			0							1	Pengra (1976)
			279					0.750 ± 0.019		11	Persson(1961)
83	Bi 205	2704	2566	$\frac{9^-}{2} \rightarrow \frac{9^+}{2}$	1.17 ± 0.16					6	Bonacalza(1962)
83	Bi 206	3652	3279	6 ⁺ -5 ⁻	0.264 ± 0.010	0.228 ± 0.007				5	Goverse(1974b)
			3403	6 ⁺ -5 ⁻	0.281 ± 0.009	0.276 ± 0.008				5	Goverse(1974b)
			3563	6 ⁺ -5 ⁻	0.509 ± 0.015	0.282 ± 0.010				5	Goverse(1974b)
83	Bi 208	2868	2615	5 ⁺ -3 ⁻				0.230 ± 0.008		11	Millar(1959)
85	At 210	3875	3726	5 ⁺ -6 ⁺					0.45 ± 0.09	8	Schima(1963)
85	At 211	793	0	$\frac{9^-}{2} \rightarrow \frac{9^+}{2}$	0.143					6	Hoff(1953)
93	Np 235	123	0	$\frac{5^-}{2} \rightarrow \frac{7^-}{2}$	30 ± 2					6	Hoffman(1956)
			0		36.7		0.46			6	Gindler(1958)
93	Np 236	977	several		2.0 ± 0.4					6	Orth(1951)

TABLE 3.2 (continued)

Z	^a Q _{EC} A (keV)	Final state (keV)	J _i ^π → J _f ^π	P _L /P _K	P _M /P _L	P _{LM...} /P _K	^b P _K ^w	P _K	^c Me- thod	Reference
94	Pu 237 233	several		1.2						Kalkstein(1957)
		60	$\frac{7^-}{2} \rightarrow \frac{5^-}{2}$	2.8	+0.8				6	Hoffman(1958)
97	Bk 245 819	250	$\frac{3^-}{2} \rightarrow \frac{5^+}{2}$				0.74	+0.03	11	Magnusson(1956)

ORIGINAL PAGE IS
OF POOR QUALITY

- a Q_{EC} values are taken from Wapstra and Gove (1971). There are some values that originate from electron capture measurements. They are replaced by values obtained from other methods, except for a few cases, indicated by an asterix, where no recent other result is available.
- b If P_K is given, the fluorescence yield used by the authors was used to calculate the measured value $P_K \omega_K$. There are some cases in which ω_K is not quoted. They are indicated by the sign "+".
- c Methods are identified by numbers explained in Table 3.1.
- d Q_{EC} value from Bertrand (1974).
- e Revised value using $k_\beta/k_\alpha=0.212$ (Salem et al., 1974) and $\omega_K=0.832$ (see Table III.V).
- f Value revised by the author, private communication to Durosinmi-Etti (1966).
- g Revised value using $k_\beta/k_\alpha=0.217$ (Salem et al., 1974) and $\omega_K=0.852$ (see Table III.V).
- h Q_{EC} value from Henry (1974).
- i Q_{EC} value from Berényi (1970).
- j Q_{EC} value from Kroger (1973).
- k Q_{EC} very uncertain.
- l Q_{EC} value from Ellis (1973).
- m Q_{EC} value from Jasinski (1963b).
- n Q_{EC} value from Auble (1971a).
- o Q_{EC} value from Auble (1971b).
- p $P_{MN...}/P_L$ value.
- q Q_{EC} value from Gopinathan (1968).
- r Q_{EC} value from Ford (1970).

TABLE 3.3 Experimental and theoretical P_L/P_K ratios

Z	A	Q_{EC}^a (keV)	Final state (keV)	$J_i^{\pi_i} - J_f^{\pi_f}$	Experimental values				Theor. values			
					P_L/P_K	$(q_{L_1}/q_K)^2$	$\frac{P_L/P_K}{(q_{L_1}/q_K)^2}$	Me- thod ^b	Reference	$\frac{P_L/P_K^c}{(q_{L_1}/q_K)^2}$	Bahcall Vatai	
<u>Allowed transitions</u> $\Delta J=0, 1 ; \pi_i \pi_f = +1$												
18	Ar	37	814.1±0.6	0	$\frac{3^+}{2} - \frac{3^+}{2}$	0.102 ±0.008	1.006	0.101 ±0.008	2	Kiser(1959)	0.098	0.095
						0.103 ±0.003		0.102 ±0.003	1	Santos-Ccampo (1960)		
						0.0971±0.0005		0.0965±0.0005	1	Manduchi(1961)		
						0.102 ±0.004		0.101 ±0.004	1	Dougan(1962a)		
						0.102 ±0.003		0.101 ±0.003	1	Winter(1964)		
						0.097 ±0.003		0.096 ±0.003	1	Heuer(1966)		
						0.098 ±0.003		0.097 ±0.003	1	Totzek(1967)		
						0.098 ±0.002		0.097 ±0.002	1	Krahn(1972)		
23	V	48	4015.4±2.8	several		0.104 ±0.004	1.007	0.103 ±0.004	1	Bertmann(1972)	0.104	0.101
				2297	$4^+ - 4^+$	0.115 ±0.015	1.005	0.114 ±0.015	1	Bertmann(1972)		
23	V	49	601.2±1.0	0	$\frac{7^-}{2} - \frac{7^-}{2}$	0.106 ±0.004	1.015	0.104 ±0.004	1	Krahn(1972)	0.104	0.101
24	Cr	51	751.4±0.9	320;0	$\frac{7^-}{2} - \frac{5^-}{2}; \frac{7^-}{2}$	0.1026±0.0004	1.014	0.1012±0.0004	1	Fasioli(1962)	0.105	0.102

TABLE 3.3 (continued)

Z	A	Q_{EC}^a (keV)	Final state (keV)	$J_i^\pi - J_f^\pi$	Experimental values				Theor. values		
					P_L/P_K	$(q_{L_1}/q_K)^2$ ^k	$\frac{P_L/P_K}{(q_{L_1}/q_K)^2}$	Me- ^b thod	Reference	$\frac{P_L/P_K}{(q_{L_1}/q_K)^2}$ ^c	Bahcall Vatai
24	Cr 51	751.4±0.9	320	$\frac{7^-}{2} - \frac{5^-}{2}$	0.1044±0.0021	1.023	0.1021±0.0021	1	Heuer(1966)		
			320;0	$\frac{7^-}{2} - \frac{5^-}{2}; \frac{7^-}{2}$	0.1033±0.0031	1.022	0.1011±0.0031	1	Heuer(1966)		
25	Mn 54	1374.9±3.6	835	$3^+ - 2^+$	0.106 ±0.003	1.020	0.104 ±0.003	1	Manduchi(1963)	0.106	0.103
26	Fe 55	231.7±0.7	0	$\frac{3^-}{2} - \frac{5^-}{2}$	0.108 ±0.006	1.052	0.103 ±0.006	1	Scobie(1959)	0.107	0.104
					0.106 ±0.003		0.103 ±0.003	1	Manduchi(1962a)		
					0.106 ±0.005		0.103 ±0.005	1	Moler(1963)		
					0.117 ±0.001		0.111 ±0.001	1	Pengra(1972)		
28	Ni 56	2133 ±11	1720	$0^+ - 1^+$	0.115 ±0.006	1.034	0.111 ±0.006	1	Winter(1967)	0.109	0.107
28	Ni 57	3243 ±7	several		0.100 ±0.006	1.008	0.099 ±0.006	1	Winter(1967)	0.109	0.107
27	Co 58	2308.0±2.5	1675;811	$2^+ - 2^+; 2^+$	0.110 ±0.008 ^f	1.009	0.109 ±0.009	1	Moler(1963)	0.108	0.106

TABLE 3.3 (continued)

Z	A	Q_{EC}^a (keV)	Final state (keV)	$J_i^\pi - J_f^\pi$	Experimental values				Theor. values		
					P_L/P_K	$(q_{L_1}/q_K)^2$	$\frac{P_L/P_K}{(q_{L_1}/q_K)^2}$	Me- ^b thod	Reference	$\frac{P_L/P_K^c}{(q_{L_1}/q_K)^2}$	Bahcall Vatai
30	Zn 65	1350.7±1.1	1115;0	$\frac{5^-}{2} - \frac{5^-}{2}; \frac{3^-}{2}$	0.119 ±0.007	1.043	0.114 ±0.007	1	Santos-Ocampo (1962)	0.110	0.108
			1115;0		0.111 ±0.006		0.106 ±0.006	1	Totzek(1967)		
			1115		0.117 ±0.007	1.071	0.109 ±0.007	5	McCann(1968)		
			1115;0		0.118 ±0.003	1.043	0.113 ±0.003	1	Krafft(1970)		
			1115		0.120 ±0.003	1.071	0.112 ±0.003	1	Krafft(1970)		
32	Ge 71	235.1±1.7	0	$\frac{1^-}{2} - \frac{3^-}{2}$	0.116 ±0.005	1.082	0.107 ±0.005	1	Drever(1959)	0.112	0.110
					0.1187±0.0008		0.1097±0.0007	1	Manduchi(1962a)		
					0.117 ±0.001		0.108 ±0.001	1	Genz(1971a)		
36	Kr 79	1631 ±9	several		0.108 ±0.005	1.017	0.106 ±0.005	1	Drever(1959)	0.115	0.113
37	Rb 83	1038 ±32	571;562	$\frac{5^-}{2} - \frac{3^-}{2}; \frac{3^-}{2}$	0.121 ±0.002	1.056	0.115 ±0.002	5	Schulz(1967a)	0.116	0.115
			571		0.128 ±0.002	1.056	0.121 ±0.002	5	Goedbloed(1970b)		
			562		0.132 ±0.002	1.056	0.125 ±0.002	5	Goedbloed(1970b)		

C.S

TABLE 3.3 (continued)

Z	A	Q _{EC} ^a (keV)	Final state (keV)	J _i ^π -J _f ^π	Experimental values				Theor. values		
					P _L /P _K	(q _{L1} /q _K) ²	P _L /P _K (q _{L1} /q _K) ²	Me- ^b thod	Reference	$\frac{P_L/P_K}{(q_{L1}/q_K)^2}$ ^c Bahcall Vatai	
48	Cd 109	182.0±3.0	88	$\frac{5}{2}^+ - \frac{7}{2}^+$	0.195 ±0.005	1.735 ±0.018	0.112 ±0.028	5	Leutz(1965)	0.125	0.124
					0.237 ±0.005		0.137 ±0.024	2	Moler(1965)		
					0.193 ±0.003		0.117 ±0.028	5	Goedbloed(1970a)		
55	Cs 131	355 ±6	0	$\frac{5}{2}^+ - \frac{3}{2}^+$	0.153 ±0.008	1.190	0.129 ±0.007	5	Joshi(1960)	0.133	0.131
					0.155 ±0.002		0.130 ±0.002	5	Schulz(1967a)		
56	Ba 131	1340 ±19	696;620	$\frac{1}{2}^+ - \frac{1}{2}^+ - \frac{3}{2}^+$	0.135 ±0.009	1.091	0.124 ±0.008	5	Smith(1963)	0.134	0.132
56	Ba 133	515.8±3.0 ^d	437	$\frac{1}{2}^+ - \frac{1}{2}^+$	0.371 ±0.007	2.914 ±0.085	0.127 ±0.004	5	Schulz(1967c)	0.134	0.132
					384	$\frac{1}{2}^+ - \frac{3}{2}^+$	0.221 ±0.005	1.732 ±0.013	0.128 ±0.003	5	Schulz(1967c)

TABLE 3.3 (continued)

Z	A	Q_{EC}^a (keV)	Final state (keV)	$J_i^\pi - J_f^\pi$	Experimental values				Theor. values		
					P_L/P_K	$(q_{L_1}/q_K)^2$	$\frac{P_L/P_K}{(q_{L_1}/q_K)^2}$	Me- thod	Reference	$\frac{P_L/P_K}{(q_{L_1}/q_K)^2}^c$	Bahcall Vatai
<u>First non-unique forbidden transitions $\Delta J=0, 1 ; \pi_i \pi_f = -1$</u>											
37	Rb 84	2679.8±2.9	880	$2^- - 2^+$	0.116 ±0.002	1.014	0.114 ±0.002	5	Schulz(1967a)	0.116	0.115
					0.119 ±0.002		0.117 ±0.002	5	Goedbloed(1970b)		
47	Ag105	1341 ±9 ^e	344	$\frac{1}{2}^- - \frac{1}{2}^+$	0.128 ±0.003	1.043	0.123 ±0.003	5	Schulz(1967d)	0.124	0.123
			1088	$\frac{1}{2}^- - \frac{3}{2}^-$	0.152 ±0.002	1.190	0.127 ±0.002	5	Schulz(1967d)		
53	I 126	2151 ±5	several		0.142 ±0.005 -0.018	1.035 ±0.015	0.137 ±0.005 -0.017	5	Scobie(1958)	0.130	0.129
55	Cs132	2099 ±23	several		0.136 ±0.001	1.048 ±0.012	0.130 ±0.002	5	Goverse(1974a)	0.133	0.131
66	Dy 159	365.4±1.0	0	$\frac{3}{2}^- - \frac{3}{2}^+$	0.198 ±0.009	1.295	0.153 ±0.007	5	Leiper(1971)	0.146	0.146

TABLE 3.3 .1. (continued)

Z	A	Q_{EC}^a (keV)	Final state (keV)	$J_i^\pi - J_f^\pi$	Experimental values				Theor. values		
					P_L/P_K	$(q_{L_1}/q_K)^2$	$\frac{P_L/P_K}{(q_{L_1}/q_K)^2}$	Me- thod	Reference	$\frac{P_L/P_K}{(q_{L_1}/q_K)^2}^c$ Bahcall	Vatai
76	Os 185	1015.0 \pm 0.7	874;880	$\frac{1}{2}^- - \frac{3}{2}^+; \frac{1}{2}^+$	0.600 \pm 0.006	3.62 \pm 0.14	0.166 \pm 0.007	5	Schulz(1967a)	0.162	0.160
			646	$\frac{1}{2}^- - \frac{1}{2}^+$	0.228 \pm 0.004	1.438	0.160 \pm 0.003	5	Schulz(1967a)		
79	Au 195	229.0 \pm 1.0*	99	$\frac{3}{2}^+ - \frac{3}{2}^-$	0.873 \pm 0.044	5.047 \pm 0.055	0.173 \pm 0.009	5	Goverse(1973)	0.168	0.165
			130	$\frac{3}{2}^+ - \frac{5}{2}^-$	3.055 \pm 0.086	16.74 \pm 0.61	0.183 \pm 0.008	5	Goverse(1973)		
			0	$\frac{3}{2}^+ - \frac{1}{2}^-$	0.337 \pm 0.007	2.040	0.165 \pm 0.003	5	Goverse(1973)		

TABLE 3.3 . (continued)

Z	A	Q _{EC} ^a (keV)	Final state (keV)	J _i ^π -J _f ^π	Experimental values				Theor. values				
					P _L /P _K	(q _{L1} /q _K) ²	$\frac{P_L/P_K}{(q_{L1}/q_K)^2}$	Me ^b thod	Reference	$\frac{P_L/P_K}{(q_{L1}/q_K)^2}$ ^c	Bahcall Vatai		
81	Tl	202	1372	+22 ^g	440	2 ⁻ -2 ⁺	0.196 ±0.002	1.167 ± 0.002	0.168 ±0.002	5	Leutz(1966)	0.171	0.169
					960	2 ⁻ -2 ⁺	0.305 ±0.020	1.458 ± 0.017	0.209 ±0.014	5	Leutz(1966)		
83	Bi	206	3652	+25 ^h	3279	6 ⁺ -5 ⁻	0.264 ±0.010			5	Goverse(1974b)	0.175	0.173
					3403	6 ⁺ -5 ⁻	0.281 ±0.009			5	Goverse(1974b)		
					3563	6 ⁺ -5 ⁻	0.509 ±0.015			5	Goverse(1974b)		
<u>Second non-unique forbidden transitions</u>					Δ J=2 ; π _i π _f =+1								
17	Cl	36	1144.1±1.7	0	2 ⁺ -0 ⁺	0.112 ±0.008			1	Dougan(1962b)			
28	Ni	59	1073.1±1.1	0	$\frac{3}{2}$ ⁻ - $\frac{7}{2}$ ⁻	0.121 ±0.002			1	Chew(1974a)			
42	Mo	93	398	+4	30;0	$\frac{5}{2}$ ⁺ - $\frac{1}{2}$ ⁻ ; $\frac{9}{2}$ ⁺	0.36 ±0.04		6	Hohmuth(1964)			
43	Tc	97	347.	+9	0	$\frac{9}{2}$ ⁺ - $\frac{5}{2}$ ⁺	0.21 ±0.14 ±0.10		6	Katcoff(1958)			

ORIGINAL PAGE IS
OF POOR QUALITY

TABLE 3.3 - (continued)

Z	A	Q _{EC} ^a (keV)	Final state (keV)	J _i ^π -J _f ^π	Experimental values					Theor. values		
					P _L /P _K	(q _{L1} /q _K) ⁴	P _L /P _K (q _{L1} /q _K) ⁴	Me ^{-b} thod	Reference	P _L /P _K ^c (q _{L1} /q _K) ⁴	Bahcall Vatai	
First unique forbidden transitions ⁱ ΔJ=2 ; π _i π _f =-1												
36	Kr 81	290	+100	0	$\frac{7^+}{2} - \frac{3^-}{2}$	0.146 ±0.005	1.179	0.124 ±0.006	1	Chew(1974b)	0.127	0.126
53	I 126	1251	+5	several		0.142 ±0.005 -0.018 ±0.016	1.071	0.133 ±0.005 -0.018	5	Scobie(1958)	0.131	0.130
81	Tl 202	1372	+22 ^g	0	2 ⁻ -0 ⁺	0.22 ±0.02 -0.015 ±0.004	1.230	0.179 ±0.016 -0.012	5	Leutz(1966)	0.173	0.171
81	Tl204	345	+4	0	2 ⁻ -0 ⁺	0.42 ±0.05	2.256 ±0.016	0.17 ±0.02	5	Joshi(1961)	0.204	0.201
				0		0.41 ±0.03		0.16 ±0.01	5	Leutz(1962)		
				0		0.60 ±0.055		0.24 ±0.02	7	Christmas(1964)		
				0		0.48 ±0.04		0.19 ±0.02		Robinson(1963)		
				0		0.43 ±0.16		0.17 ±0.06	6	Rao(1965)		
				0		0.52 ±0.02		0.20 ±0.01	5	Klein(1966)		

ORIGINAL PAGE IS
OF POOR QUALITY

- a Q_{EC} values are taken from Wapstra and Gove (1971). There are some values that originates from electron capture measurements. They are replaced by values obtained from other methods, except for a few cases, indicated by an asterix where no recent other result is available.
- b Methods are identified by numbers explained in Table 3.1.
- c The theoretical L/K ratios are derived from wave functions of Mann and Waber (1973) and exchange and overlap corrections $X^{L/K}$ as described in Sec. 2.5. For $Z > 54$ the correction factors of Suslov (1970) are used in continuation of the Bancall factors and those of Martin and Blichert-Toft (1970), in extension of the recalculated Vatai factors.
- d Q_{EC} value from Henry (1974).
- e Q_{EC} value from Bertrand (1974).
- f Revised value; see Grinberg et al. (1973).
- g Q_{EC} value from Auble (1971b).
- h The Q_{EC} value is obviously too low. No reliable comparison with theoretical values can be given.
- i First unique forbidden transitions; the factor $(q_{L1}/q_K)^2$ has been squared and in the theoretical values the contribution of the L_3 shell has been allowed for.

TABLE 3.4 Experimental and theoretical P_M/P_L ratios

Z	A	Q_{EC}^a (keV)	Final state (keV)	$J_i^{\pi_i} - J_f^{\pi_f}$	Experimental values				Theor. values			
					P_M/P_L	$(q_{M_1}/q_{L_1})^2$	$\frac{P_M/P_L}{(q_{M_1}/q_{L_1})^2}$ Me ^{-b}	thod	Reference	$\frac{P_M/P_L}{(q_{M_1}/q_{L_1})^2}$ ^c	Bahcall Vatai	
<u>Allowed transitions</u> $\Delta J = 0, 1 ; \pi_i \pi_f = +1$												
18	Ar	37	814.1 ± 0.6	0	$\frac{3}{2}^+ - \frac{3}{2}^+$	0.104 ^{+0.007} _{-0.003}	1.000	0.104 ^{+0.007} _{-0.003}	3	Renier(1968)	0.130	0.116
26	Fe	55	231.7 ± 0.7	0	$\frac{3}{2}^- - \frac{5}{2}^-$	0.157 ± 0.003	1.006	0.156 ± 0.003	1	Pengra(1972)	0.163	0.156
30	Zn	65	1350.7 ± 1.1	1115	$\frac{5}{2}^- - \frac{5}{2}^-$	0.153 ± 0.020	1.008	0.152 ± 0.020	1	Krafft(1970)	0.167	0.160
32	Ge	71	235.1 ± 1.7	0	$\frac{1}{2}^- - \frac{3}{2}^-$	0.142 ± 0.010	1.010	0.141 ± 0.010	1	Manduchi(1962b)	0.170	0.164
						0.162 ± 0.003		0.160 ± 0.003	1	Genz(1971a)		
48	Cd	109	182.0 ± 3.0	88	$\frac{5}{2}^+ - \frac{7}{2}^+$	0.205 ± 0.020 ^d	1.070	0.192 ± 0.019	2	Moler(1965)	0.206	0.202
<u>First non-unique forbidden transitions</u> $\Delta J=0, 1 ; \pi_i \pi_f = -1$												
50	Sn	113	1025 ± 15	648;393	$\frac{1}{2}^+ - \frac{3}{2}^- - \frac{1}{2}^-$	0.220 ± 0.010 ^e	1.011	0.218 ± 0.010	1	Manduchi(1964b)	0.209	0.205
76	Os	185	1015.0 ± 0.7	646	$\frac{1}{2}^- - \frac{1}{2}^+$	0.254 ± 0.005	1.055	0.241 ± 0.005	5	Schulz(1967a)	0.245	0.236

TABLE 3.4 (continued)

Z	A	Q_{EC}^a (keV)	Final state (keV)	$J_i^\pi - J_f^\pi$	Experimental values				Theor. values		
					P_M/P_L	$(q_{M_1}/q_{L_1})^2$	$\frac{P_M/P_L}{(q_{M_1}/q_{L_1})^2}$	Me- ^b thod	Reference	$\frac{P_M/P_L \cdot c}{(q_{M_1}/q_{L_1})^2}$ Bahcall Vatai.	
78	Pt 193	61.2±3.0	0	$\frac{1^-}{2} - \frac{3^+}{2}$	0.386 ±0.014	1.475	0.262±0.010	5	Ravn(1971)	0.247	0.239
81	Tl 202 1372	±22 ^f	440	$2^- - 2^+$	0.269 ±0.007	1.025	0.262±0.007	5	Leutz(1966)	0.249	0.240
83	Bi 206 3652	±25 ^g	3279	$6^+ - 5^-$	0.228 ±0.007			5	Goverse(1974b)	0.250	0.242
			3403	$6^+ - 5^-$	0.276 ±0.008			5	Goverse(1974b)		
			3563	$6^+ - 5^-$	0.282 ±0.010			5	Goverse(1974b)		

- a Q_{EC} values are taken from Wapstra and Gove (1971).
- b Methods are identified by numbers explained in Table 3.1.
- c The theoretical M/L ratios are determined from wave functions of Mann and Waber (1973) and exchange and overlap corrections $X^{M/L}$ as described in Sec. 2.5. For $Z > 54$ the correction factors of Suslov (1970) are used in continuation of the Bahcall factors and those of Martin and Blichert-Toft (1970) in extension of the recalculated Vatai factors.
- d Revised value using $k_{\beta}/k_{\alpha} = 0.212$ (Salem et al. 1974) and $w_K = 0.832$ (see Table 3.5).
- e Revised value using $k_{\beta}/k_{\alpha} = 0.217$ (Salem et al. 1974) and $w_K = 0.852$ (see Table 3.5).
- f Q_{EC} value from Auble (1971b).
- g The Q_{EC} value is obviously too low. No reliable comparator with theoretical values can be given.

TABLE 3.5 Experimental and theoretical P_K values

Z	A	Q_{EC}^a (keV)	Final state (keV)	Experimental values					Theor. P_K values ^c		
				$J_i^{\pi} - J_f^{\pi}$	P_{LM} / P_K	$P_{K^0} w_K$	w_K^b	P_K	Me- thod. Reference	Bahcall	Vatai
<u>Allowed transitions $\Delta J=0, 1; \pi_i \pi_f = +1$</u>											
23	V 48	4015.4 ± 2.8	several			0.2005 \pm 0.0030	0.225 \pm 0.009	0.891 \pm 0.036	11 Albrecht(1975)	0.892	0.896
24	Cr 51	751.4 ± 0.9	320 $\frac{7^-}{2} - \frac{5^-}{2}$			0.227 \pm 0.003	0.256 \pm 0.007	0.887 \pm 0.008	10 Taylor(1965)	0.890	0.893
25	Mn 54	1374.9 ± 3.6	835 $3^+ - 2^+$			0.257 \pm 0.004	0.283 \pm 0.007	0.908 \pm 0.008	10 Taylor(1965)	0.889	0.891
						0.243 \pm 0.012		0.859 \pm 0.014	10 Leistner(1965)		
						0.2514 \pm 0.0017		0.888 \pm 0.007	10 Bambynek(1967a)		
						0.250 \pm 0.005		0.883 \pm 0.009	10 Petel(1967)		
						0.2492 \pm 0.0017		0.881 \pm 0.009	11 Hammer(1968)		
								0.900 \pm 0.014	10 Dobrilovic(1972)		
						0.247 \pm 0.009		0.873 \pm 0.011	11 Mukerji(1973)		
27	Co 57	836.9 ± 0.7	136 $\frac{7^-}{2} - \frac{5^-}{2}$			0.3044 \pm 0.0043	0.344 \pm 0.008	0.885 \pm 0.009	11 Rubinson(1968)	0.887	0.890
					0.15 \pm 0.02			0.87 \pm 0.02	11 Bosch(1969)		
						0.317 \pm 0.006		0.922 \pm 0.010	11 Mukerji(1973)		
			706 $\frac{7^-}{2} - \frac{5^-}{2}$			0.088 \pm 0.040		0.92 \pm 0.03	11 Bosch(1969)	0.878	0.881

TABLE 3.5. (continued)

Z	A	Q_{EC}^a (keV)	Final state (keV)	$J_i^\pi - J_f^\pi$	Experimental values				Theor. P_K values ^c			
					P_{LM} / P_K	$P_K \omega_K$	ω_K^b	P_K	Me- thod	Reference	Bahcall	Vatai.
27	Co 58	2308.0 +2.5	1675; 810	$2^+ - 2^+; 2^+$		0.3050+0.0022	0.344+0.008	0.887+0.008	10	Banbynek(1968b)	0.887	0.890
30	Zn 65	1350.7 +1.1	1115	$\frac{5^-}{2} - \frac{5^-}{2}$			0.441+0.009	0.878+0.006	13	Kramer(1962a)	0.882	0.884
						0.3927+0.0026		0.890+0.009	11	Hammer(1968)		
						0.386+0.010		0.875+0.013	11	Mukerji(1973)		
			1115;	$\frac{5^-}{2} - \frac{5^-}{2}; \frac{3^-}{2}$		0.400+0.006		0.907+0.011	10	Taylor(1965)	0.882	0.884
			0			0.3894+0.0016		0.883+0.009	10	Banbynek(1968a)		
33	As 73	340 +15	67	$\frac{3^-}{2} - \frac{1^-}{2}$				0.85+0.05	16	Kyles(1970)	0.874	0.875
34	Se 75	864.7 +1.0	401	$\frac{5^+}{2} - \frac{5^+}{2}$		0.460+0.004	0.576+0.031	0.799+0.031	11	Rao(1966a)	0.876	0.878
						0.462+0.012		0.802+0.033	11	Raesian(1969)		
						0.516+0.021		0.896+0.037	11	Chew(1973)		
37	Rb 83	1038 +32	562	$\frac{5^-}{2} - \frac{3^-}{2}$	0.164+0.002			0.859+0.002	5	Goedbloed(1970b)	0.872	0.874

ORIGINAL PAGE IS
OF POOR QUALITY

TABLE 3.5 (continued)

Z	A	Q_{EC}^a (keV)	Final state (keV), $J_i^\pi - J_f^\pi$	Experimental values				Theor. P_K values ^c		
				$P_{LM..}/P_K$	$P_{K^w_K}$	ω_K^b	P_K	Method Reference	Bahcall Vatai	
38 Sr 85	1064 +7	514	$\frac{9^+}{2} - \frac{9^+}{2}$				0.88 ± 0.04	11 Bisi(1956a)	0.871	0.873
					0.5959 ± 0.0035	0.676 ± 0.008	0.882 ± 0.009	11 Grotheer(1969)		
					0.586 ± 0.003		0.867 ± 0.009	10 Bambynek(1970)		
39 Y 88	3619 +4	2734; 1836	$4^- - 3^-$ $4^- - 3^-; 2^+$		0.6290 ± 0.0032	0.700 ± 0.009	0.898 ± 0.009	11 Grotheer(1969)	0.871	0.874
					0.613 ± 0.004		0.876 ± 0.010	10 Bambynek(1973)	0.871	0.874
48 Cd 109	182.0 +3.0	88	$\frac{5^+}{2} - \frac{7^+}{2}$		0.28 ± 0.03		0.871 ± 0.018	5 Der Mateosian (1953)	0.785	0.787
							0.805 ± 0.027	8 Wapstra(1957)		
					0.228 ± 0.003		0.814 ± 0.002	5 Leutz(1965)		
					0.26 ± 0.03		0.794 ± 0.025	18 Durosini- Etti(1966)		
					0.226 ± 0.003		0.816 ± 0.002	5 Goedbloed(1970 a)		
49 In 111	826 +29	419	$\frac{9^+}{2} - \frac{7^+}{2}$				0.867 ± 0.007	17 Sparrmann(1966)	0.848	0.850

TABLE 3.5 (continued)

Z	A	Q_{EC}^a (keV)	Final state (keV)	$J_i^\pi - J_f^\pi$	Experimental values				Theor. P_K values ^c		
					P_{LM} / P_K	$P_K \omega_K$	ω_K^b	P_K	Method Reference	Bahcall Vatai	--
53 I	125	177.0 ^e ±1.2	35.5 $\frac{5}{2}^+ - \frac{3}{2}^+$		0.23 ±0.03			0.813 ±0.020	5 Der Mateosian (1953)	0.796	0.798
					0.2543 ±0.0027			0.7972 ±0.0017	5 Leutz(1964)		
					0.253 ±0.005			0.789 ±0.003	5 Smith(1966)		
						0.685 ±0.018	0.876 ±0.028	0.782 ±0.033	11 Karttunen(1969)		
						0.699 ±0.030		0.798 ±0.041	11 Tolea(1974)		
54 Xe	127	664 ±4	375 $\frac{1}{2}^+ - \frac{1}{2}^+$		0.685 ±0.012			0.782 ±0.029	11 Plch(1974a)		
					0.705 ±0.004	0.883 ±0.028	0.798 ±0.028	11 Bresesti(1964)	0.830	0.832	
						0.750 ±0.016		0.849 ±0.032	11 Bresesti(1964)	0.842	0.843
55 Cs	131	355 ±6	0 $\frac{5}{2}^+ - \frac{3}{2}^+$		0.734 ±0.006	0.889 ±0.020	0.826 ±0.020	11 Plch(1974b)	0.831	0.835	
56 Ba	133	515.8 ^f ±3.0	437 $\frac{1}{2}^+ - \frac{1}{2}^+$		0.45 ±0.04			0.69 ±0.02	19 Törnkvist(1968)	0.662	0.667
						0.576 ±0.038	0.895 ±0.012	0.652 ±0.040	14 Narang(1968)		
						0.644 ±0.034		0.72 ±0.04	11 Schmidt-Ott(1972)		
						384 $\frac{1}{2}^+ - \frac{3}{2}^+$	0.72 ±0.06		0.80 ±0.07	11 Schmidt-Ott (1972)	0.769

ORIGINAL PAGE IS
OF POOR QUALITY

TABLE 3.5 (continued)

Z	A	Q_{EC}^a (keV)	Final state (keV)	$J_i^\pi - J_f^\pi$	Experimental values				Theor. P_K values ^c							
					P_{LM} / P_K	$P_K \omega_K$	ω_K^b	P_K	Method	Reference	Bahcall	Vatai				
58	Ce 139	275 +15	165	$\frac{3^+}{2} - \frac{5^+}{2}$	0.37	+0.02	0.73	+0.01	15	Ketelle(1956)	0.724	0.729				
											+0.014	+0.014				
											0.68	+0.02	17	Marelius(1967)		
											0.750	+0.010	16	Adamowicz(1968)		
											0.69	+0.02	13	Vatai(1968a)		
											0.707	+0.018	0.906	+0.026	0.78	+0.03
0.649	+0.017	0.716	+0.031	14	Campbell(1972)											
		0.639	+0.006	0.705	+0.030	11	Pfich(1975)									
				0.726	+0.010	15	Hansen(1975)									
64	Gd 151	484 ^g +30	352	$\frac{7^-}{2} - \frac{9^-}{2}$	0.664	+0.009	0.930	+0.015	0.714	+0.017	11	Genz(1973c)	0.704	0.709		
													+0.015	+0.015		
70	Yb 166	260 +20*	82	$2^+ - 2^+$	0.68	+0.06 -0.02	0.946	+0.020	0.72	+0.06 -0.03	14	Jasinski (1963 a)	0.711	0.715		
													+0.011	+0.011		
81	Tl 201	484 ^h +17	167	$\frac{1^+}{2} - \frac{1^+}{2}$	0.67	+0.04	0.964	+0.017	0.70	+0.04	11	Gupta(1960)	0.722	0.726		
													+0.014	+0.014		

TABLE 3.5 Experimental and theoretical P_K values

Z	A	Q_{EC}^a (keV)	Final state (keV)	$J_i^{\pi_i} - J_f^{\pi_f}$	Experimental values					Theor. P_K values ^c	
					P_{LM} / P_K	$P_K^{\omega_K}$	ω_K^b	P_K	Method Reference	Bahcall	Vatai
<u>First non-unique forbidden transitions $\Delta J=0, 1 ; \pi_i \pi_f = -1$</u>											
37	Rb 84	2679.8 +2.9	880	$2^- - 2^+$		0.580 +0.025	0.653+0.030	0.888+0.039	11 Welker(1955)	0.876	0.878
61	Pm 145	170 +7*	67	$\frac{5^+}{2} - \frac{3^-}{2}$		0.558 +0.022	0.919+0.024	0.607+0.033	11 Tolea(1974)	0.676 +0.011	0.681 +0.011
			72	$\frac{5^+}{2} - \frac{5^-}{2}$		0.509 +0.022		0.554+0.033	11 Tolea(1974)	0.660 +0.011	0.665 +0.011
62	Sm 145	647 _k +14 _k	61	$\frac{7^-}{2} - \frac{5^+}{2}$	0.20 +0.02			0.833+0.014	16 Brosi(1959)	0.830	0.833
64	Gd 151	484 +30 _g	307	$\frac{7^-}{2} - (\frac{3,7}{2})^+$		0.754 +0.014	0.930+0.015	0.811+0.021	11 Genz(1973c)	0.754 +0.009	0.759 +0.009
66	Dy 159	365.4 +1.0	58	$\frac{3^-}{2} - \frac{5^+}{2}$		0.752 +0.024	0.936+0.022	0.803+0.033	11 Genz(1973c)	0.793	0.797
72	Hf 175	607 +8*	433	$\frac{5^-}{2} - \frac{7^+}{2}$		0.64 +0.04	0.950+0.020	0.67 +0.04	11 Funke(1965)	0.689 +0.005	0.693 +0.005
								0.712+0.008	16 Jasinski(1968)		
			343	$\frac{5^-}{2} - \frac{5^+}{2}$				0.767 ^{+0.030} -0.016	16 Jasinski(1968)	0.753 +0.002	0.757 +0.002

TABLE 3.5 (continued)

Z	A	Q_{EC}^a (keV)	Final state (keV)	$J_i^\pi - J_f^\pi$	Experimental values				Theor. P_K^c values		
					$P_{LM...}/P_K$	$P_{K^{\omega K}}$	ω_K^b	P_K	Method Reference	Bahcall	Vatai
78	Pt 188	540 +10*	195	$0^+ - 1^-$				0.744 ± 0.020	16 Hanson(1968)	0.748	0.752
			187	$0^+ - 1^-$				0.766 ± 0.023	16 Hanson(1968)	0.750	0.754
79	Au 195	229.0 +1.0*	130	$\frac{3^+}{2} - \frac{5^-}{2}$		0.188 ± 0.005	0.961 ± 0.018	0.196 ± 0.019	11 De Wit(1965)	0.202 +0.006	0.206 +0.006
						5.25 ± 0.66		0.160 ± 0.017	5 Goverse(1973)		
			99	$\frac{3^+}{2} - \frac{3^-}{2}$				0.458 ± 0.012	16 Jasinski(1968)	0.461 +0.003	0.466 +0.003
					1.28 ± 0.06		0.438 ± 0.011	5 Goverse(1973)			
80	Hg 197	684; +40	268;77	$\frac{1^-}{2} - \frac{3^+}{2}; \frac{1^+}{2}$		0.741 ± 0.012	0.963 ± 0.017	0.769 ± 0.021	18 Plch(1971)	0.754 +0.002	0.758 +0.002
81	Tl 202	1372 +22j	440	$2^- - 2^+$		0.76 ± 0.05	0.964 ± 0.017	0.79 ± 0.05	11 Hagedoorn (1958)	0.790	0.793
						$0.761^{+0.015}$ -0.008		$0.789^{+0.022}$ -0.019	14 Jha(1959)		
						0.751 ± 0.014		0.779 ± 0.022	14 Blok(1959)		
						0.75 ± 0.03		0.778 ± 0.034	11 Gupta(1960)		
						0.265 ± 0.010		0.791 ± 0.006	5 Leutz(1966)		

TABLE 3.5 (continued)

Z	A	Q_{EC}^a (keV)	Final state (keV)	$J_i^{\pi_i} - J_f^{\pi_f}$	Experimental values				Theor. P_K values ^c			
					P_{LM} / P_K	$P_{K^{\omega_K}}$	ω_K^b	P_K	Method	Reference	Bahcall	Vatai
82	Pb 203	982 +12	680	$\frac{5^-}{2} - \frac{5^+}{2}$	0.66	+0.04	0.69	+0.04	11	Hagedoorn (1958)	0.709	0.713
											+0.003	+0.003
											279	$\frac{5^-}{2} - \frac{3^+}{2}$
					0.750	+0.019	0.776	+0.025	11	Persson(1961)		
<u>First unique forbidden transitions</u> $\Delta J=2 ; \pi_i \pi_f = -1$												
19	K 40	1505.1 +0.7	1460; 0	$4^- - 2^+ ; 0^+$	0.34	+0.08	0.75	+0.05	5	McCann(1967)	0.741 ¹	0.749 ¹
					0.44	+0.09	0.69	+0.04	8	Azman(1968)		

ORIGINAL PAGE IS
OF POOR QUALITY

- a Q_{EC} values are taken from Wapstra and Gove (1971). There are some values that originates from electron capture measurements. They are replaced by values obtained from other methods, except for a few cases, indicated by an asterix, where no recent other result is available.
- b Fluorescence yields were calculated from the equation $[\omega_K/(1-\omega_K)]^{1/4} = A+BZ+CZ^3$. The constants A, B, C were determined by fitting the selected "most reliable" experimental values of Bambynek et al. (1972) to this equation. We have omitted from the list of the "most reliable" values those that were deduced from $P_K \omega_K$ measurements.
- c The theoretical P_K values were derived from wave functions of Mann and Waber (1973) and exchange and overlap corrections as described in Sec. 2.5. For $Z > 54$ the correction factors of Suslov (1970) are used in continuation of the Bahcall factors and those of Martin and Blichert-Toft (1970) in extension of the recalculated Vatai factors. Uncertainties are quoted only in those cases where they are significant. They originate from the uncertainties of the Q_{EC} value.
- d Methods are identified by numbers explained in Table 3.1.
- e Q_{EC} value from Gopinathan (1968).
- f Q_{EC} value from Henry (1974).
- g Q_{EC} value from Ford (1970).
- h Q_{EC} value from Auble (1971a).
- i Q_{EC} value from Jasinski (1963b).
- j Q_{EC} value from Auble (1971b).
- k Q_{EC} value from Berényi (1970).
- l Theoretical value for a unique 1st forbidden transition.

TABLE 3.6 Experimental K/β^+ and EC/β^+ Ratio

Z	Element	A	Q_{EC} (keV)	Final state (keV)	$J_i^\pi - J_f^\pi$	R_{K/β^+}	R_{EC/β^+}	Method ^b	Reference
6	C	11	1982.2 ± 1.0	0	$\frac{3}{2}^- \rightarrow \frac{3}{2}^-$	$(1.9 \pm 0.3) \times 10^{-3}$		20	Scobie (1957b)
						$(2.30^{+0.14}_{-0.11}) \times 10^{-3}$		21	Campbell(1967)
7	N	13	2220.5 ± 0.9	0	$\frac{1}{2}^- \rightarrow \frac{1}{2}^-$	$(1.68 \pm 0.12) \times 10^{-3}$		21	Ledingham(1965)
8	O	15	2759.2 ± 0.9	0	$\frac{1}{2}^- \rightarrow \frac{1}{2}^-$	$(1.07 \pm 0.06) \times 10^{-3}$		21	Leiper(1972)
9	F	18	1655.3 ± 0.9	0	$1^+ \rightarrow 0^+$	$(3.00 \pm 0.18) \times 10^{-2}$		20	Drever(1956)
10	Ne	19	5238.2 ± 0.9	0	$\frac{1}{2}^+ \rightarrow \frac{1}{2}^+$	$(9.6 \pm 0.3) \times 10^{-4}$		21	Leiper(1972)
11	Na	22	2842.3 ± 0.5	1274.6	$3^+ \rightarrow 2^+$	0.105 ± 0.009		22	McCarr(1969)
							0.10 ± 0.05	26	Bouchez(1952)
							0.110 ± 0.006	27	Sherr(1954)
							0.124 ± 0.010	26	Kreger 1954)
							0.09 ± 0.06	27	Sair(1954)
							0.122 ± 0.010	31	Allen(1955)
							0.065 ± 0.009	23	Charpak(1955)

ORIGINAL PAGE IS
OF POOR QUALITY

TABLE 3.6 (continued)

Z	Element	A	Q_{EC}^a (keV)	Final state (keV)	$J_i^{\pi_i} \rightarrow J_f^{\pi_f}$	P_K/P_{β^+}	P_{EC}/P_{β^+}	Method ^b , Reference	
11	Na	22					0.124 ± 0.012	27 Hagedoorn(1957)	
							0.109 ± 0.008	27 Konijn(1958/59)	
							0.112 ± 0.004	27 Ramaswamy(1959a)	
							0.1041 ± 0.0010	28 Williams(1964, 1968)	
							0.1048 ± 0.0007	27 Leutz(1967)	
							0.103 ± 0.018	31 Steyn(1966)	
							0.1042 ± 0.0010	27 Vatai(1968c)	
						0.1077 ± 0.0003	27 MacMahon(1970)		
13	Al	26	4004.7 ± 0.5	1810	$5^+ \rightarrow 2^+$		0.135 ± 0.023	26 Rightmire(1959)	
							0.12	31 Jastram(1961)	
15	P	30	4227.4 ± 2.6	0	$1^+ \rightarrow 0^+$	$(1.24 \pm 0.04) \times 10^{-3}$		21 Ledingham(1971)	
17	Cl	36	1144.1 ± 1.7	0	$2^+ \rightarrow 0^+$	$(1.4 \pm 0.2) \times 10^3$ $(0.6 \pm 0.6) \times 10^3$		combination of 21 and 31	Dougan(1962b)
									31 Berényi(1962) and (1963b)
21	Sc	44	3649 ± 6	several	$2^+ \rightarrow$ several		0 ± 0.1	26 Langevin(1954c)	
							0.05 ± 0.15	26 Langevin(1954c)	
							0.11 ± 0.05	26 Blue(1955)	

TABLE 3.6 (continued)

Z	Element	A	Q_{EC}^a (keV)	Final state (keV)	$J_i^\pi - J_f^\pi$	P_K/P_{β^+}	P_{EC}/P_{β^+}	Method ^b	Reference
21	Sc	44					0.073 ± 0.017	27	Blue(1955)
							0.023 ± 0.019	27	Konijn(1958/59)
							0.049	26	Dillman(1963)
23	V	48	4015.4 ± 2.8	several	$4^+ \rightarrow$ several		0.72 ± 0.11	31	Good(1946)
							0.46 ± 0.09	26	Sterk(1953)
				2295	$4^+ \rightarrow 4^+$		1.04 ± 0.17	26	Casson(1953)
							0.75 ± 0.09	31	Bock(1955)
							0.74 ± 0.07	-	van Nooijen(1957) revised by Konijn(1967b)
							0.74 ± 0.02	27	Hagedoorn(1957)
							0.43 ± 0.03	26	Ristinen(1963)
							0.77 ± 0.04	29	Biryukov(1966)
							0.77 ± 0.06	27	Konijn(1967a)
							0.83 ± 0.06	27	Konijn(1967b)
							0.76 ± 0.035	29	Konijn(1967b)
							0.69 ± 0.03	27	Albrecht(1975)
25	Mn	52	4709.8 ± 3.5	3112	$6^+ \rightarrow 6^+$		1.86 ± 0.17	31	Good(1946)

ORIGINAL PAGE IS
OF POOR QUALITY

Z	Element	A	Q_{EC}^a (keV)	Final state (keV)	$J_i^\pi - J_f^\pi$	P_K / P_{B^+}	P_{EC} / P_{B^+}	Method ^b	Reference
25	Mn	52					2.01 ± 0.24	27	Sehr(1954)
							1.95 ± 0.19	-	Konijn(1958c) revised by Konijn(1967b)
							1.84 ± 0.20	30	Wilson(1962)
							2.04 ± 0.24	26	Freedman(1966)
							1.80 ± 0.13	27	Konijn(1967b)
							2.12 ± 0.17	29	Konijn(1967b)
25	Fe	52	2372 ± 12	548	$0^+ \rightarrow (1)^+$		0.77 ± 0.18	31	Arbman(1955)
							0.82	31	Juliano(1959)
							1.6 ± 0.4	24	Friedlander(1951a)
27	Co	56	4568.2 ± 1.9	several	$4^+ \rightarrow$ several		4.3 ± 0.2	26	Cook(1956)
				3120	$4^+ \rightarrow (5)^+$		12	26	Sakai(1954)
				2085	$4^+ \rightarrow 4^+$		0.35 ± 0.07	26	Sakai(1954)
							0.014 ± 0.152	27	Berényi(1965c)
							0.23 ± 0.22	26	Berényi(1965c)
							0.117 ± 0.089	27	Vatai(1966)
27	Co	58	2308.0 ± 2.5	810.5	$2^+ \rightarrow 2^+$	4.92 ± 0.09		22	Joshi(1961)

TABLE 3.6 (continued)

Z	Element	A	Q_{EC}^{\pm} (keV)	Final state (keV)	$J_i^{\pi} \rightarrow J_f^{\pi}$	P_K / P_{β^+}	P_{EC} / P_{β^+}	Method ^b	Reference
27	Co	58				4.83 ± 0.10		20	Kramer(1962b)
						5.05 ± 0.09		24 & 31	Bambynek(1968b)
				several	$2^+ \rightarrow$ several	5.9 ± 0.2		31	Good(1946)
						5.9 ± 0.2		26	Cook(1956)
			810.5		$2^+ \rightarrow 2^+$	5.67 ± 0.14		27	Konijn(1958a)
						5.49 ± 0.18		30	Ramaswamy(1961)
						5.48 ± 0.09		29	Biryukov(1966)
						5.76 ± 0.13		28	Williams(1970) and Goodier(1971)
28	Ni	57	3243 ± 7	several	$5/2^- \rightarrow$ several	1.0 ± 0.1		24	Friedlander(1950)
						1.0 ± 0.1		26	Konijn(1956)
						1.13 ± 0.01		26	Konijn(1958a)
						1.15 ± 0.04		27	Konijn(1958b)
						1.68 ± 0.2		30	Chilosi(1962)
						1.14 ± 0.1		26	Bakhru(1967)
			1890		$5/2^- \rightarrow (5/2^-)$	18 ± 6		27	Konijn(1958b)

Z	Element	A	Q_{EC}^a (keV)	Final state (keV)	$J_i^{\pi_i} \rightarrow J_f^{\pi_f}$	P_K/P_{β^+}	P_{EC}/P_{β^+}	Method ^b	Reference
							27 ± 3	30	Chilosi(1962)
							.22	27	Bakhru(1967)
			1750		$\frac{3}{2}^- \rightarrow (\frac{3}{2}^-)$		6 ± 1	30	Chilosi(1962)
							~7	27	Bakhru(1967)
			1490		$\frac{3}{2}^- \rightarrow \frac{1}{2}^-$		1.438 ± 0.059	27	Konijn(1958b)
							2 ± 0.4	30	Chilosi(1962)
							1.5 ± 0.08	27	Bakhru(1967)
			1370		$\frac{3}{2}^- \rightarrow \frac{3}{2}^-$		0.805 ± 0.040	27	Konijn(1958b)
							1 ± 0.2	30	Chilosi(1962)
							1 ± 0.1	27	Bakhru(1967)
			1590		$\frac{3}{2}^- \rightarrow ?$		~4	30	Chilosi(1962)
							~5	27	Bakhru(1967)
			1460		$\frac{3}{2}^- \rightarrow ?$		2.5 ± 1	27	Bakhru(1967)
29	Cu	61	2245.2 ± 2.3	several	$\frac{3}{2}^- \rightarrow$ several	0.55 ± 0.06		25	Bouchez(1949)
						0.32 ± 0.03		31	Huber(1949)

TABLE 3.6 (continued)

Z	Element	A	Q_{EC}^a (keV)	Final state (keV)	$J_i^\pi - J_f^\pi$	P_K/P_{β^+}	P_{EC}/P_{β^+}	Method ^b	Reference
29	Cu	64	1677.5 ± 1.8	1340; 0	$1^+ \rightarrow 2^+; 0^+$	3.5 ± 1		23	Cook(1948)
						2.65 ± 0.4		25	Bouchez(1949)
						1.75 ± 0.2		25	Huber(1949)
						2.18 ± 0.20		23	Plassmann(1951)
							2.32 ± 0.28	31	Reynolds(1950)
30	Zn	62	1690 ± 8	several	$0^+ \rightarrow$ several		0:1	31	Hayward(1950)
				0	$0^+ \rightarrow 1^+$	4.4 ± 0.5		31	Hoffman(1969)
30	Zn	65	1350.7 ± 1.1	0	$5/2^- \rightarrow 3/2^-$	27		24	Watase(1940)
						18.8		27	Zumwalt(1947)
						25 ± 10		31	Major(1952)
						$21.3 \pm 1.$		31	Major(1952)
						$21.8 \pm 2.$		23	Yuasa(1952)
						$28.0 \pm 3.$		25	Perkins(1953)
						26 ± 3		20	Avignon(1955)
						25 ± 2		31	Gleason(1959)

TABLE 2.0 (CONTINUED)

Z	Element	A	Q_{EC}^a (keV)	Final state (keV)	$J_i^\pi \rightarrow J_f^\pi$	P_K/P_{β^+}	P_{EC}/P_{β^+}	Method ^b	Reference
30	Zn	65				27.7 ± 1.5		31	Hammer(1968)
							24	31	Good(1946)
							24.9 ± 1.5	27	Sehr(1954)
							29.6 ± 0.5	31	Steyn(1966)
31	Ga	66	5175.0 ± 3.0	several	$0^{(\pm)} \rightarrow$ several	0.52		23	Langer(1950)
31	Ga	68	2919.4 ± 3.9	1078	$1^+ \rightarrow 2^+$	1.28 ± 0.12		31	Ramaswamy(1959b)
				0	$1^+ \rightarrow 0^+$	0.1 ± 0.02		31	Ramaswamy(1959b)
32	Ge	66	2102 ± 15	several	$0^+ \rightarrow$ several		1.45 ± 0.2	31	Ricci(1960)
32	Ge	69	2225.5 ± 2.4	unknown	unknown	2		31	McCown(1948a)
33	As	71	2009 ± 7	several	$5/2^- \rightarrow$ several	2.1 ± 1		23	Thulin(1954a)
						~2		31	McCown(1948b)
33	As	74	2563.7 ± 2.9	several	$2^- \rightarrow$ several	1.42		20	Scobie(1957a)
				596	$2^- \rightarrow 2^+$	1.5		26	Johansson(1951)
						1.49		20	Scobie(1957a)
							1.32 ± 0.14	31	Grigor'ev(1958a)
							1.47 ± 0.35	26	Horen(1959)

TABLE 3.6 (continued)

Z	Element	A	Q_{EC}^a (keV)	Final state (keV)	$J_i^\pi \rightarrow J_f^\pi$	P_K/P_{β^+}	P_{EC}/P_{β^+}	Method ^b	Reference
33	As	74					1.288 ± 0.018	27	Vatai(1968c)
				1200	$2^- \rightarrow 2^+$		> 3.2	31	Horen(1959)
34	Se	73	2740 ± 10	several	$(\frac{9}{2}^+)$ \rightarrow several	0.59		23	Scott(1951)
				425	$(\frac{9}{2}^+)$ \rightarrow $\frac{9}{2}^+$	0.45		26	Scott(1951)
35	Br	75	3010 ± 20	unknown	unknown	~ 0.1		26	Baskova(1961)
35	Br	76	5100 SYST	several	$1 \rightarrow$ several	0.5 ± 0.2		24	Hirgis(1959b)
35	Br	77	1364.5 ± 2.8	several	$\frac{3}{2}^- \rightarrow$ several	20		24	Woodward(1948b)
							39.8 ± 6.2	27	Sehr(1954)
36	Kr	77	3000 ± 50	several	$(\frac{5}{2}^-)$ \rightarrow several	2.6		31	Woodward(1948a)
						0.21 ± 0.1		23	Fhulin(1955)
36	Kr	79	1631 ± 9	several	$\frac{1}{2}^- \rightarrow$ several	50		31	Woodward(1948a)
						~ 10		23	Bergström(1951)
						8 ± 4		23	Bergström(1952)
						14.1 ± 4.0		23	Radvanyi(1952b)
						9.3 ± 2		23	Fhulin(1954b)

Z	Element	A	$Q_{EC}^{\beta^-}$ (keV)	Final state (keV)	$J_i^{\pi_i} \rightarrow J_f^{\pi_f}$	P_K/P_{β^+}	P_{EC}/P_{β^+}	Method	Reference
36	Kr	79				14.1 ± 4.9 $- 3.2$		23	Radvanyi(1955b)
				261.3	$\frac{1^-}{2} \rightarrow \frac{3^-}{2}$	57 ± 10		29	Langhoff(1966)
				398	$\frac{1^-}{2} \rightarrow ?$	430 ± 100		29	Langhoff(1966)
37	Rb	84	2679.8 ± 2.9	several	$2^- \rightarrow \text{several}$	0.07		24	Karraker(1950)
				0	$2^- \rightarrow 0^+$	2.06 ± 0.36		31	Welker(1955)
						1.12 ± 0.25		31	Konijn(1958/59)
				880	$2^- \rightarrow 2^+$	5.15 ± 0.38		31	Welker(1955)
						3.96 ± 0.16		22	Goedbloed(1970c)
							5.72 ± 0.12	27	Konijn(1958a)
								26	Zoller(1969)
39	Y	87	1882 ± 7	388	$\frac{1^-}{2} \rightarrow \frac{1^-}{2}$		46		
40	Zr	89	2834.1 ± 3.0	several	$\frac{9^+}{2} \rightarrow \text{several}$		~ 3	26	Goldhaber(1951)
							4 ± 1	26	Shore(1953)
				910	$\frac{9^+}{2} \rightarrow \frac{9^+}{2}$		3.48 ± 0.15	-	Monaro(1961) revised by van Patter(1964)
							3.43 ± 0.10	26	van Patter(1964)
							3.47 ± 0.21	26	Hinrichsen(1968)

TABLE 3.6 (CONTINUED)

Z	Element	A	$Q_{\beta C}^a$ (keV)	Final state (keV)	$J_i^{\pi} - J_f^{\pi}$	P_K / P_{β^+}	$P_{\beta C} / P_{\beta^+}$	Method ^b	Reference
40	Zr	89m	3422.1 ± 3.0	1510	$\frac{1}{2}^- \rightarrow \frac{3}{2}^-$		4.7 + 2.3 - 1.8	-	derived by van Patter(1964) from results of Shore(1953)
							3.76 ± 0.19	31	van Patter(1964)
42	Mo	90	2487 ± 4	several	$0^+ \rightarrow$ several		3.0 ± 0.5	26	Cooper(1965)
42	Mo	91	4443 ± 28	0	$\frac{9}{2}^+ \rightarrow \frac{9}{2}^+$	$(5.05 \pm 0.34) \times 10^{-2}$		24	Fitzpatrick(1975)
45	Tc	93	5186 ± 13	several	$(\frac{9}{2}^+) \rightarrow$ several		7.20 ± 0.67	27	Sehr(1954)
				1350; 1500	$(\frac{9}{2}^+) \rightarrow ?$	6.7 ± 2.2		26 & 31	Levi(1954)
45	Tc	94	4260 ± 6	several	$(6^+, 7^+) \rightarrow$ several		6.1	26	Monaro(1962)
							14.9 ± 0.7	31	Matuszek(1963)
				2422	$(6^+, 7^+) \rightarrow 6^+$		7.5 ± 1.8	26	Hamilton(1964)
45	Tc	95m	1740 ± 11	several	$(\frac{1}{2}^-) \rightarrow$ several		2.5×10^2	31	Medicus(1950)
							3.8×10^2	31	Levi(1957)
							$(2.5 \pm 1) \times 10^2$	31	Unik(1959)
							$(2.3 \pm 0.2) \times 10^2$	31	Cretzu(1965)
				204.2	$(\frac{1}{2}^-) \rightarrow \frac{3}{2}^+$	78		31	Levi(1959)
							62	31	Cretzu(1965)
				0	$(\frac{1}{2}^-) \rightarrow \frac{3}{2}^+$	23		31	Levi(1959)

ORIGINAL PAGE IS
OF POOR QUALITY

Z	Element	A	Q_{EC} ^a (keV)	Final state (keV)	$J_i^\pi - J_f^\pi$	P_K/P_{β^+}	P_{EC}/P_{β^+}	Method ^b	Reference
45	Rh	100	3630 ± 20	several	$1, 2^- \rightarrow$ several		~ 19	24	Lindner(1948)
46	Pd	101	1990 ± 15	several	$(\frac{5}{2}^+) \rightarrow$ several		~ 9	24	Lindner(1948)
							~ 24	24	Katcoff(1956)
47	Ag	108	1921 ± 8	0	$1^+ \rightarrow 0^+$	9.6		25	Perlman(1953)
						5.6 ± 1		25	Frevert(1965)
							9.3	31	Wahlgren(1960)
48	Cd	107	1417 ± 4	several	$\frac{5}{2}^+ \rightarrow$ several	320 ± 20		26	Bradt(1945)
49	In	114	1431 ± 7	several	$1^+ \rightarrow$ several	5.4×10^2		31	Brodzins(1956)
50	Sn	111	2508 ± 26	several	$\frac{7}{2}^+ \rightarrow$ several	2.50 ± 0.25		26	McGinnis(1951)
							2.7 ± 0.2	25	Snyder(1965)
				0	$\frac{7}{2}^+ \rightarrow \frac{9}{2}^+$		2.20 ± 0.15	31	Rivier(1971)
51	Sb	113	3898 ± 32	several	$\frac{5}{2}^+ \rightarrow$ several	0.25 ± 0.04		26	Kiselev(1969)
51	Sb	115	3030 ± 20	several	$\frac{5}{2}^+ \rightarrow$ several		1.99	26	Vartanov(1963)
						1.22 ± 0.06		26	Kiselev(1969)
51	Sb	116	4500 ± 40	several	$(3, 2^+) \rightarrow$ several		3.5	26	Flak(1961)

TABLE 3.6 (continued)

Z	Element	A	Q_{EC} ^a (keV)	Final state (keV)	$J_i^\pi \rightarrow J_f^\pi$	P_K/P_{β^+}	P_{EC}/P_{β^+}	Method ^b	Reference
51	Sb	116m	5000 ± 40	2900	(8 ⁻) → 7 ⁻		4.22 ± 0.20	29	Bolotin(1964)
51	Sb	117	1753 ± 40	158	5/2 ⁺ → 3/2 ⁺		38.5 ± 7.4	30	McGinnis(1955)
						.977		26	Baskova(1964)
51	Sb	118m	3835 ± 6	2572	(8 ⁻) → 7 ⁻		620 ± 40	29	Bolotin(1961)
51	Sb	120	2680 ± 7	0	1 ⁺ → 0 ⁺	1.057 ± 0.035		24	Campbell(1975)
51	Sb	122	1610.1 ± 3.3	0	2 ⁻ → 0 ⁺	300 ± 130		31	Glaubman(1955)
						300 ± 50		31	Perlman(1958)
52	Te	117	3490 ± 30	several	1/2 ⁺ → several		~2.3	31	Fink(1961)
53	I	118	6100 SYST	unknown	unknown	0.76 ± 0.16		24	Andersson(1965)
53	I	119	5200 ± 400	unknown	unknown	0.86 ± 0.10		24	Andersson(1965)
53	I	120	5500 SYST	unknown	unknown	1.04 ± 0.09		24	Andersson(1965)
53	I	121	2370 SYST	several	(5/2 ⁺) → several	9 ± 1		24	Andersson(1965)
53	I	124	3160 ± 10	several	2 ⁻ → several		~2.3	31	Marquez(1950)
						2.7 ± 0.4		25	Girgis(1959a)
						2.2		25	Mitchell(1959)

ORIGINAL PAGE IS
OF POOR QUALITY

Z	Element	A	Q_{EC}^a (keV)	Final state (keV)	$J_i^\pi - J_f^\pi$	P_K/P_{β^+}	P_{EC}/P_{β^+}	Method	Reference
53	I	126	2151 ± 5	0	$2^- \rightarrow 0^+$	12.5^{+7}_{-3}		31	Marty(1953)
						21 ± 8		31	Perlman(1954)
						20.2 ± 2.0		31	Koerts(1955)
				667	$2^- \rightarrow 2^+$	>75		31	Marty(1953)
						95 ± 10		31	Koerts(1955)
						200		31	Singh(1970)
							165 ± 5	29	Harmer(1959)
53	I	128	1254 ± 4	0	$1^+ \rightarrow 0^+$	1800 ± 400		31	Langhoff(1961)
55	Cs	125	3070 ± 20	unknown	unknown		1.03 ± 0.07	25	Friedlander(1962)
55	Cs	127	2090 ± 20	several	$\frac{1}{2}^+ \rightarrow$ several		27.7 ± 1.7	25	Friedlander(1962)
55	Cs	132	2099 ± 23	667.6	$2^- \rightarrow 2^+$	78 ± 26		31	Jha(1961)
						53.5 ± 8.7		22	Goverse(1974a)
							$(1.6 \pm 0.6) \times 10^2$	26	Robinson(1962)
							$(3.3 \pm 1.7) \times 10^2$	29	Taylor(1963)
							1.7×10^2	30	Taylor(1963)

TABLE 3.6 (continued)

Z	Element	A	Q_{EC}^a (keV)	Final state (keV)	$J_i^\pi - J_f^\pi$	P_K/P_{β^+}	P_{EC}/P_{β^+}	Method	Reference
57	La	131	2960 ± 40	several	$\frac{1}{2}^+ \rightarrow$ several	2.31 ± 0.31		25	Creager(1959/60)
57	La	134	3710 ± 25	several	$1^+ \rightarrow$ several		1.3	24	Stover(1951)
				0	$1^+ \rightarrow 0^+$	0.40 ± 0.04		25	Biryukov(1965)
57	La	136	2870 ± 70	several	$1^+ \rightarrow$ several		2	24	Naumann(1950)
58	Ce	131	4300	SYST unknown	unknown		~8	26	Norris(1966)
59	Pr	136	5200	SYST several	$(2,3^+) \rightarrow$ several	1.8 ± 0.4		25	Danby(1958)
						0.65 ± 0.01		25	Ketelle(1971)
59	Pr	137	2750 ± 40	several	$(\frac{5}{2}^+) \rightarrow$ several	2.05 ± 0.3		25	Danby(1958)
						2.5 ± 0.2		25	van Hise(1967)
59	Pr	138	4437 ± 10	several	$(6,7,8) \rightarrow$ several		7.7	24	Stover(1951)
							3.35 ± 1.1	26	Fujioka(1964)
						4.5 ± 1.2		25	Danby(1958)
59	Pr	139	2112 ± 20	several	$(\frac{5}{2}^+) \rightarrow$ several		16	24	Stover(1951)
						11.3 ± 1.0		25	Danby(1958)
				0	$(\frac{5}{2}^+) \rightarrow \frac{3}{2}^+$	7.1		25	Biryukov(1963b)

ORIGINAL PAGE IS
OF POOR QUALITY

Z	Element	A	Q_{EC}^a (keV)	Final state (keV)	$J_i^\pi - J_f^\pi$	P_K / P_{β^+}	P_{EC} / P_{β^+}	Method ^b	Reference
59	Pr	140	3388 ± 6	several	$(1^+) \rightarrow$ several		2	24	Wilkinson(1949)
							0.85	-	Rasmussen(1957)
						1.0 ± 0.1		25	Browne(1952)
						0.897		23	Brabec(1960)
						0.90 ± 0.08		25	Evans(1972)
					$(1^+) \rightarrow 0^+$	0.76		25	Biryukov(1960)
						0.74 ± 0.03		25	Biryukov(1962) and (1970)
60	Nd	141	1905 ± 15	several	$\frac{3}{2}^+ \rightarrow$ several	~ 60		24	Wilkinson(1949)
						48 ± 9		25	Polak(1958)
							35.6 ± 3.6	25	Grissom(1966)
							21.9	25	Beery(1968)
						30.4 ± 2.3		25	Evans(1972)
				0	$\frac{3}{2}^+ \rightarrow \frac{5}{2}^+$	21.1 ± 1.0		25	Biryukov(1963a)
						28 ± 1		25	Biryukov(1970)

TABLE 3.6 (continued)

Z	Element	A	Q_{EC}^a (keV)	Final state (keV)	$J_i^\pi - J_f^\pi$	P_K/P_{β^+}	P_{EC}/P_{β^+}	Method ^b	Reference
61	Pm	141	3730 ± 40	unknown	unknown	~ 0.67		25	Gratot(1959)
61	Pm	142	4820 ± 100	unknown	unknown	~ 0.05		24	Gratot(1959)
62	Sm	143	3479 ± 28	several	$\frac{3}{2}^+ \rightarrow$ several	0.30 ± 0.04		25	Penev(1974)
						~ 1.7		24	Gratot(1959)
						0.98 ± 0.09		25	Belyanin(1966)
						1.27 ± 0.11		25	Evans(1972)
				0	$\frac{3}{2}^+ \rightarrow \frac{5}{2}^+$	0.92 ± 0.09		25	Biryukov(1970)
				1173.1	$\frac{3}{2}^+ \rightarrow \frac{1}{2}^+$		63 ± 10^c	31	Firestone(1974)
				1403.1	$\frac{3}{2}^+ \rightarrow$ unknown		35 ± 5^c	31	
				1515.0	$\frac{3}{2}^+ \rightarrow$ unknown		30 ± 7^c	31	
63	Eu	143	5000 ± 200	1536.7	$\frac{5}{2}^+ \rightarrow \frac{5}{2}^+$		0.62 ± 0.06^d	31	Firestone(1974)
				1565.9	$\frac{5}{2}^+ \rightarrow (\frac{3}{2}^+ \frac{5}{2}^+)$		0.69 ± 0.15^d	31	
				1715.1	$\frac{5}{2}^+ \rightarrow (\frac{5}{2}^+)$		0.75 ± 0.17^d	31	
				1912.6	$\frac{5}{2}^+ \rightarrow (\frac{3}{2}^+ \frac{5}{2}^+)$		1.07 ± 0.11^d	31	

ORIGINAL PAGE IS
OF POOR QUALITY

Z	Element	A	Q_{20}^a (keV)	Final state (keV)	$J_i^{\pi} \rightarrow J_f^{\pi}$	P_K/P_{R^+}	P_{EC}/P_{R^+}	Method ^b	Reference
63	Eu	145	2720 ± 15	0	$\frac{5}{2}^+ \rightarrow \frac{7}{2}^-$	<5		31	Avotina(1965a)
						3.4		31	Zhelev(1967)
						3.0 ± 0.5		31	Muziol(1966)
				894	$\frac{5}{2}^+ \rightarrow \frac{3}{2}^+$	100 ± 20		31	Avotina(1965a)
						120		31	Zhelev(1967)
						70 ± 9		31	Muziol(1966)
						80		31	Adam(1967b)
63	Eu	146	3872 ± 9	several	$(4^-) \rightarrow \text{several}$		21	25	Takekoshi(1964)
				1384	$(4^-) \rightarrow ?$	7.9 ± 1.2		25	Funk(1962)
				2051	$(4^-) \rightarrow ?$	19 ± 8		25	Funk(1962)
63	Eu	147	1762 ± 9	198.1	$\frac{5}{2}^+ \rightarrow \frac{3}{2}^-$	150 ± 30		31	Avotina(1966;1965b)
						155 ± 50		31	Muziol(1966)
						302 ± 150		31	Adam(1967a)

TABLE 3.6 (continued)

Z	Element	A	Q_{EC}^a (keV)	Final state (keV)	$J_i^\pi \rightarrow J_f^\pi$	P_K/P_{β^+}	P_{EC}/P_{β^+}	Method ^b	Reference
63	Eu	147		121.8	$\frac{5}{2}^+ \rightarrow \frac{3}{2}^-$	170 ± 30		31	Avotina(1966;1965b)
						165 ± 35		31	Muziol'(1966)
						257 ± 100		31	Adam(1967a)
				0	$\frac{5}{2}^+ \rightarrow \frac{7}{2}^-$	87 ± 45		31	Muziol'(1966)
						258 ± 100		31	Adam 1967a)
66	Dy	155	2099 ± 6	227.0	$(\frac{5}{2}^-) \rightarrow \frac{5}{2}^-$	44 ± 5		31	Ferguson(1963)
68	Er	161	2050 ± 40	211.1	$\frac{3}{2}^- \rightarrow \frac{1}{2}^+$	400 ± 200		31	Gromov(1965)
69	Tm	162	4700 ± 100	several	1 → several	12		25	Chu(1971)
69	Tm	166	3035 ± 12	?	2 ⁺ → 4 ⁺	9		31	Wilson(1960)

TABLE 3.6 (continued)

Z	Element	A	Q_{EC} (keV)	Final state (keV)	$J_i^\pi - J_f^\pi$	P_K/P_{β^+}	P_{EC}/P_{β^+}	Method ^b	Reference
64	Gd	145	5311 ± 120	808.5	$\frac{1}{2}^+ \rightarrow \frac{1}{2}^+$		18 ± 8	31	Firestone(1974;1975)
				1041.9	$\frac{1}{2}^+ \rightarrow \left(\frac{3}{2}^+\right)$		1.0 ± 0.1	31	
				1567.3	$\frac{1}{2}^+ \rightarrow \left(\frac{1}{2}^+ \frac{3}{2}^+ \frac{5}{2}^+\right)$		37 ± 18	31	
				1599.9	$\frac{1}{2}^+ \rightarrow \left(\frac{1}{2}^+ \frac{3}{2}^+ \frac{5}{2}^+\right)$		13 ± 6	31	
				1757.8	$\frac{1}{2}^+ \rightarrow \frac{3}{2}^+$		1.87 ± 0.09	31	
				1761.9	$\frac{1}{2}^+ \rightarrow$ unknown		2.6 ± 0.8	31	
				1845.4	$\frac{1}{2}^+ \rightarrow \left(\frac{3}{2}^+ \frac{5}{2}^+\right)$		43 ± 21	31	
				1880.6	$\frac{1}{2}^+ \rightarrow \left(\frac{1}{2}^+ \frac{3}{2}^+\right)$		2.15 ± 0.12	31	
				2048.9	$\frac{1}{2}^+ \rightarrow$ unknown		4.2 ± 1.0	31	
				2113.9	$\frac{1}{2}^+ \rightarrow \left(\frac{3}{2}^+ \frac{5}{2}^+\right)$		10 ± 4	31	
				2494.8	$\frac{1}{2}^+ \rightarrow \left(\frac{1}{2}^+\right)$		4.8 ± 0.5	31	
				2642.2	$\frac{1}{2}^+ \rightarrow$ unknown		8.1 ± 0.9	31	

TABLE 3.6 (continued)

Z	Element	A	Q_{EC}^a (keV)	Final state (keV)	$J_i^\pi - J_f^\pi$	P_K/P_{β^+}	P_{EC}/P_{β^+}	Method ^c	Reference
70	Yb	162	2500	SYST	$0^+ \rightarrow 1^+$	36		31	Abdurazakov(1974)
71	Lu	168	4360 ± 80	several	$(1^-) \rightarrow$ several		8	31	Merz(1961)
72	Hf	171	2600	syst	662.0	$\frac{7^+}{2} - \frac{7^-}{2}$	144 ± 3	25 26	Wilson(1969) Gnatovich(1974)
73	Ta	178	1910 ± 100	0	$1^+ \rightarrow 0^+$	110 ± 70		25	Gallagher(1961)
77	Ir	186	3831 ± 20	868.7	unknown $\rightarrow 6^+$	6.5 ± 3		26	Emery(1963)
				1453.1	unknown $\rightarrow (8^+)$	17		26	Emery(1963)
79	Au	190	4400	SYST	several	$1^- \rightarrow$ several	50	25	Jastrzebski(1961)
81	Tl	200	2454 ± 5	367.97	$2^- \rightarrow 2^+$	110 ± 10		31	Konijn(1960)
						102 ± 9		27	van Nooijen(1962)
83	Bi	207	2405 ± 8	569.6	$\frac{9^-}{2} \rightarrow \frac{5^-}{2}$		$(6 \pm 1) \times 10^2$	26	Rapnik(1972)

^a Q_{EC} values are taken from Wapstra and Gove(1971).

^b Methods are identified by numbers explained in Table

^c Relative measurements, normalised to the transition to the 1056.6 keV state of ^{143}Pm .

^d Relative measurements, normalised to the transition to the 1107.2 keV state of ^{143}Sm .

ORIGINAL PAGE IS
OF POOR QUALITY

TABLE 3.7 Allowed Transitions - Comparison of Selected Results with Theory
(a) Results for K/β^+ Ratios

Z	Element	A	Q_{EC}^a (keV)	Final state (keV)	$J_i^\pi - J_f^\pi$	Experimental values		Theoretical values	
						P_K/P_{β^+}	Method Reference	P_K/P_{β^+}	
6	C	11	1982.2±1.0	0	$\frac{3^-}{2} - \frac{3^-}{2}$	$(2.30^{+0.14}_{-0.11}) 10^{-3}$	21	Campbell(1967)	$(2.11 \pm 0.01) 10^{-3}$
7	N	13	2220.5±0.9	0	$\frac{1^-}{2} - \frac{1^-}{2}$	$(1.68 \pm 0.12) 10^{-3}$	21	Ledingham(1965)	$(1.800 \pm 0.006) 10^{-3}$
8	O	15	2759.2±0.9	0	$\frac{1^-}{2} - \frac{1^-}{2}$	$(1.07 \pm 0.06) 10^{-3}$	21	Leiper(1972)	$(0.911 \pm 0.002) 10^{-3}$
9	F	18	1655.3±0.9	0	$1^+ - 0^+$	$(3.00 \pm 0.18) 10^{-2}$	20	Drever(1956)	$(3.14 \pm 0.02) 10^{-2}$
10	Ne	19	3238.2±0.9	0	$\frac{1^+}{2} - \frac{1^+}{2}$	$(9.6 \pm 0.3) 10^{-4}$	21	Leiper(1972)	$(9.28 \pm 0.02) 10^{-4}$
11	Na	22	2842.3±0.5	1274.6	$3^+ - 2^+$	0.105 ± 0.009	22	McCann(1969)	0.1023 ± 0.0004
15	P	30	4227.4±2.6	0	$1^+ - 0^+$	$(1.24 \pm 0.01) 10^{-3}$	21	Ledingham(1971)	$1.233 \pm 0.005) 10^{-3}$
27	Co	58	2308.0±2.5	810.5	$2^+ - 2^+$	4.92 ± 0.09	22	Joshi(1961)	4.97 ± 0.11
						4.83 ± 0.10	20	Kramer(1962 b)	
						5.05 ± 0.09	Combination of 24 and 31		Bambynek(1963b)
30	Zn	65	1350.7±1.1	0	$\frac{5^-}{2} - \frac{3^-}{2}$	28.0 ± 3.2	23	Perkins(1953)	30.5 ± 0.4
						25 ± 2	31	Gleason(1959)	
						27.7 ± 1.5	31	Hammer(1968)	

TABLE 3.7 . (a) continued.

Z	Element	A	Q_{EC}^a (keV)	Final state (keV)	$J_i^\pi - J_f^\pi$	Experimental values		Theoretical values	
						P_K/P_{β^+}	Method Reference	P_K/P_{β^+}	
31	Ga	68	2919.4+3.9	1078	$1^- - 2^+$	1.28 +0.12	31	Ramaswamy(1959b)	1.36 +0.03
42	Mo	91	4443 +28	0	$\frac{9^+}{2} - \frac{9^+}{2}$	(5.05 +0.34) 10^{-2}	24	Fitzpatrick(1975)	(5.50 +0.22) 10^{-2}
51	Sb	120	2680 +7	0	$1^+ - 0^+$	1.057 +0.035	24	Campbell(1975)	1.24 +0.02
57	La	134	3710 +25	0	$1^+ - 0^+$	0.40 +0.04	25	Biryukov(1965)	0.48 +0.02
59	Pr	140	3388 +6	0	$(1^+) - 0^+$	0.74 +0.03	25	Biryukov(1962,1970)	0.85 +0.01
60	Nd	141	1805 +15	0	$\frac{3^+}{2} - \frac{5^+}{2}$	28 +1	25	Biryukov (1970)	35.3 +3.2
62	Sm	143	3479 +28	0	$\frac{3^+}{2} - \frac{5^+}{2}$	0.92 +0.09	25	Biryukov(1970)	0.98 +0.05
66	Dy	155	2099 +6	227.0	$(\frac{3^+}{2}) - \frac{5^-}{2}$	44 +5	31	Persson(1963)	44.0 + 1.5

ORIGINAL PAGE IS
OF POOR QUALITY

TABLE 3.7 (continued) (b) Results for EC/ β^+ Ratios.

Z	Element	A	Q_{EC}^a (keV)	Final state (keV)	$J_i^\pi \rightarrow J_f^\pi$	Experimental values			Theoretical values
						P_{EC}/P_{β^+}	^b Method	Reference	P_{EC}/P_{β^+}
11	Na	22	2842.3±0.5	1274.6	3 ⁺ -2 ⁺	0.1041±0.0010	28	Williams(1964,1968)	0.1117±0.0004
						0.1048±0.0007	27	Leutz(1967)	
						0.1042±0.0010	27	Vatai(1968c)	
						0.1077±0.0003	27	MacMahon(1970)	
23	V	48	4015.4±28	2295	4 ⁺ -4 ⁺	0.77 ±0.04	29	Biryukov(1966)	0.78 ±0.01
						0.83 ±0.06	29	Konijn(1967b)	
						0.76 ±0.035	27	Konijn(1967b)	
25	Mn	52	4709.8±3.5	3112	6 ⁺ -6 ⁺	1.86 ±0.17	31	Good(1946)	2.09 ±0.06
						2.01 ±0.24	27	Sehr(1954)	
						1.84 ±0.20	30	Wilson(1962)	
						2.04 ±0.24	26	Freedman(1966)	
						1.80 ±0.13	27	Konijn(1967b)	
						2.12 ±0.17	29	Konijn(1967b)	

TABLE 3.7 (b) continued

Z	Element	A	Q_{EC}^a (keV)	Final state (keV)	$J_i^\pi \rightarrow J_f^\pi$	Experimental values		Theoretical values
						P_{EC}/P_{β^+}	Method ^b Reference	P_{EC}/P_{β^+}
27	Co	58	2308.0±2.5	810.5	$2^+ \rightarrow 2^+$	5.67 ±0.14	27 Konijn(1958a)	5.62 ±0.12
						5.49 ±0.18	30 Ramaswamy(1961)	
						5.48 ±0.09	29 Biryukov(1966)	
						5.76 ±0.13	28 Williams(1970) and Goodier(1971)	
28	Ni	57	3243 ±7	1490	$\frac{3}{2}^- \rightarrow \frac{1}{2}^-$	1.438±0.059	27 Konijn(1958b)	1.48 ±0.07
						1.5 ±0.08	27 Bakhru(1967)	
				1370	$\frac{3}{2}^- \rightarrow \frac{3}{2}^-$	0.805±0.040	27 Konijn(1958b)	
						1.0 ±0.1	27 Bakhru(1967)	
30	Zn	65	1350.7±1.1	0	$\frac{5}{2}^- \rightarrow \frac{3}{2}^-$	24.9 ±1.5	27 Sehr(1954)	34.5 ±0.4
40	Zr	89	2834.1±3.0	910	$\frac{9}{2}^+ \rightarrow \frac{9}{2}^+$	3.48 ±0.15	- Monaro(1961) revised by van Patter(1964)	3.40 ±0.05
						3.43 ±0.10	26 van Patter(1964)	
						3.47 ±0.21	26 Hinrichsen(1968)	

TABLE 3.7 (b) continued.

Z	Element	A	Q_{EC}^a (keV)	Final state (keV)	$J_i^\pi - J_f^\pi$	Experimental values			Theoretical values
						P_{EC}/P_{β^+}	Method	Reference	P_{EC}/P_{β^+}
40	Zr	89m	3422.1 \pm 3.0	1510	$\frac{1}{2}^- - \frac{3}{2}^-$	3.76 \pm 0.19	31	van Patter(1964)	3.55 \pm 0.06
50	Sn	111	2508 \pm 26	0	$\frac{7}{2}^+ - \frac{9}{2}^+$	2.20 \pm 0.15	31	Rivier(1971)	1.87 \pm 0.16
51	Sb	116m	5000 \pm 40	2900	$(8^-) - 7^-$	4.22 \pm 0.20	29	Bolotin(1964)	5.9 \pm 1.1
51	Sb	118m	3885 \pm 6	2572	$(8^-) - 7^-$	620 \pm 40	29	Bolotin(1961)	830 \pm 80

^a Q_{EC} values are taken from Wapstra and Gove (1971).

^b Methods are identified by numbers explained in Table 3.1.

TABLE 3.8 First Forbidden Unique Transitions

Z	Element	A	Q_{EC}^a (keV)	Final state (keV)	$J_i^\pi - J_f^\pi$	Experimental values		Theoretical	
						P_K/P_{β^+}	Method Reference	1st unique forbidden values P_K/P_{β^+}	
37	Rb	84	2679.8±2.9	0	2 ⁻ -0 ⁺	1.12 ±0.25	31 Konijn(1958/59)	0.94 ±0.01	
51	Sb	122	1610.1±3.3	0	2 ⁻ -0 ⁺	300 ±50	31 Perlman(1958) and Glaubman(1955)	254 ±11	
53	I	126	2151 ±5	0	2 ⁻ -0 ⁺	20.2 ±2.0	31 Koerts(1955)	21.1 ±0.7	

a Q_{EC} values are taken from Wapstra and Gove (1971).

b Methods are identified by numbers explained in Table 3.1.

ORIGINAL PAGE IS
OF POOR QUALITY

TABLE 3-9 . First Forbidden Non-Unique Transitions
(a) K/β^+ Ratios

Z	Element	A	Q_{EC}^a (keV)	Final state (keV)	$J_i^\pi - J_f^\pi$	Experimental values		Theoretical (allowed)			
						P_K/P_{β^+}	Method Reference	P_K/P_{β^+}			
37	Rb	84	2679.8±2.9	880	$2^- - 2^+$	5.15 ±0.38	31 Welker(1955)	3.51 ±0.06			
						3.96 ±0.16	22 Goedbloed(1970c)				
53	I	126	2151 ±5	667	$2^- - 2^+$	95 ±10	31 Koerts(1955)	138 ±7			
63	Eu	145	2720 ±15	0	$\frac{5^+}{2} - \frac{7^-}{2}$	3.0 ±0.5	31 Muziol(1966)	3.39 ±0.14			
						894	$\frac{5^+}{2} - \frac{3^-}{2}$		100 ±20	31 Avotina(1965a)	43.9 ±4.2
									70 ±9	31 Muziol(1966)	
63	Eu	147	1762 ±9	198.1	$\frac{5^+}{2} - \frac{3^-}{2}$	160 ±30	31 Avotina(1966)	197 ±16			
						121.8	$\frac{5^+}{2} - \frac{5^-}{2}$		170 ±30	31 Avotina(1966)	
									165 ±35	31 Muziol(1966)	119 ±8
55	Cs	132	2099 ±23	-667.8	$2^- - 2^+$	53.5 ±8.9	22 Goverse(1974)	264 ±71			
81	Tl	200	2454 ±5	367.97	$2^- - 2^+$	110 ±10	31 Konijn(1960)	65.7 ±1.4			
						102 ±9	27 van Nooijen(1962)				

TABLE 3.9 (continued)
(b) EC/ β^+ Ratios

Z	Element	A	Q_{EC}^a (keV)	Final state (keV)	$J_i^\pi - J_f^\pi$	Experimental values			Theoretical (allowed)
						P_{EC}/P_{β^+}	Method ^b	Reference	P_{EC}/P_{β^+}
33	As	74	2563.7±2.9	596	2 ⁻ -2 ⁺	1.32 ±0.14	31	Grigor'ev(1958a)	1.24 ±0.01
						1.288±0.018	27	Vatai(1968 c)	
37	Rb	84	2679.8±2.9	880	2 ⁻ -2 ⁺	5.72 ±0.12	27	Konijn(1958a)	3.97 ±0.07
53	I	126	2151 ±5	667	2 ⁻ -2 ⁺	165 ±5	29	Harmer(1959)	159 ±8

^a Q_{EC} values are taken from Wapstra and Gove (1971).

^b Methods are identified by numbers explained in Table 3.1..

ORIGINAL PAGE IS
OF POOR QUALITY

TABLE 1. The function $L_{1s}(r)$ given by Eq. (4-24), and the associated relativistic correction factor $L_{1s}(k)$, for various values of the photon energy k , measured in units of the K-shell binding energy $E_K = (Z\alpha)^2/2$.

k	$L_{1s}(k)$	$L_{1s}(r)$
1.0	.2745	.5377
1.1	.2803	.5420
1.2	.3042	.5463
1.3	.3175	.5504
1.4	.3300	.5545
1.5	.3419	.5584
1.6	.3520	.5623
1.7	.3634	.5660
1.8	.3733	.5697
1.9	.3829	.5733
2.0	.3917	.5767
2.1	.4003	.5801
2.2	.4084	.5834
2.3	.4162	.5866
2.4	.4237	.5897
2.5	.4308	.5928
2.6	.4377	.5958
2.7	.4443	.5987
2.8	.4506	.6015
2.9	.4567	.6043

ORIGINAL PAGE IS
OF POOR QUALITY

TABLE 4.1. Continued.

k	$B_{1s}(k)$	$B_{2s}(k)$
3.0	.4626	.6070
3.2	.4738	.6122
3.4	.4842	.6177
3.6	.4940	.6220
3.8	.5032	.6266
4.0	.5118	.6313
4.2	.5200	.6352
4.4	.5278	.6393
4.6	.5351	.6432
4.8	.5421	.6470
5.0	.5488	.6506
5.5	.5642	.6592
6.0	.5780	.6670
6.5	.5905	.6743
7.0	.6018	.6811
7.5	.6122	.6874
8.0	.6218	.6932
8.5	.6307	.6989
9.0	.6389	.7041
9.5	.6466	.7090
10.0	.6537	.7137
11.0	.6653	.7223
12.0	.6754	.7301

ORIGINAL PAGE IS
OF POOR QUALITY

TABLE 4.1. Continued.

	$R_{1s}(k)$	$R_{1s}(k)$
15.0	.6200	.7571
14.0	.6932	.7450
16.0	.7746	.7554
18.0	.7235	.7654
20.0	.7405	.7742
22.0	.7510	.7820
24.0	.7602	.7890
26.0	.7685	.7953
28.0	.7759	.8010
30.0	.7826	.8053
35.0	.8070	.8171
40.0	.8080	.8271
45.0	.8183	.8352
50.0	.8272	.8422
60.0	.8411	.8537
70.0	.8520	.8629
80.0	.8609	.8705
90.0	.8635	.8770
100.0	.8747	.8825
120.0	.8850	.8916
140.0	.8930	.8988
160.0	.8996	.9046
180.0	.9051	.9096

TABLE 4.1 Continued.

N	$r_{1s}(k)$	$r_{1s}(1)$
200.0	.9077	.9136
220.0	.9138	.9175
240.0	.9173	.9207
250.0	.9204	.9236
280.0	.9232	.9261
300.0	.9257	.9285
350.0	.9310	.9334
400.0	.9354	.9374
450.0	.9389	.9408
500.0	.9420	.9437
700.0	.9502	.9520
1000.0	.9586	.9595

ORIGINAL PAGE IS
OF POOR QUALITY

TABLE 4.2. The function $\epsilon_{2s}(k)$ given by Eq. (4-25), and the associated relativistic correction factor $\delta_{2s}(k)$, for various values of the photon energy k , measured in units of the K-shell binding energy $E_K = (Z\alpha)^2/2$.

k	$\epsilon_{2s}(k)$	$\delta_{2s}(k)$
1.0	.7439	.5010
1.1	.7060	.5000
1.2	.6262	.5003
1.3	.5561	.5016
1.4	.4932	.5035
1.5	.4380	.5058
1.6	.3893	.5085
1.7	.3459	.5115
1.8	.3073	.5147
1.9	.2734	.5179
2.0	.2433	.5213
2.1	.2172	.5247
2.2	.1941	.5281
2.3	.1731	.5315
2.4	.1544	.5349
2.5	.1379	.5383
2.6	.1238	.5417
2.7	.1119	.5450
2.8	.1019	.5483
2.9	.0931	.5516

TABLE B.2. Continued.

λ	$\tau_{2s}(k)$	$\lambda_{2s}(l)$	τ
3.0	.3200	.5547	
3.2	.3402	.5670	
3.4	.3592	.5770	
3.6	.3781	.5785	
3.8	.3960	.5784	
4.0	.4134	.5730	
4.2	.4302	.5620	
4.4	.4467	.5440	
4.6	.4627	.5190	
4.8	.4781	.4835	
5.0	.4940	.4401	
5.5	.5372	.4127	
6.0	.5650	.3794	
6.5	.5923	.3375	
7.0	.6100	.2872	
7.5	.6242	.2336	
8.0	.6372	.1602	
8.5	.6470	.0776	
9.0	.6540	.0040	
9.5	.6600		.6800
10.0	.6693		.6856
11.0	.6862		.6960
12.0	.6410		.7054

ORIGINAL PAGE IS
OF POOR QUALITY

TABLE 4.2 Continued

	2s	2s
13.0	.7547	.7130
14.0	.7550	.7217
15.0	.7561	.7304
16.0	.7573	.7391
20.0	.7675	.7574
22.0	.7700	.7664
24.0	.7740	.7744
26.0	.7785	.7817
28.0	.7832	.7882
30.0	.7870	.7942
35.0	.7936	.8070
40.0	.7970	.8176
45.0	.8032	.8266
50.0	.8177	.8343
60.0	.8331	.8470
70.0	.8451	.8571
80.0	.8549	.8654
90.0	.8630	.8723
100.0	.8698	.8783
120.0	.8800	.8880
140.0	.8895	.8957
160.0	.8966	.9019
180.0	.9024	.9071

TABLE 4.2. Continued.

k	$B_{2s}(k)$	$\mu_{2s}(k)$
200.0	.9073	.9126
220.0	.9115	.9155
240.0	.9153	.9180
260.0	.9185	.9210
280.0	.9214	.9245
300.0	.9241	.9270
350.0	.9276	.9321
400.0	.9311	.9363
450.0	.9370	.9398
500.0	.9410	.9427
700.0	.9501	.9513
1000.0	.9582	.9590

TABLE 4.3: The functions $\gamma_{2p}(k)$, $\gamma_{2p}(k)$, $q_{2p}(k)$, and $\gamma_{2p}(k)$, given by eq. (4-33), for various values of the photon energy k , measured in units of the K-shell binding energy, $B_K = 6.5 \times 10^4 / Z^2$.

k	$\gamma_{2p}(k)$	$\gamma_{2p}(k)$
1.0	1.5815	1.0104
1.1	1.4737	.9370
1.2	1.3859	.8625
1.3	1.3090	.7891
1.4	1.2400	.7178
1.5	1.1769	.6481
1.6	1.1190	.5815
1.7	1.0647	.5179
1.8	1.0127	.4575
1.9	.9625	.4003
2.0	.9133	.3471
2.1	.8652	.2974
2.2	.8182	.2510
2.3	.7721	.2074
2.4	.7270	.1662
2.5	.6828	.1281
2.6	.6395	.0930
2.7	.5971	.0707
2.8	.5555	.0520
2.9	.5147	.0379
3.0	.4747	.0283

TABLE 4.3. Continued.

h	$C_{2p} (K)$	$C_{3p} (K)$
3.2	.1352	.0715
3.4	.1242	.0745
3.6	.1142	.0793
3.8	.1057	.0839
4.0	.0996	.0877
4.2	.0934	.0919
4.4	.0877	.0952
4.6	.0830	.0985
4.8	.0785	.0469
5.0	.0746	.0444
5.2	.0709	.0423
5.4	.0677	.0403
5.6	.0647	.0385
5.8	.0619	.0368
6.0	.0594	.0353
6.2	.0570	.0339
6.4	.0548	.0326
6.6	.0528	.0314
6.8	.0510	.0303
7.0	.0492	.0292
7.2	.0476	.0283
7.4	.0460	.0273
7.6	.0446	.0265

ORIGINAL PAGE IS
OF POOR QUALITY

TABLE 4.3. Continued.

λ	σ_p (K)	σ_p (°C)
7.8	.0432	.0257
8.0	.0419	.0249
8.2	.0407	.0242
8.4	.0395	.0235
8.6	.0385	.0229
8.8	.0375	.0225
9.0	.0365	.0217
9.5	.0343	.0204
10.0	.0323	.0192
10.5	.0305	.0181
11.0	.0289	.0172
11.5	.0275	.0163
12.0	.0262	.0155
12.5	.0250	.0148
13.0	.0239	.0142
13.5	.0229	.0136
14.0	.0220	.0131
14.5	.0212	.0126
15.0	.0204	.0121
15.5	.0196	.0117
16.0	.0190	.0112
16.5	.0183	.0109
17.0	.0177	.0105

TABLE 4.3. Continued.

θ	$\epsilon_{22}(\%)$	$\epsilon_{33}(\%)$
17.5	.0172	.0102
18.0	.0166	.0099
18.5	.0161	.0095
19.0	.0157	.0093
19.5	.0152	.0090
20.0	.0148	.0087

TABLE 4.4. Nuclear matrix elements $M_{Nj_v}^A$ [Eq. (4-74)], after Zou and Rapoport (1968).

Type of transition	A	Z	j_v	$M_{Nj_v}^A$	$ \Delta T $	Δc
allowed	0	1	1/2	$C_v \int r^0 Y_0$	0	No
				$-C_A \int r^0 Y_1$		
1st forbidden nonunique	0	1	1/2	$C_A \int r^2 Y_0 Y_2 - \frac{Z\alpha}{1+\lambda_N} C_A \int r^2 Y_1 Y_2$	0	Yes
				$-C_v \int r^2 Y_1 Y_2 - \frac{1}{\sqrt{5}} \frac{Z\alpha}{1+\lambda_N} \times (C_v \int r^2 Y_{110} + \sqrt{2} C_A \int r^2 Y_{111} Y_2)$		
1st forbidden unique	2	2	1/2	$(-1)^N C_A \int r^2 Y_{211} Y_2$	2	Yes
				$(-1)^N C_A \int r^2 Y_{211} Y_2$		
2nd forbidden nonunique	2	2	1/2	$(-1)^N \left[C_v \int r^2 Y_{211} + \frac{1}{\sqrt{5}} \frac{Z\alpha}{1+\lambda_N} \times (\sqrt{2} C_v \int r^2 Y_{220} + \sqrt{3} C_A \int r^2 Y_{221} Y_2) \right]$	2	No
				$(-1)^{N+1} \left[1 + \frac{1}{2} \left(\sqrt{\frac{2}{5}} - 1 \right) \times (1 - (-1)^{N+2j_v}) \right] C_A \int r^2 Y_{321} Y_2$		
2nd forbidden unique	3	3	1/2	$(-1)^{N+1} \left[1 + \frac{1}{2} \left(\sqrt{\frac{2}{5}} - 1 \right) \times (1 - (-1)^{N+2j_v}) \right] C_A \int r^2 Y_{321} Y_2$	3	No
				$(-1)^{N+1} \left[1 + \frac{1}{2} \left(\sqrt{\frac{2}{5}} - 1 \right) \times (1 - (-1)^{N+2j_v}) \right] C_A \int r^2 Y_{321} Y_2$		

TABLE 4.4. Continued.

Type of transition	Λ	Π	j_j	$\frac{1}{\sqrt{2}} \begin{matrix} i \\ j \\ v \end{matrix}$	$ \Delta J $	$\Delta \pi$
3rd forbidden nonunique	3	3	1/2	$(-1)^{N+1} \left[1 + \frac{1}{2} \left(\sqrt{\frac{6}{5}} - 1 \right) \right. \\ \left. \times (1 - (-1)^{N+2j_j} v) \right] \left[C_v \int r^2 T_{321} \right. \\ \left. + \frac{1}{\sqrt{5}} \frac{Z_c}{N+1} \left(\sqrt{3} C_v \int r^{2m} {}_{-330} + {}^{20} C_A \int r^{2m} {}_{331} Y_F \right) \right]$	3	Yes
			3/2			
			5/2			

ORIGINAL PAGE IS
OF POOR QUALITY

TABLE 4. Coefficients a_n and b_n [Eq. (4-16)], after Con and Lapointe (1967), including corrections by Zou (1971).

	a_0	a_1	a_2	a_3	b_0	b_1	b_2	b_3	b_4	$k \rightarrow \infty$
A_{1c}^{11}	1				2	$-\hat{\rho}$				$\frac{1}{2} (1+\lambda_1) \left[1 - \frac{1}{2} \left(\frac{2\hat{\rho}}{1+\lambda_1} \right)^2 \right]$
E_{1s}^{11}	1	1			2		-2			0
A_{1s}^{21}	7/4	-9/4			2	-5	9/2			$-\frac{5}{1+\lambda_1} \frac{2+\lambda_2}{\Gamma(1+2\lambda_2)} \Gamma(\lambda_2-\lambda_1)$ $\times \Gamma(\lambda_2+\lambda_1+1) \Gamma(\lambda_1+2-\lambda_2)$
F_{1s}^{21}	7/4	-19/4	4		2	-7	29/2	-8		$O(1/k)$
A_{1s}^{22}	7/4	-5/4			2	-3	5/2			0
F_{1s}^{22}	7/4	3/4	-3		2	-1	-7/2	6		0
A_{1s}^{32}	13/6	-35/6	5		2	-8	15	-10		$-\frac{4}{1+\lambda_1} \frac{3+\lambda_2}{\Gamma(1+2\lambda_3)} \Gamma(\lambda_3-\lambda_1)$ $\times \Gamma(\lambda_3+\lambda_1+2) \Gamma(\lambda_1+3-\lambda_2)$
F_{1s}^{32}	13/6	-22/33	1/2	-9	2	-10	31	-37	18	$O(1/k)$
A_{1s}^{33}	13/6	-17/6	2		2	-4	7	-4		0
B_{1s}^{33}	13/6	-1/3	-6	15/2	2	-2	-3	17	-15	0

ORIGINAL PAGE IS
OF POOR QUALITY

TABLE 4.6. Experiments on total IB spectra.

Z	Element	A	Final state (keV)	$J_i^\pi - J_f^\pi$	E_{EC}^a (keV)	Deduced quantities		Spectro meter	Method ^d	Reference
						E_{EC} (keV) ^b	others ^c			
4	Be	7	0	$3/2^- - 3/2^-$	861.75 ± 0.09	851 ± 12	I_{IB}, R_{eff}	Ge(Li)	IB/ γ	Mutterer (1973b,c)
			477.6	$3/2^- - 1/2^-$	384.1 ± 0.1	395 ± 25	I_{IB}	NaI	IB- γ -coinc.	Lancman (1971b)
						388 ± 8	I_{IB}	NaI	IB- γ -coinc.	Persson (1972)
17	Cl	36	0	$2^+ - 0^+$	1144.1 ± 1.7	1170 ± 40		NaI		Dougan (1962)
						1162 ± 45		NaI		Berényi (1962, 63 b)
						1178 ± 15		NaI		Lipnik (1964)
						1158 ± 18		NaI		Berényi (1965a,b)
						1141 ± 8	R_{eff}, DT	NaI		Smirnov (1973)
18	Ar	37	0	$3/2^+ - 3/2^+$	814.1 ± 0.6	818 ± 15		NaI		Anderson (1952, 53)
						818 ± 20		NaI		Emmerich (1954)
								NaI		Lindqvist (1955)
							I_{IB}	NaI	IB/K-Augur	Saraf (1956)
20	Ca	41	0	$7/2^- - 3/2^+$	421.2 ± 0.5		I_{IB}, R_{eff}	Ge(Li)	IB/ N_o	Myslek (1973)
23	V	49	0	$7/2^- - 7/2^-$	601.2 ± 1.0	621 ± 10		NaI		Hayward (1956)
24	Cr	51	0	$7/2^- - 7/2^-$	751.4 ± 0.9	756 ± 5		NaI		Bisi (1955b)

TABLE 4. (Continued)

Z	Element	A	Final state (keV)	$J_i^\pi - J_f^\pi$	E_{EC}^a (keV)	Deduced quantities		Spectro meter	Method ^d	Reference
						E_{EC} (keV) ^b	others ^c			
						786 ± 50	P_γ from I_{IB}	NaI	IB/ γ	Cohen (1955)
						752 ± 22		NaI		Van der Kooij (1956)
						730 ± 20	P_γ from I_{IB}	NaI	IB/ γ	Ofer (1957)
						794 ± 60	P_γ from I_{IB}	NaI	IB/ γ	Murty (1967)
						748 ± 14	P_γ from I_{IB}	Ge (Li)	IB/ γ	Ribordy (1970)
						760 ± 15	I_{IB} , R_{eff}	Ge (Li)	IB/ γ	Mutterer (1973a, c)
			320.1	$7/2^- - 5/2^-$	431.1 ± 1.0	429 ± 16	I_{IB}	NaI	IB- γ -coinc.	Koonin (1972)
25	Mn	54	835.3	$3^+ - 2^+$	540.1 ± 3.6	512 ± 25	I_{IB}	NaI	IB- γ -coinc.	Lancman (1969)
						639 ± 100	I_{IB}	NaI	IB- γ -coinc.	Kádár (1970)
						518 ± 8	I_{IB}	NaI	IB- γ -coinc.	Koonin (1972)
26	Fe	55	0	$3/2^- - 5/2^-$	231.7 ± 0.7	~ 150		GM-count.		Bradt (1946)
						212 ± 10		NaI		Maeder (1951)
						212 ± 20		NaI		Bell (1952)
						222 ± 10	I_{IB}	NaI	IB/Kx	Michalovicz (1953)
						227		NaI		Madansky (1954)
						232 ± 10		NaI		Emmerich (1954)

TABLE 4.1. (Continued)

Z	Element	A	Final state (keV)	$J_i^\pi - J_f^\pi$	E_{EC}^a (keV)	Deduced quantities		Spectro meter	Method ^d	Reference
						E_{EC} (keV) ^b	others ^c			
							I_{IB}	NaI	IB/Kx	Saraf (1956)
						227 ± 10	I_{IB}	NaI	IB/Kx	Biavati (1959, 62)
						224 ± 4	R_{eff}	NaI		Berenyi (1965b)
						248 ± 20		NaI		Raj (1969)
27	Co	57	136.3	$7/2^- - 5/2^-$	700.4 ± 0.7	434 ± 30		NaI	IB- γ -coinc.	Jung (1956)
						674 ± 30	I_{IB}	NaI	IB- γ -coinc.	Lancman (1971a)
28	Ni	59	0	$3/2^- - 7/2^-$	1073.1 ± 1.1	1073 ± 30		NaI		Emmerich (1954)
							I_{IB}	NaI	IB/Kx	Saraf (1956)
								NaI		Hayashi (1960)
							DT	NaI		Schmorak (1963)
						1075.1 ± 1.3	DT	NaI		Berényi (1976)
32	Ge	71	0	$1/2^- - 3/2^-$	235.1 ± 1.7	236 ± 12		NaI		Saraf (1953)
							I_{IB}	NaI	IB/Kx	Saraf (1954b)
						237 ± 5		NaI		Langevin (1954d)
						231 ± 3	I_{IB}	NaI	IB/Kx	Bisi (1955a)
46	Pd	103	39.7	$5/2^+ - 7/2^+$	513 ± 27	517 ± 12		NaI		Rietjens (1954)

TABLE 4.6. (Continued)

Z	Element	A	Final state (keV)	$J_i^\pi - J_f^\pi$	E_{EC}^a (keV)	Deduced quantities		Spectro meter	Method ^d	Reference		
						E_{EC} (keV) ^b	others ^c					
50	Sn	113	391.0	$1/2^+ - 1/2^-$	634	± 14	930	± 300	NaI	Phillips (1960)		
			646.5	$1/2^+ - 3/2^-$	378	± 14	108	± 5	NaI	IB- γ -coinc.	Bosch (1967)	
51	Sb	119	23.8	$5/2^+ - 3/2^+$	555	± 20	555	± 20	I_{IB}	NaI	IB/Kx	Olsen (1957)
53	I	125	35.5	$5/2^+ - 3/2^+$	112.5	± 1.0	141.5	± 2.0		Ge(Li)		Gopinathan (1968)
55	Cs	131	0	$5/2^+ - 3/2^+$	355	± 6	356	± 10	I_{IB}	NaI	IB/Kx	Saraf (1954a)
							356	± 10		NaI		Hoppes (1956)
									I_{IB}	NaI	IB/Kx	Michalowicz (1956)
									I_{IB}	NaI	IB/Kx	Biavati (1959, 62)
62	Sm	145	61.2	$7/2^- - 7/2^+$	577	± 7	584	± 15		NaI		Brosi (1959)
							547	± 10	I_{IB}^e	NaI	IB/(Kx+ γ), IB- e^- -coinc.	Sujkowski (1968)
66	Dy	159	0	$3/2^- - 3/2^+$	365.4	± 1.0	370	± 10		NaI		Ryde (1963b)
							370	± 4	I_{IB}^f	NaI	IB/(Kx+ γ)	Sujkowski (1965)
68	Er	165	0	$5/2^- - 7/2^-$	371	± 4	370	± 10		NaI	IB/Kx	Ryde (1963a)
							372	± 8	I_{IB}	NaI	IB/Kx	Zylicz (1963)
									I_{IB}	NaI	IB/Kx	Sujkowski (1965)
74	W	181	0	$9/2^+ - 7/2^+$	187	± 10	190	± 16		Ge(Li)		Rao (1966)

TABLE 4.6. (Continued)

Z	Element	A	Final state (keV)	$J_i^\pi - J_f^\pi$	E_{EC}^a (keV)	Deduced quantities E_{EC} (keV) ^b others ^c	Spectro meter	Method ^d	Reference
78	Pt	193	0	$1/2^- - 3/2^+$	61.2 ± 3.0	60.8 ± 3.0	Ge(Li)		Hopke (1969)

^acalculated using Q_{EC} values from Wapstra and Gove (1971).

^bpartly recalculated from measured $1s$ - IB end-point energies, using electron binding energies from Bearden and Burr (1967).

^csymbols are used for the bremsstrahlung intensity (I_{IB}), the effective shape function (R_{eff}), information on the influence of detour transitions (\underline{DT}) and the γ -branching ratio (\underline{P}_γ). Informations on the different spectral shapes are not indicated.

^dindicated only if normalized IB spectra have been determined.

^eincludes bremsstrahlung of the 8%- EC branch to the ground state of ^{145}Pm .

^fincludes bremsstrahlung of the 26%- EC branch to the 58.2 keV-excited state in ^{159}Tb .

TABLE 1. Electron-capturing forbidden β decay by pure
spin-parity selection rules.

Z	Element	A	$T_{1/2}$	Q_{EC}^a (keV)	$J_i^\pi - J_f^\pi$	Degree of forbiddenness
18	A	37	35 d	814.1 ± 0.6	$3/2^+ - 3/2^+$	allowed
23	V	49	330 d	601.2 ± 1.0	$7/2^- - 7/2^-$	
26	Fe	55	2.6 y	231.7 ± 0.7	$3/2^- - 5/2^-$	
32	Ge	71	11.4 d	235.1 ± 1.7	$1/2^- - 3/2^-$	
55	Cs	131	9.7 d	355 ± 6	$5/2^+ - 3/2^+$	
67	Ho	163	$>10^3$ y	9.0 ± 1.5	$7/2^- - 5/2^-$	
68	Er	163	75 min	1208 ± 6	$5/2^- - 7/2^-$	
68	Er	165	10.3 h	371 ± 4	$5/2^- - 7/2^-$	
65	Tb	157	150 y	64 ± 5	$3/2^+ - 3/2^-$	first non-unique
78	Pt	193	620 y	61.2 ± 3.0	$1/2^- - 3/2^+$	
20	Ca	41	8×10^4 y	421.2 ± 0.5	$7/2^- - 3/2^+$	first unique
36	Kr	81	2.1×10^5 y	290 ± 100	$7/2^+ - 3/2^-$	
25	Mn	53	2×10^6 y	597.3 ± 1.2	$7/2^- - 3/2^-$	second non-unique
28	Ni	59	8×10^4 y	1073.1 ± 1.1	$3/2^- - 7/2^-$	
43	Tc	97	2.6×10^6 y	346 ± 9	$9/2^+ - 5/2^+$	
57	La	137	6×10^4 y	~ 500	$7/2^+ - 3/2^+$	
52	Te	123	1.2×10^{13} y	57.2 ± 2.4	$1/2^+ - 7/2^+$	second unique

^afrom Wapstra and Gove (1971)

TABLE 4.8. 1s IB spectra measured in coincidence with β^- decay.

Z	Element	A	Final state (keV)	$J_i^\pi - J_f^\pi$	E_{EC}^a (keV)	Deduced quantities		Spectrometer	Reference	
						E_{EC} (keV) ^b	others ^c			
25	Mn	54	835.0	$3^+ - 2^+$	540.1 ± 3.6	528	± 20	NaI	Jung (1956)	
26	Fe	55	0	$3/2^- - 5/2^-$	231.7 ± 0.7			I_{IB}^{1s}	NaI	Biavati (1959, 62)
38	Sr	85	514.0	$9/2^+ - 9/2^+$	550 ± 7	493	± 30		NaI	McDonnell (1969)
48	Cd	109	87.7	$3/2^+ - 7/2^+$	94 ± 3	94	± 3		Ge (Li)	Gopinathan (1968)
50	Sn	113	646.5	$1/2^+ - 3/2^-$	378 ± 14	100	± 10		NaI	Jung (1956)
53	I	125	35.5	$5/2^+ - 3/2^+$	112.5 ± 1.0	141.5	± 2		Ge (Li)	Gopinathan (1968)
55	Cs	131	0	$5/2^+ - 3/2^+$	355 ± 6			I_{IB}^{1s}	NaI	Michalowicz (1956)
								I_{IB}^{1s}	NaI	Biavati (1959, 62)
62	Sm	145	61.2	$7/2^- - 7/2^+$	577 ± 7			$I_{IB}^{1s, d}$	NaI	Sujkowski (1968)
68	Er	165	0	$5/2^- - 7/2^-$	371 ± 4	370	± 8		NaI	Zylicz (1963)
						384	± 20		NaI	Sujkowski (1965)
74	W	181	0	$9/2^+ - 7/2^+$	187 ± 10	184	± 12		Ge (Li)	Rao (1966a)
80	Hg	197	77.3	$1/2^- - 1/2^+$	338 ± 20	686	± 40	I_{IB}^{1s}	NaI	Jasinski (1965)
81	Tl	204	0	$2^- - 0^+$	345 ± 4	335			NaI	Der Mateosian (1954)

TABLE 2.2. (Continued)

Z	Element	A	Final state (keV)	$J_i^\pi - J_f^\pi$	E_{EC}^a (keV)	Deduced quantities		Spectrometer	Reference
						E_{EC} (keV) ^b	others ^c		
						376 ± 20		NaI	Jung (1956)
						393 ± 10		NaI	Biavati (1959, 62)
								NaI	Goudsmit (1966)
						385 ± 20	I_{IB}^{1s}	NaI	Lancman (1973)

^aCalculated using Q_{EC} values from Wapstra and Gove (1971)

^bpartly recalculated from measured $1s-IB$ end-point energies, using K -electron binding energies from Bearden and Burr (1967).

^c $I_{IB}^{1s} = 1s-IB$ intensity

^dincludes bremsstrahlung of the $8\%EC$ branch to the groundstate of ^{145}Pm .

TABLE 4.9. Measured IB intensities for allowed and first nonunique forbidden transitions, compared with theoretical values.

Element	Z	A	Final-state (keV)	$J_i^\pi - J_f^\pi$	$E_{EC}^{1)}$ (keV)	Energy range (keV)	Intensity-ratio	Experiment. value ₅ ($\times 10^{-5}$)	Theoretical values ($\times 10^{-5}$)			Reference ²⁾
									MS	MG	Int	
<u>Allowed transitions</u> $\Delta J = 0, 1; \pi_i \pi_f = + 1$												
4	Be	7	0	$3/2^- - 3/2^-$	861.75 ± 0.09	$523.7 - k_{max}$	I_{IB}/W_{EC}	9.0 ± 0.6	9.35	8.56	8.57	Mutterer (1973b) ^y
			477.6	$3/2^- - 1/2^-$	384.1 ± 0.1	50 - 360	I_{IB}/W_{EC}	10.3 ± 0.6	9.95	9.19	9.20	Persson (1972) ^t
						100 - 360	I_{IB}/W_{EC}	8.6 ± 0.6	7.82	7.25	7.26	Persson (1972) ^h
						120 - 360	I_{IB}/W_{EC}	7.7 ± 0.5	6.83	6.39	6.35	Persson (1972) ^b
						120 - 360	I_{IB}/W_{EC}	$4.9 \pm 1.0^{3,4)}$	6.83	6.39	6.35	Lancman (1971b) ^c
18	A	37	0	$3/2^+ - 3/2^+$	814.1 ± 0.6	35 - k_{max}	I_{IB}/W_K	$52 \pm 13^5)$	52.1	36.9	37.6	Saraf (1956) ^d
24	Cr	51	0	$7/2^- - 7/2^-$	751.4 ± 0.9	$348.1 - k_{max}$	I_{IB}/W_{EC}	9.56 ± 0.60	14.6	9.13	9.43	Mutterer (1973a) ^x
			320.1	$7/2^- - 5/2^-$	431.1 ± 1.0	130 - 425	I_{IB}/W_{EC}	7.2 ± 0.4	8.34	5.41	5.58	Koonin (1972) ^f
25	Mn	54	835.3	$3^+ - 2^+$	540.1 ± 3.6	100 - 420	I_{IB}/W_{EC}	$5.8 \pm 1.3^{3,4)}$	16.5	10.5	10.8	Lancman (1969) ^g
						82 - k_{max}	I_{IB}/W_{EC}	$17.2 \pm 3.0^{3,4)}$	18.1	11.5	11.9	Kádár (1970) ^h
						82 - 515	I_{IB}/W_{EC}	15.4 ± 0.8	18.1	11.5	11.9	Koonin (1972) ⁱ
26	Fe	55	0	$3/2^- - 5/2^-$	231.7 ± 0.7	50 - k_{max}	I_{IB}/W_K	$4.0 \pm 1.0^4)$	3.42	2.20	2.28	Michalowicz (1953) ^j

TABLE 4.9. (continued)

Element	Final-state (keV)	$J_i^\pi - J_f^\pi$	$E_{EC}^{(1)}$ (keV)	Energy range (keV)	Intensity ratio	Experiment. value ₅ ($\times 10^{-5}$)	Theoretical values ($\times 10^{-5}$)			Reference ²⁾	
							MS	MG	Int		
				100	$-k_{max}$	I_{IB}/W_K	$1.4 \pm 0.4^{(5)}$	1.68	1.07	1.11	Saraf (1956) ^k
				0	$-k_{max}$	I_{IB}^{1s}/W_K	1.5 ± 0.8	3.76	2.15	2.26	Biavati (1959, 62) ^l
27 Co 57	136.3	$7/2^- - 5/2^-$	700.4 ± 0.7	180	-465	I_{IB}/W_{EC}	$8.8 \pm 1.8^{(3,4)}$	21.0	12.8	13.3	Lancman (1971a) ^m
32 Ge 71	0	$1/2^- - 3/2^-$	235.1 ± 1.7	70	$-k_{max}$	I_{IB}/W_K	2.3 ± 0.5	2.82	1.70	1.79	Bisi (1955a) ⁿ
51 Sb 119	23.8	$5/2^+ - 3/2^+$	555 ± 20	0	$-k_{max}$	I_{IB}^s/W_K	$10.6 \pm 1.2^{(6)}$	22.0	8.46	10.2	Olsen (1957) ^o
55 Cs 131	0	$5/2^+ - 3/2^+$	355 ± 6	0	$-k_{max}$	I_{IB}^{1s}/W_K	1.4 ± 1.0	7.61	2.25	3.14	Biavati (1959, 62) ^p
68 Er 165	0	$5/2^- - 7/2^-$	371 ± 4	93	-306	I_{IB}^{1s}/W_K	1.63 ± 0.16	4.87	1.05	1.67	Sujkowski (1965) ^r
				182	-306	I_{IB}^{1s}/W_K	0.53 ± 0.06	1.52	0.34	0.50	Sujkowski (1965) ^r
				185	-300	I_{IB}/W_K	0.9 ± 0.2	2.39	1.28	1.43	Zylicz (1963)
				185	-300	I_{IB}/W_K	0.89 ± 0.12	2.39	1.28	1.43	Sujkowski (1965)

TABLE 4.9. (continued)

Ele- ment	Z	A	Final- state (keV)	$J_i^\pi - J_f^\pi$	$E_{EC}^{(1)}$ (keV)	Energy range (keV)	Inten- sity- ratio	Experiment. value ₅ ($\times 10^{-5}$)	Theoretical ₅ values ($\times 10^{-5}$)			Reference ²⁾
									MS	MG	Int	
<u>First nonunique forbidden transitions</u>								$\Delta J = 0, 1; \pi_i \pi_f = -1$				
62	Sm	145	61.2	$7/2^- - 7/2^+$	577 ± 7	120 - 239	I_{IB}/W_K	$6.7^{+0.7(7)}$	11.9	5.87	6.73	Sujkowski (1968)
						120 - 412	I_{IB}/W_K	$10.1^{+1.0(7)}$	20.7	9.18	10.6	Sujkowski (1968)
						169 - 412	I_{IB}/W_K	$7.3^{+1.2(7)}$	15.1	6.08	7.14	Sujkowski (1968)
						129 - 412	I_{IB}^{1s}/W_K	$4.6^{+0.8}$	14.9	3.90	5.28	Sujkowski (1968) ^c
						169 - 412	I_{IB}^{1s}/W_K	$3.6^{+0.5}$	12.2	3.19	4.25	Sujkowski (1968) ^c
66	Dy	159	0	$3/2^- - 3/2^+$	365.4 ± 1.0	185 - 300	I_{IB}/W_K	$1.0^{+0.3(8)}$	2.24	1.18	1.32	Sujkowski (1965)
80	Hg	197	77.3	$1/2^- - 1/2^+$	686 ± 40	350 - 550	I_{IB}^{1s}/W_K	$1.6^{+0.3}$	5.49	0.83	1.26	Jasinski (1965) ^s

TABLE 4.10. Average experimental-to-theoretical IB yield $\langle \rho_{E,T} \rangle$ for various regions of the atomic number Z .

Region of Z	$4 \leq Z \leq 80$	$Z = 4$	$18 \leq Z \leq 32$	$51 \leq Z \leq 80$
Number of independent measurements	19	3	11	5
Theory of:	$\langle \rho_{E,T} \rangle$			
Morrison and Schiff	0.66	0.91	0.76	0.32
Martin and Glauber	1.19	0.98	1.19	1.31
Intemann	1.06	0.98	1.10	0.92

TABLE 4.11. Circular Polarization of IB in allowed EC transitions

Z	Element	A	Final state (keV)	$E_{EC}^{a)}$ (keV)	Energy range (keV)	Degree of Polarization	Polarimeter type ^{b)}	Reference
18	A	37	0	814.1 ± 0.6	200 - k_{max}	1.03 ± 0.04	f.s.m.	Hartwig(1958)
						0.97 ± 0.15	f.s.m.	Mann(1958)
24	Cr	51	0(90.2%)	751.4 ± 0.9		0.67 ± 0.07	f.s.m.	Vanderleeden (1971)
			320.1(9.8%)	431.3 ± 1.0		1.2 ± 0.1	r.t.m.	Kuphal(1974)
26	Fe	55	0	231.7 ± 0.7	85 - 220	0.98 ± 0.1	f.s.m.	Parfenova(1960)
32	Ge	71	0	235.1 ± 1.7	70 - 120	~ 0.4	f.s.m.	Bernardini(1955)

a) from Wapstra and Gove (1971)

b) f.s.m. = forward-scattering magnet
r.t.m. = radial transmission magnet.

TABLE 5.1. Electron ejection probabilities per K capture (in multiples of 10^{-5}).

Isotope	Primakoff- Porter ^a	MIKS ^b	Intemann ^c	K- or L- electron ejection ^d
$^{37}_{18}\text{Ar}$	27.7	14.2	21.12	57
$^{55}_{26}\text{Fe}$	11.2	8.81	8.26	6.4
$^{71}_{32}\text{Ge}$	6.68	4.56	4.72	3.3
$^{131}_{55}\text{Cs}$	1.62	0.709	0.92	2.6
$^{165}_{68}\text{Er}$	0.767	0.304	0.39	2.9

^aPrimakoff and Porter (1953), evaluated by Mukoyama et al. (1973).

^bMukoyama et al. (1973).

^cIntemann (1969), as evaluated by Intemann (1974).

^dK-electron ejection accompanying L capture and L-electron ejection accompanying K capture, after Mukoyama and Shimizu (1974).

TABLE 5.2. Double K-vacancy production probability (due to internal ionization and excitation), per K-capture event (in multiples of 10^{-5}).

Isotope	Theory		Experiments ^c	
	Primakoff-Porter ^a	MIKS ^b		
³⁷ ₁₈ Ar	38.6	23.0	37±9	Kiser and Johnston (1959)
			44±8	Miskel and Perlman (1954)
⁵⁵ ₂₆ Fe	18.5	15.8	38±17	Charpak (1953)
⁷¹ ₃₂ Ge	12.2	8.85	24	Briand <u>et al.</u> (1971)
			13±8	Oertzen (1964)
			13.3±1.4	Langevin (1957, 1958)
¹³¹ ₅₅ Cs	4.13	1.79	1.33±0.33	Nagy <u>et al.</u> (1972)
			2.0±1.3	Smith (1964)
			5.0±1.0	Daniel <u>et al.</u> (1960)
			2.5±0.2	Lark and Perlman (1960)
¹⁶⁵ ₆₈ Er	2.70	1.09	0.67±0.39	Nagy <u>et al.</u> (1972)
			1.5±0.4	Ryde <u>et al.</u> (1963)

^aPrimakoff and Porter (1953), as evaluated by Mukoyama et al. (1973).

^bMukoyama et al. (1973).

^cK-x-ray-K-x-ray coincidence experiments, except for K x-ray satellite measurements on ⁷¹Ge by Oertzen (1964) and Briand et al. (1971).

Figure Captions

FIG. 2-1. The function $I(l, l, l; r)$ vs. distance r from the origin (in multiples of the nuclear radius R) for various nuclear charge distributions: a) uniform charge distribution [Eq. (2-55)]; b) Fermi distribution, with $t=0.4R$ [Eq. (2-61)]; c) Gaussian distribution, with $A=0$ [Eq. (2-58)]; d) modified Gaussian distribution, with $A=1$.

FIG. 2-2. L_1/K exchange and overlap correction factors. The solid and broken curves were recalculated according to the approaches of Bahcall (1963a, b; 1965a) and Vatai (1968, 1970), respectively, with wave functions from the Hartree-Fock program of Froese-Fischer (1972a). Results of the relativistic calculation of Suslov (1970a), following Bahcall's theory, are indicated by triangles, and those of the calculation of Martin and Blichert-Toft (1970), based on the same approach as Vatai's, are indicated by crosses.

FIG. 2-3. M_1/L_1 exchange and overlap correction factors. See caption of Fig. 2-2 for details.

FIG. 3-1. Typical K, L, and M spectra from the decay of ^{71}Ge measured with a multiwire counter system. In the M spectrum, background and degradation tails were subtracted and a Poisson distribution fitted to the data (after Genz, 1971a).

FIG. 3-2. Multiwire proportional counter (after Scobie et al., 1959).

FIG. 3-3. Block diagram of multiwire-proportional-counter electronic system (after Genz et al., 1971a).

FIG. 3-4. The M region of the ^{37}Ar spectrum, with the single-electron spectrum produced by introducing ultraviolet photons from an external source, normalized to the M spectrum (after Renier et al., 1968).

FIG. 3-5. The normalized M and L spectra from ^{37}Ar decay, corrected for dead time and background (after Renier et al., 1968).

FIG. 3-6. Block diagram of single-wire proportional-counter electronic system (after Genz et al., 1972).

FIG. 3-7. Assemblies of source and enveloping crystals (after Goedbloed et al., 1970a).

FIG. 3-8. Spectrum of ^{131}Cs measured with a doped NaI(Tl) crystal. Elimination of escape effects by extrapolating to a zero surface-to-volume ratio (after Schulz, 1967a).

FIG. 3-9. M-electron capture decay to the 646-keV level of ^{185}Re . (a) Spectrum of M events. (b) Extrapolation to correct for escape effects (after Schulz, 1967a).

FIG. 3-10. Block diagram of coincidence apparatus to measure ^{193}Pt M- and L-capture peaks (after Ravn and Bøgeholt, 1971).

FIG. 3-11. Block diagram for coincidence measurements with internal solid sources (after Leutz et al., 1966).

FIG. 3-12. Comparison of experimentally determined L/K capture ratios for allowed transitions (solid circles) and first-forbidden non-unique transitions (open circles) with theoretical predictions based on wave functions of Mann and Waber (1973) and exchange and overlap corrections $X^{L/K}$ according to Bahcall (1963, 1965), Vatai (1970a) and Martin and Blichert-Toft (1970).

FIG. 3-13. Comparison of experimentally determined M/L capture ratios for allowed transitions (solid circles) and first-forbidden non-unique transitions (open circles) with theoretical predictions based on wave functions of Mann and Waber and exchange and overlap corrections $X^{M/L}$ according to Bahcall (1963, 1965), Vatai (1970a), and Martin and Blichert-Toft (1970).

FIG. 3-14. Comparison of experimentally determined P_K values for allowed transitions (solid circles), first-forbidden non-unique transitions (open circles), and first-forbidden unique transitions (squares) with theoretical predictions based on wave functions of Mann and Waber (1973) and exchange and overlap corrections according to Bahcall (1963, 1965).

FIG. 3-15. Number of allowed positron emitters, as a function of half-life.

FIG. 3-16. Continuous gas-flow system used for K/β^+ measurements

with short-lived low-Z isotopes.

FIG. 3-17. Diagram of counter used to determine K/β^+ ratios of ^{11}C , ^{13}N , ^{15}O , ^{19}Ne and ^{30}P . K-capture events and positrons are detected in the central counter; only positrons have sufficient energy to be detected in the plastic scintillator.

FIG. 3-18. Typical pulse-height spectrum from the central proportional counter in Fig. 3-17, in anticoincidence with the plastic scintillator. The counter gas, introduced in flow mode, was 90% Ar and 10% CH_4 . Radioactive phosphine (PH_3) was introduced in trace amounts (<1% of Ar/ CH_4) from an irradiation vessel to the main flow line carrying the counting mixture.

FIG. 3-19. The 870-eV K-capture peak of ^{22}Na , measured with an internal-source scintillation counter in coincidence with another NaI detector, closely located to register the 1.274-MeV deexcitation γ rays of ^{22}Ne .

FIG. 3-20. Niobium K x rays from the decay of ^{91}Mo , measured with a Si(Li) detector with a resolution of 185 eV at 5.9 keV. The Nb $K\alpha$, and $K\beta$ peaks are well-resolved, even in the presence of a β^+ spectrum twenty times as intense as the K-capture branch. The Mo $K\alpha$ peak is caused by β^+ induced fluorescence in the source.

FIG. 3-21. Molybdenum-91 K x-ray spectrum measured with a 5.7×0.63 cm NaI(Tl) of 28% resolution at 22 keV. The fine structure evident in Fig. 3-20 is no longer visible.

FIG. 3-22. Thin, self-supporting evaporated sources are placed between two $\text{CaF}_2(\text{Eu})$ crystals. Although CaF_2 has inherently a lower light output than NaI(Tl) , the crystals are nonhygroscopic and can be used without windows between source and crystal.

FIG. 3-23. Typical electronic arrangement for triple-coincidence measurements.

FIG. 3-24. Ratio of experimental to theoretical allowed K/β^+ and EC/β^+ ratios.

FIG. 3-25. Theoretical K-capture to positron-emission ratios for allowed transitions.

FIG. 3-26. Theoretical K/β^+ ratios.

FIG. 4-1. Feynman Diagrams for electronic and nuclear mode contributions to radiative electron capture.

FIG. 4-2. IB spectra for radiative capture from various atomic shells of ^{55}Fe , according to the theory of Glauber and Martin (1956).

FIG. 4-3. Relativistic correction factor $R_{1s}(k)$, according to the exact results of Martin and Glauber (1958) and Intemann (1971).

FIG. 4-4. Comparison of several theoretical results for the relativistic correction factor $R_{1s}(k)$. The exact result is deduced from Eqs. (4-44) and (4-45), the low-k expansion, from Eqs. (4-38) and (4-39), and the high-k approximation, from Eq. (4-40).

FIG. 4-5. K-capture IB spectrum for ^{55}Fe according to the theories of Morrison and Schiff (1940) (MS) [Eq. (4-14)], Glauber and

Martin (1956) (GM) [Eq. (4-22)], and Martin and Glauber (1958) (MG) [Eq. (4-36)]. GM includes relativistic effects to lowest order in $Z\alpha$, while MG is fully relativistic.

FIG. 4-6. IB spectra for radiative capture from various atomic shells of ^{165}Er . The solid curves represent the fully relativistic results of Zon (1971), while the dashed curves are deduced from the results of Glauber and Martin (1956). [After Zon (1971)].

FIG. 4-7. Screening factors s_α , according to Martin and Glauber (1958).

FIG. 4-8. Polarization and asymmetry functions, $P_{1s}(k)=\alpha_{1s}(k)$ and $P_{2s}(k)=\alpha_{2s}(k)$, and related functions for $Z=18$. The $1s$ -state curves are deduced from the exact results of Martin and Glauber (1958) and Intemann (1971), the $2s$ -state curves, from the results of Glauber and Martin (1956).

FIG. 4-9. Polarization and asymmetry functions, $P_{1s}(k)=\alpha_{1s}(k)$ and $P_{2s}(k)=\alpha_{2s}(k)$, and related functions for $Z=51$. The $1s$ -state curves are deduced from the exact results of Martin and Glauber (1958) and Intemann (1971), the $2s$ -state curves, from the results of Glauber and Martin (1956).

FIG. 4-10. Relativistic correction factors $R_{1s}^{(1)}(k)$ and $R_{1s}^{(2)}(k)$, according to Zon and Rapoport (1968), for several atomic numbers. The function $R_{1s}^{(1)}$ is the same as R_{1s} of Martin and Glauber (1958); it has been evaluated using the high- k approximation [Eqs. (4-40) or (4-76)],

$R_{1s}^{(2)}$ has also been evaluated in the high- k approximation [Eq. (4-76)]. The three points shown on the ordinate represent the results of an exact evaluation of $R_{1s}^{(1)}(0)$, using Eq. (4-41) or Table 4.5, for $Z=20, 50, 80$ (in descending order).

FIG. 4-11. Comparison of theoretical results for the K-capture IB spectrum for ^{41}Ca . The theories of Morrison and Schiff (1941) and Martin and Gläuber (1958) for an allowed transition are represented by the curves MS-A and MG, respectively. For a unique first-forbidden transition, the corresponding curves are those labeled MS-F and ZR, deduced from Eq. (4-79) and the results of Zon and Rapoport (1968), evaluated to first order in $Z\alpha$.

FIG. 4-12 IB pulse-height spectra of ^{131}Cs , measured with a 3.5 3.5-cm NaI(Tl) spectrometer. Copper absorbers were placed between source and detector, ranging from 710 mg/cm² (A) to 2200 mg/cm² (H). [From Saraf (1954a)].

FIG. 4-13 Pulse-height spectrum of ^{51}Cr , as recorded with a 1.2-cm³ Ge(Li) detector with a pileup rejector. The measured spectrum (N_{ap}) is shown in the energy range above the 320.1-keV γ -ray peak, with its individual components: internal bremsstrahlung (N_{IB}), residual pileup (N_{pu}), and background (N_B). [From Mutterer (1973a)].

FIG. 4-14 Extrapolation plot for pileup correction of ^{51}Cr spectra, recorded from sources of different strengths with a Ge(Li) spectrometer. Ratios of integral counting rates (N_{int}) for different energy ranges $E > E_1$ above the 320.1-keV γ line and total counting rates (N) are plotted against corrected total counting rates (N'). The intercepts at $N'=0$ give ratios of IB to γ counting rates above different energy thresholds E_1 . [From Mutterer (1973a)].

FIG. 4-15 IB pulse-height spectrum (n_{IB}) of ^{51}Cr , deduced from ⁴⁷² a set of spectra that were recorded with a Ge(Li) spectrometer and corrected for pileup applying the extrapolation method. The corresponding energy spectrum (w_{IB}) is shown in the inset. Solid lines represent theoretical spectra of Martin and Glauber (1958). [From Mutterer (1973a)].

FIG. 4-16 Arrangement of two 3×3-in. NaI(Tl) detectors, used for IB spectrometry in coincidence with γ rays. [From Persson and Koonin (1972)].

FIG. 4-17 Pulse-height spectra of ^7Be photons gated by γ rays, as obtained with two 3×3-in. NaI(Tl) spectrometers in close face-to-face geometry. The coincidence spectrum (open circles) is compared with the random coincidence spectrum (filled circles). The difference between the two spectra represents the pulse-height spectrum of internal bremsstrahlung that accompanies the EC transition to the excited state in ^7Li . [From Lancman and Lebowitz (1971b)].

FIG. 4-18 Electronic circuit of IB spectrometry in coincidence with γ rays, for a device with two NaI(Tl) detectors (Fig. 4-16). [From Persson and Koonin (1972)].

FIG. 4-19 IB pulse-height spectrum of ^7Be measured in coincidence with the 477-keV ^7Be γ -ray. The peak at 477 keV remained after correction for coincidences. The corresponding Compton distribution is shown as a dashed line. [From Persson and Koonin (1972)].

FIG. 4-20 Total IB spectrum of ^{131}Cs , measured with a 1×1½-in. NaI(Tl) crystal with a 0.0005-in. thick aluminum window. The 1s IB

spectrum gated by ^{131}Xe K α rays that were recorded with a 1.5x0.080-in. NaI(Tl) crystal, is also shown. [From Baiyati et al. (1962)].

FIG. 4-21 Pure higher-shell IB spectrum of ^{193}Pt , measured with a 7-cm³ coaxial Ge(Li) detector. [From Hopke and Naumann (1969), and private communication].

FIG. 4-22 Corrections applied to the predicted ^{37}Ar IB spectrum to convert it into a pulse-height spectrum as would be measured with a 1x1-in. NaI(Tl) spectrometer: (A) theoretical curve corrected for γ efficiency, and distribution curves for (B) photo electrons, (C) Compton electrons, (D) backscattered photons, (E) escaped photons, and (F) absorbed photons. [From Lindqvist and Wu (1955)].

FIG. 4-23 Compton distributions of ^{54}Mn (a) and ^{85}Sr (b) recorded with small Ge(Li) spectrometers. Measured spectra are compared with those calculated from constructed response matrices. [(a) from Ribordy and Huber (1970), courtesy of Birkhäuser Publishing Co.; (b) from Mutterer (1973c), unpublished].

FIG. 4-24 IB pulse-height spectrum of ^{54}Mn , measured with a 3x3-in. NaI(Tl) spectrometer, in coincidence with the 835-keV γ rays from ^{54}Cr . The solid line is the best fit (corresponding to the minimum value of χ^2) of the curves obtained by folding the theoretical IB spectrum with the response matrix. The endpoint energy is used as fitting parameter. [From Lancman and Lebowitz (1969)].

FIG. 4-25 The 1s IB spectrum of ^{165}Er , as measured with an $1\frac{1}{2}\times 1$ -in. NaI(Tl) spectrometer, in coincidence with Ho K x rays. Jauch plots are shown according to Eq. (4-81) (curve a) and Eq. (4-82) (curve b). [From Zylicz et al. (1963), courtesy of North-Holland Publishing Co.].

FIG. 4-26 IB spectrum of ^{49}V , measured with a well-type NaI(Tl) spectrometer. The full line represents the theoretical spectrum of Glauber and Martin (1956). The experimental points are normalized at 200 keV. [From Hayward and Hoppes (1956)].

FIG. 4-27 Total IB spectrum of ^{55}Fe , measured by Berényi et al. (1965) with a 10.2×15.2 -cm NaI(Tl) spectrometer. Data points represent the effective shape factor \bar{R}_{eff} , obtained by dividing the corrected spectrum (N_{Korr}) by the Morrison-Schiff term $k(k_0-k)^2$. [From Varga (1970), courtesy of Hungarian Academy of Science].

FIG. 4-28 Ratios $\rho_{\text{E,T}}$ of experimental to theoretical bremsstrahlung yields, calculated with theoretical IB intensities according to Morrison and Schiff (1940). Values are given for 1s IB intensities per K capture (open circles); total IB intensities in which s contributions predominate, relative to K-capture rates (triangles); and total IB intensities relative to total EC rates (filled circles). References for experimental data are given in Table 4.9.

FIG. 4-29 Ratios of experimental to theoretical bremsstrahlung yields, calculated with theoretical IB intensities from the theory of Martin and Glauber (1958), with $R_{1s}(Z,k)$ from Eqs. (4-37) and (4-38). For notation and references see caption of Fig. 4-28.

FIG. 4-30. Ratios of experimental to theoretical bremsstrahlung yields, calculated with theoretical IB intensities according to Intemann (1971) for $R_{1s}(Z,k)$ (Eq. 4-44). For notation and references see Fig. 4-28.

FIG. 4-31 IB spectrum of ^{41}Ca , measured with a Ge(Li) spectrometer in two different geometries. The spectra (W_{IB}) divided by the Morrison-Schiff spectrum $k(k_0^{1s}-k)^2$ are compared with predicted IB shape factors. [From Myslek et al., (1973), courtesy of North-Holland Publishing Co.].

FIG. 4-32 Total IB spectrum accompanying the second-forbidden nonunique EC decay of ^{36}Cl , measured with a 10x10-cm NaI(Tl) spectrometer. The spectrum is shown in Jauch coordinates, (a) and in form of the effective shape function R_{eff} (b). The latter is compared with theoretical shape functions, calculated with (1) and without (2) including detour transitions. [From Smirnov and Batkin (1973), courtesy of Nauka Press].

FIG. 4-33 Circular Polarization (P) of the IB from ^{37}Ar as function of energy, measured with a forward-scattering Compton polarimeter provided with a NaI(Tl) detector. (Hartwig and Schopper, 1958). The solid line is the theoretical curve, cal-

culated from Eq.(4-52) with the polarization functions α_{1s} and α_{2s} of Fig. 4-8. The IB spectrum of ^{37}Ar is also shown.

FIG. 4-34 Relative change $\delta(x)$ in the Compton absorption of ^{51}Cr photons in iron that is magnetized parallel and anti-parallel, respectively, to the photon momentum. The Compton polarimeter has a special radial-transmission magnet. Photons are recorded with NaI(Tl) detectors applying current integration techniques. Values of $\delta(x)$ for different Pb absorbers between source and magnet are shown. Solid lines are calculated from IB theory. [From Kuphal et al. (1974)].

FIG. 4-35 Forward-backward asymmetry $W(\pi)/W(0)$ in the emission of IB photons from polarized ^{119}Sb nuclei, as a function of sample temperature. [From Brewer and Shirley (1968)].

FIG. 4-36 Overall asymmetry coefficient $A(k)$ of IB emission from oriented ^{119}Sb nuclei, measured by Brewer and Shirley (1968). Data points are compared with theoretical predictions, calculated with the asymmetry functions α_{1s} and α_{2s} of Fig. 4-9 (full curve), and with $\alpha_{1s} = \alpha_{2s} = 1$ (dashed curve). [From Intemann (1971)].

FIG. 5-1. Theoretical momentum spectrum of K electrons ejected during K capture of ^{55}Fe . The upper curve is calculated according to Intemann and Pollock (1967), taking into account only the exchange of scalar virtual photons during transitions between spherically symmetric states. The lower curve, calculated by Intemann (1972), results if p-wave intermediate states and the exchange of longitudinal virtual photons are taken into account. (After Intemann, 1972).

FIG. 5-2. Calculated momentum spectrum of K electrons ejected during K-capture decay of ^{131}Cs . Curve A is according to the non-relativistic theory of Primakoff and Porter (1953); curve B represents the semirelativistic calculation of Intemann (1969). (From Intemann, 1969).

FIG. 5-3. Calculated energy spectra of electrons ejected in the decay of ^{55}Fe . The dashed curve labeled "K-K" represents K electrons ejected during K capture; the curves "K- L_i " indicate L_i -electrons ejected during K capture plus the exchange effect, *viz.*, K electrons ejected during L_i capture. All rates are given per K-capture event. After Mukoyama and Shimizu (1974).

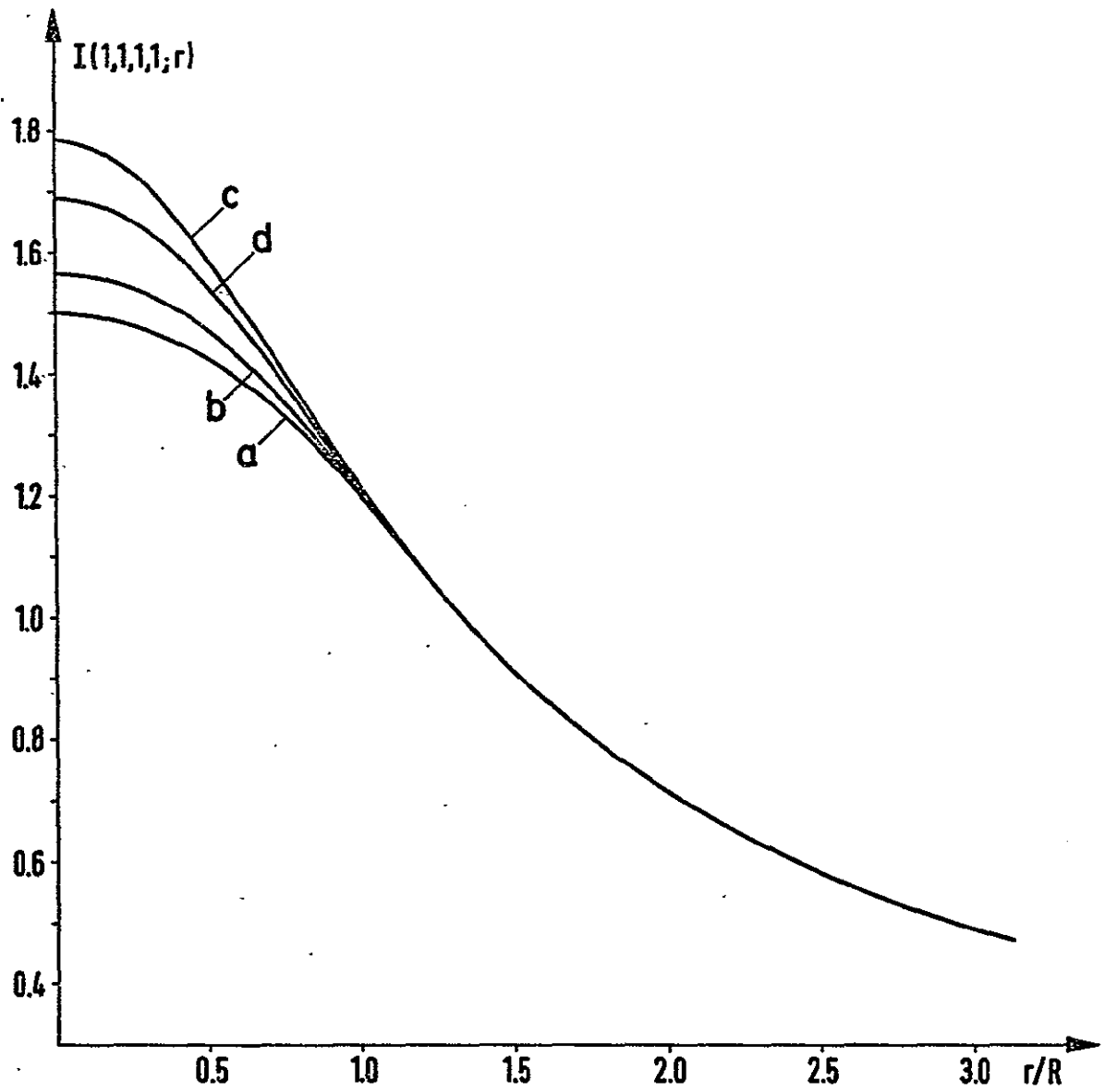


FIG. 2-1

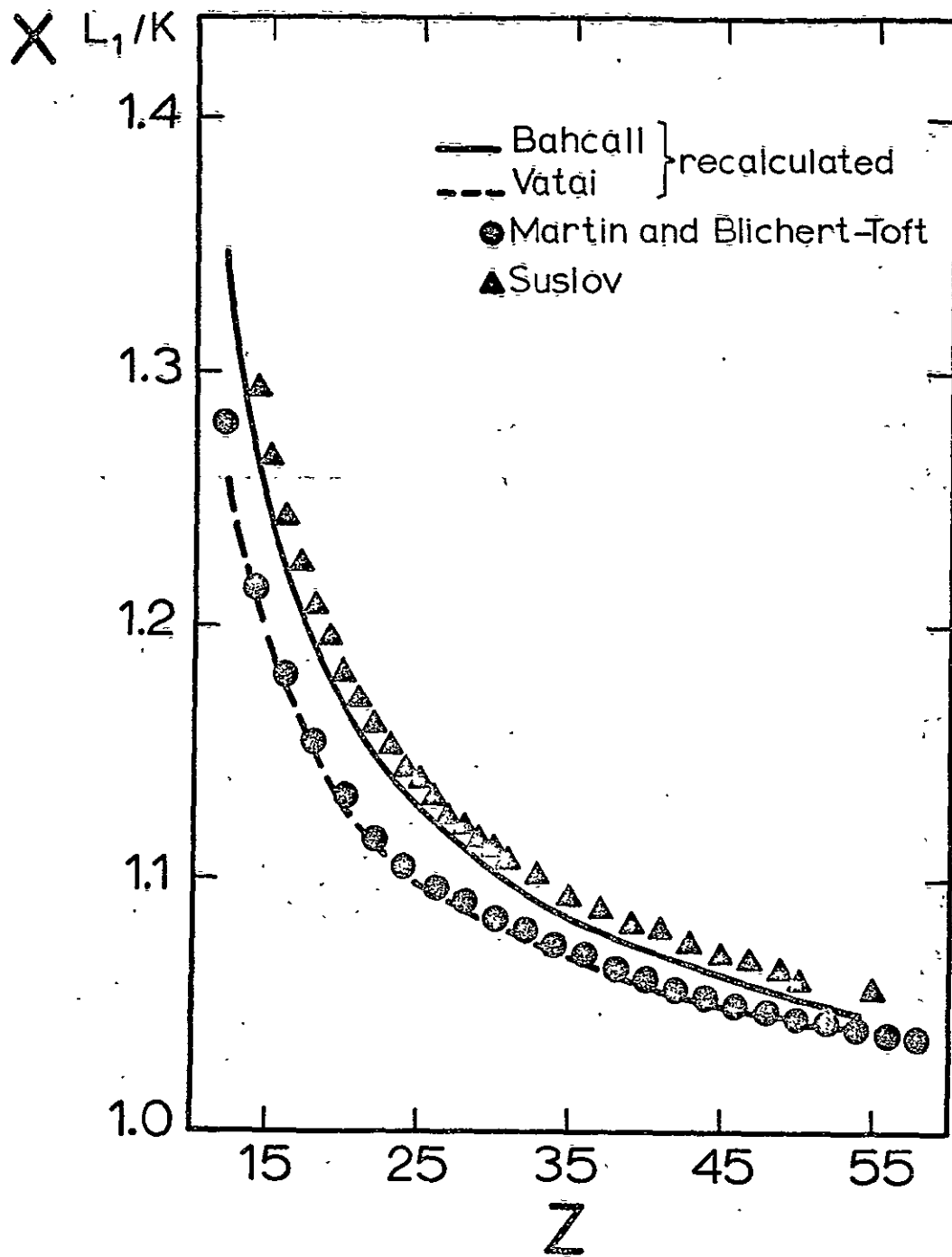


FIG. 2-2

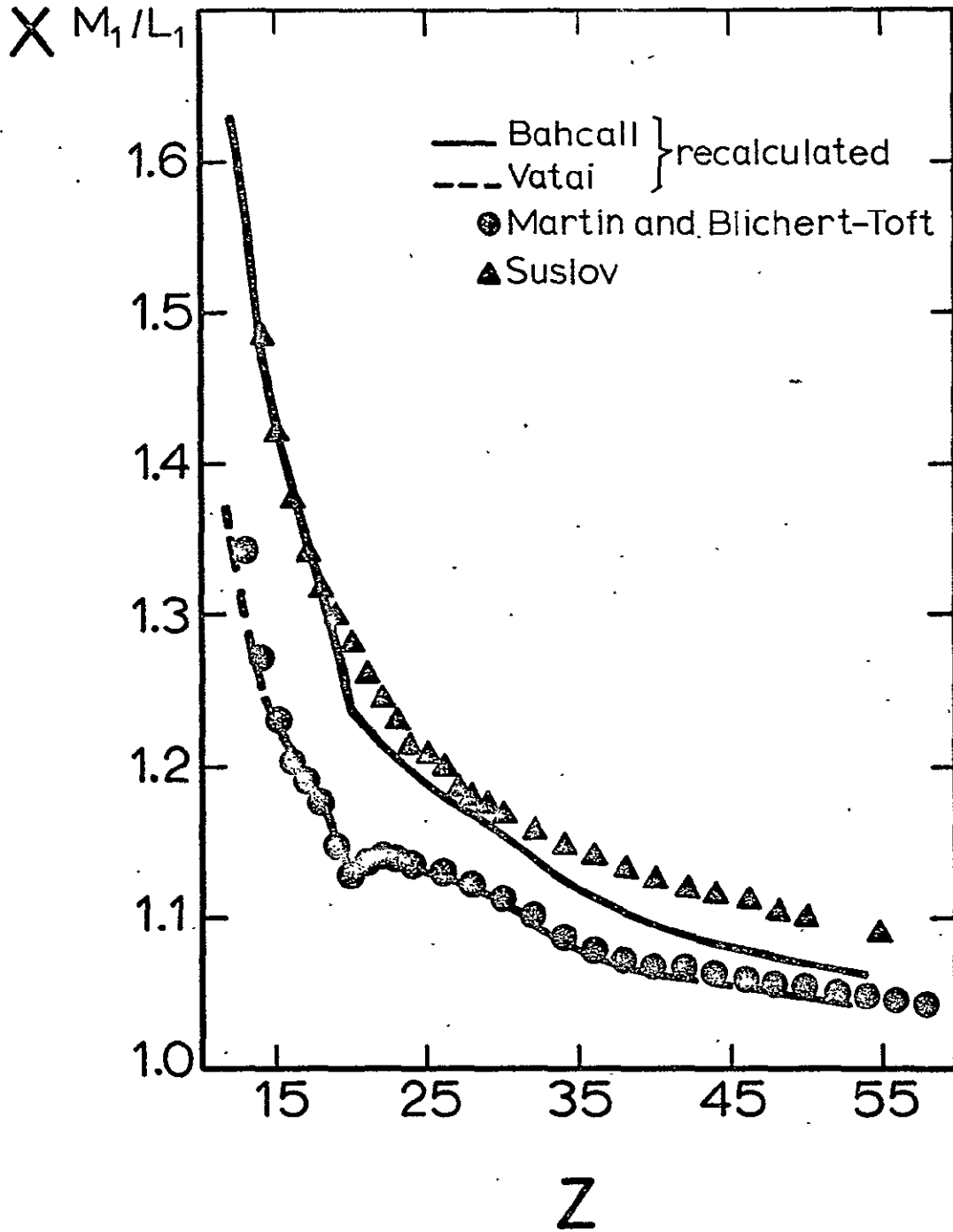


FIG. 2-3

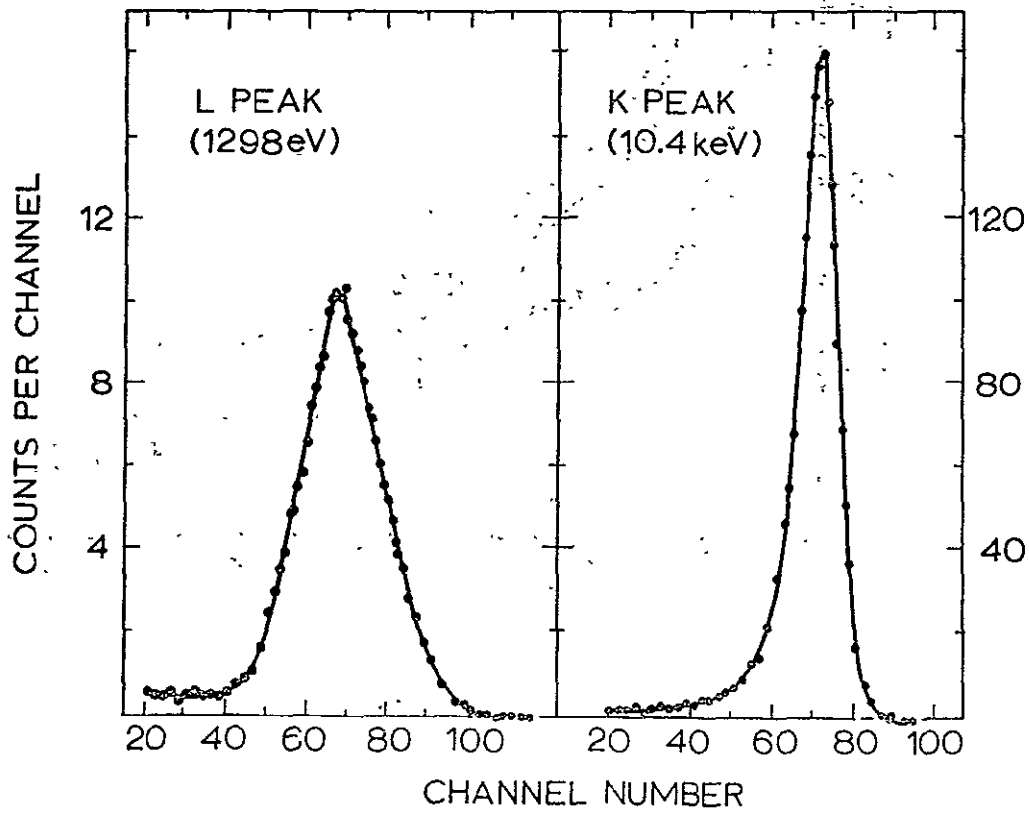
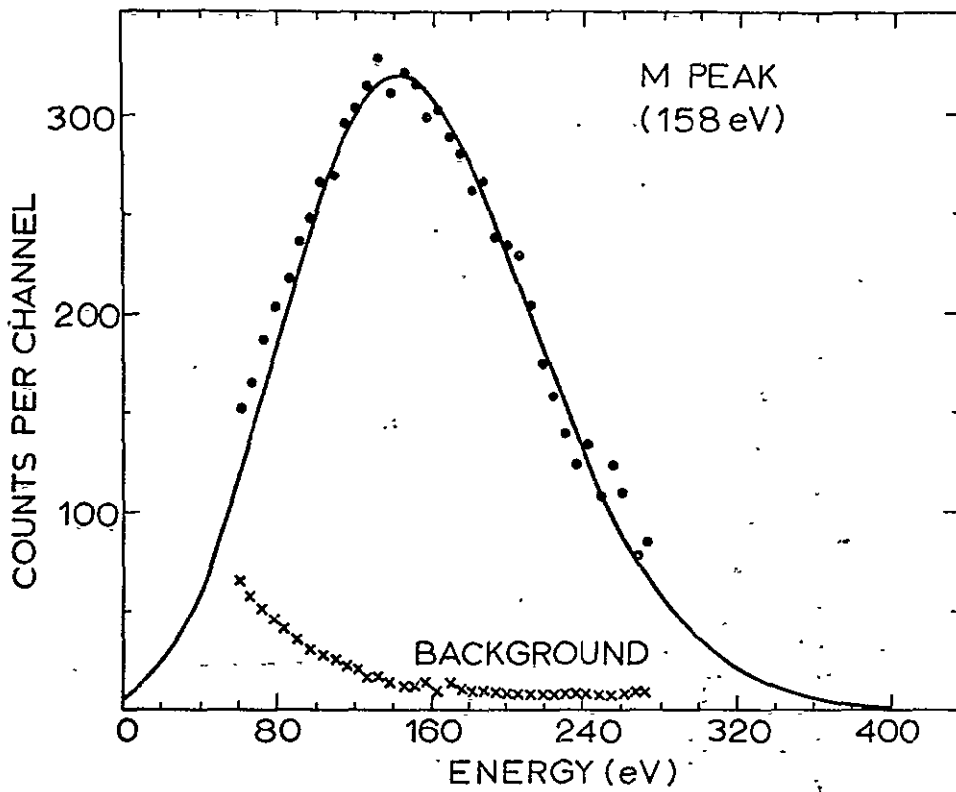


FIG. 3-1

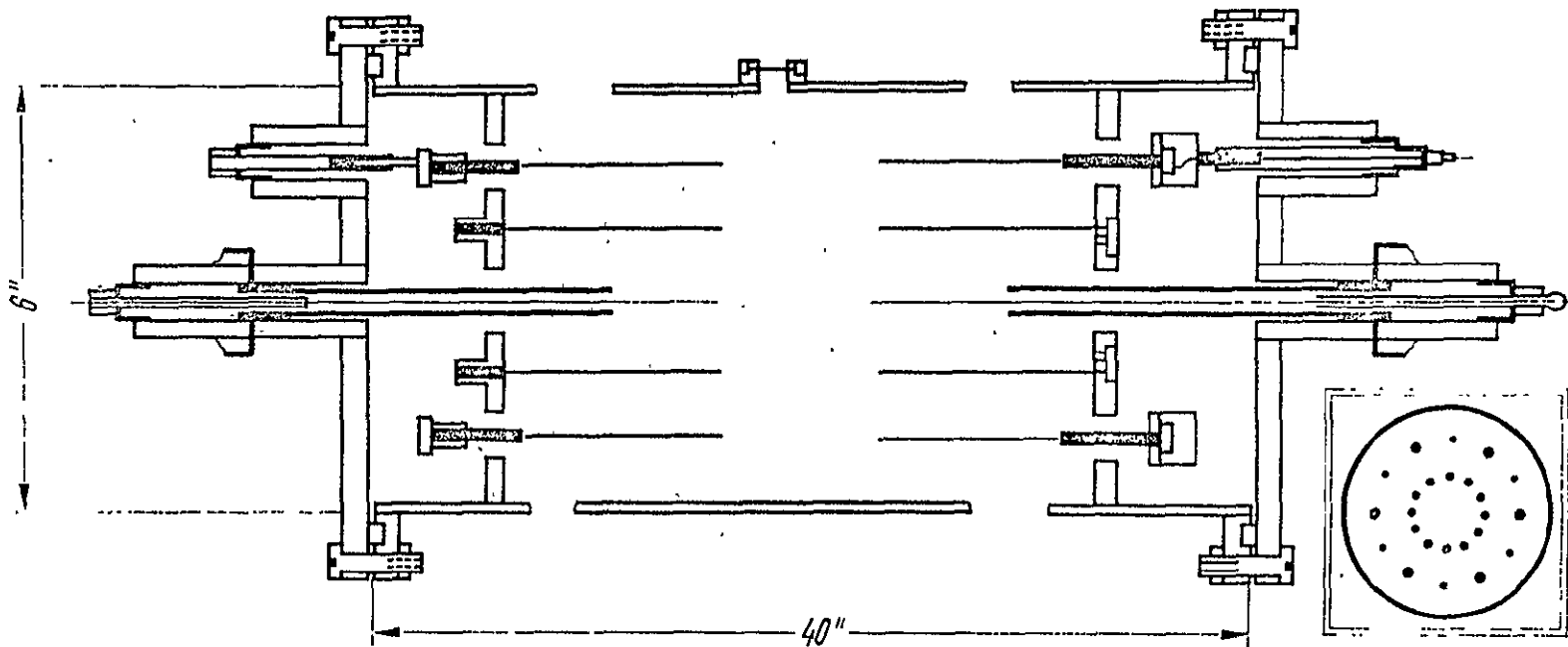


FIG. 3-2

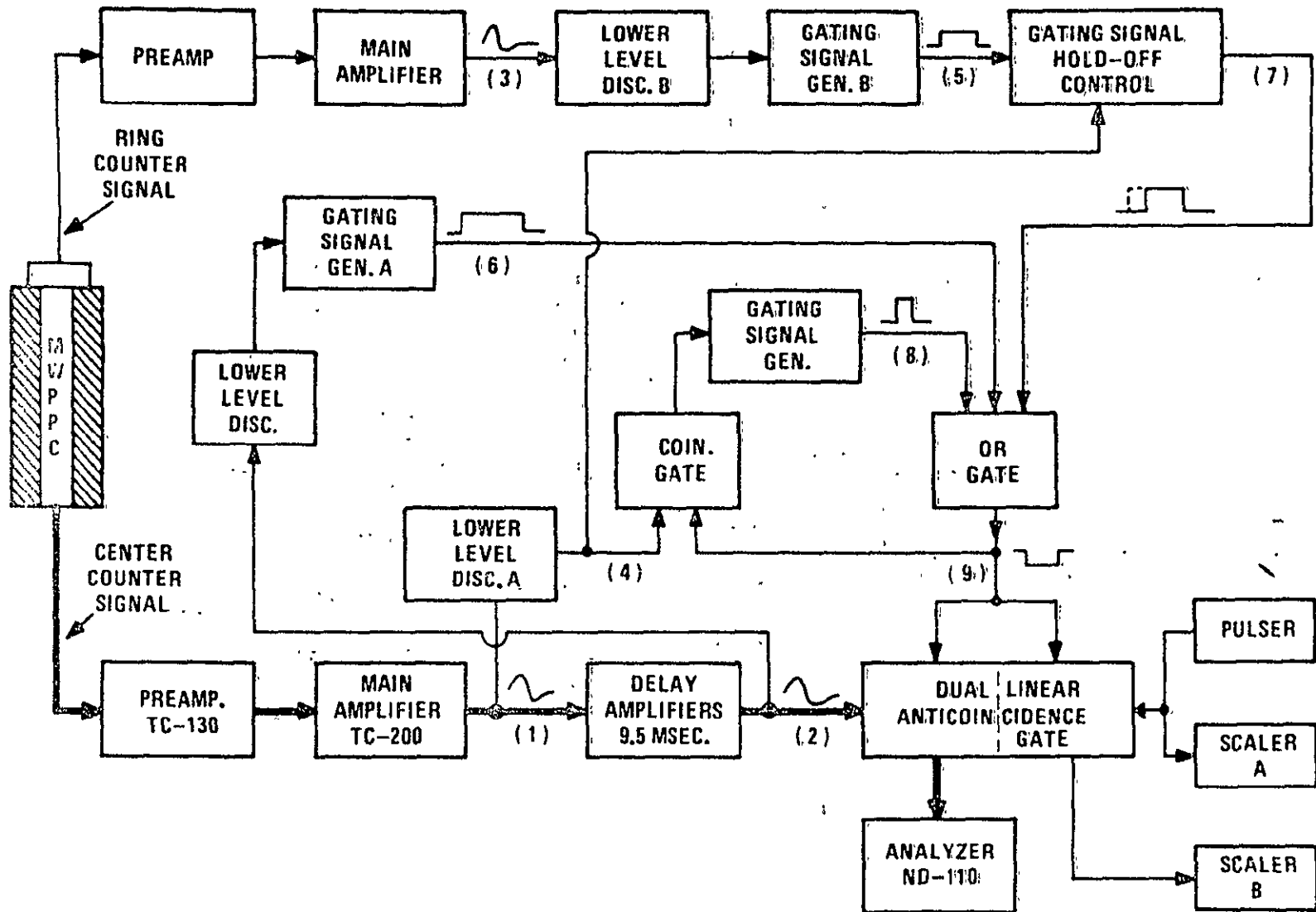


FIG. 3-3

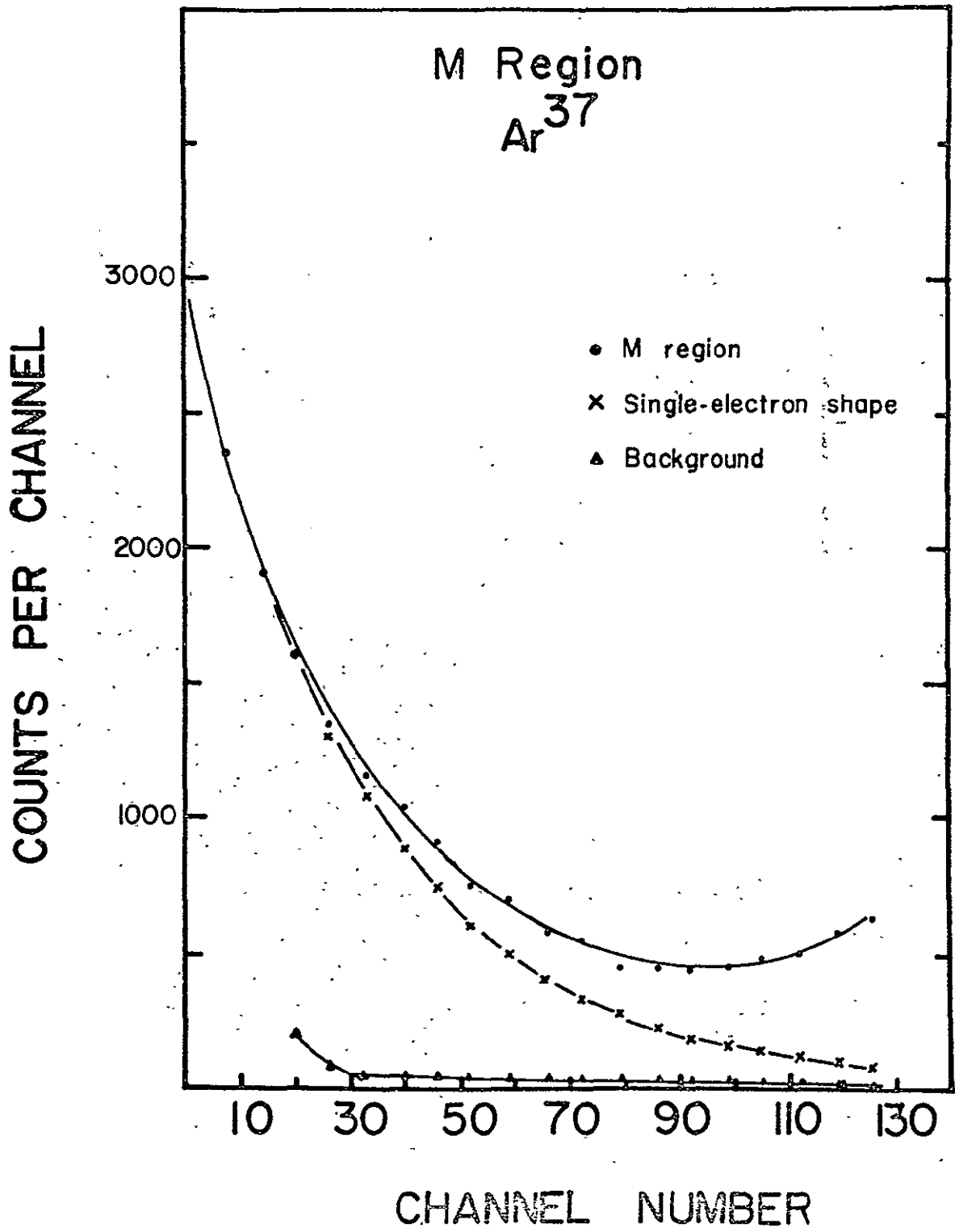


FIG. 3-4

2.6

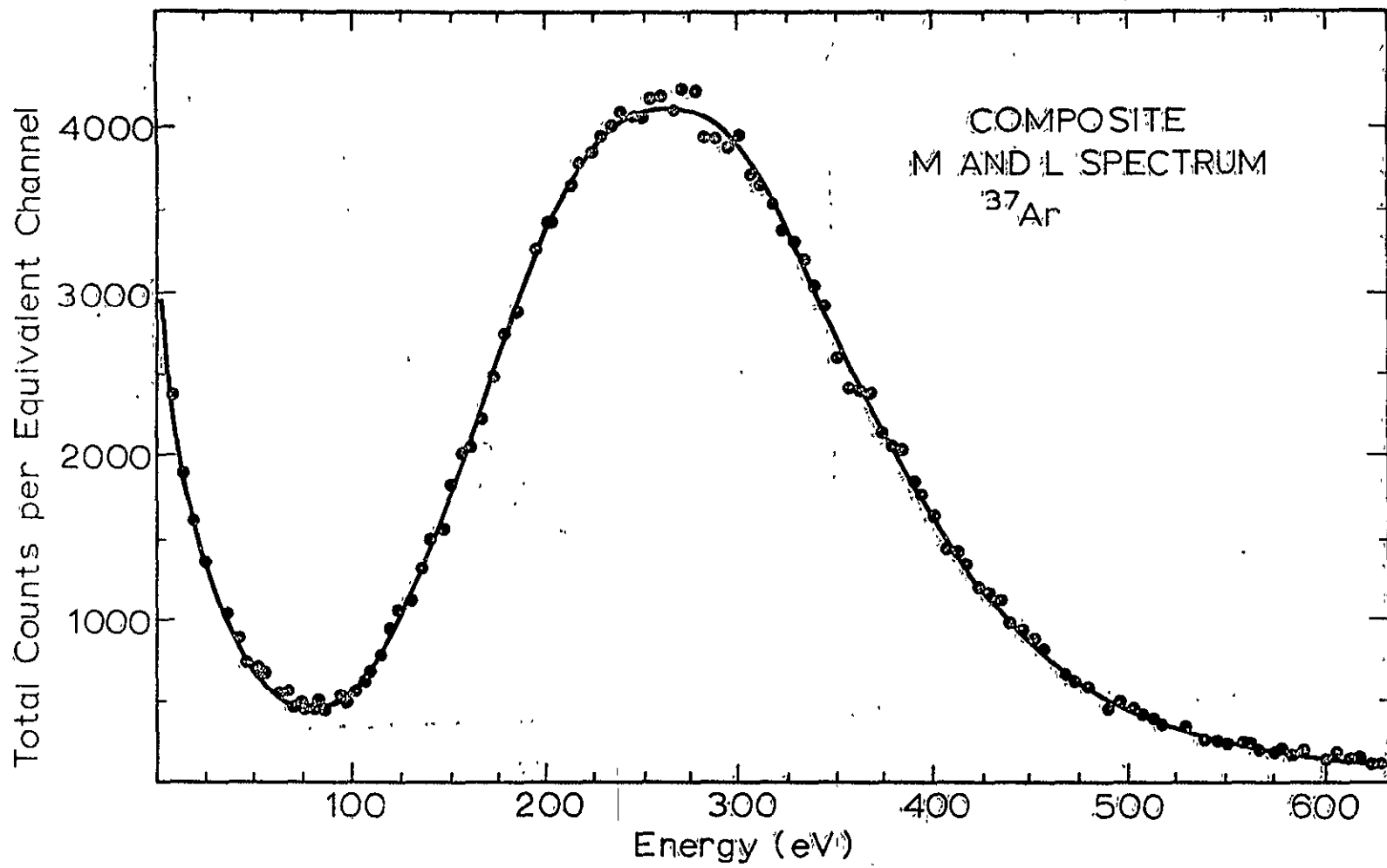


FIG. 3-5

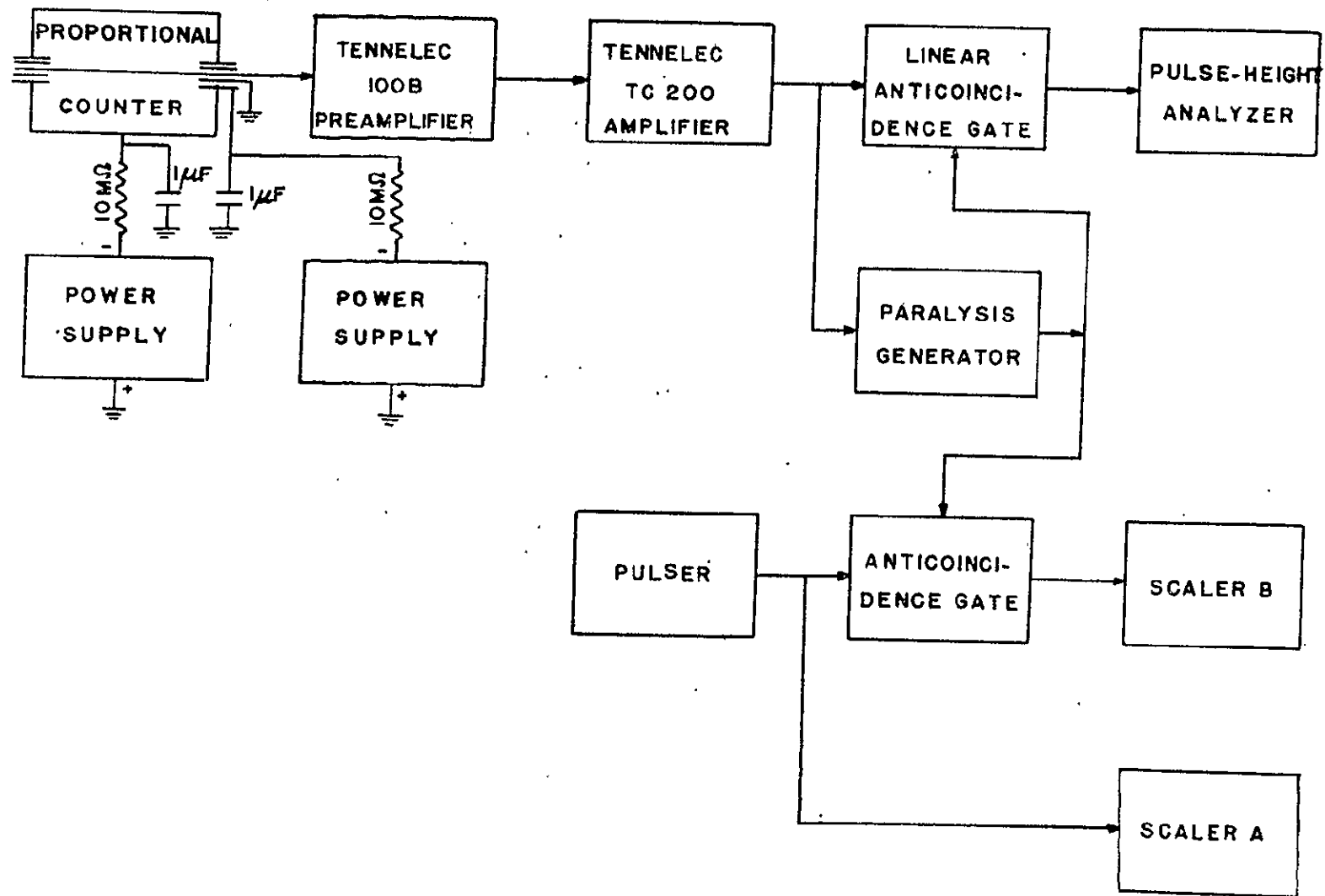


FIG. 3-6

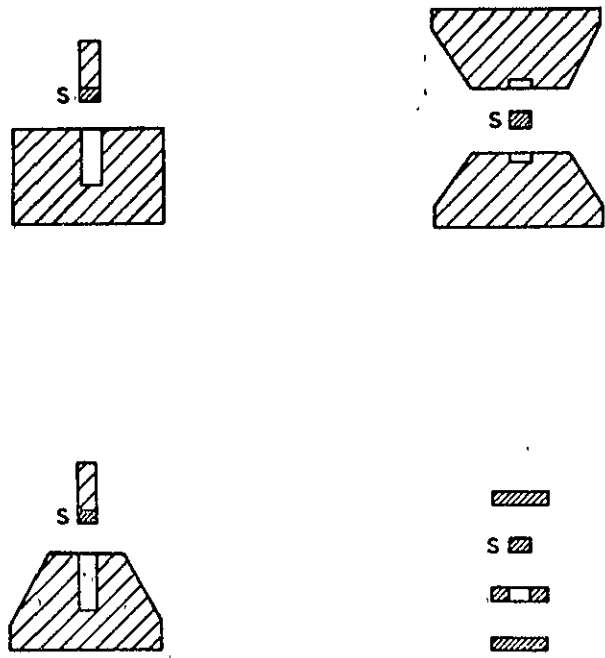


FIG. 3-7

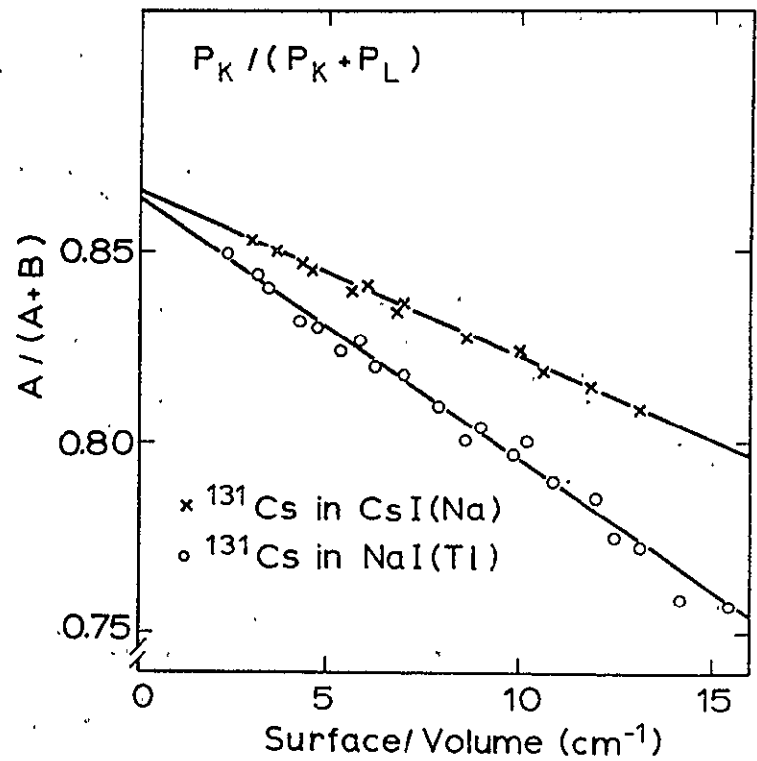
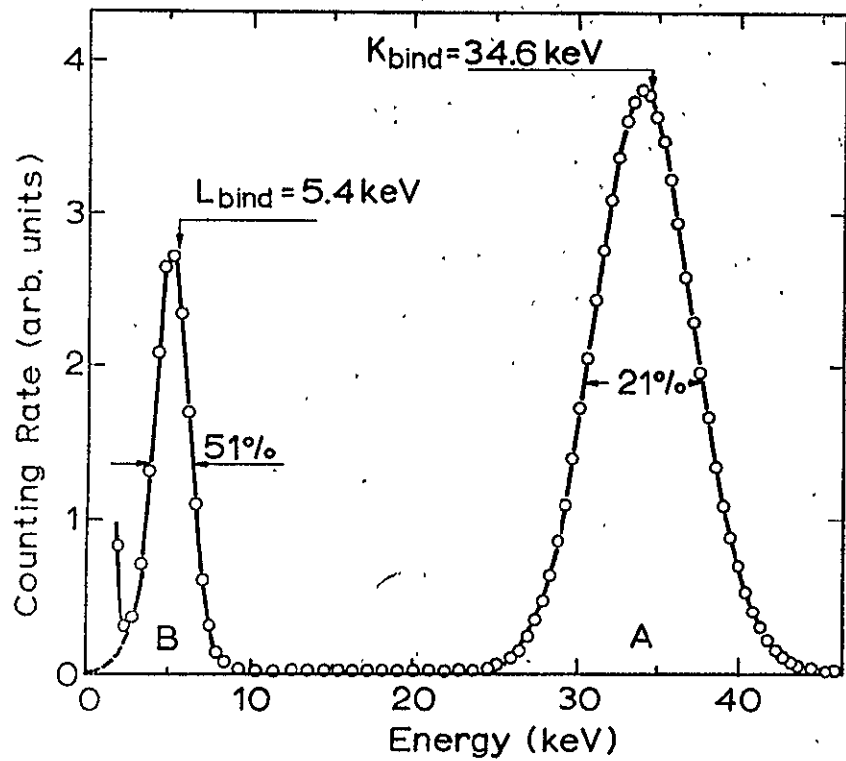


FIG. 3-8

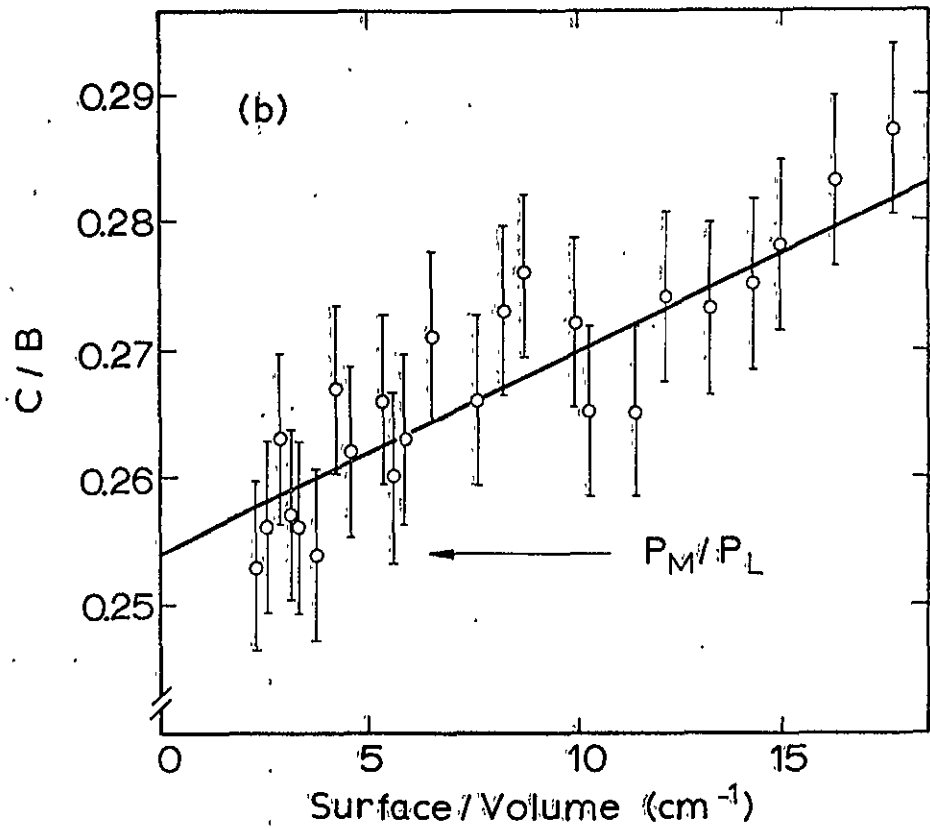
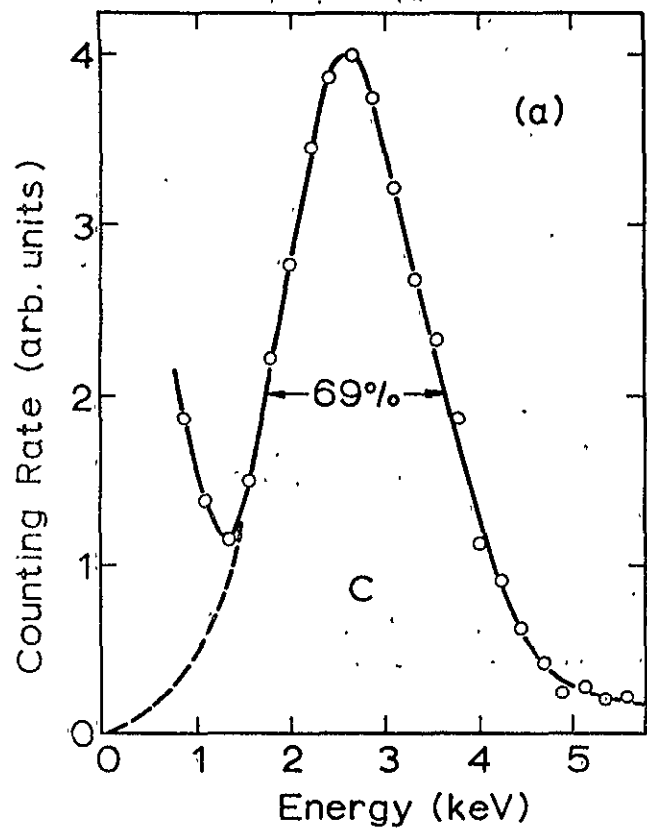


FIG. 3-9

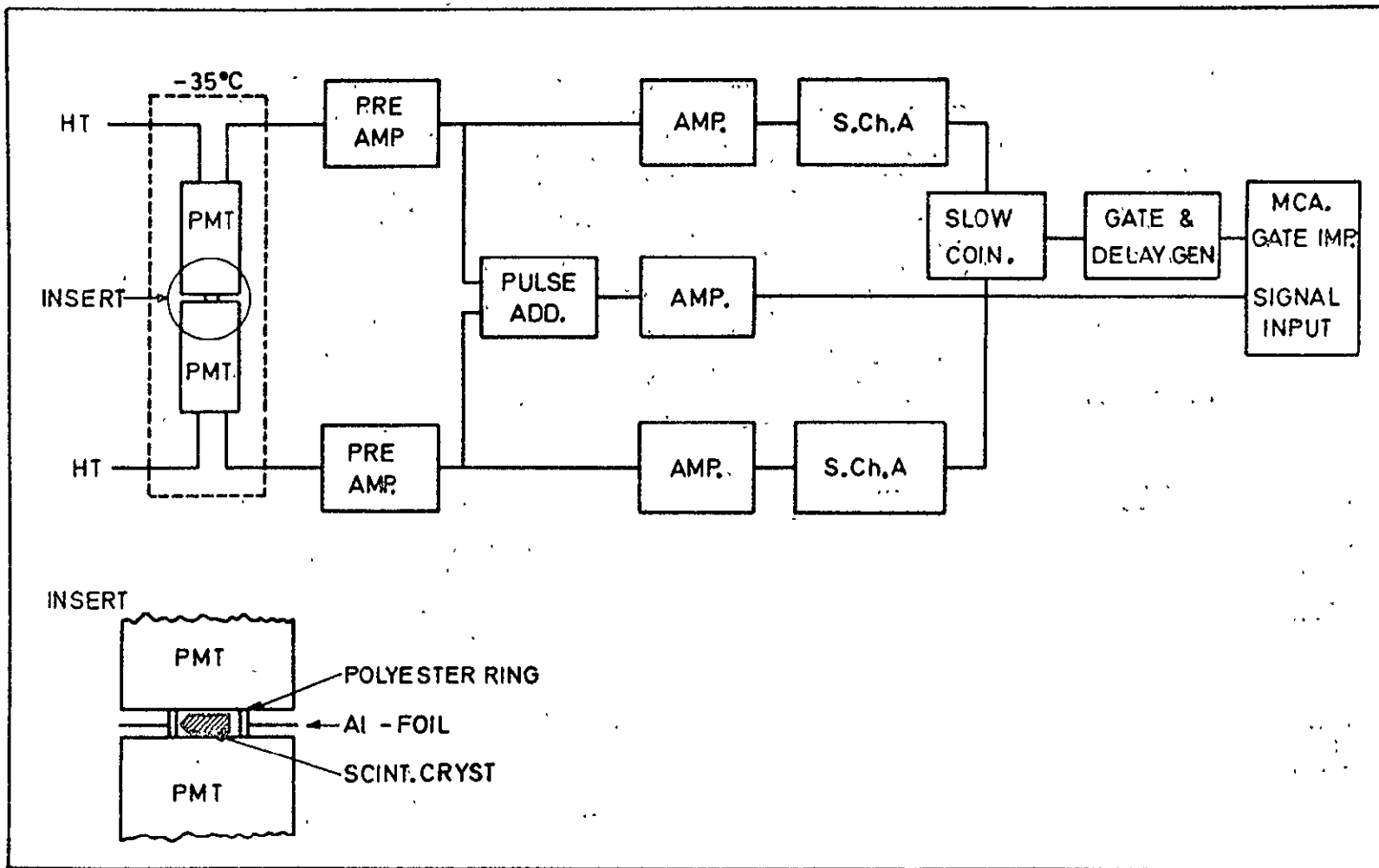


FIG. 3-10

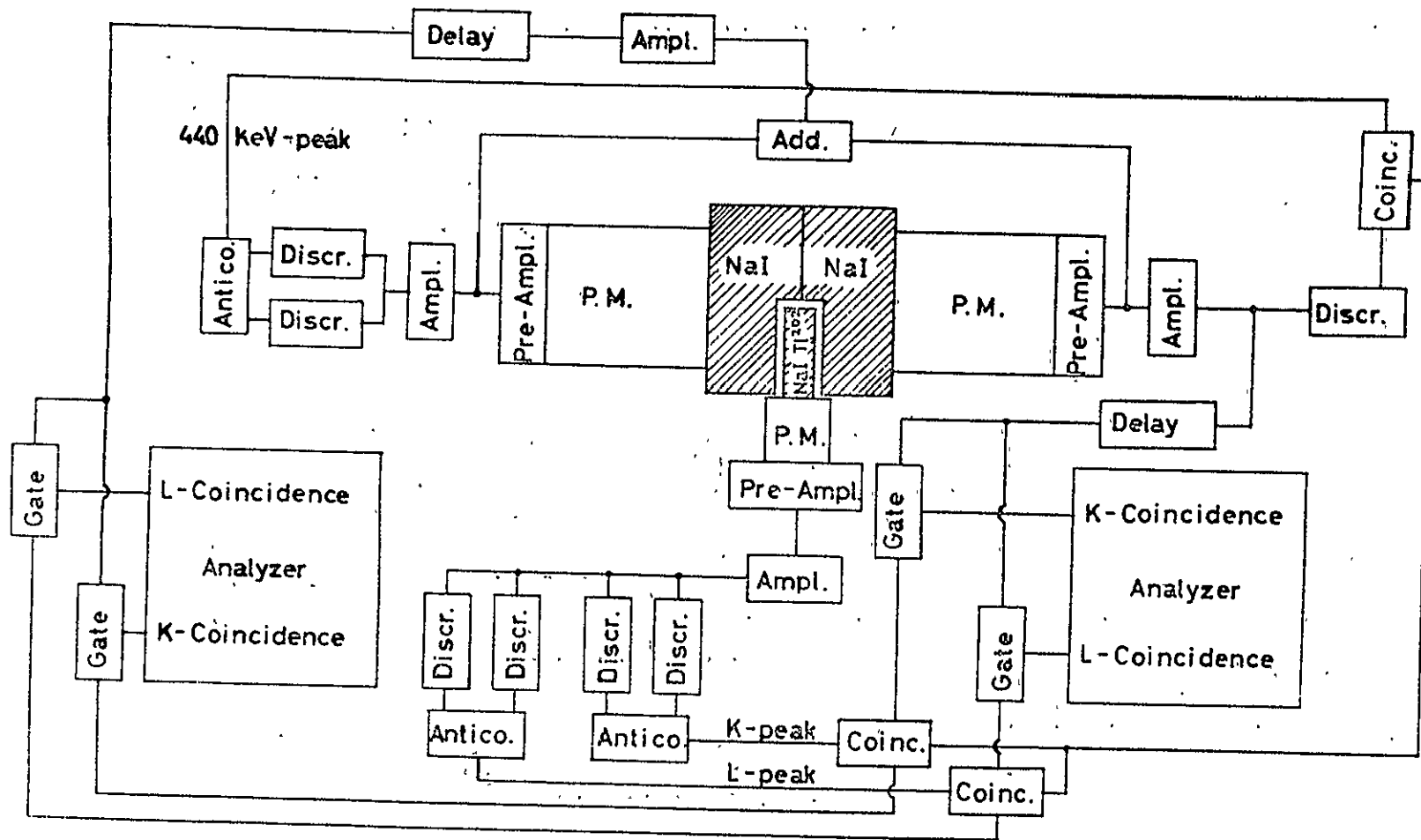


FIG. 3-11

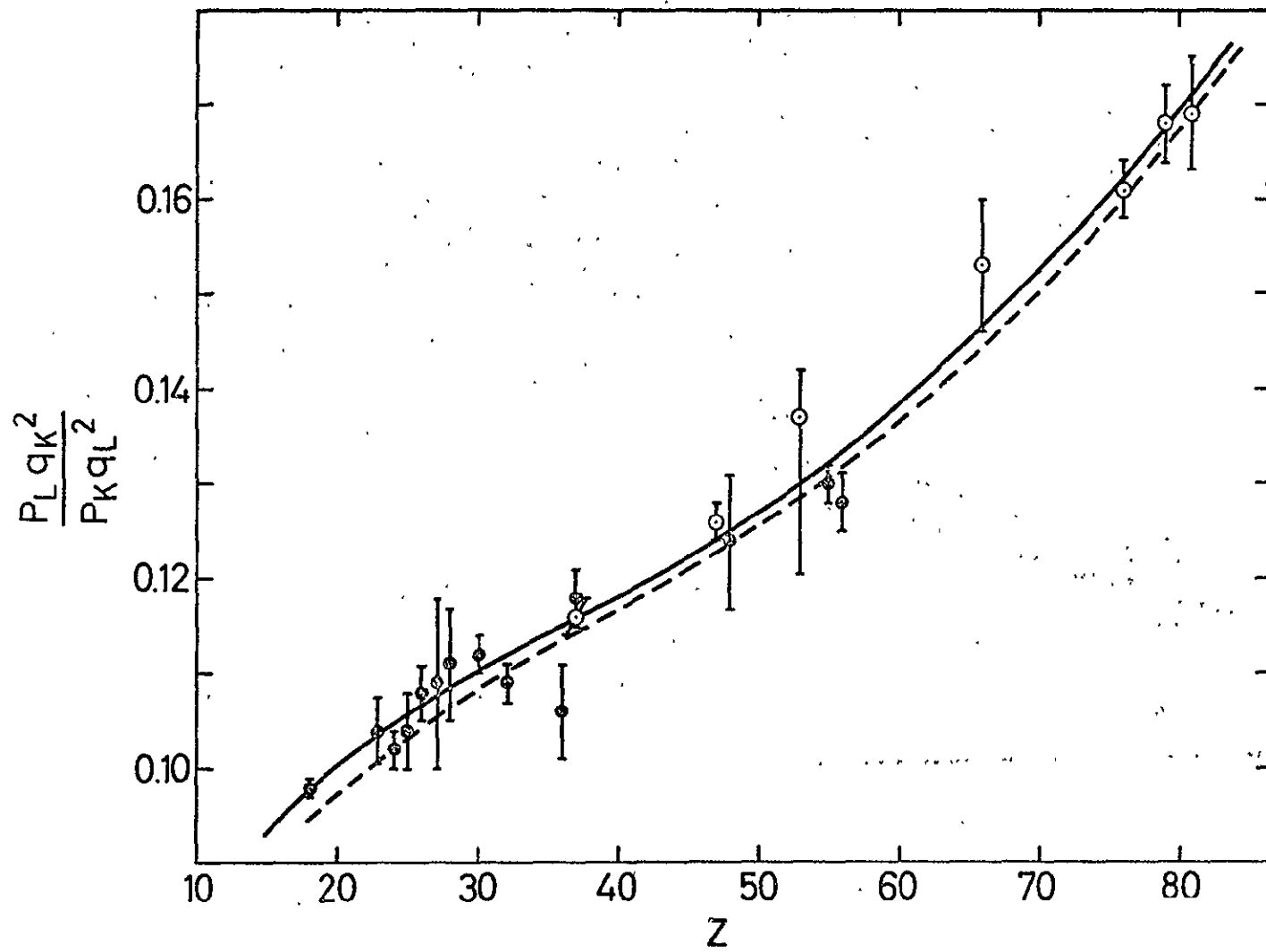


FIG. 3-12

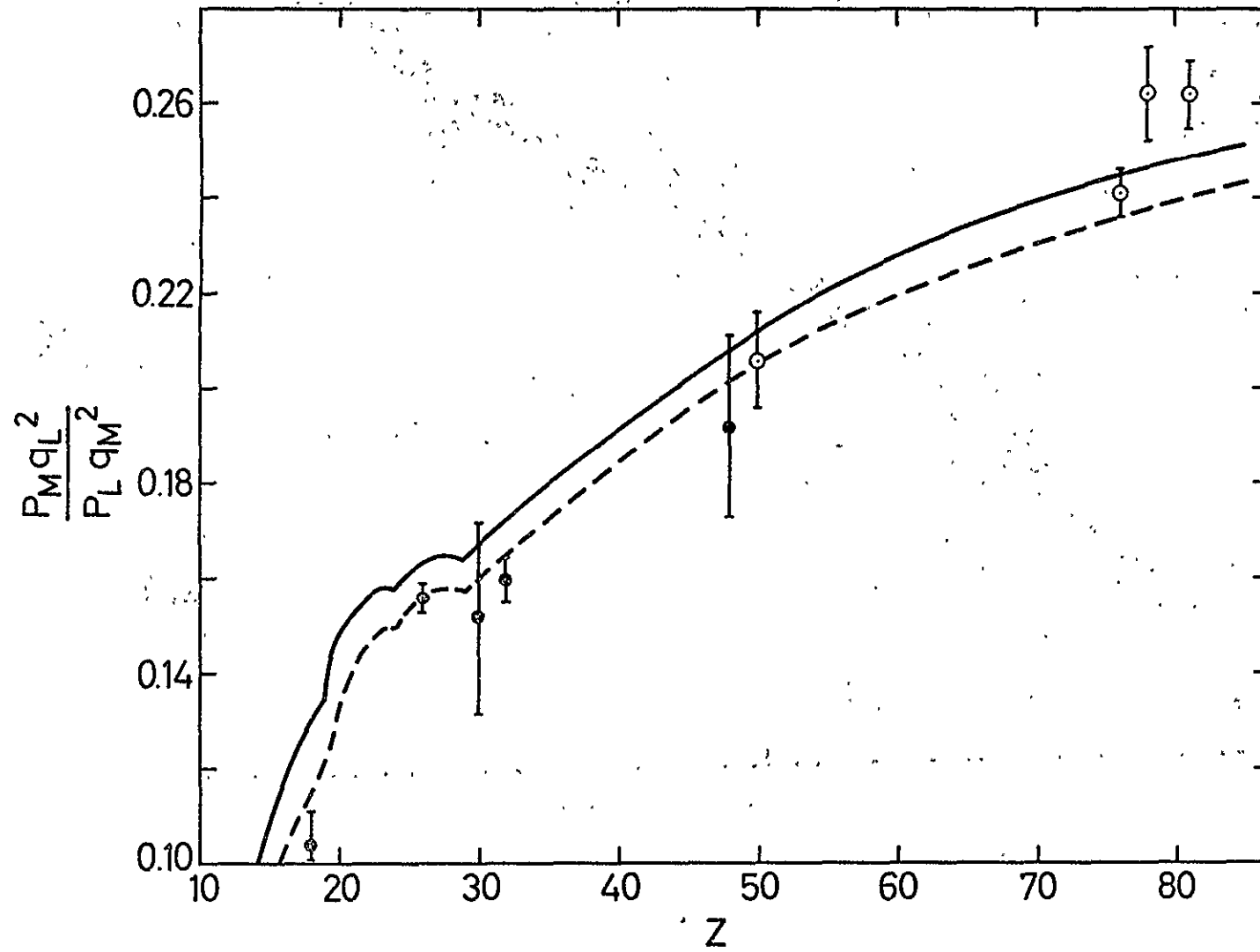


FIG. 3-13

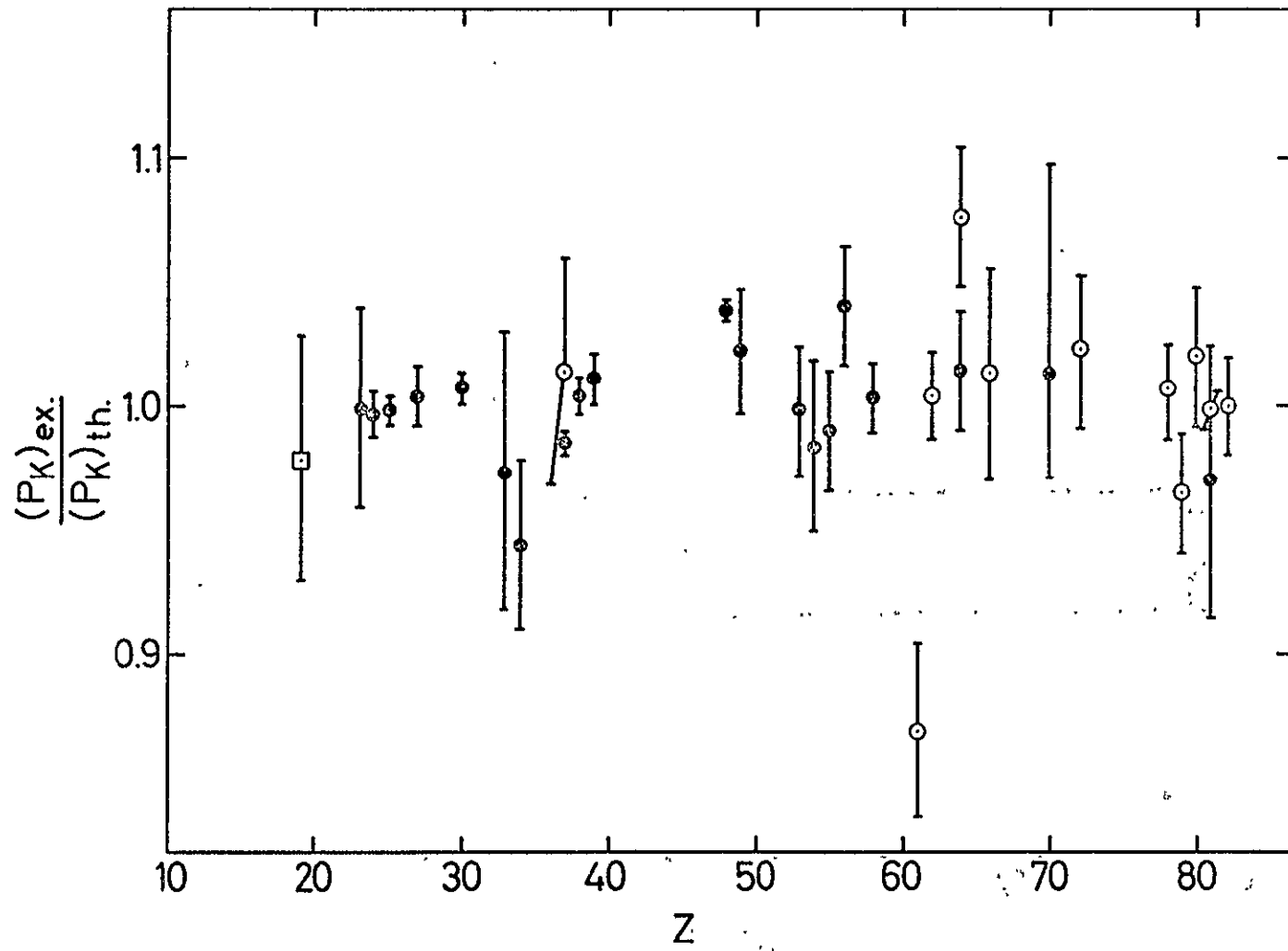


FIG. 3-14

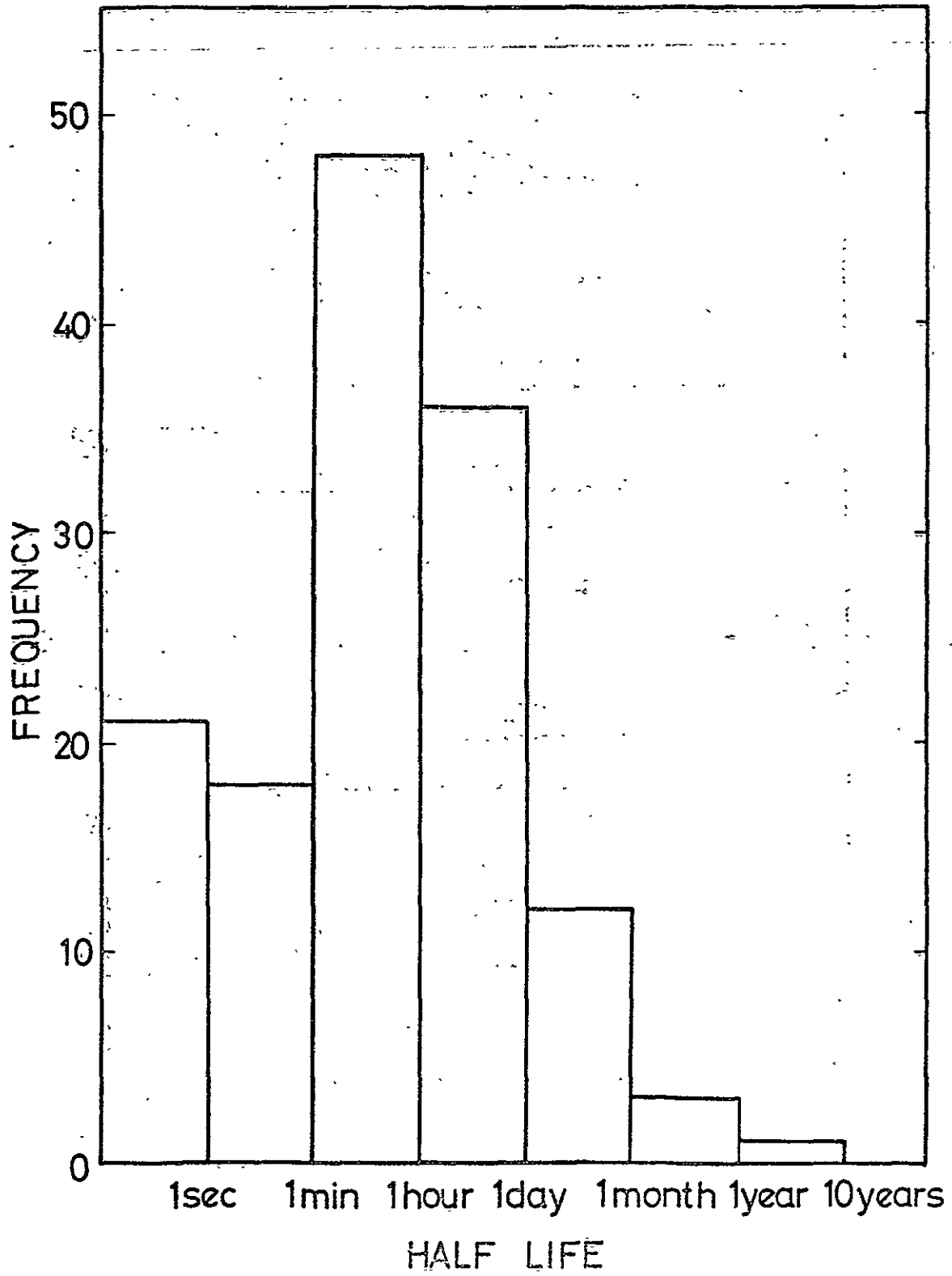


FIG. 3-15

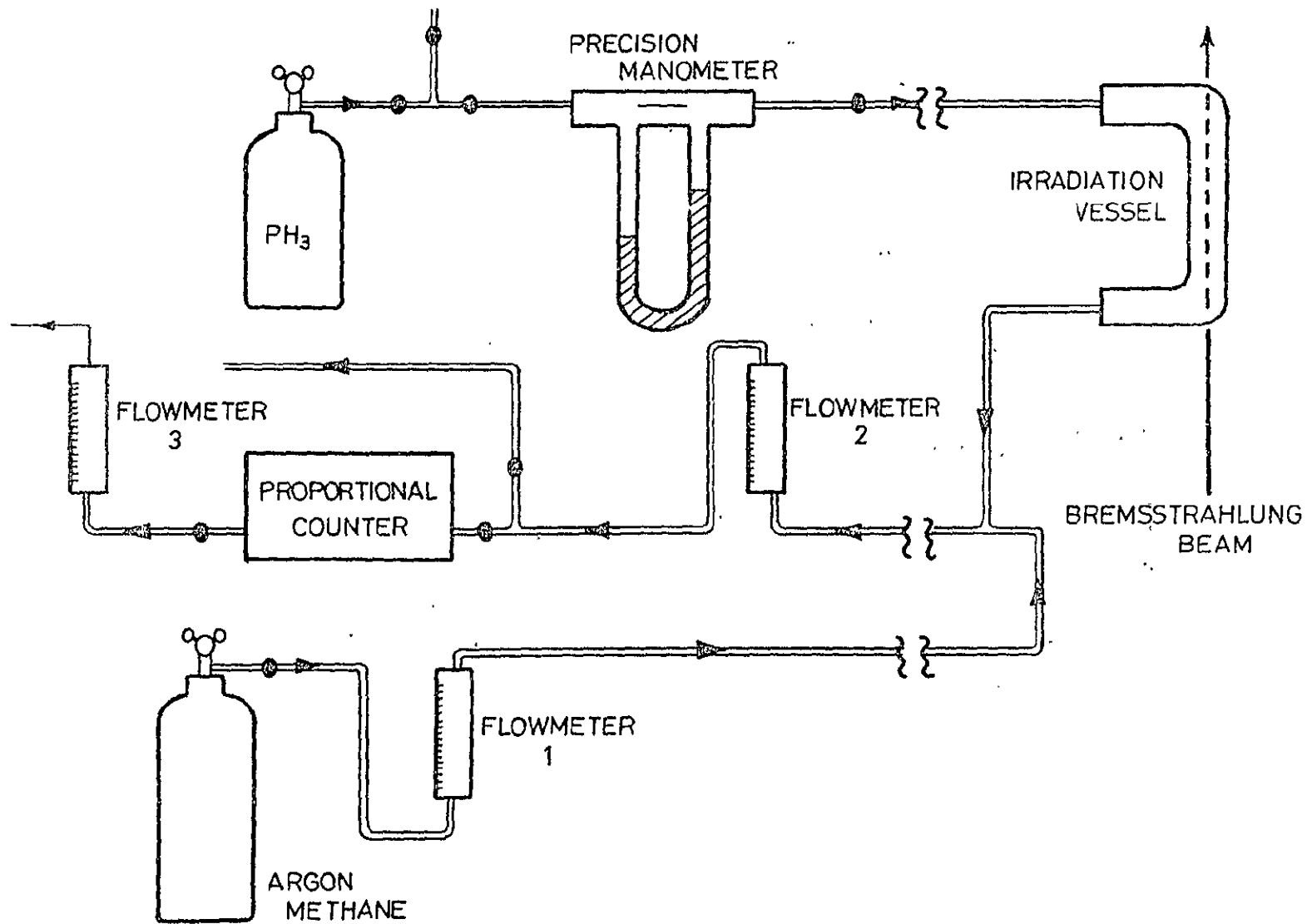


FIG. 3-16

PLASTIC COUNTER

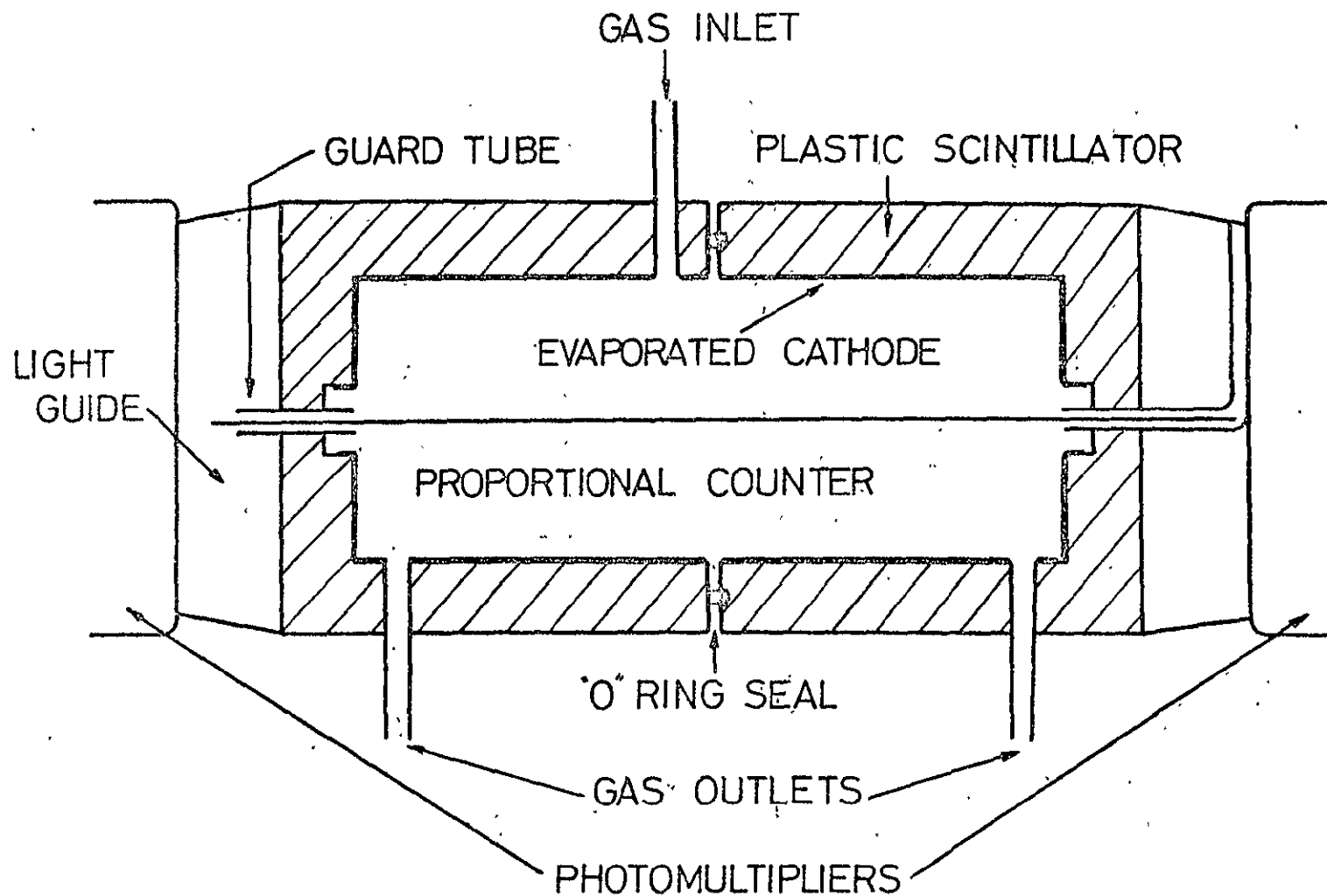


FIG. 3-17

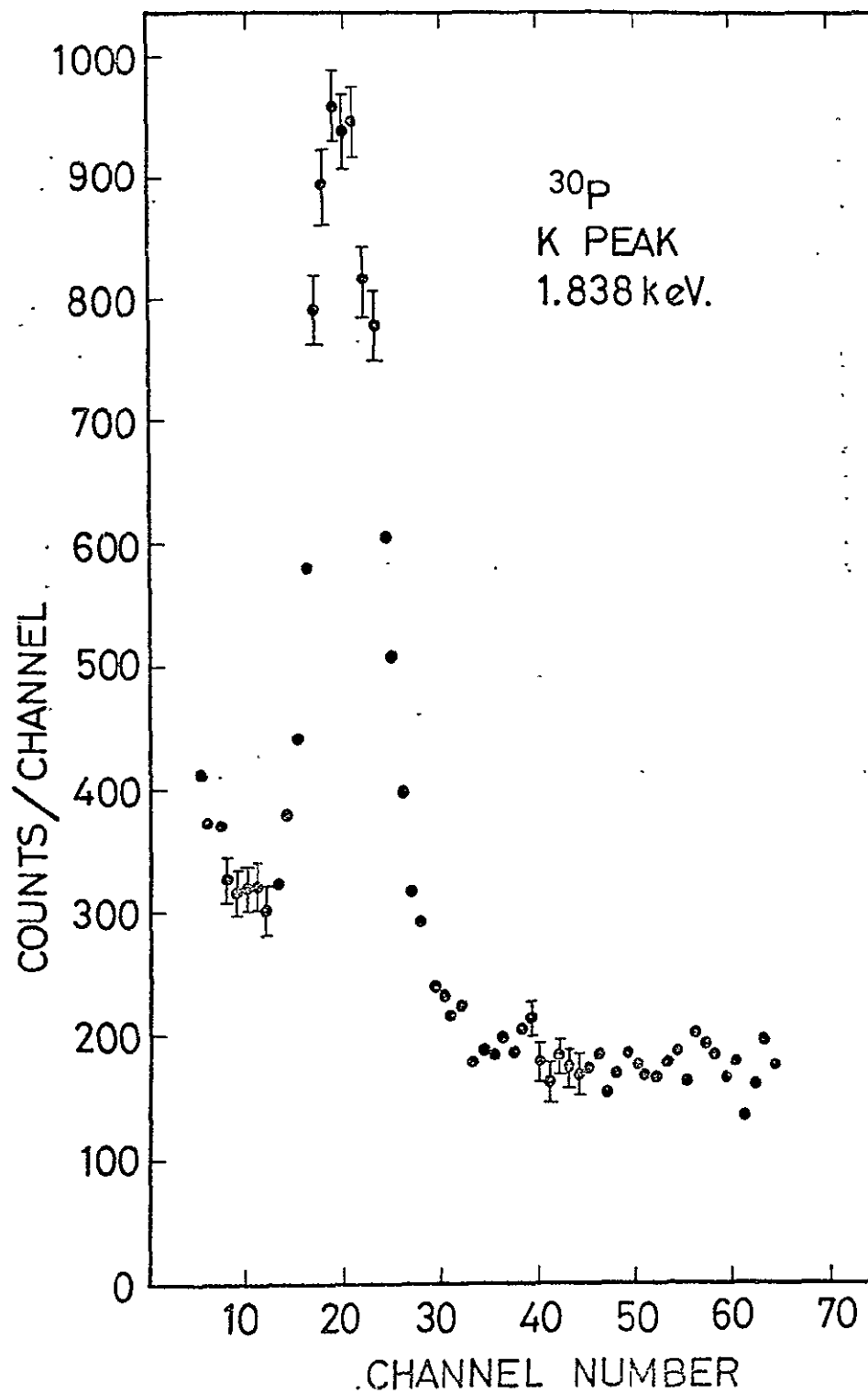


FIG. 3-18

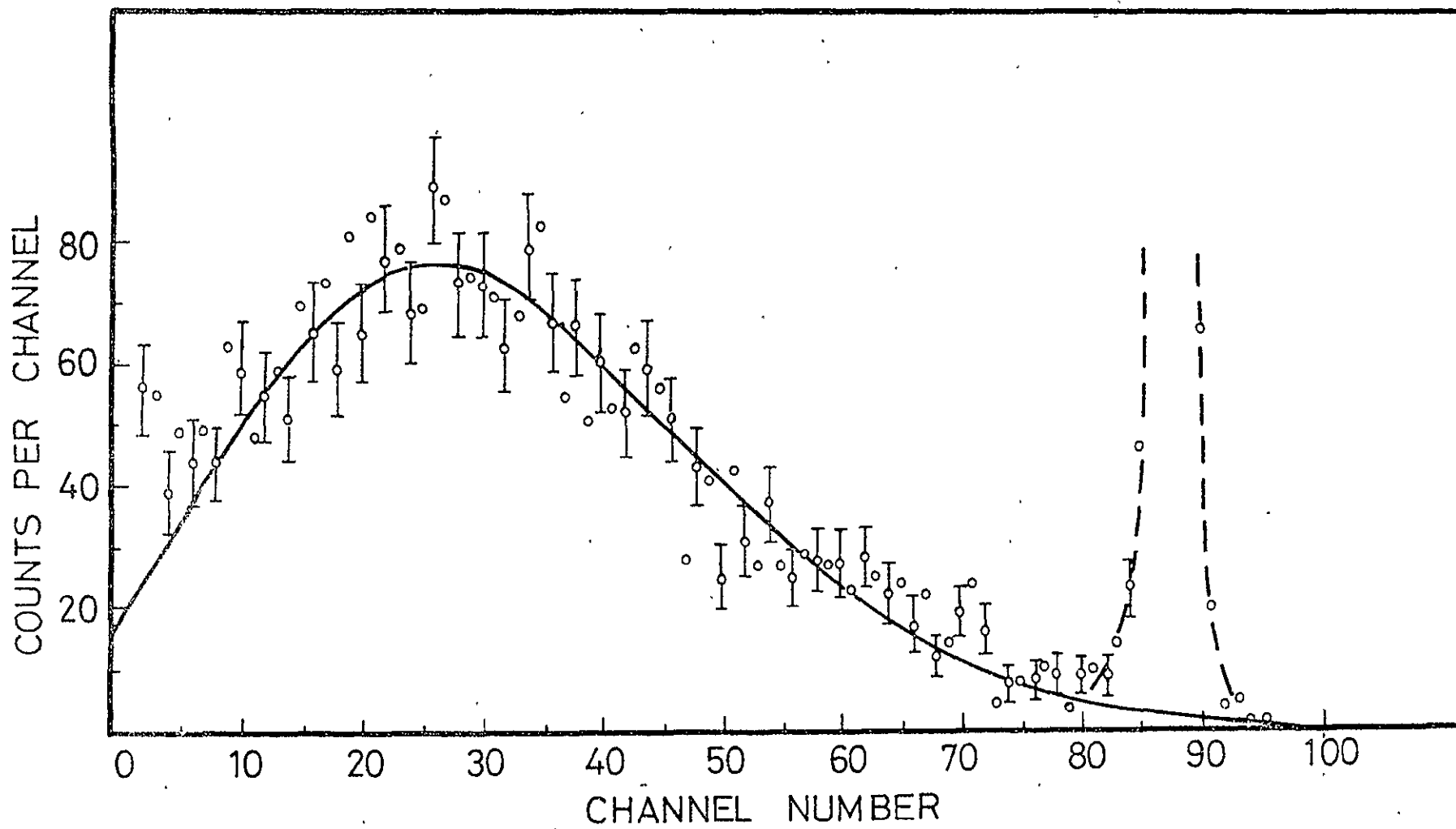


FIG. 3-19

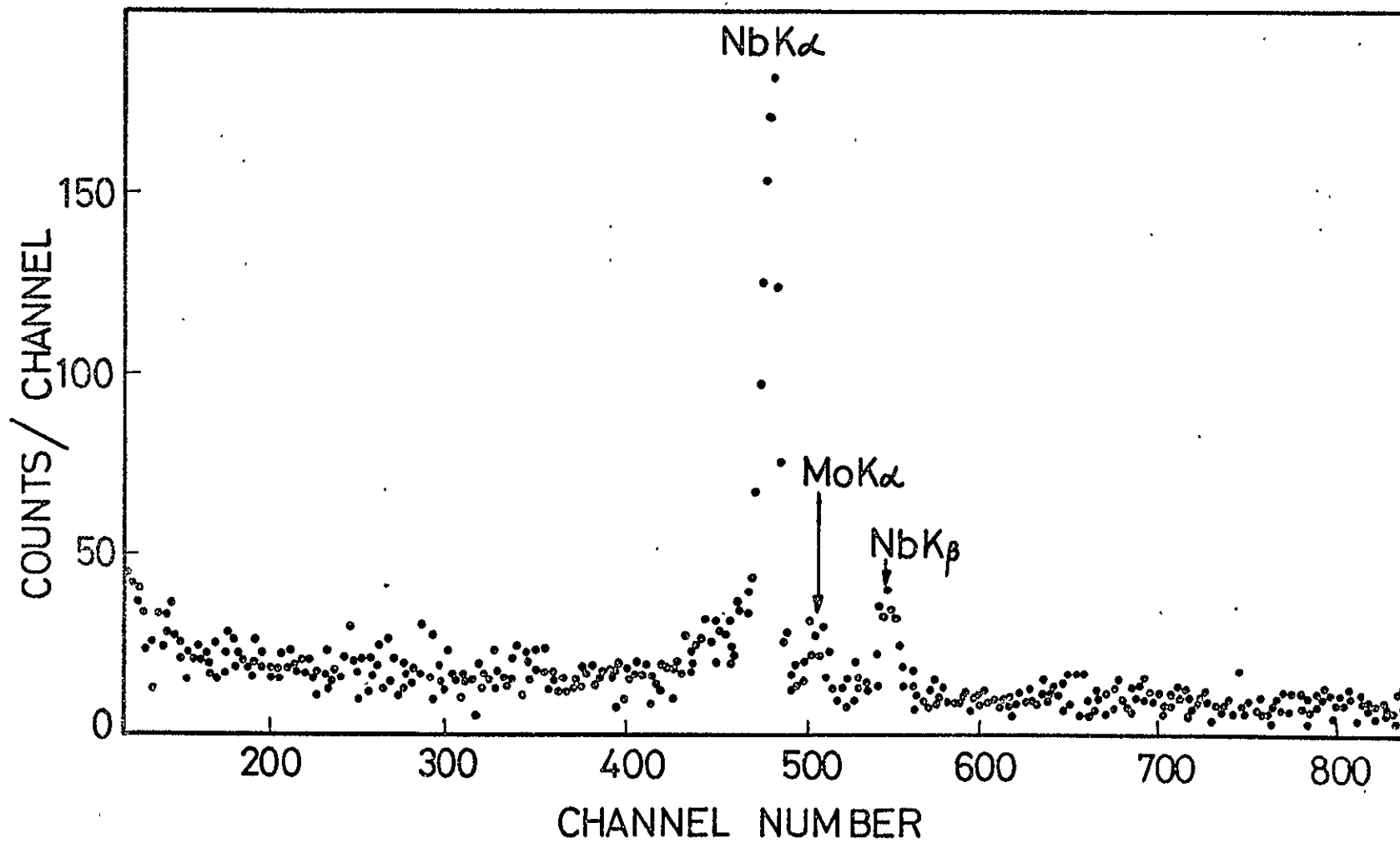


FIG. 3-20

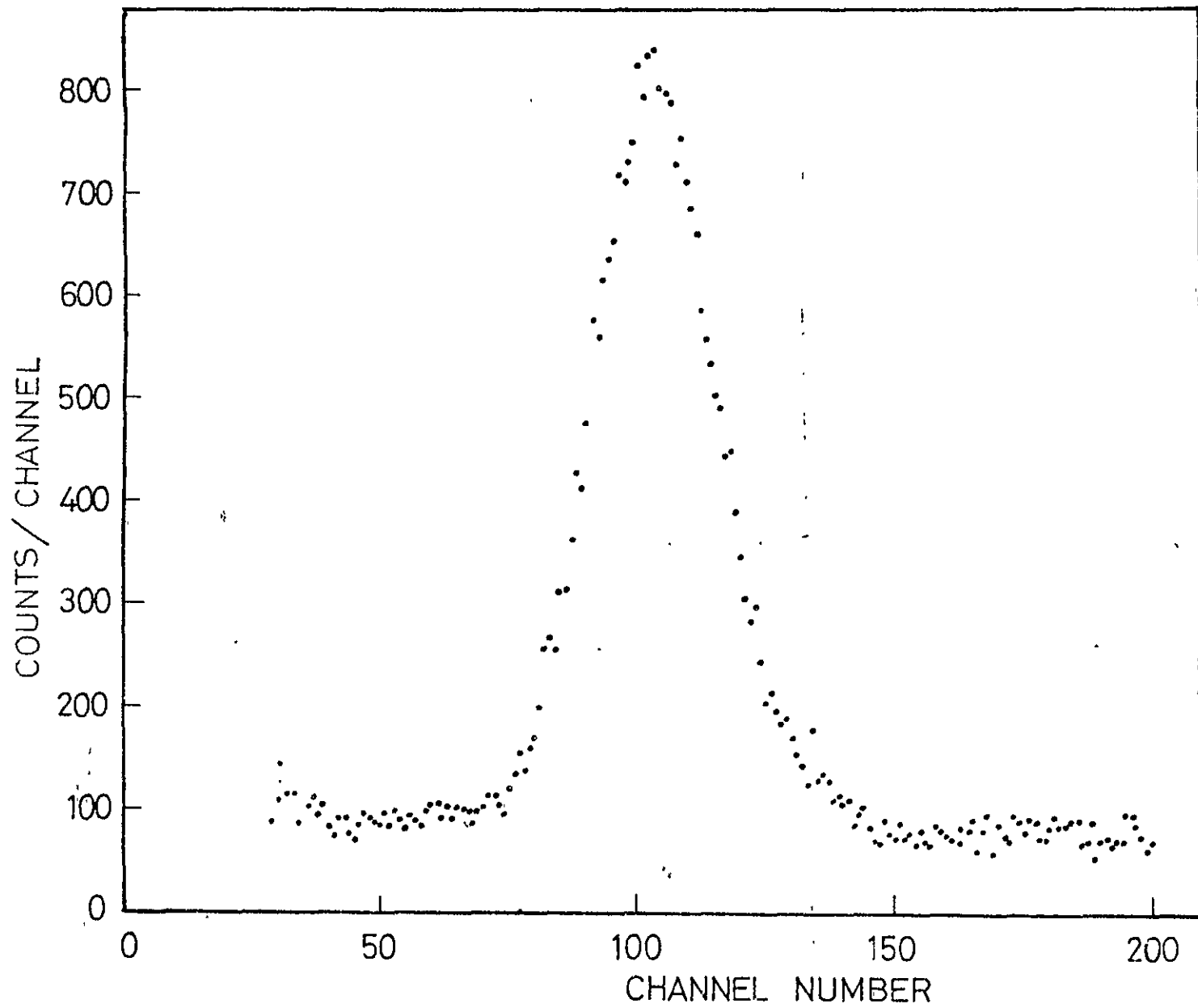


FIG. 3-21

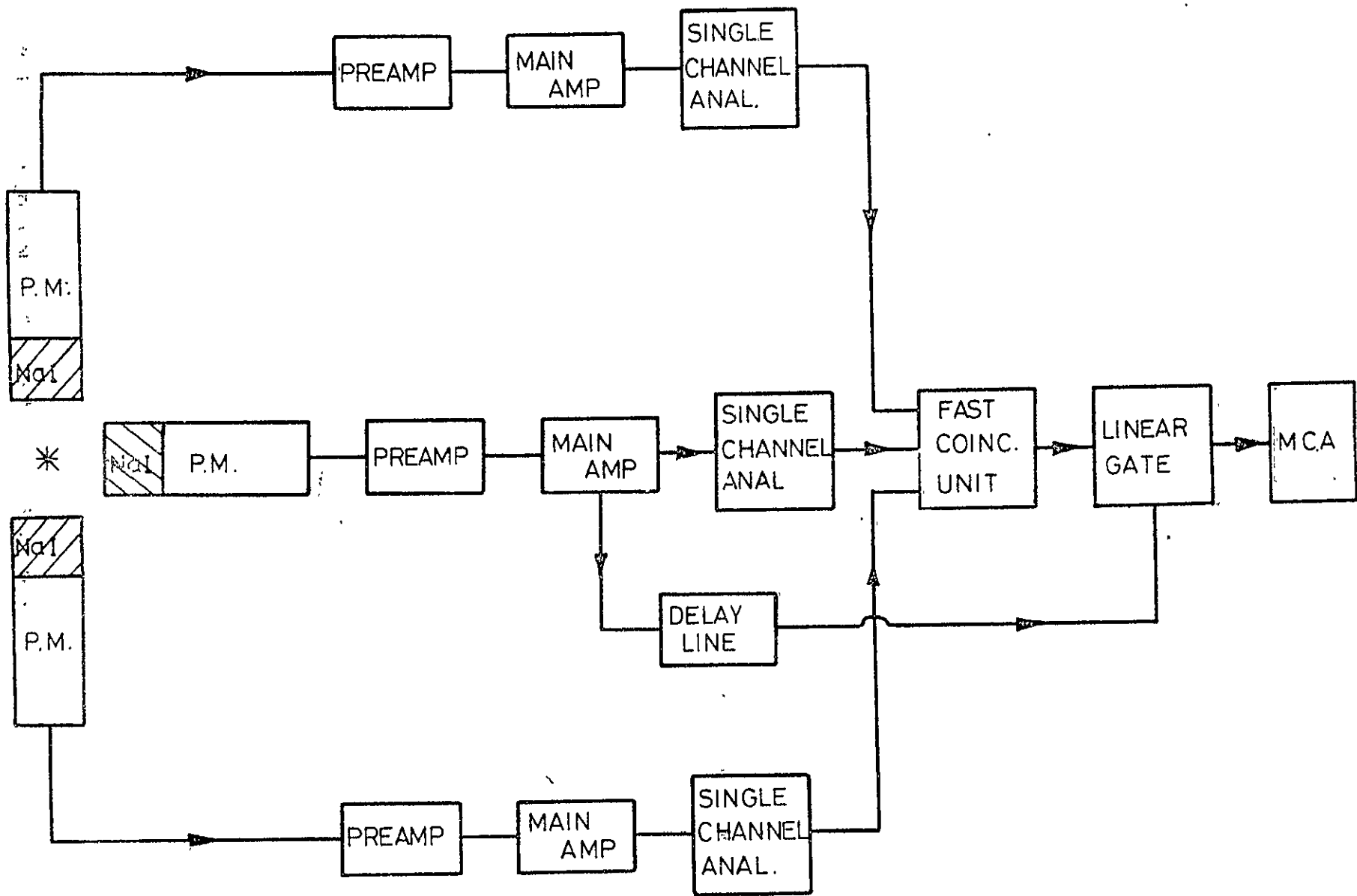


FIG. 3-23

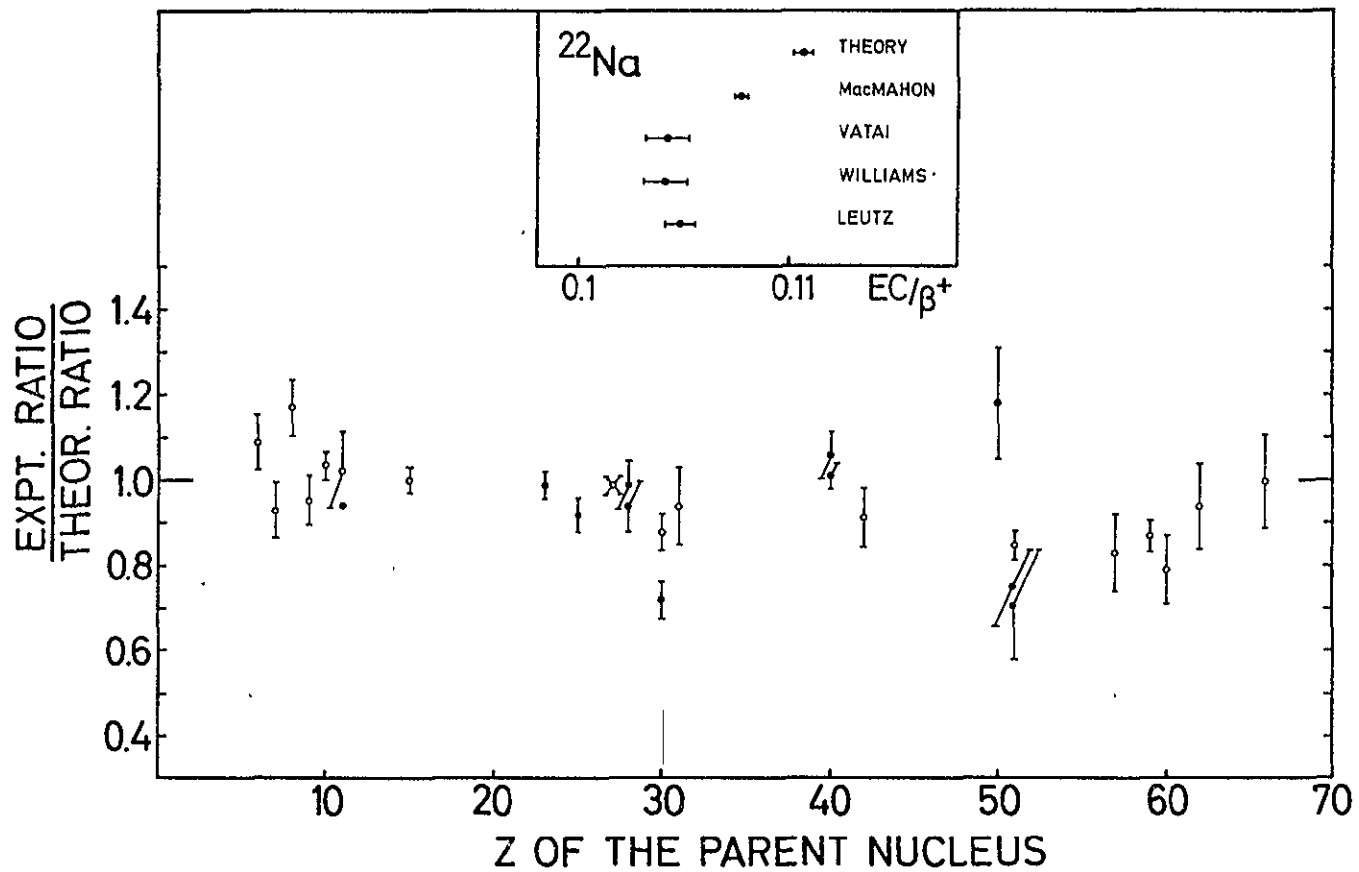


FIG. 3-24

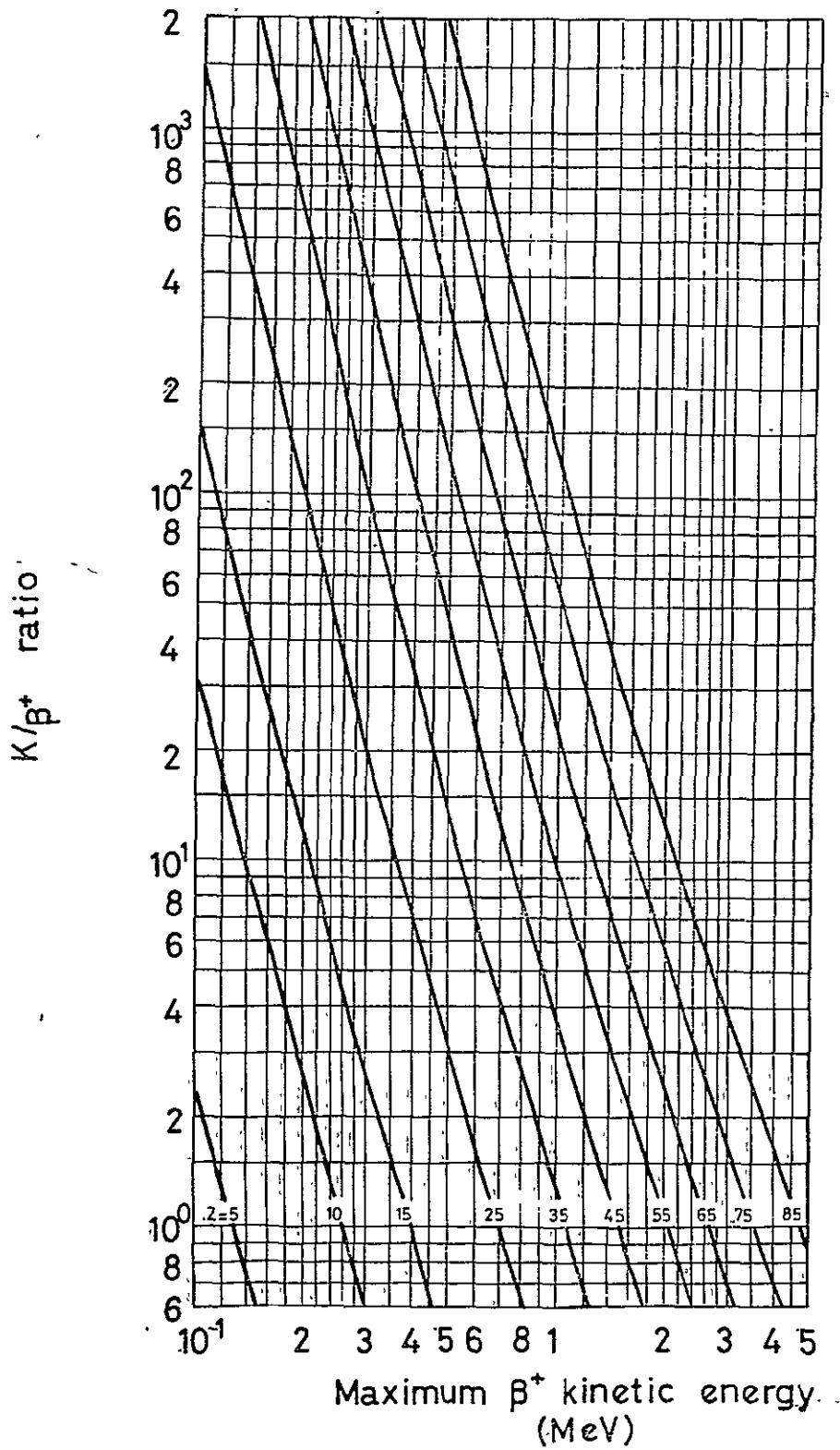


FIG. 3-25

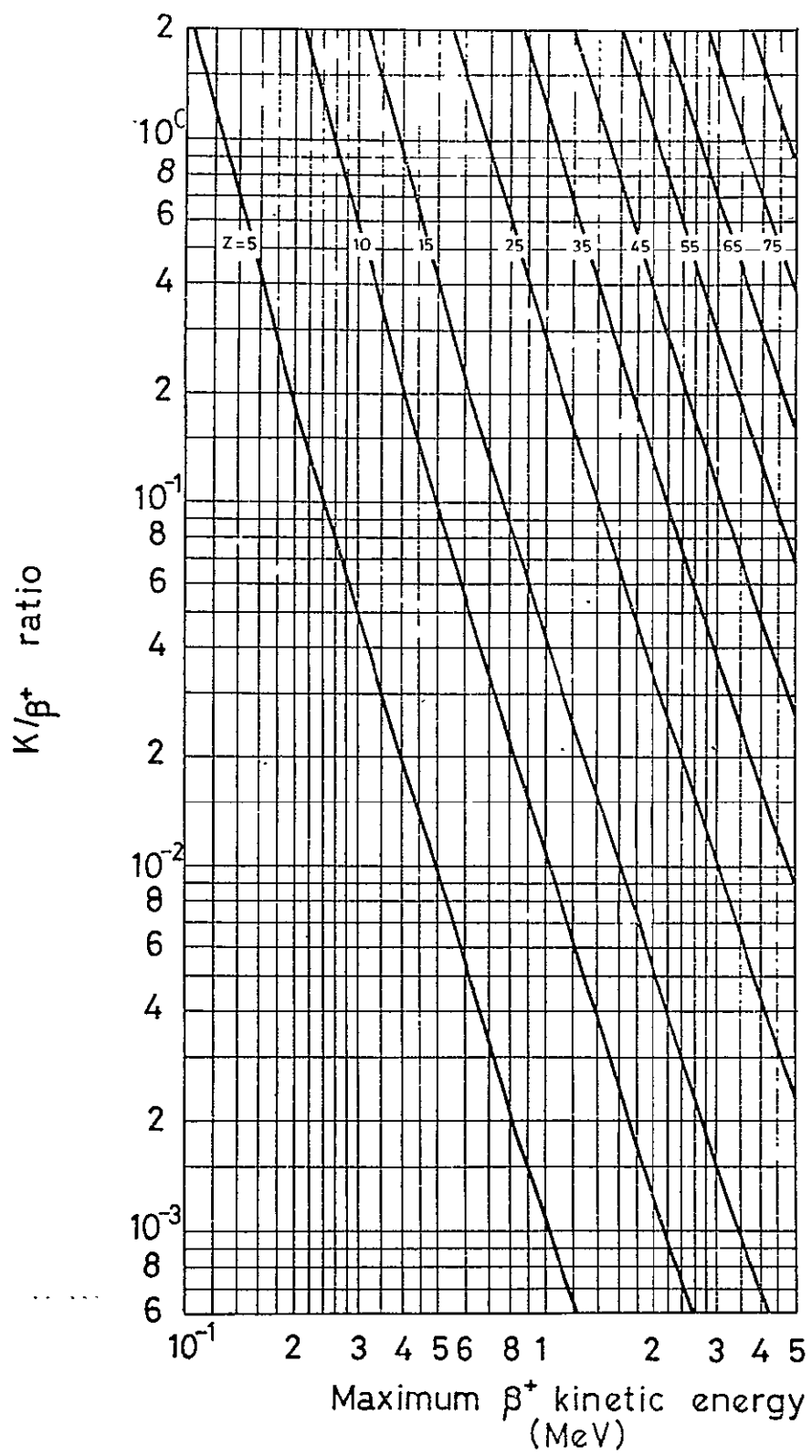
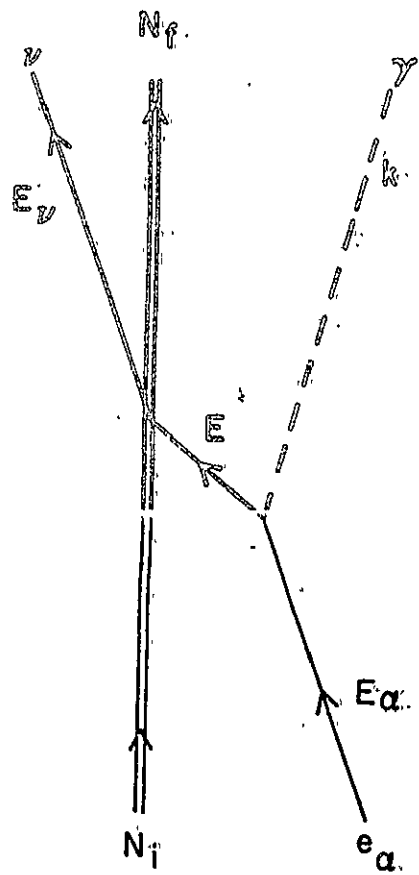
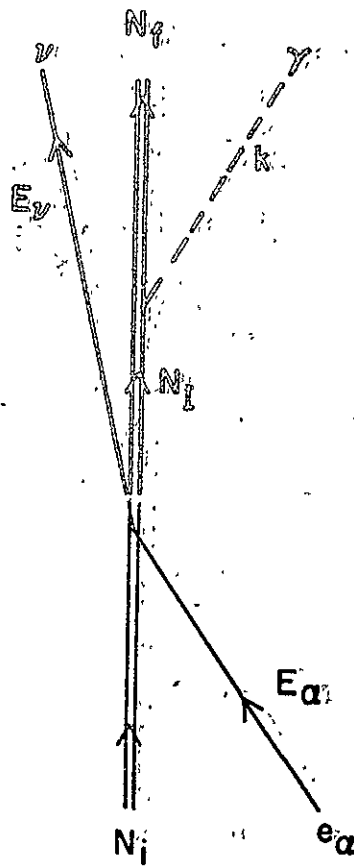


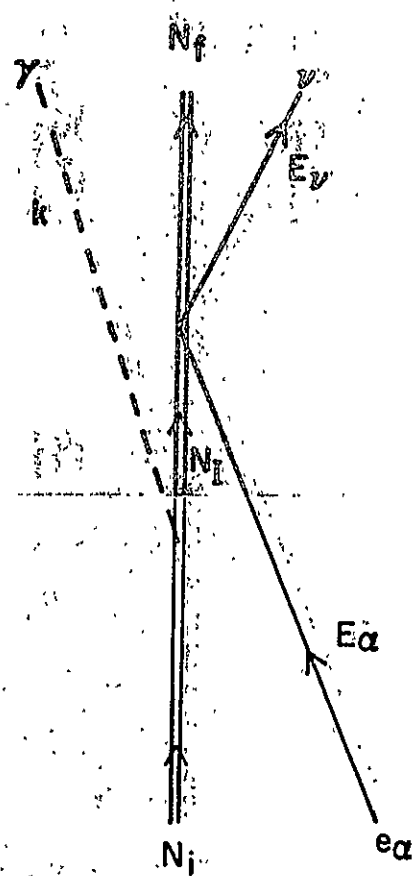
FIG. 3-26



(a)



(b)



(c)

FIG. 4-1

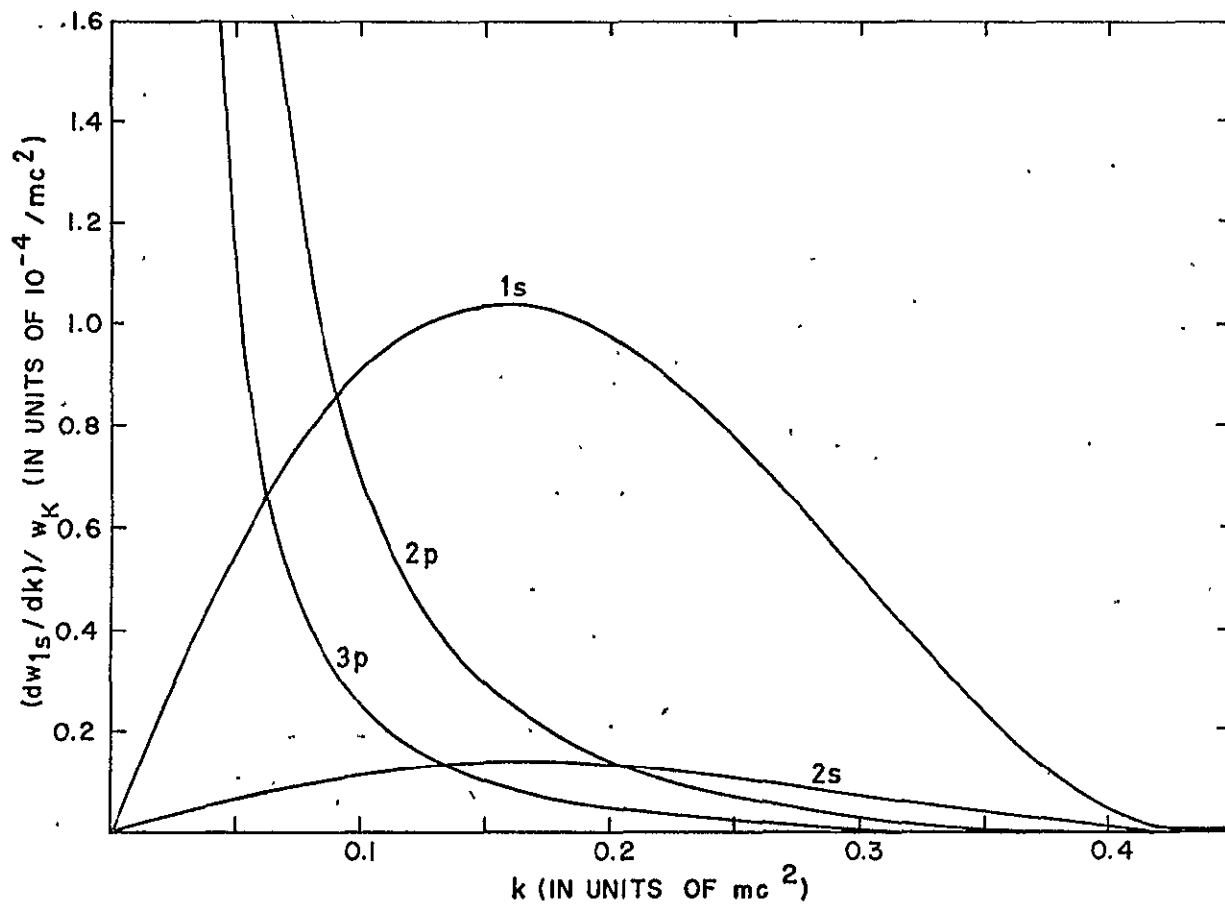


FIG. 4-2

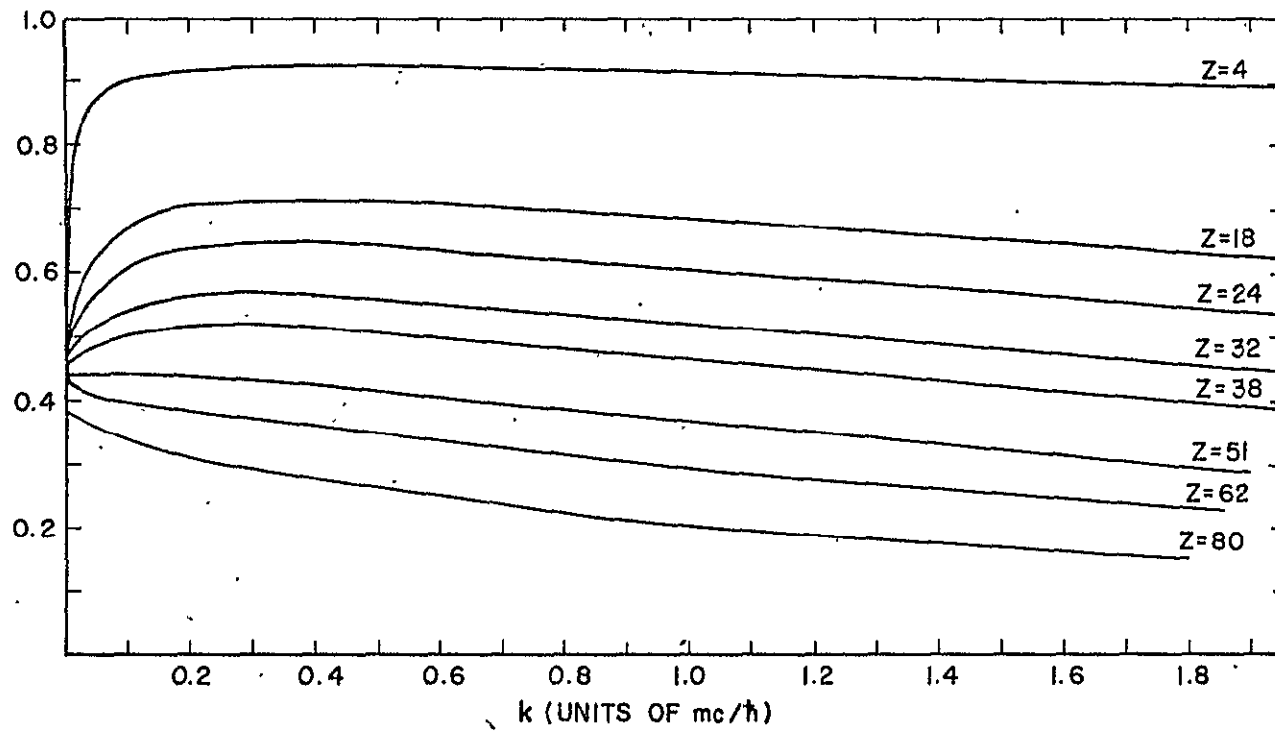


FIG. 4-3

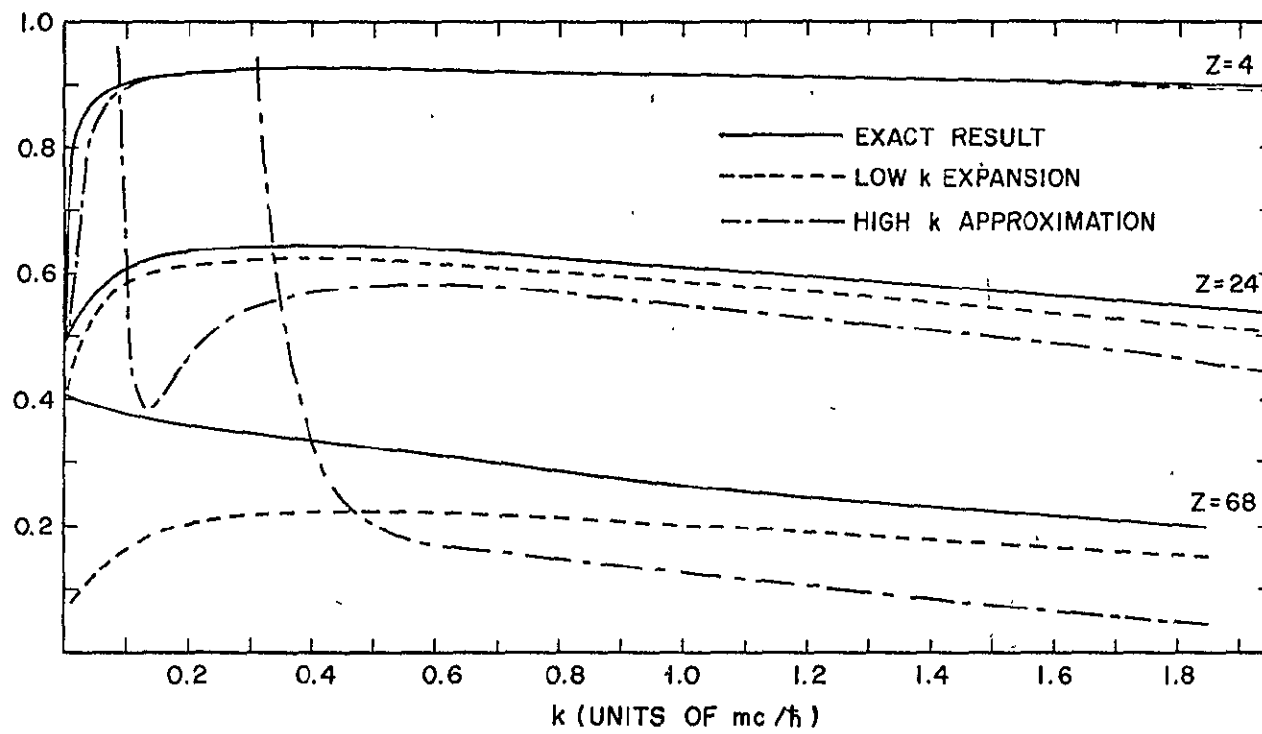


FIG. 4-4

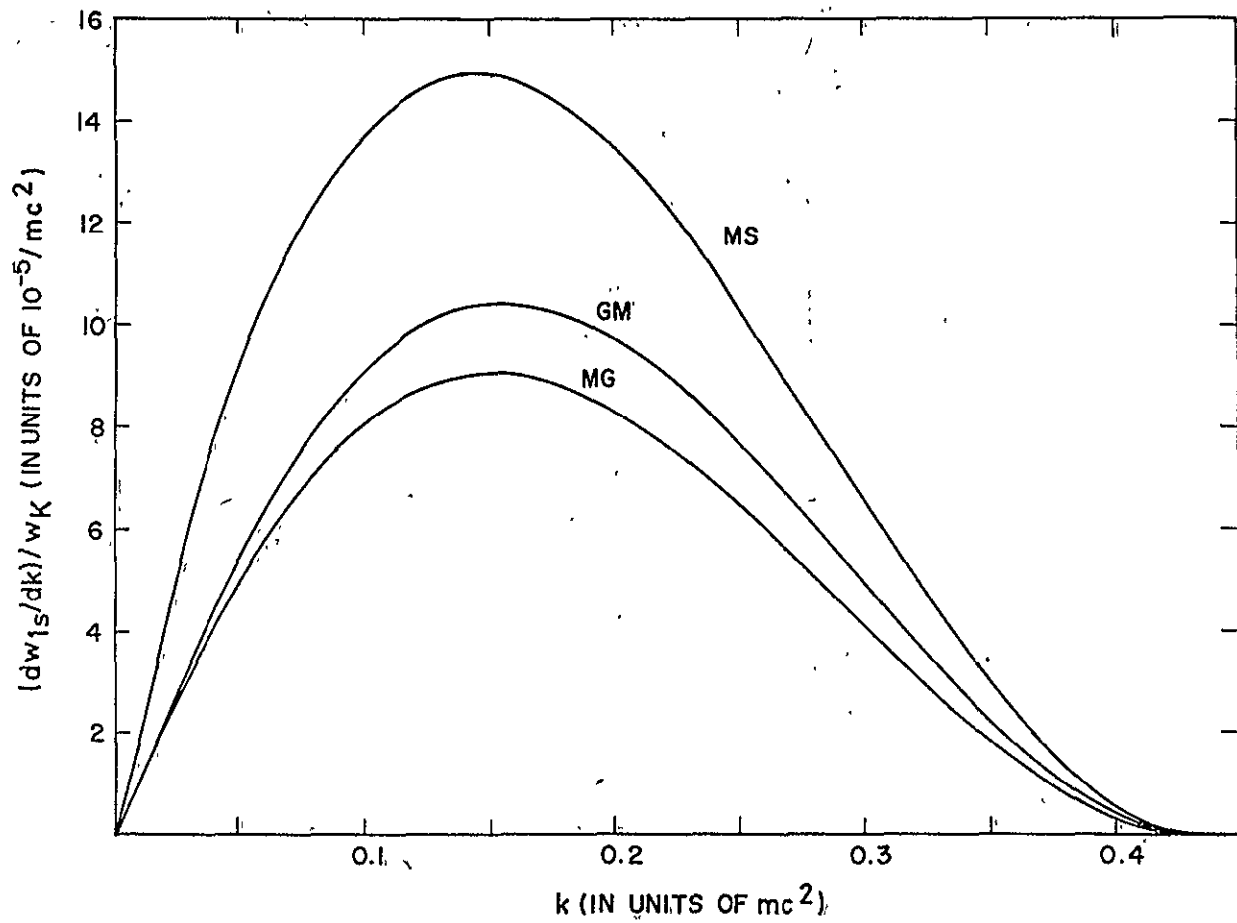


FIG. 4-5

$3 \cdot 10^4 W_E$

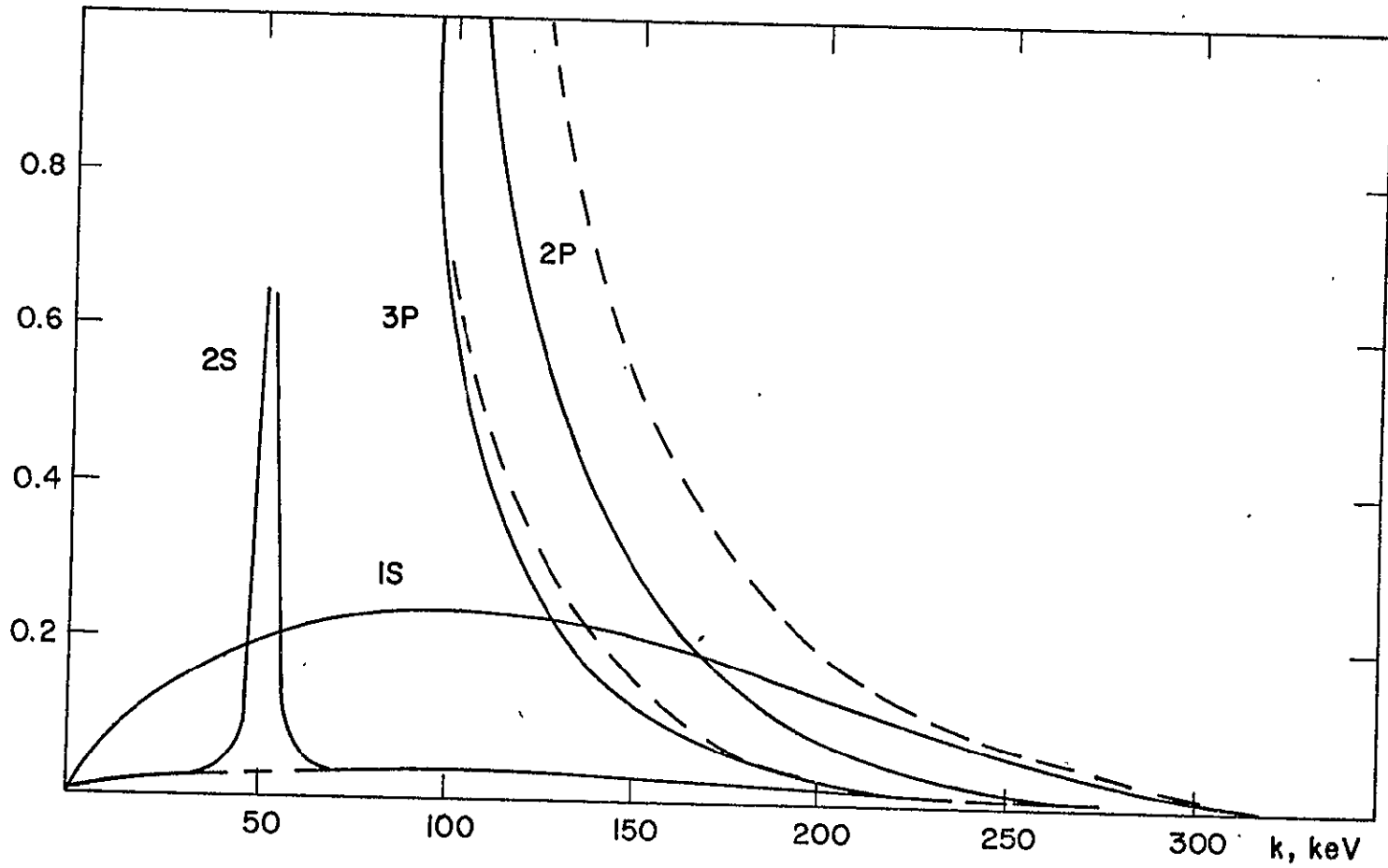
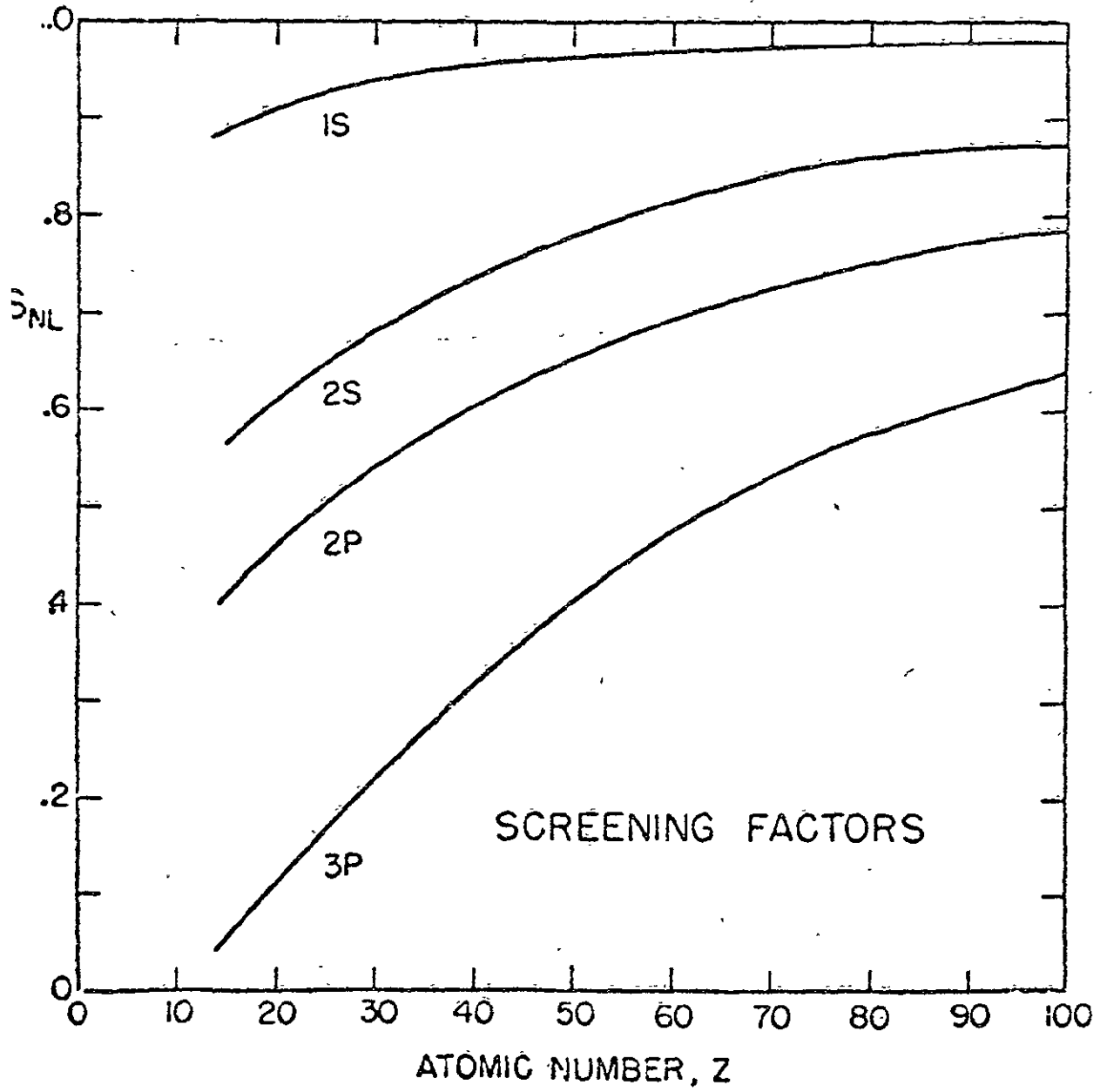


FIG. 4-6



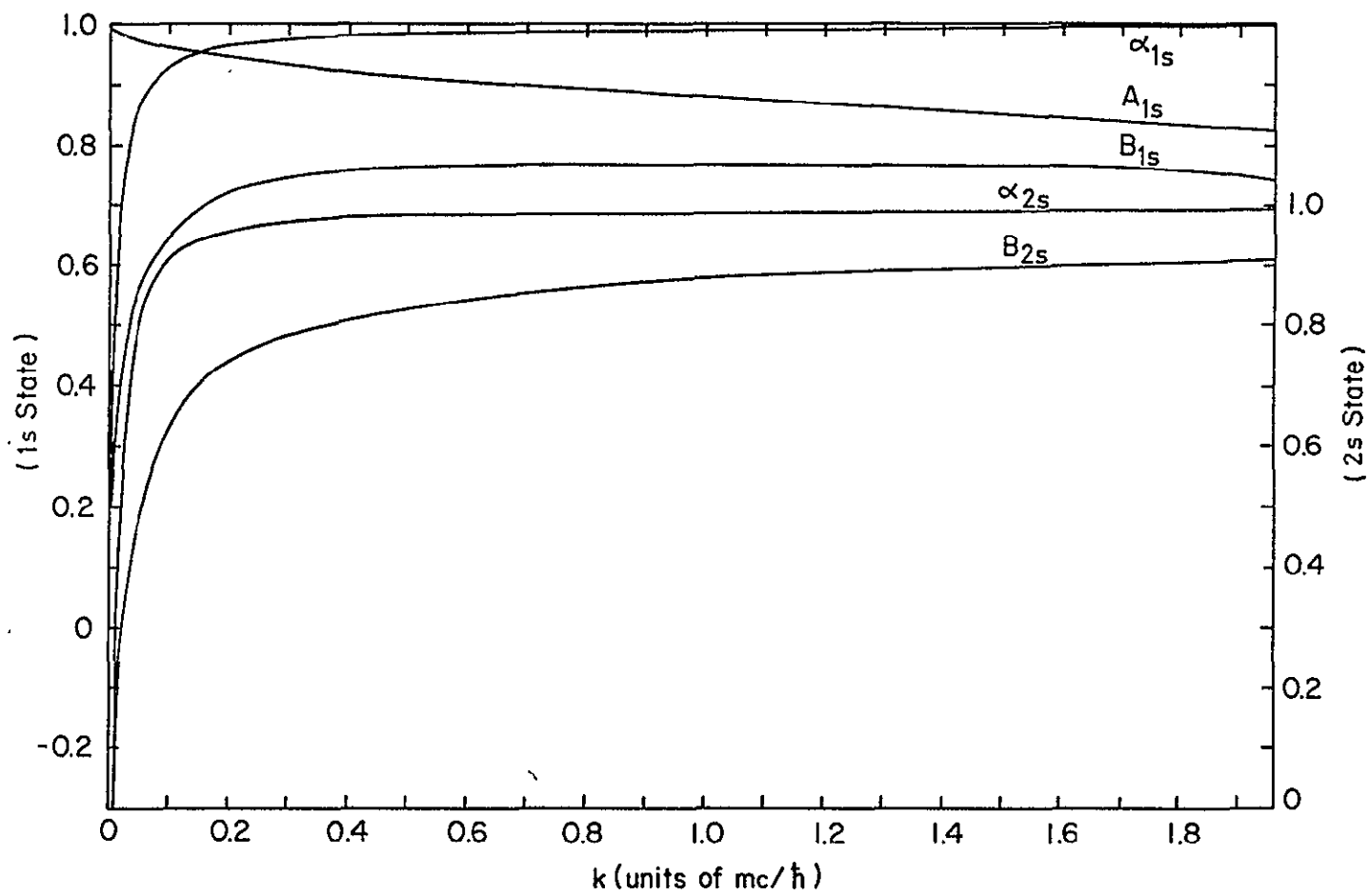


FIG. 4-8

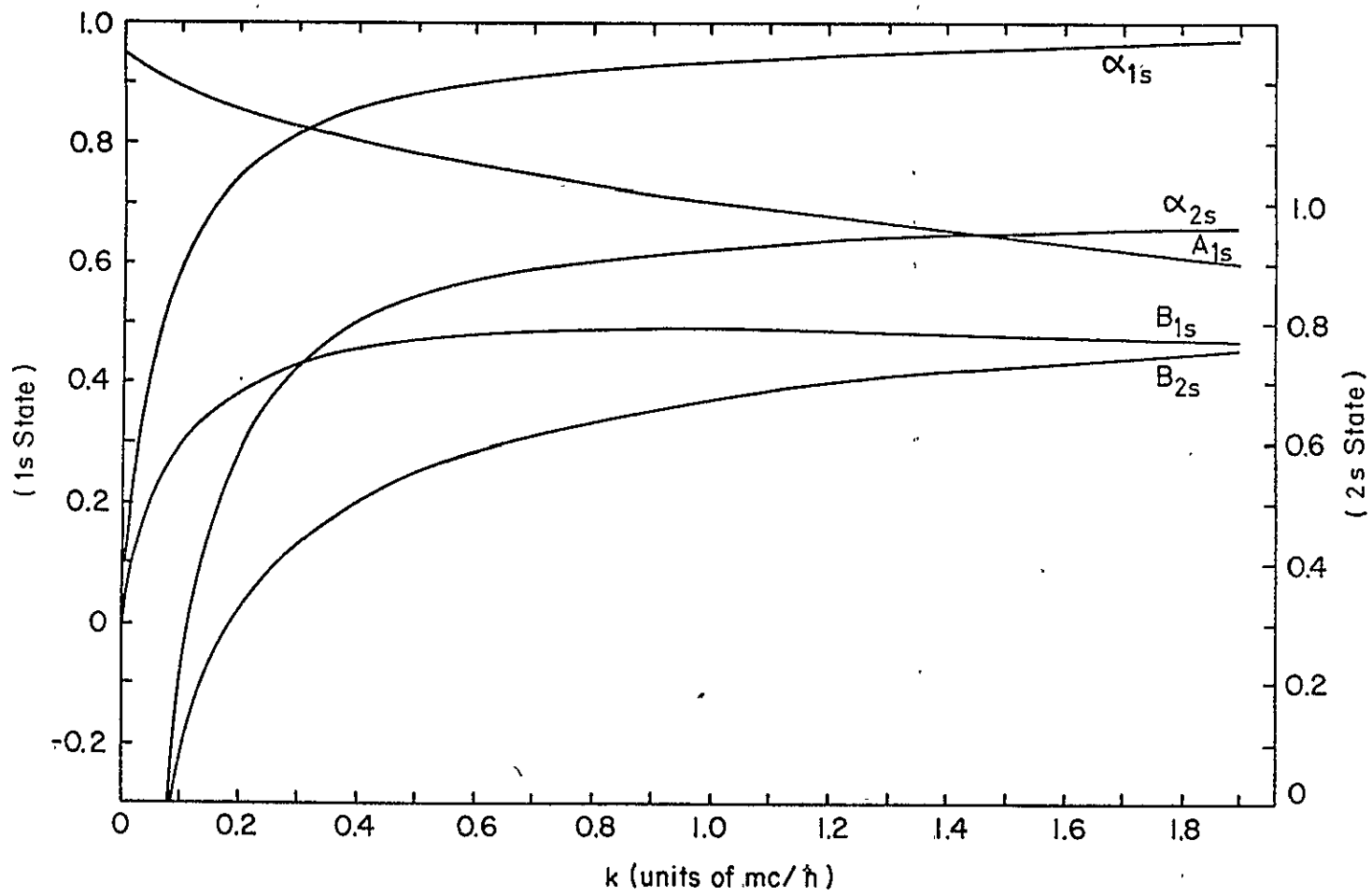


FIG. 4-9

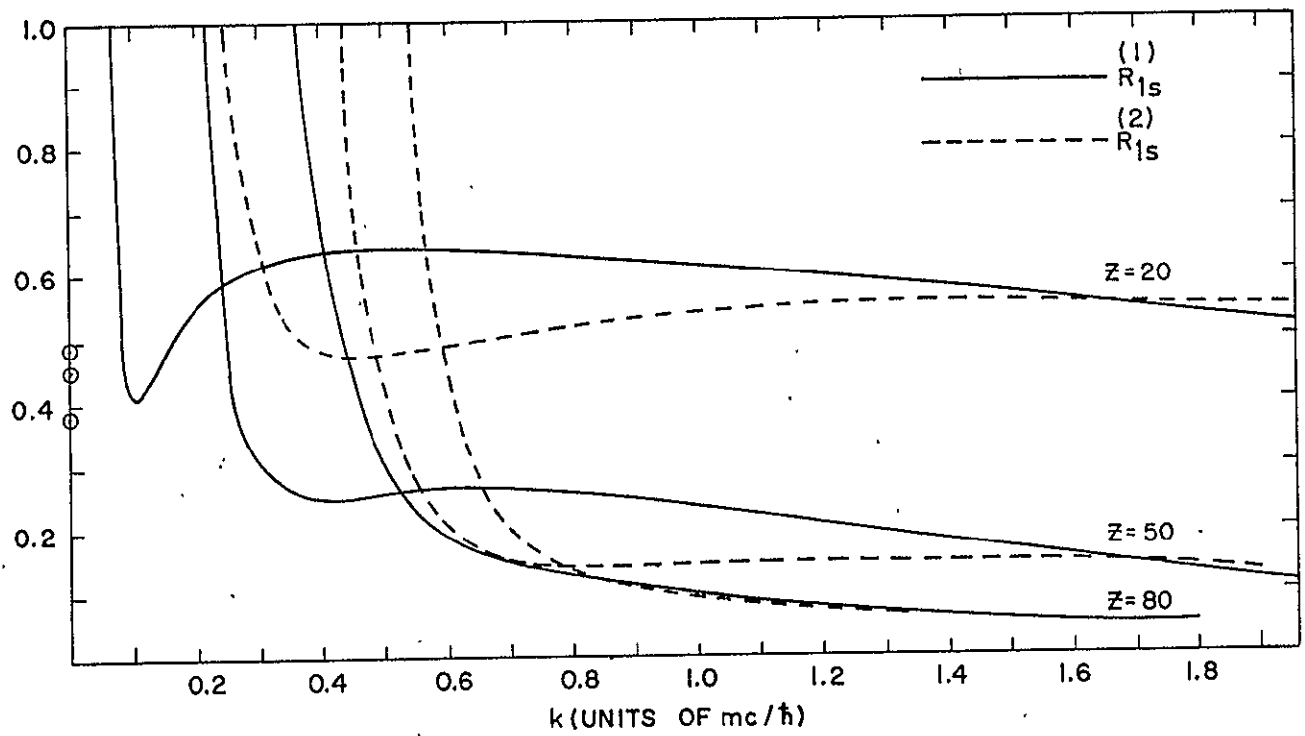


FIG. 4-10

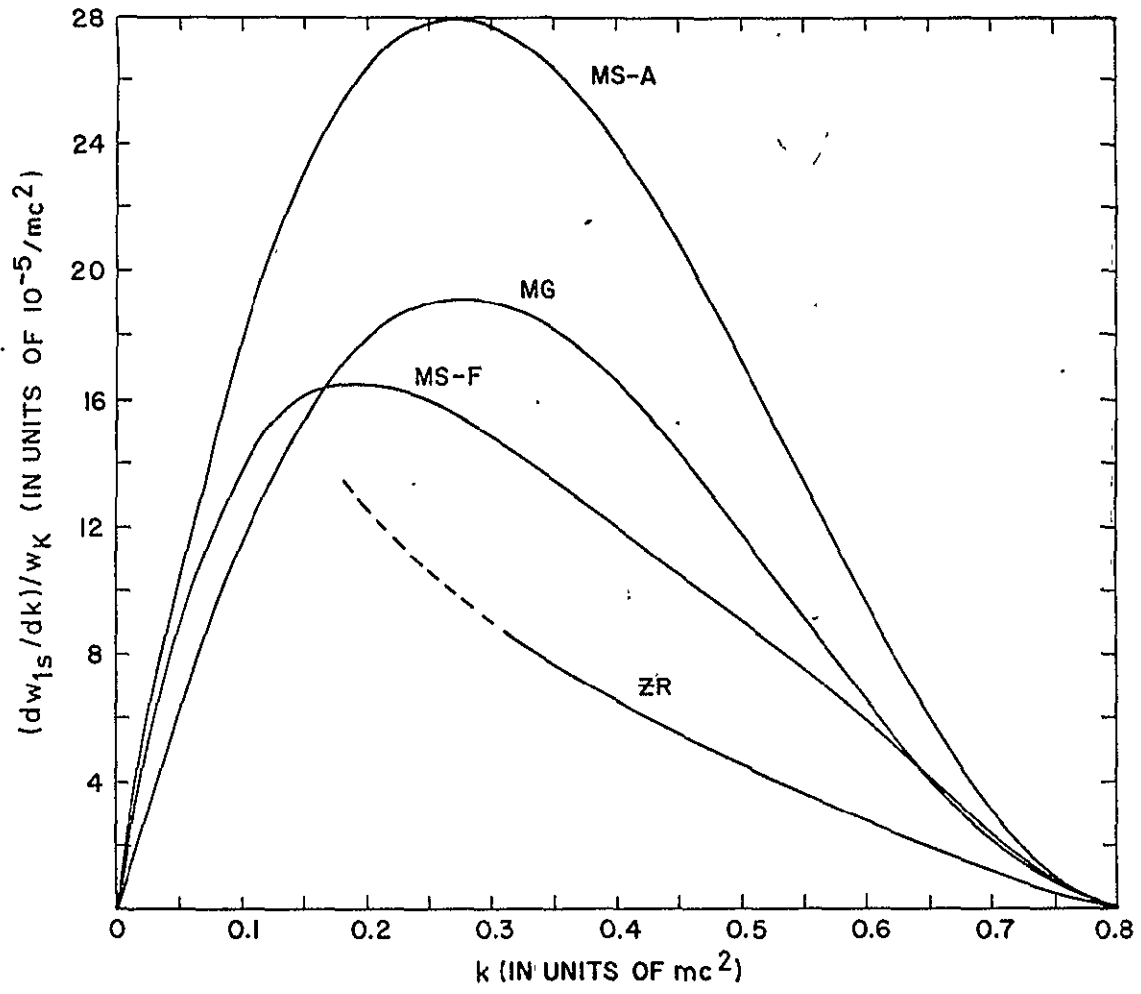


FIG. 4-11

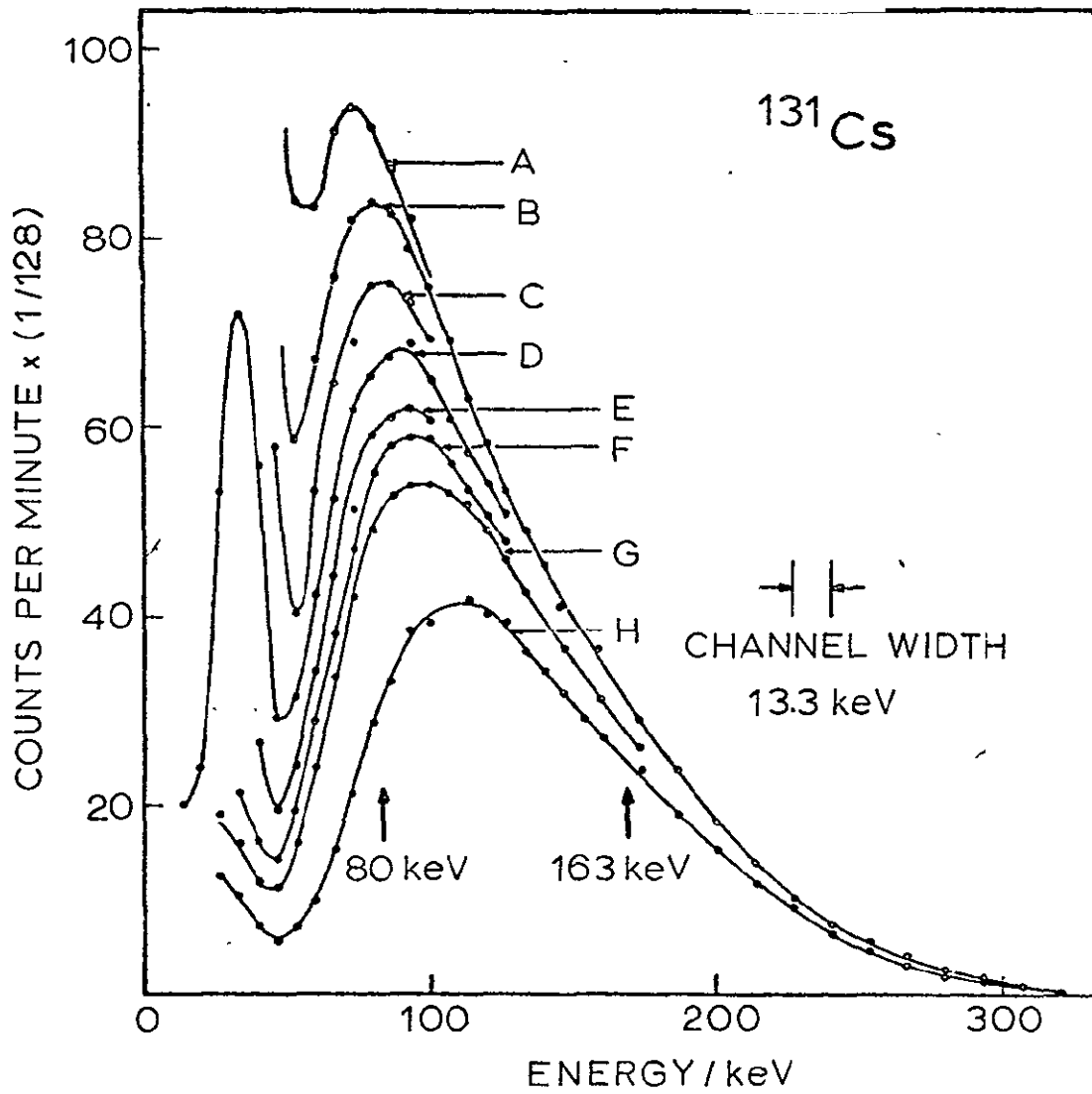


FIG. 4-12

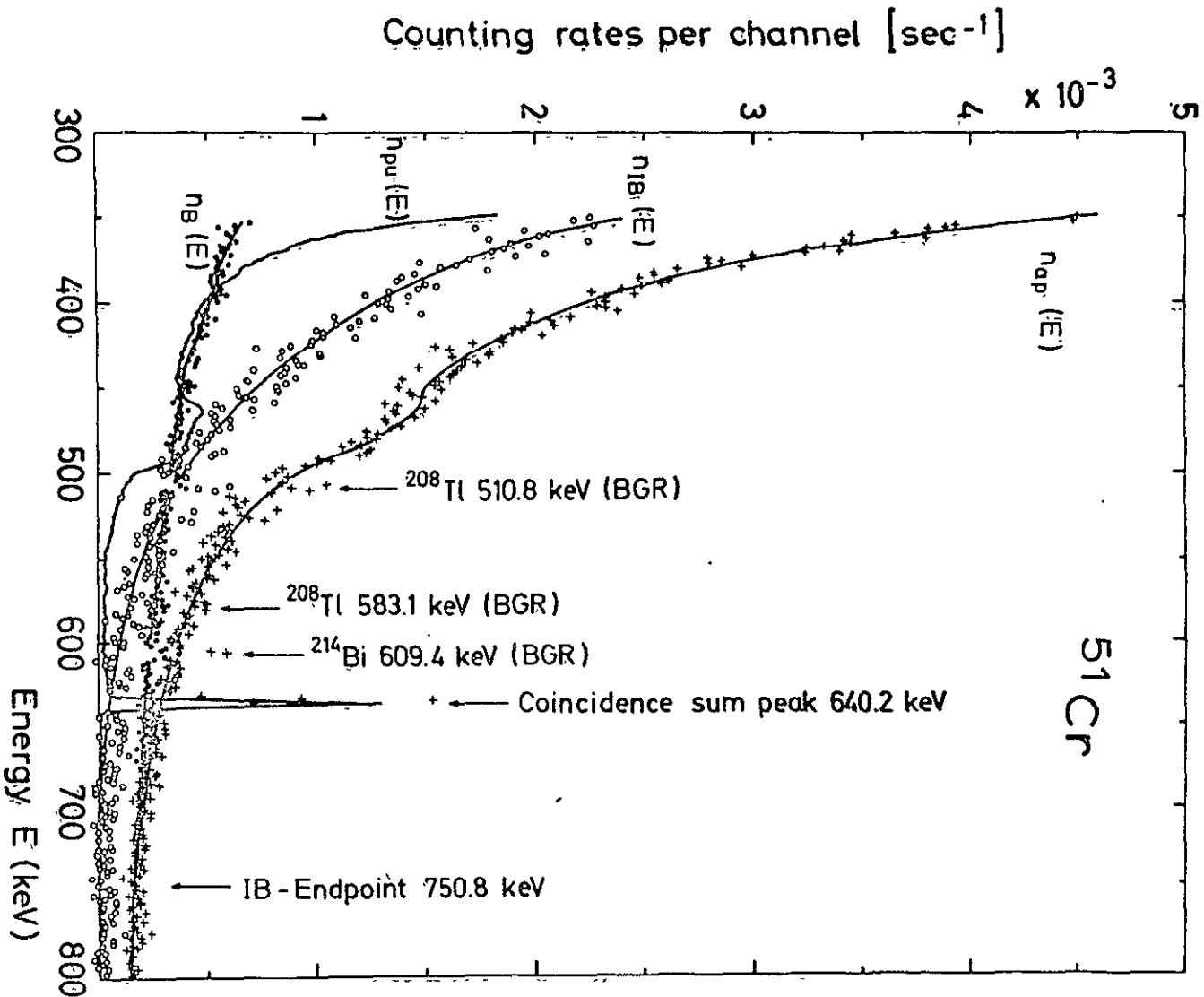


FIG. 4-13

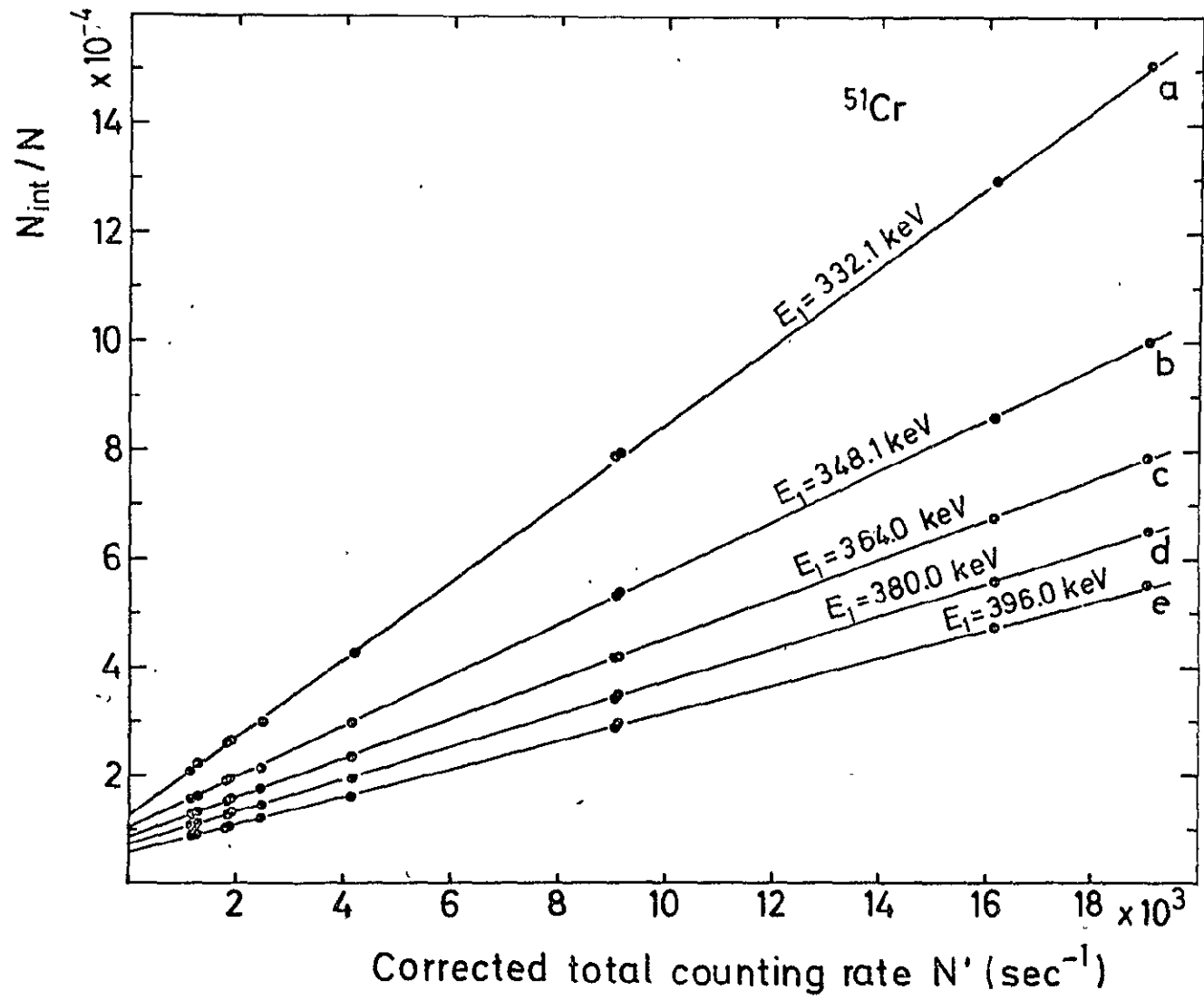


FIG. 4-14

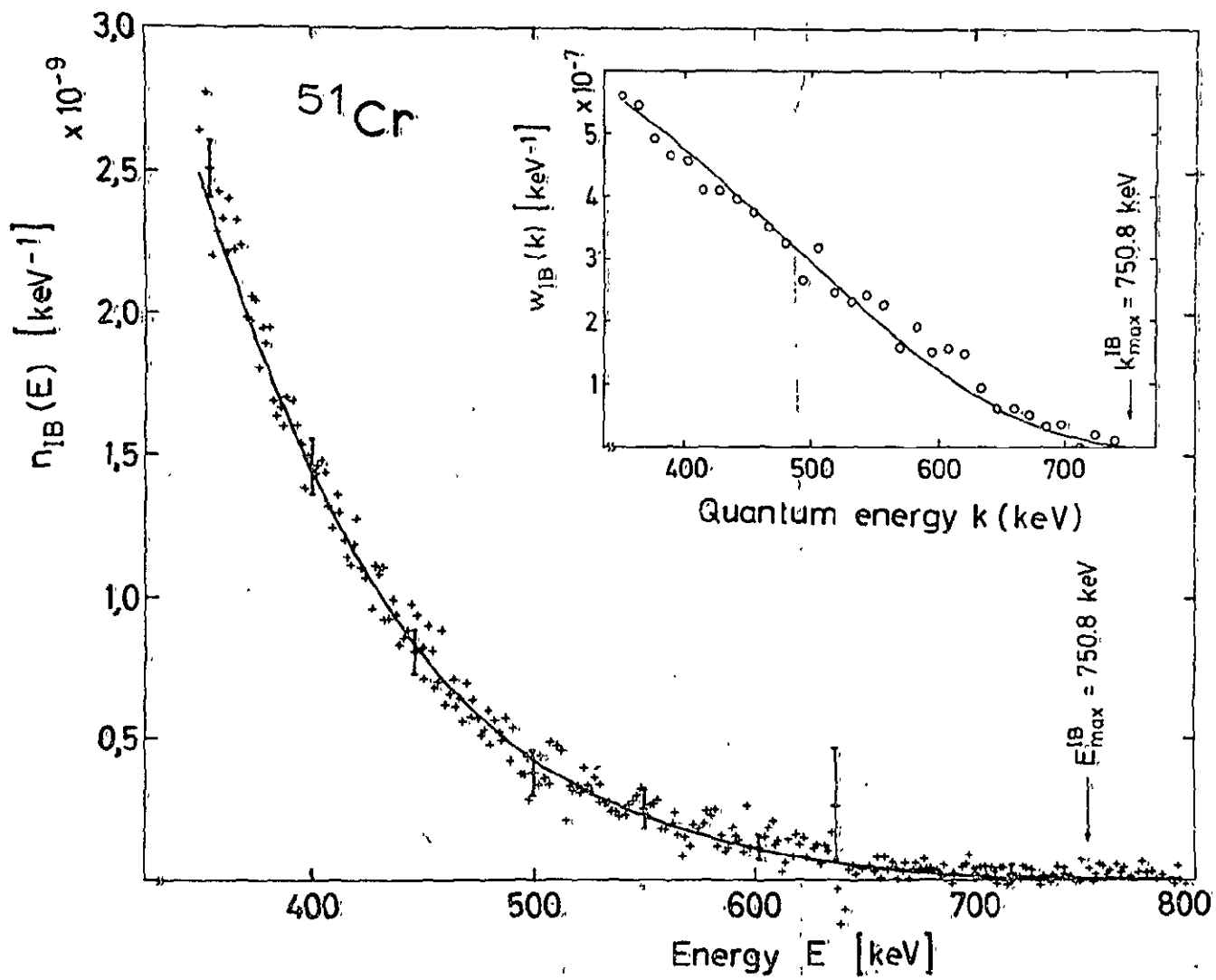


FIG. 4-15

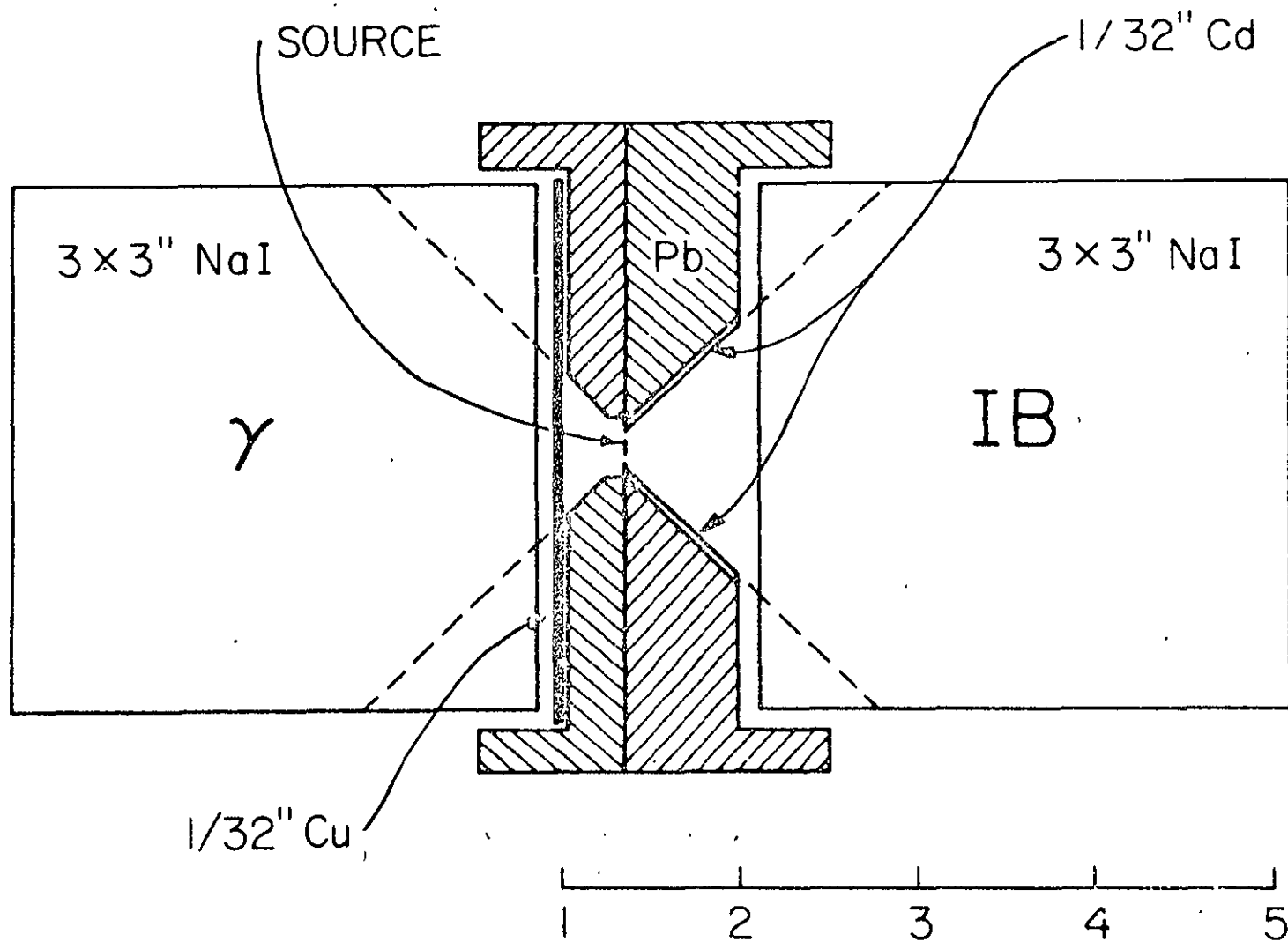


FIG. 4-16

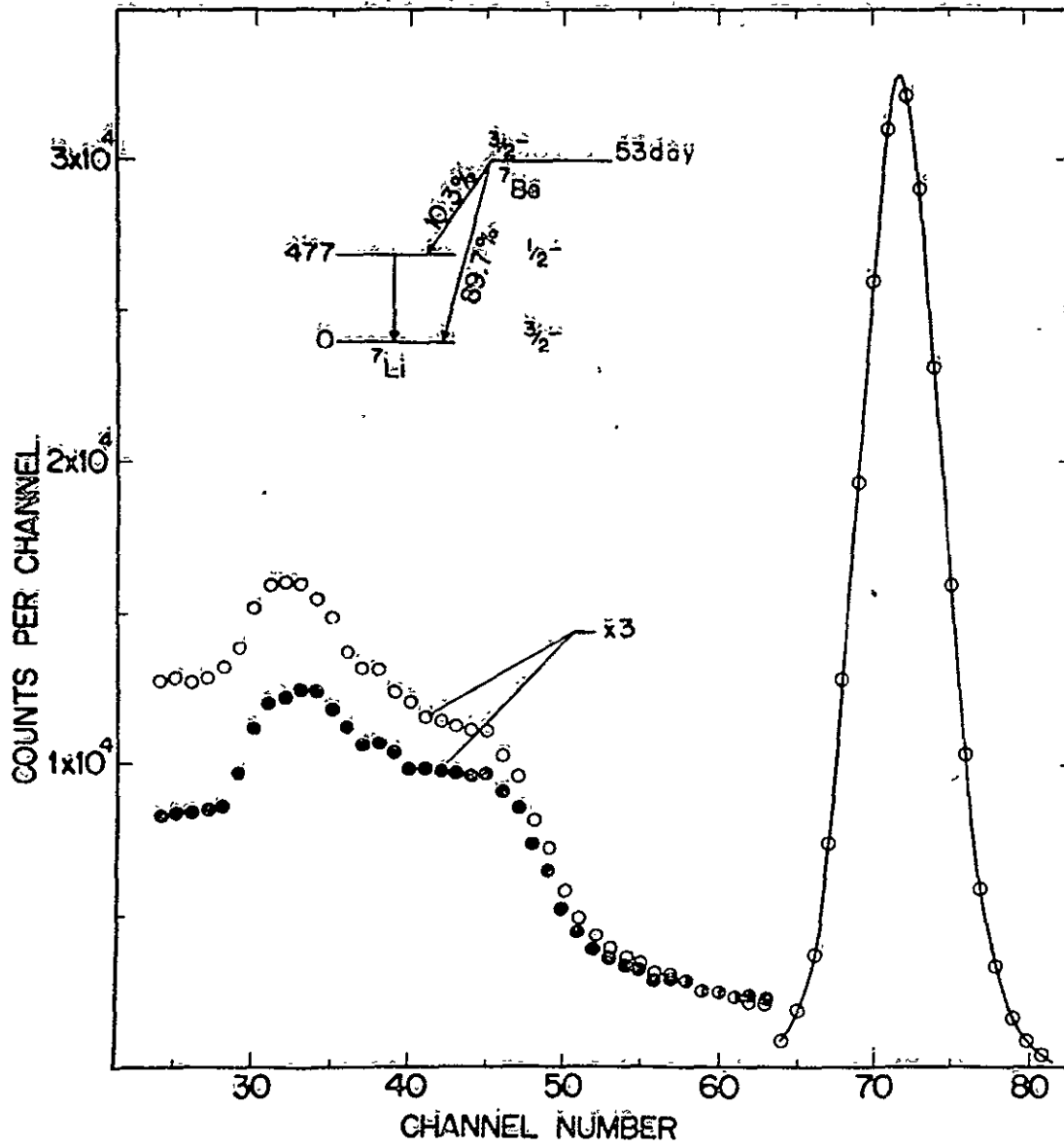


FIG. 4-17

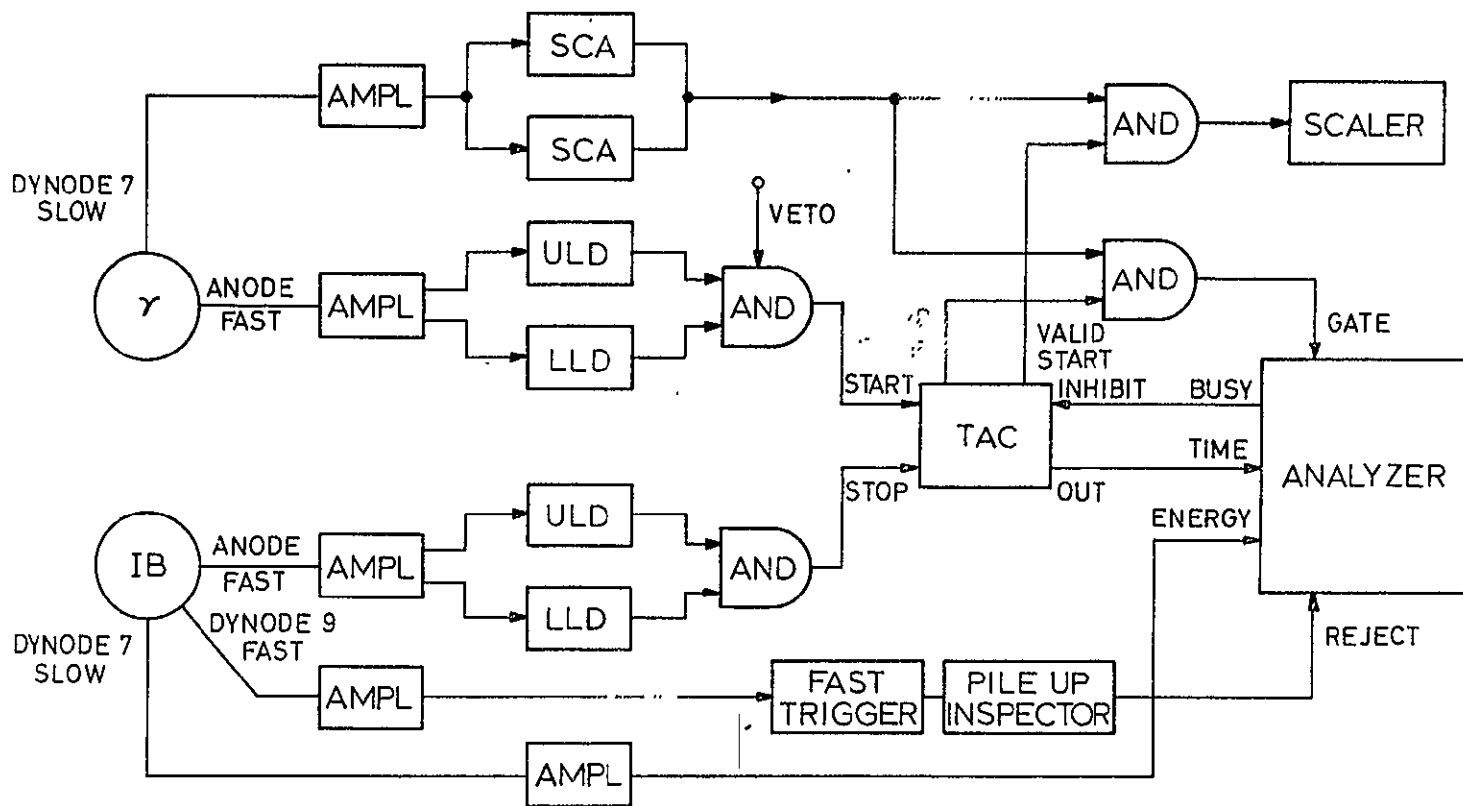


FIG. 4-18

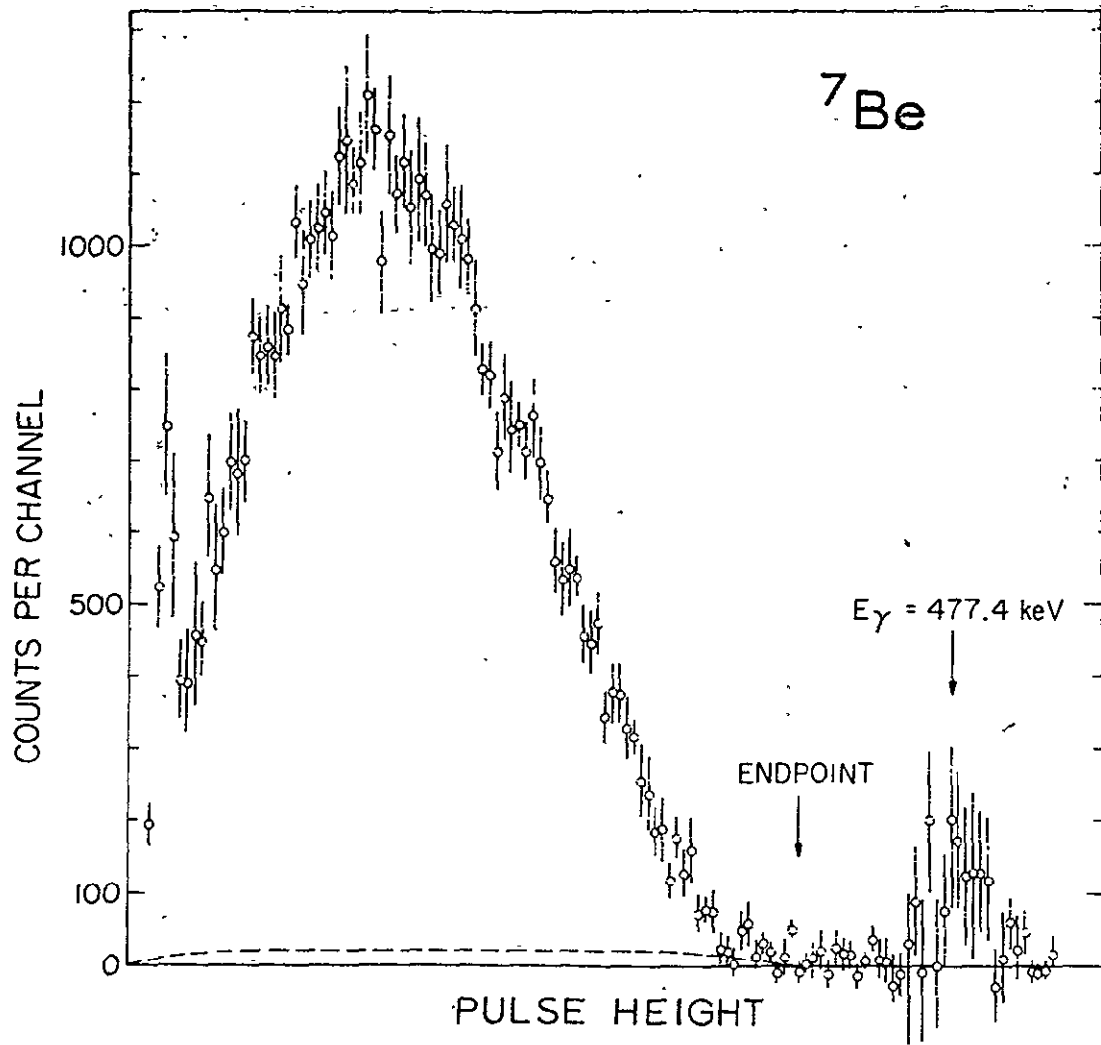


FIG. 4-19

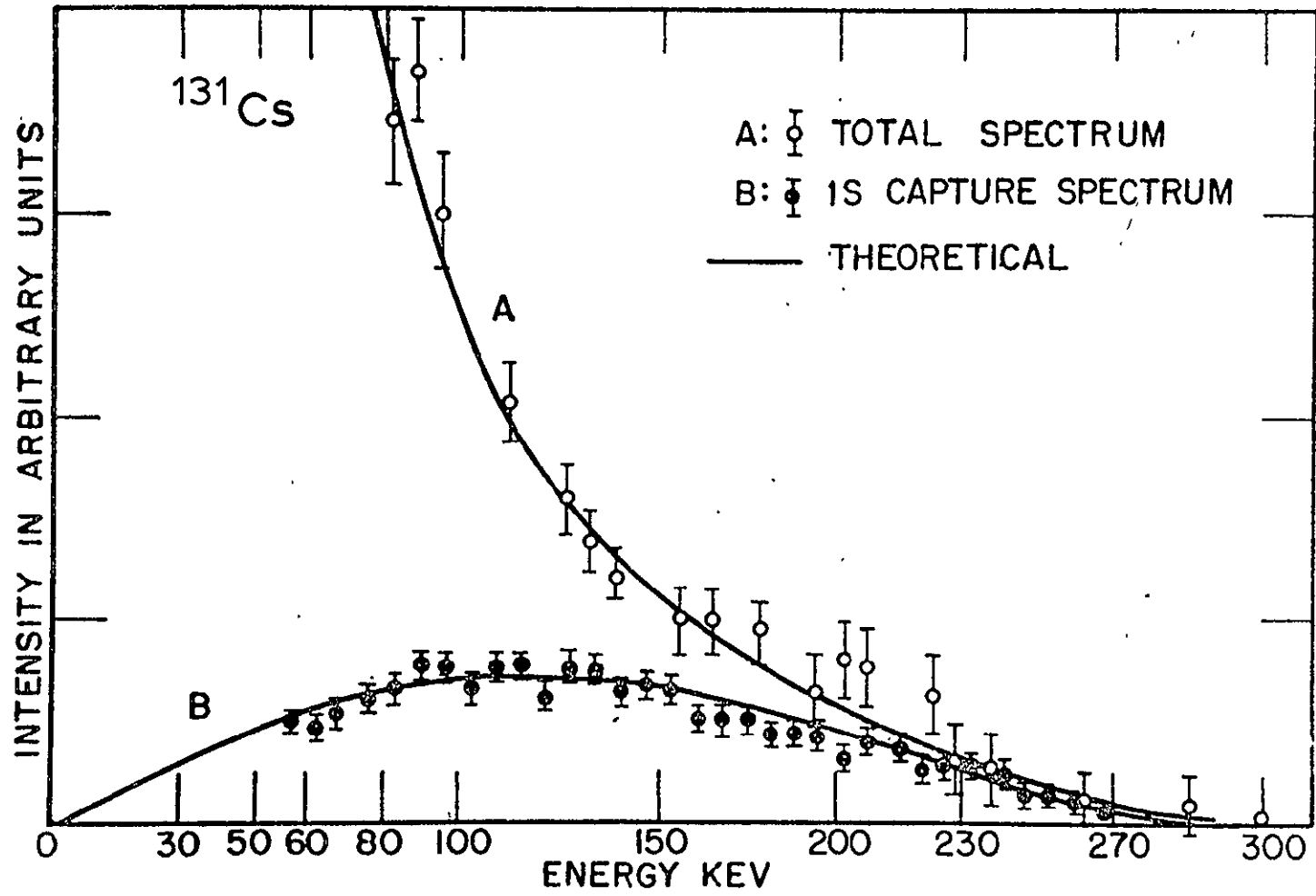


FIG. 4-20

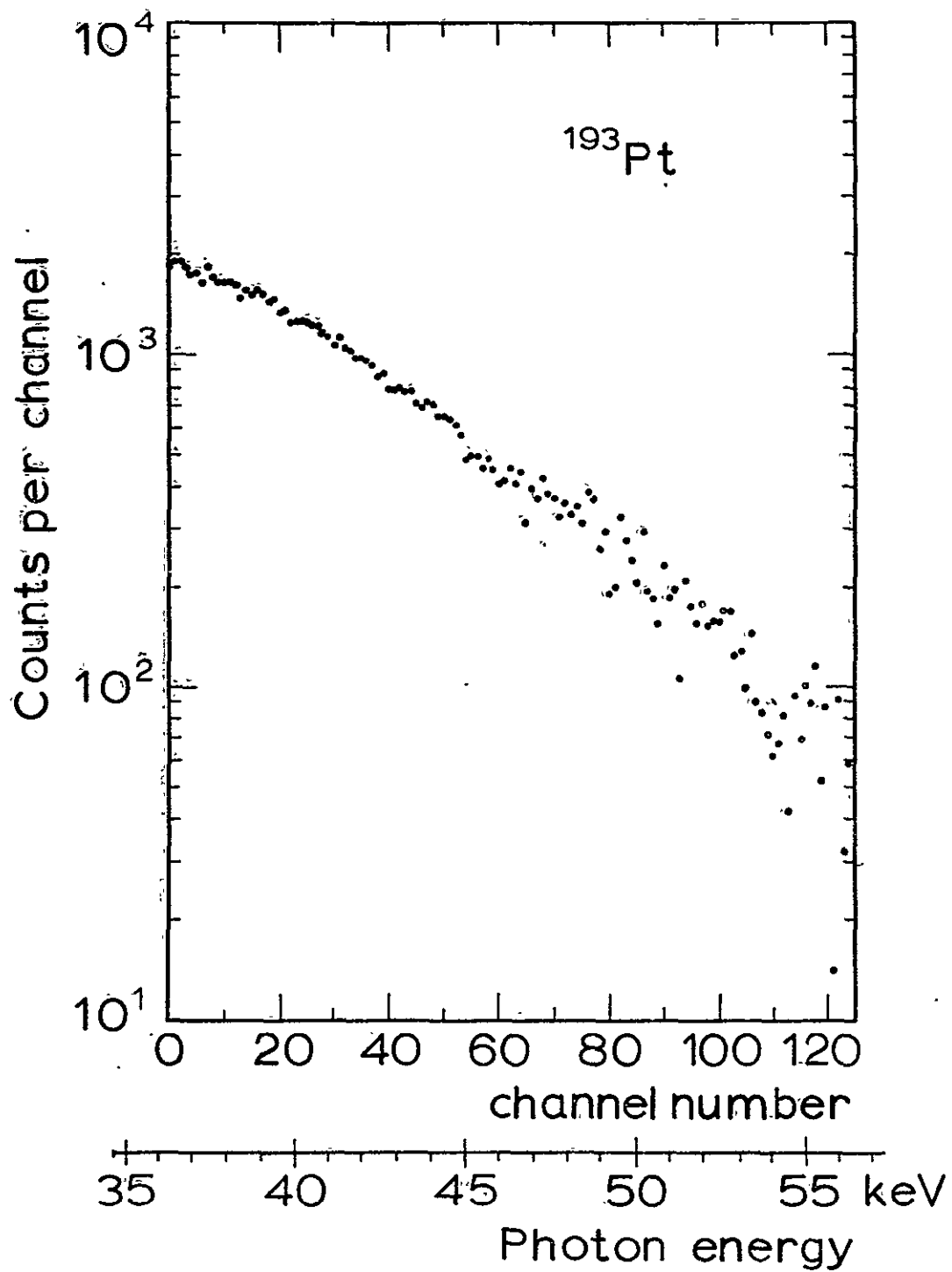


FIG. 4-21

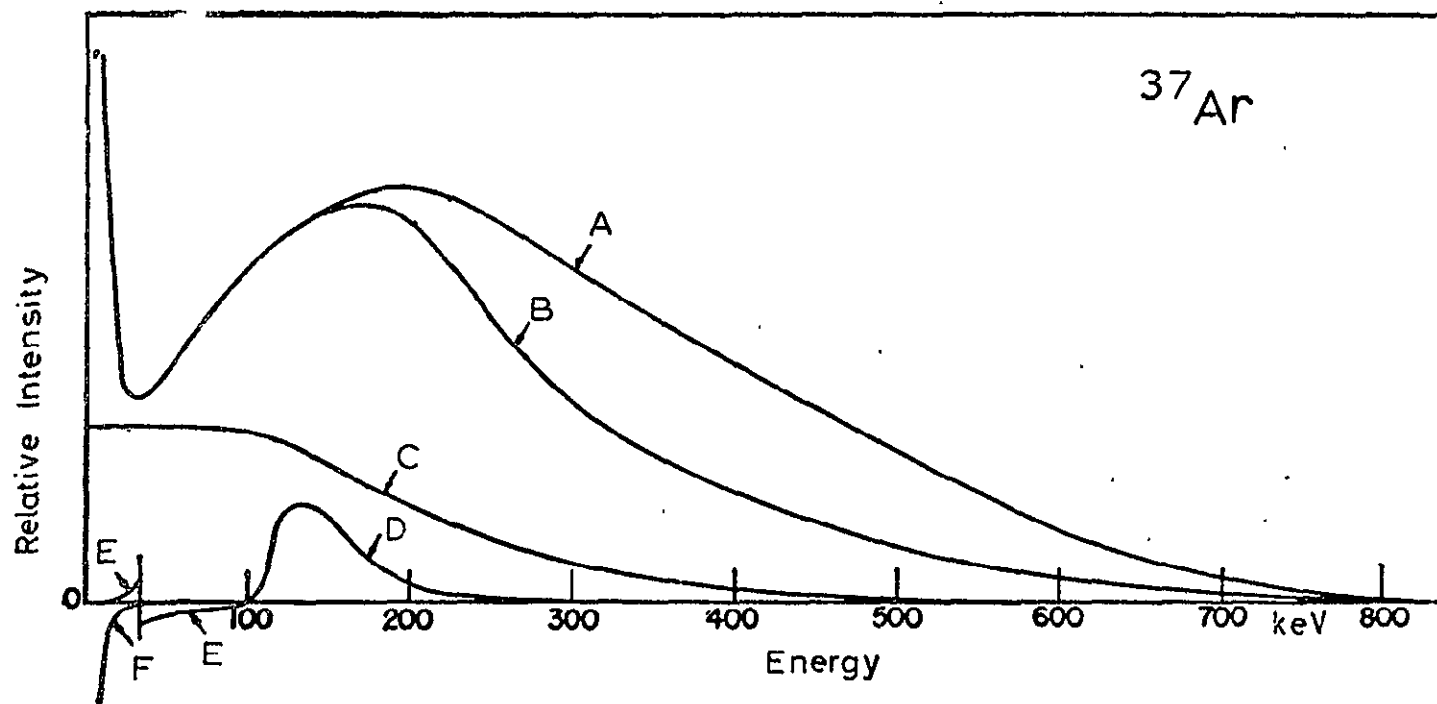


FIG. 4-22

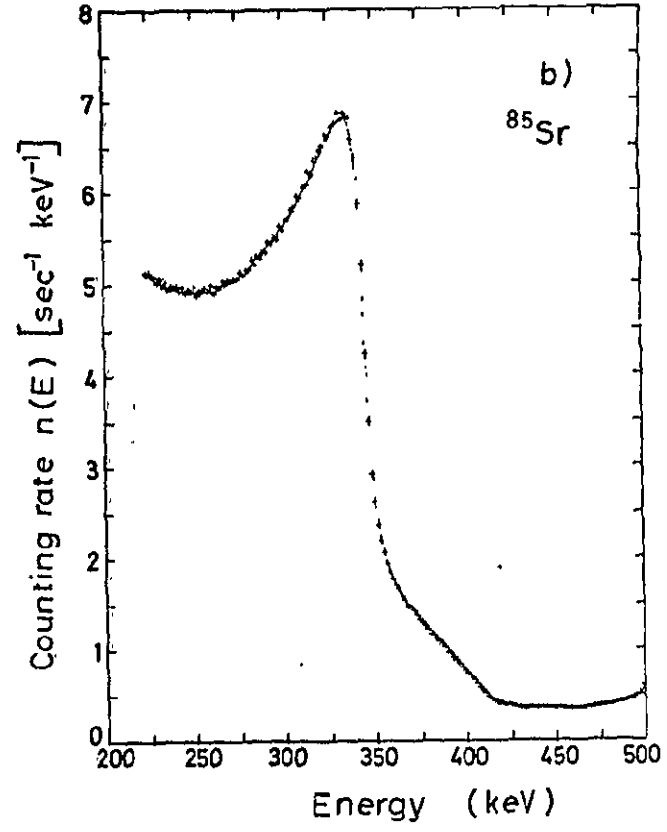
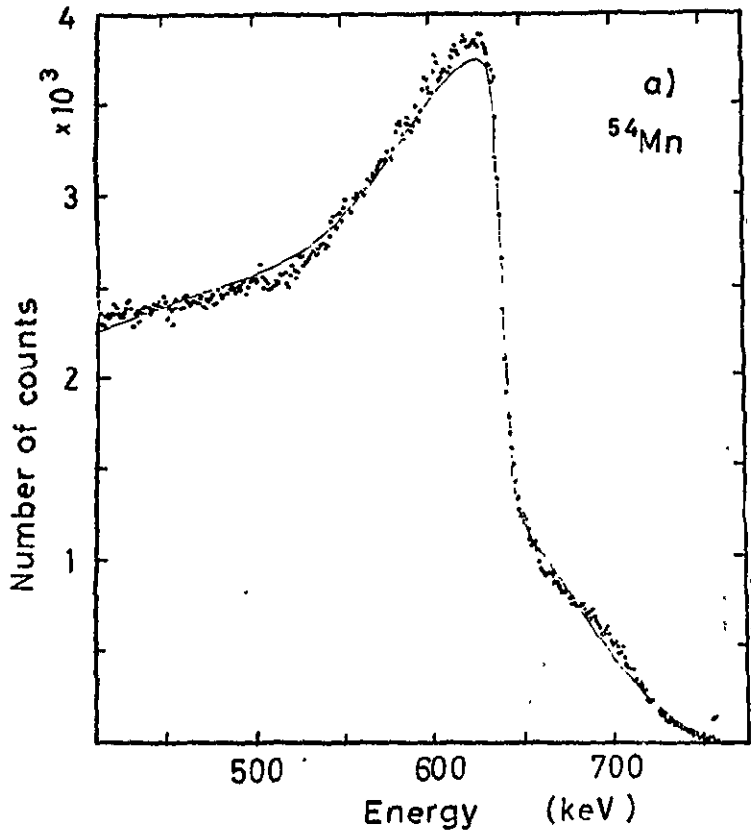


FIG. 4-23

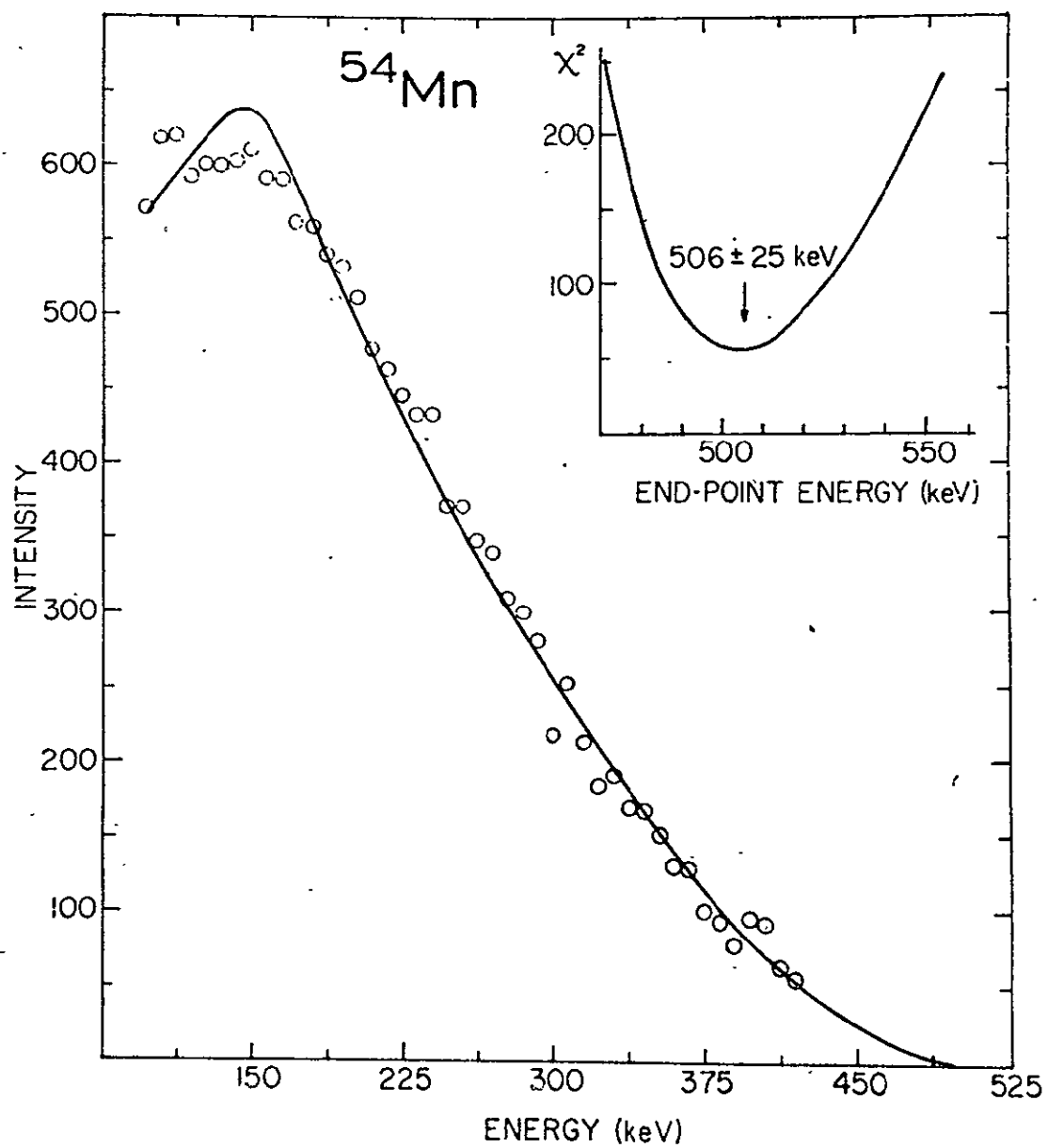


FIG. 4-24

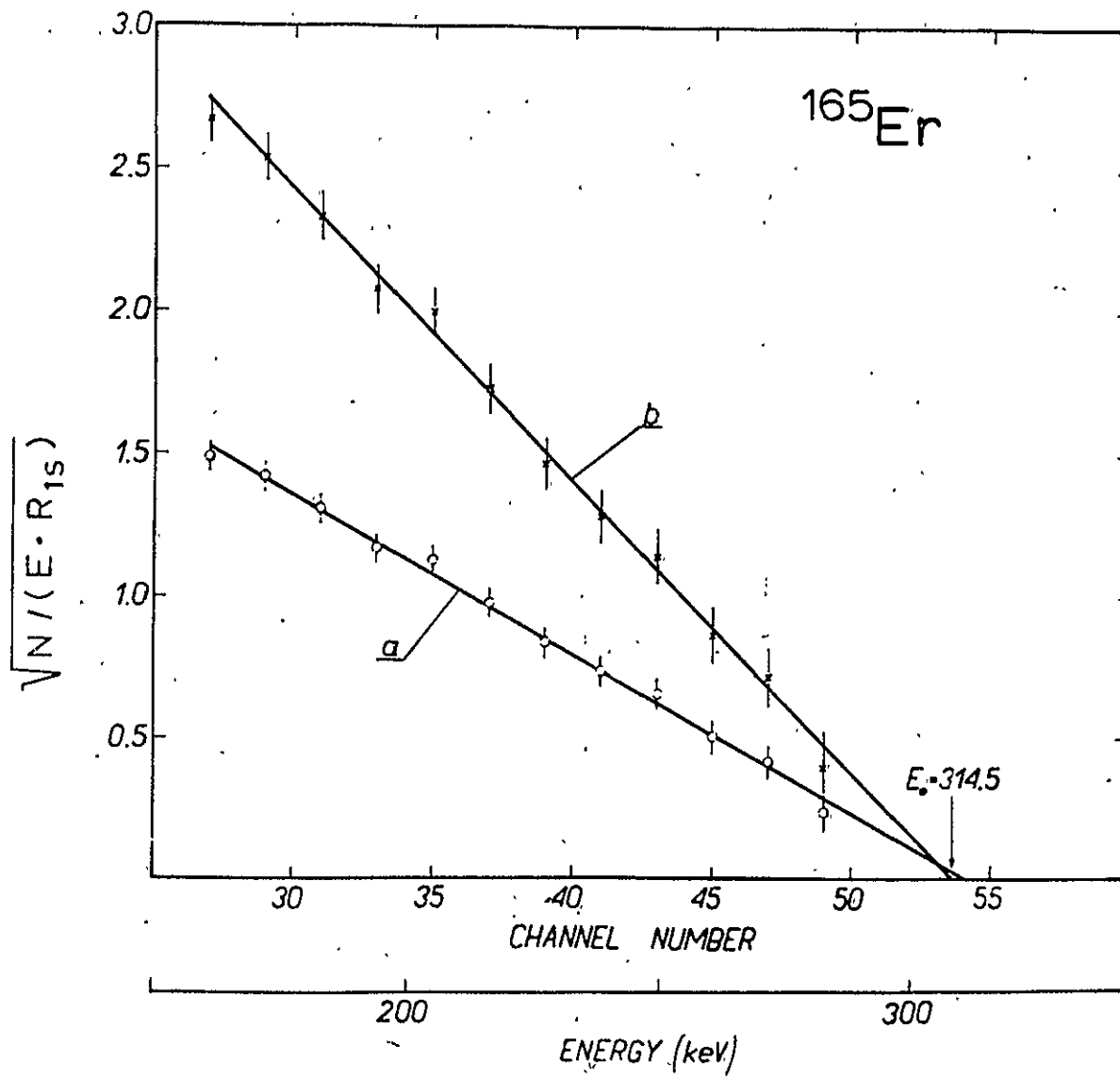


FIG. 4-25

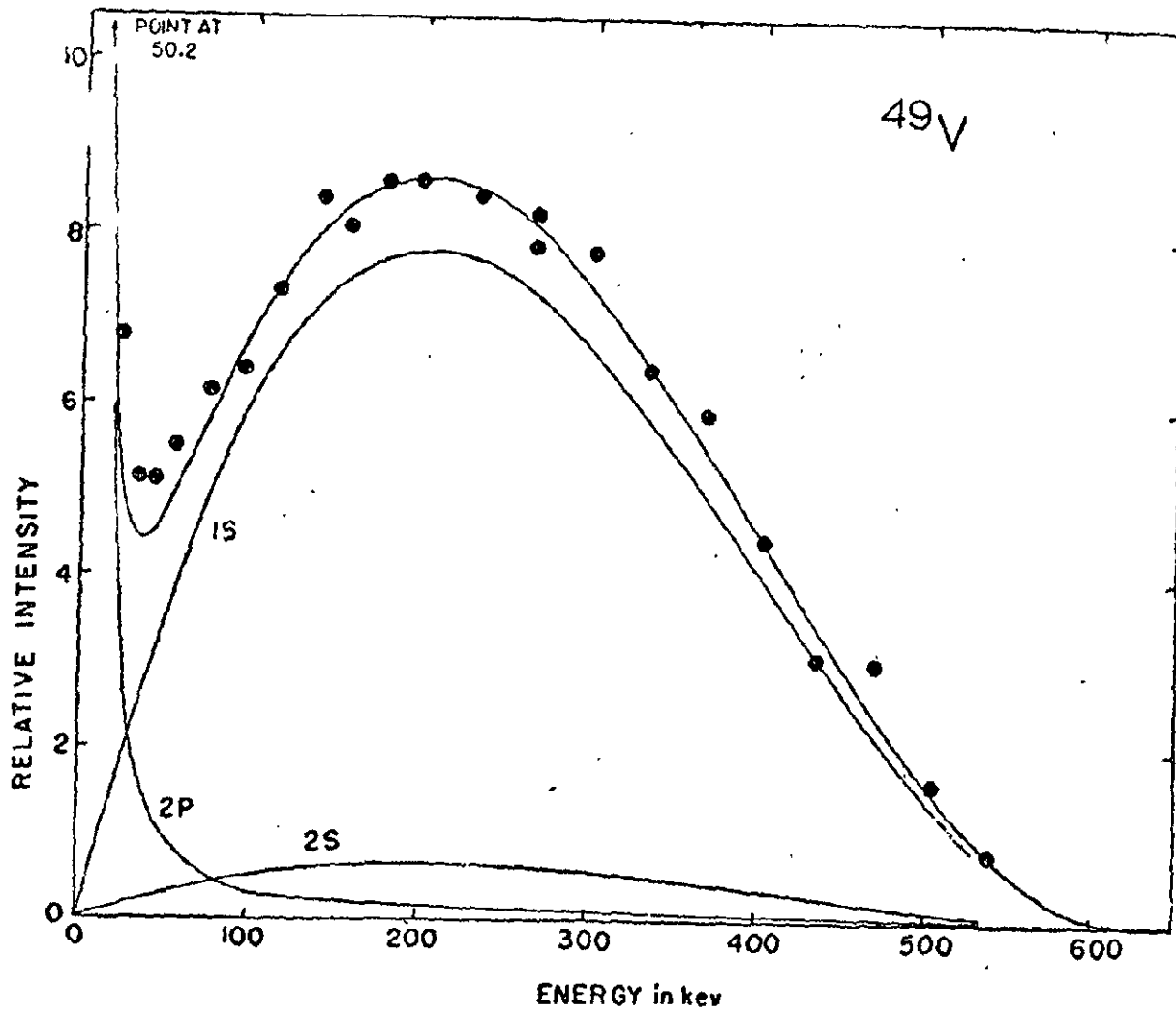


FIG. 4-26

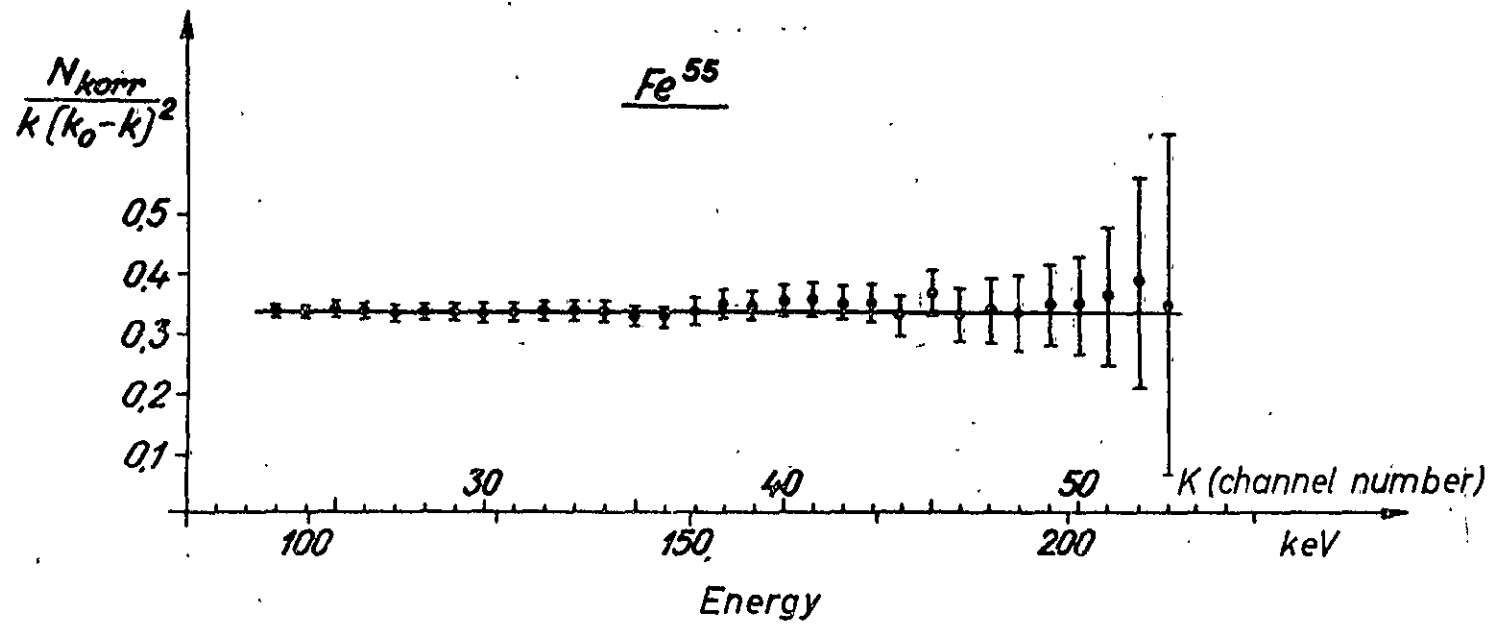


FIG. 4-27

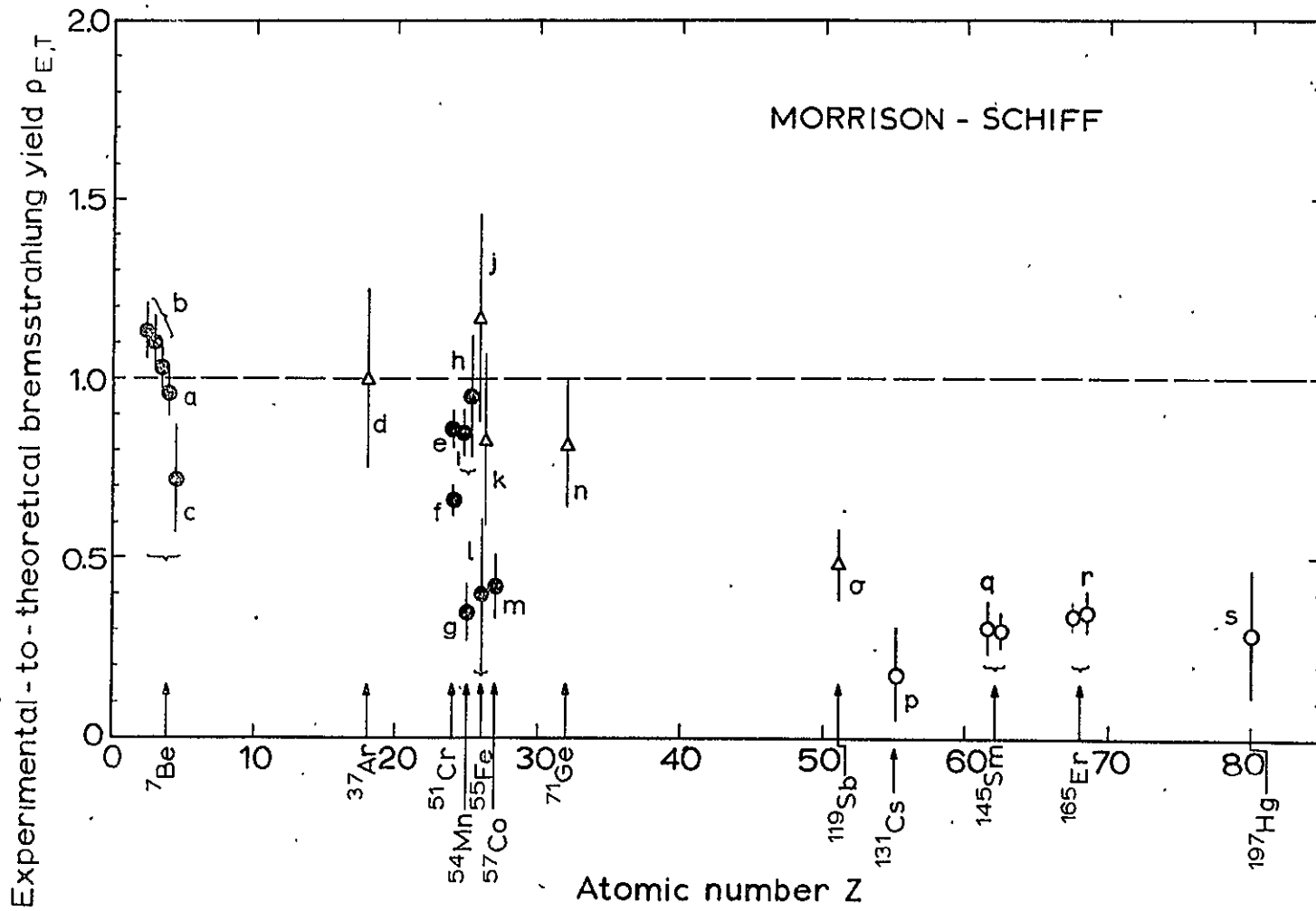


FIG. 4-28

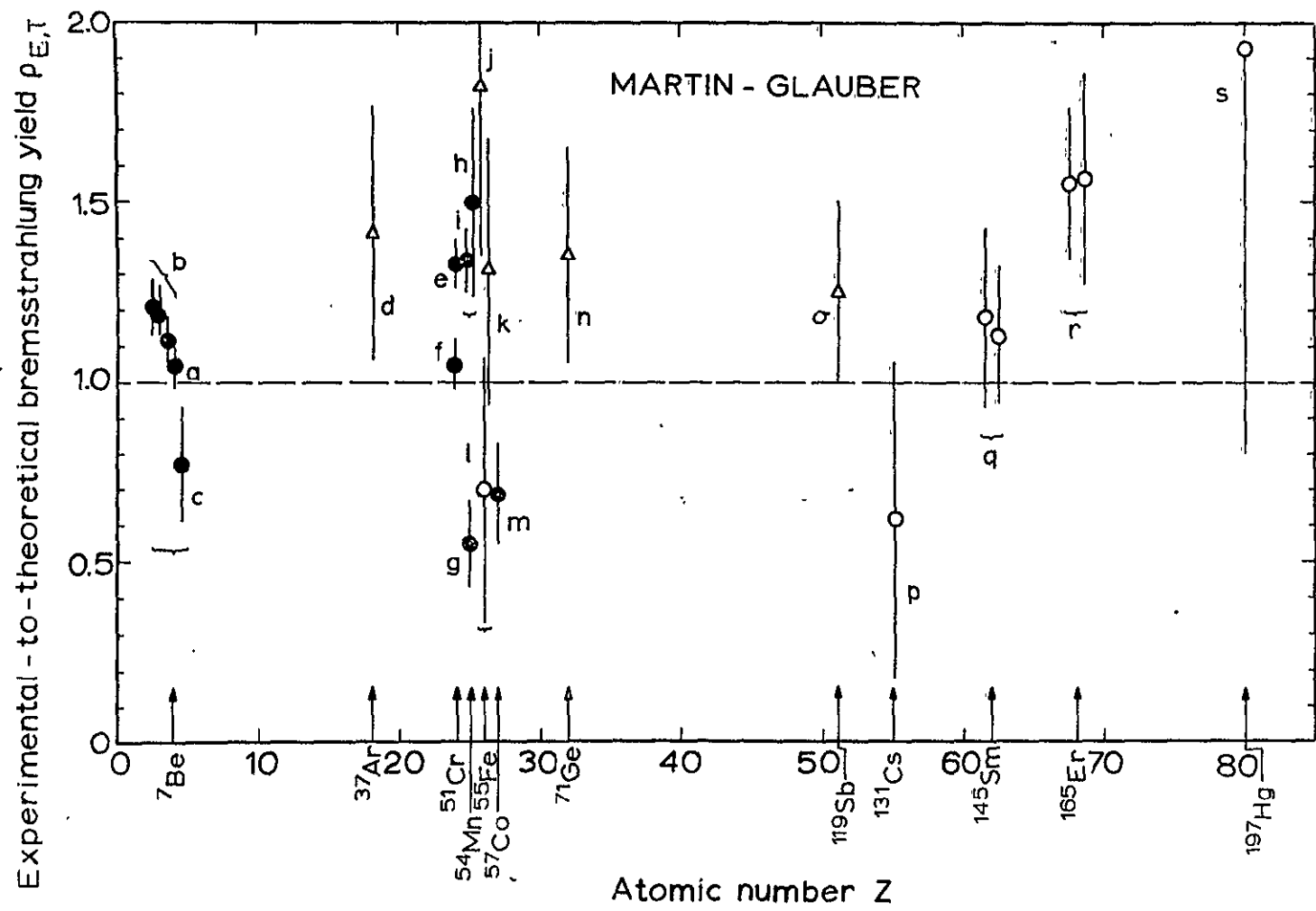


FIG. 4-29

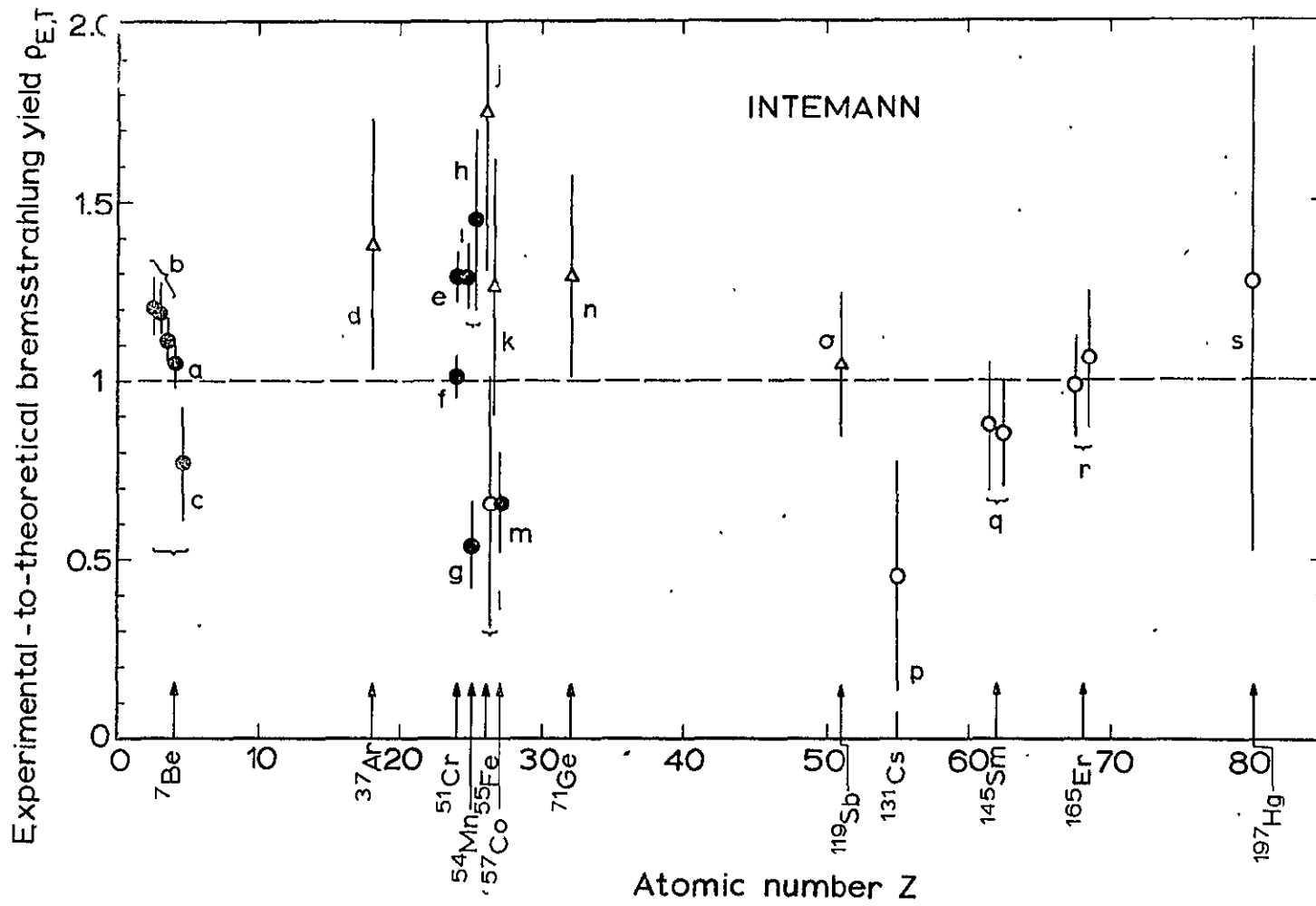


FIG. 4-30

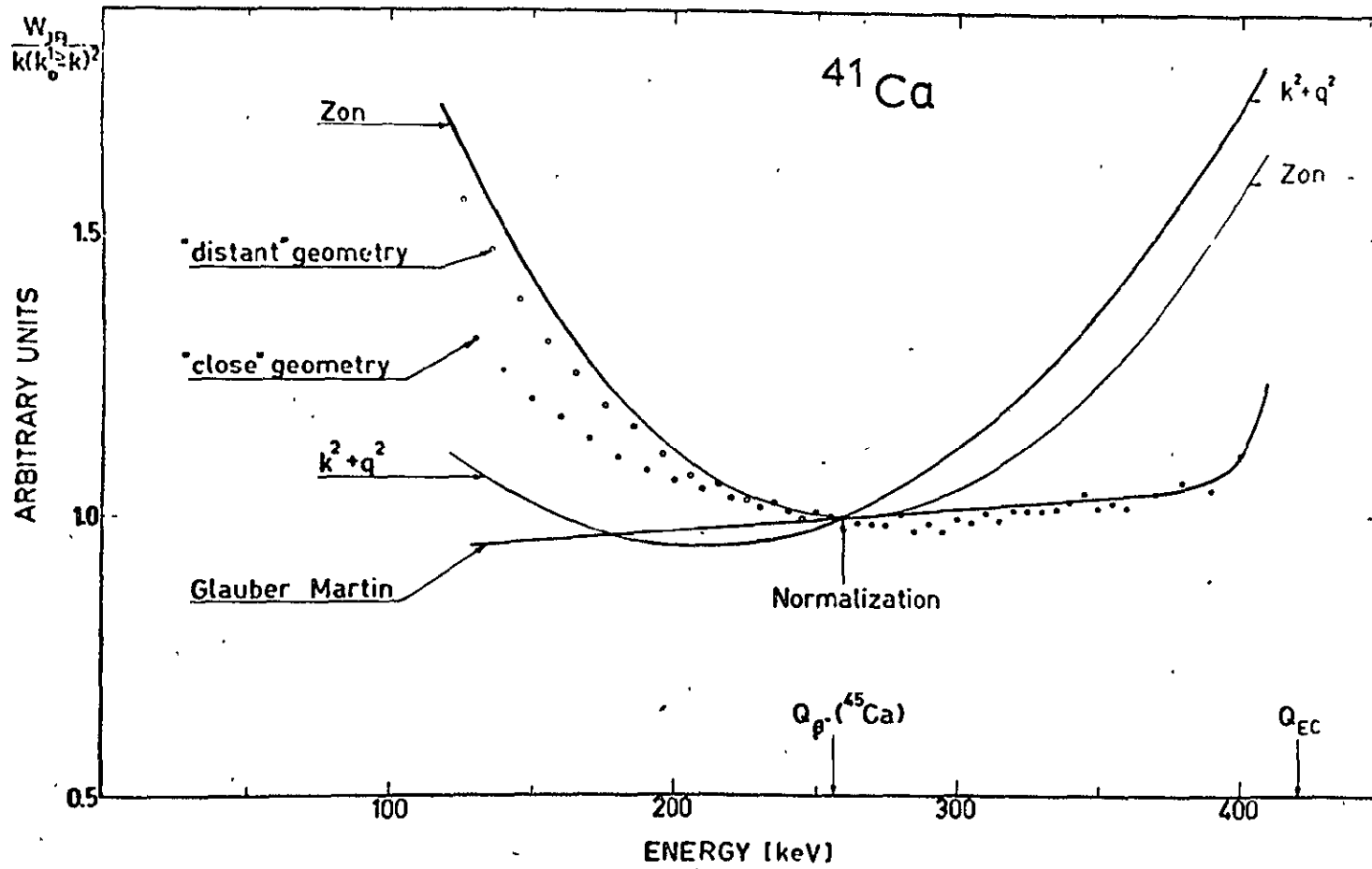


FIG. 4-31

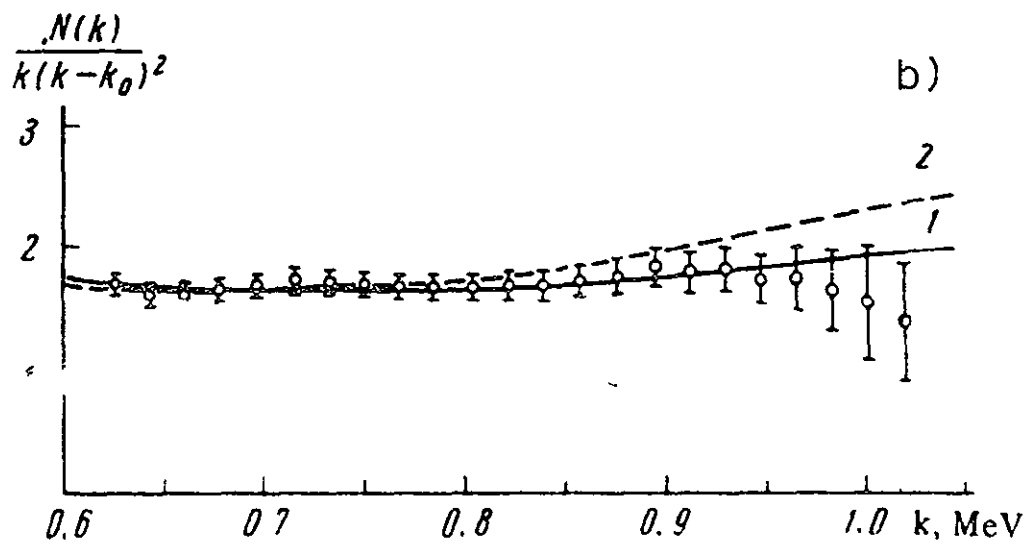
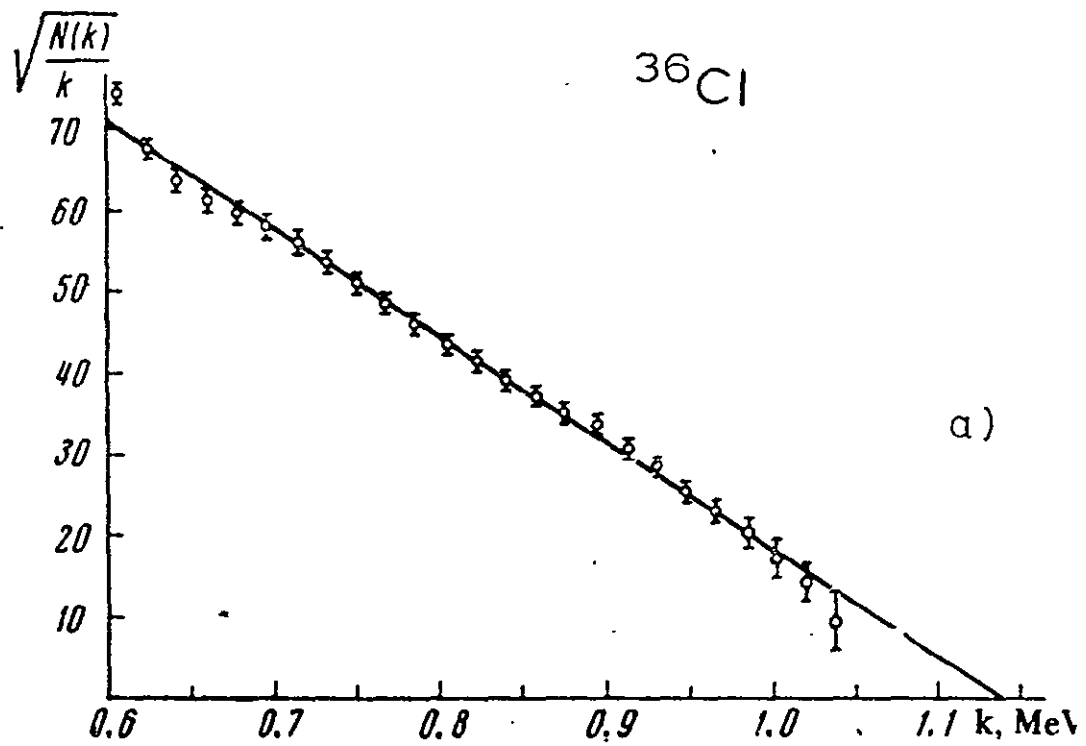
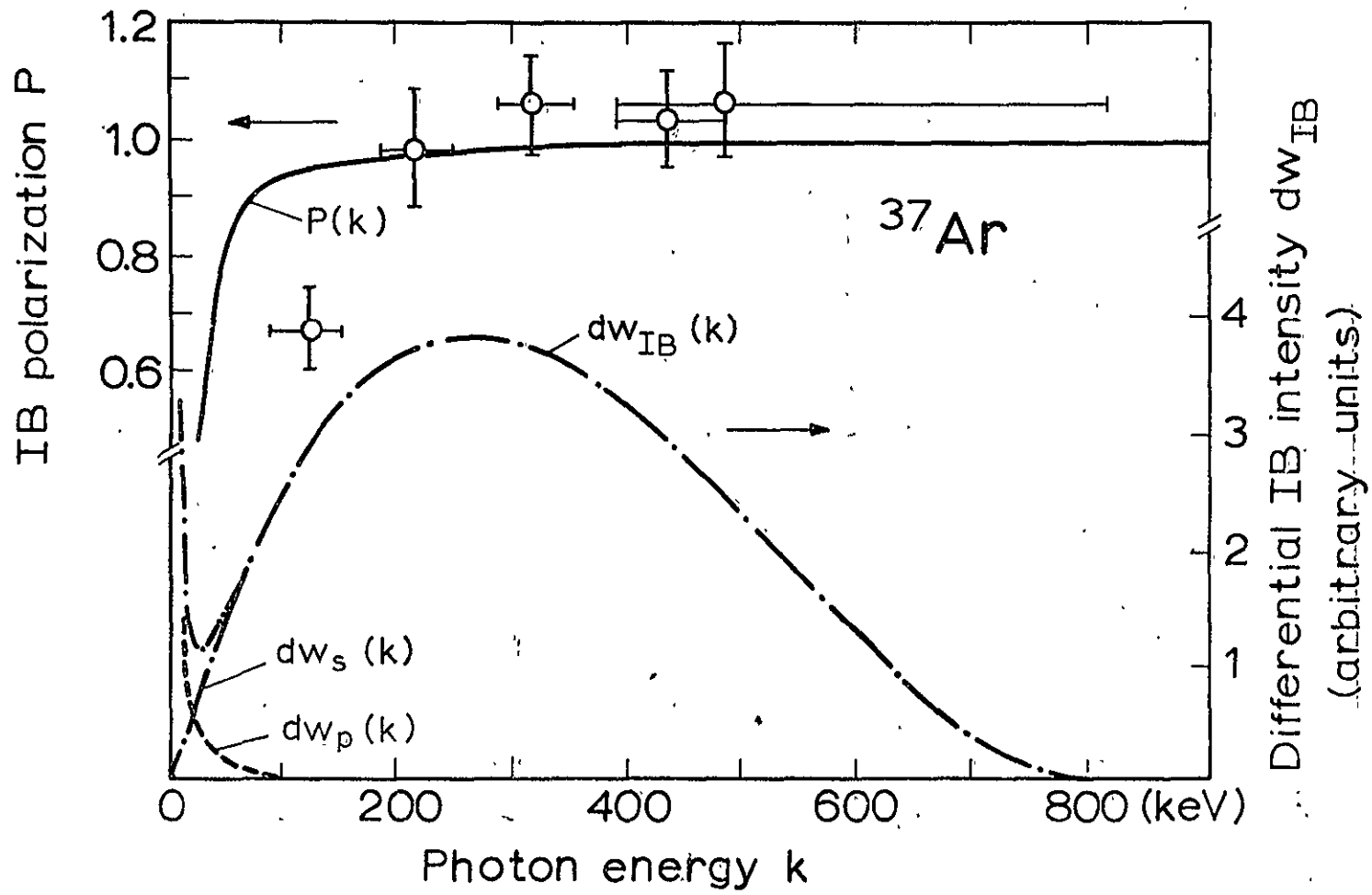


FIG. 4-32



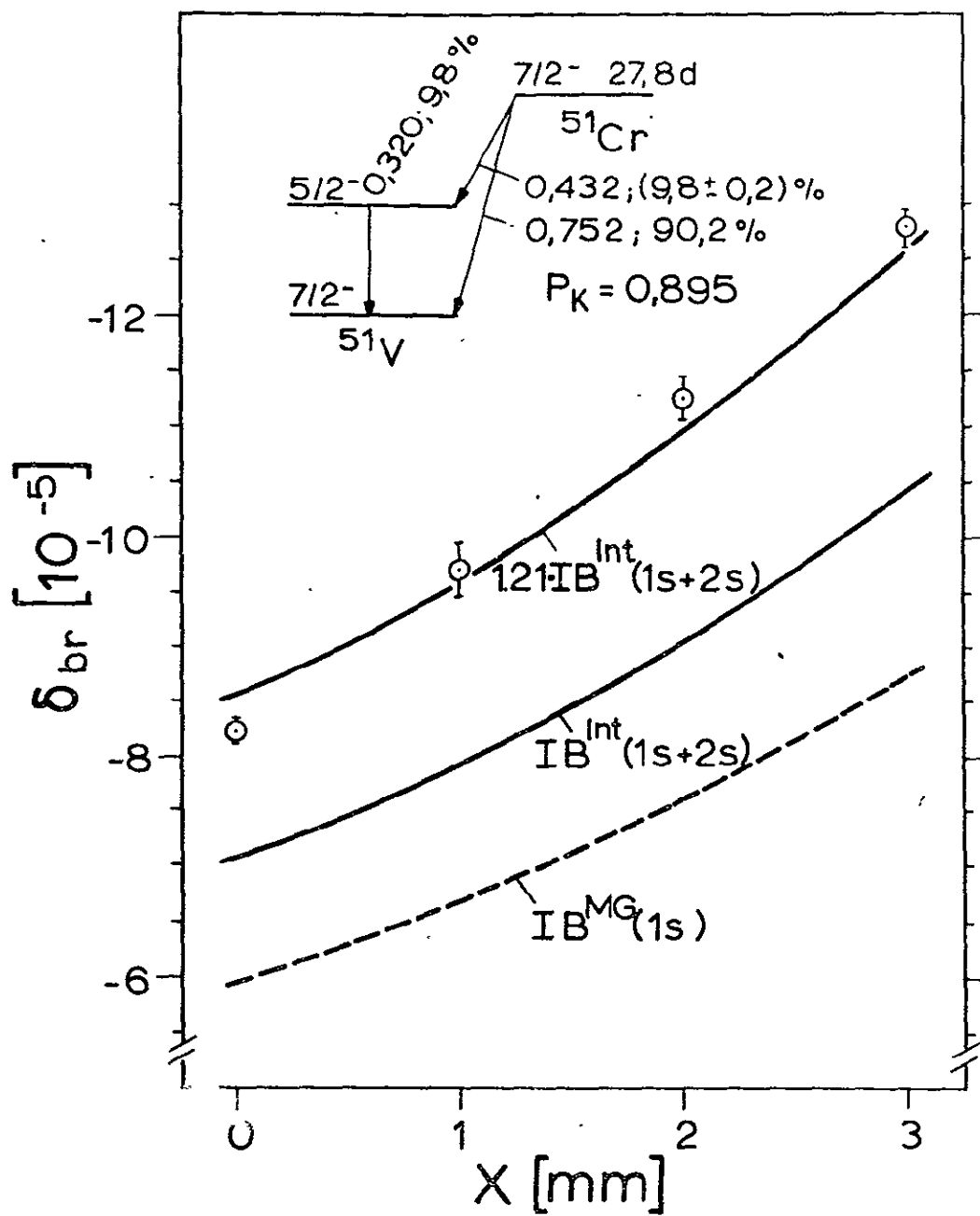


FIG. 4-34

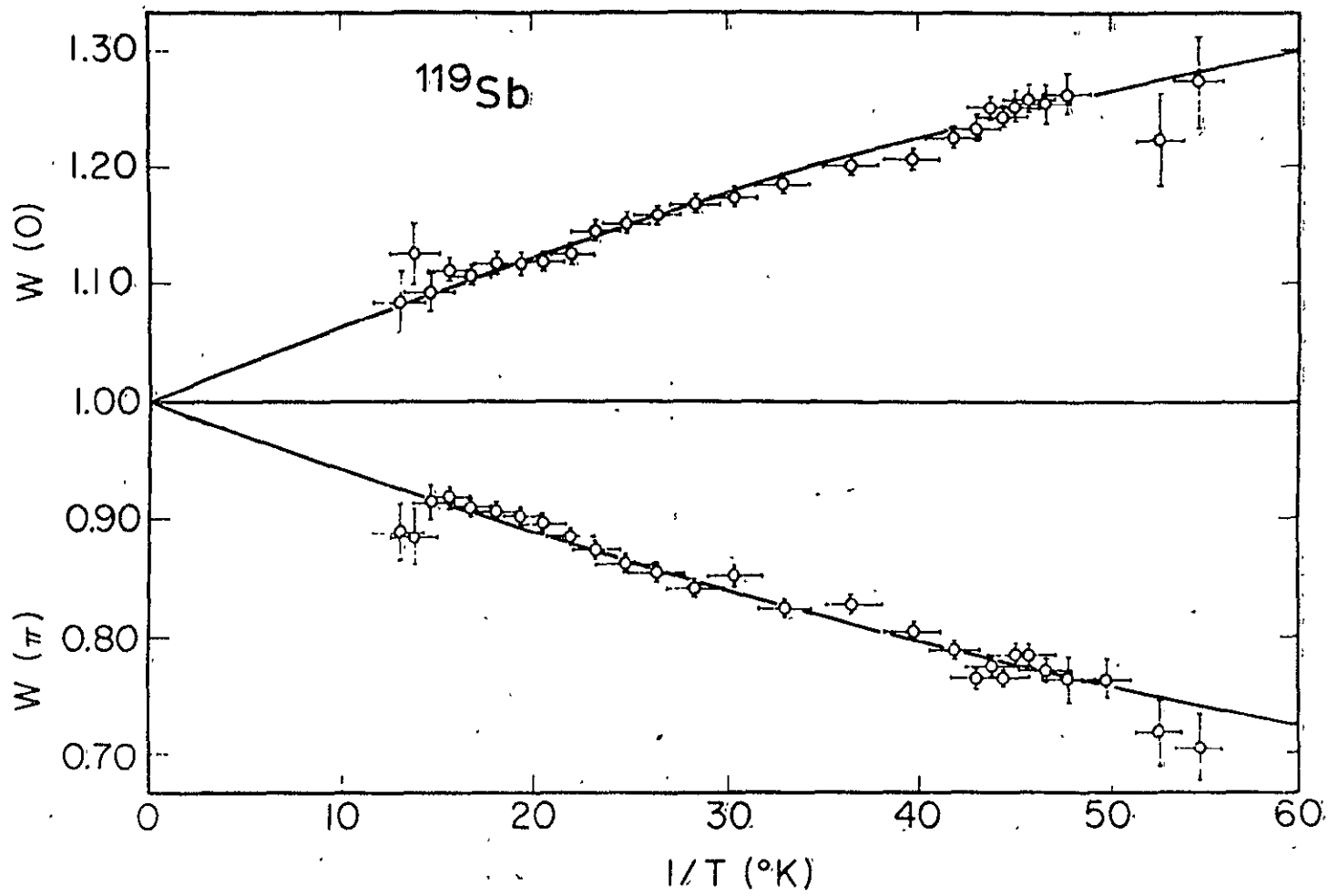
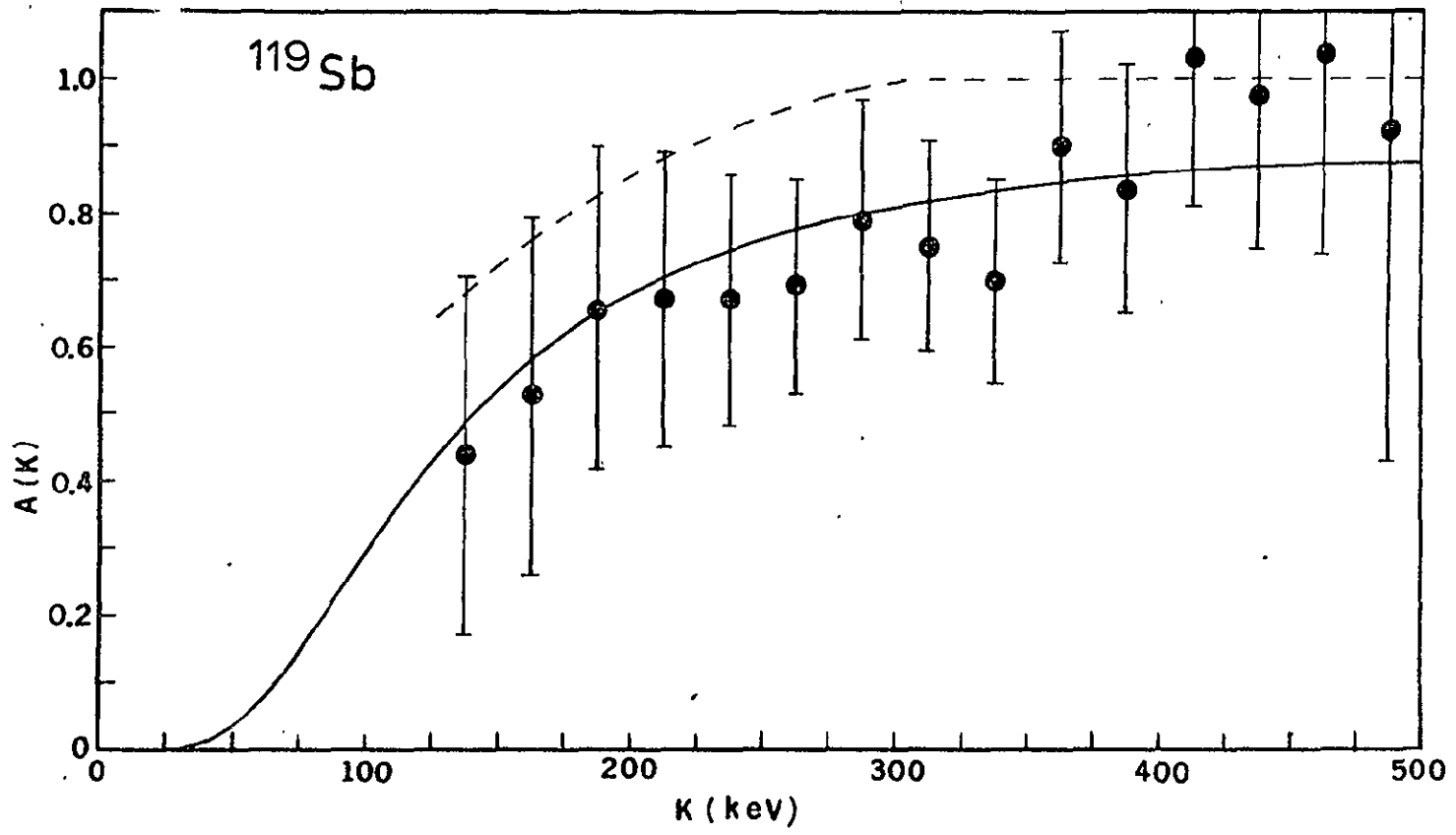


FIG. 4-35



PTC 4-36

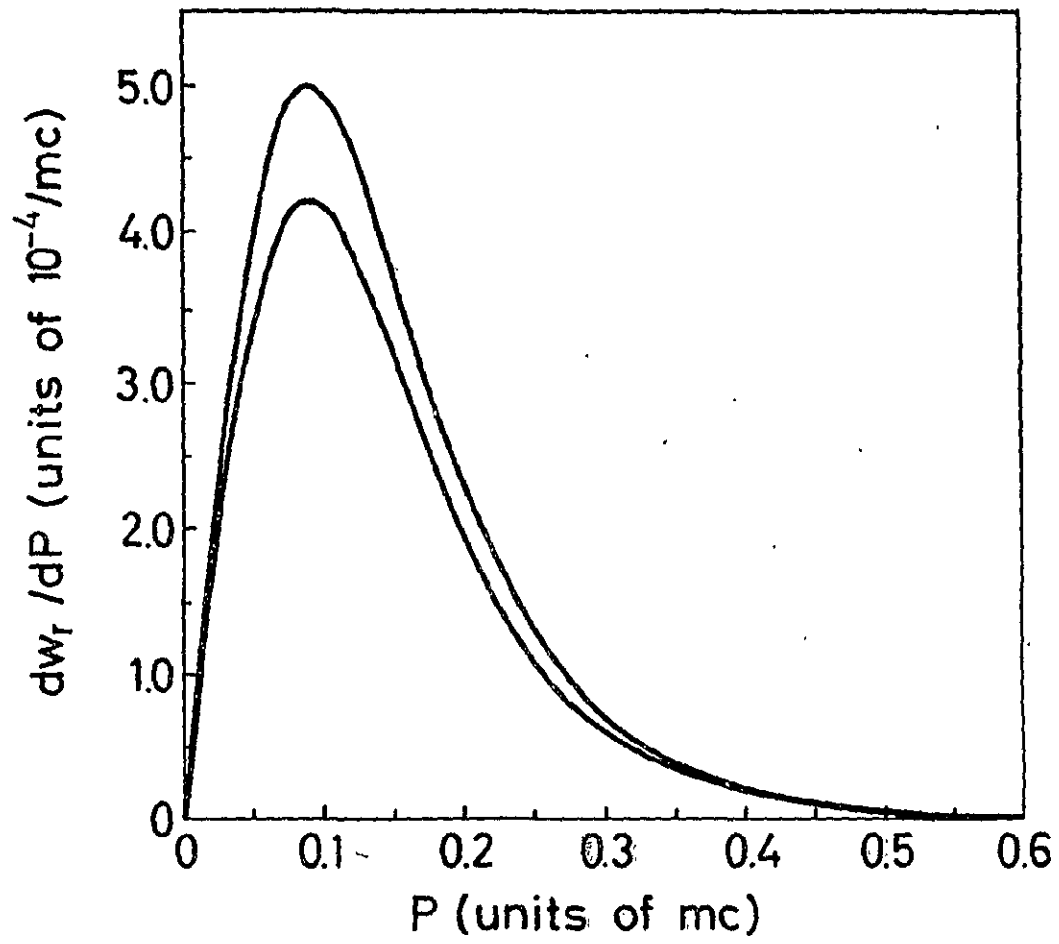


FIG. 5-1

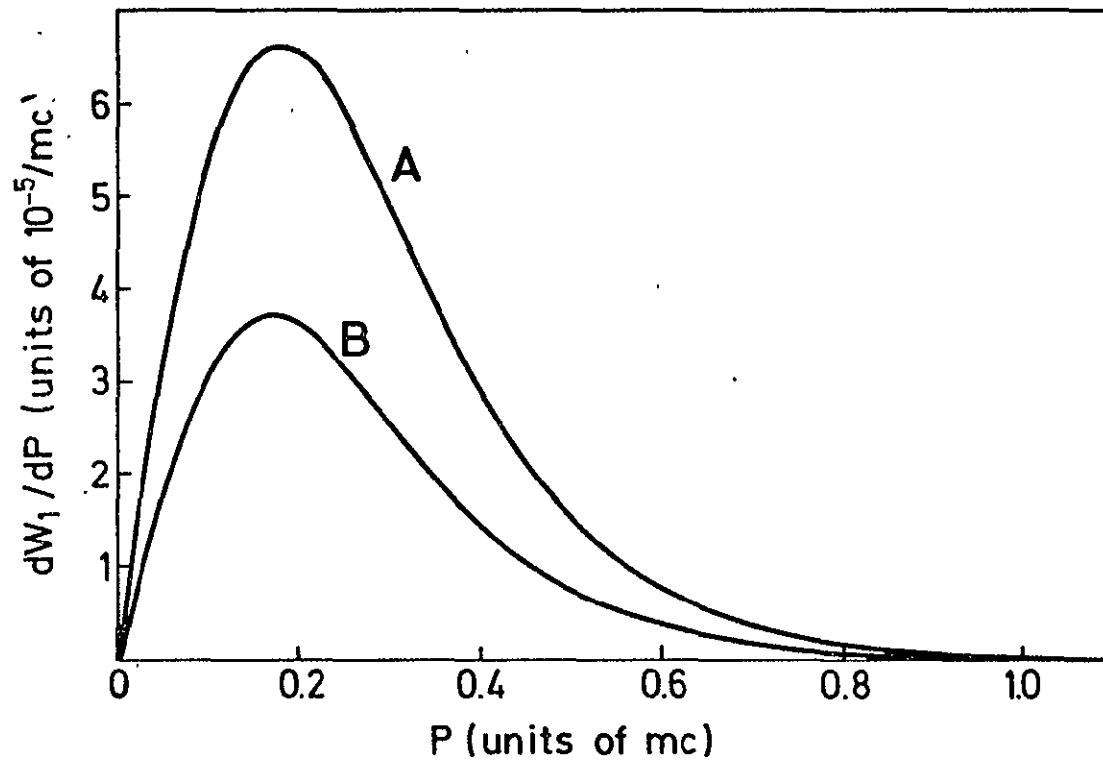


FIG. 5-2

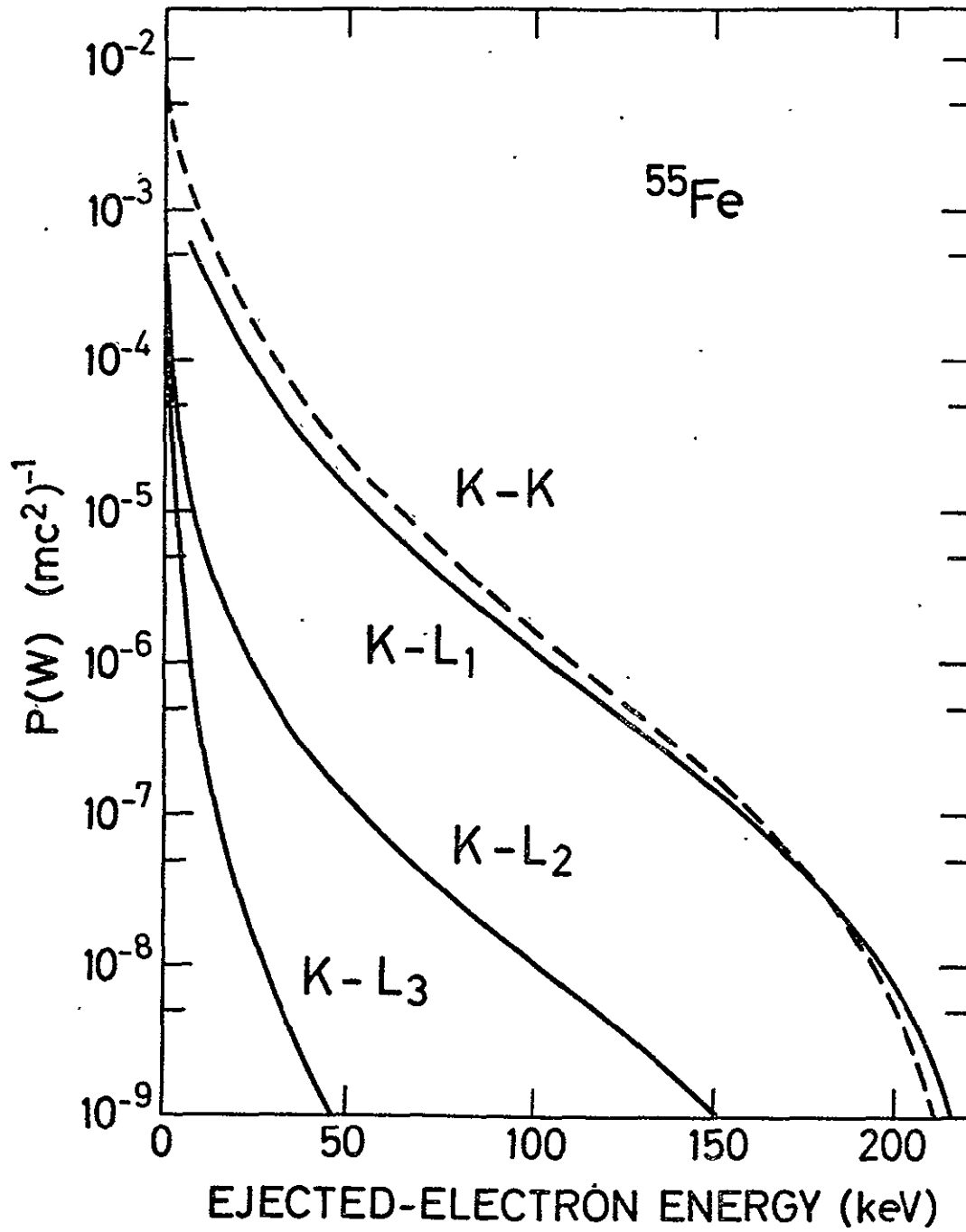


FIG. 5-3